buildings

Special Issue Reprint

Research towards the Green and Sustainable Buildings and Cities

Edited by
Haibo Guo and Bolun Zhao

mdpi.com/journal/buildings

MDPI

Research Towards the Green and Sustainable Buildings and Cities

Research Towards the Green and Sustainable Buildings and Cities

Guest Editors

Haibo Guo
Bolun Zhao

MDPI

Basel • Beijing • Wuhan • Barcelona • Belgrade • Novi Sad • Cluj • Manchester

Guest Editors

Haibo Guo
School of Architecture and Design
Harbin Institute of Technology
Harbin
China

Bolun Zhao
School of Architecture and Design
Harbin Institute of Technology
Harbin
China

Editorial Office
MDPI AG
Grosspeteranlage 5
4052 Basel, Switzerland

This is a reprint of the Special Issue, published open access by the journal *Buildings* (ISSN 2075-5309), freely accessible at: https://www.mdpi.com/journal/buildings/special_issues/5B1779A081.

For citation purposes, cite each article independently as indicated on the article page online and as indicated below:

Lastname, A.A.; Lastname, B.B. Article Title. *Journal Name* **Year**, *Volume Number*, Page Range.

ISBN 978-3-7258-5157-7 (Hbk)
ISBN 978-3-7258-5158-4 (PDF)
https://doi.org/10.3390/books978-3-7258-5158-4

© 2025 by the authors. Articles in this book are Open Access and distributed under the Creative Commons Attribution (CC BY) license. The book as a whole is distributed by MDPI under the terms and conditions of the Creative Commons Attribution-NonCommercial-NoDerivs (CC BY-NC-ND) license (https://creativecommons.org/licenses/by-nc-nd/4.0/).

Contents

About the Editors . . . . . **vii**

Preface . . . . . **ix**

Jiang Wang, Wei Fan, Bolun Zhao, Yang Yang and Zhijun Zhang
A Rule-Based Design Approach to Generate Mass Housing in Rural Areas of the North China Plain
Reprinted from: *Buildings* **2023**, *13*, 2539, https://doi.org/10.3390/buildings13102539 . . . . . **1**

Yaqi Wen, Yuyao Li, Yang Yang and Jiang Wang
Towards an Evaluation System of Disabled Individuals' Friendly Communities from the Perspective of Inclusive Development—A Case Study in Jinan
Reprinted from: *Buildings* **2023**, *13*, 2715, https://doi.org/10.3390/buildings13112715 . . . . . **17**

Yuedong Wu, Jincheng Ren and Jian Liu
Field Investigation of Water Infiltration into a Three-Layer Capillary Barrier Landfill Cover System Using Local Soils and Construction Waste
Reprinted from: *Buildings* **2024**, *14*, 139, https://doi.org/10.3390/buildings14010139 . . . . . **37**

Siyuan Chen, Zao Zhang, Cheng Wang, Lifeng Tan, Huanjie Liu, Hong Yuan, et al.
Evaluation Model of Distributed Photovoltaic Utilization in Urban Built-Up Area
Reprinted from: *Buildings* **2024**, *14*, 943, https://doi.org/10.3390/buildings14040943 . . . . . **51**

Shuhu Liu, Lin Wu, Chenlu Xiang and Wenyuan Dai
Revitalizing Rural Landscapes: Applying Cultural Landscape Gene Theory for Sustainable Spatial Planning in Linpu Village
Reprinted from: *Buildings* **2024**, *14*, 2396, https://doi.org/10.3390/buildings14082396 . . . . . **75**

Rafa Ramisha Tabassum and Jihyun Park
Development of a Building Evaluation Framework for Biophilic Design in Architecture
Reprinted from: *Buildings* **2024**, *14*, 3254, https://doi.org/10.3390/buildings14103254 . . . . . **98**

Zhongkai Zhou, Meng Liu, Jilong Zhao and Chaoxian Li
Construction and Optimization Strategies for Rural Residential Spatial Models Based on the Concept of Resource Metabolism: A Case Study of Rural Areas in the Shandong Plain
Reprinted from: *Buildings* **2024**, *14*, 3302, https://doi.org/10.3390/buildings14103302 . . . . . **119**

Ziqi Xu, Jiang Chang, Fangyu Cheng, Xiaoyi Liu, Tianning Yao, Kuntao Hu and Jingyu Sun
Examining the Impact of the Built Environment on Multidimensional Urban Vitality: Using Milk Tea Shops and Coffee Shops as New Indicators of Urban Vitality
Reprinted from: *Buildings* **2024**, *14*, 3517, https://doi.org/10.3390/buildings14113517 . . . . . **149**

Qinghong Li, Tiejian Zhang, Yingming Fang and Fengzeng Lin
A Pathological Diagnostic Method for Traditional Brick-Masonry Dwellings: A Case Study in Guangfu Ancient City
Reprinted from: *Buildings* **2024**, *14*, 3563, https://doi.org/10.3390/buildings14113563 . . . . . **180**

Jiahui Yu, Hongnan Wang, Yige Sui, Yitong Xu and Yang Chen
Optimising Ventilation Strategies Based on Predicted Mean Vote and Indoor CO_2 Concentration: A Case Study of University Teaching Spaces in Cold Region of China
Reprinted from: *Buildings* **2024**, *14*, 3822, https://doi.org/10.3390/buildings14123822 . . . . . **208**

Tianning Yao, Liang Sun, Lin Geng, Yao Xu, Ziqi Xu, Kuntao Hu, et al.
Exploring Optimisation Pathways for Underground Space Quality Under the Synergy of Multidimensional Perception and Environmental Parameters
Reprinted from: *Buildings* **2025**, *15*, 204, https://doi.org/10.3390/buildings15020204 . . . . . **230**

Jitai Li, Fan Lin, Yile Chen and Shuai Yang
Assessing and Enhancing Green Quantity in the Open Spaces of High-Density Cities: A Comparative Study of the Macau Peninsula and Monaco
Reprinted from: *Buildings* **2025**, *15*, 292, https://doi.org/10.3390/buildings15020292 . . . . . **257**

Qiaoli Ouyang, Fengxiang Liu and Yanyu Wang
Operationalizing Sustainability in Old Community Renewal: A Post-Occupancy Evaluation of Resident Satisfaction in Chengdu, China
Reprinted from: *Buildings* **2025**, *15*, 725, https://doi.org/10.3390/buildings15050725 . . . . . **283**

Lingxin Meng, Ziyao Yang, Lifeng Tan, Shulong Yan, Yukun Zhang and Xuan Wang
Research on the Dynamic Defensive Efficiency of Traditional Military Settlements in the Ming Dynasty: A Case Study of Ningbo Coastal Defense, China
Reprinted from: *Buildings* **2025**, *15*, 1077, https://doi.org/10.3390/buildings15071077 . . . . . **307**

Yicheng Zhang, Guorui Chen and Xue Yang
Research on the Evolution Characteristics of Building Space in the Central Urban Area of Tianjin Based on Multi-Source Data Collaboration: 2021–2024
Reprinted from: *Buildings* **2025**, *15*, 1142, https://doi.org/10.3390/buildings15071142 . . . . . **329**

Tengfei Ma, Huakai Ye, Yujing Lai, Haoying Han, Yangguang Song and Yile Chen
Spatiotemporal Dynamics and Driving Factors of Urban Green Space in Texas (2001–2021): A Multi-Source Geospatial Analysis
Reprinted from: *Buildings* **2025**, *15*, 1166, https://doi.org/10.3390/buildings15071166 . . . . . **349**

An Li, Chong Guo, Jian Gu, Yanyuan Hu, Zhaoyang Luo and Xunzhi Yin
Promoting Circular Economy of the Building Industry by the Use of Straw Bales: A Review
Reprinted from: *Buildings* **2024**, *14*, 1337, https://doi.org/10.3390/buildings14051337 . . . . . **370**

Lin Geng, Minghui Xue, Jia Li and Jiaoguo Ma
Historic District Conservation: A Critical Review of Global Trends, Development in the 21st Century, and Challenges Through CiteSpace Analysis
Reprinted from: *Buildings* **2025**, *15*, 1232, https://doi.org/10.3390/buildings15081232 . . . . . **396**

About the Editors

Haibo Guo

Haibo Guo is a Professor at the School of Architecture and Design, Harbin Institute of Technology (HIT), in Harbin, China. His research focuses on green building materials, building energy efficiency, and sustainable urban development, aiming to advance innovative solutions for environmentally responsible construction and urban planning. He has led or participated in 10 major national-level research projects, including grants from the National Natural Science Foundation of China (NSFC), addressing critical challenges in sustainable building and city design. His work has contributed significantly to developing practical frameworks for enhancing the ecological performance of built environments. Professor Guo actively supports academic discourse through his roles as a Guest Editor and peer reviewer for several leading international journals in the fields of sustainable architecture and urban science.

Bolun Zhao

Bolun Zhao is a doctoral candidate at the School of Architecture and Design, Harbin Institute of Technology (HIT), in Harbin, China. His research focuses on building indoor thermal comfort, computational design methodologies, and sustainable biomass materials for construction applications, with the overarching goal of advancing sustainable development in buildings and cities. As an active researcher, he has authored or co-authored more than 20 peer-reviewed publications contributing to these fields. Mr. Zhao further supports the academic community by serving as a reviewer for several leading peer-reviewed journals in architecture, building science, and sustainable materials. His work consistently bridges theoretical innovation with practical solutions for enhancing environmental performance in the built environment.

Preface

Our present era demands a radical rethinking of the built environment. Climate change, resource depletion, greenhouse gas emissions, and sustainable development imperatives compel us to embrace energy-efficient, ecologically sensitive, and sustainable practices. This Reprint, Research towards the Green and Sustainable Buildings and Cities, responds to this critical need.

The scope of this collection spans the transformative potential of emerging technologies—such as green building techniques, artificial intelligence, and digital twins—alongside the vital preservation of architectural heritage and cultural identity. It explores how innovation harmonizes with tradition to revitalize communities and redefine sustainable architecture.

The aim of this Reprint is to showcase cutting-edge research driving multidisciplinary solutions for sustainable urban futures. We are motivated by the urgency of global challenges and the opportunity to steer architectural practice toward resilience, cultural continuity, and ecological stewardship.

This Reprint presents 18 peer-reviewed papers advancing knowledge in green materials, smart building systems, heritage-sensitive retrofits, and urban sustainability frameworks. We extend our deepest gratitude to the contributing authors for sharing their expertise, the diligent reviewers for ensuring scholarly rigor, and the Buildings editorial team for their unwavering support.

We address this work to researchers, architects, urban planners, engineers, policymakers, and all stakeholders committed to forging sustainable, livable cities and buildings for generations to come.

Haibo Guo and Bolun Zhao
Guest Editors

buildings

MDPI

Article

A Rule-Based Design Approach to Generate Mass Housing in Rural Areas of the North China Plain

Jiang Wang [1,*], Wei Fan [2], Bolun Zhao [3,4], Yang Yang [1] and Zhijun Zhang [5]

[1] School of Architecture and Urban Planning, Shandong Jianzhu University, Jinan 250101, China; 24265@sdjzu.edu.cn
[2] School of Architecture, Tianjin University, Tianjin 300354, China; 1022206003@tju.edu.cn
[3] School of Architecture, Harbin Institute of Technology, Harbin 150001, China; 22b934023@stu.hit.edu.cn
[4] Key Laboratory of Cold Region Urban and Rural Human Settlement Environment Science and Technology, Ministry of Industry and Information Technology, Harbin 150001, China
[5] School of Computer Science and Technology, Shandong Jianzhu University, Jinan 250101, China; 12778@sdjzu.edu.cn
* Correspondence: wangjiang@sdjzu.edu.cn

Abstract: Affected by the development strategy of Rural Space Reconstruction in China, the demand for rural mass housing has peaked in the North China Plain in the past 20 years. However, due to the inefficiency of conventional design methods, the rural houses built appear to have a noticeable trend of urbanization and homogeneity. To propose a more effective design approach to change the hitherto unsuccessful homogenized phenomenon of rural design, the study is based on investigating the composition, configuration and characteristics of the dwellings in some traditional villages of the eastern Shandong Province, and it compares and analyzes the differences between conventional methods and generation methods through three design tests: Test 1 is for the reappearance of a general mode of planning, Test 2 is based on the definition of shape-grammar-based rules and Test 3 is mainly used for the optimizing and programming of rules. Furthermore, based on the three prototypes of homestead combination, three-level rules are determined through the three tests mentioned above: Level-1 describes the housing prototype consisting of four homesteads, which generates a variety of spatial relations through the translation of homesteads. Level-2 describes a neighborhood prototype consisting of 16 homesteads, which generates various samples through splitting prototypes and expanding homesteads. Level-3 describes a block prototype consisting of 64 homesteads, which controls open space and identifies a given base during sample filling. Through the analysis of the tests results, the rationality and feasibility of the generative design approach are verified, proving that this approach effectively solves the design monotony problem that commonly exists in rural mass housing in the North China Plain.

Keywords: rule-based approach; generative design; mass housing; rural housing; shape grammar; design process; automation; space syntax

1. Introduction

Since 2000, the Chinese government has implemented the development strategy of Rural Space Reconstruction. Through planning and control, the government has led and planned rural settlements and promoted the moderate concentration of the rural population. On this basis, it is necessary to allocate the rural infrastructure appropriately, improve the quality of human settlements in rural areas, and form a spatial structure conducive to urban–rural integration [1]. To make more compact and efficient use of rural land resources in the North China Plain, some local governments have mandated that architects design mass rural housing, which may take the form of either urban multi-story houses with upstairs living spaces or single-door, single-courtyard row houses. However, upon the completion of certain projects, the homogenized and dull image clashed with the original rural aesthetic,

leading to scrutiny from many architectural critics. This unified construction of mass rural housing appears to be evolving into a newly emerging architectural typology, thereby impacting the rural construction process in China. Because this type of building belongs to rural projects, its low price makes it difficult for architects to devote a lot of energy, and many projects are designed using simple row houses. Furthermore, in the past, rural houses were typically constructed by individual families, leading to diverse and evolving spatial relationships among households through diachronic evolution. In a unified construction cycle, if the traditional spatial relationships are to be reconstructed simultaneously, the overall planning of these small body and large quantity houses should align with the fundamental elements of traditional styles. This calls for the establishment of a set of efficient design methods, abandoning the conventional blueprint-based design approach.

With this scenario in the backdrop, the current study employed a rule-based approach to the design of rural housings and homesteads to generate a variety of layout patterns that represented the traditional Chinese rural settlement. The results of this study showed predefined, phased, hierarchical, and differentiated characteristics. The findings are expected to provide a foundation for the industrialized methods of construction which may further support automated design and mass customization.

2. Literature Review

With the advent of digital design tools, designers' awareness and handling of complex spatial issues improved significantly. Not only can a digital design produce a personalized response to real-world design issues, but it can also provide a meaningful alternative to repetitive design logic. Based on Gilles Deleuze's philosophical theory, Oxman [2] summarized five digital design models, viz. the CAD model, digital formation model, generative design model (GDM), performance model, and compound model. Among these models, the GDM is used to define the calculation rules of the formal generative mechanism, and the results obtained are more flexible and can maximize the implementation of interactional design. It has been widely used in the field of digital architecture design recently.

The GDM framework consists of several different design approaches or models, such as cellular automata (CA), genetic algorithms (GA), L-systems (LS), shape grammars (SG), and swarm intelligence (SI). Most of them, like SG, are branches of the rule-based system, which is one of the most basic automation design techniques. Although there are some similarities and overlaps between them, each approach deals with different design issues [3]. For instance, SG is generally used when there is a strong domain of knowledge [4], such as in the study of mass housing layout.

SG can be both descriptive and generative. It can be used both as an analytical tool to describe the formal structure of a corpus of existing designs, and as a synthetic tool to create new languages of design. Initially, SG was used for the generative specification of painting and sculpture [5]. Stiny and Mitchell [6] defined SG that constituted the style of Palladio's villas and translated them into concrete methods and a generative process. Chiou and Krishnamurti [7] were the first to use SG to study folk houses in Taiwan, which established the fact that SG can be applied to study Chinese traditional architecture. Duarte [8] described the grammar of Alvaro Siza's houses at Malagueira, and applied an interactive computer system to design customized mass housing. In recent years, several computational design methods have been applied on a large scale. Beirão et al. [9] defined Urban Grammar formally and developed a digital design tool to start the research of a customized city. Therefore, SG is being increasingly used to clarify any design rules of complex architectural designs and urban planning, leading to the building of a multi-level design corpus [10].

Considering Duarte [11] and Wang et al. [12], the residential design world can be described as a hierarchical structure comprising materials, components, parts, rooms, dwellings, housings, neighborhoods, blocks, settlements, and towns, of which the housing, neighborhoods, and blocks have been the focus of the present study (Figure 1). Regarding housing, the individual buildings which comprised similarly shaped elements [13] were

analyzed, such as in the case of Erem et al. [14] who added Turkish rural housing grammars to the new rules, which can improve the adaptability of traditional housing after reconstruction. With regard to neighborhood, combinations of similar housing were considered, such as in the case of Herbert et al. [15]. With respect to blocks, mainly the roads, layout, and scale were paid attention to, such as in the case of Dias [16].

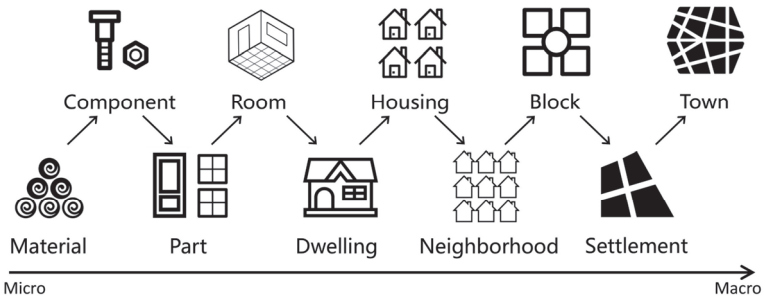


Figure 1. Hierarchical structure of mass customized housing design.

3. Methodology

To propose a more effective method, selecting an actual base for design research is necessary. Therefore, Zhuo village in the North China Plain was selected as the target, and an investigation was conducted on it and some surrounding villages to clarify the composition, configuration and characteristics of typical rural housing in the local area. And, then, we qualitatively proposed a housing prototype, core housing, and their relative relationship with homesteads. In the subsequent research on the rule-based approach, on the one hand, some design tests were conducted using the base of Zhuo village. On the other hand, a series of applicable rules have been proposed, some of which come from the investigation results and some from the professional experience of the researchers.

3.1. Investigation and Analysis Approach

The first method was a field investigation. In this method, 16 villages were selected which are distributed in the plain areas of the Wulong River, adjacent to Laiyang City of the Jiaodong Peninsula (Figure 2). These villages are all urban fringe villages with a history of more than 200 years and comprising 100 to 2000 households. Due to the rapid surge in demand for urban entertainment and rural tourism in recent years, these villages have gradually transformed their traditional farming to experiential agriculture. In our initial investigation, Google Earth images were used to analyze the boundary, road, layout and scale of each village. Next, through field research, particularly the texture of the Zhuo village was focused to systematically analyze the three levels—block, neighborhood and housing. At the block level, the roads were divided into main roads with a width of about 6 m and alleys with a width of about 3–4 m. The main road is used for household and agricultural vehicles, and the alleys are primarily used for walking. Tortuosity and cul-de-sacs are the two basic forms of the roads; the homesteads adjacent to the main road are larger because they are often used for commercial services. With regard to the neighborhood aspect, most of the blood-related families were found to live next to each other. This is due to the influence of the traditional family culture. Later, as the economy developed and population mobility increased, the closely related families split into single-family households with a small courtyard. At the housing level, five typical fragments consisting of four detached houses were selected for diagram and transformation to designate a housing-level prototype (Figure 3). In addition, the core housing faced south with a maximum of 2 floors and rooms having widths between 3 and 3.3 m. The shape of the homestead mainly included two types: long rectangle in a vertical direction and approximate square. Furthermore, the gable of the core housing and the northern boundary of the homestead were usually not provided with any gates.

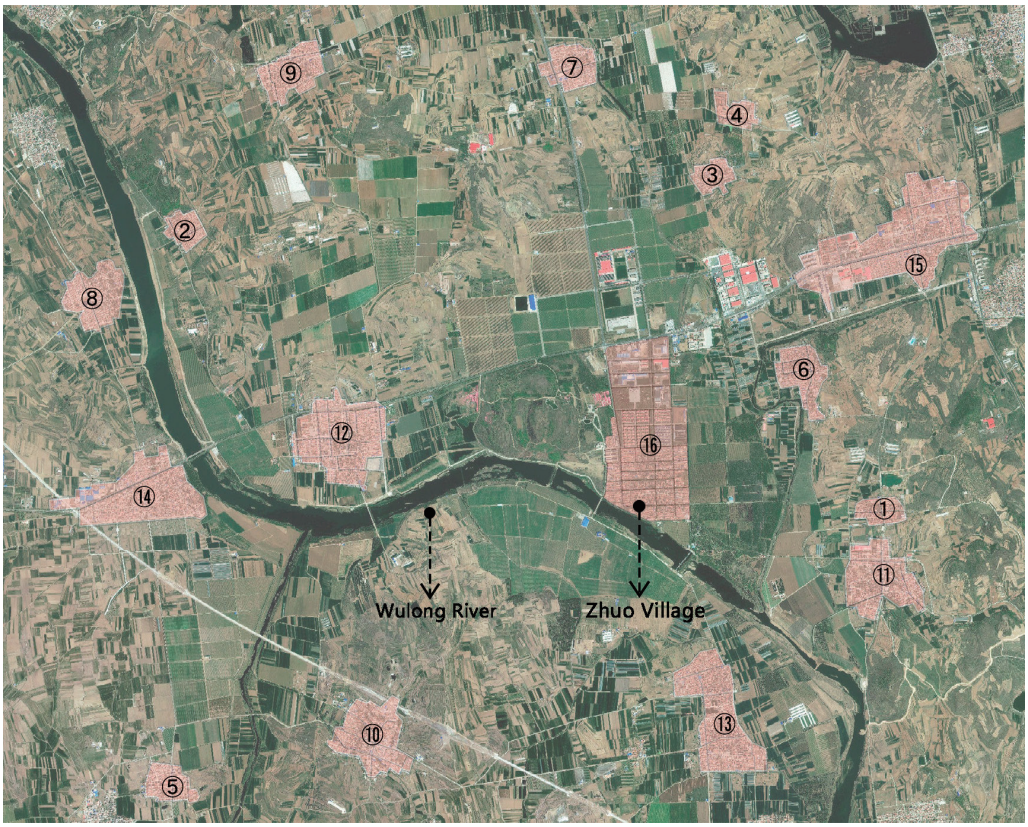


Figure 2. The distribution map of villages investigated. ① Bozhuang village. ② Yuanshang village; ③ Heshankou village. ④ Dongzhuang village. ⑤ Dongzhuanggezhuang village. ⑥ Beisonggezhuang village. ⑦ Dazhuangzi village. ⑧ Nanligezhuang village. ⑨ Beihuang village. ⑩ Xuzhuangzhuang village. ⑪ Fengtou village. ⑫ Donggezhuang village. ⑬ Heqian village. ⑭ Cuizhuang village. ⑮ Jiangzhuang town. ⑯ Zhuo village.

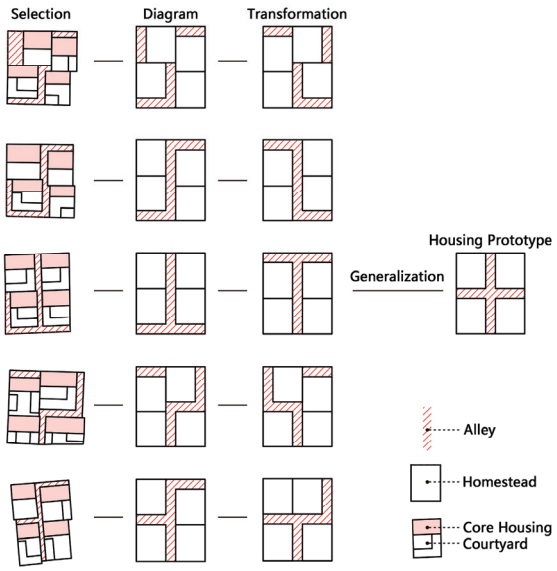


Figure 3. The evolution map of housing prototype.

3.2. Rule-Based Approach

The second method was the automation of rule-based design, which was divided into three stages (Test-1, 2, 3) of progressive implementation. Specifically, the second method included the definition of rules, implementation of rules, comprehensive analysis and

the encoding of rules. (1) In the field investigation, we used SG-based rules to derive the different housing prototypes. We also defined the rules for non-SG (non-Euclidean transformation) at all the 3 levels—the housing, neighborhood and block levels (homesteads from 4 to 16, 64). Moreover, the combination rules and filling rules were also defined. (2) Both qualitative and quantitative analyses were performed to verify the results of every test. In the qualitative analysis, the results of the tests were compared with traditional settlements, which showed whether the test results had the characteristic form and organization of a traditional residential space. In the quantitative analysis, Space Syntax was applied. The Space Syntax can be used to quantitatively analyze the spatial relationships implied in environmental design, interpret the impact of urban form and land use for pedestrians and bicycle transportation, and assist in decision-making in the planning and design of future environments. The integration value of the tests results was measured, and the high integration value represented high reachability and great potential to become a center [17]. (3) Furthermore, using the preliminary results, the filtration rules, classification rules, and adjustment rules were set to optimize the whole design process. The rules were coded via algorithms using Python and applied in a computer program to develop the design corpora. Subsequently, we selected a real base from the Zhuo village which needs to be renewed and used Pyautocad to identify its boundaries and roads. Samples from the corpora were then randomly and automatically filled into the base following the developed rules in order to realize design automation (Figure 4).

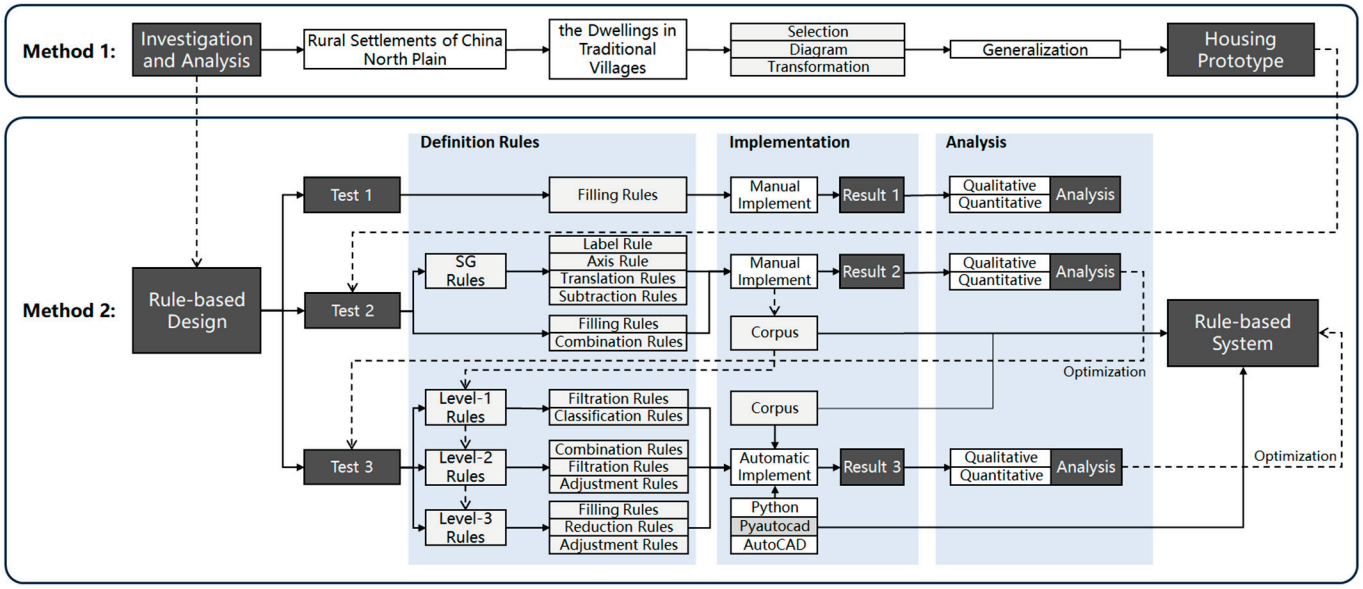


Figure 4. Process of rule-based design framework.

4. Predefinition

A basic module of 3.3 m was used to divide the grid of the homestead; the widths of the main road and the alley were considered as 6.6 m and 3.3 m, respectively. The length of the standard homestead (H0) in the north–south and east–west directions were 13.2 m and 9.9 m, respectively, and the area was 130.68 m^2. The given base, as shown in Figure 5, comprised an abandoned gated factory which was surrounded by walls. Since this land is not residential, the scope of this was excluded from the design tests. It should be emphasized that centrality is an important factor in traditional Chinese rural settlement. Therefore, in the analysis of Space Syntax, the results of tests which had a higher integration of the central area were better.

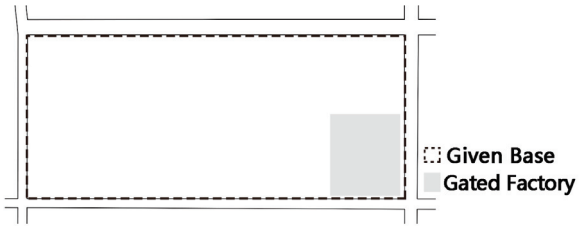


Figure 5. Given base.

5. Test 1 (Reappearance of General Mode of Planning)

Test 1 aimed to make the prevailing rural housing planning methods in China reappear. This process only involved the housing-level-based design rules, mainly by arranging and combining standard homesteads horizontally and vertically for layout.

5.1. Filling Rules

For a and b, starting from the left border, copy three (Figure 6a) or four (Figure 6b) of them horizontally to the right side and add a vertical road; repeat until the given base is filled. For c, starting from the upper border, copy two of them vertically to the lower side and add a horizontal road; repeat until the given base is filled (Figure 6c).

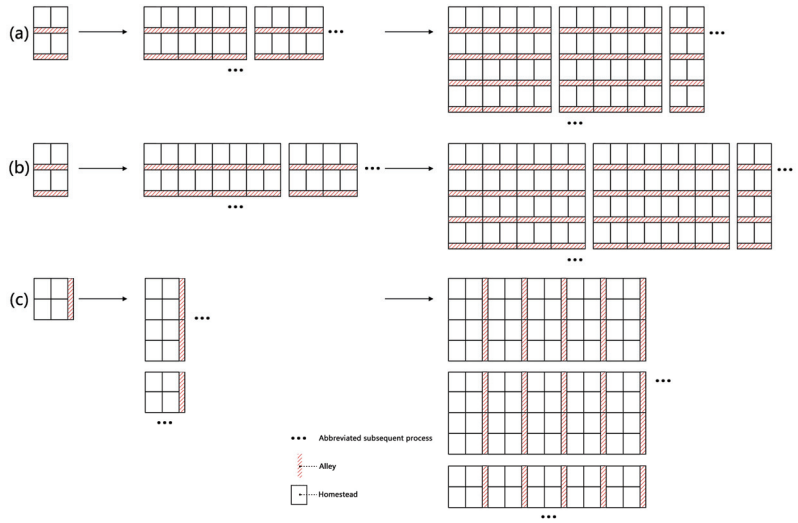


Figure 6. Filling rules. (**a**) The housing prototypes are arranged horizontally in groups of three. (**b**) The housing prototypes are arranged horizontally in groups of four. (**c**) The housing prototypes are arranged vertically in groups of four.

5.2. Implementation and Analysis

The filling rules were applied to the given base, generating three different plans to build the 3D models. Qualitatively, Figure 7a,b show the orderly form of row housing and homogeneous landscape, which displayed strong contrasts with the different styles and features of traditional villages. From a practical point of view, although this approach was conducive to mass production, the residential demands of each homestead could not be maintained as completely consistent, thereby losing the features of traditional villages. Quantitatively, while using Space Syntax to measure the integration value of the three results, the integration value showed an increase from the outer area to the central area, which indicated that the results were good with respect to integrity, centrality and enclosure (Figure 7c).

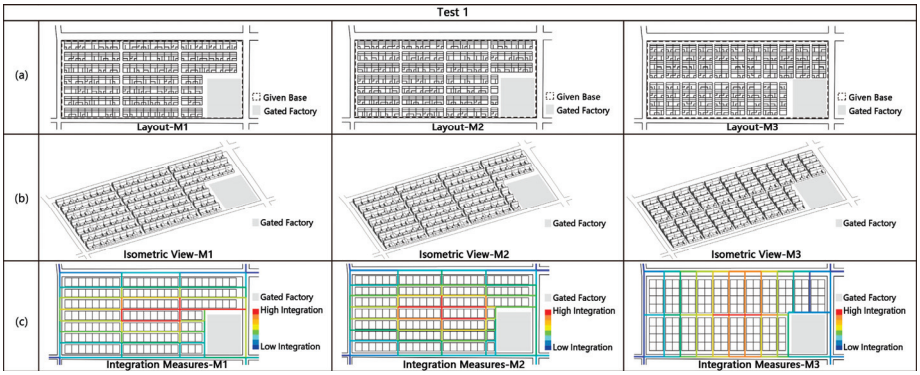


Figure 7. Results and analysis of Test 1. (**a**) Layout. (**b**) Isometric view. (**c**) The integration value of results measured.

6. Test 2 (Definition of SG-Based Rules)

More complicated rules were defined in Test 2 to address the problem of homogeneous design in Test 1. In order to improve the flexibility of the results, we not only defined the SG-based rules for housing level, but also defined the combination rules and filling rules for neighborhood and block level (Figure 8).

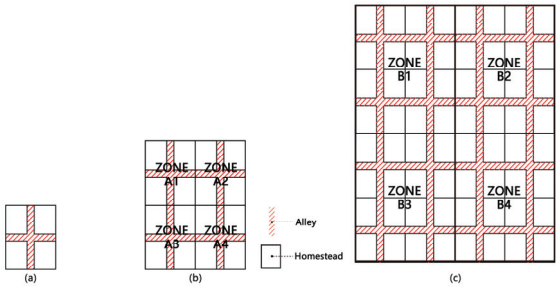


Figure 8. Prototype of neighborhood and block. (**a**) Housing prototype. (**b**) Neighborhood prototype. (**c**) Block prototype.

6.1. Housing Level: SG-Based Rules

In the housing prototype, the homesteads can be shifted horizontally or vertically by one module to form new shapes. Therefore, we used SG to define the rules to generate all the samples at the housing level. The main shape rules used are as follows (Figure 9):

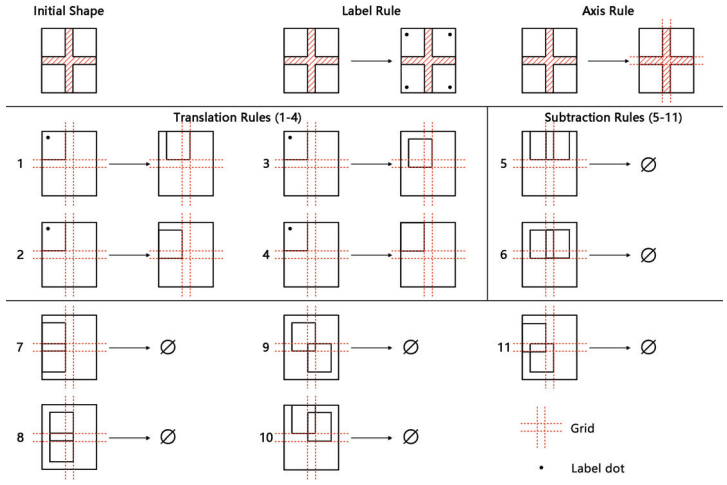


Figure 9. SG-based rules (Label rule, Axis rule, Transformation rules, Subtraction rules).

1. Label rule. Labeling homesteads of the initial shape indicated, on which the transformation rules could be applied.

2. Axis rule. This rule placed a grid over the initial shape and controlled the application of transformation rules, along with Euclidian transformations when translating the labelled (·) homesteads.

3. Transformation rules. The labels only allow for each of the homesteads to be acted on and can only be applied once to a selected homestead. Therefore, each homestead in the initial shape can only be manipulated once with the application of the four transformation rules.

4. Subtraction rules. As the purpose of the grammar was to facilitate samples of housing level development, the generation of overlapping or embedded shapes should be avoided. This is also supported by the application of subtraction rules which eliminate a complete permutation if overlapping or embedded shapes occur with the transformation of the smaller rectangles.

As permutations are progressively developed, they were categorized according to the number of applications of each of the four transformation rules. In the present study, the application of the shape rules and the subtraction rules generated 79 different samples of housing level—Set T (Figure 10).

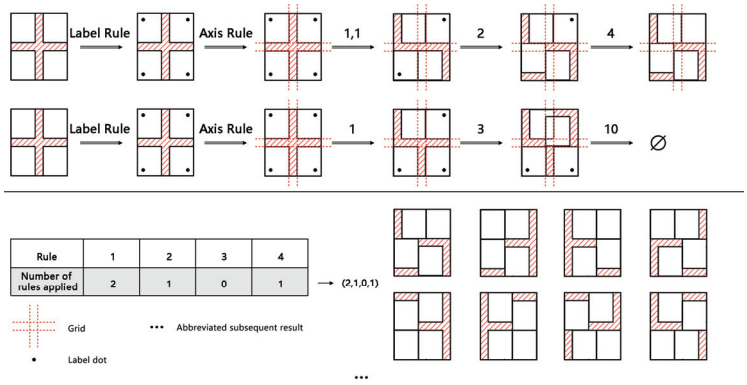


Figure 10. Implementation of rules.

6.2. Neighborhood and Block Level: Non-SG-Based Rules

1. Combination rules. The samples in Set T were randomly extracted and combined, like the neighborhood prototype, to form a new sample Set N. The samples in Set N were randomly extracted and combined, similarly to the block prototype, to form a new sample Set B.

2. Filling rules. The samples in Set B were collected and filled on the given base, and each sample was separated by a road. Moreover, during filling, 9 of the 64 homesteads were randomly transformed into open space.

6.3. Implementation and Analysis

We collected the samples from Set B and implemented the filling rules on the given base. Any extra homesteads beyond the boundary were removed to generate three different plans and build 3D models. Qualitatively, Figure 11a, b displays a repetitive and different form which has the traditional rural style and features. This shows good similarity and continuity in the results. Some shapes were identified from the traditional housing layout; however, there was only one size of homestead which did not meet the different residential demands. The results obtained were contingent, and reflected some errors that the gate could not be set up at the homestead (red-marked in Figure 11a). Quantitatively, the integration value of Test 2 was unevenly distributed within the given base, which means that the results did not show good centrality and enclosure, and the space was comparatively negative (Figure 11c). This is because some samples lacked the definition of restrictions or rules related to road connectivity in the combination process.

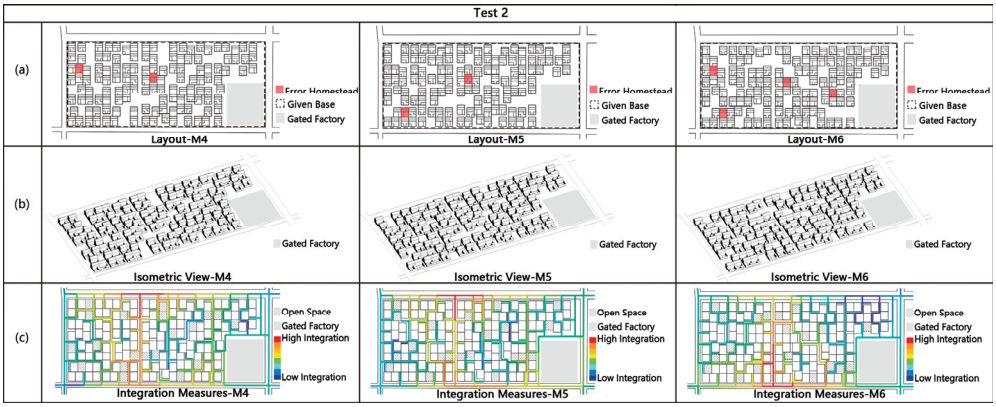


Figure 11. Results and analysis of Test 2. (**a**) Layout; (**b**) Isometric view; (**c**) The integration value of results maesured.

7. Test 3 (Optimization and Programming of Rules)

7.1. Predefinition

Based on the results of Test 1 and Test 2, the rules were optimized and coded using a computer program using Pyautocad. The samples in Set T and the housing and neighborhood prototypes were retained. Furthermore, to meet different residential demands, five sizes of homestead were predefined, including one standard type (H0), one small type (H1) and three large types (H2, H3, H4) (Figure 12a). Additionally, the block prototype was modified by adding north–south and east–west roads at the center (Figure 12b).

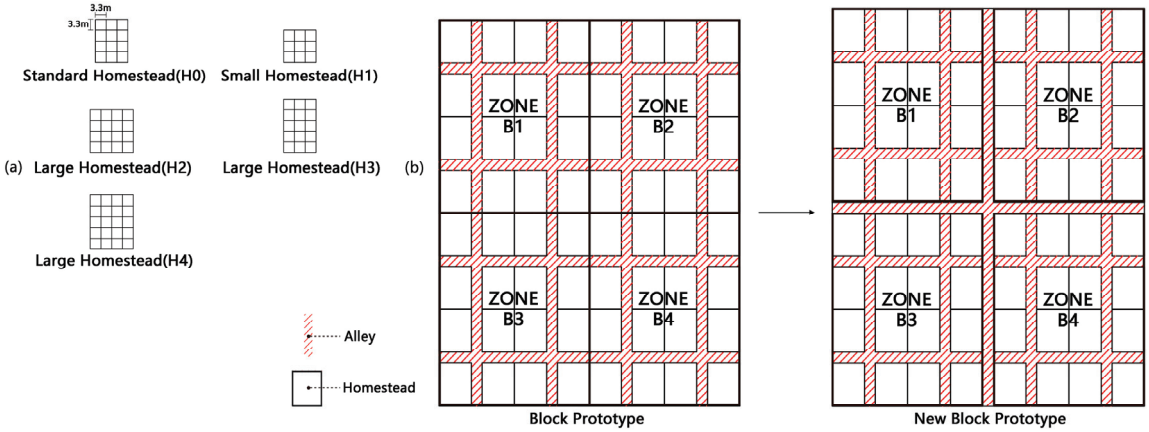


Figure 12. Adjusted prototypes of homestead and block. (**a**) Five sizes of homestead. (**b**) Modify block prototype.

7.2. Level-1 Rules (Housing Level)

1. Filtration rules. Limited by factors such as walking accessibility and gate position, Set T did not support the survey conclusions fully. Therefore, some samples were removed by setting new filtration rules, which are as follows: (1) as long as there is a homestead not close to an internal alley, filtering was necessary, (2) if the gate can only be opened on the north side of the homestead or the gable wall of the core housing, it must be filtered and (3) delete the sample of housing prototype. After filtering, 16 samples constituted the level-1 corpus (T0) (Figure 13a).

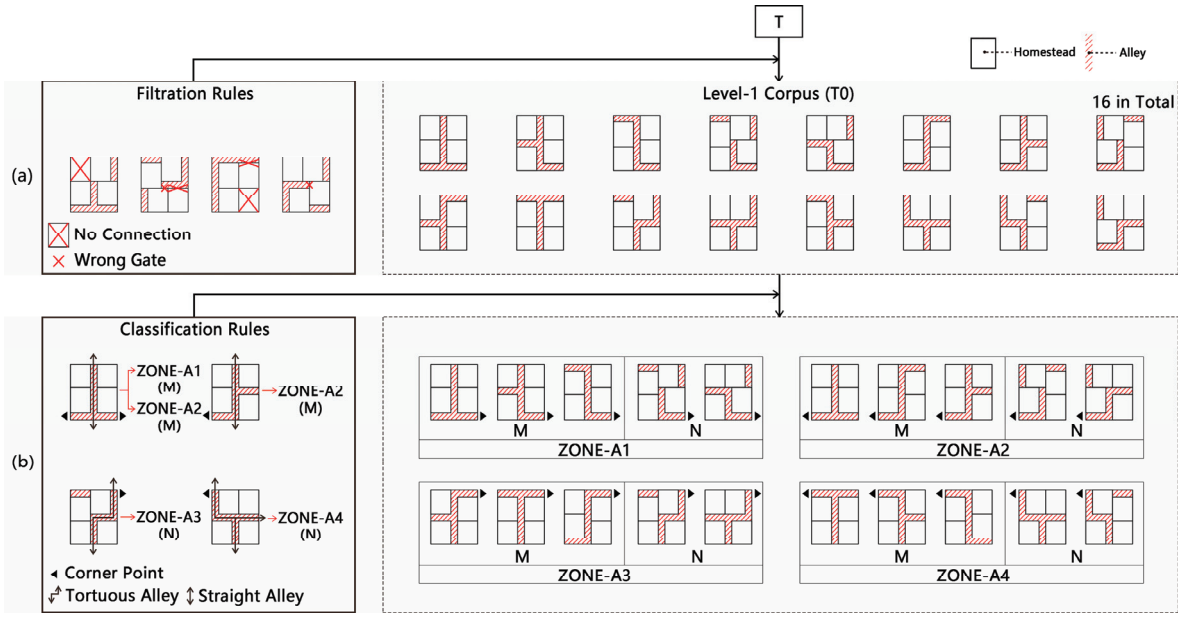


Figure 13. Level-1 rules. (**a**) Filtration rules. (**b**) Classification rules.

2. Classification rules. The level-1 corpus was divided into four quadrants for combination (ZONE-A1/A2/A3/A4), following which the four corner points could be accessed by the internal alleys. The samples that had access to the southeast corner point were placed in ZONE-A1, the ones with access to the southwest corner point were placed in ZONE-A2, while the ones with access to the northeast and northwest corner points were placed in ZONE-A3 and ZONE-A4, respectively. Since some samples' internal alleys could reach two corner points, they qualified to be placed in two quadrants equally. Also, to enrich the styles and features, the samples in each quadrant were divided into subsets M and N based on whether there were alleys running through the samples vertically (Figure 13b).

7.3. Level-2 Rules (Neighborhood Level)

1. Combination rules. First, in the neighborhood prototype, the level-1 samples of the four quadrants (ZONE-A1/A2/A3/A4) were extracted to fill. To avoid the monotonic problem caused by combinations, the following constraints were imposed during filling: (1) no adjacent ZONEs would have a mirror combination of the same samples and (2) no samples from M subsets of ZONE-A1 and ZONE-A3 can be adjacent to each other. Similarly, no samples from M subsets of ZONE-A2 and ZONE-A4 can be adjacent to each other. After imposing the above constraints, 148 combination shapes were obtained (Figure 14a).

2. Filtration rules. To improve accessibility, as long as one side of the neighborhood samples could not open the entrance to access the center, filtration became necessary. After filtering, 102 level-2 shapes were generated (Figure 14b).

3. Adjustment rules. Homesteads facing the main road often have a larger area, mainly used for selling daily necessities. There are also a small number of large homesteads in the inner areas not facing the road. Therefore, we used three larger homesteads (H2, H3 and H4), to accommodate the above possibilities. At this level, it is necessary to discuss the two cases of facing road and non-facing road. In advance, we should consider the following conditions: (1) a homestead at a corner point which did not face the main road should be selected as a labelled homestead; (2) the level-2 shapes with three or four sides facing the main road are not discussed. Furthermore, six types of adjustment rules were employed to generate the level-2 corpus, as described below.

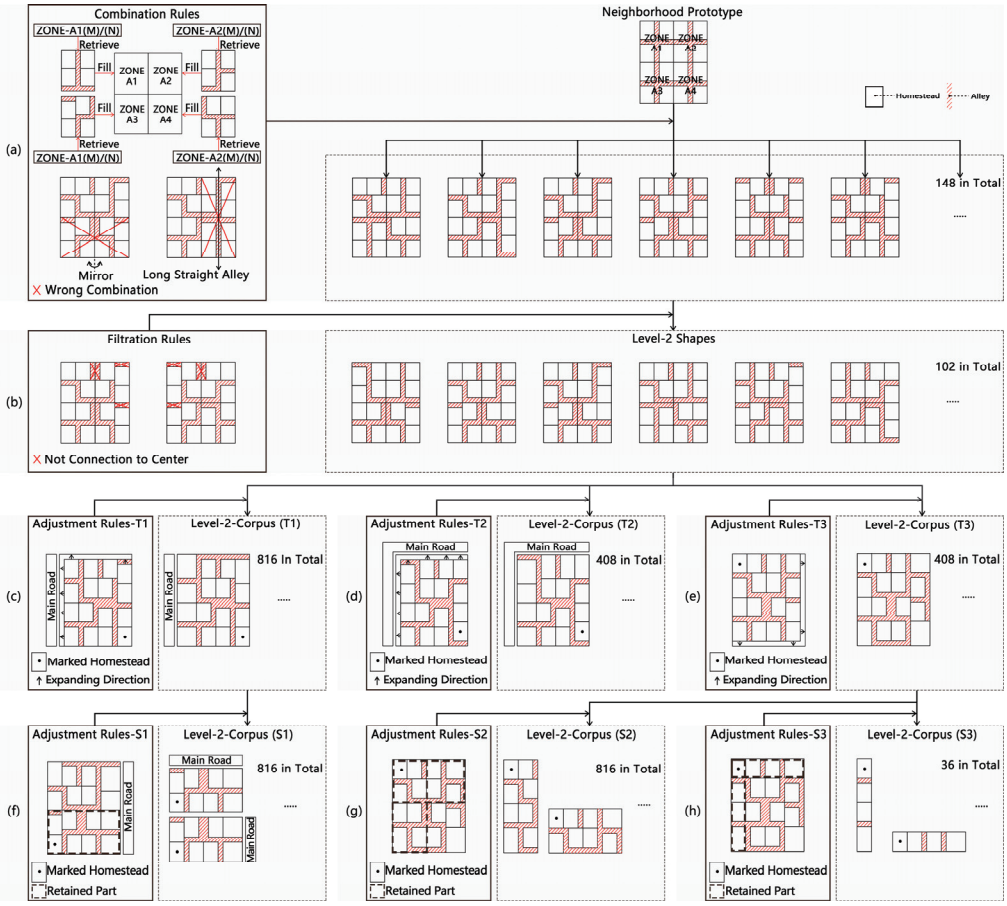


Figure 14. Level-2 rules. (**a**) Combination rules. (**b**) Filtration rules. (**c**) Adjustment rules—T1. (**d**) Adjustment rules—T2. (**e**) Adjustment rules—T3. (**f**) Adjustment rules—S1. (**g**) Adjustment rules—S2. (**h**) Adjustment rules—S3.

- Adjustment rules—T1. When only one side faced the main road, five standard homesteads turned into large homesteads, as shown in Figure 14c;
- Adjustment rules—T2. When two sides faced the main roads, seven homesteads became large homesteads, as shown in Figure 14d;
- Adjustment rules—T3. If no side faced the main road, three homesteads became large homesteads, as shown in Figure 14e;
- Adjustment rules—S1. Based on T1, the samples should be cut in half and the parts with the labeled homestead should be retained, as shown in Figure 14f;
- Adjustment rules—S2. Based on T3, the samples should be cut in half and the parts with the labeled homestead should be retained, as shown in Figure 14g;
- Adjustment rules—S3. Based on T3, the samples should be cut in quarters and the parts with the labeled homestead should be retained, as shown in Figure 14h.

Among these, the adjustment Rules S1, S2 and S3 are able to generate smaller samples of the neighborhood for filling the narrow or patchy space of a given base.

7.4. Level-3 Rules (Block Level)

The level-3 rules are the control rules for filling a given base to generate a block, so no level-3 samples were generated. We filled the block prototype facing the main road with the corpus of T1, T2 and T3 to verify how the samples of the level-2 corpus recognized the main road. Then, the following rules of reduction and adjustment control were set to recognize the number and area of homesteads in the block, and form of the block's open space.

1. Filling rules. When one side is facing a main road, the corpus of T1 and S1 can be used. When two sides are facing the main roads, the corpus of T2 and S1 can be used. When no side is facing the main roads, the corpus of T0, T3, S2 and S3 can be used. To improve the accessibility of traffic inside and outside the block, roads should also be reserved between the level-2 samples (Figure 15a).



Figure 15. Level-3 rules. (**a**) Filling rules. (**b**) Reduction rules. (**c**) Adjustment rules.

2. Reduction rules. Open space is necessary for a block, so some homesteads must be removed. This includes the following two cases: (1) homesteads that are facing the main road could be block prototype entrances, and (2) homesteads that are not facing the main road could be open spaces for landscaping. Therefore, reduction rules are an effective method for dynamically adjusting the number of homesteads according to specific situations (Figure 15b).

3. Adjustment rules. To further increase the type of homesteads, standard homesteads (H0) at the center of a block can be transformed into small homesteads (H1) (Figure 15c).

7.5. Implementation and Analysis

By analyzing Test 1 and Test 2, more reasonable rules of the three levels can be redefined in Test 3 and coded using a computer program to generate the planning solutions.

These rules and the resulting corpus are more flexible and can adapt to more complex situations of construction land. For a given base, samples are collected from T0, T1, T2, T3, S1, S2 and S3 for filling according to these rules, and three different results (2D and 3D) were generated randomly (Figure 16a,b). We used Pyautocad to automate the design in AutoCAD. The specific operating principles of the program designed in Test 1-3 are as follows:

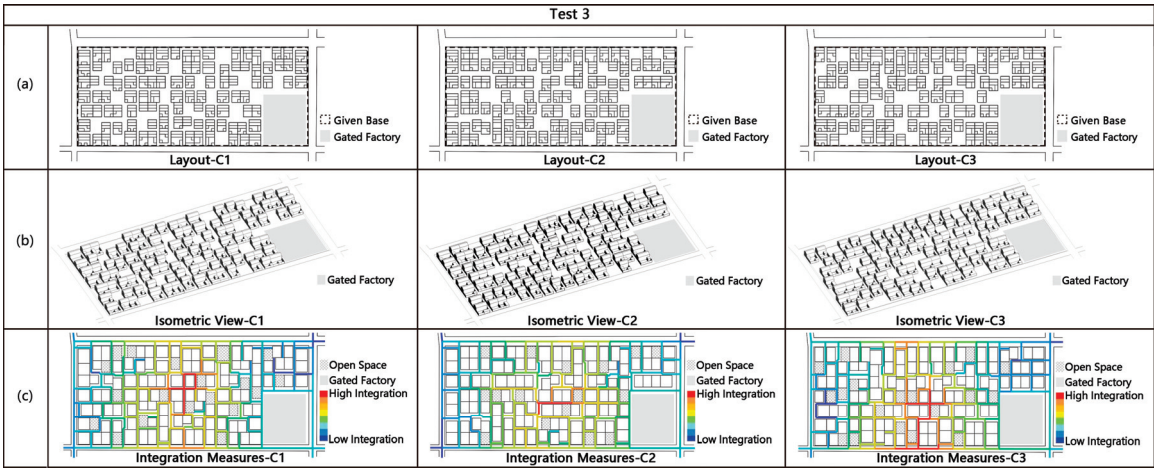


Figure 16. Results and analysis of Test 3. (**a**) Layout. (**b**) Isometric view. (**c**) The integration value of results measured.

1. Sample representation. As the module system was predefined in advance, a matrix of numbers can be used to represent the positional relationships between the homesteads, alleys and roads. For example, the level-1 samples were represented by a 9×7 matrix, where 1 represents the homestead and 0 represents the alley.

2. Sample filtration. In terms of filtration rules of level-2 rules, the sample matrices were accessed one by one using Depth-First Search (DFS), complying to the rules which allowed us to identify the unreasonable samples, such as one side of the neighborhood samples cannot open the entrance to access the center.

3. Sample combination and classification. During the combination process, the low-level samples were classified first via DFS, and the prerequisites for the high-level combined samples were analyzed using algorithms. The low-level samples were then combined with the high-level ones following matrix combinations.

4. Homestead identification and filling. When the rules were applied to a given base, the level-2 corpus should be used first, identified and filled according to the corresponding layers (base boundary and main road). Then, the level-1 corpus can be called to fill the remaining small space, in order to complete adaptive filling at the given base. Moreover, in response to the design goals, some parameters were set to control the results. For example, to render the main road accessible, the filling probability of the S1 and S3 samples can be increased to identify the boundary of the base and exclusive layer; the filling probability of the T3 and S2 samples can be increased.

Qualitatively, the results of Test 3 were similar to those of Test 2, showing the appearance of traditional rural settlements. Quantitatively, the results of Test 3 were similar to those of Test 1. The integration value of these results was higher for the central area, which meant that the central area had high accessibility (Figure 16c). In general, the results of Test 3, based on automatic design, better represented the characteristics of traditional rural self-organization and this is more reasonable in road planning.

8. Discussion

The three tests, T1, T2 and T3, applied to the given base, with a small area and relatively regular shape, were found to be suitable for the rapid qualitative and quantitative

analysis of the results of reappearing the characteristics of traditional rural settlements. However, due to the regular shape and small size of the given base, it could not be proved that a feasible layout could be generated when dealing with a larger and more irregular site. In addition, due to a small number of samples collected at all levels, it was impossible to show the mutual influence of a large number of samples at all levels during filling. As a result, to further verify the adaptability of the application of this design approach, we selected a new base (Figure 17a) for a test which had more complex site conditions. The corpus and rules of Test 3 were used. The main road and site boundary in AutoCAD were automatically identified by the computer program (Figure 17b), and the layout of the homestead was also predefined and randomly generated (Figure 17c). Both qualitatively and quantitatively, the results of the test successfully retained the traditional Chinese rural style and characteristics (Figure 17d, e). Moreover, the random filling and mutual influence of a large number of samples at all levels created a flexible and diverse road network at the block level (Figure 17b). Therefore, the test proved that the corpus and rules can reasonably and accurately generate the housing layout in accordance with the traditional rural characteristics, even on a large-sized irregular site. However, due to the size limitation of the samples, some small areas could not be filled (Figure 17b, c). In addition, since the samples have regular rectangular boundaries, they may not be well adapted to sites with various actual complex conditions, such as curved or oblique boundaries. In future work, we intend to improve the three-level rules, enrich the corpus and filling rules and make them adaptable to more complex topographic conditions, such as altitude difference and irregular site boundary. Moreover, since the main roads and alleys are only considered in this work, we plan to improve the communal-facilities-based rules corpus at the settlement level and town level, with a view to developing the generative approach.

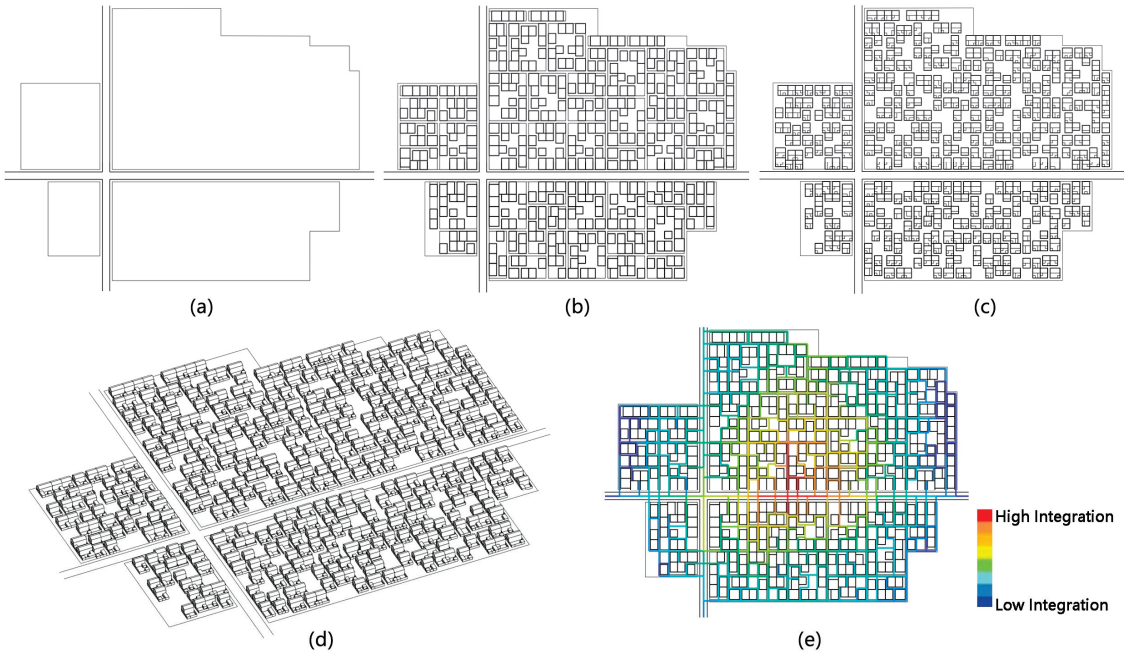


Figure 17. The results and analysis of one new test. (**a**) A new base. (**b**) Filling automatically. (**c**) Layout. (**d**) Isometric view. (**e**) The integration value of result measured.

9. Conclusions

This study explores a rule-based design approach for rural mass housing, mainly based on the results of three tests. The optimized rules and condition restrictions were coded, and a relatively reasonable result was obtained via the automatic operation of the program. Through a comprehensive analysis of the tests, the following conclusions can be drawn. First, this rule-based generative design approach can help architects solve

the design problem of the homogenization of rural mass housing, and the design results have "harmony in diversity" characteristics. The method keeps architects' role in the housing design process. It acts as a research booster, helping architects systematically explore the logic and process of generating research objects. Secondly, compared with traditional design methods, it can achieve the "emergence" and "unpredictability" of design results through rule-based reasoning, which can better meet the needs of multiple parties, especially associating architects and users. It can not only help architects use computer-aided tools to select and optimize the generated results and better control the geometric size, entrance direction and other parameters to realize the traceable and targeted research process, but also allow users to adjust the layout of their houses and their built-in building information according to their needs, depending on the family's life cycle. Thirdly, as a visual design tool based on shapes, SG has the advantages of processing multiple complex rules simultaneously, directly applying rules to functional geometry and better perceiving and expressing complex shapes. An effective relationship between abstract "spatial demands" (traditional architectural features, user design demands) and specific design rules can be established. Architects can apply this approach to control the design generation process, optimizing the design quality and improving the design efficiency.

10. Patents

The following Chinese invention patent was produced: "A Generative Design Method for Mass Housing Layout in Rural Areas of the North China Plain", with the authorization number "ZL202010327152.8".

Author Contributions: Idea, Methodology and Survey Data: J.W., W.F., B.Z. and Z.Z.; Model Analysis: J.W., Y.Y. and W.F.; Rules Definition and Verification: J.W., W.F. and B.Z., Computer Programming: Z.Z. All images are by the authors. All authors have read and agreed to the published version of the manuscript.

Funding: This work was supported by the Shandong Natural Science Foundation Project (ZR2021MF099, ZR2022MF334); the Shandong Province Teaching Reform Research Project (M2021130, M2022245, Z2022202); the Shandong Province High Quality Professional Degree Teaching Case Library Construction Project (SDYAL2022155).

Data Availability Statement: All data used in this research are available on open data sources.

Acknowledgments: We would like to give special thanks to K. Liu, L. Qiao, S. Sang and Q. Q. Qin for their support.

Conflicts of Interest: The authors declare no conflict of interest.

References

1. Wang, J.; Zhao, J.; Wu, T.; Li, J. A co-evolution model of planning space and self-built space for compact settlements in rural China. *Nexus Netw. J.* **2017**, *19*, 473–501. [CrossRef]
2. Oxman, R. Theory and design in the first digital age. *Des. Stud.* **2006**, *27*, 229–265. [CrossRef]
3. Singh, V.; Gu, N. Towards an integrated generative design framework. *Des. Stud.* **2012**, *33*, 185–207. [CrossRef]
4. Rahimian, M.; Beirão, J.N.; Duarte, J.P. A grammar-based generative urban design tool considering topographic constraints-the case for American urban planning. In Proceedings of the 37th eCAADe and 23rd SIGraDi Conference, Porto, Portugal, 11–13 September 2019.
5. Stiny, G.; Gips, J. Shape grammars and the generative specification of painting and sculpture. In Proceedings of the IFIP Congress, Ljubljana, Slovenia, 23–28 August 1971.
6. Stiny, G.; Mitchel, W.J. The Palladian grammar. *Environ. Plan. B Plan. Des.* **1978**, *5*, 5–18. [CrossRef]
7. Chiou, S.C.; Krishnamurti, R. The grammar of Taiwanese traditional vernacular dwellings. *Environ. Plan. B Plan. Des.* **1995**, *22*, 689–720. [CrossRef]
8. Duarte, J.P. Towards the mass customization of housing: The grammar of Siza's houses at Malagueira. *Environ. Plan. B Plan. Des.* **2005**, *32*, 347–380. [CrossRef]
9. Beirão, J.N.; Duarte, J.P.; Stouffs, R. Creating specific grammars with generic grammars: Towards flexible urban design. *Nexus Netw. J.* **2010**, *13*, 73–111.
10. Wang, J.; Zhao, B.; Fan, W.; Yang, Y.; Zhao, J. A combined shape grammar and housing-space demand approach: Customized mass housing design in rural areas of the North China Plain. *Nexus Netw. J.* **2022**, *24*, 5–23. [CrossRef]

11. Duarte, J.P. Customizing mass housing: Toward a formalized approach. In *Mass Customization and Design Democratization*, 1st ed.; Kolarevic, B., Duarte, J.P., Eds.; Routledge: London, UK, 2018; pp. 129–142.
12. Wang, J.; Zhang, S.; Fan, W. Application of shape grammar to vernacular houses: A brief case study of Unconventional Villages in the contemporary context. *J. Asian Archit. Build. Eng.* **2023**. [CrossRef]
13. Celani, G. Grammar form and analysis methodology and synthesis in architecture. *Connect. Commun. Cult.* **2006**, *5*, 180–197.
14. Erem, Ö.; Abbasoğlu, E.M.S. Adapted design generation for Turkish vernacular housing grammar. *Environ. Plan. B Plan. Des.* **2016**, *43*, 893–919. [CrossRef]
15. Herbert, T.; Sanders, I.; Mills, G. African shape grammar: A language of linear Ndebele homesteads. *Environ. Plan. B Plan. Des.* **1994**, *21*, 453–476. [CrossRef]
16. Dias, M.A. Informal settlements: A shape grammar approach. *J. Civil Eng. and Archit.* **2014**, *8*, 1389–1395.
17. Jiang, B.; Claramunt, C. Integration of space syntax into GIS: New perspectives for urban morphology. *Trans. GIS.* **2002**, *6*, 295–309. [CrossRef]

Disclaimer/Publisher's Note: The statements, opinions and data contained in all publications are solely those of the individual author(s) and contributor(s) and not of MDPI and/or the editor(s). MDPI and/or the editor(s) disclaim responsibility for any injury to people or property resulting from any ideas, methods, instructions or products referred to in the content.

buildings

MDPI

Article

Towards an Evaluation System of Disabled Individuals' Friendly Communities from the Perspective of Inclusive Development—A Case Study in Jinan

Yaqi Wen, Yuyao Li, Yang Yang * and Jiang Wang

College of Architecture and Urban Planning, Shandong Jianzhu University, Jinan 250101, China
* Correspondence: yangyang21@sdjzu.edu.cn

Abstract: The quality of travel for residents has improved in China's urban renewal development, but there are still barriers to the activities of disadvantaged groups like people with disabilities in the city, including challenges with accessible travel and a lack of accessible design. All urban people should have access to services and be guaranteed equal rights, according to the inclusive development theory. This study examines the travel requirements and behavioural patterns of the barrier-free groups to safeguard the right of underprivileged groups to participate equally in the urban space. It also determines the impact of various types of urban land use and service facilities on the distribution of barrier-free facilities. An evaluation system based on the needs of the disabled group is established to evaluate the degree of barrier-free facilities in the surveyed areas, summarise the problems shown by the evaluation scores, and propose improvement strategies for the shortcomings of accessibility to residential areas and the controversy through web data crawling and a geographically weighted analysis. From the standpoint of inclusive development, the goal is to lessen the travel issues faced by underprivileged groups and to improve their capacity to take advantage of opportunities and have access to resources.

Keywords: inclusive development; disability friendly; accessible facilities evaluation; Jinan

1. Introduction

1.1. Backgrounds

At the end of 2022, the urbanisation rate of China's resident population was 65.22%, which has stepped into the middle and late stages of the rapid development of urbanization. The development of urbanization has entered an important period of urban renewal, with the development path switching from "quantity" to "quality", and from large-scale incremental construction to stock-quality renovation focusing on improving urban quality [1]. In the context of urban renewal, the 2030 Agenda for Sustainable Development puts forward goals for building inclusive and sustainable cities, including the following goal: by 2030, to strengthen inclusive and sustainable cities and capacities for participatory, integrated, and sustainable human settlements planning and management in all countries and to provide universal access to safe, inclusive, accessible, and green public spaces for all, in particular, for women, children, older persons, and persons with disabilities [2]. Where the development of urban accessibility will immediately affect the travelling conditions of the elderly and persons with disabilities, etc., the construction of an accessible travelling environment is, therefore, an important part of inclusiveness. The 14th Five-Year Plan emphasises strengthening service facilities for persons with disabilities and comprehensive service capacity building, and improving the construction of barrier-free environments [3]. The State gives considerable attention to vulnerable groups, and the necessity to improve the barrier-free environment opens the way to the building of inclusive cities.

People with disabilities are a typical vulnerable group in society, and their needs must be seriously considered in the process of raising the quality of urban development.

More than 85 million Chinese citizens are disabled, and there are more than 64 million senior individuals who are disabled or semi-impaired. The design of accessible travel has emerged as a key issue in urban redevelopment since there is a sizable but unmet demand for it and significant challenges in the areas of basic life safety and social participation.

China began to build an accessible environment relatively late, with the concept of "accessibility" appearing for the first time in 1985 in a seminar on "Persons with Disabilities and the Social Environment". Some scholars have concluded that although the barrier-free design in China is being gradually improved, at the same time, there are still a lot of places that need to be improved: from the perspective of society, the designers do not have a sufficient understanding of accessible facilities, and all parties do not attach enough importance to the research and construction of the design of barrier-free access; from the perspective of management, there are often cases where barrier-free access is piled up with sundry things or damaged by road construction [4]. From a theoretical point of view, the overall research is still insufficiently emphasised, and there is a lack of better and more systematic design methods [5]. Overall, China's construction of an accessible travelling environment is insufficient because of the lack of attention to the perspectives of persons with disabilities and the psychology of persons with disabilities, as well as the lack of quantitative statistics and quantitative analyses of the degree of uniformity of the construction of accessibility facilities.

A nation's ability to advance economically and socially depends heavily on its infrastructure. However, it is crucial to evaluate the condition of the infrastructure, determine the regions that require the greatest care, and allocate the government's constrained budget to those areas [6]. More specifically, it would be effective and crucial to evaluate the present state of accessibility in a city to identify the areas that require updating and more relevance to the actual needs of people with disabilities.

The inclusive design of urban space is inextricably linked to the social component, which emphasises the city's openness, acceptance, recognition, and respect for all groups and classes of residents [7]. Current divisions should be improved to reduce the exclusion and segregation of disadvantaged groups in urban spaces, to guarantee equal power for every resident, and to promote equity and justice [8,9]. This paper analyses the travel needs and behavioural patterns of the accessible groups based on the theory of inclusive perspectives, focusing on the needs and problems of disadvantaged public groups in the context of urban regeneration and urban construction. The goals of this paper are to improve the quality of urbanisation, guarantee the right of disabled groups to use urban resources equally, and reduce the travel problems of disabled people. It proposes improvement strategies for the management of barrier-free facilities in combination with the needs of disabled groups, measuring the degree of perfection of the barrier-free environment through the establishment of an assessment system for the degree of perfection of barrier-free road facilities, to draw attention to the underprivileged groups and increase their opportunities for participation in public life.

1.2. Research Framework

Based on previous research, the urban accessibility update section is deepened, and quantitative analyses of the degree of urban accessibility improvement are conducted, an evaluation system is established, and the results of the research on the needs of persons with disabilities are made more intuitive, so as to assist in the analysis of the subsequent data and provide the basis for urban renewal. It then proposes urban renewal strategies and recommendations to make urban renewal services better and more inclusive. Figure 1 shows the flowchart of the paper's research.

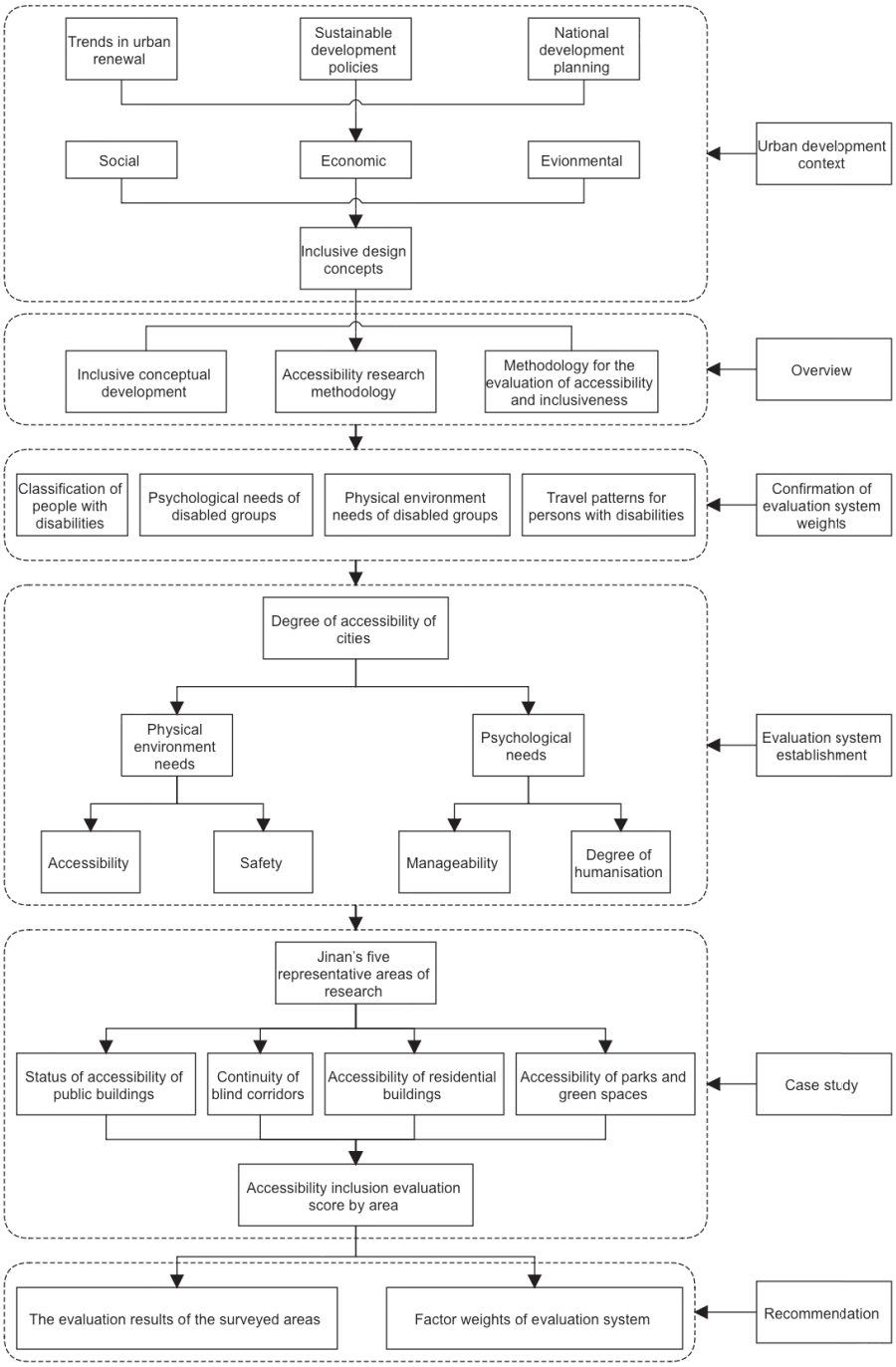


Figure 1. Research flow chart (source: the authors).

2. Overview

2.1. The Definition and Evolution of Inclusive Design Concepts

Inclusive development involves various aspects. From a social perspective, UN-Habitat first formally proposed the "inclusive city" initiative in the *World Cities Report* in 2000, emphasising the equal rights, resource sharing, and spatial balance of different urban subjects in the process of urban development, and promoting the equal participation of urban citizens in the development process under the guidance of the concept of inclusiveness; at the 2016 United Nations Conference on Housing and Sustainable Urban Development, inclusiveness was incorporated into the New Urban Agenda as a core concept, with "Cities for All, Equal Use and Enjoyment of Cities and Human Settlements by All" as a common vision to promote prosperity and improve the quality of life for all, by promoting social

cohesion, inclusiveness, and security in peaceful and pluralistic societies in which the needs of all inhabitants are met and the special needs of those in vulnerable situations are recognised [10]. The obstacles to travelling by vulnerable groups, such as the disabled and the elderly, should be eliminated and their right to participate in normal life should be guaranteed.

The notion of inclusive growth was initially introduced by the Asian Development Bank (ADB) in 2007 from an economic standpoint. Its objective was to enhance the accessibility of impoverished individuals to markets and essential productive assets, as well as to ensure their meaningful involvement in decision-making regarding resource management [11]. Within the framework of China's urban development agenda, inclusive growth entails the equitable distribution of economic development benefits throughout the urban development process, fostering coordinated and balanced development, and ultimately achieving shared prosperity [12].

In the spatial environment perspective, inclusive thinking first appeared in 1984 when Richard Hatch introduced the idea of inclusive design, defining it as "the ability of the public to participate in and control the environment". Later in 1994, Roger Coleman proposed inclusive design as an offshoot of disability design to create a friendlier future for all in terms of environmental design and assessment [13].

2.2. An Overview of Accessible Design from the Perspective of Inclusive Development

2.2.1. Introduction to Research Methods in Accessibility Studies

Previous scholarly investigations on accessibility design have employed various research methods such as questionnaires, simulations of disabled individuals' travel experiences, analysis of population characteristics, user research through zonal random sampling surveys, and others. These studies have focused on examining the current issues related to accessibility, the satisfaction levels of disabled populations, the challenges posed by obstacles, and the fairness of participation in social activities. Additionally, these studies have proposed specific strategies to address these issues. However, it is important to acknowledge that these investigations have certain limitations. For instance, they tend to overlook other types of disabilities when studying a specific group of disabled individuals. Moreover, these studies heavily rely on subjective human judgement and a qualitative analysis, lacking a quantitative analysis and the establishment of a comprehensive evaluation system. Specific literature arrangements are summarized in Table 1.

Table 1. Accessibility research methods review form.

Target	Methodology	Contents	Strategies
Utilisation rate of accessible facilities [14]	In-depth interviews and fieldwork	Socio-economic characteristics of persons with disabilities, travelling activities, living space, facility utilisation influencing factors	Universal design, optimising accessibility, frequency of use
Continuity and safe accessibility for accessible travelling [15]	Questionnaires, simulated trips for people with disabilities	Sample survey on travelling by people with disabilities, status and problems	Safeguard and regulatory system, promoting information accessibility
Status of facilities in the quarter-hour community service circle [16]	Questionnaire, factor analysis of population characteristics	Characteristics of the physically disabled population, characteristics of place needs, correlation between environmental needs and satisfaction	Addressing systemic issues, improve the education level of people with physical disabilities.

Table 1. *Cont.*

Target	Methodology	Contents	Strategies
Ordinary citizens, sanitation workers, the visually impaired [17]	Random sampling by district	Restrictions on the use of blind alleys, status of low travelling rate of visually impaired persons	Strengthening publicity, strengthening construction and maintenance, provide rehabilitation training for the visually impaired
Travelling life patterns of people with disabilities [18]	User research, environmental studies	Participation in social equity, assistive technology for travelling	Incorporate assistive technology for travelling

2.2.2. Introduction to Inclusive Evaluation

The evaluation of urban inclusiveness is a further deepening of the evaluation of accessibility. The design of accessible facilities necessitates the involvement and assessment of disability groups to ensure that their intentions and needs are comprehended and fulfilled, thereby fostering a more participatory and inclusive approach. Previous suggestions have emphasised the importance of recognising the diversity within the disabled community, promoting understanding and respect for individuals with disabilities, facilitating their active participation and cocreation in the design process, and conducting participatory observations to assess the actual usability of facilities by people with disabilities as part of the overall quality control. This research paper aims to contribute to the development of an evaluation system by investigating the specific usage requirements of individuals with disabilities. Relevant literature are summarized in Table 2 below.

Table 2. Inclusive accessibility design review form.

Concept Proposal	Participation of the Disabled	Methodology
Promote inclusive development and strengthening systematization [19].	Processes of policymaking	An analytical framework to study design and processes
Create community participation and boundary objects [20].	Participant observation Processes participation and cocreation	Two participatory agenda-setting projects
Recognize the diversity of disabilities. Expand the participation of marginalized groups in tourism decision-making [21].	Tourism producers, tourism consumers	Applying the conceptual framework for inclusive tourism development
Explore innovative barrier-free design methods [5].	Interaction with the design team	Conceptual and developmental overview Generalisation of methods and theoretical models
Inside the barrier-free community participatory planning [22]	Participation in community public hearings	Pattern language

3. Evaluation System

3.1. Establishment of the Evaluation

After consulting the pertinent policy manuals and papers in a previous article, it is necessary to research and compile the travel requirements and behavioural patterns of the

barrier-free groups to obtain the corresponding and more accurate impact indicators and weighting values. This will help with the renewal and construction of barrier-free facilities as well as the evaluation of the impact of various types of urban service facilities.

3.2. Needs of the Disabled Population

The direct aim of accessibility is to solve the mobility problems of disabled people, and through literature references, the needs of disabled people were collated from different perspectives in order to serve as a basis for the establishment of evaluation factors.

As users of barrier-free facilities and as special people in society, persons with disabilities need a change in perspective, the full consideration of their needs, the satisfaction of their needs as much as possible, and assistance in having their demands "seen and heard". Persons with disabilities have the same basic and generic needs as all human beings and the same needs to be met. Thus, in conjunction with Maslow's theory of needs, the analysis focuses on the integration of the five areas of physiology, safety, socialisation, respect, and self-actualisation [23]. The introduction and ranking of these five aspects are shown in Figure 2.



Figure 2. Maslow's hierarchy of needs.

Firstly, the most basic physiological needs for people with disabilities are equivalent to their reliance on accessible facilities in social and urban construction, which requires designers to accurately plan the application and layout of accessible facilities in public facilities. Secondly, the same low-level safety needs for people with disabilities are the need for the safe use of accessible facilities and a safe arrival at destinations, and to ensure their safety, it is necessary to focus on the need for a regular maintenance, a reasonable design, the ease of use, and the effective use of public facilities. Social needs and respect needs

are relatively high-level needs which belong to psychological aspects. The highest level of self-fulfilment needs refers to the process by which the individual's various talents and potentials can be brought into full play in a suitable social environment and the individual's ideals and ambitions can be realised, and in the case of a person with disabilities whose physical disabilities have already become a relative limitation, the limitations on their inner pursuits should be reduced to a minimum.

Based on this theory, and taking into account the realities of the situation, evaluation factors were determined on the basis of the needs of the different categories of the disabled groups themselves, the needs of the physical environment of the disabled, the psychological needs of the disabled, and their travelling patterns.

3.2.1. Categorization of Individuals with Disabilities

Through cooperation with the Jinan Disabled Persons' Federation, theoretical training, practical research, and classification of disabled groups were completed and the types of disabilities were categorised into four types: physical (A1), visual (A2), hearing (A3), and cognitive (A4) [24].

Persons with disabilities have different levels of disability and have different requirements for environmental accessibility. Among them, persons with physical disabilities who use mobility aids and wheelchairs and persons with visual disabilities have higher accessibility requirements: Persons with physical disabilities may have some difficulty in walking, climbing steps or slopes, and standing for long periods; persons with visual disabilities who have functional impairments in their vision or field of view mostly rely on their senses of touch and hearing to perceive their surroundings, or they use crutches or service animals to assist them in getting around. People with cognitive disabilities due to slow intellectual development have higher accessibility requirements, may have difficulty in using various service facilities, and have a limited range of activities, mainly in the residential area. Therefore, the main needs of this group of people are accessible facilities with strong environmental features and simple and clear flow lines in residential areas. On the other hand, persons with hearing disabilities and persons with upper-limb disabilities, who have difficulties in verbal communication, do not have walking difficulties, and have a high degree of self-care, have less issues with the accessibility of the built environment in terms of mobility, have lower accessibility requirements for the environment, and mainly require sufficient light and a quiet acoustic environment for hearing aids.

Through the categorisation study of different disability groups, the factors affecting the mobility of people with disabilities were compiled in descending order of influence: the continuity of blind corridors, the presence of ramp connections at height differences, the simplicity and ease of use of barrier-free facilities, the flow lines within the living area, and the light and acoustic environments.

3.2.2. Physical Environmental Requirements of Inclusive Communities

The physical demand primarily pertains to the need for accessible facilities and buildings, necessitating the implementation of appropriate design and management standards to address the physiological and safety requirements of individuals with disabilities. This encompasses various aspects, such as the inclusion of accessible entrances in residential buildings, the provision of flyovers and zebra crossings on pavements, and the construction of blind alleys within residential areas. Additionally, specific considerations must be made for certain facilities, such as designing wider accessible public toilets to accommodate wheelchair access and appropriately labelling parking spaces as barrier-free in car parks [25].

Travelling safety is the common mentality of all participants in urban transport, and it is the most basic requirement for all travelling activities [26]. Compared with ordinary people, disabled people are usually less capable of self-protection in traffic accidents than ordinary people due to their physiological insufficiency, so the probability and degree of injuries are higher than those of ordinary people.

The accessibility of information and communication also satisfies the physiological and safety requirements of people with disabilities. This is primarily reflected in the media facilities in public spaces that can communicate information to people with disabilities, enabling people with various types of disabilities to obtain information, primarily necessitating the consideration of both the visual and auditory senses [25]. Therefore, the weights of transport station services, public management and service facilities, and parks and green spaces should be moderately increased. Affected by the demand for community services and the shortcomings in accessibility services and awareness, the demand for accessible facilities in public utilities, commercial service facilities, and parks should also be moderately increased.

3.2.3. Psychological Requirements of Demographically Inclusive Cohorts

The user's control over the environment and the state of things is called controllability. Among them, psychological security is an important influencing factor [26]. For example, the continuity of the distribution of accessible facilities in transport venues and the availability of simple and easy-to-use accessible facilities affect the psychological needs of people with disabilities. Satisfying these psychological needs and providing a stable and humane experience for people with disabilities during travelling is conducive to helping people with disabilities overcome or even eliminate some of their psychological barriers, which in turn increases the likelihood of travelling in the future [26]. Among the previous needs by disability group, whether the barrier-free facilities are simple and easy to use, the flow line, light, and acoustic environment in a residential area can be used as controllable travelling factors, and the degree of universality of barrier-free facilities and the degree of appropriateness for different groups of disabled people can be used to evaluate whether the facilities are humanised or not.

3.2.4. Travel Behaviours Exhibited by Individuals with Disabilities

Accessibility refers to the ease of getting from one location to another and is often used to describe how human activities can maximise access using minimal activity and is an important basis when public facilities are built and planned [27]. Many factors in the city affect the accessibility of travelling for people with disabilities, and the higher the frequency of travelling, the higher the demand for this factor by people with disabilities, and the more important it is in the evaluation system. The research used data-collation field visits to the disabled and online questionnaires to summarise the travel patterns of the disabled; a total of 200 questionnaires were distributed, and the results showed that leisure trips and shopping trips accounted for the highest proportion of travel frequency, so when assigning weights affecting the distribution of accessible facilities, the proportion of parks, green spaces, and commercial service facilities should be increased as appropriate.

Based on the data shown in the aforementioned chart about the activity requirements of individuals with disabilities, it is evident that there is a greater occurrence of leisure and shopping excursions; however, the likelihood of engaging in other forms of travel is comparatively diminished. These results are summarized in Figures 3 and 4.

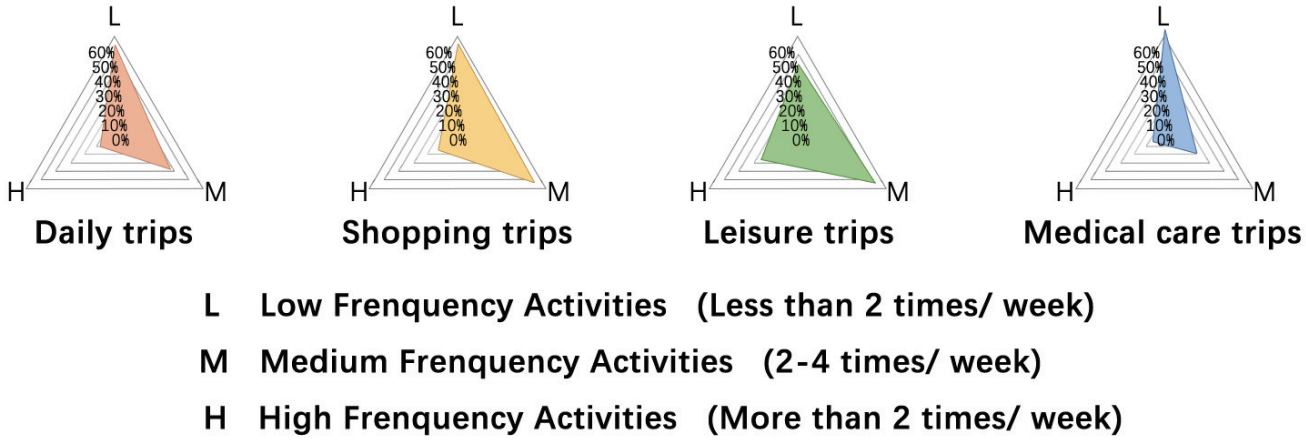


Figure 3. Radar map of frequency of travelling for different types of activities for persons with disabilities (source: the authors).

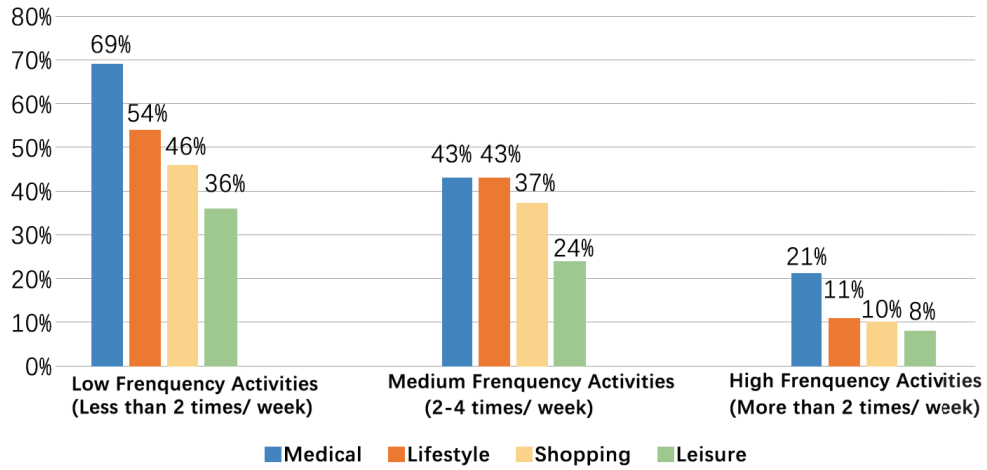


Figure 4. Histogram of travelling to different types of activities by persons with disabilities (source: the authors).

The chart illustrates the distribution of activity trips for disabled individuals across various categories. It reveals that medical and life service facilities exhibit the highest proportion in the likelihood of low-frequency trips. In terms of medium-frequency trips (2–4 days per week), both medical and life service facilities, as well as shopping facilities, demonstrate the highest proportion. As for high-frequency trips (more than 4 days per week), the proportion of medical, life, shopping, and leisure categories collectively decreases, although medical facilities remain predominant.

In conjunction with the previous section, public services and buildings for high-frequency travel were included in the accessibility factor for public buildings. Considering the constraints associated with travel distances for individuals with disabilities and the recommendations regarding the organisation of three-tier living areas, the public service facilities should consist of a blend of medical service facilities and living service facilities that are conveniently accessible to individuals with disabilities who travel by foot or wheelchair. These facilities should be accorded the highest priority compared with other service facilities.

3.2.5. Assessment of the Accessibility Scenario

In brief, the assessment of the level of adequacy of accessible facilities was conducted based on two dimensions: physical environment requirements and psychological needs. The former encompassed accessibility within buildings, road traffic safety, and the effectiveness of information exchange. The latter pertained to controllability and humanization. The specific factors for the evaluation are depicted in Figure 5.

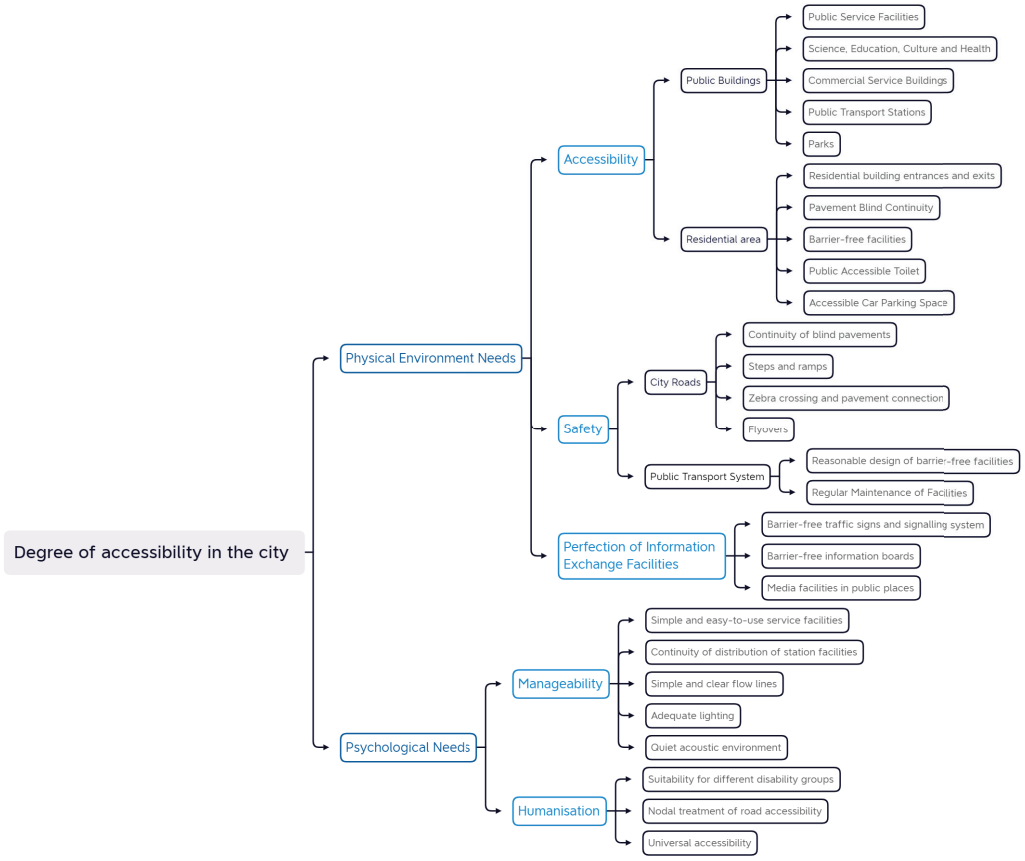


Figure 5. Factors of the evaluation (source: the authors).

In the preceding section, the hierarchical analysis approach was employed to develop an evaluation system for assessing the level of adequacy of urban accessible facilities, taking into consideration the travel and psychological requirements of individuals with disabilities. The evaluation formula was as follows:

$$Final\ Score = \sum(\sum(Initial * level3\ factor\ weight) * level2\ factor\ weight) * level1\ factor\ weight \quad (1)$$

The specific weight values are shown in the Tables 3–5.

Table 3. Primary evaluation factors.

Classification	Primary Evaluation Factor	Weight
Physical environment needs	Accessibility	0.443
	Security	0.316
Psychological needs	Controllability	0.168
	Humanisation	0.072

Table 4. Secondary evaluation factors.

Primary Evaluation Factor	Secondary Evaluation Factor	Weight
Accessibility	Public Buildings	0.413
	Residential areas	0.259
Security	City roads	0.178
	Public transport system	0.094
	Information-exchange facilities	0.056
Controllability		
Humanisation		

Table 5. Tertiary evaluation factors.

Secondary Evaluation Factor	Tertiary Evaluation Factor	Weight
Public buildings	Public service facilities	0.587
	Science, education, culture and health buildings	0.226
	Commercial service buildings	0.100
	Public transport stations	0.051
	Parks and green spaces	0.035
Residential areas	Residential building entrances and exits	0.605
	Continuity of blind pavements	0.214
	Accessibility facilities	0.097
	Public accessible toilets	0.005
	Barrier-free car parking spaces	0.034
City roads	Continuity of blind pavements	0.698
	Steps and ramps	0.186
	Zebra crossing and footpath junction	0.069
	Footbridge	0.046
Public transport system	Reasonable design of accessible facilities	0.800
	Regular maintenance of facilities	0.200
Information-exchange facilities	Barrier-free traffic signs and signalling systems	0.742
	Barrier-free information boards	0.183
	Media facilities in public places	0.075
	Simple and easy-to-use service facilities	0.499
	Continuity of distribution of station facilities	0.285
	Simple and clear flow lines	0.128
	Adequate lighting	0.057
	Quiet acoustic environment	0.032
	Suitability for different disability groups	0.528
	Nodal treatment of road accessibility	0.333
	Universal accessibility	0.140

4. Case Study

Jinan possesses a rich historical background, and the city is continuously undergoing modernization and advancement. The spatial configuration and economic progress of its districts exhibit significant disparities, particularly between the ancient cultural urban areas and the newly developed districts, which feature distinct environments and varying levels of construction quality. Furthermore, the policies governing these districts are subject to frequent updates. Consequently, the research on Jinan's districts encompassed a diverse range of sample types.

4.1. The Progression of Accessible Facilities Construction in Jinan City

Starting from 2006, after more than five years of unremitting efforts, the provincial capital Jinan's barrier-free construction policies, laws, regulations, and standards system was initially established, the number of accessible facilities further increased, the quality

was further improved, the layout was further rationalised, the whole society cared more and more about and supported a barrier-free development of the city, and the construction of urban-area accessible facilities saw some results. In September 2009, the Jinan Municipal People's Government issued The Measures for the Administration of Barrier-Free Facilities Construction in Jinan [28]. The measures established uniform provisions on the responsible departments, construction requirements, and construction projects of accessible facilities in Jinan, thus placing the construction of barrier-free facilities at the institutional level based on evidence and rules. The introduction of the regulations guaranteed and directed the significance of the promotion and improvement of accessible facilities construction in downtown Jinan as well as other areas under its jurisdiction. Taking this as a guide, Jinan began to strive to become a national barrier-free city, responding to the call of the Ministry of Housing and Construction, the China Disabled Persons' Federation, and the Committee on the Elderly, and began to create a "National Barrier-Free City" in a systematic manner. During this period, downtown pavements, major attractions, large shopping malls, and other places underwent an unprecedented large-scale barrier-free transformation.

The Municipal Construction Commission has issued a comprehensive repair plan that includes the renovation of 139 public buildings and facilities, such as Walmart, to make them barrier-free. Additionally, 10 parks and scenic spots, including Daming Lake and Baotu, will have barrier-free entrances, ramps, passages, aisles, staircases, and steps installed. Quancheng Square will also have a barrier-free lift platform established. Furthermore, 15 public transport facilities, such as the Remote Wall International Airport and East Railway Station, will undergo renovations based on their specific requirements. Major public places will see the installation of 530 Braille bus stops, while 934 major bus stops in urban areas will have passenger boarding and alighting guardrails implemented. Moreover, major bus stops in urban areas will have 2349 bus shelter seats installed. Lastly, the city's 196 residential neighbourhoods and corresponding residential buildings will be retrofitted with barrier-free pavements, green spaces, and public service facilities. Figure 6 is several real scenes of barrier-free facilities taken during the research.

4.2. Methods of Research

This paper summarises the behavioural characteristics, psychological features and group needs of disabled groups by investigating the awareness of various groups through a literature search and field observations to understand the needs and travelling characteristics of the barrier-free groups, and through field research, combined with interview and questioning methods to investigate the views of the disabled on the accessibility of the district's medium view of the trend of renewal. We explored the construction of accessible facilities in 26 subdistricts within the 5 main city districts of Jinan and analysed the current distribution of accessible facilities in the main city districts of Jinan, including the continuity, uniformity, and perfection of their distribution. Through this accessibility infrastructure research, the public's perception of the overall situation of accessibility in each area was analysed, and a visual analysis of the overall accessibility infrastructure construction in each area of Jinan City was obtained.

4.3. Research Material

This study covered 26 districts in Jinan City, including Guaiyin, Tianqiao, Shizhong, Lixia, and Lixiancheng, as well as five representatives of the central business district. There were also more than 240 research roads, 384 public buildings (including 125 bus stops, 7 large public parking lots, and 5 underground stations), 159 residential neighbourhoods, 17 parks and green spaces, and 11 historical structures. The study's overall mileage was approximately 169 km.



Figure 6. Partial accessibility facilities in the research area (**a**) Accessible ramp. (**b**) Accessible public toilet. (**c**) BRT accessible ramp and blind path. (**d**) Barrier-free elevator. (Source: Author).

4.4. Initial Examination of Research Findings

The prevailing public sentiment centred around the road infrastructure, residential structures, and commercial amenities situated alongside the park. This emphasis highlights the constrained nature of barrier-free construction efforts within the historic district, which is hindered by the need to preserve historical buildings and showcase external attractions. Consequently, the accessibility needs of disadvantaged residents and their corresponding psychological need for safety have been overlooked.

4.5. Assessment of Accessibility Infrastructure in Jinan Municipality

4.5.1. Examination of the Current State of Accessibility Features in Public Structures

The condition of accessible facilities in the three pavilions within the scope of the study was good; road sections such as Dongying Road, Xingfusi North Road, Weihai Road, Qingdao Road, Weifang Road, and other sections in Huaiyin District achieved a full coverage of blind alleys, and the setting of ramp edges was relatively perfect; recreational public buildings such as Wanshiang City, Evergrande Fortune Centre, Impression Jinan-Quanworld, Hongyang Plaza of Jinan, and Shandong Provincial Congress Theatre achieved a full coverage of barrier-free entrances and exits; and public buildings such as Hengyuan School, BeiduoYi Kindergarten, the Second Experimental Kindergarten in

Huaiyin District, Hengxin Primary School, and Majiyuan Kindergarten in Huaiyin District, and other educational public buildings also set up barrier-free entrances and exits. Other key facilities in other districts, including seven Tianqiao districts, three Shizhong districts, six Lixia districts, and four Licheng districts, also showed a generally good progress in terms of barrier-free construction. Many public places in Jinan were equipped with accessible facilities to protect the rights and interests of the disabled, such as the construction of ramps to ensure the smooth passage of prams and wheelchairs, the construction of barrier-free toilets in some parks to ensure the normal physiological needs of the disabled, the addition of barrier-free access at bus stops, and the setting up of guided tours for the blind at intersections to meet the needs of the blind.

This study analysed three distinct areas, namely the Quancheng Square area, the Quancheng Park area, and the Old Shangfu area, in order to identify the distribution of problematic points related to accessible facilities within each subarea. The analysis focused on various urban elements such as roads, bus stations, residential buildings, parks, green spaces, and buildings with historical and cultural significance. The aim was to provide a refined and systematic understanding of the identified issues, which is visualized in Figure 7.



Figure 7. Distribution of problematic accessibility points and sections in the old town area (source: the authors).

Through the picture analysis, the continuity of the roads on the south and north sides of the park belt was good; however, the perfection and distribution were not good enough, which was reflected in the better degree of perfection of the barrier-free facilities on the south side of the base. A comparison with the buffer zone showed that there were localised areas of missing barrier-free facilities within 300–500 m of the buffer zone for public service facilities. In older neighbourhoods, such as the public service facilities around the settlement of the city of Zakyn, the accessibility index was poor and there were many missing locations, while the ageing phenomenon was serious, and the proportion of elderly residents with weak mobility was even higher, which required a more complete configuration of barrier-free facilities.

In the context of privately owned communities and real estate, as well as distant places like the southern highland areas, there persisted a prevalent deficiency in accessibility and inconsistencies in the development of accessible infrastructure.

4.5.2. Examination of Visual Impairment Continuity

Through research interviews with several handicapped individuals, it was revealed that the degree of continuity of accessible roads was a very major hurdle to disabled people's travelling. The resulting bar chart is shown below in Figure 8.

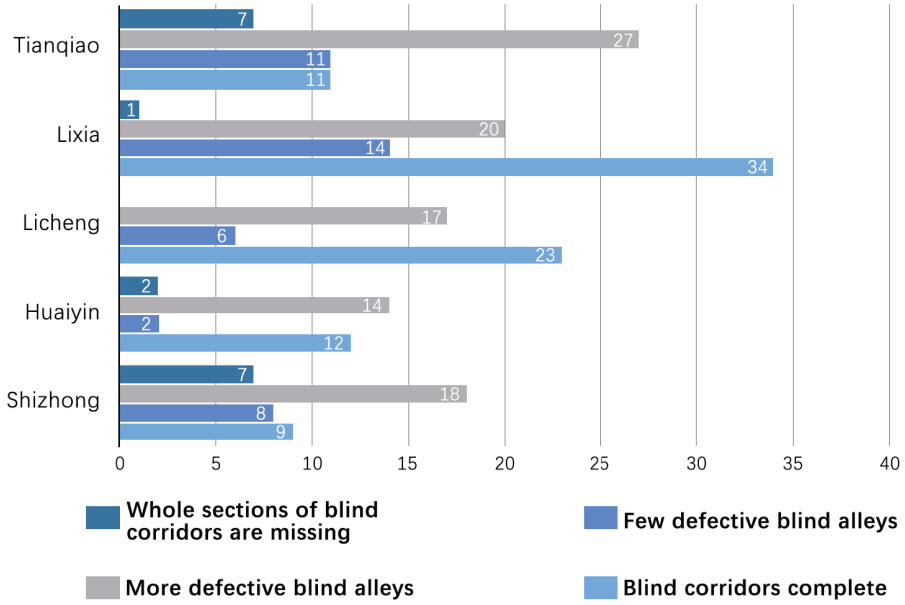


Figure 8. Road accessibility analysis (source: the authors).

Statistics on road facilities for the blind in each sub-district of the five districts in the main urban area of Jinan City found that the overall situation of the integrity of the blind on the roads accounted for a small percentage of the total roads researched, as each district was below 35%. Figure 9 shows the situation of blind access facilities in different areas on a map.

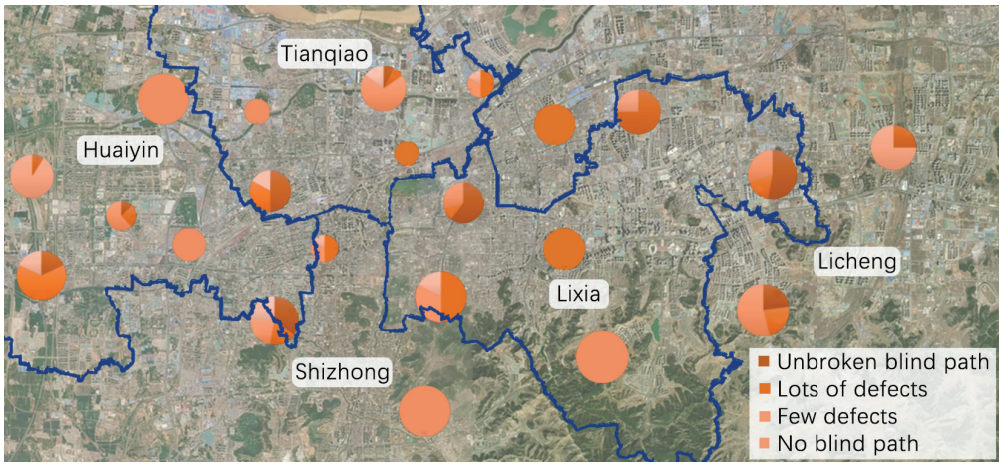


Figure 9. Summary map of Jinan Road facilities' accessibility analysis (Source: Author).

4.5.3. Examination of Accessible Facilities in Residential Structures

We conducted an in-depth investigation into the state of accessible infrastructure in residential buildings, including the examination of facilities such as lift shafts and public places within the community.

The distribution of accessible facilities in residential buildings exhibited a pattern similar to that observed in road transport facilities (Figure 10). Specifically, Lixia District demonstrated the most favourable overall situation, which was roughly commensurate with the level of economic development in each respective region. However, there were relatively fewer areas that boasted superior overall accessible facilities, indicating the need for a further improvement in the overall barrier-free environment.

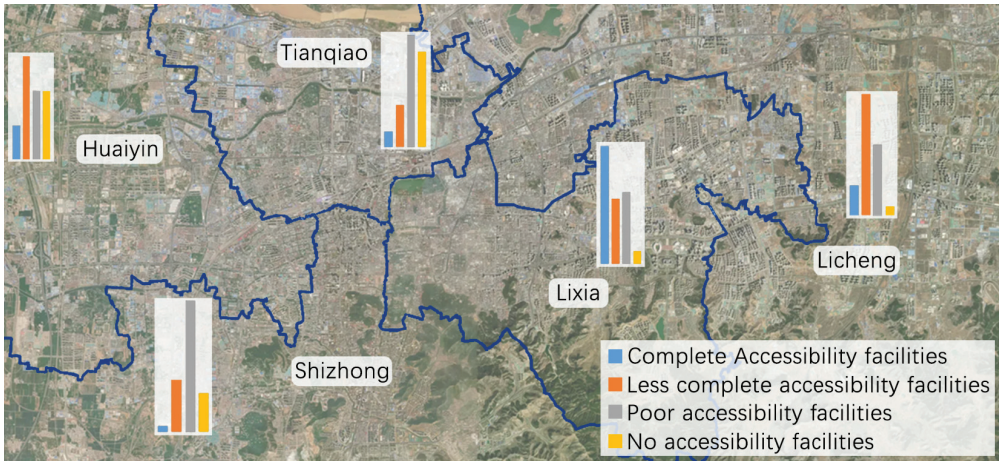


Figure 10. Summary map of analysing accessibility in residential neighbourhoods (source: the authors).

4.5.4. Examination of Accessible Facilities in Environmentally Friendly Parks

The parks were divided into seven gradients using a gradient division method, which was based on the development of barrier-free services in green areas. To visually represent this division, a map was utilised with a visualisation technique.

A visual analysis showed in Figure 11 that the accessibility of parks and green spaces in Jinan City was not good enough. According to this analysis, it could be seen that the areas with better accessible facilities were concentrated in the central area of Jinan City, and the accessible facilities in the old city areas were improved based on the existing ones, such as the Gucheng, Honglou, and Tianqiao areas, while the new city areas, such as the Hanyu and Long'ao areas, had a low degree of improvement of accessible facilities; in addition, the remote areas not part of the centre of the urban area of Jinan City, such as the Longdong area, were generally free of barriers, and the southern mountainous areas had a low degree of improvement. From this, it could be seen that the coverage of barrier-free facilities in Jinan City was not wide enough, and the areas with perfect barrier-free facilities were only limited to the central urban area, historical preservation areas, and areas with a better economic development, while the coverage and perfection of remote areas were insufficient. Figure 12 shows some areas where the accessibility facilities are incomplete.

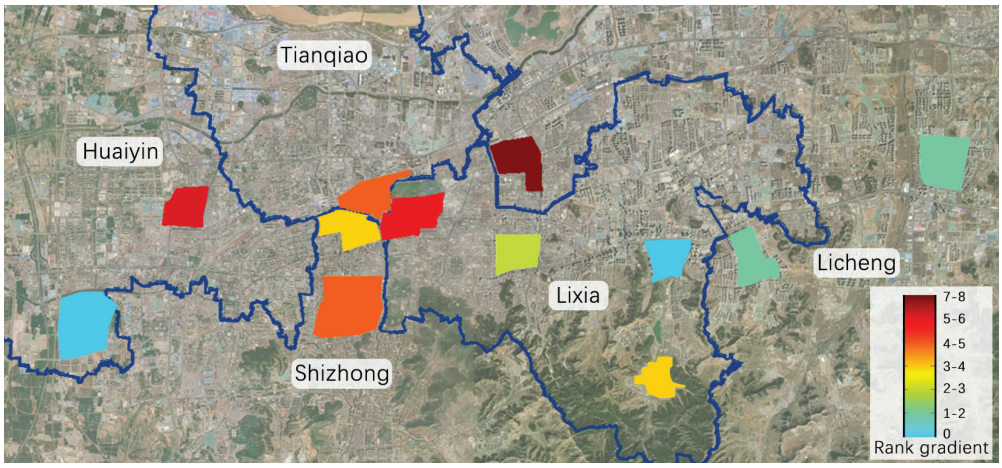


Figure 11. Summary chart of the analysis of the accessibility improvement of parks and green spaces (source: the authors).



Figure 12. Some inadequate accessibility facilities. (**a**) There are still no ramps in some small parks and there is a large height difference. (**b**) The blind path ended abruptly (source: the authors).

4.6. Assessment of Accessible Infrastructure in Researched Environments

Based on the findings of the study, the evaluation of accessible facilities in Huaiyin, Tianqiao, Shizhong, Lixia and Licheng was conducted utilising the assessment framework outlined in the preceding section whose results are arranged in Figure 13.

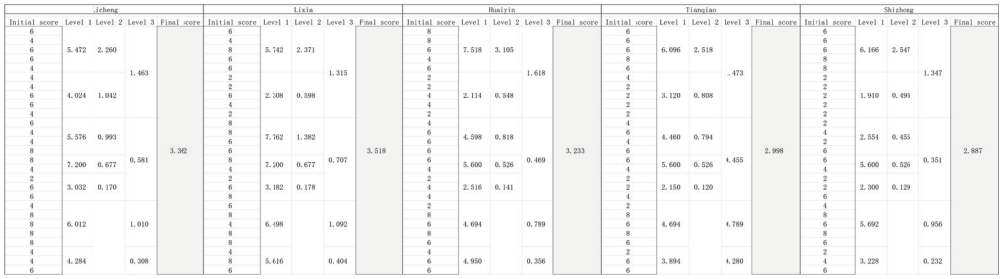


Figure 13. Score by region (source: the authors).

The districts' scores, arranged in descending order, were as follows: Lixia: 3.518, Lixing: 3.362, Huaiyin: 3.233, Tianqiao: 2.998, Shizhong: 2.887. The accessibility was the highest in the locality of Huaiyin, and the safety, controllability, and humanisation were all the highest in Lixia. Based on the evaluation results, the corresponding factors will be updated or improved.

5. Conclusions and Recommendations

This study presents conclusions and recommendations regarding the existing issues surrounding accessible facilities. The recommendations primarily emphasise two aspects. On the one hand, it is to propose improvement strategies for the accessibility of Jinan's researched area based on the results of the research and evaluation, and on the other hand, it is to make suggestions for an inclusive urban renewal based on the factor weights in the evaluation system.

5.1. Strategies for Increasing Accessibility in Selected Jinan Districts Based on Evaluation Results

Bar charts as shown in Figure 14 were made to visually compare the district-level factor-weighted scores , and generalised improvement strategies were proposed for each of the five research areas.

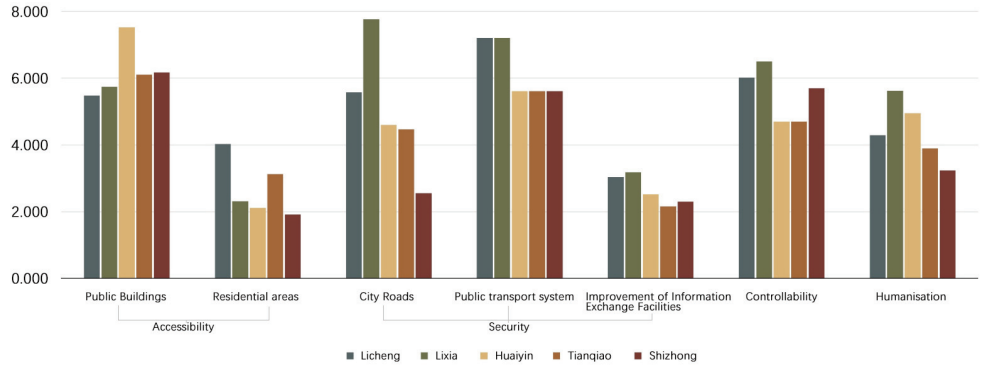


Figure 14. Comparison of level 1 scores of the five districts (source: the authors).

The five districts were all poor in terms of accessibility, information-exchange facilities, and humanisation of residential areas, and should be updated with accessible services such as bus stops, traffic signal systems, and accessible nodes, as well as maintaining blind alleys at entrances and exits of buildings and pavements in residential areas. The continuity of urban roads in the central district was also poor, and blind facilities, pavements, and zebra crossings should be managed and corrected to improve the continuity of roads.

5.2. Urban Renewal Recommendations Based on Evaluation Systems

Based on the evaluation scores, recommendations were made for the renewal of barrier-free facilities: priority was given to the renovation of barrier-free facilities in public buildings and the planning of barrier-free environments in residential areas, followed by the improvement of the accessibility of urban roads and the accessibility of the public transport system, and lastly, the management and maintenance of small-scale barrier-free service facilities, and so on.

1. New public buildings should strictly comply with barrier-free design norms and build barrier-free facilities with high quality; old public buildings with substandard facilities should be rectified and supervised within a limited period and follow-up maintenance management should be strengthened [29];
2. In residential areas, the barrier-free facilities that should be paid attention to include ramps, passages, doors, handrails and lifts, etc.; road accessible facilities should be improved with kerb ramps, blind corridors, etc.; and ancillary public service facilities, such as public toilets, accessible parking spaces, low-level service facilities and lifting platforms, etc., should also be fully equipped [30];
3. The improvement of road continuity should focus on the management and maintenance of blind alleys, connecting height differences with ramps, etc.; the standardisation strategy of the transport system includes: regulating the taxi industry to eliminate the phenomenon of taxis refusing to carry the disabled, transforming bus stop signs set in a high position and with a small font, and in terms of traffic management, increasing the punishment of vehicles occupying blind alleys, etc. [31];
4. Other accessible service facilities should be more user-friendly, easier to use, and regularly maintained and managed, and nonstandard facilities should be remedied to reduce inaccessibility or poor accessibility [32];
5. With the development of information technology and intelligence, intelligent assistive facilities for disabled people travelling have been paid attention to and researched, and various intelligent accessible facilities such as smart blind canes, smartphones with accessibility functions, and smart wheelchairs have appeared one after the other; some scholars have also researched the monitoring of high-risk zones for vulnerable groups, such as the elderly, who are prone to fall in outdoor environments [33], which provides a scientific basis for the construction of the public service field and enhances the convenience and safety of disabled people's travels as well as the efficiency and accuracy of the improvement of the barrier-free environment.

6. Conclusions and Prospect

At present, Chinese cities are in the stage of quality improvement, and there is still room for exploring research on urban renewal. The evaluation system established in this paper is only a tool and basis for one branch of this renewal. On this basis, more in-depth and comprehensive research will be carried out at a later stage to gradually build more inclusive and livable cities.

Author Contributions: Methodology, Y.W.; software, Y.Y. and J.W.; validation, Y.W. and Y.L.; formal analysis, Y.W. and Y.Y.; investigation, Y.L.; writing—original draft preparation, Y.W.; writing—review and editing, Y.Y. and J.W. All authors have read and agreed to the published version of the manuscript.

Funding: This research received no external funding.

Data Availability Statement: All data used in this research are available on open data sources.

Conflicts of Interest: The authors declare no conflict of interest.

References

1. Wang, P. *Wang Pingping: The Total Population Decreased Slightly and the Level of Urbanization Continued to Improve*; State Statistics Bureau: Beijing, China, 2023.
2. 2030 Agenda for Sustainable Development. New York, USA, 2016; Available online: https://sdgs.un.org/2030agenda (accessed on 20 October 2023)
3. National Development and Reform Commission. *Outline of the 14th Five-Year Plan (2021–2025) for National Economic and Social Development and Vision 2035 of the People's Republic of China*; National Development and Reform Commission: Beijing, China, **2021**.
4. Huang, B.; Lv, X.; Fang, Y. Survey and Reflection on the Status of accessibility facilities. *For. Sci. Technol. Intell.* **2023**, *55*, 165–167.
5. He, X.; Yang, Y. A Review of the Current Research Status of Accessible Design Methods. *Packag. Eng.* **2023**, *44*, 60–73. [CrossRef]
6. Boix-Cots, D.; Pardo-Bosch, F.; Pujadas, P. Analysis and Comparison of the Infrastructure Report Cards as a Decision Making Tool for Sustainable Development. *Buildings* **2023**, *13*, 2166. [CrossRef]
7. Huang, X.; White, M.; Langenheim, N. Towards an Inclusive Walking Community—A Multi-Criteria Digital Evaluation Approach to Facilitate Accessible Journeys. *Buildings* **2022**, *12*, 1191. [CrossRef]
8. Tang, Y.; Liu, Y.; Wang, Y. From Growth to Inclusion: The Multidimensional Connotation and Assessment of Inclusive Cities from the Perspective of the Right to the City. *J. Shanghai Adm. Coll.* **2023**, 48–64.
9. Harris, E.; Franz, A.; O'Hara, S. Promoting Social Equity and Building Resilience through Value-Inclusive Design. *Buildings* **2023**, *13*, 2081. [CrossRef]
10. United Nations. New Urban Agenda. In Proceedings of the Section III United Nations Conference on Housing and Sustainable Urban Development, Quito, Ecuador, 20 October 2016.
11. Asian Development Bank. *Strategy 2020: The Long-Term Strategic Framework of the Asian Development Bank 2008–2020*; Asian Development Bank: Manila, Philippines, 2008.
12. Xiang, D. Implications of the Concept of Inclusive Development for the Construction of Social Policy in China. *Soc. Sci.* **2012**, *1*, 70–74.
13. Xu, J. Multi-dimensional analysis and visualisation of inclusive design methodology. *Design* **2021**, *34*, 102–105.
14. Jing, X.; Xia, J.; Chen, H.; Wang, X. A study on the low utilisation rate of barrier-free facilities from the perspective of disabled people—A case study of Nanjing city. *Urban Plan.* **2020**, *44*, 47–56.
15. Zhao, P.; Chen, J. Study on the continuity of barrier-free design at the boundary of public space in old urban areas–Hangzhou City as an example. *Intell. Build. Smart City* **2022**, *8*, 160–164. [CrossRef]
16. Yuan, Z.; Liu, T.; Shao, L. Accessibility Needs and Satisfaction of the Physically Disabled in Beijing's Quarter-hour Community Service Circles. *Planner* **2019**, *35*, 25–31.
17. Wu, Y.; Gao, G.; Wu, M.; Wang, X.; Xue, P.; Gou, B. Investigation and analysis of the application status of urban barrier-free facilities (blind passage). *Chin. Tissue Eng. Res.* **2020**, *24*, 271–275.
18. Zhang, M.; Fu, J.; Liu, J.; Yan, M. Research on Urban Public Transport Travelling Service for Disabled People. *Packag. Eng.* **2022**, *43*, 199–207. [CrossRef]
19. Andersen, A.D.; Andersen, P.D. Foresighting for inclusive development. *Technol. Forecast. Soc. Chang.* **2017**, *119*, 227–236. [CrossRef]
20. Hinrichs, M.M.; Johnston, E.W. The creation of inclusive governance infrastructures through participatory agenda-setting. *Eur. J. Futures Res.* **2020**, *8*, 15. [CrossRef]
21. Gillovic, B.; McIntosh, A. Accessibility and Inclusive Tourism Development: Current State and Future Agenda. *Sustainability* **2020**, *12*, 15. [CrossRef]
22. Sun, J. *A Pattern Language-based Participatory Planning Approach for Barrier-free Communities*; Harbin Institute of Technology: Harbin, China, 2021.
23. Maslow, A.H. *Motivation and Personality*; Harper and Row: New York, NY, USA, 1970.

24. Hong, C.; Donghui, Z. Barrier-free design of residential areas and characteristics of disabled people. *Sichuan Archit. Sci. Res.* **2009**, *35*, 259–261.
25. Jin, C. A Study on Barrier-Free Travelling for People with Disabilities from a Systems Perspective. Master's Thesis, Guangxi Normal University, Guilin, China, 2019.
26. Cai, Y. Research Review on the Mobility Psychology of Disabled People and Suggestions on Urban Transport Planning. In Proceedings of the Annual Conference on Urban Planning in China 2016, Shenyang, China, 24–27 September 2016; p. 12.
27. Karlqvist, A. *Some Theoretical Aspects of Accessibility-Based Models//Dynamic Allocation of Urban Traffic Models*; Columbia University Press: New York, NY, USA, 1971.
28. General Office of Jinan Municipal People's Government .*Jinan City Barrier-Free Facilities Construction Management Measures*; General Office of Jinan Municipal People's Government: Jinan, China, 2009; pp. 8–9.
29. Sun, Z. A Study on Enhancing the Satisfaction of Barrier-Free Facilities Construction. Master's Thesis, Tianjin University, Tianjin, China, 2021.
30. Zhang, W. Standardised Construction Practice of Barrier-Free Facilities in Urban Residential Areas. *China Stand.* **2021**, *2*, 145–149.
31. Ye, H. Jinan: Barrier-Free Facilities for the Disabled Are Difficult to Satisfy. *China Disabl. People* **2013**, *12*, 6.
32. Zhang, S.; Xu, B. Barrier-free facilities still face the "three no-uses" barrier. *Beijing Dly.* **2023**, *8*.
33. Meng, J.; Yang, L.; Lei, H. Promoting Elderly Care Sustainability by Smart Village Facilities Integration—Construction of a Public Service Field with Introduction of Fall Posture Monitoring. *Buildings* **2023**, *13*, 2144. [CrossRef]

Disclaimer/Publisher's Note: The statements, opinions and data contained in all publications are solely those of the individual author(s) and contributor(s) and not of MDPI and/or the editor(s). MDPI and/or the editor(s) disclaim responsibility for any injury to people or property resulting from any ideas, methods, instructions or products referred to in the content.

buildings

MDPI

Article

Field Investigation of Water Infiltration into a Three-Layer Capillary Barrier Landfill Cover System Using Local Soils and Construction Waste

Yuedong Wu [1,2], Jincheng Ren [1,2] and Jian Liu [1,2,3,*]

[1] Key Laboratory of Ministry of Education for Geomechanics and Embankment Engineering, Hohai University, Nanjing 210098, China; hhuwyd@163.com (Y.W.); 211604010056@hhu.edu.cn (J.R.)
[2] Geotechnical Engineering Research Center of Jiangsu Province, Nanjing 210098, China
[3] Engineering Research Center of Dredging Technology of Ministry of Education, Hohai University, Changzhou 213000, China
* Correspondence: 20170053@hhu.edu.cn; Tel.: +86-1836-296-0323

Abstract: In response to the rapid urban expansion and the burgeoning number of landfill sites, managing water infiltration in these areas has become a critical challenge, especially in cities like Shenzhen, Hong Kong, and Singapore where traditional cover materials such as silt, clayey gravel, and sand are scarce. A three-layer (silt/gravelly sand/clay) capillary barrier cover system has been proposed to address this issue in humid climates. As an alternative to scarce traditional materials, using local soils and construction waste (CW) for this system presents a viable solution. However, the real-world performance of this adapted three-layer system, constructed with local soils and CW under natural rainfall conditions, remains to be fully evaluated. This paper presents a field test evaluating the water infiltration behavior of a three-layer capillary barrier landfill cover system under natural conditions. The tri-layered system is comprised of a 0.6 m loose local unscreened soil layer, covered by a 0.4 m CW layer and topped by a 0.8 m heavily compacted local screened soil layer. Monitoring findings reveal that, during the wet season, infiltration through the top two layers was staved off until the third rainfall, after which these layers retained moisture until 15 September 2016. The fluctuation in pore water pressure in the topmost layers showed each rainfall was contingent not only on the day's precipitation but also the hydraulic state. Beyond the hydraulic state's influence, a deeper tensiometer showed resulted in a diminished correlation between the surge in pore water pressure and daily rainfall. This declining correlation with depth can be attributed to the capillary effect and the reduced permeability of the screened soil layer. Rainfall patterns significantly affect percolation, with the combination of a short-duration, intense rainfall and prolonged weak rainfall resulting in a marked increase in percolation. In the foundational screened soil layer, the pore water pressure remained relatively low, with the cumulative percolation over six months (June to December) registering approximately 10 mm. These findings suggest a promising performance of the three-layer capillary barrier cover system, integrating local soils and CW, in the year of the study conducted in a humid environment.

Keywords: capillary barrier; infiltration; field test; local soil; construction waste

1. Introduction

Recently, a three-layer capillary barrier cover system has been proposed to minimize water infiltration into municipal solid waste in humid climates [1,2]. The three-layer cover system consists of a fine-grained soil layer (e.g., silt layer) overlying a coarse-grained layer (e.g., gravelly sand layer), which in turn overlies a fine-grained soil layer such as clay layer. Results obtained from numerical simulations [1], soil column tests [3], and physical flume model tests [2] show that the three-layer cover system performed well under heavy rainfalls. The breakthrough of the upper two layers occurred after heavy rainfalls. The

percolation through the three-layer capillary barrier cover system was negligible, primarily because the low permeability of the bottom clay layer redirected most of the infiltrated rainwater laterally along the gravelly sand layer. This transformation meant that the gravelly sand layer's role shifted from a capillary barrier to a lateral diversion passage, due to the influence of the clay layer following the upper layers. Recently, construction waste has been extensively used in engineering construction. An optimized system based on the three-layer capillary barrier cover has been proposed [4], particularly addressing the challenges of material availability in urban areas such as Shenzhen, Hong Kong, and Singapore. To reduce costs in a landfill cover system, construction waste was used instead of gravel in the middle layer, and local soil replaced kaolinite. Additionally, a vegetative layer was added on top. A field test was conducted to assess the system's impermeability. However, the performances of this three-layer capillary barrier system in responding to different rainfall patterns in field tests are limited.

Field monitoring programs have been carried out extensively on traditional landfill covers, for instance, compacted clay cover [5], evapotranspiration cover [6,7], two-layer capillary barrier [8,9], and multi-layered cover [10]. In these field sites, monitoring data were usually recorded by a data logger or collected manually at a low frequency. However, some rainfalls only lasted a few hours and thus the data may be missed. Moreover, landfills usually are located far away from downtown and thus lack computers and electricity for the data logger. To solve these difficulties, a wireless system based on a General Packet Radio Service (GPRS) network was used to establish the monitoring system at a high frequency [11]. In this system, the computer could be fixed far away from the testing site (e.g., landfill) and the instruments can be installed in the testing site where the GPRS network covers. However, the GPRS network may not be stable sometimes due to the interference from significant noise and impairments at the site [12]. Under such conditions, the monitoring system in the landfill may not work effectively.

In this study, an architecture with local and GPRS networks at a high logging frequency was established in the landfill where the GPRS network may not be good sometimes. Based on this architecture, the study investigated the performance of a three-layer cover system using local soils and construction waste (CW) under various natural rainfall conditions in a humid climate. Additionally, the research explored the performances of the three-layer capillary barrier system responding to different types of rainfall. For each heavy rainfall, the responses of measured pore water pressure in the local soils and CW were measured. In addition, the percolation was directly measured with drain gauges to better understand the performance of the three-layer cover system using the local soils and CW.

2. Materials and Methods

2.1. Testing Site

The testing site is located at the Xiaping solid waste landfill in Shenzhen, Guangdong China, as shown in Figure 1. The Xiaping landfill, the largest one in Shenzhen, receives an average of 5300 t of domestic waste per day. More than 6 Mt domestic wastes have been dumped in the landfill. After the landfill reaches the designed height, a final cover system has been installed over the waste.

This testing site is in a humid region with an average annual rainfall of about 1932.9 mm. The daily evaporation potential values are about 4.6 and 3.3 mm in wet and dry seasons, respectively. The average monthly maximum and minimum temperatures range from 19.8 °C to 32.3 °C and from 12.5 °C to 26.3 °C, respectively. No freezing temperature was observed at the site.

An area, 6 m wide by 20 m long, was selected on a slope along the western side of the Xiaping solid waste landfill. The test area has an average slope angle of about 15° and a height of 5 m. Based on the conceptual framework from Ng et al. [1,2], the three-layer capillary barrier cover system in this study consisted of a 0.6 m thick loose local unscreened soil layer overlying a 0.4 m thick construction waste layer and a 0.8 m thick heavily local

compacted screened soil layer. The screened local soil was obtained by screening the local soil through a layer of metal mesh with a 10 mm aperture.

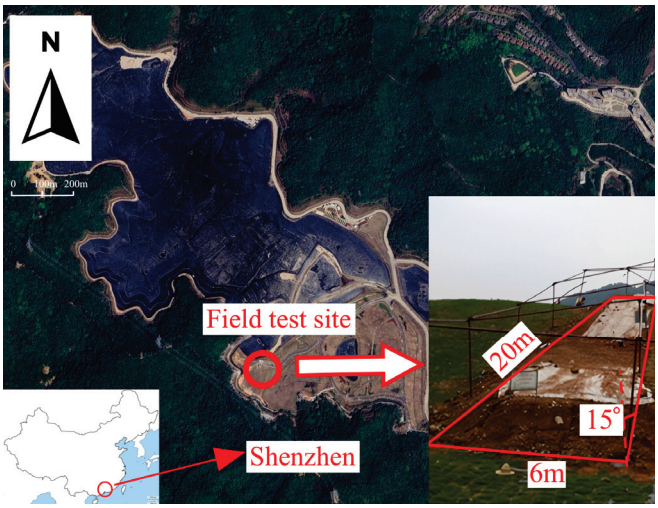


Figure 1. Overview of the field test site.

The cover system primarily consists of three layers: unscreened soil, construction waste, and screened soil. The unscreened and screened soils are sourced locally, while the construction waste predominantly comprises waste concrete and bricks. These types of construction waste are generally considered to be environmentally inert. This implies that under natural conditions, they are less prone to chemical reactions.

2.2. Materials and Construction Methods

A sampling program was conducted during the construction of the cover. The samples were analyzed for particle size distribution (ASTM D 422) [13], Atterberg limits (ASTM D 4318) [14], compaction characteristics (ASTM D 698) [15], and saturated permeability properties (ASTM D 5084) [16]. Table 1 summaries the physical properties of the three soils (i.e., unscreened soil, CW, and screened soil). The unscreened soil exhibited D60, D30, and D10 values of 0.298 mm, 0.091 mm, and 0.006 mm, respectively, while the screened soil showed values of 0.165 mm, 0.032 mm, and 0.003 mm. The fine content was 25.2% for the unscreened soil and 40% for the screened soil. After screening, an increase in fine content was observed, leading to a decrease in the saturated hydraulic conductivity (k_s). The main difference between the CW layer and the local soil lies in the overall larger particle size, with D60, D30, and D10 values of 20.1 mm, 8.9 mm, and 2.3 mm, respectively. The saturated hydraulic conductivity of the CW layer is 6–7 orders of magnitude higher than that of the screened soil, enabling it to form a cover system with capillary barrier effects (CCBE) with the unscreened soil. Construction waste mainly consists of inert waste, non-inert waste, and contaminated waste; the CW chosen for this study mainly consists of recycled crushed concrete and bricks. The particle size of these materials determines their hydraulic properties. These are classified as inert waste and have no environmental impacts under natural conditions [17,18]. For the upper two layers, the relative densities of unscreened soil and CW were 80% and 94%. For the bottom layer, the screened soil was compacted to 95% of its maximum dry density, aiming to obtain a low coefficient of water saturated permeability and porosity.

The three-layer landfill cover was constructed from July 2015 to May 2016. The soils were compacted at four sublayers for the bottom layer, three sublayers for the middle layer, and three sublayers for the top layer using a mini roller compactor with a weight of 1 t. As suggested by Ng et al. [2], geotextiles were installed at the interface between the two soil layers at depths of 0.6 and 1.0 m to prevent soil particle migration. The geotextiles used in our study were non-woven, with a thickness of 0.9 mm, and had an equivalent pore size

ranging from approximately 0.07 mm to 0.2 mm, the saturated permeability of geotextile (i.e., 7×10^{-2} m/s) was significantly higher than that of the uppermost soil layer (i.e., $5 \times 10^{-7} \sim 9 \times 10^{-7}$ m/s), water penetration was not affected. After the construction of the cover system, the instrumentation and monitoring system were installed at the testing site.

Table 1. Properties of local soils and construction waste used in the field test.

Soil Type		Unscreened Soil	Construction Waste	Screened Soil
Unified soil classification system		SC	GW	SC
Liquid limit, *LL* (%)		37	/	37
Plastic limit, *PL* (%)		20	/	20
Grain size distribution	D_{60} (mm)	0.298	20.1	0.165
	D_{30} (mm)	0.091	8.9	0.032
	D_{10} (mm)	0.006	2.3	0.003
	Fine content (0.075 mm; %)	25.2	/	40.0
	Coefficient of uniformity, C_u	49.6	8.7	55
	Coefficient of curvature, C_c	4.6	1.7	2.1
Maximum dry density, ρ_d (Mg/m^3)		1.86	1.89	1.82
Saturated coefficient of permeability, k_s (m/s)		5×10^{-7}–9×10^{-7}	6×10^{-2}–1×10^{-1}	1.0×10^{-8}–3.0×10^{-8}

2.3. Instrumentation Program

2.3.1. Layout of Instruments

Figure 2 shows the layout of all instruments used in the field monitoring program. The instruments included a rain gauge for recording precipitation, jet-filled tensiometers with pore pressure transducer for negative pore water pressure, and drain gauges for percolation. The details for each instrument are summarized in Table 2.

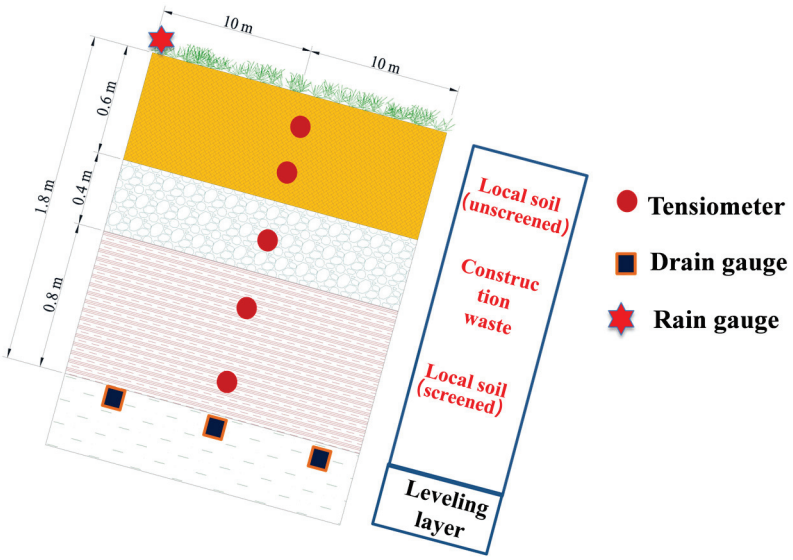


Figure 2. Layout of instruments in the landfill cover.

Five tensiometers were installed only at the middle section of the cover system. These tensiometers were spaced 0.5 m apart. For each depth (i.e., 0.2 m, 0.4 m, 0.8 m, 1.2 m, and 1.6 m), there was one tensiometer to study water seepage characteristics in the three-layer cover system. The rain gauge was installed at the crest of the slope. These instruments

were connected to a wireless network system for data collection. For detailed information on the Data Transmission System, please refer to the Appendix A.

Table 2. Summary of instruments.

No.	Measurement	Type of Instrument	Quantity	Measuring Range/Accuracy
1	Pore water pressure	Jet-fill tensiometers	5	−90–100 kPa/0.1 kPa
2		Pore pressure transducers	5	
3	Percolation	Drain gauge	3	No limit/0.1 mm
4	Precipitation	Rain gauge	1	0–50 mm/min/0.2 mm/min

2.3.2. Instruments, Calibrations, and Installing Methods

Rain gauge—The rain gauge is a freestanding receptacle for measuring precipitation. As water is collected, the tipping bucket fills to the point that it tips over, causing a momentary closure of a switch to incrementally measure rainfall accumulation. This action empties the bucket in preparation for additional measurement. Water discharged by the tipping bucket passes out of the rain gauge with no need for emptying. A simple device consisting of a peristaltic pump with transparent hose was used for calibration as presented by Vasvári [19].

Jet-filled tensiometer—Negative pore water pressure was measured by jet-filled tensiometer manufactured by the Soil moisture Equipment Corporation [20]. In order to increase the accuracy and automatically record data, a pore pressure transducer (PPT) was employed, taking the place of a vacuum gauge. Different from the traditional artificial reading for the vacuum gauge, the use of PPT could decrease the workload of reading and increase the recording frequency to meet the requirements for recording water infiltration during the process of rainfall. Before installation, all tensiometers with PPT were calibrated using the method proposed by Chen et al. [21] and Feng et al. [22]. The measurement accuracy of PPT was 0.1 kPa, about 5% of the accuracy of vacuum gauge.

Drain gauge—The drain gauge was a buried tank with an open top that collected any infiltrated water from the overlying soil mass. The diameter of the tank was designed as 1 m. In the tank, the soil mass was compacted with a water content to a dry density identical to the surrounding soil mass. At the bottom of the tank, a drain tube with porous stone was connected to carry water from the tank to a collection tank. The mass of the infiltrated water collected in the collection tank was measured by a balance. Then, the infiltration rate can be calculated by the mass changes of the collection tank over the measuring duration. The accuracy of mass measurements is 0.5 g. it has been widely adopted and confirmed to exhibit outstanding reliability and high precision [23].

3. Results

3.1. Pore Water Pressure

Figure 3 shows the record of daily precipitation from 1 June 2016 to 1 December 2016. After construction, the cover system was first subjected to a wet season lasting about five months and then a dry season lasting about 1 month. According to data from the Shenzhen Meteorological Bureau [24], the total precipitation in Shenzhen for the year 2016 was 2490.6 mm. The maximum and minimum annual rainfalls recorded over the past 50 years in Shenzhen were 2747.3 mm and 1269.7 mm, respectively, indicating that the 2016 precipitation level is representative of the typical climatic conditions in Shenzhen. During the wet season, the condition was a relatively high humidity and the total precipitation was 1551 mm, approximately 65% of Shenzhen's annual rainfall. According to the meteorological report formulated by the Shenzhen Meteorological Bureau [24], the number of rainy days in the rainy season is 64, which accounts for about 45% of the total

number of days in this period. To study the effectiveness of the cover system under natural rainfall conditions over a year, daily rainfall data were selected as the metric. It should be noted that eight heavy rainfalls (or rainstorms) whose daily precipitation (labeled in the figure) was higher than 50 mm [25] occurred during the wet season. The maximum daily precipitation was as large as 217.8 mm (No. 7). In the dry season, the soil humidity was low and the total precipitation was only 162.3 mm, with the heavy rainfall event No. 9 contributing 52.2 mm to this total. In the dry season, the number of no-rainfall days reached 23 and the number of the maximum continuous no-rainfall days was 11.

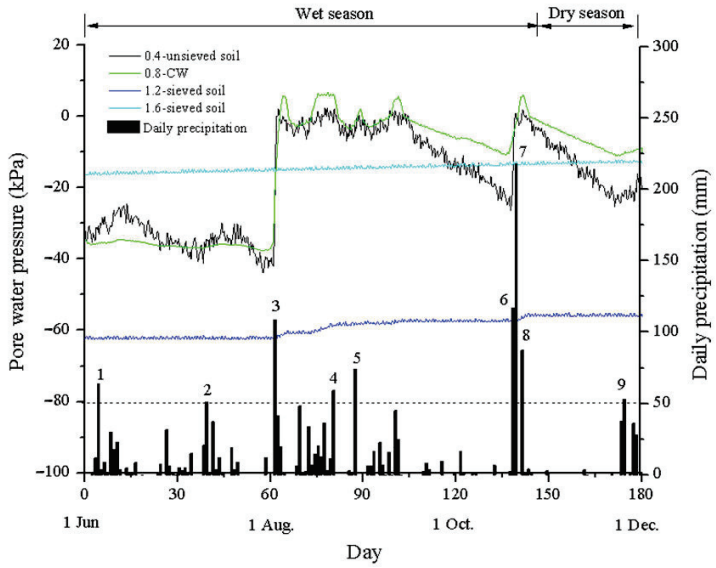


Figure 3. Changes of pore water pressure in the three-layer cover system at different soil depths under natural conditions.

The development of pore water pressure at each depth was also included in Figure 3. Due to the evaporation, the cavitation in the tensiometer at a depth of 0.2 m occurred and its data were not shown in the figure. As expected, the pore water pressure increased in response to each rain at depths of 0.4 and 0.8 m, particularly subjected to nine heavy rainfalls. At a depth of 1.2 m, the increases in the pore water pressure were smaller than those at depths of 0.4 m and 0.8 m. It indicates that little water infiltrated into the screened layer at the bottom [2]. On the other hand, the pore water pressure in the upper two layers decreased in the no-rainfall days, e.g., from 15 September 2016 to 16 October 2016 and from 22 October 2016 to 21 November 2016. In the upper two layers, the pore water pressure in the top layer decreased more than in the layer beneath during periods without rainfall. At depths of 1.2 m, the pore water pressure was maintained as constant. It was due to the low permeability in the CW layer during drying and thus the water loss in the underlying screened soil layers was small. Similar changes in pore water pressure were obtained using numerical simulations by Ng et al. [26]. In this study, "breakthrough" refers to the movement of water through the top two soil layers under rainfall conditions. In this three-layer system, when a breakthrough occurs in the top two layers, the presence of a low-permeability soil layer impedes the infiltration of rainwater. A breakthrough is characterized by pore water pressure, correlating with field capacity. Correspondingly, pore water pressure shows increased sensitivity during rainfall events as soil approaches saturation [27]. It should be noted that before 2 August 2016, the total precipitation was 423 mm, approximately 21% of Shenzhen's annual rainfall. However, the pore water pressure remained relatively low (ranging from −25 to −45 kPa) at the depths of 0.4 and 0.8 m. The breakthrough of the upper two layers did not occur. It may be because the maximum daily precipitation was 63.8 mm, smaller than the rain intensity when the breakthrough of the upper two layers occurred (e.g., No. 3 with 108.8 mm, No. 6 with

116.3 mm, and No. 7 with 217.8 mm). At a depth of 1.2 m, the pore water pressure remained at −62 kPa. After the breakthrough (e.g., No. 3 rainfall with 108.8 mm), the pore water pressure remained near zero until 15 September 2016. In this period, positive pore water pressure was observed in the upper two layers subjected to each heavy rainfall.

The Xiaping solid waste landfill generates landfill gas (LFG) primarily through the biodegradation of municipal solid waste (MSW). The gas composition predominantly consists of approximately 60% methane (CH_4) and 40% carbon dioxide (CO_2). The LFG production rate at this landfill is approximately 1.109×10^3 m^3/h, based on estimates [28]. At a depth of 1.6 m in the screened soil layer, the pore water pressure varied from −10 kPa to −22 kPa, unrelated to the daily precipitation. Its value was approximately 40 kPa larger than that at a depth of 1.2 m in the same soil layer. It may be induced by the high humidity of landfill gas under the cover [29]. In other words, wet landfill gas may be important for a minimum of landfill gas emission [26].

As previously mentioned, the heavy rainfalls were important for the breakthrough of the upper two layers. Figures 4–6 summarize the change in pore water pressure subjected to the nine heavy rainfalls at a depth of 0.4 m (unscreened soil layer), 0.8 m (CW layer), and 1.2 m (screened soil layer). At a depth of 0.4 m, the maximum increase in the pore water pressure was 42.2 kPa subjected to a No. 3 heavy rainfall. However, the daily precipitation of No. 3 rain was 108.8 mm (not maximum). The daily precipitation seemed not to be the sole factor to the change in pore water pressure. It may be due to the hydraulic state of the cover system. After the rains of No. 3, 7, and 8, the unscreened soil was wet. In the wet state, it was easy to reach the maximum pore water pressure for the cover system. The maximum pore water pressure was approximately 2 kPa at a depth of 0.4 m. It should be noted that the maximum pore water pressure was smaller than its hydrostatic pressure (i.e., 4 kPa for the tensiometers at a depth of 0.4 m) by assuming that the cover system was saturated. It may be due to desiccation cracking near the top of the unscreened soil layer [5]. A similar change to pore water pressure also occurred at a depth of 0.8 m. The maximum pore water pressure of 5.5 kPa also occurred after No. 3 rain.

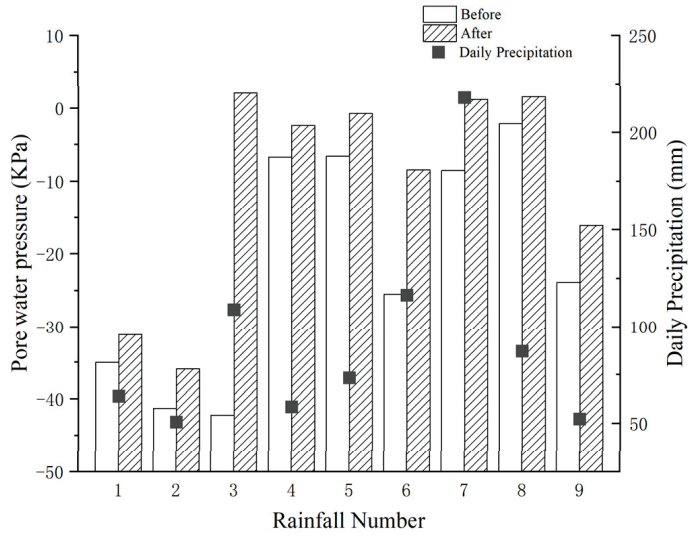


Figure 4. Change in pore water pressure subjected to heavy rainfalls at depth of 0.4 m in unscreened soil layer.

Different from the depths of 0.4 and 0.8 m, the increase in the pore water pressure at a depth of 1.2 m changed only slightly after each heavy rainfall. The wetter the CW layer, the larger the increase in the pore water pressure, for example, No. 3, 4, 5, and 8 rainfalls. The maximum increase in pore water pressure was 1 kPa. It may be because the wet CW layer increased the pore water pressure in the top boundary of the underlying screened soil layer.

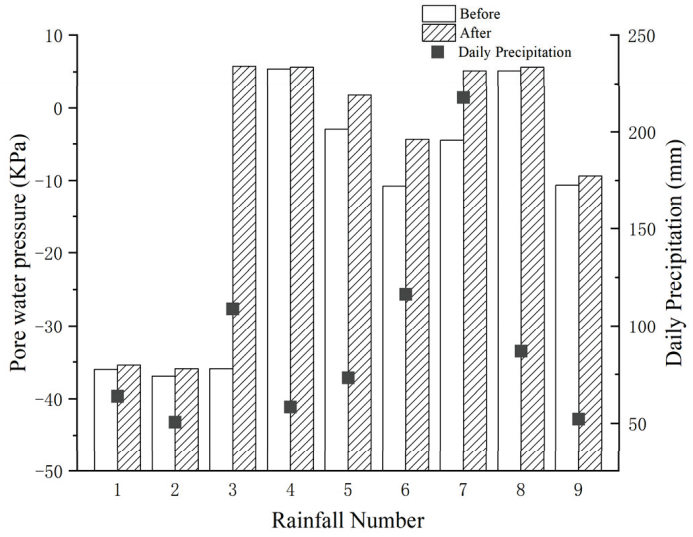


Figure 5. Change in pore water pressure subjected to heavy rainfalls at depth of 0.8 m in CW layer.

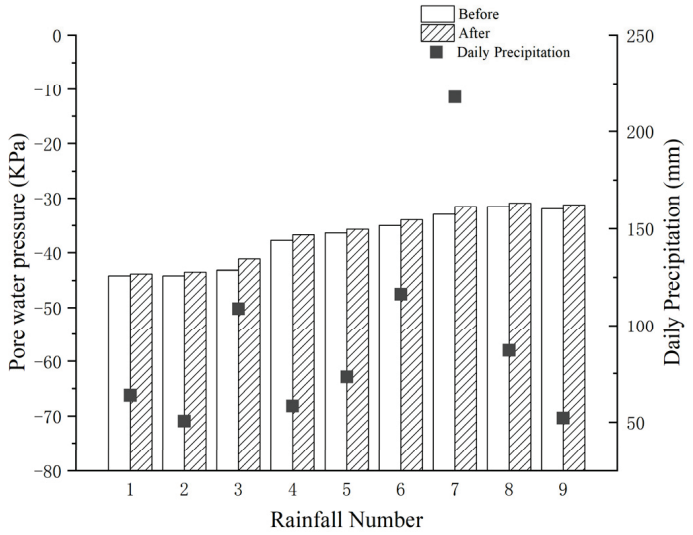


Figure 6. Change in pore water pressure subjected to heavy rainfalls at depth of 1.2 m in screened soil layer.

The No. 3, 7, and 8 rainfall events, although of different intensities (108.8 mm, 217.8 mm, and 86.9 mm), all caused the soil to reach the maximum pore water pressure, which will be maintained regardless of the amount of rainfall. Except for these three rainfalls, Figure 7 shows the relationship between daily precipitation and the increase in pore water pressure. As expected, increases in the daily precipitation and increases in pore water pressure in each soil layer were observed. The deeper the tensiometer, the smaller the ratio between the increase in pore water pressure and daily precipitation. As water seeped from the unscreened soil layer into the CW layer, this ratio decreased by approximately 48% (from 0.1771 to 0.0918). It was due to the capillary effect formed by the upper two layers. Once water seeped from the CW layer into the screened soil layer, the ratio decreased by approximately 98% (from 0.0918 to 0.0018). It was due to the low permeability of the screened soil. It indicates that the screened soil layer served as the major function for preventing water seepage in the three-layer cover system.

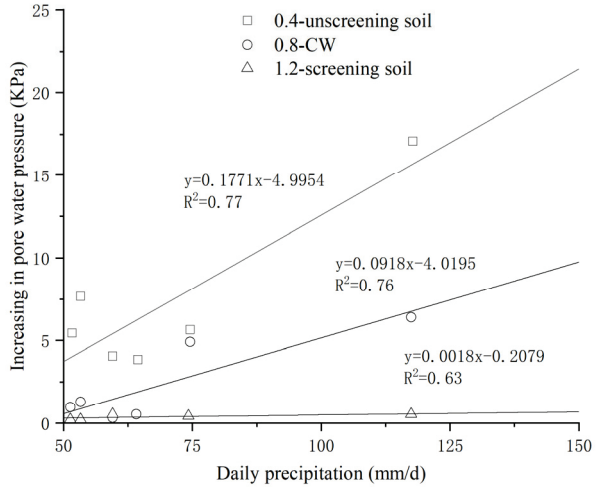


Figure 7. Relationship between daily precipitation and increase in pore water pressure except No. 3, 7, and 8 rains.

3.2. Percolation

Figure 8 shows the cumulative percolation at three sections. It should be noted that the cumulative percolation in a 6-month duration (i.e., from June to December) was about 10 mm. It indicates that the performance of the three-layer capillary barrier cover system using local soils and CW in the field condition was satisfactory under a humid climate where an annual rainfall is about 2000 mm.

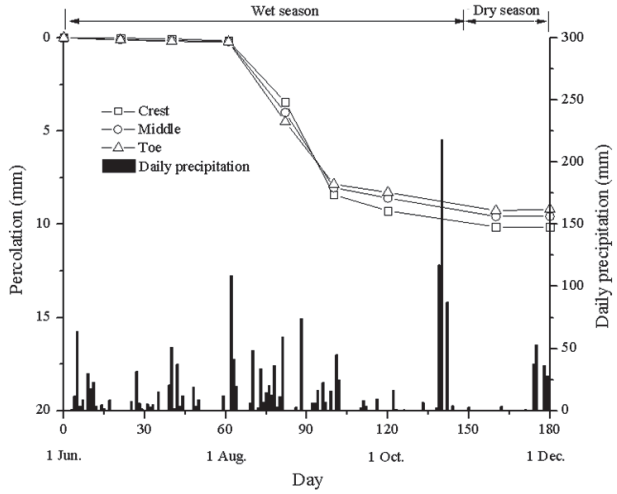


Figure 8. Development of percolation under daily precipitation condition.

From 1 June to 1 December 2016, the cumulative percolation development underwent distinct phases under varying rainfall conditions. In the initial phase (1 June–2 August), the initial pore water pressures from top to bottom were approximately −30 kPa, −35 kPa, −62 kPa, and −18 kPa. Characterized by prolonged weak rainfall, despite a total rainfall of 423.2 mm, the pore water pressure in the top two layers remained low, ranging from −25 kPa to −45 kPa at the 0.4 m (unscreened soil layer), while the pore water pressures in the other layers remained largely unchanged. No breakthroughs were observed, resulting in a negligible increase in cumulative percolation. The subsequent phase (2 August–5 September) experienced a combination of short-duration, high-intensity rainfall and continued prolonged weak rainfall. During this phase, the initial pore water pressures from top to bottom were approximately −30 kPa, −35 kPa, −60 kPa, and −18 kPa. After experiencing short-duration, high-intensity rainfall, the pore water pressures in the unscreened soil layer and CW layer increased to around 0 kPa, followed by a prolonged period of weak rainfall

where the top two layers' pore water pressures remained persistently around zero. This condition led to breakthrough events, with a total rainfall of 602.2 mm and a significant cumulative percolation increase of approximately 8 mm. The final phase (5 September–1 December) was marked by a predominantly short-term intense rainfall, with initial pore water pressures from top to bottom of approximately −20 kPa, −10 kPa, −55 kPa, and −12 kPa. After experiencing a short-duration, high-intensity rainfall, the top two layers' pore water pressures briefly rose to around 0 kPa, with most pore water pressure readings remaining negative. Despite the total rainfall in this phase being higher at 687.8 mm than in the previous phase, the additional cumulative percolation was around 2 mm, which is less than the 8 mm increase observed in the second phase.

Regarding the percolation process, the pore water pressure in the CW layer, which serves as the top boundary of the screened soil layer, plays a crucial role. Figure 9 shows the relationship between percolation rate and average pore water pressure in the CW layer. As expected, the percolation rate increased as the average pore water pressure in the CW layer increased. It indicates that even in the period without rainfall, water will percolate when the CW layer is wet. According to the design criterion recommended by the US EPA, the percolation rate should not exceed 30 mm/year [30]. Following the U.S. EPA's ACAP guidelines, our study indicates that the CW layer's pore water pressure should remain below −3 kPa in humid climates.

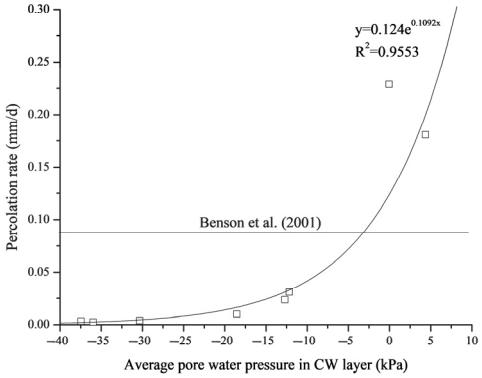


Figure 9. Relationship between percolation rate and average pore water pressure in CW layer [30].

4. Discussion

This field test examined a three-layer capillary barrier cover system, employing unscreened soil (25.2% fines content) and screened soil (40.0% fines content), combined with construction waste (CW), under natural rainfall. The focus was on the dynamics of pore water pressure and percolation across varying depths and under different rainfall intensities.

Below 1.2 m, pore water pressure remained largely constant, mirroring the simulated trends by Ng et al., (2015) [26], indicating minimal water infiltration to the lower layer. In high-rainfall scenarios, pore water pressures in the upper layers were positive, aligning with Ng et al.'s indoor model findings [2]. A notable deviation from these models was the slight rise in pore water pressure below 1.2 m during ongoing rainfall, attributed to increased pressure within the CW layer due to extended precipitation. Analysis revealed a direct proportionality between the percolation rate in the CW layer and the average pore water pressure.

Figures 4 and 8 reveal that prolonged weak rainfall, without breakthrough in the top two layers, results in minimal changes in cumulative percolation. However, breakthroughs occur when these layers transition from unsaturated to saturated states during short-duration, high-intensity rainfall, and continued weak rainfall prevents the layers from returning to an unsaturated state promptly, leading to percolation. Although short-duration, high-intensity rainfall was found to have a lesser impact on percolation, when followed by prolonged weak rainfall, it resulted in significant percolation. Despite the top two layers being in a saturated state, the CW layer, acting as a drainage layer, still effectively reduces

percolation [4]. The effect of short-duration, high-intensity rainfall in elevating moisture levels substantially influences the landfill's response to further rainfall events.

The high relative humidity in landfill gas might influence the pore water pressure in the screened soil at the bottom [29], which could in turn affect landfill gas emissions [26].

The measured data and parameters of our study, conducted on a three-layer capillary barrier landfill cover system using local soils and construction waste, are subject to various environmental uncertainties. For example, measurement errors during heavy rain due to the inertia of tipping buckets, and factors like evaporation, wind effects, surface runoff generation, and lateral drainage were not fully incorporated in our boundary conditions. These elements could affect the system's performance under diverse environmental scenarios [31]. Future research should focus on quantifying these uncertainties to better predict system behavior.

Future research should focus on exploring the applicability of the cover system in different regions, particularly considering variations in soil and climate. Conducting long-term experiments under a variety of environmental conditions is crucial for understanding the system's response to climate change and aging. This includes a detailed analysis of the aging characteristics of materials, such as studying the changes in physical and chemical properties over time of materials used in the cover system, and how these changes affect the overall performance of the system. Additionally, the long-term monitoring of structural integrity is essential, requiring assessment of how structural damages (such as cracks and collapses) develop over time and impact the system's permeability and effectiveness.

5. Conclusions

A field test was carried out to study the performance of a three-layer cover system using local soils and construction waste. The detailed response of pore water pressure and percolation during rainfalls could be captured. Based on the measured results, the following conclusions may be drawn:

(1) In the wet season, the breakthrough of the upper two layers did not occur until a No. 3 rainfall whose daily precipitation was 108.8 mm. After the breakthrough, the upper two layers were wet until 15 September 2016. In this period, the pore water pressure in the underlying screened soil layer increased slightly and thus a major percolation occurred.

(2) The pore water pressure in the screened soil layer near the bottom was at a high level, and not correlated with daily precipitation. It may be due to the influence of the high humidity of the landfill gas.

(3) The increase in the pore water pressure in the upper two layers subjected to heavy rainfalls depended on not only the daily precipitation, but also the hydraulic state. Rainfall patterns significantly impact pore water pressure and percolation, with the combination of a short-duration, intense rainfall and prolonged weak rainfall notably extending the duration of saturated conditions and leading to significant percolation.

(4) Over the six-month period from June to December, the cumulative percolation in the study measured approximately 10 mm. These results indicate that the three-layer capillary barrier cover system, which integrates local soils and construction waste (CW), demonstrated initial effectiveness under the field conditions of a humid climate observed during the study period.

(5) The percolation rate increased as the average pore water pressure in the CW layer increased. In order to satisfy the allowable percolation rate of 30 mm/year, the pore water pressure in the CW layer should be smaller than -3 kPa.

Author Contributions: Conceptualization: J.L. and Y.W.; methodology: J.L. and Y.W.; software: J.R.; validation: J.R. and Y.W.; formal analysis: J.L., J.R. and Y.W.; investigation: J.L.; resources: Y.W. and J.R.; data curation: J.L. and J.R.; writing—original draft preparation: J.L. and J.R.; writing—review and editing: Y.W.; visualization: J.R.; supervision: Y.W.; project administration: J.L.; funding acquisition: J.L. All authors have read and agreed to the published version of the manuscript.

Funding: This work was supported in part by the National Natural Science Foundation of China under Grant 52378337.

Data Availability Statement: The data presented in this study are available in this article.

Conflicts of Interest: The authors declare no conflicts of interest.

Appendix A

Data Transmission System:

Figure A1 shows the architecture of the network system. The network system consisted of several analog-to-digital converters, a microcontroller, a data terminal unit (DTU) based on GPRS, a base transceiver station, a data center server, a computer, a solar panel, and a battery.

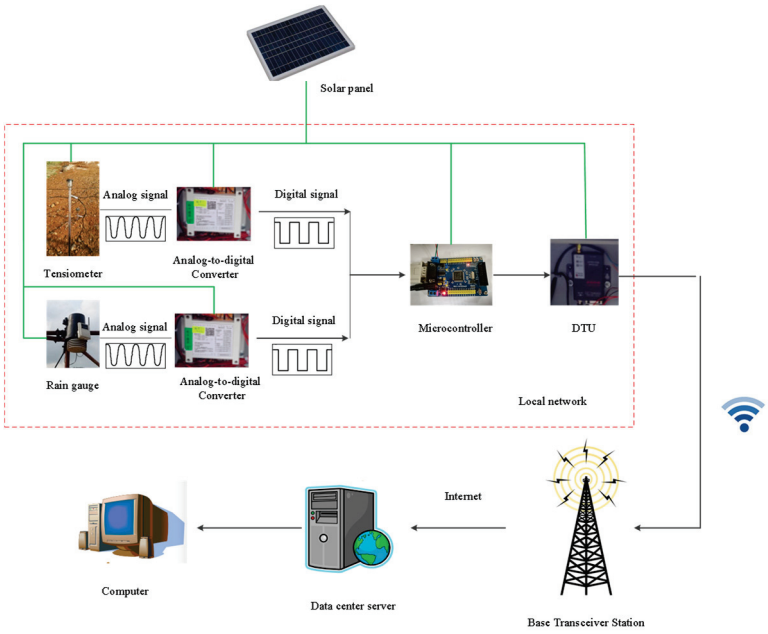


Figure A1. Architecture of network system.

In this architecture, the analog signal from each instrument was first sampled at regular time intervals in the analog-to-digital converter. Each sample was then evaluated in terms of a binary number and output in the form of the digital signal. This process may introduce errors, because a continuously varying analog signal was replaced by a discrete set of points at each time interval. In order to reduce the sample error to a level which could be accepted in field monitoring of the landfill cover system, the sample frequency was set as 1 Hz. The measuring range and accuracy of the analog-to-digital converter used in this study were ±60 mV and 0.01 mV, respectively.

All the analog-to-digital converters were connected to a microcontroller to establish a local area network. In this network, each analog-to-digital converter was a slave whereas the microcontroller was a master. The microcontroller would send a request message to all the analog-to-digital converters and receive reply messages from the analog-to-digital converters with the desired address. All the received messages would be first saved to a storage unit in the microcontroller. It should be noted that even if the GPRS was not good, the local area network still worked. In other words, the data from each instrument were recorded and saved to the storage units and were independent of the GPRS network. On the other hand, the microcontroller was also connected to a DTU to form another area GPRS network. Based on this GPRS network, the microcontroller would send the data saved in the storage unit to a data center server. It should be noted that the results are saved in the storage unit during the period of poor GPRS quality.

The DTU is a wireless device which is applied to transmit the digital signal through the GPRS networks. Therefore, the DTU needed a build-in subscriber identification module (SIM) card which was used to apply for GPRS services. One of the advantages of GPRS networks is that it supports the DTU to permanently stay online. Another is that the GPRS network has covered almost all the provinces, municipalities, and autonomous regions. Once the DTU powered on, DTU first connected to a mobile station nearby and kept this communication link online. Subsequently, the digital signal from the analog-to-digital converter was read out by the DTU and saved in its cache. Finally, the DTU encapsulated the information in the cache into an information packet and sent the packet to a fixed internet protocol (IP) address which was configured in advance.

The base transceiver station is a piece of equipment that operates in the 3.5 GHz band for fourth-generation (4 G) mobile communication between user equipment (e.g., DTU, mobile phone) and a network. Via the communication, the base transceiver station could receive the information packet from DTU and then send it to the external public internet.

The data center server maintained online with a fixed IP address and could receive the information packets from DTUs. Once receiving the packets, the server would extract the useful data from the information packets and save it on the hard drive. When the data were required to be analyzed, a computer could be used to connect the server and download the data.

The solar panel and battery could supply enough electric energy for all instruments which were installed in the landfill cover. The solar panel first absorbed the sunlight as a source of energy to generate electricity. This electricity was then stored in a battery. The battery was connected to all instruments and supplies enough electricity for them.

References

1. Ng, C.W.W.; Liu, J.; Chen, R.; Lim, C.J. Numerical parametric study of an alternative three-layer capillary barrier cover system. *Environ. Earth Sci.* **2015**, *74*, 4419–4429. [CrossRef]
2. Ng, C.W.; Liu, J.; Chen, R.; Xu, J. Physical and numerical modeling of an inclined three-layer (silt/gravelly sand/clay) capillary barrier cover system under extreme rainfall. *Waste Manag.* **2015**, *38*, 210–221. [CrossRef] [PubMed]
3. Ng, C.W.; Coo, J.L.; Chen, Z.K.; Chen, R. Water Infiltration into a New Three-Layer Landfill Cover System. *J. Environ. Eng.* **2015**, *142*, 04016007. [CrossRef]
4. Ng, C.W.W.; Guo, H.; Ni, J.; Chen, R.; Xue, Q.; Zhang, Y.; Feng, Y.; Chen, Z.; Feng, S.; Zhang, Q. Long-term field performance of non-vegetated and vegetated three-layer landfill cover systems using construction waste without geomembrane. *Geotechnique* **2022**. *ahead of the print*. [CrossRef]
5. Albrecht, B.A.; Benson, C.H. Effect of Desiccation on Compacted Natural Clays. *J. Geotech. Geoenviron. Eng.* **2001**, *127*, 67–75. [CrossRef]
6. Barnswell, K.D.; Dwyer, D.F. Two-year performance by evapotranspiration covers for municipal solid waste landfills in northwest Ohio. *Waste Manag.* **2012**, *32*, 2336–2341. [CrossRef] [PubMed]
7. Zhan, G.; Lattin, D.; Keller, J.; Milczarek, M. 20 Years of Evapotranspiration Cover Performance of the Leach Pads at Richmond Hill Mine. *Mine Water Environ.* **2019**, *38*, 402–409. [CrossRef]
8. Rahardjo, H.; Santoso, V.A.; Leong, E.C.; Ng, Y.S.; Hua, C.J. Performance of an Instrumented Slope Covered by a Capillary Barrier System. *J. Geotech. Geoenviron. Eng.* **2012**, *138*, 481–490. [CrossRef]
9. Zhan, L.T.; Li, G.Y.; Jiao, W.G.; Lan, J.W.; Chen, Y.M.; Shi, W. Performance of a compacted loess/gravel cover as a capillary barrier and landfill gas emissions controller in Northwest China. *Sci. Total Environ.* **2020**, *718*, 137195. [CrossRef]
10. Shaikh, J.; Bordoloi, S.; Yamsani, S.K.; Sekharan, S.; Rakesh, R.R.; Sarmah, A.K. Long-term hydraulic performance of landfill cover system in extreme humid region: Field monitoring and numerical approach. *Sci. Total Environ.* **2019**, *688*, 409–423. [CrossRef]
11. Yu, Y.; Zhao, X.; Shi, Y.; Ou, J. Design of a real-time overload monitoring system for bridges and roads based on structural response. *Measurement* **2013**, *46*, 345–352. [CrossRef]
12. Kraimeche, B. Performance of a GSM/GPRS System Subject to Interference. In Proceedings of the 2005 5th International Conference on Information Communications & Signal Processing, Bangkok, Thailand, 6–9 December 2005; pp. 249–252. [CrossRef]
13. *ASTM D 422*; Standard Test Methods for Particle-Size Analysis of Soils. ASTM International: West Conshohocken, PA, USA, 2007.
14. *ASTM D 4318*; Standard Test Methods for Liquid Limit, Plastic Limit, and Plasticity Index of Soils. ASTM International: West Conshohocken, PA, USA, 2017.
15. *ASTM D 698*; Standard Test Methods for Laboratory Compaction Characteristics of Soil Using Standard Effort [12,400 ft-lbf/ft3 (600 kN-m/m^3)]. ASTM International: West Conshohocken, PA, USA, 2021.
16. *ASTM D 5084*; Standard Test Methods for Measurement of Hydraulic Conductivity of Saturated Porous Materials Using a Flexible Wall Permeameter. ASTM International: West Conshohocken, PA, USA, 2016.

17. Simion, I.M.; Fortuna, M.E.; Bonoli, A.; Gavrilescu, M. Comparing environmental impacts of natural inert and recycled construction and demolition waste processing using LCA. *J. Environ. Eng. Landsc. Manag.* **2013**, *21*, 273–287. [CrossRef]
18. Chen, Z.; Feng, Q.; Yue, R.; Chen, Z.; Moselhi, O.; Soliman, A.; Hammad, A.; An, C. Construction, renovation, and demolition waste in landfill: A review of waste characteristics, environmental impacts, and mitigation measures. *Environ. Sci. Pollut. Res.* **2022**, *29*, 46509–46526. [CrossRef] [PubMed]
19. Vasvári, V. Calibration of tipping bucket rain gauges in the Graz urban research area. *Atmos. Res.* **2005**, *77*, 18–28. [CrossRef]
20. Soilmoisture. *Model 2725A Jet Fill Tensiometer Operating Instructions*; Soilmoisture Equipment Corp.: Santa Barbara, CA, USA, 1997.
21. Chen, R.; Liu, J.; Ng, C.W.W.; Qiao, J. Development of a new assembled-type tensiometer. *Rock Soil Mech.* **2013**, *34*, 3028–3032. [CrossRef]
22. Feng, W.Q.; Liu, Z.Y.; Tam, H.Y.; Yin, J.H. The pore water pressure sensor based on Sagnac interferometer with polarization-maintaining photonic crystal fiber for the geotechnical engineering. *Measurement* **2016**, *90*, 208–214. [CrossRef]
23. Wang, L.; Liu, S.; Shen, C.; Lu, Y. Laboratory test and modelling of gas pressure under geomembrane subjected to the rise of groundwater in plain reservoirs. *Geotext. Geomembr.* **2020**, *49*, 81–96. [CrossRef]
24. Shenzhen Statistics Bureau, NBS Survey Office in Shenzhen. *Shenzhen Statistical Yearbook*; China Statistics Press: Beijing, China, 2017.
25. Wu, M.; Lam, H.; Li, K. Characterization and indexing of heavy rainstorms in Hong Kong. *Meteorol. Appl.* **2015**, *22*, 25–36. [CrossRef]
26. Ng, C.W.; Liu, J.; Chen, R. Numerical Investigation on Gas Emission from Three Landfill Soil Covers under Dry Weather Conditions. *Vadose Zone J.* **2015**, *14*, vzj2014.12.0180. [CrossRef]
27. Avzalshoev, Z.; Uchimura, T. An experimental approach to investigating Quasi-Saturation using Darcy's Law. *Sustainability* **2023**, *15*, 10459. [CrossRef]
28. Yang, J.; Ma, X.Q. The benefit of landfill gas power generation to the reduction of the greenhouse gas emission. *Environ. Pollut. Control* **2006**, *28*, 461–464.
29. Piechota, G.; Hagmann, M.; Buczkowski, R. Removal and determination of trimethylsilanol from the landfill gas. *Bioresour. Technol.* **2012**, *103*, 16–20. [CrossRef] [PubMed]
30. Benson, C.; Abichou, T.; Albright, W.; Gee, G.; Roesler, A. Field Evaluation of Alternative Earthen Final Covers. *Int. J. Phytoremediat.* **2001**, *3*, 105–127. [CrossRef]
31. Baker, E.A.; Manenti, S.; Reali, A.; Sangalli, G.; Tamellini, L.; Todeschini, S. Combining noisy well data and expert knowledge in a Bayesian calibration of a flow model under uncertainties: An application to solute transport in the Ticino basin. *arXiv* **2022**, arXiv:2210.17388. [CrossRef]

Disclaimer/Publisher's Note: The statements, opinions and data contained in all publications are solely those of the individual author(s) and contributor(s) and not of MDPI and/or the editor(s). MDPI and/or the editor(s) disclaim responsibility for any injury to people or property resulting from any ideas, methods, instructions or products referred to in the content.

buildings

MDPI

Article

Evaluation Model of Distributed Photovoltaic Utilization in Urban Built-Up Area

Siyuan Chen [1,2], Zao Zhang [1,*], Cheng Wang [3,*], Lifeng Tan [4], Huanjie Liu [1], Hong Yuan [1], Rui Zhang [1] and Rui Hu [1]

[1] School of Architecture, Tianjin University, Tianjin 300384, China; liuhuanjie_arch@163.com (H.L.)
[2] China Northeast Architectural Design & Research Institute Co., Ltd., Shenzhen 518057, China
[3] School of Art, Tianjin Chengjian University, Tianjin 300384, China
[4] School of Architecture, Tianjin Chengjian University, Tianjin 300072, China; tanlf_arch@163.com
* Correspondence: zao.zhang@tju.edu.cn (Z.Z.); cheng_gsa@163.com (C.W.)

Abstract: Photovoltaic (PV) power generation is emerging as a key aspect of the global shift towards a more sustainable energy mix. Nevertheless, existing assessment models predominantly concentrate on predicting the overall capacity of PV power generation, often neglecting temporal dynamics. Drawing upon the urban energy substitution rate, utilization rate, and power supply stability, this study has devised a comprehensive evaluation model for the utilization of distributed photovoltaic systems (SUS). This model integrates the quantification of spatio-temporal features inherent in urban settings and buildings. Using Hohhot city as a case study, this study conducted simulations to analyze how the installation of PV systems affects the electricity consumption patterns across different land plots within the urban core. The study additionally examines how urban planning influences the adoption of PV power, taking into account both the timing of PV power usage and the stage of PV technology development. The evaluation model surpasses the constraints of current urban PV assessments, which primarily emphasize enhancing power generation potential without adequately quantifying supply–demand dynamics or spatial and temporal variations. This breakthrough significantly improves the precision and reliability of assessing the efficiency of distributed PV systems. Its implications extend widely to subsequent comprehensive evaluations of urban PV applications.

Keywords: distributed photovoltaic; evaluation model; sustainable energy; quantitative analysis

1. Introduction

Today, 80% of the world's GDP comes from 2% of the world's cities, but they consume nearly 75% of the world's resources [1]. Renewable energy has become a crucial issue that must be addressed in the national development process, as energy security is directly linked to economic growth [2,3].

As of 2018, the total global installed PV capacity has grown to 480 GW (from only 1 MW in 1979), accounting for approximately 2% of global energy consumption [4]. This demonstrates a rapid development trend. In the future, until 2050, PV power generation will continue to drive the structural transformation of renewable energy worldwide due to its abundant resource availability, substantial market potential, and cost competitiveness [5]. One of the most important forms of photovoltaic power generation is distributed photovoltaic power generation, which involves installing photovoltaic modules on the surfaces of buildings in cities to generate electricity [6].

However, regarding distributed photovoltaics in urban built-up areas, energy spatial planning and urban planning will both play crucial limiting roles [7]. The current indicators focus on enhancing the production potential of generation, but there are significant shortcomings in considering the energy supply-and-demand relationship, as well as spatial and temporal variations.

In the past, the assessment of urban PV potential focused on the installable area for PV systems and the power generation capacity in different urban areas. Firstly, evaluation indicators should be established. At present, several common evaluation indicators or standards are shown in Table 1. However, the established research indicators are relatively single, only consider the total amount of power generation/total amount of power consumption, ignoring the temporal sequence of PV power consumption and the stage of development.

Table 1. Main application indicators of current urban PV potential assessment work.

Indicators	Definition of Indicator	Index Source
PV area per capita	Area PV available roof area/area total population	IEA-PVPS [8]
Per capita installed PV capacity	Total installed PV capacity/total population of the region	Izquierdo, S. [9]
$SAFAR_n$	Photovoltaic available area on building exterior surface/building area	Jouri, K. [10]
Photovoltaic permeability	Regional total installed PV capacity/regional peak load	Zhao, B., Xiao, C.H., et al. [11]
PV cost/PV utilization	Regional photovoltaic installation cost and electricity sales revenue by weight comprehensive comparison	Cheng, M., Zhao, S.H., et al. [12]
Solar energy grading factor	Area available for photovoltaic power generation/area of land use	Sigrid Lindner of Ecofys [13]
RPVID	Area of photovoltaic available on the regional roof/area of land use	Zhang, H. [14]

In addition to the relevant indicators, the methodology for potential assessment is at the core of the research. The urban PV potential is usually assessed by giving a percentage of the building surface that is suitable for urban PV development (usually the roof utilization factor). In terms of the scope of the assessment, calculations are conducted for specific building types. For instance, Enongene et al. analyzed and modeled typical buildings to calculate the PV potential of urban areas in Nigeria [15]. There are also projections on a national scale. For example, Rosas-Flores et al. assessed the energy potential of Mexican city pools and rural households through large-scale grid-connected and interconnected PV systems [16]. Bodis et al. assessed the potential PV power generation for the entire European Union, estimating 680 TWh per year [17]. In terms of assessment calculation methods, accurate quantitative studies incorporating GIS systems have also been used by an increasing number of scholars for assessing urban PV potential [18–21]. Alaa Alhamwi et al. proposed the establishment of a GIS open-source platform for optimizing urban distributed energy systems [22]. Mariela Tapia et al. utilized GIS and associated building feature extraction algorithms to evaluate rooftop solar PV potential in various cities in Ecuador [23]. Jiang Liu et al. combined 3D building data with GIS to accurately assess the solar PV potential of rural roofs and facades [24]. Most of these potential assessment studies focus on a city scale or specific building types to maintain the high accuracy provided by the aforementioned methods. There are also uncertain predictions for intricate cities, such as the study by Diana Bernasconi and Giorgio Guariso on surface quantities and the potential of rooftop PV in complex cities. This study utilized morphological clustering methods instead of relying on remote sensing data for large-scale studies [25].

Most of the previous studies on PV potential have focused on estimating the capacity of PV power generation by predicting the ratio of PV power production to the current urban electricity consumption. However, the discussion focusing on the theoretical increase in the total power generated has also contributed to overly optimistic expectations. On the one hand, PV power output is greatly influenced by environmental factors. Without considering the impact of specific climatic conditions such as clouds and rain, PV power output typically peaks at midday and follows a clear normal distribution. As the primary source of urban energy consumption, the pattern of electricity load change is associated

with users' behavioral characteristics and exhibits variations based on the diverse functions of buildings. The two do not always show a similar trend of change due to the simultaneity of power output and consumption behavior. The excess PV power output cannot be effectively consumed immediately.

The primary solution to this problem is to depend on different energy storage technologies to maintain the balance between system supply and demand, thereby enhancing its overall stability. However, due to cost constraints, energy storage facilities cannot be widely used for commercial purposes in urban areas. This creates a significant technological bottleneck that hinders the utilization of photovoltaics [26]. The excess PV power can be transferred to other urban areas through grid-connected methods. However, in the future, when the city relies on PV energy as the primary source of electricity, the excess power cannot be transferred and consumed within the city. Therefore, it is necessary to propose a dynamic indicator to introduce the concept of PV consumption timing. This indicator, known as the PV Utilization Assessment Method (SUS), is based on the energy substitution rate, PV utilization rate, and PV utilization stability. It aims to comprehensively reflect the current status of PV application and integration in all regions of the city.

2. Materials and Methods

2.1. Research Materials

In the research of distributed PV in urban built-up areas, we selected the central city of Hohhot as the primary research object (Figure 1). Hohhot is classified as a second-tier region for solar energy sunshine resources in China, indicating better potential for PV development. It is considered a priority region for large-scale PV installations in the future. At the same time, Hohhot's three types of industrial structure ratios are very similar to those of China, and its urban function ratio can reflect the characteristics of China's urban economic development.



Figure 1. Location of the study area. (The map of China (left) was provided by Ministry of Natural Resources of China (Approval number: GS(2019)1673)).

Hohhot city in Inner Mongolia is located between 110°46′–112°10′ E and 40°51′–41°8′ N. It belongs to the primary solar resource distribution area of China. The total annual solar radiation is 6241.19 MJ/m^2 (about 1734 kWh/m^2), and the effective sunshine time is 2599.7 h. This indicates promising prospects for PV development. Meanwhile, in terms of electricity consumption load in Hohhot, the total area of various types of construction land

reached 329,554,000 square meters. The entire society in Hohhot used 33,084,270,000 kWh of electricity in 2022. The city mentioned above has a high electricity demand, coupled with abundant sunshine energy, that holds great potential for development [27].

The information on the urban built-up area of Hohhot was obtained from the planning data and relevant policies and regulations of the relevant departments. The building load information was calculated and summarized based on the meter readings provided by the state power department. In addition, all relevant data, including the comparison of photovoltaic technology characteristics, the land-cover status of centralized photovoltaic land, the data on protected areas and global sunshine radiation, the distribution of population density, per capita electricity consumption, meteorological data, and other information, were sourced from open data provided by countries and various global organizations.

2.2. Research Methods

2.2.1. Formulate SUS PV Potential Assessment Indicators

Energy Substitution Rate

The concept of energy substitution rate (ESR) considers the time sequence and actual situation of photovoltaic electricity consumption to reflect the degree of substitution of renewable energy for traditional electricity consumption. It measures the degree of spontaneous self-use after the integrated application of photovoltaic systems in various urban areas. Specifically, it can be divided into the overall energy substitution rate (ESR) and the hourly energy substitution rate (ESR_i) of regional plots, as shown in Equations (1) and (2).

The hourly energy substitution rate (ESR_i) is as follows:

$$ESR_i = \frac{Pe_i}{Load_i} \tag{1}$$

The overall energy substitution rate (ESR) is as follows:

$$ESR = \frac{\sum_i^n Pe_i}{\sum_i^n Load_i} \tag{2}$$

ESR_i is the hourly energy substitution rate of a block area in the city at the ith time. ESR is the overall energy substitution rate in the period from 0 to 23 points in a certain area of the city. Pe_i (kWh) is the consumption of photovoltaic power produced by a block in a city at the ith time. $Load_i$ (kWh) is the electricity consumption load at the ith moment of a block in a city. PV_i (kWh) is the photovoltaic power generation at the ith moment of a block in a city.

Photovoltaic Utilization Rate (PUR)

In addition to considering the replacement degree of traditional energy sources, the daily load curve patterns in various urban areas will change according to the different building functions (residential, office, commercial, etc.). In this paper, the photovoltaic utilization rate [28] (PUR, PV utilization ratio) is a supplement to the PV utilization ratio index (ESR), which is defined as the ratio of actual available photovoltaic power generation to the maximum allowable power generation under theoretical conditions within a specific operating period.

$$PUR = \frac{\sum_i^n Pe_i}{C \cdot T} \tag{3}$$

PUR is the photovoltaic utilization rate of a certain area in the city. C (kWh) is the installed photovoltaic capacity of a certain area in the city. T (h) is the theoretical working hours of PV module in a certain area of the city.

Standard Deviation of Hourly Replacement Rate

Photovoltaic power generation technology is significantly influenced by climate change factors. The stability of power supply output exhibits considerable volatility with

changes in weather and time. This instability is evident in the variation of the photovoltaic daily hourly replacement rate (ESR_i) over time. In this study, the standard deviation (Stdev) of the hourly PV replacement rate was used to reflect the power supply stability of each urban parcel after PV application, as shown in Formula (4):

$$\text{Stdev} = \sqrt{\frac{1}{n} \cdot \sum_{i}^{n} (ESR_i - R_i)^2} \quad (4)$$

Stdev is the standard deviation of the hourly PV replacement rate. R_i is the arithmetic average of daily hourly PV replacement rate. n is the number of power generation hours during the photovoltaic available period of the plot.

2.2.2. SUS PV Potential Assessment Model

The PV potential assessment of SUS mainly includes four steps: basic data collection, data processing, SUS index, and formulation of regional planning and adjustment strategies.

The basic data collection part includes load information data such as, daily load rate curves of various buildings and their peak load densities; urban model information data such as, the building floor area ratio, building density, and functional ratio of each building; and meteorological information data such as, annual sunshine hours and annual hourly sunshine radiation intensity.

Firstly, the corresponding hourly load and hourly power generation of each block are calculated. Based on this data, the ESR, PUR, and Stdev indexes of each block are calculated, respectively.

Finally, through the classification and analysis of the three indicators, the priority of photovoltaic development in each region is evaluated. In this way, it can be determined which land parcel's functional form is more suitable for the future energy structure transformation. Then, the location layout and urban planning can be adjusted for the unfavorable areas of photovoltaic development to optimize the overall utilization of photovoltaics in the city (Figure 2).

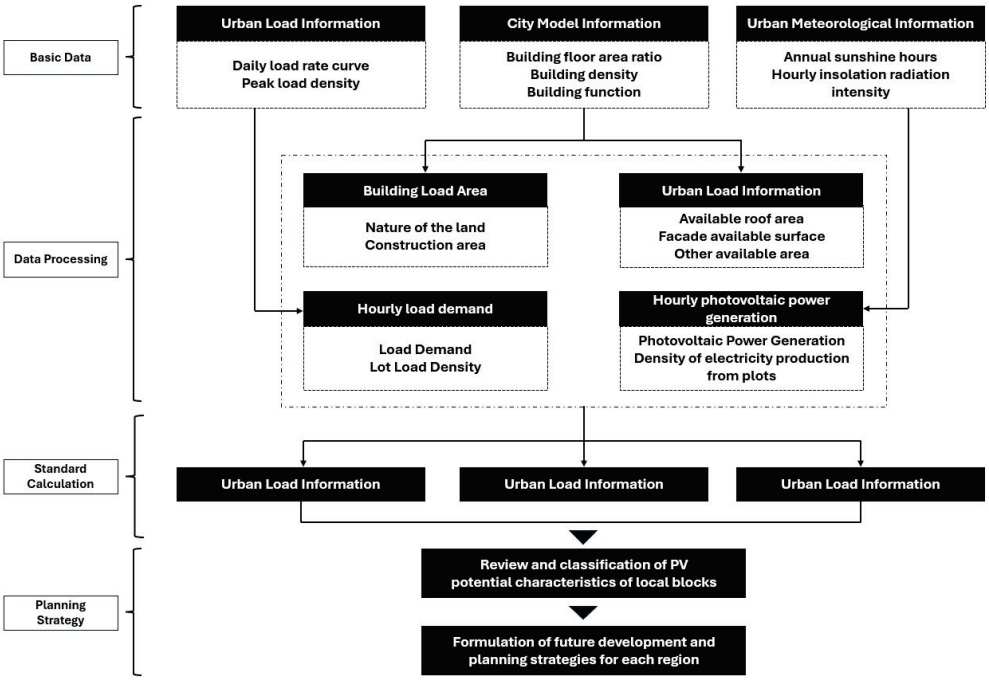


Figure 2. Framework diagram of SUS PV potential assessment procedure. Source: Drawn by the author.

2.2.3. Urban Basic Form Calculation

Based on the overall urban plan and zoning regulations of Hohhot City for 2020–2030, this paper examines the three indices of building function, building density, and floor area ratio for each block within the designated planning area.

Building Volume Rate for a Certain Area

The basic data was provided by the Hohhot Urban and Rural Planning and Design Institute. The overall plan (2020–2030) includes vector information such as land use boundaries, land use characteristics, and road network planning for various areas. The zoning plan includes Huhhot Hui District, Saihan District, Xincheng District, and Yuquan District. The controlled range of land use intensity (plot ratio) is as follows: A plot ratio >4.5, B plot ratio 3.5–4.5, C plot ratio 2.0–3.4, and D plot ratio <2.0 (Figure 3).



Figure 3. Plot ratio simulation results of each block. Source: Drawn by the author. Building density of a certain area.

Building density (BD) refers to the ratio between the total base area of a building and the land area of a plot within a certain range. It is an important indicator that reflects the building form information of different blocks. Since it is still in the planning stage, this paper adopts a calculation method for building density based on the characteristics of a typical urban plot layout. The building density of each block can be roughly calculated by Equation (5):

$$BD' = (1 - G - R - S - P) \times 100\% \quad (5)$$

BD′ means the preliminary estimated building density of a certain block. G is the green land rate of a place. R is the land use rate of a block of roads. S is the rate of supporting public construction land for a residential parcel. P is the percentage of ground parking land in a certain area.

Draw up the Number of Building Floors and Adjust Building Density

According to Equations (4) and (5), the building density (BD′) of each block can be preliminarily estimated. At the same time, according to the relationship between floor area

ratio and building density, the average floor number (F′) of each block building can be further calculated. To facilitate further prediction and analysis, we assume that buildings in each given land parcel have the same number of building floors and in turn adjust the preliminary calculated building density (BD′) results for each parcel. Finally, the proposed building density (BD) and the number of building floors (F) of each block can be used for calculation. The calculation process is shown in Equations (6)–(8).

$$f' = \frac{FAR}{BD'} \tag{6}$$

$$f = \text{roundup}(f' + 0.5) \tag{7}$$

$$BD = \frac{FAR}{f} \tag{8}$$

FAR is the volume ratio of a certain area. F′ means the average number of building floors preliminarily calculated for a certain block. BD′ is the building density preliminarily calculated for a certain block. f is the proposed number of building floors after adjustment of a certain block and is the result of f′ rounded up. BD is the proposed building density after the adjustment of a place block.

2.2.4. Calculation of Available PV Area

Available Rooftop PV Area

The rooftops of various buildings in the city are the primary locations for photovoltaic applications. For specific buildings, the available roof area can be determined through software simulation or manual screening. However, for a large range of urban areas, it is usually calculated by the rooftop photovoltaic utilization coefficient (Kr). The roof utilization coefficient refers to the research results of Zhang Hua in 2017 (Table 2). The available area of rooftop PV (Sr) of each building block can be calculated by Equation (9).

$$Sr = BD \times A \times Kr \tag{9}$$

Sr (m^2) is the available rooftop photovoltaic area of a block building. A (m^2) is the land area of a certain place. Kr is the rooftop photovoltaic utilization coefficient corresponding to a block type.

Table 2. PV roof utilization factor at a glance and the values taken in this paper [29].

Land Use Category		City Discount Rate	Neighborhood Discount Rate	Monomeric Discount Rate	Rooftop PV Utilization Factor (Kr)	Mean Value (Kr) Values
Residential buildings	Low-rise residential area	1	1	0.3–0.5	0.3–0.5	0.4
	Multi-story residential area	0.85–1	0.95–0.98	0.55–0.7	0.44–0.69	0.57
	High-rise residential area	0.9–1	0.7–0.95	0.4–0.6	0.25–0.57	0.41
Multi-story public buildings		1	1	0.7–0.85	0.7–0.85	0.78
High-rise public buildings		0.85–1	0.51–0.8	0.5–0.7	0.22–0.56	0.39
Single/low-rise industrial buildings		1	1	0.8–0.9	0.8–0.9	0.85

Assessment of Photos

According to the layout characteristics of general urban buildings, each block area can be divided into two layout modes, multi-block layout and single-family/tower layout, to simplify the complex changes in urban building forms, as shown in Figure 4. Among them, the former is applicable to the general land use properties such as low multi-story/small high-rise buildings with an average building level (F) below 10, while the latter is applicable to land use properties of individual buildings such as commercial buildings, wholesale markets, and high-rise tower layouts with an average building level (F) above 10.

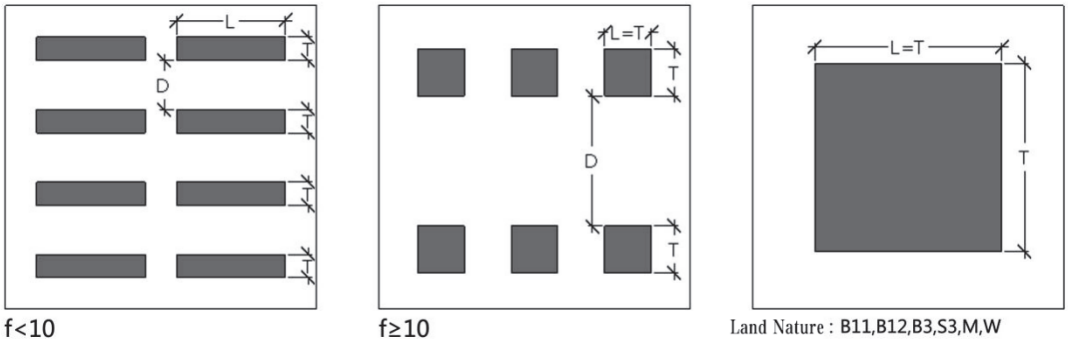


Figure 4. Simplified urban plot layout: Multi-block layout (**left**), tower layout (**middle**), single-family layout (**right**). Source: Drawn by the author.

The azimuth angle of the layout of each block is oriented towards the south to ensure that the south facade can receive maximum solar radiation. When each block has the same land use property, if multiple buildings are arranged in a row, each building has the same building depth (T). For energy conservation, single-family/tower layout buildings have the same building depth (T) and face width (L) to minimize their building size factor [30]. The values of general depth (T) and height (H) of reference buildings are determined from relevant codes, design regulations, and design experience values (Table 3). The area of the south facade of each block in the city can be roughly and statistically evaluated using Equations (10) and (11).

Table 3. In this paper, the depth (T) and height (h) of each type of building are taken from [31–33].

Nature of Land Use	Site Code	Floor Height h (m) Average	Depth of Entry T (m)
Administrative office land	A1	3.9	16
Cultural facilities land	A2	4.2	16
Educational and research land	A3	3.9	18
Primary school land	A33	3	10
Medical and health land	A5	3	24
Social welfare land	A6	3.6	16
Retail commercial land	B11	4.5	Single building layout T = L
Mixed commercial/hotel land	B11/B14	3.9	20
Mixed commercial/office land	B11/B2	3.9	16
Wholesale market land	B12	4.5	Single building layout T = L
Hotel land	B14	3.9	20
Business office land	B2	3.9	16
Recreation and sports land	B3	4.5	Single building layout T = L
Public utility business land	B4	3.9	18
Other service facilities land	B9	3.9	18
Industrial land	M1	6	Single building layout T = L
Residential land	R	3	15
Residential/commercial land	R/B11	3.2	15
Comprehensive transportation hub land	S3	4.5	Single building layout T = L
Storage and logistics land	W	6	Single building layout T = L

Statistics for the area of the south facade of multiple townhouses are calculated as follows:

$$Sn = f \cdot h \cdot \frac{Ar}{T} \quad (10)$$

Statistics for the area of the south facade of a single-family/tower layout are calculated as follows:

$$Sn = f \cdot h \cdot \sqrt{Ar} \quad (11)$$

Sn (m^2) is the statistical value of the south elevation area of a block. f is the number of proposed building floors for a certain block. h (m) is the general building height selected

according to the nature of land. Ar (m^2) is the roof area/floor area. T (m) is the general building depth selected according to the nature of land use.

Describe the window reduction coefficient (Kf) of the facade and the shadow reduction coefficient (Ks) of the facade. That is, the photovoltaic available area (Sf) of the south facade of each block can be expressed as follows:

$$Sf = Sn \cdot Kf \cdot Ks \tag{12}$$

For the value of Kf, we ignored the influence of shadow occlusion caused by the changes in the concave and convex shape of building facades, such as shading and projection, and calculated it only with the area ratio of window to wall (100%—window–wall area ratio). In combination with relevant codes [34], the value of Kf can be set as 0.55 for general buildings and as 1 for commercial buildings (B11). However, for general commercial building plots (B11) or mixed plots including commercial functions (B11/B14, B11/B2, R/B11), the first 1–2 floors of commercial building parts are usually not suitable for photovoltaic module installation due to their extremely high commercial value and should be excluded in the assessment of photovoltaic available facade area. In other words, the value of the proposed building floor (F) in each commercial and mixed parcel containing commerce in Equations (10) and (11) shall be considered by subtracting 1–2 floors.

As for the value of Ks, according to the standard, the sunshine duration of 6 h during the winter solstice should be guaranteed [35]. Therefore, in this paper, the elevation shadow reduction coefficient (Ks) of the multi-block layout was calculated at the most unfavorable time point (9:00 a.m. on the winter solstice). As shown in Figure 5, the ratio of photovoltaic available facade area to facade area (Ks) can be expressed as AB/AC and can also be expressed as C′c/C′o, according to the similar triangle theorem. The detailed calculation process is shown in Equations (13)–(16).

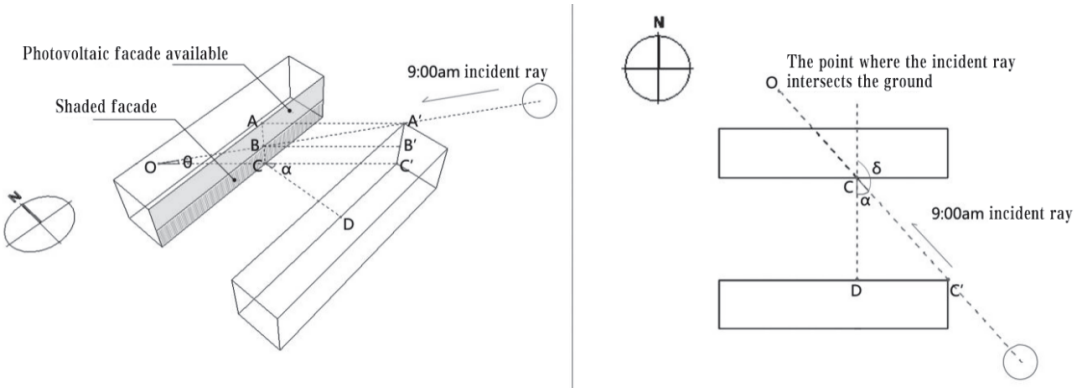


Figure 5. Calculation of the shadow reduction coefficient Ks of the multi-block layout facade. Source: Drawn by the author.

The Ks calculation process of multi-building row layout is determined as follows [35]:

$$Ks = \frac{AB}{AC} = \frac{A'B'}{A'C'} = \frac{B'B}{C'O} = \frac{C'C}{C'O} \tag{13}$$

$$C'C = \frac{CD}{\cos(180^\circ - \delta)} = \frac{L0 \cdot h \cdot f}{\cos(180^\circ - \delta)} \tag{14}$$

$$C'O = \frac{A'C'}{\tan\theta} = \frac{h \cdot f}{\tan\theta} \tag{15}$$

By substituting Equations (14) and (15) into Equation (13), we can get the following:

$$Ks = \frac{L0 \cdot \tan\theta}{\cos(180^\circ - \delta)} \quad (16)$$

Ks is the shadow reduction coefficient of the south-central facade of a multi-block layout. L0 is the reference sunshine spacing coefficient. h (m) is the general building height selected according to the nature of the land. f is the number of proposed building floors. δ means the azimuth angle of the sun at a certain time. θ is the height angle of the sun at a certain time.

At the same time, it is known that the sunshine spacing coefficient (L0) of Hohhot City is 1.73 (2 h on a major cold day) [36], the sun azimuth angle (δ) is 138.19° at 9:00 a.m. on the winter solstice, and the sun altitude angle (θ) is 13.34° (calculated according to the method in the literature [37]). By substituting Equations (5)–(15), we can calculate that the value of the facade shadow reduction coefficient (Ks) for the multi-building row layout in Hohhot is 0.55.

Assessment of Photovoltaic Available Area of a Parking Lot Surface

Approximately 10% of the land area of the parking lot and 20% of the canopy area cannot be utilized for photovoltaic installation. Finally, the available photovoltaic area of various parking lots can be expressed by Equation (17). The calculation results are shown in Figure 6.

$$St = 0.72 \cdot A \cdot P \quad (17)$$

St (m^2) is photovoltaic available area of a parking lot. P is the rate of ground parking land, assuming that the social parking lot and bus station are 100%.



Figure 6. Total available PV area of various blocks in Hohhot (roof, south facade, and ground parking area). Source: Drawn by the author.

2.2.5. Evaluation of Hourly Photovoltaic Power Generation

Under the condition that the available PV area of each block in the city is known, we can evaluate and calculate the hourly electricity production of each area. Considering the feasibility of urban distributed photovoltaic installations in the future, this paper selects a relatively common and cost-effective polysilicon solar cell module (with an average photoelectric conversion efficiency of about 16%) for calculation. It is also assumed that the roofs, facades, and ground parking areas of block buildings around the city are all

installed with a relatively common tilt, and photovoltaic applications are carried out in a south-facing arrangement. The optimal tilt angle (β) of a photovoltaic installation is 37.78° (latitude 40.78° for Hohhot) according to the relevant provisions of the grid connection system. This is calculated by subtracting 3 from the local latitude, as specified in the design specification of a photovoltaic power station.

In terms of statistical capacity per unit area (Cp) [38], we consulted the relevant specification for horizontal photovoltaic installations (roofs, various ground parking areas) and photovoltaic facade installations. We selected two distinct points in time during the year that represent the most unfavorable conditions to assess the spacing of photovoltaic modules, photovoltaic coverage, and capacity per unit area for each installation type.

The statistics of installed capacity per unit area can be calculated by determining the ratio between the projected area of PV modules and the available area of PV, that is, the PV coverage rate (Pr). This paper briefly describes the indicator as the ratio between the PV module projection length and the PV array spacing, as illustrated in Figures 7 and 8. The PV coverage of the horizontal plane and elevation can be calculated by referring to Equations (13)–(16). After substituting the local parameters in Hohhot, (at 9:00 on the winter solstice, the sun's altitude angle θ = 13.34° and the sun's azimuth angle δ = 138.19°; at 12:00 on the summer solstice, the solar altitude angle θ = 72.62°, and the solar azimuth angle δ = 180°), it can be determined that the photovoltaic coverage rate of the horizontal plane is 75.4% and the photovoltaic coverage rate of the facade is 19.5%. According to Equations (18) and (19), the installed capacity per unit area of the horizontal plane (Cph) in Hohhot is 158 W/m^2, and the installed capacity per unit area of the facade (Cpv) is 53 W/m^2.

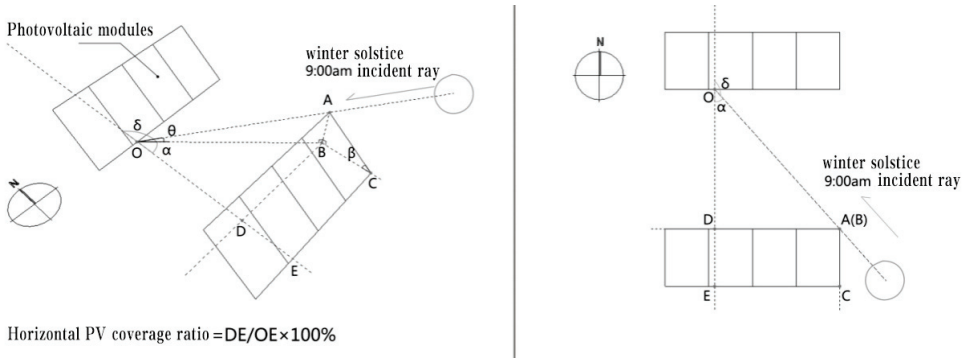


Figure 7. Calculation of the PV coverage when installed on an inclined horizontal plane. Source: Drawn by the author.

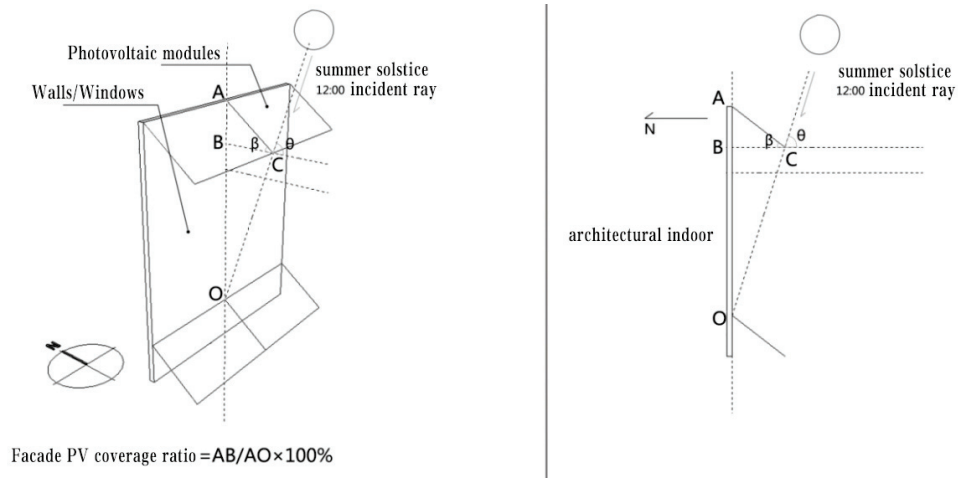


Figure 8. Calculation of the PV coverage when installed on a tilted facade. Source: Drawn by the author.

The installed capacity per unit area of the horizontal plane is as follows [35]:

$$Cph = \frac{Pw \cdot Pr}{Ap \cdot \cos\beta} \quad (18)$$

The installed capacity per unit area of facade plane is determined by the following:

$$Cpv = \frac{Pw \cdot Pr}{Ap \cdot \sin\beta} \quad (19)$$

Cph (W/m^2) is the estimated installed capacity per unit area of the horizontal plane of the proposed area. Cpv (W/m^2) is the estimated installed capacity per unit area of the proposed area facade. Pw (Wp) means the peak power (rated power) of the selected PV module. Pr is the PV coverage rate of the PV module installation area. Ap (m^2) is the area of the selected PV module. **β** is the best angle selected for photovoltaic module installation (37.78° in Hohhot).

3. Results and Discussion

3.1. Hourly Electricity Generation Calculation

After determining the installed capacity per unit area of the horizontal plane and facade, we can proceed to calculate the hourly power generation per unit area of photovoltaic panels. Firstly, the hourly meteorological forecast data for Hohhot City from 0:00 on 1 January 2019 to 23:00 on 31 December 2019 was selected from EnergyPlus. Then, we combined the SAM (System Advisor Model) PV Model analysis software (2015.1.30) provided by the United States National Renewable Energy Laboratory (NREL) to analyze the variation in hourly PV output power per unit area on the horizontal plane and facade in Hohhot city throughout the year (Figure 9).

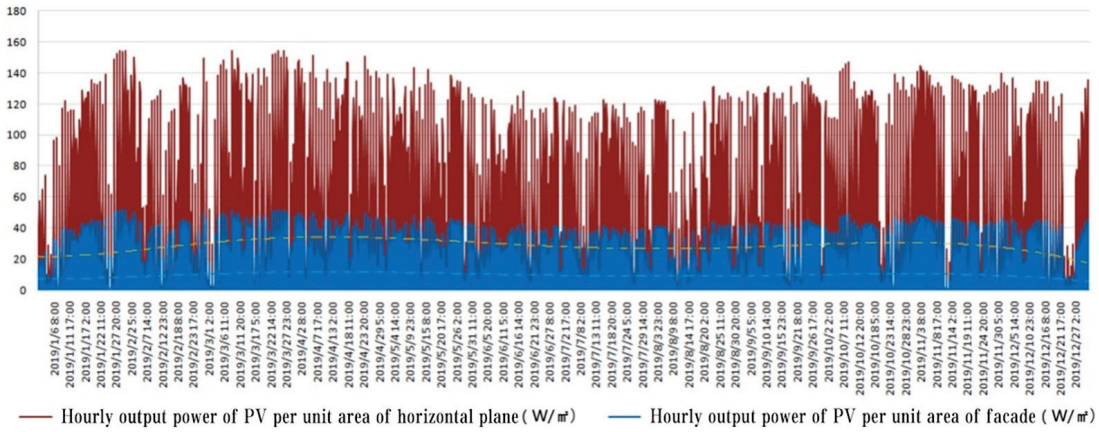


Figure 9. Annual hourly PV output per unit area of horizontal plane and facade of Hohhot. Source: exported by the author according to the analysis result of SAM.

The results indicate that the overall variation throughout the year remains stable, with a slight increase in photovoltaic electricity production observed during the periods from March to May and September to November. By utilizing SPSS software (26.0), we conducted k-means cluster analysis on the hourly PV output per unit area of Hohhot City throughout the year on a daily basis. This analysis helped us categorize the days with similar characteristics in terms of hourly PV output fluctuations. With this clustering (K = 10), we obtained a 10-category clustering result (as shown in Figure 10, arranged in descending order of occurrence days).

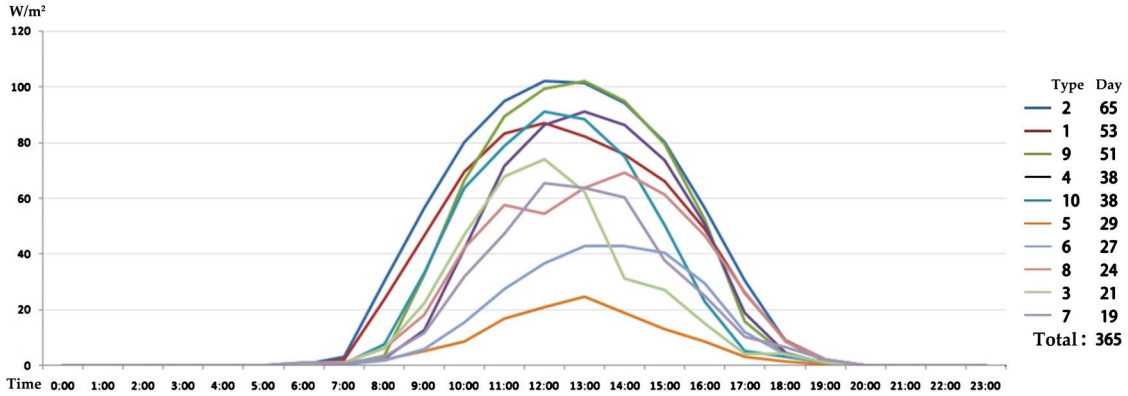
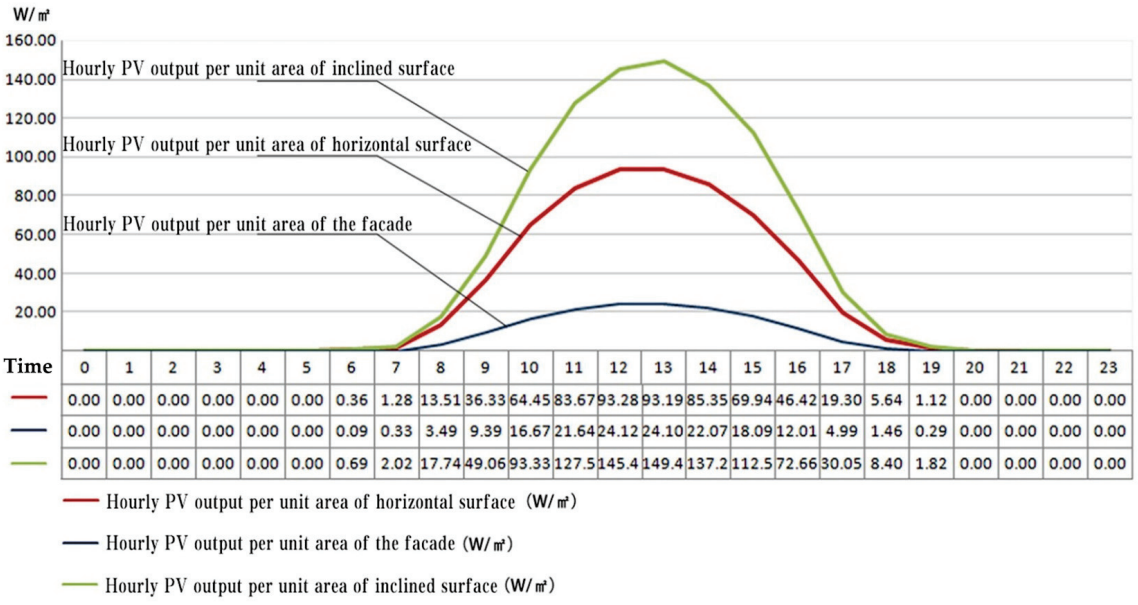


Figure 10. Classification results of annual hourly photovoltaic output changes per unit area of horizontal plane (clustering center). Source: Drawn by the author.

Categories 5, 6, 8, 3, and 7 are heavily affected by weather factors such as overcast rain, and their hourly photovoltaic power generation decreases in different periods. On the other hand, categories 2, 1, 9, 4, and 10 represent typical hourly photovoltaic power generation conditions on sunny days, with power generation being less affected by the weather. The average value of PV power output per unit area at each time point of these five types of curves is used as the standard hourly PV power output per unit area per day curve developed in this paper to reflect the local situation throughout the year (refer to Figure 11 for the results). Then, based on the installed capacity per unit area and the available PV area of the roof, facade, and ground parking area of each block, the total installed PV capacity, the total hourly PV power generation, and the hourly PV power generation density of each block can be calculated, as shown in Equations (20)–(22).



Time	0	1	2	3	4	5	6	7	8	9	10	11	12	13	14	15	16	17	18	19	20	21	22	23
	0.00	0.00	0.00	0.00	0.00	0.00	0.36	1.28	13.51	36.33	64.45	83.67	93.28	93.19	85.35	69.94	46.42	19.30	5.64	1.12	0.00	0.00	0.00	0.00
	0.00	0.00	0.00	0.00	0.00	0.00	0.09	0.33	3.49	9.39	16.67	21.64	24.12	24.10	22.07	18.09	12.01	4.99	1.46	0.29	0.00	0.00	0.00	0.00
	0.00	0.00	0.00	0.00	0.00	0.00	0.69	2.02	17.74	49.06	93.33	127.5	145.4	149.4	137.2	112.5	72.66	30.05	8.40	1.82	0.00	0.00	0.00	0.00

Figure 11. Hourly output power curve of standard daily PV per unit area used in this paper. Source: Drawn by the author.

The assessment of total installed PV capacity of each block is performed as follows:

$$C = Sr \cdot Cph + Sf \cdot Cpv + St \cdot Cph \quad (20)$$

The assessment of hourly photovoltaic power generation in various blocks is performed as follows:

$$PV_i = \frac{Sr \cdot Oph_i + Sf \cdot Opv_i + St \cdot Oph_i}{1000} \quad (21)$$

The assessment of hourly photovoltaic power generation density in various blocks is performed as follows:

$$PVd_i = \frac{1000 \cdot PV_i}{A} \quad (22)$$

C (W) is the total installed photovoltaic capacity of a certain block. Cph (W/m^2) is the estimated installed capacity per unit area of the horizontal plane of the proposed area. Cpv (W/m^2) is the estimated installed capacity per unit area of the proposed area façade.

Sr (m^2) is the available rooftop photovoltaic area. Sf (m^2) is the photovoltaic available area for a block building facade (south). St (m^2) is the photovoltaic available area of a block of ground parking area. PV_i (kWh) is the photovoltaic power generation of a certain area at the ith moment. Oph_i (W/m^2) is the photovoltaic output power per unit area of the horizontal plane at the ith time. Opv_i (W/m^2) is the photovoltaic output power per unit area of the facade at the ith time. PVd_i (Wh/m^2) is the photovoltaic power generation density at the ith moment.

3.2. Hourly Electricity Load Calculation

3.2.1. Load Density Index Method

In this paper, the power load forecasting method recommended in the Urban Power Planning Code [39], known as the load density index method (also referred to as the power per unit area method), is utilized to depict the electricity consumption of different buildings in the city. According to a survey conducted in cities of various sizes, focusing on urban planning and development, population planning, and the growth of residents' income levels, this method utilizes the general peak load power per unit area (W/m^2 or kW/km^2), known as the load density index [40], to assess the urban load level. This provides a reference for the power supply capacity configuration in this area. At the same time, since this method directly reflects the power load situation by the product of the building area or regional occupation area and load density index (Equation (23)), it is easier to effectively combine with the GIS geographic information system in terms of operation. This allows for a quick realization of the assessment of power load for various urban buildings.

In order to conduct hourly load assessments of different buildings in the city, this paper introduces the concept of hourly load rate (Lr_i) and the daily hourly load rate curve, drawing on the idea of power grid load rate. This approach aims to illustrate the variations in hourly load magnitude across different buildings. Finally, this paper provides a brief evaluation of the hourly power load of blocks in Hohhot City using two indices: load density and hourly load rate, as shown in Equation (24).

$$P_C = Ld \cdot A_{built} = Ld \cdot FAR \cdot A \quad (23)$$

$$Load_i = Lr_i \cdot Ld \cdot A_{built} \quad (24)$$

P_C (kW) is the peak load power (active power) of each building. Ld (W/m^2) is the load density of each building. A_{built} (m^2) is the building area. FAR is the floor area ratio of each block. A (m^2) is the land area of a certain place. $Load_i$ (kWh) is the power load at the ith moment of each block. Lr_i is the load rate at the ith moment of each block.

3.2.2. Load Density Index

The load density index is typically utilized to predict the power supply capacity configuration of different blocks, and its value also indicates the peak load of a block. In this paper, the proposed values of the load density index for various land uses are shown in Table 4.

Table 4. Partial land load density indicators selected in this paper [41–43].

Nature of the Land	Coding	Average Load Density <Ld> (W/m^2)	Simultaneous Factor (Kt)	Demand Factor (Kd)	Proposed Load Density Ld (W/m^2)
Residential land	R	55.00	0.95	0.43	22.09
Public administration and public service	A	74.44	0.98	0.75	54.44
Retail commercial land	B11	96.00	0.98	0.85	79.56
Wholesale market land	B12	62.50	0.98	0.85	51.80
Land for catering industry	B13	100.00	0.98	0.85	82.88
Land for the hotel	B14	70.00	0.98	0.85	58.01
Commercial office land	B2	81.00	0.98	0.85	67.13
Category I industry	M1	53.71	0.97	0.35	18.24
Category II industry	M2	59.43	0.97	0.38	21.62
Category III Industry	M3	74.00	0.97	0.43	30.51
Logistics and storage land	W	24.60	0.95	0.38	8.76
Municipal utility facilities	U	42.20	0.95	0.38	15.03
Green land and square land	G	2.00	0.95	0.75	1.43

Data Source: collated and calculated by the author according to relevant literature.

3.2.3. Daily Hourly Load Rate Curve

Analyzing the electricity load curves of various sections provided by Hohhot National Grid, we utilized SPSS software to classify the daily hourly load rate curves of 290 land samples based on the land use characteristics. Subsequently, we analyzed the clustering results to extract the most representative daily load rate curves of different land use types. These representative curves were then considered the typical daily load rate curves proposed in this paper (Figure 12).

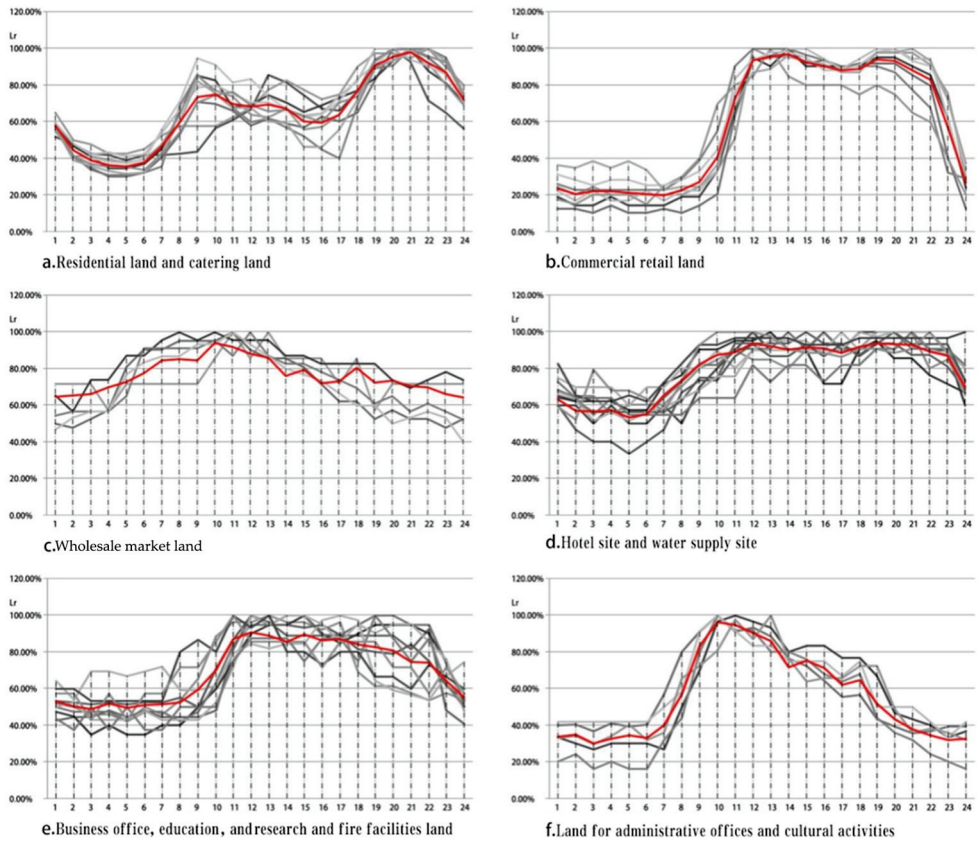


Figure 12. *Cont.*

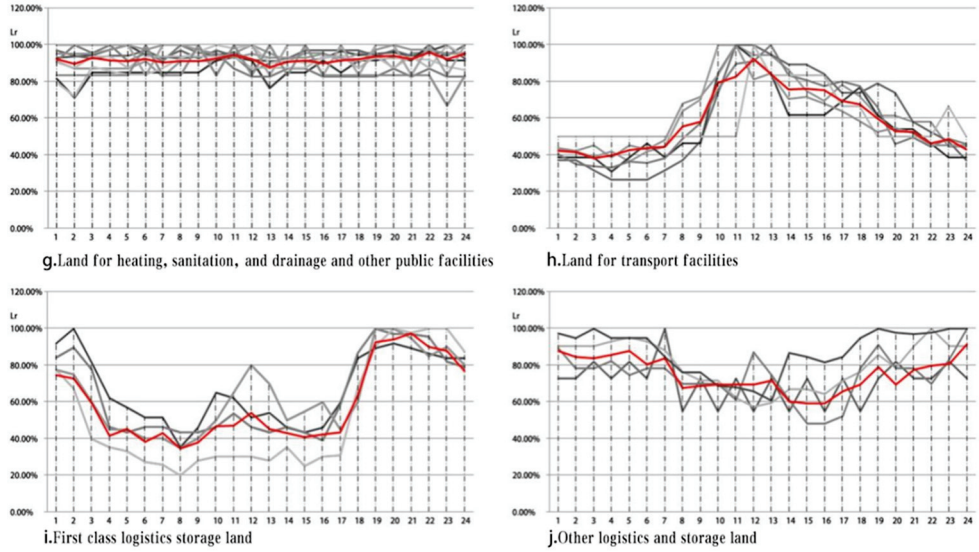


Figure 12. Daily load rate curve of each civil building block proposed in this paper (red): (**a**) Residential land and catering land; (**b**) Commercial retail land; (**c**) Wholesale market land; (**d**) Hotel site and water supply site; (**e**) Business office, education, and research and fire facilities land; (**f**) Land for administrative offices and cultural activities; (**g**) Land for heating, sanitation, and drainage and other public facilities; (**h**) Land for transport facilities; (**i**) First class logistics storage land; (**j**) Other logistics and storage land. Data source: Drawn by the author according to the results of SPSS cluster analysis.

3.2.4. Hourly Load Assessment for Mixed-Function Plots

In addition to the properties of all kinds of single-function land use, there are also various mixed-use plots in the city. These plots do not have a dominant single building function; instead, they showcase a variety of building functions coexisting. The mixed-function plot mainly combines horizontal and comprehensive functions. On a smaller scale (single building), it is primarily a combination of vertical and temporal dimensions. On a block scale, all four hybrids can be achieved.

Therefore, this paper selected 12 mixed commercial and other functional plots in Hohhot City and analyzed the proportion of the floor area of their respective commercial parts (Figure 13). The results show that most businesses account for between 20% and 40%. In order to facilitate the assessment of potential, this paper adopts the proportion of 30% commercial buildings as the standardized metric for all mixed-use plots. This means that the ratio of commercial to other building functional areas is 3:7. The peak load density and hourly daily load rate of all mixed-use plots are then calculated based on this standard. The peak load density values are B11/R: 39.67 W/m^2, B11/B14: 61.47 W/m^2, B11/B2: 65.72 W/m^2.

It is important to note that this article has established an ideal standard curve for photovoltaic power generation, depicting the hourly output per unit area. The results are derived from a year-long simulation of photovoltaic hourly output over 365 days. The analysis includes the calculation of the similarity to the average output power over 245 days, specifically focusing on the period from 6 to 7 p.m. Therefore, in the three indicators of daytime photovoltaic replacement rate (ESRd), photovoltaic utilization rate (PUR), and standard deviation of hourly replacement rate (Stdev), this paper uses a 13-hour period as the standard for calculation. The hourly PV power generation of each block is calculated based on the assessment results of the available PV area of each block and the proposed hourly PV power output curve per unit area of the standard daily area (Figure 12). The hourly power load of each block is determined by the proposed curve of hourly load rate for each functional building and the proposed index of load density for each functional building (Table 4), which is calculated using Equation (24). Then, according to Equations (1)–(3), the three indicators of ESRd, PUR, and Stdev of each block can be calculated, as shown in Figures 14–16.

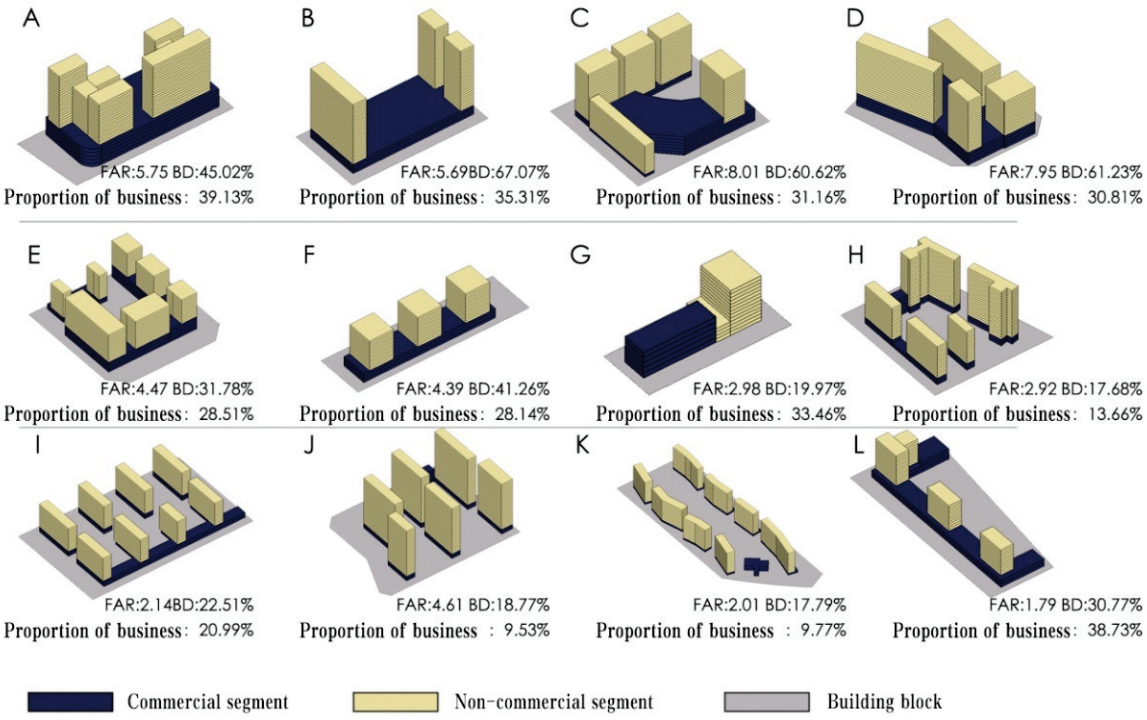


Figure 13. (**A**–**L**) Commercial area proportion of 12 commercial and other functional mixed plots selected in this paper: Source: Drawn by the author.



Figure 14. Daytime photovoltaic replacement rate (ESRd) of blocks in Hohhot.



Figure 15. Photovoltaic utilization rate of various blocks in Hohhot (PUR).



Figure 16. Standard deviation of inter-day displacement rate (Stdev) of blocks in Hohhot.

From the perspective of PV installation potential, the total area of suitable land for PV installation in all types of construction land in Hohhot is 1898.18 million square meters, accounting for 57.6% of the total construction land area. The total available rooftop PV area is 604,447,647 square meters, with an installed capacity of 95,507,028 kW. The total available PV area on the south elevation is 249,144,454 square meters, with an installed capacity of 132,046 kW. The total available PV area in the ground parking area is 49,499,580 square meters, with a total installed PV capacity of 78,203,034 kW. The total installed PV capacity in the city is about 10,464 MW. According to the typical daily hourly PV power generation, the theoretical average daily power generation can reach 44,015,000 kWh when tilt installation is adopted, accounting for approximately 73.7% of the daily electricity consumption of the entire society.

In terms of total photovoltaic power generation, Hohhot city presents optimistic development prospects due to its excellent solar radiation resources. In this paper, the average daytime PV replacement rate for all types of industrial sites is 82.9%, based on the daytime PV replacement rate (ESRd). This reflects the application of PV to replace traditional energy sources during off-peak production periods in all types of plants, even when there is excess power output. After considering the hourly electricity usage per unit of land for PV generation, the actual daily shipments in the city amount to 31,281 million kWh, representing approximately 52.4% of the total electricity consumption (citywide PV replacement rate). In other words, around 28.9% of the PV generation is theoretically wasted due to mis-match with the electricity load, which is equivalent to an indirect loss of 12,734 million kWh of electricity output per day.

The stability of hourly photovoltaic power supply is determined by the standard deviation of the hourly photovoltaic replacement rate (Stdev). Spatial quantification of photovoltaic energy using urban data is becoming an important element of future smart cities and sustainable development. On the whole, the average Stdev of the city is 23.8%, which indicates relative stability in terms of the overall variability within the city. The average Stdev level of all types of industrial land is the highest at 38.9%, indicating significant instability. Residential and office space occupancy rates are relatively stable at 21.8% and 15.9%, respectively. The most stable type of land is commercial land, with an average Stdev of 8.8%. The main reason is that the land has a high load density, and the impact of photovoltaic power is not significant. Even after the implementation of photovoltaic systems, urban distribution networks still need to maintain a high level of capacity allocation and power supply to ensure reliable electricity distribution.

3.3. Cluster Analysis of Power Characteristic Laws of Different Plots

In order to summarize the evolving patterns of daily power characteristics following the implementation of PV power generation at various sites, this study conducted a cluster analysis of 5023 plots in the city using three indicators: daytime PV replacement rate, PV utilization rate, and PV utilization stability (Table 5). Additionally, a regression analysis was carried out to examine the relationship between each indicator and the floor area ratio (FAR) (Figure 17).

Table 5. Cluster analysis of daily power characteristics after PV installation.

Category	Center of Clustering			Major Building Features and Their Corresponding Floor Area Ratio Ranges
	ESRd/%	PUR/%	Stdev/%	
1	0.00	0.00	0.00	Cultural relics, monuments, religious facilities, special sites, various types of plazas, green spaces, water bodies, and other areas where photovoltaic installation is not feasible
2	88.52	1.20	24.79	Various types of social car parks
3	79.67	5.12	37.01	Primary and secondary schools (0.8–1.19), logistics warehouses (0.8)
4	79.25	11.43	40.27	Executive offices (0.8–0.99), primary and secondary schools (1.2–2.2), various industrial buildings (0.8), integrated traffic hubs (0.86–1.49)
5	52.32	26.58	40.55	Executive offices (1.11–2.13), educational research (0.84–2.1), medical and health (0.81–1.47), residences (0.85–1.78), mixed residential/commercial (0.82–1.04), integrated traffic hubs (1.71–2.58)
6	29.31	28.66	25.70	Executive offices (2.19–3.21), educational research (2.12–3.82), medical and health (2.22–3.57), commerce (0.96–1.31), mixed commercial/offices (0.97–1.29), business offices (0.83–1.18), residences (1.82–2.94), mixed residential/commercial (1.44–1.84)
7	19.18	28.25	15.67	Executive offices (3.53–4.33), educational research (3.8–4.15), medical and health (3.65–4.38), commerce (1.42–1.76), mixed commercial/offices (1.34–2.32), business offices (1.2–2.1), residences (2.95–4.39), mixed residential/commercial (1.89–3.4)
8	10.73	28.80	7.59	Executive offices (5.92–5.98), educational research (4.24–4.38), commerce (1.93–3.8), mixed commercial/hotels (2.53–5.74), mixed commercial/offices (2.34–6.0), business offices (2.19–5.64), residences (5.74–5.94), mixed residential/commercial (3.32–5.81)

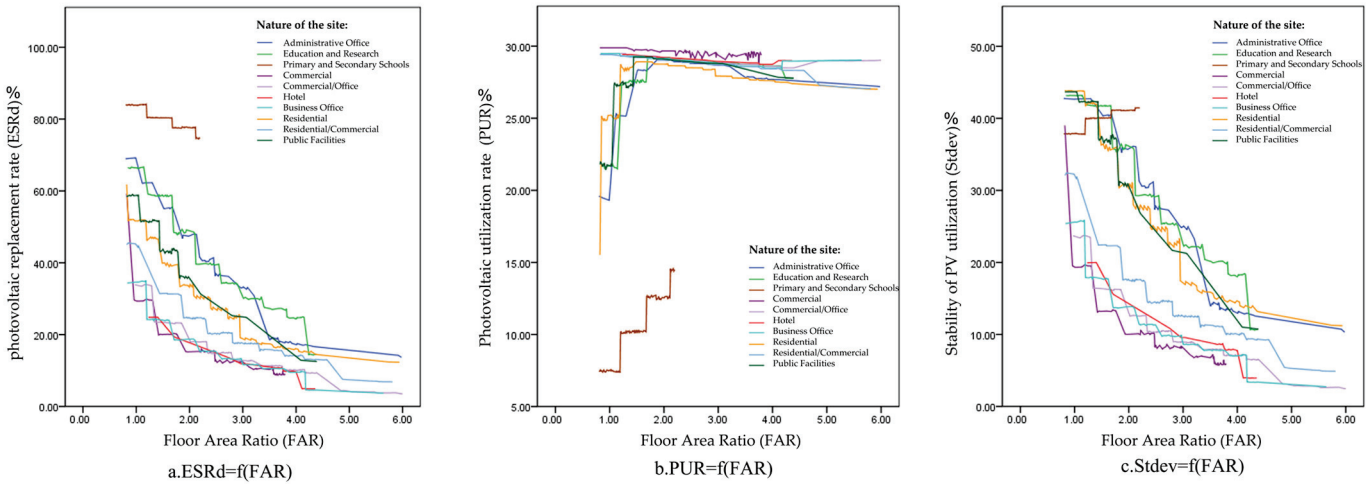


Figure 17. Regression analysis of ESRd = f(FAR), PUR = f(FAR), Stdev = f(FAR).

After considering the time sequence of PV power consumption, all urban land plots can be categorized into three main types: PV unsuitable land plots (category 1), PV excess power land plots (categories 2 to 4), and general PV application land plots (categories 5 to 8). Among them, the areas with excess PV power mainly include industrial areas, warehouses, car parks, primary and secondary schools, and other building plots with insufficient power consumption. The replacement rate of PV systems is excessively high, and the surplus

power cannot be consumed during the peak hours of PV power generation. As a result, the PV utilization rate is very low, and the replacement rate fluctuates significantly throughout the day (categories 3 and 4). The general PV application areas mainly include commercial, office, residential, and other civil buildings. Based on the results of the evaluation and analysis (Table 5, Figure 17), it is evident that the variation in electricity load demand due to differences in plot ratio will significantly influence the electricity consumption patterns following the installation of photovoltaic systems in each plot. Therefore, it is of great significance to enhance the overall PV potential of the city by effectively controlling the planning layout and plot ratio of each site.

As far as the stage of PV development is concerned, traditional fossil energy generation, mainly thermal power, will continue to dominate as a reliable energy source for an extended period. However, the current thermal turbines are generally characterized by slow start-up and shutdown, high minimum technical output requirements, lack of flexibility in system regulation, and rigidity in power scheduling. These limitations may pose challenges in meeting the future demands of renewable energy development. Considering its development goals, this paper takes the 40% daytime PV replacement rate as the best criterion to measure the proportion of PV power consumption in each urban area. During the daytime when PV energy is available, 40% of the load demand is supplied by PV in combination with a small amount of energy storage to ensure voltage stability. The remaining load demand is met by 40% of the minimum thermal power output and 20% from other renewable energy sources. As can be seen in Table 4, the daytime PV replacement rate in the areas of plot 5 and plot 6 has a better match with this criterion, with ESRd values of 52.32% and 29.31%, respectively. Meanwhile, it can be seen from Figure 17 that under different plot ratios, there is a theoretical maximum peak value of the PV utilization rate for each plot. However, due to the relatively low plot ratio of category 5, its economic return from PV systems is poor. At the same time, the stability of the power supply also reflects a significant disadvantage, with a Stdev value as high as 40.55%. This high variability is relatively unfavorable for regulating the thermal system, given the substantial demand of the grid connection. After a comprehensive comparison, the building plot ratio interval for each type of building will serve as the standard for the sixth type of land, which will be more favorable to the overall PV potential of Hohhot. The corresponding values of the functional plot ratios for each type of building in this category will become the primary focus for adjusting urban planning in the future. It can be further seen that various types of small high-rise (average number of floors 6–9) building forms in the city may be better suited to meet the needs of urban PV utilization and will likely become the primary spatial layout for future urban development. These building forms include residential buildings, administrative office buildings, and more.

In addition, as shown in Table 5, the PV replacement rate is high for all types of industrial land (Class 3 and 4) in the city, indicating a clear surplus of electricity output. The paper examines the impact of the demand coefficient, which indicates that not all power equipment is activated simultaneously. The power load is only represented by daily office, lighting, and other non-production loads. In fact, various types of industrial buildings require significant power loads during peak production hours. Typically, these power needs are met by specific power plants through dedicated lines to ensure a consistent power supply. However, photovoltaic power faces challenges in meeting these demands due to its inherent instability and intermittency characteristics. Hence, industrial plants situated far from other urban functions and centrally located in isolated patches may experience minimal actual benefits from PV applications.

In addition, due to the higher load density in commercial, hotel, business office, and other land areas in the city (categories 7, 8), the overall rate of photovoltaic replacement is low. According to this paper, various types of building functions need to adjust the volume ratio interval. The average volume ratio needs to be adjusted downward to 0.96–1.31 (for instance, in commercial buildings, the average number of floors is typically 2–3). Otherwise, the shape of the building will exceed the reasonable design range and be challenging to

realize. Therefore, it is difficult to realize the future urban development of the above area. Therefore, for future adjustments to urban planning in the aforementioned areas, more consideration should be given to facilitating the layout of neighborhoods or even the organic integration of these areas while ensuring that the normal operation of the city is not disrupted.

4. Conclusions

The strategic deployment of installed PV systems within built environments is paramount for driving future urban renewable energy structural transformations. Simply focusing on guiding PV planning and construction based on total power generation at a singular level cannot fully exploit the potential benefits of this approach. The urban distributed photovoltaic energy evaluation model introduced in this paper offers a more comprehensive integration of future energy needs with sustainable urban development. It lays the groundwork for incorporating Internet of Things and big data technologies, which are crucial for maximizing future urban energy potential. However, as this paper solely addresses the optimization of PV potential in Hohhot city concerning a single spatial layout issue of volume ratio adjustment, several limitations remain regarding parameter selection, data accuracy, and influencing factors. Future research should encompass a broader spectrum of practical social development issues, such as economic growth, urban planning, and industrial adaptations. This holistic approach will facilitate strategic planning of urban energy spatial layouts, fostering the transformation of photovoltaic power energy structures and advancing sustainable urbanization.

Author Contributions: Conceptualization, Z.Z.; methodology, S.C. and C.W.; software, S.C.; validation, L.T., H.L. and R.H.; date analysis, S.C. and Z.Z.; investigation, S.C. and C.W.; resources, S.C. and R.Z.; data curation, H.L. and H.Y.; writing-original draft preparation, S.C.; writing-review and editing, H.L., H.Y. and R.H.; visualization, Z.Z. and R.H.; supervision, C.W., H.Y. and R.Z.; project administration, L.T.; funding acquisition, L.T. and R.Z. All authors have read and agreed to the published version of the manuscript.

Funding: This work was supported by the National Natural Science Foundation of China (52078324); the National Natural Science Foundation of China (52078322); Tianjin University Graduate Students' Award Program for Outstanding Innovation in Arts and Sciences (A1-2022-005) and Tianjin Graduate Student Research Innovation Program (2022BKY093).

Data Availability Statement: The raw data supporting the conclusions of this article will be made available by the authors on request.

Conflicts of Interest: Author Siyuan Chen was employed by the company China Northeast Architectural Design & Research Institude Co., Ltd. The remaining authors declare that the research was conducted in the absence of any commercial or financial relationships that could be construed as a potential conflict of interest.

Nomenclature

Ar (m^2)	Roof area/floor area
Ap (m^2)	Area of selected PV module
A_{built} (m^2)	Building area
β	Best angle (37.78° in Hohhot)
BD′	Building density
BD	Proposed building density
Cph (W/m^2)	Installed capacity per unit area of the horizontal plane
Cpv (W/m^2)	Installed capacity per unit area of the facade
C (W)	Installed photovoltaic capacity
ESR_i	Hourly Energy Substitution Rate
ESR	Overall Energy Substitution Rate
FAR	Floor area ratio

F′	Average number of building floors
F/f	Proposed number of building floors
G	Green land rate
H (m)	Building height
Kf	Window reduction coefficient
Ks	Facade and shadow reduction coefficient
Kr	Rooftop photovoltaic utilization coefficient
Ld (W/m^2)	Load density of each building
$Load_i$ (kWh)	Power load at the ith moment
Lr_i	Load rate at the ith moment
L0	Reference sunshine spacing coefficient
N	Number of power generation hours
Oph_i (W/m^2)	Photovoltaic output power per unit area of the horizontal plane at the ith time
Opv_i (W/m^2)	Photovoltaic output power per unit area of the facade at the ith time
PUR	Photovoltaic utilization rate
Pw (Wp)	Peak power (rated power)
Pr	PV coverage rate
PV_i (kWh)	Photovoltaic power generation at the ith moment
PVd_i (Wh/m^2)	Photovoltaic power generation density at the ith moment
Pc (kW)	Peak load power (active power)
P	Percentage of ground parking land
Pe_i (kWh)	Consumption of photovoltaic power
PV_i (kWh)	Photovoltaic power generation
R	Land use rate
R_i	Arithmetic average of daily hourly PV replacement rate
Stdev	Standard deviation of hourly PV replacement rate
Sr (m^2)	Available rooftop photovoltaic area
Sf (m^2)	Available area for photovoltaic of a block building facade (south)
St (m^2)	Photovoltaic available area of a block of ground parking area
Sn (m^2)	Statistical value of the south elevation area
Sf	Photovoltaic available area
S	Rate of supporting public construction land
T (m)	Building depth
δ	Sun azimuth

References

1. UN-Habitat. *World Cities Report 2020: The Value of Sustainable Urbanization*; United Nations Human Settlements Programme: Nairobi, Kenya, 2020.
2. Kartal, G. The Effects of Positive and Negative Shocks in Energy Security on Economic Growth: Evidence from Asymmetric Causality Analysis for Turkey. *Econ. Comput. Econ. Cybern. Stud. Res.* **2022**, *56*, 223–240.
3. Yoon, J.; Joung, S. Environmental self-identity and purchasing ecofriendly products. *J. Logist. Inform. Serv. Sci.* **2021**, *8*, 82–99.
4. IRENA. *Future of Solar Photovoltaic: Deployment, Investment, Technology, Grid Integration and Socio-Economic Aspects (A Global Energy Transformation: Paper)*; International Renewable Energy Agency: Abu Dhabi, United Arab Emirates, 2019.
5. Root, L.; Perez, R. *Photovoltaic Covered Parking Lots: A Survey of Deployable Space in the Hudson River Valley, New York City, and Long Island, New York*; Atmospheric Sciences Research Center: Albany, NY, USA, 2006.
6. Xiong, Y.; Liu, X.; Ma, S. Analysis on application conditions of urban scale photovoltaic power generation in China. *Renew. Energy Resour.* **2012**, *30*, 123–126.
7. Manni, M.; Formolli, M.; Boccalatte, A.; Croce, S.; Desthieux, G.; Hachem-Vermette, C.; Kanters, J.; Ménézo, C.; Snow, M.; Thebault, M.; et al. Ten questions concerning planning and design strategies for solar neighborhoods. *Build. Environ.* **2023**, *246*, 110946. [CrossRef]
8. IEA. *PVPS Task VII, Potential for Building Integrated Photovoltaics*; International Energy Agency: Paris, France, 2002.
9. Izquierdo, S.; Rodrigues, M.; Fueyo, N. A Method for Estimating the Geographical Distribution of the Available Roof Surface Area for Large-Scale Photovoltaic Energy-Potential Evaluations. *Sol. Energy* **2008**, *82*, 929–939. [CrossRef]
10. Jouri, K. *Planning for Solar Buildings in Urban Environments an Analysis of the Design Process, Methods and Tools*; Department of Architecture and Built Environment, Faculty of Engineering LTH, Lund University: Lund, Sweden, 2015.
11. Zhao, B.; Xiao, C.; Xu, C. Analysis of absorptive capacity of distributed photovoltaic grid connection in regional distribution network based on permeability. *Electr. Power Syst.* **2017**, *21*, 111–117.

12. Cheng, M.; Zhao, S.; Wu, L. Comprehensive evaluation of urban photovoltaic power generation projects based on AHP-TOPSIS. *Electr. Power* **2016**, *49*, 171–175.
13. Sigrid Lindner of Ecofys. Solar Urban Planning Berlin [EB/OL]. Available online: http://www.pvupscale.org/IMG/pdf/Berlin.pdf (accessed on 10 May 2020).
14. Zhang, H. *Study on the Evaluation of Photovoltaic Utilization Potential of Urban Building Roofs*; Tianjin University: Tianjin, China, 2017.
15. Enongene, K.E.; Abanda, E.H.; Otene, I.J.J.; Obi, S.I.; Okafor, C. The potential of solar photovoltaic systems for residential homes in Lagos city of Nigeria. *J. Environ. Manag.* **2019**, *244*, 247–256. [CrossRef] [PubMed]
16. Rosas-Flores, J.A.; Zenon-Olvera, E.; Galvez, D.M. Potential energy saving in urban and rural households of Mexico with solar photovoltaic system using geographical information system. *Renew. Sustain. Energy Rev.* **2019**, *116*, 109412. [CrossRef]
17. Bodis, K.; Kougias, I.; Jager-Waldau, A.; Taylor, N.; Szabo, S. A high-resolution geospatial assessment of the rooftop solar photovoltaic potential in the European Union. *Renew. Sustain. Energy Rev.* **2019**, *114*, 109309. [CrossRef]
18. Verso, A.; Martin, A.; Amador, J.; Dominguez, J. GIS-based method to evaluate the photovoltaic potential in the urban environments: The particular case of Miraflores de la Sierra. *Sol. Energy* **2015**, *117*, 236–245. [CrossRef]
19. Saadaoui, H.; Ghennioui, A.; Ikken, B.; Rhinane, H.; Maanan, M. Using GIS and photogrammetry for assessing solar photovoltaic potential on Flat Roofs in urban area case of the city of Ben Guerir/Morocco. In Proceedings of the 5th International Conference on Geoinformation Science—GeoAdvances 2018, Casablanca, Morocco, 10–11 October 2018; Copernicus Publications: Göttingen, Germany, 2019; Volume XLII-4/W12, pp. 155–166.
20. Wang, L.Z.; Tan, H.W.; Ji, L.; Wang, L. A method for evaluating photovoltaic potential in China based on GIS platform[C]//IOP Conference Series: Earth and Environmental Science. *IOP Publ.* **2017**, *93*, 012056.
21. Kozlovas, P.; Gudzius, S.; Ciurlionis, J.; Jonaitis, A.; Konstantinaviciute, I.; Bobinaite, V. Assessment of technical and economic potential of urban rooftop solar photovoltaic systems in Lithuania. *Energies* **2023**, *16*, 5410. [CrossRef]
22. Alhamwi, A.; Medjroubi, W.; Vogt, T.; Agert, C. Development of a GIS-based platform for the allocation and optimisation of distributed storage in urban energy systems. *Appl. Energy* **2019**, *251*, 113360. [CrossRef]
23. Tapia, M.; Ramos, L.; Heinemann, D.; Zondervan, E. Power to the city: Assessing the rooftop solar photovoltaic potential in multiple cities of Ecuador. *Phys. Sci. Rev.* **2023**, *8*, 2285–2319. [CrossRef]
24. Liu, J.; Wu, Q.; Lin, Z.; Shi, H.; Wen, S.; Wu, Q.; Zhang, J.; Peng, C. A novel approach for assessing rooftop-and-facade solar photovoltaic potential in rural areas using three-dimensional (3D) building models constructed with GIS. *Energy* **2023**, *282*, 128920. [CrossRef]
25. Bernasconi, D.; Guariso, G. Rooftop PV: Potential and Impacts in a Complex Territory. *Energies* **2021**, *14*, 3687. [CrossRef]
26. Fu, R.; Timothy, R.; Robert, M. *2018 U.S. Utility—Scale Photovoltaics-Plus-Energy Storage System Costs Benchmark*; National Renewable Energy Laboratory: Oak Ridge, TN, USA, 2018.
27. Inner Mongolia Hohhot Bureau of Statistics. *2023 Hohhot City Statistical Yearbook [EB]*; Hohhot Bureau of Statistics: Huhehaote, China, 2023.
28. Andson, K.; Coddington, M.; Burman, K. *Interconnecting PV on New York City's Secondary Network Distribution System*; National Renwable Energy Laboratory: Golden, MO, USA, 2009.
29. Hua, Z. *Research on the Assessment of the Potential of Urban Building Rooftop Photovoltaic Utilization*; Tianjin University: Tianjin, China, 2017.
30. Ren, B. *Research on Low Energy Consumption Design Prototype of Multi-Storey Office Buildings in Cold Regions*; Tianjin University: Tianjin, China, 2014.
31. Hang, Z. *Zhejiang Province of Planning Bureau, Rules for Building Storey Height Control and Floor Area Ratio Index Calculation*; Hangzhou Municipal Planning Bureau: Hangzhou, China, 2010.
32. *GB50099-2011*; Ministry of Housing and Urban-Rural Construction of the People's Republic of China. Code for Design of Primary and Secondary Schools. Guangming Daily Press: Beijing, China, 2011.
33. *GB 51039-2014*; National Health and Family Planning Commission of the People's Republic of China. Code for Design of Polyclinic Buildings. China Planning Press: Beijing, China, 2014.
34. *GB50189-2015*; China Academy of Building Sciences. Design Standard for Energy Efficiency of Public Buildings. China Building Industry Press: Beijing, China, 2015.
35. *GB50797-2012*; China Electricity Council. Code for Design of Photovoltaic Power Station. China Planning Press: Beijing, China, 2012.
36. *GB50180-93*; Ministry of Housing and Urban Rural Development of the People's Republic of China. Code for Planning and Design of Urban Residential Areas. China Building Industry Press: Beijing, China, 2002.
37. Brito, M.; Freitas, S.; Guimar, E. The importance of facades for the solar PV potential of a Mediterranean city using LiDAR data. *Renew. Energy* **2017**, *111*, 85–94. [CrossRef]
38. *JGJ203-2010*; Ministry of Housing and Urban Rural Development of the People's Republic of China. Technical Code for Application of Solar PV System in Civil Buildings. China Construction Industry Press: Beijing, China, 2010.
39. *GB/T50293-2014*; Ministry of Housing and Urban Rural Development of the People's Republic of China. Code for Urban Power Planning. China Construction Industry Press: Beijing, China, 2014.
40. The General Institute of Electric Power Planning and Design. *Ministry of Electric Power Industry, Power System Design Manual*; China Electric Power Press: Beijing, China, 1998.

41. China Institute of Building Standards Design. *Technical Measures for National Civil Building Engineering Design: 2009 Edition, Electrical*; China Planning Press: Beijing, China, 2009.
42. Ye, X. *Research on Power Load Index of Ningbo Unit Construction Land, Urban Times, Collaborative Planning—2013 China Urban Planning Annual Conference*; China Urban Planning Society: Beijing, China, 2013.
43. Liu, D.; Zhu, Y.; Zhang, Q. Discussion on the Value of Load Index, Demand Coefficient and Synchronization Coefficient in Urban Power Planning. *Archit. Eng. Technol. Des.* **2014**, *10*, 16.

Disclaimer/Publisher's Note: The statements, opinions and data contained in all publications are solely those of the individual author(s) and contributor(s) and not of MDPI and/or the editor(s). MDPI and/or the editor(s) disclaim responsibility for any injury to people or property resulting from any ideas, methods, instructions or products referred to in the content.

buildings

MDPI

Article

Revitalizing Rural Landscapes: Applying Cultural Landscape Gene Theory for Sustainable Spatial Planning in Linpu Village

Shuhu Liu [1], Lin Wu [1], Chenlu Xiang [1] and Wenyuan Dai [2,*]

[1] Institute of Urban and Rural Planning, School of Architecture and Town and Country Planning, Fuzhou University, Fuzhou 350108, China; liushuhu@fzu.edu.cn (S.L.); 231520024@fzu.edu.cn (L.W.); 231520027@fzu.edu.cn (C.X.)
[2] Institute of Geography, School of Geographical Sciences, Fujian Normal University, Fuzhou 350117, China
* Correspondence: dwygeo@fjnu.edu.cn

Abstract: In the context of rapid urbanization, it is imperative to address the preservation and sustainable development of rural landscapes. This study introduces a novel framework using cultural landscape gene theory to enhance the landscape spatial pattern of Linpu Village, China. Employing a multi-method approach, including data collection and historical data analysis, GIS analysis, and field surveys, we analyze the village's landscape features and identify a well-preserved "one core, two wings" spatial configuration with diminishing accessibility from the center to the periphery. The study uncovers significant challenges to landscape coherence and legibility, including landscape element discontinuity, inadequate maintenance, and fragmented information. To address these issues, we propose optimization strategies aimed at revitalizing weakened cultural landscape genes, repairing disrupted elements, ensuring corridor integrity, and improving spatial organization. The extraction–construction–analysis–preservation model established in this research not only delivers a comprehensive analysis of Linpu's cultural landscape but also offers a scalable framework for preserving the ecological and cultural integrity of traditional villages. This study contributes to the practical implementation of sustainable landscape strategies, enhancing the ecological adaptability and resilience of rural environments in the face of urban encroachment.

Keywords: cultural landscape; sustainable development; human environment; livelihoods

1. Introduction

Traditional villages are vital custodians of cultural heritage, encapsulating the historical and architectural progression of societies worldwide [1]. These villages—from the ancient towns of Europe to the heritage settlements in Africa and the rural landscapes in Asia—are under increasing threat from rapid urbanization [2–4]. This phenomenon leads to the degradation of cultural landscapes and disrupts historical continuity, posing significant challenges to the sustainable development of traditional villages globally [5].

Historically, global preservation efforts have predominantly concentrated on tangible elements, such as architectural styles and the structural conservation of buildings [6]. However, these efforts often neglect the broader landscape structures and cultural contexts integral to the villages' identities [7]. This oversight can result in fragmented and sometimes ineffective conservation practices. Therefore, it is crucial to adopt a holistic approach that encompasses both the physical and cultural dimensions of these landscapes.

Cultural Landscape Genes of Traditional Settlements (CLGTS) provides a robust framework for analyzing and preserving the essence of traditional village landscapes [8]. This theory, which conceptualizes 'Cultural Landscape Genes' as the cultural, physical, and historical narratives embedded within traditional settlements, offers a way to maintain the identity and continuity of these landscapes [9]. By treating these 'genes'—comprising physical features like buildings and roads, cultural practices, and historical narratives—as components that define a landscape's character and resilience, landscape gene theory

enables a nuanced conservation strategy that preserves regional cultural attributes in an integrated and sustainable manner.

Despite advancements, cultural landscape gene theory faces critical research gaps. Firstly, its application in rural planning remains limited, with a significant need to integrate this theoretical framework into practical, scalable conservation strategies [10]. Secondly, the predominant qualitative nature of current analysis methods highlights a pressing need for systematic quantitative approaches [11]. Thirdly, the application of this research has predominantly been confined within China, specifically to traditional villages in provinces such as Hunan and Shaanxi [12,13], resulting in geographical concentration and limiting broader applicability.

This study addresses these gaps by employing Linpu Village in Fuzhou, in southeastern China, as a case study to develop a sustainable model for traditional village landscapes using landscape gene theory. This research has three objectives. The first is to establish an "extraction-construction-analysis-preservation" model to enhance the practical application of the theory in rural planning. The second is to enhance analytical methods using Geographic Information Systems (GIS) to analyze key spatial characteristics of cultural landscape genes. These include density, integration, and accessibility, which will enhance the scientific validity and generalizability of the results of the genetic characterization of cultural landscapes. Thirdly, the research will be expanded to Southeast China to enrich the cultural landscape gene pool and verify the applicability of landscape gene theory in different cultural contexts.

Through a combination of quantitative and qualitative methods, this research details the specific cultural landscape genes of Linpu Village. It demonstrates how these genes can inform effective conservation and development strategies. This approach not only promises sustainable solutions for the preservation and enhancement of traditional villages globally, but also provides a scalable model that showcases the broader applicability of cultural landscape gene theory in cultural landscape preservation.

2. Literature Review

To further deepen the understanding of cultural landscape gene theory, this section thoroughly explores the research overview of settlement landscapes, the basic concepts of cultural landscape gene theory, its historical development, and its application in modern research. This comprehensive examination aims to better grasp the practical significance and potential application of cultural landscape gene theory in global village conservation strategies.

2.1. Overview of Research on Settlement Landscapes

The study of settlement landscapes can be traced back to the 19th century, with Johann Georg Kohl's systematic study from a geographical perspective, which made settlement landscapes a hotspot in academic research [14]. By the 1980s, the purpose of conservation shifted from purely historical significance to heritage culture, and the study content began to diversify gradually [15]. Entering the 21st century, interdisciplinary convergence became increasingly evident, concentrating research on several major fields, including the economic promotion of settlement development [16], spatial research on settlement landscapes [17], and the sustainable development of settlements [18]. Recently, international research has focused on settlement landscape characteristics [19], the ecological construction of settlements [20], and the spatial patterns of settlements [21,22]. These studies have promoted the development of cultural diversity in settlement landscapes and provided a rich practical basis for applying cultural landscape gene theory.

2.2. Underlying Concepts

To better understand the theory of cultural landscape gene, it is necessary to clarify a few relevant foundational concepts (Table 1).

Table 1. Comparison of Genes, Cultural Genes, CLGTS, and Landscape Genetics.

Comparison Item	Genes	Cultural Genes	CLGTS	Landscape Genetics
Concept Origin	Biology, Genetics	Genetic Theory, Cultural Heritage	Cultural Gene Theory, Human Geography	Landscape Ecology, Population Genetics
Definition	Hereditary unit controlling biological traits, with replication, mutation, and variation	The basic unit of cultural transmission, with replication, variation, and selection	Cultural elements in traditional settlements, with uniqueness, replication, and variation	Study of how landscape features affect gene flow, population structure, and species adaptation
Application Fields	Biology, Medicine, Agriculture, Evolutionary Studies	Social Sciences, Cultural Studies, Information Dissemination	Traditional Settlement Preservation, Rural Planning, Cultural Heritage Protection	Biodiversity Conservation, Species Management, Ecosystem Restoration
Research Methods	Laboratory Experiments, Gene Sequencing, Molecular Biology Techniques	Observation, Experiments, Theoretical Modeling, Interdisciplinary Methods	GIS, Remote Sensing, Field Surveys	GIS, Remote Sensing, Genomic Tools, Mathematical Modeling
Research Background	Understanding genetic mechanisms and biological evolution, studying genetic diseases, and breeding	Exploring mechanisms of cultural transmission and evolution, understanding cultural and information dissemination patterns	The need for cultural heritage protection in the face of rapid urbanization	The impact of landscape changes on the genetic structure and connectivity of natural populations
Main Goals	Understanding genetic mechanisms, improving breeds, treating genetic diseases	Explaining cultural phenomena and their dissemination and evolution, understanding information and cultural dissemination patterns	Extracting and protecting cultural landscape genes in traditional villages to achieve sustainable cultural heritage development and revival	Understanding and managing the impact of landscape features on gene flow and species adaptation

Genes: The concept of a "gene" originated in the 1960s, when Gregor Mendel proposed that hereditary factors are the key units controlling organism traits. The term "gene" officially appeared in the 1909 book *Principles of Precision Genetics* by Danish geneticist Wilhelm Johannsen [23].

Cultural Genes: Inspired by the hereditary properties of genes, social scientists began exploring the basic elements of cultural inheritance and their properties. In the 1950s, Alfred L. Kroeber and Clyde Kluckhohn hypothesized "cultural genes", arguing that they are the basic units of human culture, subject to self-replication, "mutation", and variation [24]. Richard Dawkins's 1976 book *The Selfish Gene* introduced the concept of "meme", which brought the idea of cultural genes into social science research, later leading to the theory of "memetics" [25]. Currently, the main research areas related to modality theory include linguistic and network modality research [26], providing valuable insights for the genetic study of cultural landscapes [11].

Landscape Genetics: This interdisciplinary field combines landscape ecology and population genetics to understand how landscape features affect gene flow, population structure, and species adaptation [27]. Conceptualized by Manel et al. and formalized as a research area, landscape genetics has made significant progress utilizing GIS, remote sensing, and genomics tools [28]. Despite the similarity in name, landscape genetics and cultural landscape genes focus on distinctly different areas. The former studies natural populations and their genetic connectivity influenced by landscape structure [29], while the latter explores the cultural transmission and evolution of traditional human settlements and cultural landscapes, examining culture–environment interactions in human contexts [30].

2.3. Formation and Development of Cultural Landscape Gene Theory

The concept of the cultural landscape gene is mainly inspired by cultural genes. Chinese scholar Liu Peilin combined the concept of "cultural genes" with practical research in human geography and related disciplines, proposing the concept of "cultural landscape genes". He posits that cultural landscape genes distinguish one cultural landscape from another, akin to biological genes' uniqueness, replicability, and variability [31]. Strictly speaking, landscape genes refer to cultural factors in traditional settlements with specific material carriers or specialized reference objects [11].

From a methodological perspective, the cultural landscape gene analyzes the spatial imagery characteristics of traditional settlement landscapes and their geographic significance, drawing on cultural gene theory. Historically, research results before 2015 were relatively few, focusing mainly on landscape gene characteristics and concentrating on Liu Peilin and his academic team [11]. Post 2015, research has spread to various institutions and individuals, expanding the thematic scope. Currently, landscape gene research spans three aspects: architectural culture [32], settlement patterns [33], and regional culture [34], primarily focusing on traditional settlements with distinctive landscapes across China, particularly in the southwest and central regions [11]. Research scales include architectural monoliths, architectural groups, villages, and settlements [12,35]. The research content is divided into three major fields: cultural landscape gene identification and classification, map construction and expression, and the practical application of landscape genes.

Cultural Landscape Gene Identification and Classification: This field extracts the most characteristic landscape genes by deconstructing landscape elements of traditional settlements. Liu Peilin pioneered four basic principles for identifying a cultural landscape gene: "intrinsic uniqueness, extrinsic uniqueness, local uniqueness, and overall dominance" [36]. He elucidated the biologically similar characteristics of traditional settlement cultural factors, significantly impacting subsequent research. Shen Xiuying et al. proposed four extraction methods—pattern, element, structure, and meaning—based on these principles [37]. However, this method has operational limitations, particularly for extracting unique landscape elements and cultural factors. Hu and colleagues later proposed a feature deconstruction–extraction method, distinguishing cultural landscape elements by category, merging similar elements, and classifying them into four categories of feature genes, optimizing extraction and classification methods [38].

Mapping Construction and Expression: Cultural landscape gene mapping involves researchers processing the identified and extracted cultural landscape gene information of traditional settlements, coding and recording it, importing it into a basic database, and visualizing it with GIS tools [30]. Cultural landscape gene mapping contains information such as spatial positioning, carrier history, and culture [33]. Currently, most research on the cultural landscape genes of traditional settlements stops at the construction stage, with fewer studies combining quantitative analysis methods to reveal spatial characteristics of landscape genes [39].

Practical Application of Cultural Landscape Genes: Application mainly focuses on traditional settlement landscape inheritance and protection and minority settlement cultural landscape gene analysis [40]. For instance, Liu Peilin remodeled the image of village cultural landscapes based on extracting and identifying cultural landscape genes, presenting each attraction as a complete thematic tour line to shape a recognizable cultural tourist place [41]. However, most studies are limited to extracting and identifying cultural landscape genes and collecting and integrating local cultural and geographic information data, without further application to traditional cultural inheritance and revitalization or proposing specific, effective paths and methods compared to past efforts [39].

To summarize, the theory of landscape genetics has moved from initial exploration to rapid development. However, several issues still need scrutiny and resolution:

Improvement of Analytical Methods: Current research mainly employs qualitative analysis through literature reviews and field research to confirm the characteristics of cultural landscape genes [11]. Further analysis of spatial characteristics is limited [10].

Introducing mathematical models and spatial analysis techniques is necessary to deeply analyze spatial distribution laws and dynamic changes, providing a scientific basis for protecting and revitalizing cultural landscape genes.

Deepening Practical Applications: Most research stops at collecting raw data on cultural landscape genes of traditional villages [42], lacking depth in processing and utilizing these data for further planning and application in sustainable village development [43]. Future research should focus on specific applications of cultural landscape genes in ecological protection, cultural tourism, and community development, proposing practical operational paths and methods to transform theoretical results into practice and achieve sustainable rural development.

Addressing Research Limitations and Geographic Imbalance: Current research primarily focuses on China, particularly traditional villages in the southwest and central regions [44,45]. This concentration limits the application and generalizability of the cultural landscape gene theory, hindering the summarization of revitalization paths for traditional villages globally. Expanding the scope to cover diverse cultural landscapes and traditional villages worldwide is crucial for building a comprehensive and universal theoretical framework for cultural landscape genes. Additionally, international cooperation should be strengthened to promote the application and development of cultural landscape gene theory on a global scale, exploring paths for protecting and revitalizing traditional villages in other countries and regions.

3. Methods

3.1. Study Region

Linpu Village, situated in Chengmen Town, Cangshan District, Fuzhou City, Fujian Province, is in the northeast corner of Nantai Island. It is bordered by the Lian River to the north and Jiuqu Mountain to the south, with a view of Gushan Mountain across the river. This geographic setup forms a scenic landscape where mountains and water intertwine seamlessly, as illustrated in Figure 1. With a dense population of approximately 7000 across its 2.9 km^2, the village comprises four administrative subdivisions: Lianjiang, Shishan, Fulian, and Shaoqi [46].

Historically, Linpu has been a vibrant community since the Ming Dynasty, with a notable legacy of contributing scholars to imperial courts. By the Qing Dynasty, leveraging its advantageous location for land and water transport, it evolved into a critical hub within the Minjiang River Basin for waterborne trade, agriculture, and the broader socioeconomic development of the region. This development is documented in various historical records. Linpu Village serves as a repository for diverse regional cultures, encompassing the Shangshu culture and the patriotic culture of the Southern Song Dynasty, among others. This blend aligns with the traditional village ethos prevalent in Fuzhou and highlights Linpu's distinct cultural identity. It boasts 14 cultural heritage units and 32 listed protected buildings. Recognizing its historical and cultural significance, Linpu Village was designated as a historical and cultural village of note in Fujian Province in 2007. It was included in the seventh batch of national-level historical and cultural villages in 2019 [47]. This distinction places it among the few millennium-old villages surviving within an urban context in China.

However, recent rapid urbanization in Fuzhou has posed significant threats to Linpu's architectural integrity and landscape. Unplanned development and insufficient regulatory oversight have led to substantial alterations in village texture and aesthetics, characterized by intrusive construction and the encroachment of new development zones. These changes urgently call for concerted efforts to preserve the traditional landscapes that embody Linpu's historical and cultural essence.



(**a**) Location of Fujian Province in China

(**b**) Location of Linpu Village in Fujian Province

(**c**) Spatial layout plan of Linpu Village

(**a**)The map available at http://bzdt.ch.mnr.gov.cn/, which is publicly accessible and not subject to copyright restrictions.
(**b**,**c**) This map was generated using ArcGIS software, version 10.6. For more details, please visit https://www.esri.com/en-us/arcgis/about-arcgis/overview.

Figure 1. Location and overall landscape of Linpu Village.

3.2. Research Methods

Identifying and extracting cultural landscape genes involve extracting elements or factors that reflect regional cultural features from complex landscape phenomena. Due to this, any element or factor can be considered a cultural landscape gene theoretically; the identification and extraction of cultural landscape genes must follow certain principles and theoretical methods. Liu Peilin introduces four fundamental principles for extracting cultural landscape genes from his research on traditional Chinese settlement landscapes, namely "intrinsic uniqueness, extrinsic uniqueness, local uniqueness, and overall dominance" [36]. Moreover, he maintains that extracting cultural landscape genes from traditional village landscapes requires specific technical methods. The methods proposed by Hu Zui et al. [38] for extracting material and non-material cultural landscape genes based on the cultural landscape of Xuanzhou Ancient Town, as well as the methods proposed by Yin Zhiyi et al. [33] for Huangpi Dayu Bay, offer certain valuable guidance for this study. Based on the above identification principles and extraction methods, a cultural landscape gene extraction system for Linpu Village has been established to extract cultural landscape genes. After the extraction of cultural landscape genes, the principles of typology are adopted to classify and explain landscape elements, deriving corresponding cultural landscape genes. The understanding of village cultural landscape genes is further enhanced by constructing a landscape gene information chain. This spatial organizational form reflects certain cultural symbolic features of cultural landscapes [26]. For a more intuitive and accurate analysis of the spatial features of village cultural landscape genes, quantitative research methods such as spatial syntax theory and kernel density analysis

were combined to fully explore the features of traditional villages and propose relevant strategies for the preservation and sustainable development of traditional village features. In line with the principles mentioned above, as well as theories and methods, the integrated research process of "extraction-construction-analysis-preservation" of cultural landscape genes was established, as shown in Figure 2.

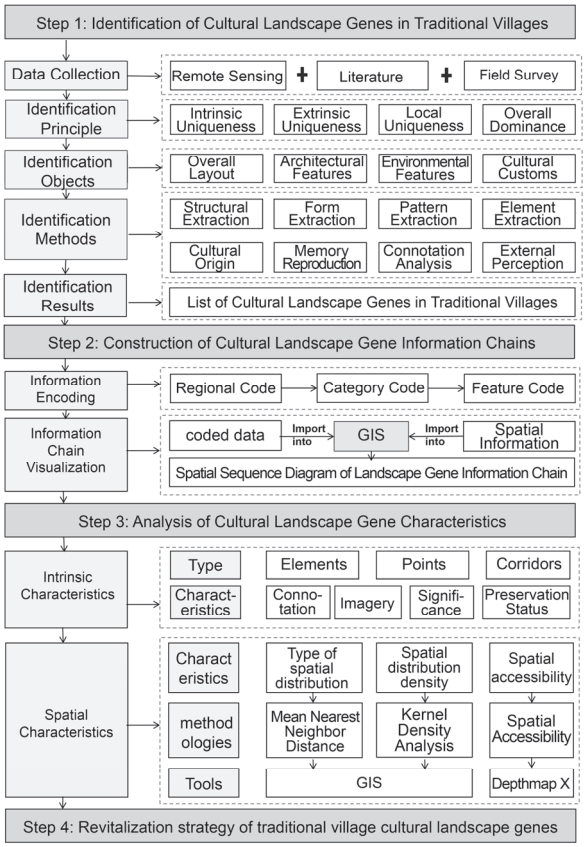


Figure 2. Research framework of sustainable inheritance of landscape features.

3.2.1. Identification and Encoding Methods of Cultural Landscape Genes

- Gene Identification and Extraction Method

The cultural landscape genes of Linpu Village mainly fall into two categories based on different material forms: material cultural genes and non-material cultural genes. The methods for extracting material elements include structural extraction, form extraction, pattern extraction, and element extraction. In contrast, those non-material elements include cultural context tracing, memory reproduction, connotation interpretation, and external perception [48]. The specific means of identification of cultural landscape genes is mainly through the visual and perceptual analyses of the researchers, specifically the perceptual identification of the cultural landscape genes of the villages through a variety of ways, such as viewing, field visits, surveys, reviewing historical and cultural data, and examining the characteristics of the natural environment. Based on the principles of typology and the "Guidelines for Strengthening the Preservation of Chinese Traditional Villages" [49], the identification and extraction results of material cultural landscape genes are classified into three identification factors, including overall layout, architectural features, and environmental references, and 10 identification indicators, including village form, street layout, and architectural style, etc. In comparison, the non-material cultural landscape genes are formed based on field research and classified into three identification factors, including regional culture, custom activities and traditional crafts, and four identification indicators, which ultimately establish the identification system for cultural landscape genes in Linpu Village (Table 2).

Table 2. Cultural landscape gene identification system in Linpu Village.

Gene Category	Identification Factor	Identification Sub-Indicators
Material cultural genes	Overall Layout	Landscape Pattern
		Street Layout
		Village Form
	Architectural Features	Plane Layout
		Public Building
		Architectural Style
		Architectural Decoration
		Architectural Texture
	Environmental References	Cultural Environment
		Natural Environment
Non-material cultural genes	Regional Culture	Surname Clan
		Object of Faith
	Custom Activities	Entertainment Customs
	Traditional Crafts	Inheritance Level

- Gene Information Chain Construction Method

This method is used to accurately categorize and elucidate the affinities among various cultural landscape genes, as well as to systematically record and manage the corresponding data. Based on the identification results of cultural landscape genes in Linpu Village, the encoding structure of cultural landscape genes is divided into region, category, and feature codes. The region code for Linpu Village is set as X. The category code, according to Richard Dawkins's concept of "Meme" [50], is set as M to represent cultural landscape genes, while distinguishing material cultural genes as M1 and non-material cultural genes as M2, respectively. The feature code follows the "Classification and Code of Fundamental Geographic Information feature" [51], categorizing the cultural landscape gene information of Linpu Village into "primary elements, secondary elements, tertiary elements, and landscape elements" and encoding them in Arabic numerals [36] (Figure 3). Our research team, which includes experienced researchers in relevant fields, conducted the cultural landscape gene encoding for Linpu Village. Our encoding method is based on established techniques referenced in several vital studies [33,52], which have been applied by other scholars in similar contexts. To ensure the accuracy and consistency of our encoding, two team members independently conducted the encoding process. Their results were compared, and discrepancies were discussed and resolved through consensus. Senior researchers reviewed and finalized this step to ensure alignment with established standards.

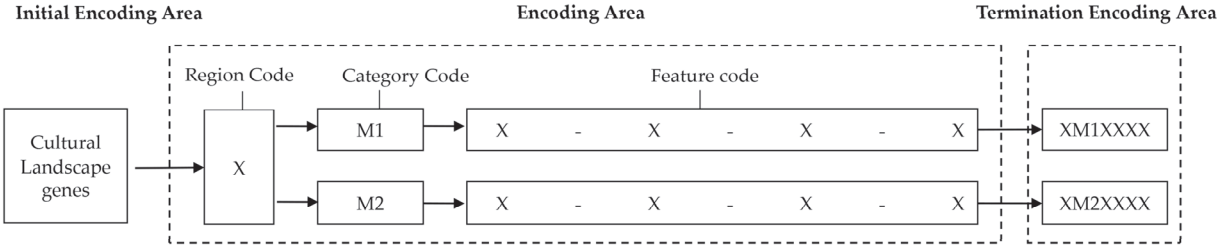


Figure 3. Encoding structure of cultural landscape genes.

3.2.2. Analysis Methods for Spatial Features of Cultural Landscape Genes

This study employs multiple analysis methods to comprehensively understand the spatial features of cultural landscape genes in Linpu Village. These methods include

analyzing the spatial distribution types, density, and accessibility of cultural landscape genes. Through these methods, we can reveal the spatial organization and distribution patterns of cultural landscape genes, assess the concentration of their cultural value, and optimize their accessibility, thereby formulating scientific conservation and sustainable development strategies. These analyses also help identify areas that need prioritized protection and provide data support for improving infrastructure and enhancing the visitor experience.

- Analysis Method for Spatial Distribution Types of Genes

To evaluate the spatial organization of cultural landscape genes, this study first needs to determine their distribution types. Understanding the spatial arrangement of cultural landscape genes within the village can reveal the influence of natural and human factors on their distribution, aiding in developing targeted management and conservation strategies. Therefore, we employed the "average nearest neighbor" (*ANN*) method. On a macro level, the cultural landscape gene units in Linpu Village are point elements. The spatial distribution types of point elements can be categorized into three types: random, clustered, and uniform. The "average nearest neighbor" method is often used to determine the spatial distribution types of point elements [53], which is also suitable for determining the spatial distribution types of cultural landscape genes. The calculation formula for the average nearest neighbor (*ANN*) ratio is as follows:

$$ANN = \frac{\overline{D_O}}{D_E} \tag{1}$$

$$D_E = \frac{1}{\sqrt[2]{n/A}} \tag{2}$$

where $\overline{D_o}$ is the actual average distance between each cultural landscape gene unit and its nearest neighbor; D_E is the expected average distance between the cultural landscape gene units, assuming a random distribution pattern; n is the number of landscape gene units; and A is the village scope, including all cultural landscape gene units. When $ANN = 1$, the cultural landscape genes tend to be randomly distributed; when $ANN > 1$, the cultural landscape genes tend to be discrete; when $ANN < 1$, the cultural landscape genes tend to be clustered.

- Analysis Method for Spatial Distribution Density of Genes

To identify and prioritize areas with high cultural and historical value, this study needs to understand the spatial density distribution of cultural landscape genes. High-density areas typically indicate a concentrated distribution of cultural heritage, which is crucial for formulating graded conservation strategies and optimizing resource allocation. Therefore, we employed the kernel density analysis method [54]. The kernel density analysis method is commonly used to calculate the spatial density of point elements [53], and this method is also applicable for analyzing the spatial distribution density of cultural landscape genes. When calculating kernel density, cultural landscape gene units are assigned values according to the number of cultural landscape genes represented by the cultural landscape gene unit. Where a cultural landscape gene unit represents more than one cultural landscape gene, the landscape unit is weighted with a weight determined by the ratio of the number of cultural landscape genes in the unit to the total number of genes in all units, ensuring that units with a higher number of genes have a greater impact on the overall density estimate. This weighting approach helps emphasize culturally and historically significant areas due to a higher concentration of cultural landscape genes. The formula for calculating the kernel density, taking into account the weights (*W_KD*), is given below: The calculation formula for kernel density, considering the weights (*W_KD*), is as follows:

$$W_KD(x) = \frac{1}{\sum_{i=1}^{n} W_i} \sum_{i=1}^{n} W_i K(\frac{x - X_i}{h}) \tag{3}$$

where x represents a position in the spatial domain for which we estimate the density. W_i defines the weight for the i^{th} unit, calculated as the proportion of cultural landscape genes within that unit relative to the sum of cultural landscape genes across all units. K denotes the kernel function. X_i is the location of the i^{th} cultural landscape gene unit. h stands for the bandwidth.

A spatial distribution model of cultural landscape genes in Linpu Village is constructed using ArcGIS version 10.6 (Esri, Redlands, CA, USA). The cultural landscape genetic elements within the village are assigned values, and the kernel density analysis method is adopted to calculate the spatial model of cultural landscape genes. The results of the kernel density calculation are presented in the form of images, and the gene density levels are graded based on the distribution results of landscape units. The color depth represents the difference in kernel density values, with darker colors indicating higher kernel density values.

- Analysis Method for Spatial Accessibility of Genes

Spatial accessibility analysis aims to examine the capacity of cultural landscape genes to attract traffic flow. High accessibility areas are more likely to attract visitors, promoting the display and conservation of cultural heritage. In traditional villages, cultural landscape genes are interconnected via existing traffic paths, constituting a transportation network. Within this network, the transportation cost associated with accessing each cultural landscape gene unit varies. The concept of "topological depth" quantifies transportation costs, whereas a higher topological depth value indicates increased costs for a cultural landscape gene unit and reduced accessibility. To quantify the spatial accessibility of cultural landscape gene units, the method of calculating their global integration was adopted. Global integration is the aggregate of the reciprocals of topological depth values from a given cultural landscape gene unit to all others within its historical and cultural village town. Consequently, spaces exhibiting high integration are characterized by enhanced accessibility [29]. This analysis was conducted using Depthmap X version 0.8.0 (Space Syntax Laboratory, The Bartlett School of Architecture, University College London, UK) to assess the global integration of Linpu Village's spatial axes. The formula to calculate the global integration of cultural landscape genes is as follows:

$$I_i = \frac{(n-2)D_n}{2\left(nD\mathrm{i}^{-1}\right)} \tag{4}$$

where MD_i is the average topological depth value of cultural landscape gene i, and its calculation formula is:

$$MD_i = \frac{TD_i}{n-1} = \frac{\sum_{j-1}^{n} \mathrm{d}_{ij}}{n-1} \tag{5}$$

$$Dn = \frac{2\{n[log((n+2)/3)-1]+1\}}{(n-1)(n-2)} \tag{6}$$

n is the total number of cultural landscape genes in the historical and cultural village. D_N is the mean distance between cultural landscape genes; TD_i is the total depth of the i^{th} cultural landscape genes, summing the steps from that gene to all others; and d_{ij} is the distance from the i^{th} cultural landscape gene to the j^{th} cultural landscape gene.

3.3. Data Sources

The data required for this study and their sources include:

(1) Remote Sensing Image Data

The 2020 remote sensing images of Linpu Village, obtained from ResourceSat-1, were sourced from the Geospatial Data Cloud site [55]. These images were collected using the vectorization of geographic information, including buildings, road networks, and rivers, using ArcGIS version 10.6. This process aids in analyzing and interpreting the village's

natural environment and spatial configuration. These data provide the foundation for the subsequent identification of cultural landscape gene locations in Linpu Village and the visualization of the quantitative analysis of cultural landscape gene spatial features.

(2) Literature Data

Various literature sources were collected, including documents such as the "Historical and Cultural City Preservation Plan of Fuzhou City" [56], "Historical and Cultural City, Town, and Village Chronicles of Fuzhou City" [57] and "Preservation Plan for Linpu Village in Chengmen Town, Cangshan District, Fuzhou City, a Historical and Cultural Village of Fujian Province" [58], to analyze the cultural features of Linpu Village. The data obtained from the literature review were organized and summarized using the literature analysis method.

(3) Field Surveys

The field surveys comprised two main components: observational surveys and structured interviews. These were conducted to gather comprehensive data on the cultural landscape genes and the villagers' perception of their cultural heritage.

Survey Process: Field surveys were conducted between January and February 2023 to observe the physical and cultural landscape features of Linpu Village directly. These involved on-site visits to various cultural landscape gene locations to document their current state, spatial characteristics, and accessibility. GPS devices and cameras were used to record precise locations and visual conditions.

Interviews: Semi-structured interviews were conducted with 36 participants, including 27 villagers, 2 village committee members, and 7 tourists. Each interview lasted between 10 and 90 min, depending on the depth of the discussion and the availability of the interviewee. Villagers were asked about their views on the protection of traditional culture, opinions on tourism development, perceptions of changes in the village landscape, and challenges in maintaining cultural heritage. Village committee members were asked about the basic conditions of the village, the maintenance of cultural heritage, and the integration of cultural preservation with development plans. Tourists were asked about their sensory experiences, perceptions of the village's cultural landscape, and suggestions for improving the visitor experience (Table 3). The interviews aimed to understand the significance of various landscape genes from the perspective of the community, capturing their views on preservation needs and future development. These insights were then used to inform the development of strategies for revitalizing the cultural landscape genes, ensuring they meet the needs and expectations of the village.

Table 3. Interviewee information and focus of interviews.

Code	Interviewee Group	Number of Participants	Description	Key Focus of Interviews
RI~R27	Villagers of Linpu Village	27	R1~R13 (ordinary villagers), R14~R19 (shop owners), R20~R23 (stallholders), R24~R25 (intangible cultural heritage bearers), R25~R27 (guesthouse receptionists)	Views on the Protection of Traditional Culture and Tourism Development of Villages
G1~G2	Village Committee Members	2	G1 (Village Party Secretary), G2 (Women's Director)	Basic conditions of the village and maintenance of culture
VI~V7	Tourists	7	V1~V7 (Tourists)	Sensory experiences of tourists

Note: 'R' denotes villagers, 'G' for government workers, and 'V' for tourists.

4. Results

4.1. Identification and Encoding of Cultural Landscape Genes

4.1.1. Identification and Extraction of Cultural Landscape Genes in Linpu Village

The identification results of cultural landscape genes are shown in Table 4. In terms of overall layout, Linpu Village exhibits a landscape pattern featuring mountains and water, a network layout of streets and alleys, and a clustered village form. In terms of architectural features, Linpu Village's buildings are mainly traditional buildings from the Ming Dynasty, Qing Dynasty, and the Republican period, with typical features of Fuzhou residential buildings. In terms of environmental references, the cultural heritage of Linpu Village is mainly reflected in cultural relics such as memorial archways, cliff inscriptions, and ancient bridges. At the same time, the natural environment is represented by ancient trees and water systems. Regarding intangible cultural genes, these mainly include regional cultures represented by Shangshu culture, hero worship, and religious beliefs, custom activities represented by welcoming the God of Mount Tai and the pageant of gods, and traditional crafts represented by Annan instrumental performance.

Table 4. Identification of cultural landscape gene in Linpu Village.

Category	Factor	Indicators	Result	
Material cultural genes	Overall layout	Landscape Pattern	Surrounded by mountains and waters	
		Street Layout	Grid structure	
		Village Form	Clustered	
	Architectural features	Plane Layout	Multiple-courtyard style	
		Public Buildings	Ancestral temple	
			Ancient academy	
			Clan hall	
		Architectural Style	Facade Form	Double-slope roof with dovetail ridge
			Gable Design	Corresponding to the five-element theory
			Roof Truss Structure	Column and tie construction
		Architectural Decoration	Decoration techniques	Wood carving, stone carving, brick carving, etc.
		Architectural Texture	Building materials	Rammed earth walls with gray tiles
	Architectural Features	Architectural Texture	Color	Mainly gray and brown
	Environmental references	Cultural Environment	Memorial archway	
			Ancient bridge	
			Cliff inscriptions	
		Natural Environment	The Lian Jiang River	
			Centuries-old banyan tree	
Non-material cultural genes	Regional culture	Surname Clan	Shangshu culture (genealogy culture)	
		Object of Faith	Hero worship	
			Religious belief	

Table 4. *Cont.*

Category	Factor	Indicators	Result
Non-material cultural genes	Custom activities	Entertainment Customs	Welcoming the God of Mount Tai
			Pageant of gods in Ruiji Temple
	Traditional craft	Level of Inheritance	Annan instrumental performance

4.1.2. Construction of Cultural Landscape Gene Information Chain in Linpu Village

The independent encoding results from the two team members showed a high degree of consistency. Initial comparisons revealed minor discrepancies in categorization, primarily due to subjective interpretations of certain landscape features. These discrepancies were thoroughly discussed in joint sessions, where the team members reconciled differences through consensus, ensuring a unified and accurate final encoding.

Figure 4 provides examples of the encoded cultural landscape genes, demonstrating the application of our method. These examples illustrate the robustness and applicability of our coding framework. The final encoding results reflect a comprehensive and consistent categorization of the cultural landscape genes in Linpu Village, as validated by senior researchers.

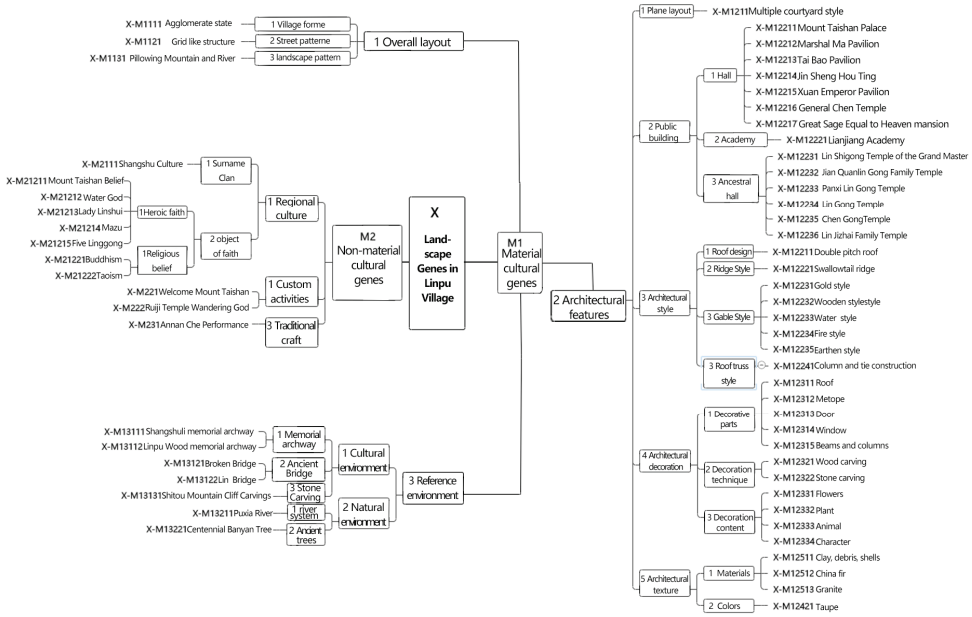


Figure 4. Cultural landscape gene information chain in Linpu Village.

On this basis, the spatial location of cultural landscape gene elements was extracted using a geographic information system (GIS), providing parameters such as ID name, coding information, coordinate information, etc.; the cultural landscape genes and the spatial distribution characteristics of cultural landscape genes were visualized (Figure 5). It can be drawn from the construction results that there are four landscape corridors in the cultural landscape gene information chain of Linpu Village, one running north to south and three running east to west. The grid-like layout of the streets and alleys reflect the overall layout gene, the architectural feature gene and regional culture gene are mainly distributed in the northern and central–southern parts of the village, and the reference environment gene is distributed primarily in the northern and southern parts of the village.

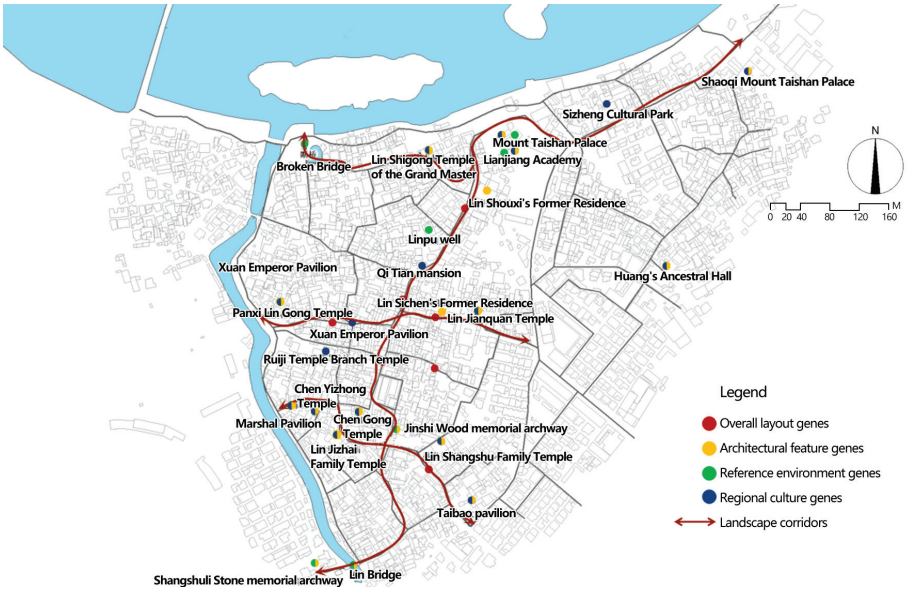


Figure 5. Spatial sequence diagram of cultural landscape gene information chain in Linpu Village.

4.2. Analysis of Intrinsic Characteristics of Cultural Landscape Genes in Linpu Village

The landscape information elements are the cultural elements of a landscape, while the landscape information points embody these elements. Landscape information elements and points serve as the fundamental elements and units for constructing a landscape information chain. In contrast, landscape information corridors represent the spatial manifestation of the landscape information chain [59], as shown in Figure 6. Through the identification and extraction of the cultural landscape genes in Linpu Village (Table 4), the main features of the information elements, information points, and information corridors in Linpu Village can be derived from the construction of the cultural landscape gene chain (Figure 4) and information graph (Figure 5).

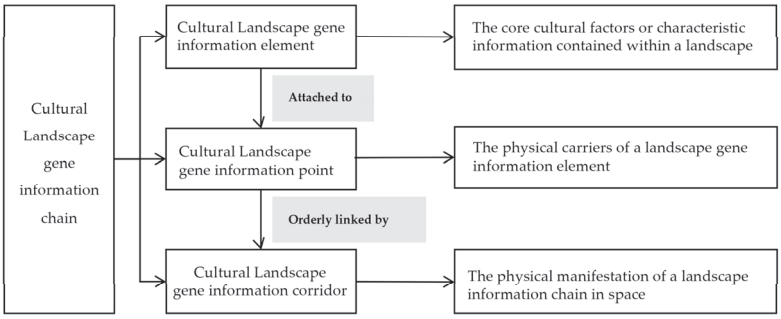


Figure 6. The intrinsic composition of cultural landscape gene information chain.

4.2.1. Features of Cultural Landscape Gene Information Elements

The landscape information elements in Linpu Village include the Shangshu culture, the patriotic culture of the Southern Song Dynasty, clan culture, religious culture, and folk culture. These elements are deeply rooted in the local cultural perspectives, enriching a rich historical context of the village's culture with the splendid "Shangshu Culture" of the Ming Dynasty and the patriotic culture of the Southern Song Dynasty. This amalgamation creates a complex historical context that shapes the village's cultural landscape. However, the village faces challenges in maintaining this heritage. Traditional customs such as clan sacrifices are in decline due to the loss of genealogies and fading clan consciousness. Similarly, the art of Annan instrumental performance is at risk as the older generation of performers dwindles and the younger generation shows less interest. Additionally, there is an imbalance in how cultural diversity is displayed. While there is a significant emphasis

on Shangshu and patriotic cultures, lesser-known cultural elements and regional crafts receive limited attention, risking a loss of cultural diversity.

4.2.2. Features of Cultural Landscape Gene Information Points

The landscape information points in Linpu Village include architectural structures such as Taishan Temple and Lianjiang Academy that embody the features of Shangshu culture and patriotic culture, as well as residential houses and ancestral temples that showcase folk culture and clan culture, and architectural relics representing diverse cultures. The existing buildings mainly reflect the traditional courtyard architecture of Ming Dynasty, Qing Dynasty, and Republican periods, while the new constructions have an impact on the overall style and features [60]. The natural landscapes, such as water systems and ancient trees, blend with cultural landscapes such as cliff stone inscriptions, broken bridges, and Lin Bridge, bearing historical research value.

4.2.3. Features of Cultural Landscape Gene Information Corridors

The internal corridors in Linpu Village are divided into primary and secondary corridors. The primary corridor is Linpu Avenue, which runs from south to north, serving as the basic framework of the village's layout. It connects Yudao Street to the north and stretches from Jin Shenghou (Qianliyan) Pavilion to Shaoqi Ferry to string various nodes in the village together, such as the Shangshuli Memorial Archway and Qitian Temple along Yudao Street, ensuring a complete cultural connotation to Linpu Village. The secondary corridor is the road network that links the internal residential buildings, forming a cultural tourism belt of Linpu that connects residential buildings, the ancestral temple, and the clan temple. The main and secondary corridors intersect with ancestral temples, residential houses, and community temples, forming a "fishbone-shaped" street layout in Linpu Village [19]. Nowadays, the original green slab stone on the corridors of Linpu Village has been replaced by cement pavement. The modern-style buildings constructed on both sides of the corridors are incongruous with the entire village's traditional style, which has affected the consistency and coherence of the landscape information chain and undermined its integrity in Linpu Village. Compared with the primary corridor, the marginal landscape information corridor that is supported by the remaining alleys, such as Houjie Street and Taibao Lane, and connects the landscape information points, such as pavilions and the clan temple, bears a lower readability of cultural landscape information and underestimated value, leaving some potential points of landscape information unexplored.

4.3. Analysis of Spatial Features of Cultural Landscape Genes in Linpu Village

4.3.1. Analysis of Spatial Distribution Types of Cultural Landscape Genes

The "nearest neighbor ratio" method in ArcGIS is adopted to analyze the spatial distribution types of cultural landscape genes in Linpu Village. The calculation results show that the nearest neighbor ratio of cultural landscape genes in Linpu Village is 1.1815, which is greater than 1, indicating that the natural geographic conditions with uniform landscape elements in the village are the main factors affecting the spatial distribution types of cultural landscape genes. Linpu Village is located in a flat coastal delta region, with regular and symmetrical residential clusters, which also contributes to the uniform spatial distribution of cultural landscape genes. However, this dispersion, lack of centralization, and clear spatial layout make it difficult for tourists to fully and systematically grasp and understand the cultural characteristics of Linpu Village.

4.3.2. Analysis of Spatial Distribution Density of Cultural Landscape Gene

After thoroughly evaluating the spatial scale of landscape patterns and the distribution of cultural landscape gene units within our study area, we selected a bandwidth of 20 km for the kernel density estimation. This bandwidth was chosen to adequately capture the broad-scale spatial patterns of cultural significance without overemphasizing local variations that might result from isolated or outlier cultural landscape gene units. It strikes a balance

between providing sufficient detail to discern meaningful clusters of cultural landscape genes and ensuring a smooth density surface that reflects the overarching distribution trends. This choice is consistent with the spatial extent of our study area and the average dispersion of cultural landscape gene units, thereby allowing us to generate a density map that accurately represents the density gradients of cultural heritage significance across the landscape. The calculation results of kernel density of cultural landscape genes indicate that the density of landscape information points in Linpu Village exhibits a clustered distribution, specifically characterized by the "one core, two clusters" pattern (Figure 7). The highest kernel density is located in the northern part of Linpu Village, forming the "gateway core area" composed of Taishan Temple and Lianjiang Academy, reaching the highest level of 9. The other two clusters are located in the central "residential and ancestral temple cluster" and the southern "diverse culture cluster", with cultural landscape gene densities ranging from levels 2 to 5. Apart from these concentrated areas, the distribution of cultural landscape genes in the surrounding village is more scattered, with densities mainly ranging from levels 1 to 3.

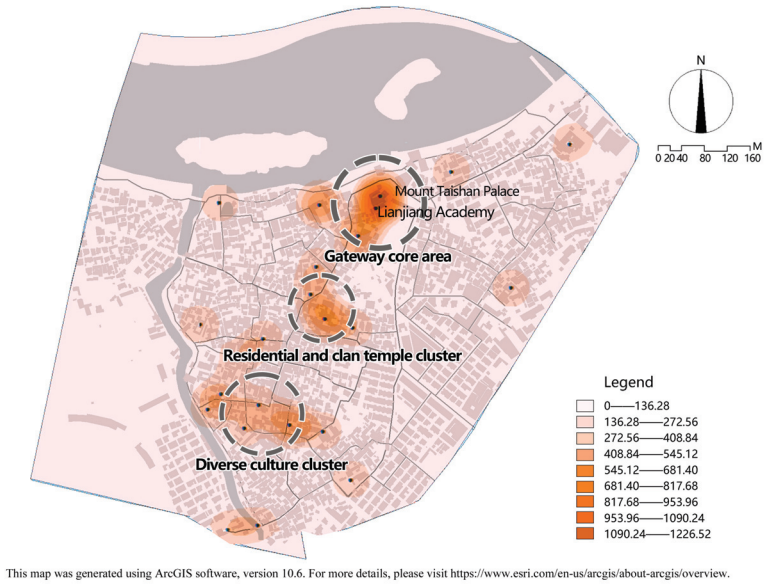


Figure 7. Kernel density map of cultural landscape genes in Linpu Village.

4.3.3. Analysis of Spatial Accessibility of Cultural Landscape Genes

The calculation results of the global integration of cultural landscape genes in Linpu Village show a gradual decrease in spatial accessibility from the center to the periphery (Figure 8). The areas with the highest global integration in Linpu Village are concentrated around Linpu Street, Jinshi Lane, Houjie Street, and their surroundings, corresponding to the highest spatial accessibility of cultural landscape genes near the "residential and ancestral temple cluster". The northern part, represented by Taishan Temple and Lianjiang Academy, is the "gateway core area" that embodies the Shangshu culture and the patriotic culture of Linpu Village, and, with the southern "diverse culture cluster", are the two areas with higher concentrations of cultural landscape genes in the village. Despite these features, both areas show comparatively low global integration, which limits visitor engagement with these culturally rich locations and adversely affects the overall portrayal of Linpu's landscape attributes. This disparity poses challenges for the effective communication and study of the village's cultural heritage.

This section may be divided by subheadings. It should provide a concise and precise description of the experimental results, their interpretation, and the experimental conclusions that can be drawn.

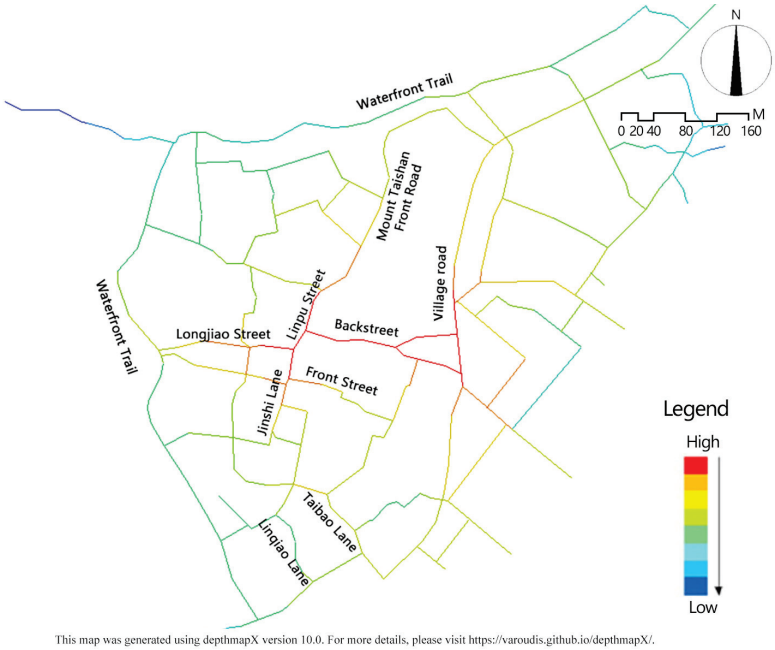


Figure 8. Global integration analysis of Linpu Village.

5. Discussion

This study systematically identified and analyzed the cultural landscape genes of Linpu Village, employing a method and coding system that have been adopted by other researchers [33,52], thus enhancing the reliability and scientific rigor of our approach. By combining an in-depth examination of the connotative characteristics of these genes with an innovative spatial attribute quantification method—including spatial distribution type, density, and accessibility—we address limitations present in previous studies that focused solely on connotative analysis [11].

Our findings reveal that Linpu Village's cultural landscape genes are diverse and rich, displaying typical Fuzhou characteristics and unique local charm. These attributes are crucial for the village's protection and revitalization. However, some genes risk disappearing, necessitating enhanced protection measures. Spatially, these genes exhibit a uniform group distribution with a pronounced core, and accessibility diminishes from the center to the periphery, hampering the effective dissemination and utilization of cultural information.

To facilitate the sustainable development of traditional villages, we propose integrating the connotative characteristics and spatial distribution patterns of cultural landscape genes and suggest revitalization strategies. The practical application of landscape gene theory remains in its infancy, with limited research available [39]. Existing studies primarily focus on connotative protection, with scant attention to strategies for revitalizing cultural inheritance [61]. Furthermore, there is a lack of empirical research on rural landscape planning and tourism development, necessitating deeper investigation [43].

Based on our comprehensive analysis, we propose a strategy to transform Linpu Village's cultural landscape resources into economic vitality. This strategy integrates cultural inheritance, spatial optimization, and industrial development to revitalize these resources sustainably. It aligns with Linpu Village's cultural distinctiveness, the well-being of the local population, and tourist expectations. The specific process is illustrated in Figure 9.

The integrated planning of connotative features and spatial distribution patterns is essential for the better protection and utilization of these resources. Using kernel density and accessibility analysis, we identified landscape nodes to ensure scientifically sound selection. Information corridors highlight Linpu Village's cultural axis, establishing a spatial pattern for protection. The central node, due to its high accessibility and rich cultural elements, should be the primary focus of development, equipped with public spaces,

infrastructure, and landscape design. The northern node, reflecting Shangshu culture and patriotism, forms a corridor with riverside genes rich in natural and cultural attributes. The southern node embodies ancestral temple culture, forming a key cultural landscape. Future developments should restore and maintain these traditional characteristics. The "three horizontal and one vertical" corridors connect Linpu Village's cultural landscapes, providing tourists with a comprehensive traditional village experience. The preservation and enhancement of these corridors should be prioritized, as indicated in Figure 10.

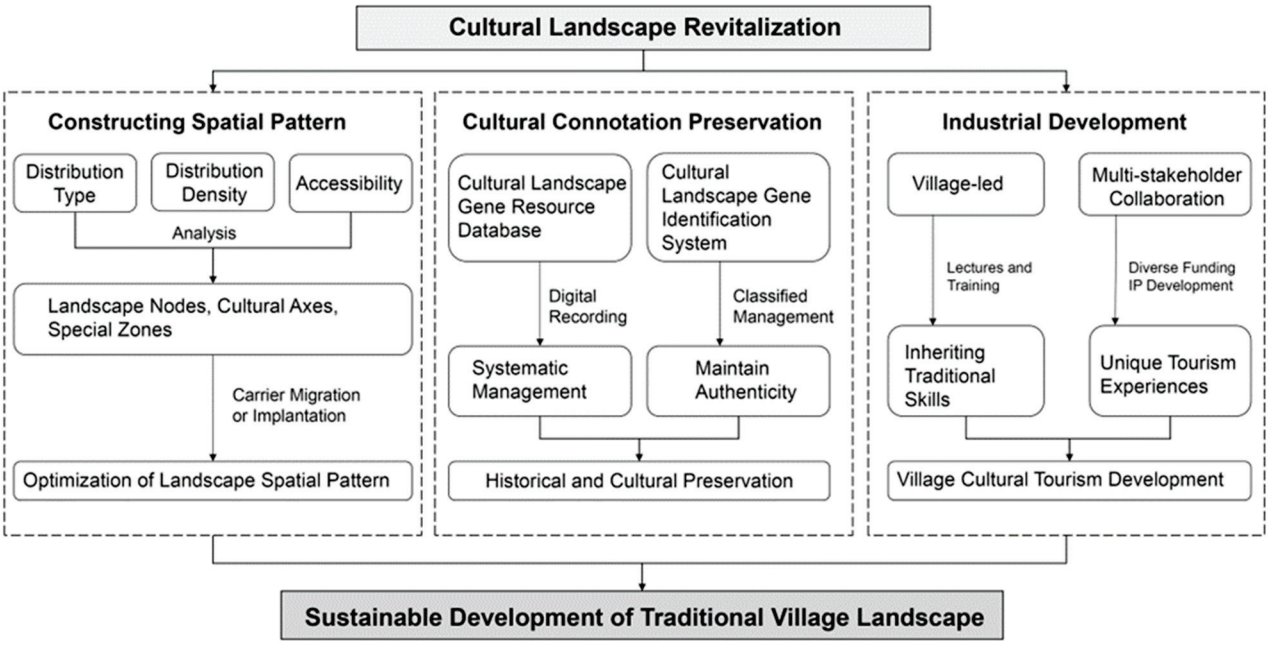
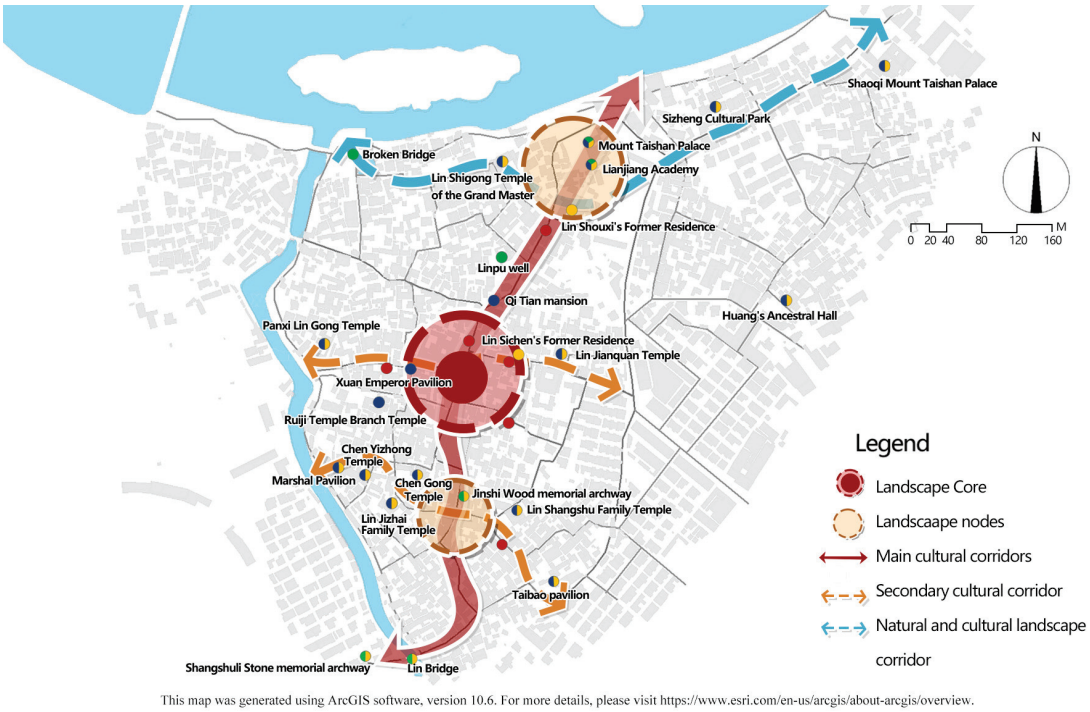


Figure 9. The model for the sustainable development of traditional village landscapes.



This map was generated using ArcGIS software, version 10.6. For more details, please visit https://www.esri.com/en-us/arcgis/about-arcgis/overview.

Figure 10. The pattern of the spatial protection of the village landscape.

Spatial optimization can be achieved through cultural landscape gene carrier migration and implantation. In regions with limited accessibility and low gene agglomeration,

relocating cultural landscape gene carriers to higher concentration areas ensures better protection and resource utilization. Establishing historical and cultural corridors in accessible alley spaces and introducing new carriers can enhance traditional alley spaces and preserve the historical and cultural narrative, further strengthening the village's identity and sense of belonging.

For the protection of cultural connotations, a cultural landscape gene resource database should be established to systematically manage and digitally monitor Linpu Village's elements. By integrating multiple data sources, a 3D cultural landscape gene database can protect the village's history and culture's integrity, authenticity, and sustainability [42]. Establishing a cultural landscape gene identification system supplemented by manual diagnosis can examine the inheritable variation, clonal variation, or mutation of Linpu Village's cultural landscape genes [13]. Different conservation methods should be adopted based on the characteristics of these elements. Inherited cultural landscape genes refer to features and structures that have remained unchanged throughout their evolution, preserving original traits or historical continuity. Important inherited elements like Taishan Temple and Lianjiang Academy should maintain their integrity and continuity, preserving their original appearance and historical information. Clonal variations, which are morphological changes adapting to social or human-induced influences, need adjustment to align with the overall landscape. For instance, variations in traditional commercial streets' architectural forms and materials should be harmonized with surrounding landscapes. Mutated cultural landscape genes, which have transformed into completely new forms unrelated to their original state, such as modern restaurants and shops, should be replaced or refurbished to maintain Linpu Village's traditional cultural style.

Regarding tourism and cultural industry development, Linpu Village should learn from successful rural development experiences in Japan, emphasizing the central role of villagers [62,63]. Organizing cultural lectures and vocational training can transmit traditional skills and customs. Collaborating with businesses in tourism projects can diversify villagers' income. Leveraging Linpu Village's unique cultural landscape genes to create high-value cultural and economic products involving artists and designers can enhance visibility and attractiveness. Collaborating with digital media professionals can also build the village's cultural IP. Traditional tours should evolve into interactive dynamic models, creating thematic routes to enhance consistency and memorability. Regularly adding interactive platforms and cultural activities can encourage repeat visits and highlight the village's unique features.

This study's theoretical contributions extend beyond Linpu Village, offering significant insights into cultural landscape studies and rural development. The innovative methodological framework we developed, combining connotative and spatial analyses, can be applied to other rural contexts to assess and preserve cultural landscapes. Our approach integrates tangible and intangible heritage elements into a cohesive analytical model, enhancing the understanding of cultural landscapes' spatial dynamics. The strategies proposed for sustainable rural development provide a replicable model for other traditional villages, emphasizing the importance of cultural sustainability alongside economic and social dimensions. By validating our theoretical models in the practical context of Linpu Village, we bridge the gap between theory and practice, encouraging further application and refinement in diverse settings. This interdisciplinary research advances theoretical discourse across cultural studies, geography, spatial analysis, and rural development, promoting a holistic understanding of cultural landscapes and encouraging future interdisciplinary collaborations.

Despite the significant contributions of this study, several limitations need to be acknowledged. Firstly, the research is confined to a single village, Linpu, which may limit the generalizability of the findings. While the methodologies and frameworks developed are theoretically applicable to other contexts, further research is needed to test and validate these approaches in diverse cultural and geographical settings. Secondly, the data collection relied heavily on qualitative methods, which, while providing deep insights, may introduce

subjectivity. Future studies could benefit from incorporating more quantitative data to enhance the robustness of the findings.

Additionally, the study primarily focuses on preserving and revitalizing cultural landscape genes without fully exploring the economic impacts of the proposed strategies. Longitudinal studies assessing the economic outcomes of implementing these strategies would provide valuable insights. Furthermore, the dynamic nature of cultural landscapes, influenced by ongoing social, economic, and environmental changes, necessitates continuous monitoring and adaptive management strategies. Future research should explore the development of real-time monitoring systems and adaptive management frameworks to ensure the sustainable preservation and utilization of cultural landscapes.

Finally, the role of community engagement and participation in the preservation and revitalization process was highlighted. However, further investigation is needed to understand the most effective ways to engage local communities and stakeholders in these efforts. Understanding the social dynamics and fostering strong community involvement is crucial for the success and sustainability of cultural landscape preservation initiatives.

By addressing these limitations and exploring these future research directions, we can further enhance our understanding and application of cultural landscape theory, contributing to the sustainable development and preservation of cultural heritage worldwide.

6. Conclusions

This study systematically identified and analyzed the cultural landscape genes of Linpu Village, utilizing a method and coding system widely adopted by other researchers, thereby enhancing the reliability and scientific rigor of our approach. By integrating connotative characteristics and spatial attribute quantification, our findings reveal the diverse and rich cultural landscape genes that exhibit typical Fuzhou characteristics and unique local charm. These attributes are crucial for the village's protection and revitalization.

Our research makes several key contributions to the field of cultural landscape studies and rural development. Firstly, the innovative methodological framework combining connotative and spatial analyses can be applied to other rural contexts, providing a comprehensive tool for cultural landscape research and planning. Secondly, the strategies proposed for transforming cultural landscape resources into economic vitality offer a replicable model for sustainable rural development, emphasizing the integration of cultural, economic, and social dimensions.

Despite these contributions, the study has several limitations. The focus on a single village, Linpu, may limit the generalizability of the findings. Future research should test and validate these approaches in diverse cultural and geographical settings. Additionally, the reliance on qualitative data introduces subjectivity, which can be mitigated by incorporating more quantitative data in future studies. Moreover, the economic impacts of the proposed strategies were not fully explored, suggesting the need for longitudinal studies to assess the long-term outcomes.

Future research should also develop real-time monitoring systems and adaptive management frameworks to address the dynamic nature of cultural landscapes. The effective engagement of local communities and stakeholders in the preservation and revitalization process remains a critical area for further investigation, as understanding social dynamics and fostering community involvement are essential for sustainable cultural landscape preservation.

In conclusion, this study advances the theoretical and practical understanding of cultural landscape genes and their role in sustainable rural development. By addressing the identified limitations and exploring the suggested future research directions, we can further enhance the application of cultural landscape theory, contributing to the preservation and development of cultural heritage worldwide.

Author Contributions: Conceptualization, S.L. and W.D.; Methodology, S.L. and L.W.; Software, L.W.; Validation, S.L. and C.X.; Formal analysis, L.W. and C.X.; Investigation, S.L., L.W. and W.D.; Resources, W.D.; Data curation, W.D.; Writing—original draft, L.W.; Writing—review and editing, S.L., L.W., C.X. and W.D.; Visualization, L.W. and C.X.; Supervision, W.D.; Project administration, S.L.; Funding acquisition, S.L. All authors have read and agreed to the published version of the manuscript.

Funding: This research was funded by (1) National Natural Science Foundation of China (NSFC), Grant No. 51778145; (2) National Natural Science Foundation of China (NSFC), Grant No. 52308054; (3) Fujian Provincial Social Science Foundation, Grant No. FJ2024B214; (4) Fujian Provincial Social Science Foundation, Grant No. FJ2023B100.

Data Availability Statement: Data are contained within the article.

Conflicts of Interest: The authors declare no conflict of interest.

References

1. Qiu, B.; Li, H.; Tang, Z.; Chen, C.; Berry, J. How cropland losses shaped by unbalanced urbanization process? *Land Use Policy* **2020**, *96*, 104715. [CrossRef]
2. Antrop, M. Landscape change and the urbanization process in Europe. *Landsc. Urban Plan.* **2004**, *67*, 9–26. [CrossRef]
3. Park, E.; Choi, B.-K.; Lee, T.J. The role and dimensions of authenticity in heritage tourism. *Tour. Manag.* **2019**, *74*, 99–109. [CrossRef]
4. Mokoena, L.G. Cultural tourism: Cultural presentation at the Basotho cultural village, Free State, South Africa. *J. Tour. Cult. Chang.* **2020**, *18*, 470–490. [CrossRef]
5. Thinh, N.K.; Gao, Y. Understanding the Informal Morphology of Villages-in-the-City: A Case Study in Hanoi City, Vietnam. *Sustainability* **2021**, *13*, 13136. [CrossRef]
6. Wang, T.; He, Q.; Wang, D.; Adeyeye, K.; Yu, P. Extension Theory for the Reconstruction of Traditional Villages: Case example in Dawa Village. In Proceedings of the 7th International Conference on Information Technology and Quantitative Management (ITQM)—Information Technology and Quantitative Management Based on Artificial Intelligence, Granada, Spain, 3–6 November 2019; pp. 191–198.
7. Ryberg-Webster, S. Heritage amid an urban crisis: Historic preservation in Cleveland, Ohio's Slavic Village neighborhood. *Cities* **2016**, *58*, 10–25. [CrossRef]
8. Jiang, Y.J.; Li, N.; Wang, Z.Y. Parametric Reconstruction of Traditional Village Morphology Based on the Space Gene Perspective-The Case Study of Xiaoxi Village in Western Hunan, China. *Sustainability* **2023**, *15*, 2088. [CrossRef]
9. Hu, Z.; Josef, S.; Min, Q.W.; Tan, M.; Cheng, F.L. Visualizing the cultural landscape gene of traditional settlements in China: A semiotic perspective. *Herit. Sci.* **2021**, *9*, 115. [CrossRef]
10. Hu, Z.; Wu, X. An Object-oriented Algorithm for Constructing the Conceptual Lattice of Cultural Landscape Genes of Traditional Settlements. *J. Geo-Inf. Sci.* **2024**, *26*, 604–619.
11. Jiang, S.; Fan, Y.; Zheng, W. Research Progress on Landscape's Gene Theory and Its Utilization in China. *J. Hum. Settl. West China* **2021**, *36*, 84–91.
12. Zheng, W.; Li, B.; Liu, P.; Zeng, R.; Deng, Y.; Zeng, C. Gene Identification and Zoning of Traditional Village Landscape Groups in Hunan Province. *Econ. Geogr.* **2021**, *41*, 204–212.
13. Xiang, Y.; Cao, M.; Qin, J.; Wu, C. Study of traditional rural settlements landscape genetic variability in Shaanxi Province based on accurate-restoration. *Prog. Geogr.* **2020**, *39*, 1544–1556. [CrossRef]
14. Muir, R. Geography and the history of landscape: Half a century of development as recorded in The Geographical Journal. *Geogr. J.* **1998**, *164*, 148–154. [CrossRef]
15. Zuo, D.; Li, C.; Lin, M.; Chen, P.; Kong, X. Tourism, Residents Agent Practice and Traditional Residential Landscapes at a Cultural Heritage Site: The Case Study of Hongcun Village, China. *Sustainability* **2022**, *14*, 4423. [CrossRef]
16. Haller, A.; Borsdorf, A. Huancayo Metropolitano. *Cities* **2013**, *31*, 553–562. [CrossRef]
17. Duncan, D.H.; Kyle, G.; Race, D. Combining facilitated dialogue and spatial data analysis to compile landscape history. *Environ. Conserv.* **2010**, *37*, 432–441. [CrossRef]
18. Owen, S.; Herlin, I.S. A Sustainable Development Framework for a Landscape of Dispersed Historic Settlement. *Landsc. Res.* **2009**, *34*, 33–54. [CrossRef]
19. Bazan, G.; Castrorao Barba, A.; Rotolo, A.; Marino, P. Vegetation series as a marker of interactions between rural settlements and landscape: New insights from the archaeological record in Western Sicily. *Landsc. Res.* **2020**, *45*, 484–502. [CrossRef]
20. Duan, Y.; Zhang, L.; Fan, X.; Hou, Q.; Hou, X. Smart city oriented Ecological Sensitivity Assessment and Service Value Computing based on Intelligent sensing data processing. *Comput. Commun.* **2020**, *160*, 263–273. [CrossRef]
21. Burghardt, K.; Uhl, J.H.; Lerman, K.; Leyk, S. Road network evolution in the urban and rural United States since 1900. *Comput. Environ. Urban Syst.* **2022**, *95*, 101803. [CrossRef]

22. Bergen, K.M.; Loboda, T.; Newell, J.P.; Kharuk, V.; Hitztaler, S.; Sun, G.; Johnson, T.; Hoffman-Hall, A.; Ouyang, W.; Park, K.; et al. Long-term trends in anthropogenic land use in Siberia and the Russian Far East: A case study synthesis from Landsat. *Environ. Res. Lett.* **2020**, *15*, 105007. [CrossRef]
23. Chi, X.; Sartor, M.A.; Lee, S.; Anurag, M.; Patil, S.; Hall, P.; Wexler, M.; Wang, X.-S. Universal concept signature analysis: Genome-wide quantification of new biological and pathological functions of genes and pathways. *Brief. Bioinform.* **2020**, *21*, 1717–1732. [CrossRef] [PubMed]
24. O'Brien, M.J. Genes, memes, and human history: Darwinian archaeology and cultural evolution. *J. Anthropol. Res.* **2003**, *59*, 380–381. [CrossRef]
25. Stent, G.S. You can take the ethics out of altruism but you can't take the altruism out of ethics. *Hastings Cent. Rep.* **1977**, *7*, 33–36. [CrossRef] [PubMed]
26. Pakendorf, B.; Stoneking, M. The genomic prehistory of peoples speaking Khoisan languages. *Hum. Mol. Genet.* **2021**, *30*, R49–R55. [CrossRef] [PubMed]
27. Holderegger, R.; Wagner, H.H. Landscape genetics. *Bioscience* **2008**, *58*, 199–207. [CrossRef]
28. Manel, S.; Schwartz, M.K.; Luikart, G.; Taberlet, P. Landscape genetics: Combining landscape ecology and population genetics. *Trends Ecol. Evol.* **2003**, *18*, 189–197. [CrossRef]
29. Anderson, C.D.; Epperson, B.K.; Fortin, M.-J.; Holderegger, R.; James, P.M.A.; Rosenberg, M.S.; Scribner, K.T.; Spear, S. Considering spatial and temporal scale in landscape-genetic studies of gene flow. *Mol. Ecol.* **2010**, *19*, 3565–3575. [CrossRef]
30. Hu, Z.; Liu, P. The conceptual model and characterizations of landscape genome maps of traditional settlements in China. *Acta Geogr. Sin.* **2015**, *70*, 1592–1605.
31. Hu, Z.; Liu, P.; Shen, X.; Deng, Y.; Li, B. Expression Mechanism of Landscape-Gene Information Unit of Traditional Settlement. *Geogr. Geo-Inf. Sci.* **2010**, *26*, 96–101.
32. Yin, L.; Liu, P. Type expression and spatial differentiation of planar archetype genes of traditional dwellings of the Xiangjiang River Basin. *Geogr. Res.* **2023**, *42*, 2191–2210.
33. Yin, Z.; Li, J. Identification and mapping of landscape gene in historic and cultural villages and towns: A case study of Dayuwan village, Huangpi district. *City Plan. Rev.* **2023**, *47*, 97–104, 114.
34. Chen, Q.; Yang, J.; Luo, S.; Sun, D. Identification and Extraction of the Linpan Culture Landscape Gene. *Trop. Geogr.* **2019**, *39*, 254–266.
35. Li, B.; Li, Z.; Liu, P.; Dou, Y. Activation path of human settlement environment of traditional villages from the perspective ofdouble repair: A case study of Zhang-Guying village in Hunan province. *Geogr. Res.* **2020**, *39*, 1794–1806.
36. Liu, P. On Construction and Utilization of Chinese Traditional Settlements Landscape's Genetic Map. Ph.D. Thesis, Peking University, Beijing, China, 2011.
37. Shen, X.; Liu, P.; Deng, Y.; Wang, L. Landscape communities of traditional settlement in southern China and their values of conservation and utilization. *Geogr. Res.* **2006**, *25*, 485–494.
38. Hu, Z.; Liu, P.; Deng, Y.; Zheng, W. A Novel Method for Identifying and Separating Landscape Genes from Traditional Settlements. *Sci. Geogr. Sin.* **2015**, *35*, 1518–1524.
39. Hu, Z. Retrospects and Outlooks on the Research of Cultural Landscape Gene of Traditional Settlements. *Geogr. Geo-Inf. Sci.* **2024**, 1–9. Available online: http://kns.cnki.net/kcms/detail/13.1330.P.20240612.0904.002.html (accessed on 2 August 2024).
40. Li, X.; Huang, H.; Wang, S. Study on the Identification and Application of Landscape Gene in the Promotion and Construction of Local Cultural Landscape. *Chin. Landsc. Archit.* **2022**, *38*, 29–34.
41. Liu, P.; Liu, Y.; Yang, L.; Li, X. Digital Transmission of Traditional Village Landscape Gene and Its Tourism Value Promotion: A Case Study of Zhangguying Village. *Econ. Geogr.* **2022**, *42*, 232–240.
42. Li, X.; Lei, A. Construction of Traditional Village Cultural Landscape Spatial Database from the Perspective of Landscape Gene: A Case Study of Gaochun District, Nanjing. *J. Hum. Settl. West China* **2023**, *38*, 110–116.
43. Wang, Z.; Zhang, Q.; Chen, Q. Spatial Reconstruction of Tourism-based Traditional Village Settlements and Rural Revitalization: A Case Study of Chongmudang Village in Xuefeng Mountain. *Econ. Geogr.* **2023**, *43*, 229–238.
44. Zhai, Z.; Chang, F.; Li, T.; Li, J.; Shi, Y.; Wu, P. Research on the Cultural Heritage Landscape Genome Maps of Traditional Villages in Shaanxi Province. *Geogr. Geo-Inf. Sci.* **2018**, *34*, 87–94, 113.
45. Zhang, Z.; Dong, G.; Wang, Y. Research on Local Knowledge Graph of Traditional Village Landscape in Dangjia Village, Hancheng City, Shaanxi Province. *Urban Stud.* **2021**, *28*, 25–31.
46. Zhang, P.; Lin, H. *Ancient Fujian Towns: Ancient Rural Commodity Markets in Fujian and Taiwan*; Fujian Map Publishing House: Fuzhou, China, 2008.
47. The Collaborating Organization for This Reference Is the Ministry of Housing and Urban-Rural Development of the People's Republic of China. The Seventh Batch of Chinese Historical and Cultural Towns and Villages List. Available online: https://www.gov.cn/zhengce/zhengceku/2019-09/27/content_5434160.htm (accessed on 18 April 2023).
48. Li, L. Establishment of Characteristic Atlas of Traditional Settlements Landscape in Multicultural Area: Take Southern Shaanxi for Example. *Areal Res. Dev.* **2020**, *39*, 175–180.
49. The Collaborating Organization for This Reference Is the Ministry of Housing and Urban-Rural Development of the People's Republic of China. Guiding Opinions on Effectively Strengthening the Protection of Traditional Chinese Villages. Available online: https://www.mohurd.gov.cn/gongkai/zhengce/zhengcefilelib/201409/20140912_218993.html (accessed on 20 May 2023).

50. Dawkins, R.L. The Selfish Gene. In *Evolution*; Oxford University Press: Oxford, UK, 1976; Volume 32, pp. 245–260.
51. Ministry of Natural Resources of the People's Republic of China. Classification and Codes for Fundamental Geographic Information Feature. Available online: https://std.samr.gov.cn/gb/search/gbDetailed?id=DD3D95E5C18271EBE05397BE0A0AF33F (accessed on 28 May 2023).
52. Wei, N.; Feng, X. Genetic Information Coding and Mapping of Traditional Settlement Landscapes in Northern Shaanxi. *South Archit.* **2023**, 88–97. [CrossRef]
53. Zhou, T.; Long, Y.; Tang, G.; Hu, L. Research on the Hybrid Index Structure for Aggregated Spatial Data. *Geogr. Geo-Inf. Sci.* **2010**, *26*, 7–10.
54. Zhang, G. A Logical Analysis of the Traditional Settlement Living Space from the Perspective of Syntax: Taking Linpu Village as an Example. *J. Minjiang Univ.* **2021**, *42*, 96–104. [CrossRef]
55. Geospatial Data Cloud. Available online: https://www.gscloud.cn/ (accessed on 14 October 2022).
56. Bureau, Fuzhou Natural Resources and Planning Bureau Fuzhou Historical and Cultural City Protection Plan (2021–2035). Available online: https://zygh.fuzhou.gov.cn/zwgk/ghjh/tdlyztgh/202209/t20220923_4439934.htm (accessed on 22 May 2023).
57. Zhang, T. *Historical and Cultural City, Town, and Village Chronicles of Fuzhou City*; Haichao Photography Art Publishing House: Fuzhou, China, 2004.
58. Fujian Provincial People's Government. Preservation Plan for Linpu Village in Chengmen Town, Cangshan District, Fuzhou City, a Historical and Cultural Village of Fujian Province. Available online: https://zygh.fuzhou.gov.cn/zfxxgkzl/gkml/ywgz/cxgh/201903/t20190328_2791942.htm (accessed on 13 May 2023).
59. Hu, H.; Hu, Z.; Wang, F.; Yi, Z. Features of Gene Information Chain of Traditional Village Landscape and Its Identification. *Econ. Geogr.* **2019**, *39*, 8.
60. Zhu, H.; Liu, J.; Wang, L.; Sun, D. Influence factors of residents' attitude and support to tourism development in ancient and cultural village: A case study of Linpu. *World Reg. Stud.* **2018**, *27*, 166–176.
61. Yang, L.; Hu, Y. Production and Inheritance of Intangible Cultural Landscape Gene in Traditional Villages: A Case Study of Huangdu Village in Tongdong Autonomous County. *Econ. Geogr.* **2022**, *42*, 208–215.
62. Kuroda, N. Conservation Design for Traditional Agricultural Villages: A Case Study of Shirakawa-go and Gokayama in Japan. *Built Herit.* **2019**, *3*, 7–23. [CrossRef]
63. Cai, G.; Xu, L.; Gao, W.; Hong, Y.; Ying, X.; Wang, Y.; Qian, F. The Positive Impacts of Exhibition-Driven Tourism on Sustainable Tourism, Economics, and Population: The Case of the Echigo-Tsumari Art Triennale in Japan. *Int. J. Environ. Res. Public Health* **2020**, *17*, 1489. [CrossRef] [PubMed]

Disclaimer/Publisher's Note: The statements, opinions and data contained in all publications are solely those of the individual author(s) and contributor(s) and not of MDPI and/or the editor(s). MDPI and/or the editor(s) disclaim responsibility for any injury to people or property resulting from any ideas, methods, instructions or products referred to in the content.

buildings

MDPI

Article

Development of a Building Evaluation Framework for Biophilic Design in Architecture

Rafa Ramisha Tabassum and Jihyun Park *

Department of Architecture, Ewha Womans University, 52 Ewhayeodae-gil, Seodaemun-gu, Seoul 03760, Republic of Korea; ramisha.rafa@ewhain.net
* Correspondence: jh.park@ewha.ac.kr

Abstract: Biophilic design has gained prominence in architecture as a strategy to integrate natural elements into built environments, aiming to improve human comfort, well-being, and environmental sustainability. This paper critically reviews existing biophilic design frameworks, identifying gaps in their integration of health outcomes and the relationship between indoor and outdoor environments, with a primary focus on indoor environmental quality (IEQ) factors such as air quality, natural light, thermal comfort, and acoustics. The review was conducted systematically, comparing frameworks using criteria such as health benefits, human–nature connections, and user satisfaction. Key findings highlight a lack of comprehensive frameworks that explicitly link biophilic design to measurable improvements in human health, comfort, and satisfaction. To address this gap, the study proposes an enhanced biophilic design framework that bridges IEQ-focused indoor environments with urban outdoor elements, prioritizing human comfort alongside environmental sustainability. The framework also emphasizes the role of post-occupancy evaluation (POE) in assessing the real-world performance of biophilic interventions, particularly in achieving user satisfaction and ensuring long-term effectiveness. This research contributes to the advancement of biophilic design by offering actionable strategies for architects, urban planners, and policymakers to adopt biophilic principles that create resilient, healthy, and sustainable spaces. Additionally, the study emphasizes the need for empirical testing and validation of the proposed framework, including POE and user surveys, to assess its real-world impact on human well-being and satisfaction, thus setting the stage for future research.

Keywords: biophilic design; indoor environmental quality; human comfort; urban sustainability; environmental features; nature integration; well-being in architecture; sustainable urban development; human–nature connection; health and well-being; resilient environments

1. Importance of Biophilic Design in Architecture

Biophilic design has emerged as a crucial approach in sustainable architecture, emphasizing the integration of natural systems into the built environment to enhance both human well-being and ecological sustainability [1–5]. By embedding natural elements into urban structures, biophilic design promotes spaces that are not only ecologically responsible but also psychologically fulfilling [6–8]. This approach effectively addresses urban challenges such as the heat island effect by increasing vegetation cover, shading, and evapotranspiration. These strategies reduce environmental impact while enhancing human comfort and satisfaction [9,10].

This disconnect between nature and urban settings is evident in various fields, including education, healthcare, architecture, and urban development. This underscores the need to design buildings that not only respond to sustainability challenges but also positively contribute to the surrounding environment [6,11–15].

As global climate change continues to intensify, there is a growing need to reevaluate traditional architectural practices. Newer methods must contribute positively to sustainability while prioritizing human comfort [16–18]. In this context, biophilic design

stands out compared to other sustainable architectural concepts such as Green Architecture, Climate-Responsive Architecture, Net-Zero Architecture, and Vernacular Architecture (see Table 1). These approaches each address specific aspects of sustainability; however, biophilic architecture provides a more holistic solution for fostering long-term resilience in urban environments [19–25].

Table 1. A Comparative review of architectural concepts that aim to achieve sustainability.

		Architecture with the Concepts of Sustainability				
		Green Architecture	**Climate-Responsive Architecture**	**Net-Zero Architecture**	**Vernacular Architecture**	**Biophilic Architecture**
Sustainable Components	Durability	●	◍	●	◍	●
	Indoor Air Quality (IAQ)	●	●	●	●	●
	Health and Well-being	◍	◍	◍	●	●
	Energy and CO_2 Emissions	●	●	●	◍	●
	Sustainable Materials	●	●	●	●	●
	Water Conservation	●	○	○	●	●
	Surface-water Run-off Pollution	○	○	○	○	●
	Waste Reduction	●	○	●	○	●
	Management	●	◍	●	◍	●
	Ecology	○	○	○	○	●

● Fully integrated. ◍ Partially considered with limitations. ○ Not emphasized.

A key aspect of this reassessment involves focusing on indoor environmental quality (IEQ), which plays a vital role in optimizing occupant health, comfort, and productivity [26–29]. Given that modern humans spend approximately 90% of their time indoors [30], the quality of indoor environments—particularly in the integration of natural elements—becomes pivotal to overall well-being [8,14]. While biophilic design shows promise in addressing these concerns, more empirical studies are needed to validate its impact on health outcomes [5,8,14,31]. By addressing the needs people seek to fulfill through their built environments, architects can create spaces that are both sustainable and ecologically regenerative [3,27,32,33].

While other approaches, such as Green Architecture, emphasize energy efficiency and material sustainability, or focus on adapting buildings to climate conditions, like Climate-Responsive Architecture, biophilic architecture is distinguished by its holistic integration of sustainable components. These include durability, indoor air quality (IAQ), health and well-being, energy and CO_2 emissions, sustainable materials, water conservation, surface-water run-off pollution, waste reduction management, and ecology [3,34–38]. This broad focus on both environmental and human well-being sets biophilic architecture apart from other sustainable design concepts. For instance, Green Architecture often prioritizes measurable environmental outcomes like CO_2 emission reduction, while biophilic architecture focuses more holistically on integrating natural elements to enhance the emotional and psychological comfort of occupants [11,39–41]. Moreover, when compared to Net-Zero Architecture, which is primarily driven by energy efficiency and minimizing CO_2 emissions, biophilic architecture takes a broader approach by addressing not only energy and environmen-

tal performance but also the human experience within the space [3,42–44]. Additionally, while Vernacular Architecture is grounded in local materials and traditional techniques, biophilic architecture incorporates ecological principles to foster a strong connection with nature, addressing both the physical and emotional dimensions of the human experience in buildings [31,43–45].

The need for beneficial contact with nature is well documented, with substantial evidence linking it to improved health and well-being. However, achieving this in the built environment presents significant challenges, particularly in ensuring adequate exposure to natural light, ventilation, natural materials, and green spaces [6,8]. This disconnection has profound implications, not only for individual well-being but also for the broader goal of environmental sustainability. Therefore, biophilic design addresses these gaps by offering a more integrated approach that harmonizes indoor and outdoor experiences, particularly through elements such as natural light, ventilation, and green spaces. This integration improves the overall quality of life for building occupants [10,11,46–49].

The biophilic framework proposed in this study aims to fill the gaps left by existing frameworks, particularly by integrating both indoor and outdoor environmental factors. Existing approaches may excel in specific areas, such as energy conservation in Net-Zero Architecture or cultural responsiveness in Vernacular Architecture, but biophilic architecture incorporates a broader range of sustainable components, making it a comprehensive and flexible solution for urban development [50,51].

In conclusion, biophilic design not only addresses the pressing issues of sustainability but also enhances the quality of life for building occupants by fostering a stronger connection to nature. Its holistic approach ensures that the built environment caters to both ecological and human needs, making it an essential framework for the future of sustainable architecture [31].

2. Materials and Methods

This study employed a structured methodology to develop a comprehensive biophilic design framework, focusing on human comfort, well-being, and environmental sustainability, with a slight inclusion of outdoor elements. The methodology was divided into two key phases: (1) a systematic literature review and (2) framework development.

2.1. Systematic Literature Review

The first phase of the methodology involved a systematic review of existing biophilic design frameworks, particularly in architectural and urban planning contexts. The aim was to identify key gaps and limitations, particularly regarding human health, well-being, and environmental sustainability. This process followed a rigorous structure, detailed below.

Search Strategy

The literature search targeted peer-reviewed articles, books, and authoritative reports on biophilic design using databases such as Scopus, Web of Science, and Google Scholar. Keywords included “biophilic design”, “human comfort”, “well-being in architecture”, “sustainable urban development”, “nature integration”, and “Indoor Environmental Quality (IEQ)”. A particular focus was placed on frameworks that directly connected biophilic elements with measurable impacts on human health and environmental performance.

Inclusion/Exclusion Criteria

The following criteria guided the inclusion of studies:

- Published between 1980 and 2024.
- Direct focus on biophilic design frameworks in urban and architectural settings.
- Empirical or theoretical analysis of the impact of biophilic design on human health, well-being, or environmental outcomes.
- Studies focusing solely on natural landscapes or unrelated to built environments were excluded, ensuring the review remained relevant to architectural applications and human comfort.

Data Extraction and Synthesis

Key data were extracted on biophilic elements (e.g., natural light, vegetation, air quality), methodologies for assessing their impact, and their outcomes related to human comfort, health, and environmental performance. The comparative analysis of existing frameworks highlighted strengths, weaknesses, and areas for improvement, particularly in connecting indoor and outdoor environments and linking biophilic elements to human health benefits. Specific attention was given to frameworks that had measurable outcomes, addressing the gap identified in earlier studies.

2.2. Development of the Biophilic Design Framework

Building on the findings from the systematic literature review, this study developed an enhanced biophilic design framework, addressing gaps in the current frameworks. This phase focused on three primary areas.

Human Comfort and Well-being

The new framework prioritized measurable outcomes related to human health and comfort, including metrics such as visual comfort, air quality, stress reduction, and thermal comfort. Key biophilic design elements—such as natural ventilation, daylighting, green spaces, and water features—were integrated to enhance these outcomes in both indoor and outdoor environments.

Indoor–Outdoor Connection

A key feature of the proposed framework was the seamless integration of indoor and outdoor environments, promoting a holistic connection with nature. The framework incorporated design strategies like open spaces, balconies, rooftop gardens, and visual access to natural surroundings, aiming to foster a stronger connection between occupants and nature, thereby enhancing well-being.

Sustainability and Practical Considerations

The framework also addressed the practical challenges of biophilic design, including cost-effectiveness, scalability, and maintenance. It proposed flexible solutions that could be adapted to a range of urban settings, from residential to commercial spaces. Sustainable materials, water conservation, energy efficiency, and waste management strategies were emphasized to support the environmental sustainability component of biophilic design.

Framework Evaluation: To ensure the robustness of the proposed biophilic design framework, this study recommends empirical validation through future research, using methods such as case studies, user surveys, or experimental evaluations. These tests would assess the practical applicability of the framework across diverse built environments and its effectiveness in improving human comfort, satisfaction, and environmental performance.

3. Review of Existing Biophilic Design Frameworks

3.1. Historic Context and Evolution

The concept of biophilic design, which has been gaining increasing attention in recent architectural discourse, has deep historical roots, tracing back to humanity's inherent connection with nature. Before the industrialization and urbanization eras, human societies relied heavily on interaction with natural environments for both survival and well-being. Historically, human settlements were multi-sensory environments, where natural elements such as light, air, greenery, water, and sound played a central role in daily life [10,52,53]. These natural settings provided essential experiences that shaped emotional and psychological well-being, a connection that neuroscientific studies now confirm as a fundamental human need [54–56]. Research employing modern neuroimaging techniques has shown that contact with nature positively influences brain activity, reducing stress and promoting cognitive restoration [54–56].

The term "Biophilia", foundational to biophilic design, originates from the Greek words "philia" (love) and "bios" (life or living things). Introduced by German psychoanalyst Erich

Fromm in 1973, it describes humanity's inherent "love for life" and attraction to the natural world. This concept was popularized by American biologist Edward O. Wilson in his seminal work *Biophilia* (1984), which introduced the "Biophilia Hypothesis" [6,50]. This theory posits that humans possess an innate affinity for living systems, shaped by evolutionary processes that foster psychological and physical well-being through close interactions with nature [57–61]. Wilson's hypothesis has catalyzed further philosophical and scientific inquiries into how reconnecting with nature can enhance human health, comfort, and satisfaction.

Despite its formal recognition in the late 20th century, biophilic design is not a novel architectural concept. The integration of natural forms and elements into built environments has been prevalent throughout history, long before the term "biophilia" existed. The Art Nouveau movement of the late 19th century, for example, drew heavily on organic and natural motifs, with architects and designers like Victor Horta, Hector Guimard, Louis Comfort Tiffany, and Antonio Gaudí creating works inspired by the natural world. Their use of flowing lines, plant-like structures, and biomorphic forms served not only as decorative features but also aimed to harmonize human-built environments with nature, fostering a deeper emotional connection to the surrounding world [5,17].

Biophilic design, as it is understood today, represents a re-emergence of this long-standing human tradition of integrating natural elements into architecture. From ancient civilizations to the Art Nouveau movement and contemporary biophilic design, the use of natural forms in architecture has persisted as a means of promoting human well-being. This historical evolution underscores the critical importance of biophilic principles in modern architecture, particularly in urban contexts where nature is often absent. By integrating natural elements into urban spaces, biophilic design offers a path to enhancing human comfort, satisfaction, and health in environments increasingly detached from nature due to urbanization and technological advancements [26,62,63].

In conclusion, the historical context of biophilic design reveals a continuous effort to reconnect built environments with the natural world. As urbanization continues to reshape human living spaces, the re-integration of biophilic elements emerges not only as an aesthetic choice but as a necessary design strategy for promoting human well-being and environmental sustainability. This evolution demonstrates that biophilic design is not merely a modern trend but a fundamental design principle central to architectural practices throughout history [5,10,64].

3.2. Analysis of Biophilic Design Frameworks

Biophilic design frameworks have evolved over time, offering diverse methods to integrate natural elements into built environments with the overarching goal of enhancing human comfort, health, and well-being. This section presents a comparative analysis of seven prominent frameworks, detailing their focus areas, key dimensions, and strategies [11,65,66].

Table 2 outlines the main features of each framework, highlighting how they approach biophilic design and human–nature interaction in architectural and urban settings. The frameworks range from Kellert et al.'s focus on environmental features and natural forms to Ryan et al.'s emphasis on multi-sensory biophilic interventions. While each framework brings unique strengths, there are variations in how they address key design patterns and human well-being [11,12,32,66].

A comprehensive review of existing biophilic design frameworks reveals significant gaps, especially regarding their application to urban environments and the explicit connection between design elements and health benefits. While these frameworks emphasize biophilic principles, they often lack clarity in defining how specific urban design elements correlate with health improvements, such as enhanced air quality, stress reduction, and cognitive function [3,67].

Table 2. Comparative analysis of biophilic design frameworks.

Research	Main Focus	Dimensions/Attributes	Key Patterns/Strategies
Kellert et al. [2]	Connection between humans and nature via architecture	6 attributes: Environmental features, Natural shapes and forms, Natural patterns, Light, Place, Evolutionary perspectives	3 types of experience: direct, indirect, symbolic interaction with nature
Ryan and Browning (14 Patterns) [39]	Framework to enhance human well-being in the built environment	14 patterns: Visual connection, Non-visual stimuli, Airflow variability, etc.	Strategies for sensory experiences, restorative environments
Kellert & Calabrese (Experiences) [6]	Expands on Kellert's 2008 work by detailing direct experiences with nature	Direct (water, plants, light), Indirect (images, colors, shapes), Experience of place	Comprehensive link between environment and human interaction
Makes and Sense (Economic Benefits of Biophilic) [65]	Stress reduction, cognitive function improvement	4 major areas: Nature in space, Natural analogs, Nature of space	Patterns for sensory balance, space configuration
Brielmann et al.(Fractal Effects in Urban Design) [55]	Neuroscience of human comfort and aesthetics	Biophilic elements based on cognitive response to the environment	Principles related to fractals, complexity, and mental stimulation
Ryan and Browning, (Seven Dimensions) [18]	Framework focused on enhancing health and well-being through biophilia	7 dimensions: Visual, Non-visual, Auditory, Olfactory, Tactile, Thermal, Spatial	Multi-sensory biophilic interventions
Untaru et al. (Biophilic Interventions) [66]	Biophilic design for urban environments	Urban biophilic interventions for well-being and sustainability	Focus on green infrastructure, urban integration

For example, design elements like green courtyards, rooftop gardens, and water features are frequently recommended but without a clear articulation of their direct health benefits. This omission makes it difficult for practitioners to understand how these elements can be strategically implemented to maximize both physical and mental health outcomes [68–72]. As a result, practitioners may struggle to implement biophilic design strategies that deliver tangible health benefits, particularly in complex urban environments where these considerations are most crucial [42,73].

By explicitly linking biophilic design elements to their health benefits, as demonstrated in Table 3, this structured approach enhances the practical application of biophilic principles in urban environments. For instance, incorporating plants and natural ventilation into buildings not only improves air quality but also regulates humidity and reduces noise, contributing to overall well-being [63,74]. Similarly, green streets and pedestrian-friendly spaces foster a sense of connection with nature, improve air quality, and alleviate stress—key for urban dwellers [5,75–77].

Moreover, this structured approach addresses the need for a more user-friendly framework, where each category is clearly organized and presented. Such organization provides a comprehensive view of how biophilic design can be strategically implemented across various urban scales, ultimately benefiting the well-being of city inhabitants [8,78,79].

To fully unlock the potential of biophilic design in urban settings, future frameworks must provide clear, actionable strategies that link design elements to health outcomes. By doing so, architects and urban planners can create sustainable, resilient environments that support human well-being and ecological balance [10,80].

Table 3. Integration of biophilic design elements and health benefits into urban design components.

Urban Design Components	Biophilic Design Elements	Health Benefits
Buildings	- Green Courtyards and Roofs	- Better Air Quality - Humidity Regulation - Noise Reduction- Stress Reduction - Enhanced Cognitive Function
	- Indoor and Outdoor Plants	- Better Air Quality - Stress Reduction - Enhanced Immune System
	- Water Features/Reservoirs	- Humidity Regulation - Stress Reduction - Faster Recovery
	- Natural Daylight and Ventilation	- Better Air Quality - Stress Reduction
	- Nature Images and Paintings	- Stress Reduction - Improved Life Satisfaction
Public Spaces	- Green Areas and Pocket Parks	- Stress Reduction - Enhanced Cognitive Function—Sense of Connection
	- Ecology Parks and Native Species Yards	- Enhanced Immune System - Faster Recovery
	- Water Features/Reservoirs	- Stress Reduction - Humidity Regulation
	- Natural Sounds/Creating Artificial Nature Sounds	- Stress Reduction
Streets	- Green Streets and Road-side Parks	- Better Air Quality - Sense of Connection
	- Skinny Streets and Vegetated Swales	- Better Air Quality - Noise Reduction
Transport	- Accessibility/Pedestrian Connections	- Stress Reduction - Sense of Connection
	- Proper Road, Rail, Bicycle, and Pedestrian Networks	- Improved Life Satisfaction
Landscape	- Native and Edible Landscaping	- Enhanced Immune System - Sense of Connection
	- Thermally Treated Timber and Natural Materials	- Enhanced Cognitive Function—Improved Life Satisfaction

3.2.1. Strengths and Limitations Regarding IEQ and POE

In this section, we evaluate the strengths and limitations of these frameworks (Table 2) concerning indoor environmental quality (IEQ) and post-occupancy evaluation (POE), two critical areas for assessing building performance and human comfort.

a. Kellert et al. (Attributes) [2]

Strengths: The framework emphasizes enhancing human well-being through natural elements and evolutionary perspectives. This indirectly supports IEQ by improving the emotional and cognitive experience of users through natural light, air quality, and access to views.

Limitations: While it touches on environmental features, it does not specifically address IEQ parameters like thermal comfort, acoustics, or air quality in depth, nor does it incorporate POE for evaluating user satisfaction post-occupancy.

b. Ryan and Browning (14 Patterns) [39]

Strengths: This framework, with its 14 patterns, is more explicit about improving aspects related to IEQ, such as thermal variability, airflow, and natural ventilation, aligning directly with physical comfort factors. Some patterns also implicitly support POE through adaptability in design.

Limitations: Although it improves certain IEQ aspects, the framework doesn't offer specific guidance on post-occupancy evaluation to assess the success of these interventions over time.

c. Kellert and Calabrese (Experiences) [6]

Strengths: Their framework integrates direct and indirect experiences of nature, fostering environments that can enhance sensory experiences tied to air quality, lighting, and thermal comfort.

Limitations: The framework lacks explicit mention of IEQ standards or a structured approach to conducting POE to measure how well the space performs for users after occupancy.

d. Makes and Sense (Economic Benefits of Biophilic) [65]

Strengths: This work focuses on stress reduction and cognitive function, with some consideration of acoustic comfort and natural ventilation, tying into IEQ elements. This framework could be adapted for ongoing user evaluation via POE.

Limitations: Although it touches on comfort-related aspects of IEQ, the framework does not comprehensively cover all IEQ factors (e.g., thermal comfort and lighting quality) or provide detailed mechanisms for POE.

e. Brielmann et al. (Fractal Effects in Urban Design) [55]

Strengths: Salingaros connects biophilia to neuroscience, emphasizing mental well-being and cognitive engagement with space, which supports the psychological dimension of IEQ.

Limitations: Physical IEQ aspects like air quality and thermal conditions are not explicitly addressed. There is also no mention of post-occupancy evaluation to validate user satisfaction or comfort.

f. Ryan and Browning(Seven Dimensions) [18]

Strengths: This framework is particularly strong in addressing multi-sensory biophilic interventions, including non-visual sensory stimuli that align with IEQ. It focuses on auditory, thermal, and spatial experiences, making it relevant for enhancing indoor comfort.

Limitations: While it addresses IEQ aspects, it lacks formalized methods for evaluating the success of these interventions through POE, leaving a gap in post-occupancy assessment.

g. Untaru et al. (Biophilic Interventions) [66]

Strengths: Han's framework is more urban-focused but includes interventions such as green infrastructure and urban greenery, which can contribute to improving outdoor IEQ. It can also incorporate POE through community engagement and satisfaction metrics in urban settings.

Limitations: The framework lacks detailed strategies for evaluating indoor IEQ in buildings and does not provide structured POE techniques to track ongoing user satisfaction.

3.2.2. Identified Key Gaps

a. IEQ Gaps: Many frameworks acknowledge sensory aspects, such as natural light, air quality, and temperature regulation, but fail to address IEQ comprehensively, particularly with regard to acoustics, thermal comfort, and detailed indoor air quality standards. More integration of IEQ standards such as the ASHRAE or the WELL Building Standard® could strengthen their applicability [3,62].
b. POE Gaps: None of the frameworks explicitly includes methods or tools for post-occupancy evaluation, which is a critical gap. POE could provide valuable feedback on how biophilic interventions perform in real-world settings, guiding future improvements and ensuring sustained user comfort and satisfaction [8,31,81].
c. Recommendations for Improvement

Integrate Comprehensive IEQ Standards

Frameworks should incorporate more robust IEQ standards, ensuring a holistic approach to indoor environments that considers acoustics, thermal comfort, and air quality. The incorporation of standards from organizations such as the ASHRAE or the WELL Building Standard® would enhance the frameworks' effectiveness and applicability in various settings [3].

Establish Structured POE Mechanisms

There is a critical need for frameworks to include methods for conducting structured POE, which can help in assessing user comfort and satisfaction after occupancy. By integrating feedback mechanisms and evaluation tools, these frameworks could be continuously improved based on real-world performance and user feedback [8].

Strengths

The frameworks excel in integrating nature-based design strategies that promote well-being, stress reduction, and sensory engagement. These contribute to the overall comfort of occupants, even if IEQ and POE are not explicitly mentioned.

The use of multi-sensory design patterns is a major strength, as it encourages designers to consider more than just visual aesthetics when integrating biophilia, extending to auditory and tactile experiences.

In conclusion, while these biophilic design frameworks offer valuable approaches to enhancing human–nature interaction in architecture, they often fall short in providing comprehensive guidelines on IEQ and lack structured POE mechanisms to assess user comfort post-occupancy. Expanding these frameworks to include rigorous IEQ standards and incorporating POE would improve their application in contemporary architectural practice.

4. Biophilic Design Aspect for Human Comfort

4.1. Indoor and Outdoor Design Elements

Biophilic design presents a comprehensive approach that integrates natural elements into both indoor and outdoor environments, thereby enhancing occupant well-being and promoting sustainability. Table 4 below summarizes key aspects of indoor and outdoor biophilic design, categorizing their primary foci, key elements, benefits, challenges, and essential considerations for implementation.

Indoor biophilic design emphasizes the integration of natural elements such as plants, natural light, and water features within confined spaces, contributing to improved air quality, stress reduction, and increased productivity [3,37,81–83]. This approach is highly adaptable to various climates and locations, allowing customization based on user preferences and needs [8,53,84,85]. However, challenges such as limited space, reliance on artificial lighting, and the maintenance of indoor plants present notable obstacles [17,53,62,86–88].

Conversely, outdoor biophilic design integrates buildings and open spaces with natural surroundings. This approach factors in landscaping, weather, and biodiversity preservation, which are critical for urban planning and the conservation of green spaces [3,15,75,89–91]. While outdoor designs can be unpredictable due to natural variations, they offer significant benefits, including improved mental well-being, physical health, and community bonding [64,92–94]. These features are particularly valuable in urban settings, where access to nature may be limited [95–98].

Table 4. Aspects of indoor and outdoor biophilic design.

Aspect	Indoor Biophilic Design	Outdoor Biophilic Design
Primary Focus	Enhancing interior spaces	Integrating natural elements into outdoor environments
Key Elements	Living walls, indoor plants, natural light, water features	Green roofs, gardens, parks, natural water features, landscaping
Human Benefits	Improved air quality, stress reduction, increased productivity	Enhanced mental well-being, physical health, and community bonding
Design Integration	Incorporating nature into architecture and interior elements	Landscaping, urban planning, preservation of green spaces
Challenges	Limited space, artificial lighting, maintenance of indoor plants	Weather considerations, biodiversity preservation
Sensory Experience	Aroma, touch, visual appeal, sounds of nature	Sounds of nature, visual aesthetics, tactile experiences
Application Scales	Homes, offices, commercial spaces	Parks, public spaces, urban planning projects
Accessibility	Available in various climates and locations	Dependent on outdoor space availability, weather conditions
Cost Considerations	Initial setup costs, maintenance expenses	Initial landscaping costs, ongoing maintenance, and upkeep
Sustainability Focus	Sustainable materials, energy-efficient designs	Preservation of natural ecosystems, eco-friendly landscaping
Community Impact	Indoor green spaces within communities	Public parks, communal outdoor spaces
Wellness Connection	Mental and emotional well-being, connection to nature indoors	Physical health benefits, community well-being outdoors

4.2. Impact on Psychological and Physiological Comfort

Biophilic design, both indoors and outdoors, has a profound impact on human comfort by addressing psychological and physiological well-being. By connecting occupants with nature, this design approach transcends aesthetic appeal and fulfills the innate human need for natural interaction.

(1) Psychological Comfort: Indoor biophilic design creates calming environments that reduce stress and anxiety. The inclusion of plants, natural light, and water features indoors supports mental well-being, enhances cognitive function, and increases creativity and productivity [3,37,42,44,99,100]. Given that people spend a significant portion of their lives indoors, connecting with nature inside these spaces helps mitigate the disconnect from the natural world experienced by many urban dwellers [101–103].

Outdoor biophilic design, on the other hand, enhances psychological comfort by providing spaces for physical activity, social interaction, and relaxation in natural settings. Exposure to natural sounds, visual aesthetics, and tactile experiences outdoors significantly reduces stress, promotes mental clarity, and improves overall mood [17,26,81,104,105]. This design fosters community bonding by creating accessible natural spaces where people can gather and interact, contributing to collective well-being [5,14,18,40,106].

(2) Physiological Comfort: Biophilic design also positively influences physical health. Indoors, it improves air quality, regulates humidity, and creates more comfortable thermal environments. For example, indoor plants act as natural air purifiers, absorbing toxins and releasing oxygen, which contributes to better respiratory health and overall physical well-being [3,74,107–111]. Natural light and water features support circadian rhythms and reduce dependence on artificial lighting, promoting a healthier living or working environment [5,44,85,112].

Outdoors, biophilic design mitigates urban heat island effects through vegetation and green spaces [5,89,113,114]. Parks and gardens designed with biophilic principles provide essential spaces for exercise, relaxation, and social interaction, all of which contribute to physical well-being. Additionally, the inclusion of natural elements such as water bodies

and vegetation in urban settings helps moderate temperatures, reduce pollution, and create a healthier environment for communities [63,64,81,115].

In conclusion, biophilic design integrates nature into both indoor and outdoor spaces, significantly enhancing human comfort by addressing psychological and physiological needs. By connecting people with nature, this design approach not only improves individual well-being but also promotes a healthier, more sustainable built environment.

5. Development of a Biophilic Evaluation Framework

The newly developed framework (Table 5), Integrated Biophilic Design for Human Comfort and Sustainability, addresses critical gaps in previous biophilic design frameworks by combining indoor and outdoor design strategies with a strong focus on human comfort, sustainability, and the integration of indoor environmental quality (IEQ) and post-occupancy evaluation (POE). This framework is unique because it extends beyond traditional indoor-centric approaches by incorporating outdoor dimensions while maintaining a primary focus on indoor spaces, where people spend 90% of their time. It also prioritizes empirical data collection through POE, making it not just a design guideline but a dynamic evaluation tool that can adapt to evolving building environments and occupant needs.

Table 5. Integrated biophilic design for human comfort and sustainability.

Design Dimension	Components	Human Comfort Factors	Sustainability Factors	Integration of IEQ and POE	Performance Metrics
Direct Experiences of Nature	Natural light, plants, water features, outdoor views, fresh air	Visual comfort, air quality, emotional well-being	Energy efficiency, biodiversity, water conservation	IEQ: Focus on natural ventilation, daylight, and air quality. POE: User satisfaction with light levels, air quality, and environmental controls, extended to outdoor views and fresh air.	- Daylight availability (lux) - CO_2 concentration (ppm) - Thermal comfort (°C) - Glare index (DGI) - User satisfaction with natural features (indoor and outdoor)
Indirect Experiences of Nature	Natural materials, views of nature, nature-inspired shapes, green roofs	Cognitive engagement, psychological relaxation	Use of sustainable materials, reduced waste, integration of urban green infrastructure	IEQ: Use of low-VOC, sustainable materials indoors, green roofs for better thermal insulation. POE: Feedback on material quality, engagement with nature (views, greenery).	- VOC concentration (mg/m^3) - Visual satisfaction (survey) - Thermal resistance (R-value) - Survey: engagement with nature (views, indoor plants)
Dynamic and Diffuse Light	Daylight, circadian lighting, shading systems, skylights	Visual comfort, stress reduction, circadian support	Energy reduction, adaptability of lighting systems	IEQ: Focus on circadian lighting, dynamic daylight integration. POE: Impact of lighting on sleep cycles, mood, and productivity (indoors), with some outdoor considerations for shade.	- Circadian stimulus (CS) - Illuminance (lux) - Luminance contrast ratio - Melatonin suppression (%) - Sleep quality surveys (indoor environment focus)
Thermal and Airflow Variability	Adaptive ventilation, outdoor breezeways, natural cooling systems	Thermal comfort, cognitive performance, air quality	Energy efficiency through natural cooling, reduced HVAC demand	IEQ: Enhance thermal comfort with adaptive systems indoors, extend airflow strategies to outdoor spaces. POE: Measure satisfaction with temperature control, airflow indoors and outdoors.	- Air speed (m/s) - Operable windows usage (%) - Survey: thermal satisfaction (indoor and outdoor spaces) - Radiant temperature asymmetry (°C)
Non-visual Sensory Stimuli	Soundscapes, textured materials, natural sounds (water, wind)	Auditory comfort, tactile engagement	Reduced noise pollution, enhanced material durability	IEQ: Focus on acoustic comfort, especially with natural sound elements. POE: Evaluate responses to soundscapes and tactile materials indoors and in semi-outdoor spaces (courtyards, atriums).	- Background noise level (dBA) - Tactile response to materials (survey) - Surface texture coefficient - Sound masking and absorption (indoor and outdoor sound quality)
Spatial Variability and Prospect-Refuge	Enclosed spaces, open vistas, urban gardens, rooftop retreats	Psychological comfort, sense of safety, cognitive restoration	Flexible use of space, efficient land use	IEQ: Offer variety in spatial experiences, including enclosed and open areas, indoors and out. POE: Surveys on comfort and sense of security in enclosed vs. open spaces (indoors/outdoors).	- Occupant density (per m^2) - Privacy score (survey) - Visual connection to outdoors (window-to-wall ratio) - Sense of security and comfort (survey: indoor and outdoor)
Biophilic Urban Integration	Urban green spaces, street trees, water management systems, biodiversity	Outdoor comfort, social interaction, overall well-being	Urban biodiversity, stormwater management, pollution control	IEQ: Leverage green infrastructure for better air quality and outdoor comfort. POE: Community engagement and feedback on outdoor spaces, integration with the indoor environment.	- Pollution reduction (PM2.5/PM10) - Stormwater retention rate (mm/hr) - Urban biodiversity index (species count) - Satisfaction with outdoor spaces (surveys)

5.1. Development of Biophilic Framework and Key Strengths

(1) Holistic Integration of Indoor and Outdoor Environments

One of the most significant strengths of this framework is its inclusion of both indoor and outdoor biophilic design elements. Many existing frameworks focus primarily on indoor spaces, addressing direct and indirect experiences with nature, but often fall short in connecting these experiences with the outdoor environment. The current table bridges this gap by including outdoor strategies like urban gardens, green roofs, and outdoor views, which improve both psychological well-being and environmental performance [3].

This holistic approach is particularly innovative because it recognizes that outdoor spaces—such as rooftop gardens, green walls, or tree-lined walkways—can be as vital as indoor spaces in promoting well-being [31]. The focus on urban integration through features like biodiversity and stormwater management positions this framework as more environmentally comprehensive than many earlier models [31].

(2) Detailed Focus on Human Comfort and Well-being

Unlike earlier frameworks that are more general in their approach to human comfort [52], this table is explicitly geared towards ensuring various forms of comfort—visual, thermal, acoustic, and psychological—while also addressing cognitive and emotional needs. For instance, the Direct Experiences of Nature dimension focuses on comfort factors such as visual comfort and emotional well-being, supported by specific design interventions like natural lighting and air quality improvement [5].

What sets this table apart is the incorporation of non-visual sensory stimuli and prospect-refuge theory to create a more inclusive and adaptable environment. Non-visual sensory experiences, such as soundscapes or tactile textures, go beyond traditional frameworks that focus predominantly on the visual connection to nature [64]. These deeper sensory experiences are crucial in reducing stress and increasing occupant satisfaction, as highlighted in the table's Non-Visual Sensory Stimuli dimension.

(3) Rigorous Performance Metrics

A key differentiator of this framework is its extensive performance metrics, which are designed to be measurable and evidence-based. Existing frameworks provide qualitative strategies for implementing biophilic design, but they often lack detailed metrics for measuring success. By contrast, this table incorporates quantifiable metrics such as daylight availability (lux), CO_2 concentration (ppm), and circadian stimulus (CS). These metrics allow for the empirical evaluation of biophilic design outcomes, making it more robust and adaptable to future innovations in design and technology.

The emphasis on post-occupancy evaluation (POE) is another unique strength. POE allows for continuous feedback from occupants, enabling designers and architects to adapt the built environment to real-time needs and preferences. While POE is mentioned in other frameworks, it is often underutilized or lacks specificity [81,116]. This table, however, makes POE central by including user satisfaction surveys related to various comfort factors and performance metrics.

(4) Sustainability and IEQ Synergy

This table also successfully integrates sustainability factors with Indoor Environmental Quality (IEQ), something many older frameworks treat as separate or secondary. The Dynamic and Diffuse Light dimension, for example, focuses on the energy efficiency of lighting systems while simultaneously promoting circadian rhythm support for human health. This dual focus ensures that design choices do not just meet environmental targets but also contribute directly to occupant comfort and well-being [3,64].

Additionally, the integration of green infrastructure (such as green roofs or urban gardens) in the Biophilic Urban Integration dimension emphasizes sustainability in a way that surpasses previous models. Urban integration is also present in other frameworks, but this table adds a stronger connection between indoor and outdoor spaces by tying stormwater management, air pollution reduction, and urban biodiversity directly to human

comfort outcomes, ensuring that sustainability goals do not compromise occupant well-being [31].

5.2. Comprehensive Biophilic Design Factors for Human Comfort and Satisfaction

This section introduces a newly developed biophilic design framework aimed at enhancing human comfort and satisfaction. Building on existing frameworks, this new model integrates insights from previous analysis sections while addressing identified gaps in current biophilic design approaches. The framework's goal is to offer a more comprehensive solution that effectively targets multiple dimensions of human comfort and satisfaction within both architectural and urban spaces.

The framework was constructed by synthesizing key findings from Table 2 (Comparative analysis of biophilic design frameworks) and Table 6 (Integration of biophilic design elements and health benefits into urban design components). It categorizes biophilic elements into factors that contribute to human comfort and satisfaction while presenting both direct and indirect biophilic experiences in architecture. Additionally, the framework suggests specific biophilic elements that can be implemented to improve well-being [17,18,117].

Table 6. Comprehensive biophilic design Factors for human comfort and satisfaction.

Human Comfort and Satisfaction Factors	Direct and Indirect IntegrationExperiences in Architecture	Biophilic Elements in Architecture and Urban Design	Health and Well-Being Benefits
Visual Comfort	- Design for Natural Light - Quality and Quantity of Illumination (Natural and Artificial Light) - Access to Outdoor Views - Color and Form Harmony - Comfort Distance and Orientation	- Allowing Daylight and Balancing Artificial Light - Green Courtyards and Roofs - Vertical Green Walls and Façades - Nature Images and Paintings - Botanical Motifs - Green Streets and Pedestrian Connections	- Stress Reduction - Cognitive Enhancement - Improved Life Satisfaction
Air Quality	- Design for Natural Ventilation - Effective CO_2 Control - Integration of Plantable Resources - Ecosystem Balance - Clean Air Solutions	- Natural Airflow Distribution via Green Atriums - Indoor and Outdoor Plants - Pocket Parks and Public Landscaping - Low Impact Development (LID) - Sustainable Waste Management	- Better Air Quality - Respiratory Health Improvement - Enhanced Immune System - Humidity Control
Thermal Comfort	- Design for Natural Light and Ventilation - Selection of Thermal Mass Materials - Heat Exchange Surfaces - Water-absorbent Features - Vegetation Integration	- Allowing Natural Light and Ventilation - Thermally Treated Timber and Natural Materials like Clay, Wood, Stone - Vegetated Swales - Urban Parks and Trees - Water Features/Reservoirs	- Thermal Balance - Energy Efficiency - Reduced Heat Stress - Enhanced Comfort in Diverse Climates
Acoustics	- Sounds of Nature - Proper Sound Placement - Noise Control/ Sound Absorption - Decorative Acoustic Solutions	- Natural Soundscapes (Water, Wind, Wildlife) - Green Walls for Sound Absorption - Vegetative Buffers for Noise Reduction - Outdoor Quiet Zones - Green Streets and Roadside Parks	- Noise Reduction - Stress Relief - Acoustic Comfort - Improved Cognitive Function
Ergonomics	- Safe and Accessible Design - Human-Centered Spatial Planning - Productivity and Efficiency Focus - Aesthetic and Functional Integration	- Universal Design Principles - Human-centered Safety Measures - Gender and Age Considerations in Design - Flexible and Adaptable Spaces	- Enhanced Safety and Security - Increased Productivity - User Satisfaction - Sense of Belonging and Comfort

(1) Visual Comfort

Visual comfort emphasizes the importance of natural light, access to outdoor views, and the harmonious use of color and form [28,116]. The design incorporates elements such as green courtyards, vertical gardens, and nature-inspired aesthetics like botanical motifs,

which together create visually stimulating and relaxing environments. These strategies reduce stress, enhance cognitive functions, and increase overall comfort [44,118,119]. By ensuring that users have access to nature, either directly or indirectly, through design, spaces become more inviting and reduce mental fatigue [31,43,120,121].

(2) Air Quality

Air quality is an essential aspect of human well-being, as poor air quality is associated with respiratory issues and overall discomfort [29,67,116]. This framework emphasizes natural ventilation, CO_2 control, and the integration of plants to purify the air. Biophilic design elements such as green atriums, pocket parks, and green roofs help filter pollutants, improve air circulation, and contribute to respiratory health and the immune system's strength. Enhanced air quality fosters a healthier and more productive environment in both residential and commercial spaces [74,107,108,122].

(3) Thermal Comfort

Thermal comfort is crucial for maintaining a balanced indoor environment [123,124]. This framework enhances thermal comfort by integrating natural materials, sustainable design practices, and features such as water bodies and vegetative cover. Elements such as vegetated swales, urban parks, and green walls help regulate temperature, reduce the urban heat island effect, and provide passive cooling, making the environment more comfortable in varying climates [12,44]. These strategies not only support human comfort but also improve energy efficiency and sustainability [3,87,125].

(4) Acoustics

Acoustic comfort focuses on minimizing noise pollution and enhancing natural soundscapes. The use of natural sounds, green walls, vegetative buffers, and quiet outdoor zones promotes a tranquil environment conducive to relaxation and cognitive function [126–128]. By reducing noise levels, biophilic design helps mitigate the stress associated with urban noise pollution, thereby improving occupant well-being [129,130].

(5) Ergonomics

Ergonomics in this biophilic framework ensures that environments are safe, accessible, and conducive to productivity. By applying universal design principles and integrating human-centered safety measures such as Crime Prevention Through Environmental Design (CPTED), spaces can cater to diverse needs while enhancing safety, accessibility, and satisfaction [63,131,132]. These considerations are essential in designing spaces that accommodate users' physical and psychological comfort, thus improving both functional and emotional experiences within built environments [37,133,134].

The newly developed biophilic design framework integrates research findings with innovative strategies to effectively target human comfort and satisfaction. By addressing visual, air quality, thermal, acoustic, and ergonomic factors, the framework offers a holistic approach to enhancing the well-being of occupants. Moreover, the inclusion of urban design elements broadens its applicability across various scales, from individual buildings to entire city blocks. As a result, this framework presents a flexible, comprehensive model for biophilic design that supports human health, comfort, and sustainable urban development.

5.3. Limitations and Gaps

While this framework is a significant advancement, it does have some minimal limitations:

(1) Outdoor Focus Could Be Enhanced: Although this table introduces a more balanced approach between indoor and outdoor design elements, the outdoor components could benefit from further development, particularly in urban contexts where outdoor space is limited. Future research could explore how to optimize outdoor biophilic interventions in dense urban areas where space constraints make it difficult to implement larger green infrastructure projects [116].

(2) Empirical Validation: While the performance metrics provided are detailed and measurable, further empirical validation through long-term studies will strengthen the framework. Existing frameworks often lack this kind of empirical backing, and while this table makes a step forward, its widespread adoption will require robust, data-driven evidence that demonstrates its effectiveness in various building types and climates.

This newly developed framework is more efficient in bridging the gap between biophilic design theory and practical application. It enhances the existing frameworks from Table 7 (a comparative analysis of biophilic design frameworks) by integrating specific human comfort and sustainability factors, offering measurable performance metrics and a structured approach for implementation. However, it also presents limitations, such as potential complexity, which might challenge designers in applying these concepts effectively. Overall, the integrated design in the Integrated Biophilic Design for Human Comfort and Sustainability framework addresses the shortcomings of earlier frameworks while emphasizing the need for a comprehensive and measurable approach to biophilic design.

Table 7. Comparative analysis of previously developed and newly developed biophilic design frameworks: fostering human comfort and sustainability.

Aspect	Existing—Biophilic Design Frameworks	Newly Developed—Integrated Biophilic Design for Human Comfort and Sustainability	Comparison
Main Focus	Connection between humans and nature; enhancing well-being.	Integration of various design dimensions for comfort and sustainability.	Integrated Biophilic Design builds on the foundational principles of the existing biophilic design frameworks but provides a more comprehensive and integrated approach that directly links comfort with sustainability goals.
Dimensions/Attributes	Attributes focus on environmental features and experiences with nature.	Incorporates multiple dimensions (e.g., direct and indirect experiences) with specific components related to comfort and sustainability.	Integrated Biophilic Design's detailed components, such as dynamic lighting and thermal variability, enhance the understanding of how biophilic design can be practically applied in architectural design.
Key Patterns/Strategies	Emphasize types of experiences and strategies for sensory engagement.	Provides actionable strategies linked to specific performance metrics for each design dimension.	While the existing biophilic design frameworks outline broader strategies, Integrated Biophilic Design translates these strategies into measurable performance metrics, enhancing its practical application in design and evaluation.
Integration of IEQ and POE	Limited discussion on indoor environmental quality (IEQ) and post-occupancy evaluation (POE).	Explicitly integrates IEQ and POE for all components, focusing on user satisfaction and environmental quality.	Integrated Biophilic Design's emphasis on IEQ and POE makes it more suitable for contemporary design practices that prioritize user experience and environmental sustainability, addressing a gap in the existing biophilic design frameworks.
Performance Metrics	No performance metrics provided.	Specifies quantitative and qualitative metrics for evaluating comfort and sustainability.	Integrated Biophilic Design offers a robust framework for measuring success, which is crucial for validating biophilic design principles and their impact on human comfort and environmental performance.
Limitations	Provide a foundational understanding of biophilic design frameworks but lack specific applications.	While it includes comprehensive metrics and factors, it may become overly complex, making implementation challenging.	Integrated Biophilic Design, despite its strengths, risks overwhelming designers with too many components and metrics, which may hinder practical application in some contexts.

6. Conclusions

The comprehensive review of biophilic design frameworks highlights the significant potential of integrating natural elements into the built environment to enhance human comfort, satisfaction, and well-being. While existing frameworks, provide valuable insights into the psychological and physiological benefits of biophilic design, gaps remain in their application, particularly in urban contexts. These gaps include the need for clearer linkages between specific biophilic design elements and measurable health benefits, especially in dense urban areas where access to nature is limited.

This paper proposes an enhanced biophilic design framework that systematically categorizes and links biophilic elements to their corresponding psychological, physiological, and environmental benefits. By integrating both indoor and outdoor environmental factors, this framework offers a more holistic approach than previous models, ensuring a comprehensive application across varying scales—from individual buildings to broader urban settings. The framework emphasizes not only direct experiences of nature, such as natural light and vegetation, but also indirect experiences, such as views of nature and non-visual sensory stimuli, to foster deeper connections to nature.

The findings suggest that biophilic design contributes not only to environmental sustainability by improving energy efficiency and indoor air quality (IEQ) but also plays a crucial role in enhancing mental health, reducing stress, and fostering social well-being. This aligns with the growing recognition of biophilic design as a vital tool for creating resilient, healthy, and sustainable environments, particularly as urbanization continues to accelerate globally. The integration of outdoor urban elements, such as green roofs, biodiversity, and stormwater management, further extends the relevance of biophilic principles in achieving both human-centered and ecological design goals.

Future research should focus on refining and expanding this framework, particularly by exploring its application in diverse cultural and climatic contexts. Additionally, the development of standardized metrics for evaluating the long-term impacts of biophilic design on both human well-being and environmental health will be critical. Post-occupancy evaluation (POE) and user surveys will play a crucial role in validating the framework and ensuring its adaptability. This will facilitate the widespread adoption of biophilic design as a core component of sustainable urban development, ultimately improving the quality of life for urban inhabitants across the globe.

Author Contributions: Conceptualization, R.R.T. and J.P.; Data curation, R.R.T.; Formal analysis, R.R.T.; Methodology, R.R.T. and J.P.; Supervision, J.P.; Validation, J.P.; Writing—original draft, R.R.T.; Writing—review and editing, J.P. All authors have read and agreed to the published version of the manuscript.

Funding: This research received no external funding.

Data Availability Statement: The original contributions presented in the study are included in the article, further inquiries can be directed to the corresponding author.

Acknowledgments: The authors wish to express their sincere gratitude to the members of the Humans, Environment, and Architecture Lab (HEAL) at Ewha Womans University for their invaluable research guidance and support throughout the preparation of this paper.

Conflicts of Interest: The authors declare no conflicts of interest.

Abbreviations

IAQ	Indoor Air Quality
IEQ	Indoor Environmental Quality
POE	Post-occupancy Evaluation
ASHRAE	American Society of Heating, Refrigerating and Air-Conditioning Engineers

References

1. Kellert, S.R. *Building for Life: Designing and Understanding the Human-Nature Connection*; Island Press: Washington, DC, USA, 2012.
2. Kellert, S.R. Building for life: Designing and understanding the human-nature connection. *Renew. Resour. J.* **2006**, *24*, 8.
3. Wijesooriya, N.; Brambilla, A. Bridging biophilic design and environmentally sustainable design: A critical review. *J. Clean. Prod.* **2020**, *283*, 124591. [CrossRef]
4. Söderlund, J. *The Emergence of Biophilic Design*; Springer: Cham, Switzerland, 2019.
5. Zhong, W.; Schröder, T.; Bekkering, J. Biophilic design in architecture and its contributions to health, well-being, and sustainability: A critical review. *Front. Archit. Res.* **2022**, *11*, 114–141. [CrossRef]
6. Kellert, S.; Calabrese, E. *The Practice of Biophilic Design*; Terrapin Bright LLC: London, UK, 2015; Volume 3.
7. Yassein, G.; Ebrahiem, S. Biophilic design in the built environment to improve well-being: A systematic review of practices. *J. Urban Res.* **2018**, *30*, 128–146. [CrossRef]
8. Andreucci, M.B.; Loder, A.; Brown, M.; Brajković, J. Exploring challenges and opportunities of biophilic urban design: Evidence from research and experimentation. *Sustainability* **2021**, *13*, 4323. [CrossRef]
9. Bowler, D.E.; Buyung-Ali, L.M.; Knight, T.M.; Pullin, A.S. A systematic review of evidence for the added benefits to health of exposure to natural environments. *BMC Public Health* **2010**, *10*, 456. [CrossRef]
10. Kabinesh, V.; Vennila, S.; Baranidharan, K.; Ravi, R.; Krishnamoorthi, S.; Thirunavukkarasu, M. Sustainable Spaces-The Evolution of Biophilic Design in Modern Architecture: A Review. *Asian J. Environ. Ecol.* **2024**, *23*, 64–77. [CrossRef]
11. Kellert, S.R.; Heerwagen, J.; Mador, M. *Biophilic Design: The Theory, Science and Practice of Bringing Buildings to Life*; John Wiley & Sons: Hoboken, NJ, USA, 2011.
12. Africa, J.; Heerwagen, J.; Loftness, V.; Balagtas, C.R. Biophilic design and climate change: Performance parameters for health. *Front. Built Environ.* **2019**, *5*, 28. [CrossRef]
13. Kaplan, S. The restorative benefits of nature: Toward an integrative framework. *J. Environ. Psychol.* **1995**, *15*, 169–182. [CrossRef]
14. Kaplan, R.; Kaplan, S. *The Experience of Nature: A Psychological Perspective*; Cambridge University Press: Cambridge, UK, 1989.
15. Beatley, T. *Biophilic Cities: Integrating Nature into Urban Design and Planning*; Island Press: Washington, DC, USA, 2011.
16. Calabrese, E.F.; Dommert, A. Biophilia and the Practice of Biophilic Design. In *Pathways to Well-Being in Design*; Routledge: London, UK, 2018; pp. 97–127.
17. Browning, W.D.; Ryan, C.O. *Nature Inside: A Biophilic Design Guide*; Routledge: London, UK, 2020.
18. Ryan, C.O.; Browning, W.D. Biophilic design. In *Sustainable Built Environments*; Springer: New York, NY, USA, 2020; pp. 43–85.
19. Daroda, K.S. Climate responsive architecture: Creating greater design awareness among architects. *J. Environ. Issues Agric. Dev. Ctries.* **2011**, *3*, 33.
20. Sinha, A. Building orientation as the primary design consideration for climate responsive architecture in urban areas. *Archit. Urban Plan.* **2020**, *16*, 32–40. [CrossRef]
21. Ragheb, A.; El-Shimy, H.; Ragheb, G. Green architecture: A concept of sustainability. *Procedia-Soc. Behav. Sci.* **2016**, *216*, 778–787. [CrossRef]
22. Aliamin, Y. Pathways toward sustainable architecture: Green architecture and circular built environment. In *IOP Conference Series: Earth and Environmental Science*; IOP Publishing: Bristol, UK, 2021.
23. Bielek, B. Green building–towards sustainable architecture. *Appl. Mech. Mater.* **2016**, *824*, 751–760. [CrossRef]
24. Guzowski, M. Biophilic Net-Positive Architecture: Integrating Nature, Health, Wellbeing and Passive Design. In Proceedings of the Architectural Research Centers Consortium, Virtual, 15–18 June 2016; Volume 21.
25. Hootman, T. *Net Zero Energy Design: A Guide for Commercial Architecture*; John Wiley & Sons: Hoboken, NJ, USA, 2012.
26. Downton, P.; Jones, D.; Zeunert, J.; Roös, P. Biophilic design applications: Putting theory and patterns into built environment practice. *KnE Eng.* **2017**, *2*, 59–65. [CrossRef]
27. Lei, Q.; Lau, S.S.Y.; Yuan, C.; Qi, Y. Post-occupancy evaluation of the biophilic design in the workplace for health and wellbeing. *Buildings* **2022**, *12*, 417. [CrossRef]
28. Park, J.; Loftness, V.; Aziz, A.; Wang, T.-H. Strategies to achieve optimum visual quality for maximum occupant satisfaction: Field study findings in office buildings. *Build. Environ.* **2021**, *195*, 107458. [CrossRef]
29. Park, J.; Loftness, V.; Aziz, A.; Wang, T.H. Critical factors and thresholds for user satisfaction on air quality in office environments. *Build. Environ.* **2019**, *164*, 106310. [CrossRef]
30. Ryan, M.M. (Ed.) *Handbook of US Labor Statistics 2015: Employment, Earnings, Prices, Productivity, and Other Labor Data*; Bernan Press: Lanham, MD, USA.
31. Hung, S.-H.; Chang, C.-Y. Health benefits of evidence-based biophilic-designed environments: A review. *J. People Plants Environ.* **2021**, *24*, 1–16. [CrossRef]
32. Heerwagen, J. Biophilia, health, and well-being. In *Restorative Commons: Creating Health and Well-Being through Urban Landscapes*; Government Printing Office: Washington, DC, USA, 2009; 39, pp. 39–57.
33. Bolten, B.; Barbiero, G. Biophilic Design: How to Enhance Physical and Psychological Health and Wellbeing in Our Built Environments. 2020. Available online: https://ojs.unito.it/index.php/visions/article/view/3829 (accessed on 8 September 2024).
34. Staszowska, A. Application of Biophilic Installations for Indoor Air Quality Improvement. *Rocz. Ochr. Sr.* **2020**, *22*, 716–726.
35. Al-Dmour, Y. *Flourishing the Indoor Environment Quality of Workplaces Using the Biophilic Architectural Design*; Brunel University London: London, UK, 2023.

36. Kavathekar, A.; Bantanur, S. Study of the influence of indoor plants as an indicator of biophilic design on CO2 concentrations in a classroom of higher education institute. *J. Sustain. Archit. Civ. Eng.* **2022**, *31*, 96–108. [CrossRef]
37. Lei, Q.; Yuan, C.; Lau, S.S.Y. A quantitative study for indoor workplace biophilic design to improve health and productivity performance. *J. Clean. Prod.* **2021**, *324*, 129168. [CrossRef]
38. Dalay, L. The impact of biophilic design elements on the atmospheric perception of the interior space. *Uluslararası Peyzaj Mimarlığı Araştırmaları Dergisi (IJLAR)* **2020**, *4*, 4–20.
39. Ryan, C.O.; Browning, W.D.; Clancy, J.O.; Andrews, S.L.; Kallianpurkar, N.B. Biophilic design patterns: Emerging nature-based parameters for health and well-being in the built environment. *ArchNet-IJAR Int. J. Archit. Res.* **2014**, *8*, 62. [CrossRef]
40. Richardson, M.; Butler, C.W. Nature connectedness and biophilic design. *Build. Res. Inf.* **2022**, *50*, 36–42. [CrossRef]
41. Grinde, B.; Patil, G.G. Biophilia: Does visual contact with nature impact on health and well-being? *Int. J. Environ. Res. Public Health* **2009**, *6*, 2332–2343. [CrossRef] [PubMed]
42. Gillis, K.; Gatersleben, B. A review of psychological literature on the health and wellbeing benefits of biophilic design. *Buildings* **2015**, *5*, 948–963. [CrossRef]
43. Berto, R.; Barbiero, G.; Pasini, M.; Pieter, U. Biophilic design triggers fascination and enhances psychological restoration in the urban environment. *J. Biourbanism* **2015**, *1*, 27–34.
44. Yin, J.; Zhu, S.; MacNaughton, P.; Allen, J.G.; Spengler, J.D. Physiological and cognitive performance of exposure to biophilic indoor environment. *Build. Environ.* **2018**, *132*, 255–262. [CrossRef]
45. Edwards, B. *Sustainable Architecture: European Directives and Building Design*; Architectual Press: New York, NY, USA, 1999.
46. Makram, A.; Abou Ouf, T. Biomimetic and biophilic design as an approach to innovative sustainable architectural design. In Proceedings of the AR-UP 2019: Third International Conference of Architecture and Urban Planning, Cairo, Egypt, 24–26 October 2019; Department Faculty of Engineering, Ain Shams University,: Cairo, Egypt.
47. Jaheen, N.U.; El-Darwish, I. Biophilic Design Elements in Modern Buildings Influenced by Islamic Architecture Features. *JES J. Eng. Sci.* **2022**, *50*, 41–54. [CrossRef]
48. Abdelaal, M.; Soebarto, V. History matters: The origins of biophilic design of innovative learning spaces in traditional architecture. *ArchNet—IJAR* **2018**, *12*, 108–127. [CrossRef]
49. Dalay, L.; Aytaç, G. Biophilic design: Integrating nature into the urban environment. In *Emerging Approaches in Design and New Connections with Nature*; IGI Global: Hershey, PA, USA, 2022; pp. 1–19.
50. Kellert, S.R.; Wilson, E.O. *The Biophilia Hypothesis*; Island Press: Washington, DC, USA, 1995.
51. Lefosse, D.; van Timmeren, A.; Ratti, C. Biophilia upscaling: A systematic literature review based on a three-metric approach. *Sustainability* **2023**, *15*, 15702. [CrossRef]
52. Kellert, S.R. *Nature by Design: The Practice of Biophilic Design*; Yale University Press: New Haven, CT, USA, 2018.
53. Barbiero, G.; Berto, R. Biophilia as evolutionary adaptation: An onto-and phylogenetic framework for biophilic design. *Front. Psychol.* **2021**, *12*, 700709. [CrossRef] [PubMed]
54. Biederman, I.; Vessel, E.A. Perceptual pleasure and the brain: A novel theory explains why the brain craves information and seeks it through the senses. *Am. Sci.* **2006**, *94*, 247–253. [CrossRef]
55. Brielmann, A.A.; Buras, N.H.; Salingaros, N.A.; Taylor, R.P. What happens in your brain when you walk down the street? implications of architectural proportions, biophilia, and fractal geometry for urban science. *Urban Sci.* **2022**, *6*, 3. [CrossRef]
56. Valentine, C.; Steffert, T.; Mitcheltree, H.; Steemers, K. Architectural Neuroimmunology: A Pilot Study Examining the Impact of Biophilic Architectural Design on Neuroinflammation. *Buildings* **2024**, *14*, 1292. [CrossRef]
57. Hartig, T.; Berg, A.E.V.D.; Hagerhall, C.M.; Tomalak, M.; Bauer, N.; Hansmann, R.; Ojala, A.; Syngollitou, E.; Carrus, G.; van Herzele, A.; et al. Health benefits of nature experience: Psychological, social and cultural processes. In *Forests, Trees and Human Health*; Springer: Dordrecht, The Netherlands, 2011; pp. 127–168.
58. Wyles, K.J.; White, M.P.; Hattam, C.; Pahl, S.; King, H.; Austen, M. Are some natural environments more psychologically beneficial than others? The importance of type and quality on connectedness to nature and psychological restoration. *Environ. Behav.* **2019**, *51*, 111–143. [CrossRef]
59. Ward Thompson, C.; Aspinall, P.A. Natural environments and their impact on activity, health, and quality of life. *Appl. Psychol. Health Well-Being* **2011**, *3*, 230–260. [CrossRef]
60. Hartig, T.; Evans, G.W. Psychological foundations of nature experience. In *Advances in Psychology*; Elsevier: Amsterdam, The Netherlands, 1993; pp. 427–457.
61. Thompson Coon, J.; Boddy, K.; Stein, K.; Whear, R.; Barton, J.; Depledge, M.H. Does participating in physical activity in outdoor natural environments have a greater effect on physical and mental wellbeing than physical activity indoors? A systematic review. *Environ. Sci. Technol.* **2011**, *45*, 1761–1772. [CrossRef]
62. Tekin, B.H.; Corcoran, R.; Gutiérrez, R.U. A systematic review and conceptual framework of biophilic design parameters in clinical environments. *HERD Health Environ. Res. Des. J.* **2023**, *16*, 233–250. [CrossRef]
63. Soderlund, J.; Newman, P. Biophilic architecture: A review of the rationale and outcomes. *AIMS Environ. Sci.* **2015**, *2*, 950–969.
64. Buceta-Albillos, N.; Ayuga-Téllez, E. The State of the Art in the Biophilic Construction of Healthy Spaces for People. *Buildings* **2024**, *14*, 491. [CrossRef]
65. Makes, N.I.M.; Sense, F. *The Economics of Biophilia*; Terrapin Bright Green, LLC: New York, NY, USA, 2012.

66. Untaru, E.-N.; Han, H.; David, A.; Chi, X. Biophilic design and its effectiveness in creating emotional well-being, green satisfaction, and workplace attachment among healthcare professionals: The hospice context. *HERD Health Environ. Res. Des. J.* **2023**, *17*, 190–208. [CrossRef] [PubMed]
67. Loftness, V.; Aziz, A.; Choi, J.; Kampschroer, K.; Powell, K.; Atkinson, M.; Heerwagen, J. The value of post-occupancy evaluation for building occupants and facility managers. *Intell. Build. Int.* **2009**, *1*, 249–268. [CrossRef]
68. Zijlema, W.L.; Triguero-Mas, M.; Smith, G.; Cirach, M.; Martinez, D.; Dadvand, P.; Gascon, M.; Jones, M.; Gidlow, C.; Hurst, G.; et al. The relationship between natural outdoor environments and cognitive functioning and its mediators. *Environ. Res.* **2017**, *155*, 268–275. [CrossRef]
69. Johnson, P. Growing physical, social and cognitive capacity: Engaging with natural environments. *Int. Educ. J.* **2007**, *8*, 293–303.
70. Berman, M.G.; Jonides, J.; Kaplan, S. The cognitive benefits of interacting with nature. *Psychol. Sci.* **2008**, *19*, 1207–1212. [CrossRef]
71. Schertz, K.E.; Berman, M.G. Understanding nature and its cognitive benefits. *Curr. Dir. Psychol. Sci.* **2019**, *28*, 496–502. [CrossRef]
72. Bailey, A.W.; Allen, G.; Herndon, J.; Demastus, C. Cognitive benefits of walking in natural versus built environments. *World Leis. J.* **2018**, *60*, 293–305. [CrossRef]
73. Gullone, E. The biophilia hypothesis and life in the 21st century: Increasing mental health or increasing pathology? *J. Happiness Stud.* **2000**, *1*, 293–322. [CrossRef]
74. Moslehian, A.S.; Roös, P.B.; Gaekwad, J.S.; Van Galen, L. Potential risks and beneficial impacts of using indoor plants in the biophilic design of healthcare facilities: A scoping review. *Build. Environ.* **2023**, *233*, 110057. [CrossRef]
75. Albert, C.; Schröter, B.; Haase, D.; Brillinger, M.; Henze, J.; Herrmann, S.; Gottwald, S.; Guerrero, P.; Nicolas, C.; Matzdorf, B. Addressing societal challenges through nature-based solutions: How can landscape planning and governance research contribute? *Landsc. Urban Plan.* **2019**, *182*, 12–21. [CrossRef]
76. Hähn, N.; Essah, E.; Blanusa, T. Biophilic design and office planting: A case study of effects on perceived health, well-being and performance metrics in the workplace. *Intell. Build. Int.* **2021**, *13*, 241–260. [CrossRef]
77. Chen, Y. *The Impact of Biophilic Design on Health and Wellbeing of Residents through Raising Environmental Awareness and Nature Connectedness*; University of Georgia Athens: Athens, GA, USA, 2017.
78. Hung, S.-H.; Chang, C.-Y. How do humans value urban nature? Developing the perceived biophilic design scale (PBDs) for preference and emotion. *Urban For. Urban Green.* **2022**, *76*, 127730. [CrossRef]
79. Reeve, A.C.; Desha, C.; Hargreaves, D.; Hargroves, K. Biophilic urbanism: Contributions to holistic urban greening for urban renewal. *Smart Sustain. Built Environ.* **2015**, *4*, 215–233. [CrossRef]
80. Nejade, R.M.; Grace, D.; Bowman, L.R. What is the impact of nature on human health? A scoping review of the literature. *J. Glob. Health* **2022**, *12*, 04099. [CrossRef] [PubMed]
81. Yildirim, M.; Gocer, O.; Globa, A.; Brambilla, A. Investigating restorative effects of biophilic design in workplaces: A systematic review. *Intell. Build. Int.* **2023**, *15*, 205–247. [CrossRef]
82. Gray, T. Retrofitting biophilic design elements into office site sheds: Does' going green'enhance the well-being and productivity of workers. In *Landscape Architecture: The Sense of Places, Models and Applications*; Jönköping University: Jönköping, Sweden, 2017; pp. 105–126.
83. Topgül, S. The impact of biophilic designs on worker efficiency. *Sos. Araştırmalar Davranış Bilim.* **2019**, *5*, 11–26.
84. Novosadová, L.; van der Knaap, W. The role of biophilic agents in building a green resilient city; the case of Birmingham, UK. *Sustainability* **2021**, *13*, 5033. [CrossRef]
85. Parsaee, M.; Demers, C.M.; Hébert, M.; Lalonde, J.-F.; Potvin, A. A photobiological approach to biophilic design in extreme climates. *Build. Environ.* **2019**, *154*, 211–226. [CrossRef]
86. Zhong, W.; Schröder, T.; Bekkering, J. Implementing biophilic design in architecture through three-dimensional green spaces: Guidelines for building technologies, plant selection, and maintenance. *J. Build. Eng.* **2024**, *92*, 109648. [CrossRef]
87. Parsaee, M.; Demers, C.M.; Hébert, M.; Lalonde, J.-F.; Potvin, A. Biophilic, photobiological and energy-efficient design framework of adaptive building façades for Northern Canada. *Indoor Built Environ.* **2021**, *30*, 665–691. [CrossRef]
88. Sadick, A.-M.; Kamardeen, I.; Vu, X.P. Challenges for implementing biophilic strategies in Australian building design. *J. Build. Eng.* **2023**, *74*, 106849. [CrossRef]
89. Gill, S.E.; Handley, J.F.; Ennos, A.R.; Pauleit, S. Adapting cities for climate change: The role of the green infrastructure. *Built Environ.* **2007**, *33*, 115–133. [CrossRef]
90. Bush, J.; Doyon, A. Building urban resilience with nature-based solutions: How can urban planning contribute? *Cities* **2019**, *95*, 102483. [CrossRef]
91. Isimbi, D.; Park, J. The Analysis of the EDGE Certification System on Residential Complexes to Improve Sustainability and Affordability. *Buildings* **2022**, *12*, 1729. [CrossRef]
92. Beatley, T. Biophilic urbanism: Inviting nature back to our communities and into our lives. *Wm. Mary Envtl. L. Pol'y Rev.* **2009**, *34*, 209.
93. Lee, E.J.; Park, S.J. Toward the biophilic residential regeneration for the green new deal. *Int. J. Environ. Res. Public Health* **2021**, *18*, 2523. [CrossRef]
94. Browning, W. *Constructing the Biophilic Community*; The MIT Press: Cambridge, MA, USA, 2013.
95. Threlfall, C.G.; Mata, L.; Mackie, J.A.; Hahs, A.K.; Stork, N.E.; Williams, N.S.G.; Livesley, S.J. Increasing biodiversity in urban green spaces through simple vegetation interventions. *J. Appl. Ecol.* **2017**, *54*, 1874–1883. [CrossRef]

96. Aronson, M.F.; Lepczyk, C.A.; Evans, K.L.; Goddard, M.A.; Lerman, S.B.; MacIvor, J.S.; Nilon, C.H.; Vargo, T. Biodiversity in the city: Key challenges for urban green space management. *Front. Ecol. Environ.* **2017**, *15*, 189–196.
97. Hu, X.; Lima, M.F. The association between maintenance and biodiversity in urban green spaces: A review. *Landsc. Urban Plan.* **2024**, *251*, 105153. [CrossRef]
98. Sadler, J.; Bates, A.; Hale, J.; James, P. Bringing cities alive: The importance of urban green spaces for people and biodiversity. In *Urban Ecology*; Cambridge University Press: Cambridge, UK, 2010; pp. 230–260.
99. Fukumoto, H.; Shimoda, M.; Hoshino, S. The effects of different designs of indoor biophilic greening on psychological and physiological responses and cognitive performance of office workers. *PLoS ONE* **2024**, *19*, e0307934.
100. Tharim, A.H.A.; Ahmad, A.C.; Saarani, P.S.N.; Haossain, N.Q.R.; Purwanto, E.; Tafridj, I.S.I.; Purisari, R.; Prasetio, T. The determinant factors of biophilic design strategies and occupants'psychological performance in office building. *Malays. J. Sustain. Environ.* **2022**, *9*, 87–106.
101. Pedersen Zari, M. Understanding and designing nature experiences in cities: A framework for biophilic urbanism. *Cities Health* **2023**, *7*, 201–212. [CrossRef]
102. Lin, B.B.; Egerer, M.H.; Ossola, A. Urban gardens as a space to engender biophilia: Evidence and ways forward. *Front. Built Environ.* **2018**, *4*, 79. [CrossRef]
103. Totaforti, S. Emerging biophilic urbanism: The value of the human–nature relationship in the urban space. *Sustainability* **2020**, *12*, 5487. [CrossRef]
104. Klotz, A.C.; Bolino, M.C. Bringing the great outdoors into the workplace: The energizing effect of biophilic work design. *Acad. Manag. Rev.* **2021**, *46*, 231–251. [CrossRef]
105. Barbiero, G.; Berto, R.; Venturella, A.; Maculan, N. Bracing Biophilia: When biophilic design promotes pupil's attentional performance, perceived restorativeness and affiliation with Nature. *Environ. Dev. Sustain.* **2021**, 1–15. [CrossRef]
106. Zhong, W.; Schroeder, T.; Bekkering, J. Designing with nature: Advancing three-dimensional green spaces in architecture through frameworks for biophilic design and sustainability. *Front. Archit. Res.* **2023**, *12*, 732–753. [CrossRef]
107. Yeo, N.L.; Elliott, L.R.; Bethel, A.; White, M.P.; Dean, S.G.; Garside, R. Indoor nature interventions for health and wellbeing of older adults in residential settings: A systematic review. *Gerontologist* **2020**, *60*, e184–e199. [CrossRef]
108. Thatcher, A.; Adamson, K.; Bloch, L.; Kalantzis, A. Do indoor plants improve performance and well-being in offices? Divergent results from laboratory and field studies. *J. Environ. Psychol.* **2020**, *71*, 101487. [CrossRef]
109. Han, K.-T.; Ruan, L.-W. Effects of indoor plants on self-reported perceptions: A systemic review. *Sustainability* **2019**, *11*, 4506. [CrossRef]
110. Bringslimark, T.; Hartig, T.; Patil, G.G. The psychological benefits of indoor plants: A critical review of the experimental literature. *J. Environ. Psychol.* **2009**, *29*, 422–433. [CrossRef]
111. Larsen, L.; Adams, J.; Deal, B.; Kweon, B.S.; Tyler, E. Plants in the workplace: The effects of plant density on productivity, attitudes, and perceptions. *Environ. Behav.* **1998**, *30*, 261–281. [CrossRef]
112. Huntsman, D.D.; Bulaj, G. Healthy dwelling: Design of biophilic interior environments fostering self-care practices for people living with migraines, chronic pain, and depression. *Int. J. Environ. Res. Public Health* **2022**, *19*, 2248. [CrossRef] [PubMed]
113. Dodman, D.; Bicknell, J.; Satterthwaite, D. *Adapting Cities to Climate Change: Understanding and Addressing the Development Challenges*; Routledge: London, UK, 2012.
114. Ramyar, R.; Ackerman, A.; Johnston, D.M. Adapting cities for climate change through urban green infrastructure planning. *Cities* **2021**, *117*, 103316. [CrossRef]
115. Watchman, M.; Demers, C.M.; Potvin, A. Biophilic school architecture in cold climates. *Indoor Built Environ.* **2021**, *30*, 585–605. [CrossRef]
116. Loftness, V.; Hartkopf, V.; Aziz, A.; Choi, J.H.; Park, J. Critical Frameworks for Building Evaluation: User Satisfaction, Environmental Measurements and the Technical Attributes of Building Systems (POE + M). In *Building Performance Evaluation: From Delivery Process to Life Cycle Phases*; Preiser, W.F.E., Hardy, A.E., Schramm, U., Eds.; Springer International Publishing: Cham, Switzerland, 2018; pp. 29–48.
117. Park, J.; Aziz, A.; Loftness, V. Post-occupancy evaluation for energy conservation, superior IEQ & increased occupant satisfaction. In *IFMA's World Workplace 2013*; Ifma: 2013; International Facility Management Association: Pennsylvania, PA, USA, 2013.
118. Yin, J.; Yuan, J.; Arfaei, N.; Catalano, P.J.; Allen, J.G.; Spengler, J.D. Effects of biophilic indoor environment on stress and anxiety recovery: A between-subjects experiment in virtual reality. *Environ. Int.* **2020**, *136*, 105427. [CrossRef]
119. Gaekwad, J.S.; Moslehian, A.S.; Roös, P.B. A meta-analysis of physiological stress responses to natural environments: Biophilia and Stress Recovery Theory perspectives. *J. Environ. Psychol.* **2023**, *90*, 102085. [CrossRef]
120. Loftness, V.; Aziz, A.; Lam, K.P.; Lee, S.; Cochran, E.; Park, J.; Srivastava, R. *State of the Art in Enclosure Technologies and Integrated Systems for 50% Energy Savings in Existing Commercial Buildings*; REPORT-CBEI: Pittsburgh, PA, USA, 2012.
121. Aristizabal, S.; Byun, K.; Porter, P.; Clements, N.; Campanella, C.; Li, L.; Mullan, A.; Ly, S.; Senerat, A.; Nenadic, I.Z.; et al. Biophilic office design: Exploring the impact of a multisensory approach on human well-being. *J. Environ. Psychol.* **2021**, *77*, 101682. [CrossRef]
122. Schweighart, R.; Bettinger, L. Psychological and physiological effects of visual stimulation with artificial natural structures and indoor plants: A randomized controlled trial. *J. Urban Des. Ment. Health* **2023**, *8*, 513–522.
123. Park, J.; Loftness, V.; Aziz, A. Post-Occupancy Evaluation and IEQ Measurements from 64 Office Buildings: Critical Factors and Thresholds for User Satisfaction on Thermal Quality. *Buildings* **2018**, *8*, 156. [CrossRef]

124. Tham, K.W.; Willem, H.C. Room air temperature affects occupants' physiology, perceptions and mental alertness. *Build. Environ.* **2010**, *45*, 40–44. [CrossRef]
125. Nitu, M.A.; Gocer, O.; Wijesooriya, N.; Vijapur, D.; Candido, C. A biophilic design approach for improved energy performance in retrofitting residential projects. *Sustainability* **2022**, *14*, 3776. [CrossRef]
126. Newsham, G.; Birt, B.; Arsenault, C.; Thompson, L.; Veitch, J.; Mancini, S.; Galasiu, A.; Gover, B.; Macdonald, I.; Burns, G. Do green buildings outperform conventional buildings? Indoor environment and energy performance in North American offices. In *Research Report (National Research Council of Canada. Construction)*; no. RR-329; National Research Council of Canada: Ottawa, ON, Canada, 2012.
127. Park, J. Are Humans Good Sensors?: Using Occupants as Sensors for Indoor Environmental Quality Assessment and for Developing Thresholds that Matte. In *Architecture*; Carnegie Mellon University: Pittsburgh, PA, USA, 2015.
128. Park, J.; Loftness, V.; Wang, T.-H. Examining In Situ Acoustic Conditions for Enhanced Occupant Satisfaction in Contemporary Offices. *Buildings* **2022**, *12*, 1305. [CrossRef]
129. Pallasmaa, J. *The Eyes of the Skin: Architecture and the Senses*; John Wiley & Sons: Hoboken, NJ, USA, 2024.
130. Hadjiphilippou, P. *The Contribution of the Five Human Senses towards the Perception of Space*; Department of Architecture, University of Nicosia: Nicosia, Cyprus, 2013.
131. Söderlund, J.; Newman, P. Improving mental health in prisons through biophilic design. *Prison. J.* **2017**, *97*, 750–772. [CrossRef]
132. Shepley, M.; Sachs, N.; Sadatsafavi, H.; Fournier, C.; Peditto, K. The impact of green space on violent crime in urban environments: An evidence synthesis. *Int. J. Environ. Res. Public Health* **2019**, *16*, 5119. [CrossRef] [PubMed]
133. Sanchez, J.A.; Ikaga, T.; Sanchez, S.V. Quantitative improvement in workplace performance through biophilic design: A pilot experiment case study. *Energy Build.* **2018**, *177*, 316–328. [CrossRef]
134. Inglese, G.; Mura, A.L.; Alves, S.; Bonaiuto, M.; Villani, T. Biophilic design for remote studying environments: Analysis of case studies involving a collaboration between ergonomics and environmental psychology. *Connectivity* **2023**, *98*.

Disclaimer/Publisher's Note: The statements, opinions and data contained in all publications are solely those of the individual author(s) and contributor(s) and not of MDPI and/or the editor(s). MDPI and/or the editor(s) disclaim responsibility for any injury to people or property resulting from any ideas, methods, instructions or products referred to in the content.

buildings

MDPI

Article

Construction and Optimization Strategies for Rural Residential Spatial Models Based on the Concept of Resource Metabolism: A Case Study of Rural Areas in the Shandong Plain

Zhongkai Zhou [1,2], Meng Liu [3,*], Jilong Zhao [1] and Chaoxian Li [1,*]

[1] School of Architecture and Urban Planning, Shandong Jianzhu University, Jinan 250101, China
[2] School of Architecture, Tianjin University, Tianjin 300072, China
[3] School of Architecture and Engineering, Qingdao Binhai University, Qingdao 266555, China
* Correspondence: 06843@qdbhu.edu.cn (M.L.); 13946@sdjzu.edu.cn (C.L.)

Abstract: Rural communities can be conceptualized as spatial organisms interconnected by optimized resource utilization systems. Investigating the efficient utilization of rural resources and spatial construction methods grounded in resource metabolism is a pivotal step toward achieving the ecological transformation of rural spaces. This paper examined rural settlements in the Shandong Plain as a case study, exploring the relationships among three scales: village, neighborhoods, and courtyards. This analysis was based on elucidating the interaction mechanisms between "space and resource" and the integration of key resources and spatial elements. From the perspective of resource circulation and metabolism, this study aimed to elucidate the equilibrium of each resource element within three resource metabolism subsystems: the agricultural production system (core element), the ecological technology system (technological link), and the human life system (spatial carrier) in Shandong Plain's villages, considering general climatic conditions. To achieve this, this research utilized the resource production volume, the utilization and transformation volume of resource metabolism technology facilities per unit area, and the average per capita resource consumption as fundamental measurement units. The concept of a rationing relationship is introduced to clarify resource allocation. Combining the aforementioned research on spatial resource metabolism in ecological villages in Shandong Province with the material flow analysis method, this study constructed a bottom–up spatial model of resource metabolism at three scales, courtyards, neighborhoods, and villages, under various resource metabolism scenarios. This study is anticipated to significantly contribute to the theoretical understanding of rural habitat environments, offering novel methods and perspectives for constructing ecological rural settlements.

Keywords: resource metabolism; Shandong Plain-Type Rural Area; spatial modelling; Optimal Design Strategy; material flow analysis

1. Introduction

Exploring efficient and sustainable patterns of resource use and spatial construction methods is a significant avenue for alleviating urban–rural conflicts and achieving the transformation and development of rural areas. The current approach to resource utilization in China's rural areas is characterized by imprecision, hindering the rational allocation and efficient use of resources. Consequently, this increases in both per capita and overall resource consumption in rural areas poses significant challenges to their resource carrying capacity and energy transformation. Furthermore, the integration of rural production, living styles, and spatial elements is deficient, resulting in uniform spatial patterns of rural settlements and a trend toward "urbanization". As a major agricultural province in northern China, Shandong boasts diverse rural habitats and natural resources. Its sustainable remediation strategy and development model for rural settlements in the plains, the most prevalent rural settlement type in the province, has long served as a

valuable reference and exemplar for similar initiatives across China. Therefore, it is crucial to consider the potential positive impact on enhancing the quality of the rural habitat environment in China, particularly in the northern region. However, a key challenge remains in achieving the ecological transformation of rural settlement spaces, based on understanding the intrinsic flow laws of rural resource elements and the characteristics of suitable resource utilization technologies. Nevertheless, there is a dearth of systematic theoretical research and practical investigation into achieving the ecological transformation and rational construction of rural settlements, based on the intrinsic flow laws of rural resource elements and the technical characteristics of suitable resource utilization.

Rural settlements are the most important spatial carriers for the lives of rural residents, and they are also the common object of research in a number of disciplines. In the early stages of research in related fields, fewer studies crossed disciplinary boundaries to pay in-depth attention to the construction of rural human settlements. In recent years, based on the cross-disciplinary perspective, taking the efficient utilization of resources as the goal and the quantitative analysis of resource flow as the main method, we have devoted ourselves to exploring the theory of "resource metabolism", which integrates the efficient utilization of resources and human settlements, opening up a brand-new perspective of systematically examining the coupled and coordinated relationship between the human settlement environment and the natural environment. It has become an important theory for solving the problem of sustainable development in rural settlements. It has opened up a new perspective for systematically scrutinizing the coupled and coordinated relationship between human settlements and the natural environment, and it has become an important theory and frontier perspective for solving the sustainable development of rural settlements. In terms of theoretical research on the connection between human habitat space and resource metabolism, the American ecologist Abel Wolman put forward the concept of "Urban Metabolism", which combines the concept of resource metabolism and related methods with the study of urban human habitat space [1]. Since then, relevant scholars and institutions have extended the concept of resource metabolism to the urban economy and industrial system, studying the metabolic flow process of various elements such as capital, raw material, water, waste, and other factors at different scales within the boundaries of urban and rural systems, as well as their impact assessment on the environment [2–5]. Agudelo-Vera pointed out that the cyclic efficiency and balanced management of resource metabolism are key factors in optimizing the sustainable development of urban and rural human settlements [6] and that recycling and the efficient use of resources reduces the dependence and impact of human settlements on external resources [7]. Based on the concept of resource metabolism, Kennedy has established indicators for the sustainable development of built spaces, which can be used to account for greenhouse gas emissions, construct dynamic analytical models, and set up sustainable design tools to dynamically evaluate the sustainable development of human settlements [8]. Researchers at the University of Groningen proposed the FEW-Nexus design tool and methodology based on the concept of resource metabolism from the perspective of the interaction between food, energy, and water resources, which affects the function of the human environment system. They furthermore carried out experimental design explorations on objects at different scales, such as neighborhoods, blocks, and districts, in some areas of the Netherlands and Japan [9]. The Dutch design office "upuse Studio", together with a team of researchers (REAP), proposed the "Cyclifiler" design strategy, which takes into account the characteristics of the transformation, distribution, and consumption processes of various types of resources, in an attempt to construct a spatial operation model that was compatible with the metabolism of resources and that advanced layer by layer from the bottom to the top [10,11]. Based on the theory of urban metabolism, Zhao Qianjun explored the driving relationship, optimization path, and evaluation mechanism of the metabolic process and efficiency on the functional layout and spatial form of urban settlements from a cross-disciplinary perspective [12].

From the systematic view of resource metabolism, the space of rural settlements can be regarded as a metabolic organism, which is in essence an ecosystem of various resource

and energy flows. Incorporating metabolic thinking implies the synergistic integration of resource management and sustainable design of rural space, which in essence explores the way of efficient utilization of various resources in the countryside under the support of an appropriate spatial system. Metabolic research is therefore more direct and closer to the essence. Metabolism research, which focuses on the flow process and efficiency of resource elements, is more direct and close to the essence perspective method, which can reveal the dynamic change mechanism of rural settlements from a deeper level. The eco-village constructions developed in Europe and the United States since the 1970s can be regarded as the initial practice of combining the rural habitat with resource metabolism, and their distinctive feature is that a large number of cash crops have been planted in the countryside to act as greening, which is organically integrated with passive solar energy, a good walking environment, and natural drainage to form a complete ecosystem [13]. With the popularization and application of eco-agriculture in China's rural areas in the 1980s, Chinese scholars in the field of agricultural economics paid early attention to the energy flow and material cycle of rural ecosystems, laying a theoretical foundation for the application of resource metabolism analysis to the study of rural spatial problems [14]. For example, Wombach pointed out that eco-villages should make full use of natural resources within their spatial boundaries, accelerating material circulation and energy transformation, so as to realize simultaneous improvement in eco-agriculture and the living environment of human beings [15]. Some scholars have summarized the four models, construction principles, and technical components of eco-village construction in China [16], or the construction of an eco-village resource metabolism technology system containing energy, nutrient, and water cycles based on the principles of ecology, with agricultural production as the core [17]. The theory of resource metabolism has been applied to the study of rural human settlement space, but so far, there is a lack of systematic quantitative research methodology and effective application at the level of rural settlements with small scales.

Based on the above considerations, this study used resource cycle metabolism as an entry point. By integrating theoretical studies on resource metabolism with practical cases of urban and rural settlements, it explores the metabolic flow processes of resource elements such as water, energy, food, and waste in rural settlements in the plain area of Shandong Province. Additionally, it examines the interaction and integration characteristics of spatial form elements at three scales, courtyards, neighborhoods, and villages within rural settlement systems, from the bottom up. By combining appropriate resource utilization technologies and their basic resource metabolism data, this study set a resource metabolism target scenario of "complete organic waste elimination". This study then constructed a multi-scale resource metabolism flow model and spatial morphology model, proposing a spatial optimization strategy for rural settlements accordingly. The results and conclusions of this study strengthen the role of resource optimization in adjusting and guiding the spatial structure of rural settlements in China. They hold theoretical significance and practical value in promoting the integrated development of urban and rural areas, while broadening the concepts of rural construction design.

2. Overview of the Concept of Resource Metabolism in Rural Areas

Resource metabolism, originating from the biological term "metabolism", encompasses both "material metabolism" and "energy metabolism" [18]. The concept of resource metabolism in rural areas is predicated on the premise that a village functions as the boundary of the system. This includes the flow, accumulation, transformation, and other input and output processes related to the primary resources within the production and living systems of the area. Rural settlements can be conceptualized as human habitat spatial units with a fully integrated resource metabolism mechanism. In the early development of the field, resource metabolism was predominantly studied within urban contexts. American ecologist Abel Wolman initially introduced the concept of "urban metabolism", which integrates the flow processes of resource metabolism with the spatial elements of human settlements [1]. Currently, the theory of resource metabolism encompasses all

scales, ranging from macro urban agglomerations to micro urban and rural settlements. Through interdisciplinary exploration, research on resource metabolism has developed a range of relatively mature analytical methods. Notably, the quantitative analysis method represented by material flow analysis (MFA), which quantifies mass fluxes of resource storage and flow conditions, has been employed to analyze the intrinsic characteristics and operational mechanisms of various resource flows within spatial systems and to elucidate the interactions between resource flows and the environment at specific locations. This approach elucidates the interactive relationship between resource flows and the environment at specific locations, facilitating the rational allocation and optimization of spatial resources. Such insights are significant for developing spatial construction strategies and methods for rural settlements aimed at the efficient utilization of resources.

The comprehensive recycling of resources has long embodied traditional ecological wisdom and remains a core concept in rural China. This principle aligns with the concepts and methods of urban resource metabolism applied in rural areas. Since the era of agrarian society in China, rural villagers have engaged in resource recycling and intensive land use within the framework of a self-sufficient small farm economic model. They have leveraged limited technology and space to develop various sustainable practices, including courtyard economy, household biogas production, and four-in-one facility agriculture. Numerous examples of eco-village construction have emerged, with Beijing's Illumining Village serving as a prominent representative. These villages have collectively amassed a wealth of invaluable experience [19]. From the perspective of resource elements and spatial composition, the configuration of rural settlements is more conducive to constructing an ideal resource metabolism and spatial modelling in rural areas. Firstly, the metabolic processes in rural areas are characterized by a comprehensive range of resource elements, a relatively straightforward spatial hierarchy, and a small scale. The agricultural space, forming the core link in the ago-ecological system, is capable of fulfilling multiple functions, including food production and the consumption and transformation of biomass resources. Furthermore, the metabolic processes in rural areas are based on three fundamental elements of resource metabolism: production, life, and ecology. Additionally, a complete cyclic path is in place, making it relatively straightforward to establish a resource production and utilization mode of "local resource recycling". Conversely, the spatial elements within the settlement are highly integrated, with production, living, and ecological spaces permeating and integrating with each other, and their boundaries are less defined. The spaces dedicated to agricultural production, water resource treatment, and human life are multifaceted and complex, making them more conducive to the integrated metabolic function of various resource elements in a complementary and symbiotic manner (Figure 1) [20].





Fruit and vegetable planting in front of village houses as a public productive landscape.



A lotus root planting pool with rainwater collection and purification functions is used as the village public space.

Figure 1. Integration of production and living space in rural residential areas.

3. Characteristics of the Interaction between Resource Metabolism in Rural Settlements and Spatial Elements

The layout of rural settlements is characterized by small and dispersed sites, complicating the direct application of traditional centralized spatial construction and infrastructure layout models to rural spaces. Findings from related research, exemplified by urban metabolism and agricultural resource management, have established a hierarchical recycling model of multiple resource mixing and a bottom–up distributed spatial operation method in terms of both technology and space [21]. These findings can effectively inform the study of resource metabolism characteristics in rural areas, the integration of spatial elements, and the rational allocation of spatial resources, in a manner closely aligned with the characteristics of agricultural resource utilization.

3.1. Spatial Layout Based on Resource Complementarity

The relative positioning of spatial elements in rural settlements necessitates comprehensive consideration of the economic and physical properties of resource elements. Enhanced spatial proximity of relevant functional facilities can ensure resource utilization efficiency and foster collaborative sharing [22]. Given the relatively loose and flat spatial characteristics of villages and the abundance of biomass resources, the distributed integration of resource treatment technology facilities with the spatial distribution of various living and production functions can reduce resource transmission and distribution losses. For example, biogas production facilities can be situated near courtyards and greenhouse planting facilities that require biogas. Small greenhouses and water resource collection systems can be integrated with courtyards, while solar water-heating devices can be installed on the sloping roofs of village buildings to provide domestic hot water or house heating. These arrangements enable the production, use, and recycling of resources in close proximity to the village, leveraging spatial proximity.

3.2. Bottom–Up Cascading Metabolic Flow of Resources

Resource metabolism in rural settlements operates at three spatial levels, the courtyard, the neighborhood, and the village, each of which can be structured to incorporate social, energy, food, and organic waste elements [23]. Interventions starting at the courtyard level are suitable for integrating resource utilization technologies, facilities, and spatial form elements. A bottom–up progressive approach allows resources that are not fully metabolized at lower levels to be transferred upward for recycling. This iterative process effectively reduces resource depletion, improves utilization efficiency, and ultimately controls and reduces the waste exported outside of a settlement system (Figure 2).

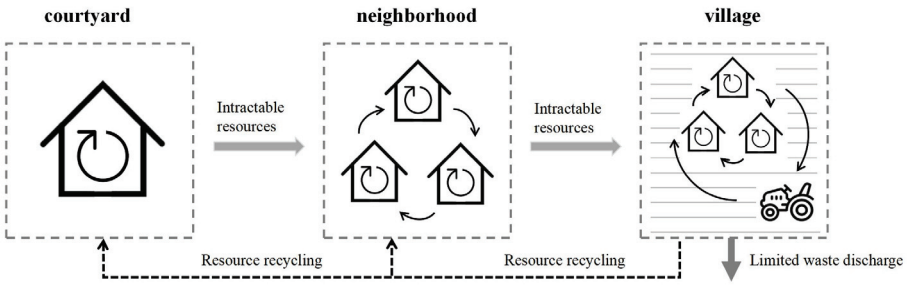


Figure 2. Bottom–up rural space optimization method.

3.3. Integration of Resource Metabolism Technology and Spatial Element Distribution

The distributed integration of appropriate resource utilization technologies and facilities with the spatial elements of rural settlements can facilitate resource recycling and preserve the rural landscape. This approach effectively reduces the input of manpower and material resources, and it better adapts to the decentralized and flat spatial layout of villages [24]. Some scholars have proposed strategies for optimizing the functional spatial layout of courtyards based on the "four-in-one" courtyard ecosystem operation model,

which integrates biogas production and use [25]. A practical example is the Schoonschip design in Amsterdam, the Netherlands, which integrates a wide range of resource recycling technology facilities with small-scale grouped living spaces (Figure 3) [26]. Another example, the reconstruction project of Jintai Village in Sichuan, designed by Kenneth Lam of the University of Hong Kong, integrates various resource recycling technologies and facilities, such as livestock farming, rainwater collection, biogas production and use, and plant-based water purification systems, at the village unit and neighborhood levels. This project created a rural community space with efficient resource metabolism [27] (Figure 4).



Figure 3. Schoonschip ecological community in the Netherlands (available online at: https://schoonschipamsterdam.org/en/) accessed on 1 May 2024.

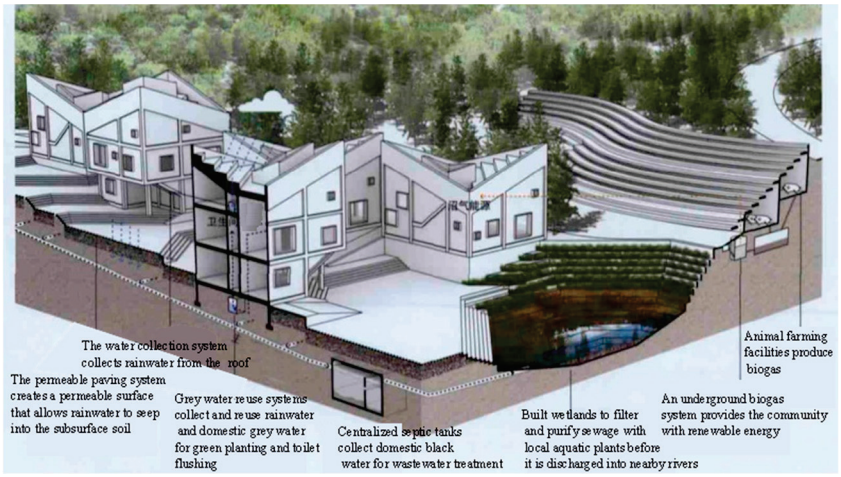


Figure 4. Resource metabolism system of spatial integration between Jintai Village and its neighbors in Sichuan Province (available online at: https://www.archdaily.cn/) accessed on 30 May 2024.

4. Research on the Methodology of Resource Metabolism Modelling

On the basis of elucidating the flow law of resource metabolism in rural settlements and its interaction with spatial patterns, resource metabolism in rural areas can be modelled based on the interdependence of resource elements and their quantitative flow dynamics, combined with the target state of resource metabolism in rural areas. The construction method of resource metabolism models has evolved from qualitative models based on the optimization of resource metabolism pathways to quantitative models grounded in the quantitative flow of resource metabolism accounting and spatial occupation.

Research on model construction based on quantitative resource flow metabolism accounting involves the quantitative analysis of the equilibrium-rationing relationship between the demand and supply of various types of resources at different process stages within a system, combined with the visualization of resource metabolism flow charts, to achieve quantitative model construction. Liu Changan constructed the resource metabolism model of an "agricultural community", based on rural production and nutrient metabolism, optimizing and improving the resource cycle system of the associated production and living space at the scale of an urban community [28]. Some scholars have employed the system dynamics method to establish a resource metabolism model for eco-villages under the zero-waste paradigm by measuring the quantitative correspondence between resource consumption and spatial occupation, based on the "3R" principles of resource reduction, reuse, and recycling (Figure 5) [29].

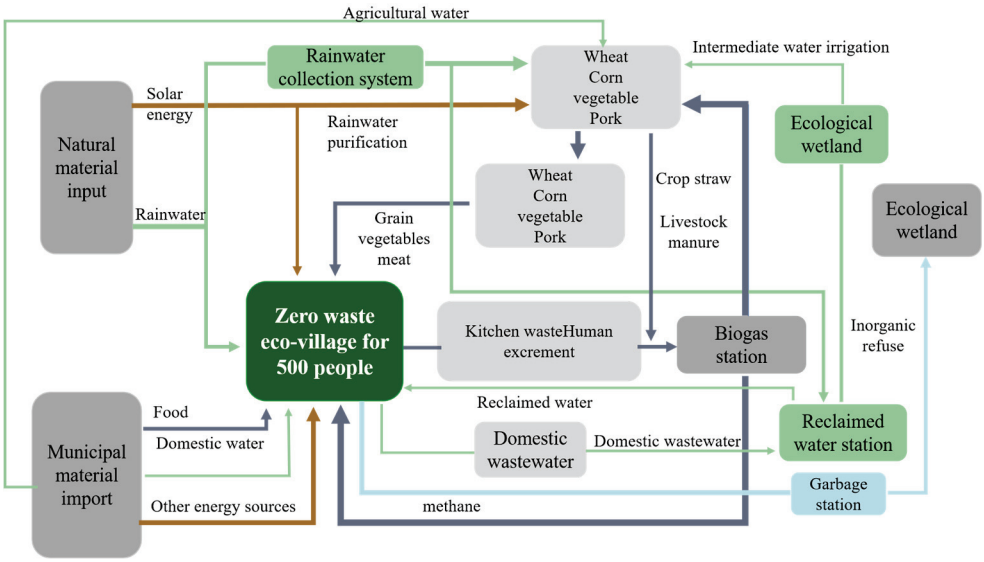


Figure 5. Resource metabolism modelling for "zero-waste" eco-villages.

Research on the construction of spatial occupancy models based on the quantitative metabolic flow of resources involves measuring and establishing a quantitative model of a functional spatial land use scale to achieve balanced resource metabolism rationing, grounded in the analysis of the resource demand, transformation, and output of relevant spatial elements. For example, Edward Yiu of the Chinese University of Hong Kong, through quantitative calculations of the cyclic metabolism of energy, water, food, and organic waste, demonstrated that 40 hectares of land were required to satisfy the food demand of 10,000 people in a zero-waste community. He established a novel planning model aimed at creating a zero-food and zero-organic waste community (ZFW community) [30]. In the Synergy between Regional Planning and Exergy (SREX) Project, Wageningen University in the Netherlands introduced the concept of "Urban Tissue", which is based on the utilization of energy and water resources. The "Urban Tissue" concept uses a 1-hectare land area (100 m × 100 m) as a proposed spatial unit. Its goal is to achieve a closed cycle of resources, using per capita resource consumption and waste emissions as basic data. This concept determines various types of functional space and land area indicators to construct a metabolic spatial model of the urban functional unit [31] (Figure 6). At the scale of rural settlements, the Netherlands' "Regen Village" project, based on the concept of resource metabolism, integrated community size with the per capita consumption of major resources. This project established a small ecological community resource metabolism model covering an area of 15,500 m^2 to meet the basic living needs of 60 residents, by combining appropriate functional space layouts and technical facilities for resource use. Japanese scholars, such as Takeuchi, regard rural space as an area capable of self-sufficiency. By combining the characteristics of rural resources with the flow of urban and rural factors

and considering the distance from urban areas, they constructed three types of ecological rural spatial models: suburban villages, peri-urban villages, and natural villages, each with a self-cycling resource metabolism mechanism [32] (Figure 7).

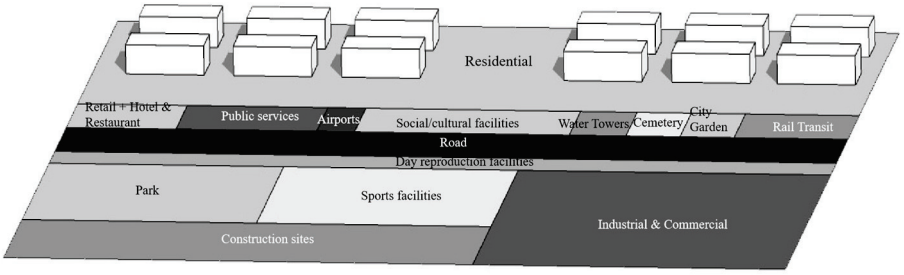


Figure 6. Conversion of quantitative metabolic values for resource metabolism balancing categories in the "Urban Functional Unit" into land area indicators.

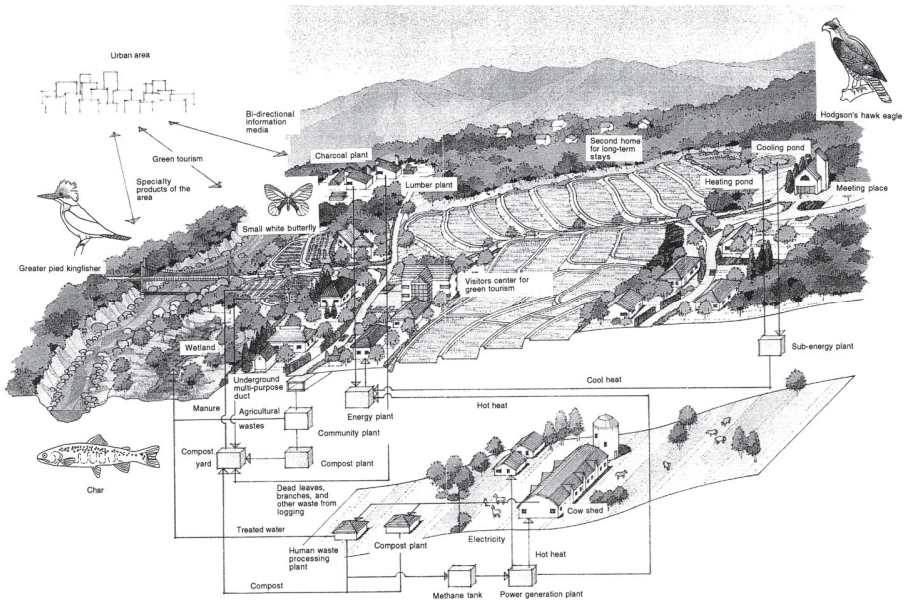


Figure 7. A spatial model of a Japanese eco-village based on the concept of in situ recycling of resources (source from: reference [16]).

5. Modelling of Resource Metabolism in Rural Settlements in the Shandong Plain Area

5.1. Characteristics of the Habitat Environment and Current Status of Resource Utilization in the Shandong Plain Region

The plain terrain of Shandong Province comprises approximately 55% of the province's total land area [33]. Additionally, the number of villages, the size of the agricultural population, and the economic volume in these plain areas are proportionally higher [34]. These settlements, representing the quintessential rural habitat of Shandong, are characterized by relatively complete infrastructure and public service facilities. They are anticipated to survive and develop over the long term and thus are a central focus of both current and future rural development efforts in Shandong. Although the villages in Shandong's plain areas have a relatively plain character, they benefit from convenient transportation and location. This proximity fosters closer interactions with urban areas in terms of economy, population, space, and resources. Consequently, these villages are more susceptible to urban influences, exacerbating the conflict between human settlement development and resource utilization [35]. Combined with a large number of case field studies in plain villages, a large amount of basic information looking into ways of utilizing the four types of resources associated with the living and production systems, namely water, organic

waste, energy, and agriculture, has been collected (Figure 8), which mainly contained the following characteristics.



Figure 8. Types of resource metabolism in research cases.

With regard to water resource utilization, the penetration of piped water facilities in rural Shandong Province has achieved 97% coverage [36], Nonetheless, numerous farmers continue to rely on personal or communal wells due to the costs associated with piped water. Furthermore, sewage collection and treatment are predominantly managed by small-scale centralized facilities. In some villages, ecological sewage treatment is integrated with landscaping and agricultural practices; however, overall water use remains relatively unsophisticated, with insufficient recycling and tiered utilization. Regarding organic waste treatment, plain villages are abundant in biomass resources. Most villages have implemented on-site resource utilization strategies, converting agricultural organic waste into straw biogas or biomass fuels, thereby enhancing the connection between production and living systems. However, the sorting and recycling rates of domestic organic waste remain inadequate. Concerning energy use (heat and electricity), with the exception of a few peri-urban villages employing centralized heating systems, most villages depend primarily on ambient heat or electricity for winter heating. Additionally, some villages utilize centralized biogas stations or small household digesters for biogas production for cooking purposes. Distributed solar photovoltaic and solar thermal systems, integrating with the roofs of village houses and unused land, are increasingly prevalent. Regarding agricultural production, traditional large-field cultivation, greenhouse planting, and large-scale farming are predominant methods in plain villages. Continuous greenhouses have emerged as prominent features in the rural landscape on the periphery of some villages. These practices utilize both courtyard areas and previously underutilized vacant land for small-scale "production and residence integration" farming methods, thereby contributing to a distinctive productive landscape.

5.2. Resource Metabolism Spatial Modelling Path

To investigate the mechanism of resource metabolism in rural settlements, it was imperative to examine both resource and spatial elements comprehensively. Resource metabolism in rural areas begins with fundamental material elements that sustain the normal function of the rural environment. It involves analyzing the mechanisms of nutrient, water, and energy cycles within the community, with particular emphasis on the nutrient cycle, which focuses primarily on food production and the cyclic metabolism of organic waste [37]. The resource elements addressed in this study, excluding inorganic waste (e.g., solid waste and old building material) that are challenging to recycle effectively within the spatial and technological constraints of villages, encompass four primary categories: water, energy (both electrical and thermal), food (agricultural production), and organic waste (nutrients). Regarding spatial elements, the typical rural spatial framework comprises four main categories: built-up elements (roads, courtyards, public buildings), natural environmental components (vegetation, water bodies), agricultural production elements (arable land, greenhouses), and infrastructural components (electric power transmission and distribution facilities, water and sewage systems). These elements are interwoven and integrated at various scales. The courtyard comprises the residence and its ancillary functional rooms, hardscaped areas, planted vegetable gardens, small greenhouses or livestock spaces, integrated solar photovoltaic and solar thermal facilities on roofs, walls, or underground, rainwater catchment areas, and organic waste collection ponds (septic tanks). The neighborhood extends beyond basic courtyard elements to include the road in front of residences, public spaces, and areas where resource metabolism can be integrated, such as agricultural greenhouses, open vegetable gardens, small ecological wetlands, breeding spaces, and underground biogas facilities. The village encompasses additional functional elements outside the courtyard, including rural public service buildings, large public open spaces, medium- to large-scale biogas and sewage treatment stations, agricultural land, extensive greenhouses, and various natural water bodies. Adhering to the principle of achieving balanced resource metabolism across varying spatial scales, this study approached the task from three hierarchical levels—the courtyard, neighborhood, and village. Following the framework of "resource metabolism data and spatial indicator calculation—resource metabolism scenario setting—balanced rationing model analysis—resource metabolism and spatial model construction", this study developed a comprehensive resource metabolism model and spatial morphology model incorporating agricultural production factors, ecological and technological facilities, and human living systems (Figure 9).

(1) Data Accounting

Data accounting encompasses both resource and spatial data related to resource metabolism in rural areas. Concerning resource metabolism data, basic information on the rural per capita or household consumption within the agricultural system, ecological facility system, and human living system was obtained from sources such as the China Statistical Yearbook, the Shandong Statistical Yearbook, and the China Household Energy Consumption Research Report. These data, covering the metabolic flow of four primary resource elements—water, food, energy, and organic waste—formed the foundational basis for constructing the resource metabolism model. By integrating spatial occupancy data for open land and greenhouses used in the production of major crops and livestock under the typical environmental and climatic conditions of the Shandong Plain, along with spatial data for land or buildings equipped with appropriate resource processing technologies, the basic spatial data indices for resource metabolism in rural areas were established.

(2) Situation Setting

Compared to the resource metabolism in urban areas, which primarily involves a unidirectional input of resources, plain-type rural settlements generally function as resource output systems due to their agricultural production roles. In these settlements, the volume of agricultural output typically exceeds the consumption levels within the villages (consid-

ering only the essential food requirements of residents and livestock). Therefore, addressing the villages' self-sustaining development needs and habitat remediation goals—focusing on the utilization of organic waste resources—and considering the village development model and spatial resource needs required the establishment of different resource metabolism scenarios. This included evaluating various types of resource metabolic flows, balanced ration data, quantitative resource flow, the degree of functional integration at different scales, resource self-sufficiency rates, and spatial element diversity.

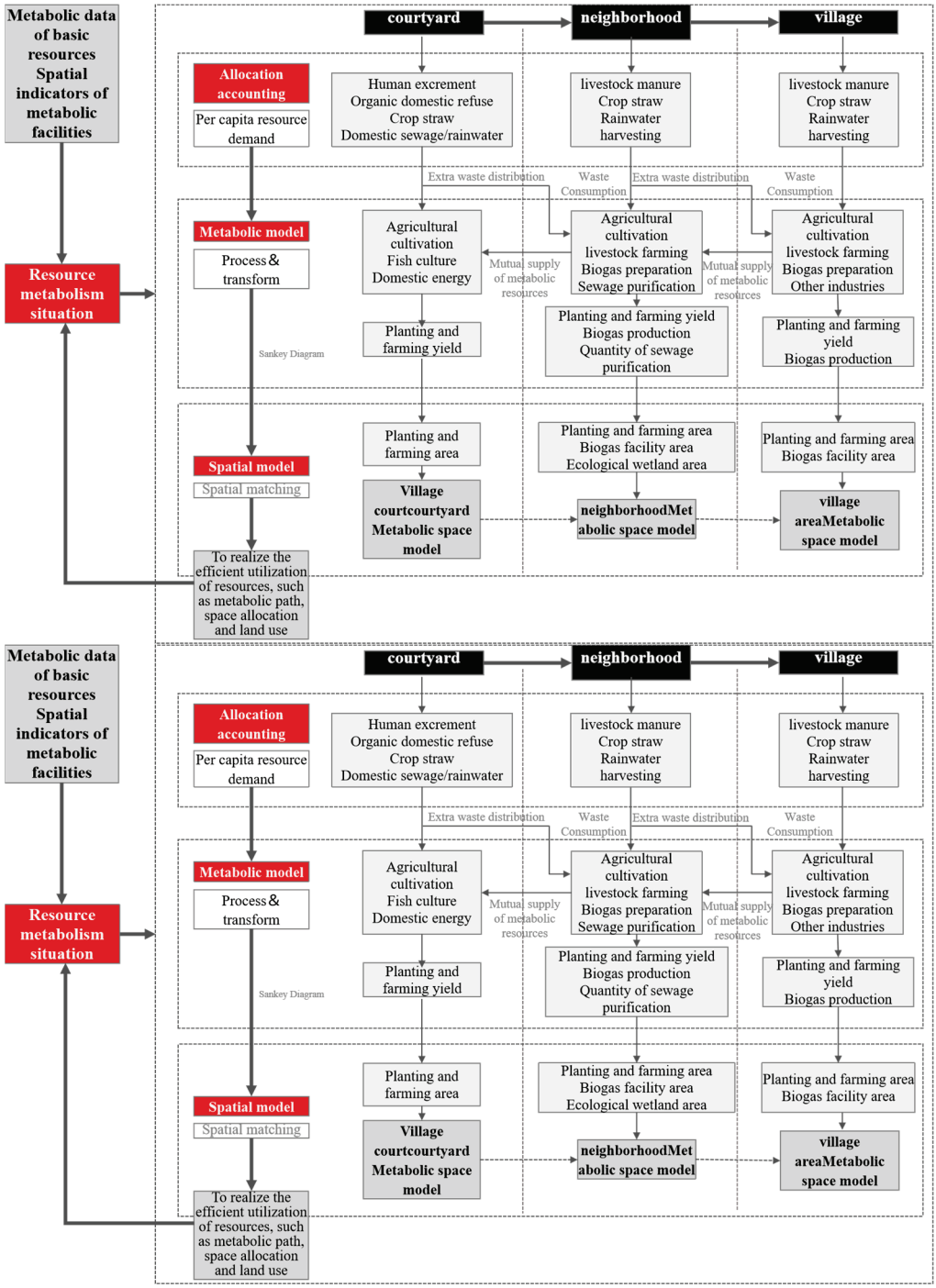


Figure 9. Resource metabolism in rural areas and spatial model construction ideas.

(3) Modelling

Quantitative Metabolic Analysis. By integrating the interaction characteristics of appropriate resource metabolism technologies and rural spatial elements, and utilizing resource metabolism quotas derived from human resource consumption data, this study performed a bottom–up analysis of resource metabolism objectives at three spatial scales—the courtyard, neighborhood, and village. This analysis considered the capacity of ecological technology systems (resource metabolism facilities) applicable to these scales. This study assessed the metabolic flow of major resources and their balanced quota relationships within and between different scales, employing Sankey diagrams for visualization. This balanced quota analysis helped determine resource flow statuses and established a model of resource metabolism in rural areas.

Spatial Modelling. Constructing a spatial model for rural resource metabolism required integrating the abstract resource metabolism model with the tangible spatial morphology of the village. This involved translating quantitative resource flow data at various scales into categorized spatial morphology indices which included relevant technological facilities. For example, this included the area occupied by photovoltaic installations on village roofs, road space used for domestic wastewater transmission, and courtyard or neighborhood open spaces allocated for small greenhouses. By converting quantitative resource indicators into spatial form indicators, this study could develop a spatial model that achieved balanced resource metabolism within the village boundaries (Figure 10).

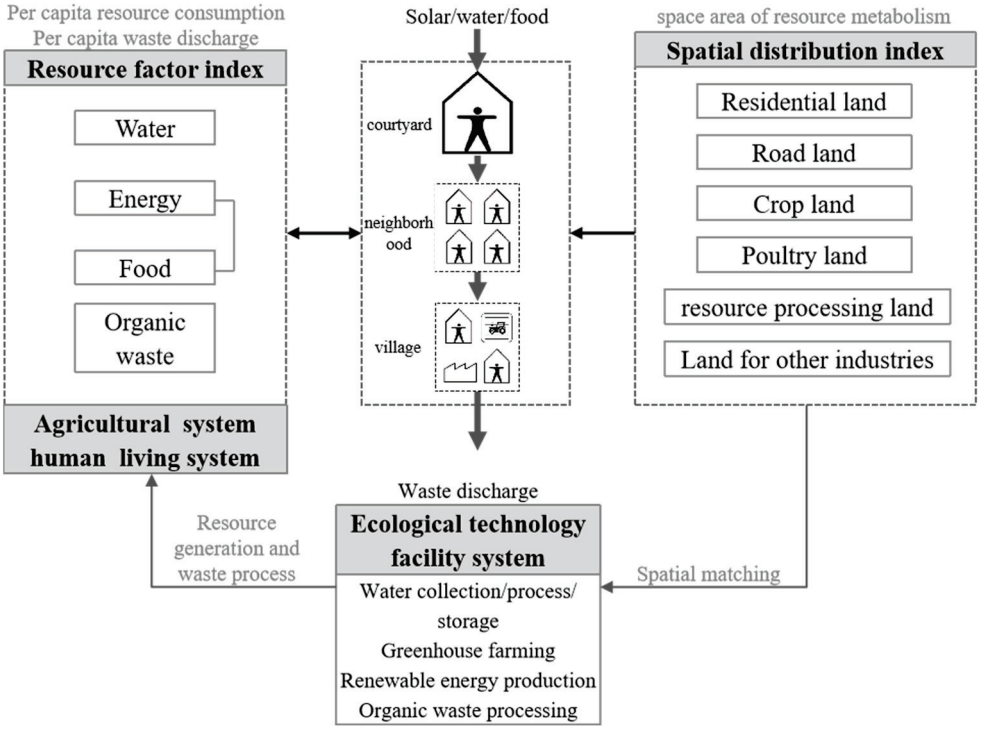


Figure 10. "Resource-space" rationing of rural human space.

5.3. Setting of Relevant Technical and Spatial Indicators for Resource Metabolism Systems in Rural Areas

The resource metabolism in the rural areas was quantitatively assessed with a focus on the needs of individuals, addressing their fundamental production, living, and ecological requirements. The analysis categorized resource metabolism into three subsystems: the human living system, the agricultural production system, and the ecological and technological system. This assessment was informed by data from statistical yearbooks of China and Shandong Province, along with the relevant literature [38,39]. Basic consumption data for the four primary resources—water, energy (both thermal and electrical), food (planting and

breeding), and organic waste—were compiled separately. Additionally, data on the production and conversion of resources through agricultural and ecological technologies (such as biogas production, solar photovoltaic systems, and ecological sewage treatment) were integrated to achieve balanced resource rationing. This approach provided the foundation for constructing robust resource metabolism models.

5.3.1. Basic Data on the Resource Elements of the Three Living Systems

Given that this study aimed to achieve metabolic spatial modelling through quantitative resource metabolism analysis, the focus of data screening was not on pursuing exact precision but on establishing the reasonable availability of data. According to the 2021 Shandong Statistical Yearbook, the average number of permanent residents in Shandong's rural areas was 3.1 per household. Consequently, resource consumption for courtyard households was calculated based on this average, and resource quantities such as those related to livestock breeding were adjusted in accordance with the general population of villages and the spatial scale of courtyard areas (Tables 1–3).

Table 1. Resource element ratios for human living systems.

Resource Type			Use	Annual Resource Consumption per Capita	Average Annual Resource Consumption per Household (Calculated for 3.1 Persons)	Marginal Notes
Resource input	Energy	Electric	Living electricity	714 kwh/yr	2213 kwh/yr	Included water for drinking, washing, cooking, etc.
		Heat	Cooking	106 m^3/yr (biogas)	317 m^3/yr (biogas)	
			Heating	61 kg/yr	184 kg/yr	
			Total amount of energy	135.06 kg/person/yr	405 kg/person/yr	
	Water		Domestic water use	24.6 m^3/yr	76 m^3/yr	Included water for drinking, washing, cooking, etc.
			Natural precipitation		114 m^3/household/yr	The average precipitation in Shandong was 710 mm/year, and the area of precipitation collection per household was calculated according to the average household's hard interface area of 160 square meters
	Food needs		Cereal consumption	168.4 kg/yr	522 kg/yr	Contained grains, potatoes, beans
			Meat consumption	27.4 kg/yr	85 kg/yr	Reference to the China Statistical Yearbook (2020) and China Food and Nutrition Development Program (2014–2020)
			Fish consumption	11.2 kg/yr	34.72 kg/yr	
			Vegetable consumption	140 kg/yr	434 kg/yr	
Resource output	Organic waste		Human excreta	164.25 kg/yr	509 kg/yr	
			Domestic sewage	21.4 m^3/yr	66 m^3/yr	
			Organic waste	182.5 kg/yr	566 kg/yr	

Table 2. Resource factor rations for agricultural production systems.

Resource Type				Average Annual Resource Production	Average Household Resources	Volume of Resources for the Cluster	Volume of Resources in the Village Area	Notes
Resource input	Nutrients	Greenhouse		Biogas: 3.5 kg/m^2/yr Residue: 3 kg/m^2/yr	–	–	–	1. Priority was given to the use of rainwater harvesting for watering agricultural plantations, and any shortfalls were mainly imported from outside the system using municipal pipeline networks or river and lake water bodies 2. The use of greenhouse intensive cultivation on the roofs of village houses and public sites of neighboring groups could produce 12.69 kg/m^2/year (8452 kg/mu/yr) of vegetables per square meter of the rooftop greenhouse 3. Feeding cycles: 365 days for cattle and sheep, 180 days for pigs, 50 days for broilers 4. Needed to be measured in relation to specific acreage
		Open-air vegetable plots						
		Cropland		Biogas: 5000 kg/mu/yr Biogas: 3750 kg/mu/year				
	Food	Pigs		Digestate: 1460 kg/pc				
		Poultry		36.5 kg/pc				
Resource output	Food and vegetables	Greenhouse vegetables		8452 kg/mu	–	–	–	
		Open-air garden		3330 kg/mu				
		Cropland grains		416 kg/mu				
	Meats	Hog		70 kg/head	–	11 heads	–	
		Meat and poultry		3.5 kg/pc		13 pc		
		Cow		250 kg/pc		–	17 pc	
		Goats		20 kg/pc			186 pc	
	Caviar	Pond aquaculture		11.2 kg/yr	34.7 kg/household/yr	–	–	
	Organic waste	Pig manure		1930 kg	–	21,230 kg	-	
		Poultry manure		36.5 kg		475 kg		
		Cattle manure		9855 kg		–	167,535 kg	
		Sheep manure		865 kg			160,890 kg	
		Quantity of straw	Greenhouse vegetables	740 kg/mu (1.54 kg/m^2)			–	
			Open-air garden	633 kg/mu (0.95 kg/m^2)				
			Grains	376 kg/mi				

Table 3. Eco-technology system resource element rations.

Resource Type	Use		Resource Handling Capacity	Appropriate Scale			Notes
				Courtyard	Neighborhood	Village	
Electricity	Solar photovoltaic installations		262.8 kwh/m^2/yr	•	•	•	1. Based on an average of 6 h of effective light per day 2. Rooftop greenhouses integrated with village buildings could transport some of the heat to the building interior 3. Processing 1 m^3 (tons) of domestic wastewater required an approximate footprint of 1.7–2 m^2 4. Treatment of 10,000 m^3 of sewage per day, with a treatment facility covering an area of approximately 17,900 square meters 5. According to the calculation of a 6 m^3 small-scale biogas digester, the annual gas production was about 288.72 m^3, and then the annual biogas production of the 1 m^3 biogas digester was 48.12 m^3 6. The biogas production of animal manure was 0.06 m^3/kg, the biogas production of domestic organic waste was 0.1 m^3/kg, and the biogas production of straw was 0.28 m^3/kg 7. A total of 1 m^3 biogas could produce 3.42 kg of digestate and 2.28 kg of digestate 8. Average annual consumption of organic waste per unit area of cultivation space
Heat energy	Solar thermal facilities		304 kwh/m^2/yr	•	•		
	Rooftop greenhouse		255 kwh/m^2/yr	•			
Sewage treatment	Small-scale artificial ecological wetland sewage treatment		2 m^2/m^3	○	•		
	Artificial sewage treatment plant		17,900 m^2 = 10,000 m^3 wastewater treatment capacity			•	
Organic waste treatment	Landfill gas	Household biogas facilities	48.12 m^3/yr		•		
		Medium and large biogas plants	418.75 m^3/m^3/yr			•	
	Plantation	Small-scale greenhouse cultivation	Organic waste 1.53 kg/m^2/yrWastewater 2.92 m^3/m^2/yr	•	•		
		Open-air garden planting		•	•		

Clarification: • indicates the optimal scale for a resource metabolism technology facility, ○ indicates a more appropriate scale.

5.3.2. Spatial Hierarchy of Rural Settlements and Indicator Setting

The balance quota accounting of the resource metabolism system, which involved tracking the flow of various resource elements at different scales within the village, had to be integrated with rural community planning and relevant technical specifications. This integration included setting spatial indicators for the three scales, the courtyard, neighborhood, and village, and defining their resource metabolism spatial layouts. This process provided a spatial operational basis for the subsequent transition from quantitative resource metabolism indicators to spatial morphology indicators of resource metabolism.

(1) Courtyard

Spatial indicator setting. According to the Technical Guidelines for the Construction of New Rural Communities in Shandong Province (for trial implementation), the land control indices for village settlements (Table 4) indicated that the average residential land area in the plain regions was 200 m^2 per household. Combining this with the 2021 statistical data showing an average per capita residential floor area of 43.41 m^2 for rural residents in Shandong Province, the average household floor area was approximately 135 m^2. This figure was used as the minimum spatial index for the village building model [40]. Regarding basic spatial form control, current regulations stipulate that rural settlements should feature 2–3-story low-rise townhouses and multi-story residential units not exceeding six stories. Considering the traditional rural landscape, which primarily consists of low-rise buildings, the proposed model for courtyard spaces utilizes low-rise townhouses as the fundamental residential units. The architectural design combines flat and sloping roofs, with flat roofs for the south-facing main houses and sloping roofs for the main rooms facing south. Auxiliary rooms on the east and west have flat roofs. This design reflects the traditional architectural style of Shandong Province's plains while accommodating ecological and technological facilities, such as solar photovoltaic panels and small greenhouses. The integration of these elements with courtyard walls creates an open space suitable for family activities, outdoor vegetable gardens, family farming, and resource metabolism facilities like rainwater collection.

Table 4. Spatial indicators for courtyards (basic spatial units).

Type of Village	Households per Capita Homestead	Average Household Floor Area	Story	Plot Ratio
Plain-type villages	$\leq$200 m^2	135 square meters	2–3 floors	$\geq$0.3

Note: This indicator was calculated on the basis of the land control indicators for the construction of village settlements in the Technical Guidelines for the Construction of New Rural Communities in Shandong Province (for trial implementation), combined with the data from the Statistical Bulletin on National Economic and Social Development of Shandong Province in 2022.

Space Usage Settings. Based on the aforementioned spatial control indices and the morphological characteristics of low-rise courtyards and physical buildings in the Shandong Plain, the spatial allocation and area index range for resource metabolism in rural courtyards were established. To meet basic access requirements, a small rooftop greenhouse, approximately 24 m^2 in area, was installed on the roofs of the east and west rooms on the first floor. An open vegetable garden, not exceeding 30 m^2, and a pond (fish pond), not exceeding 8 m^2, were positioned in the adjacent open space. Additionally, solar photovoltaic or solar thermal panels were installed on the south side of the sloping roof of the main house, sized according to the energy needs for living and production. These spatial and quantitative indices for various resource metabolism facilities are outlined, with specific ranges to be refined through subsequent metabolism accounting under different resource metabolism scenarios. The greenhouse planting and open vegetable gardens were designed to be adaptable and replaceable (Figures 11 and 12).

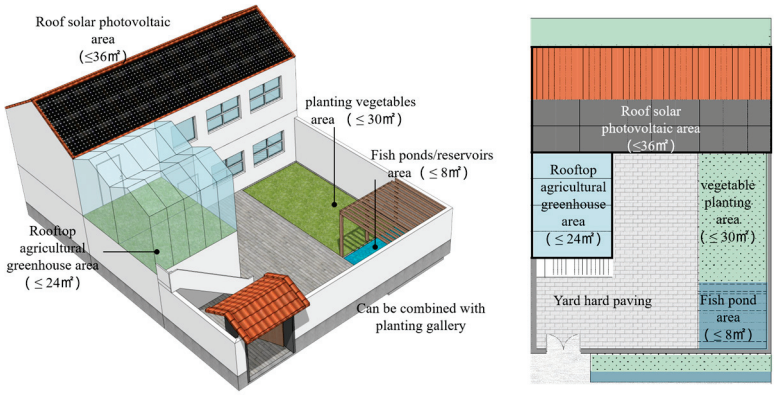
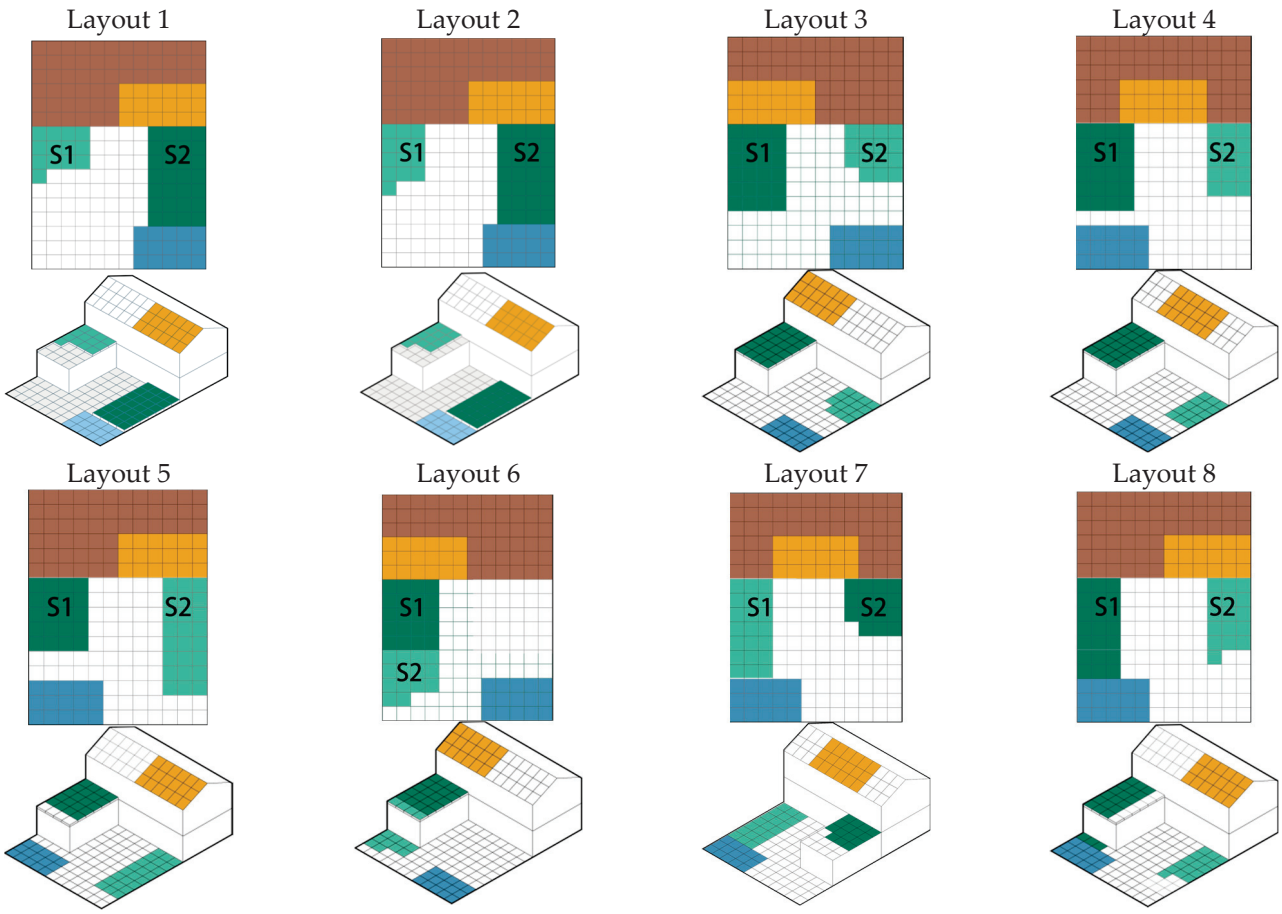


Figure 11. Basic model of the courtyard and setting of the spatial use model.



Description: 200 m² (16 m × 12.5 m) of residential area, 135 m² of building area of village house, S1 is greenhouse planting combined with the roof of the village house, S2 is the ground vegetable garden in the courtyard, yellow is solar photovoltaic and solar thermal panels combined with the south-facing sloped roof, and blue is the water-collecting fish pond in the courtyard.

Figure 12. Schematic layout of the courtyard to realize the balance of resource metabolism.

(2) Neighborhood

Spatial Indicator Setting. Neighborhoods in rural settlements are medium-scale spatial aggregates comprising multiple courtyards, public spaces, and community facilities. These clusters serve as crucial links between individual courtyards and the broader spatial-scale resource metabolism. The number of courtyards within a neighborhood must be evaluated from both technical and social perspectives. Technically, the use of "household biogas" systems for balancing resource production and consumption provides a key basis for determining the appropriate scale of neighborhoods. By integrating technology and spatial

considerations, and minimizing the distance for biomass resource transfer, the total amount of organic waste input and biogas output could be calculated to estimate the number of courtyards within a cluster. Practical examples and feedback from research supported this approach: for instance, 32 households in Jiangfang Xincun, Yongyang townships shared a biogas digester and an 8 m^3 storage tank; seven households in Longpi Village shared a 10 m^3 digester; and eight households in the EVA-Lanxmeer settlement in the Netherlands had a biogas production unit for every eight households [41]. Additionally, considering the social dynamics of "acquaintance societies", where neighborly interaction and a sense of community are significant, research indicates that residential clusters of 8–12 households foster a positive social atmosphere [42,43]. Thus, balancing both technical and social factors, the recommended number of courtyards in a neighborhood was set at 10 (Figure 13).

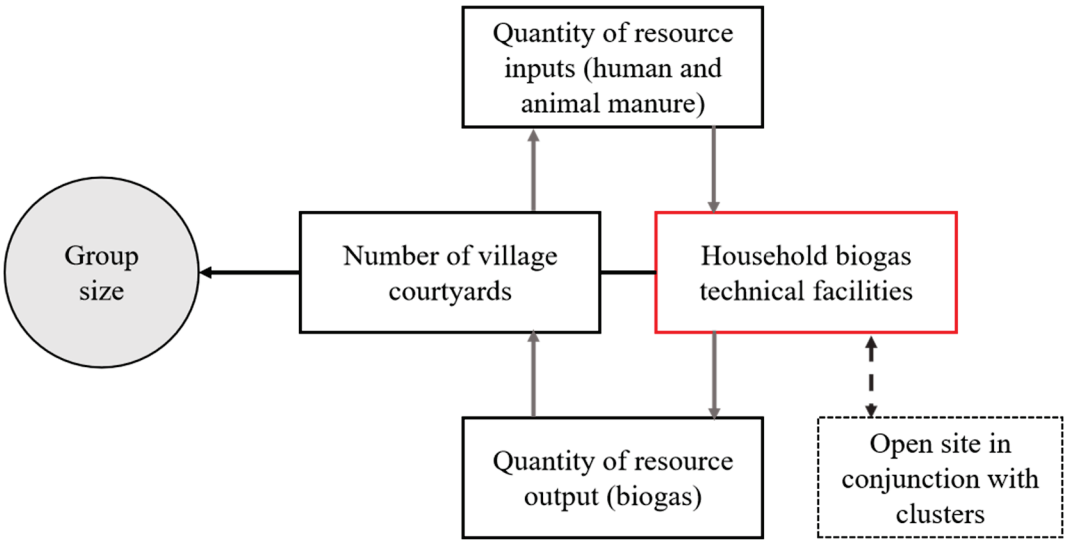


Figure 13. Flow chart outlining the determination of neighborhood sizes.

Space Use Mode Setting. Taking as an example the proposed enclosed neighborhood composed of 10 courtyards, the spatial components included two main categories: courtyards and neighborhood open spaces. Besides the road interface, which was dedicated to precipitation collection, the remaining areas between the courtyard walls and the road, as well as the open spaces (primarily unused vacant or residential land), could be utilized for various purposes. These included vegetable gardens, greenhouses, livestock breeding (such as pigs and poultry), and small-scale artificial wetlands integrated with hydroponics and vegetable cultivation (encompassing water transfer and distribution ditches, anaerobic ponds, regulating ponds, ecological oxidation ponds, and other components). The spatial indices for resource metabolism, excluding the road (which covered approximately 10–15% of the total area) and the roadside productive greenery (around 235 m^2), should be precisely determined based on the specific metabolic targets for each resource through rationing calculations (Figure 14). Additionally, for the 10 courtyards and public open spaces, different combinations of organic waste metabolism technologies should be integrated. Depending on the current situation, these spaces can be fully occupied and utilized for various scales and types of unused open areas, leading to different layout patterns such as enclosing groups, rows, and columns, to accommodate or develop diverse village morphologies (Figure 15).

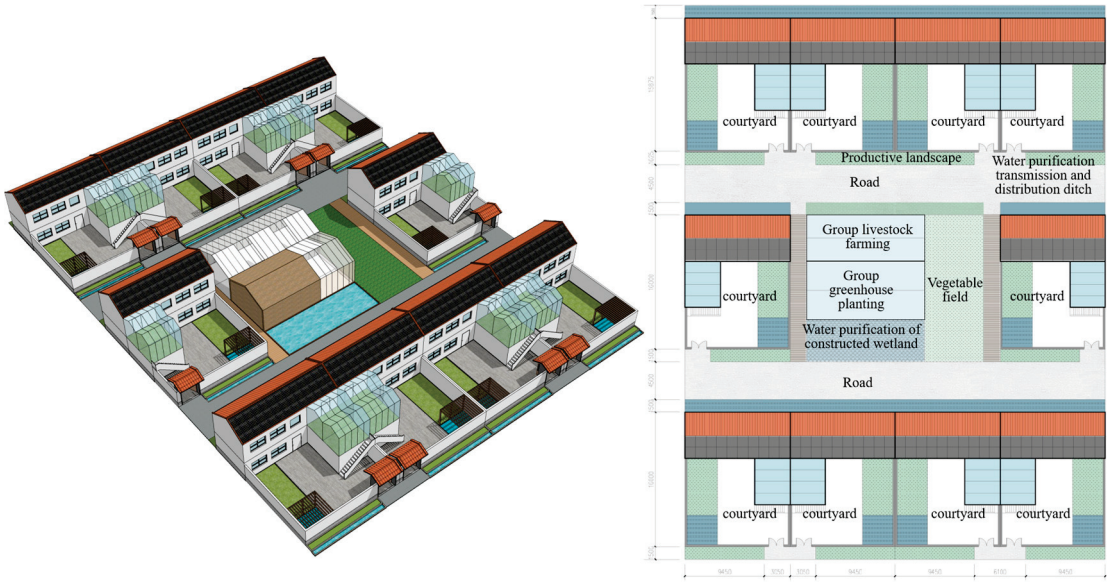


Figure 14. Basic layout setting for a neighborhood space.

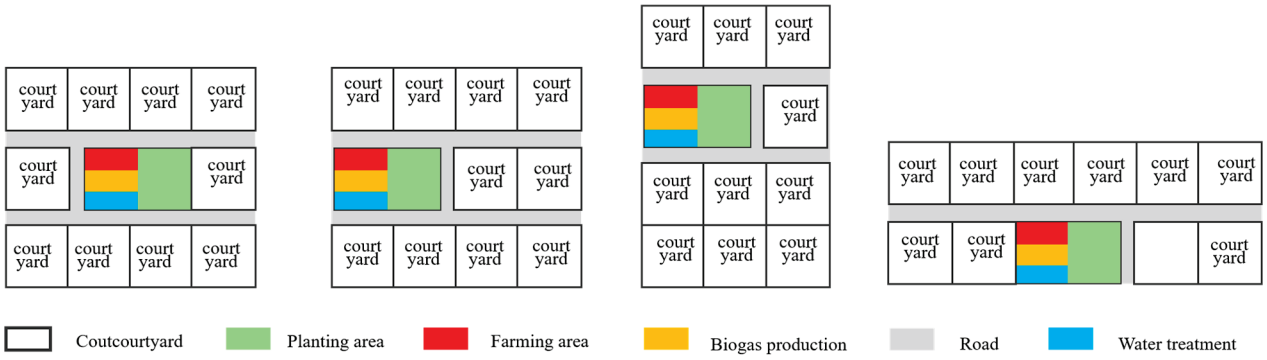


Figure 15. Schematic illustration of the metabolic spatial layout approach for neighborhoods.

(3) Whole Village

Area Allocation of Spatial Elements. To facilitate the measurement of overall resource metabolism within a village, it was essential to determine the village size and land use indicators. The village scale was based on population or household numbers. Using data from Shandong Province, where the average village population was 530 and the average household size was 3.1 in 2020, it was estimated that each village had approximately 170 courtyards. With a basic residential land area of 200 m^2 per household, the total residential land area amounted to about 34,000 m^2. Given the per capita arable land in Shandong Province was approximately 1.21 mu (3.75 mu per household), the total agricultural land within the village was estimated to be around 638 mu (424,575 m^2). Dividing the village into groups of 10 households each resulted in 17 neighborhood spaces. Public buildings and green spaces should accommodate centralized resource metabolism functions, while other spaces should be allocated based on quantitative resource metabolism accounting results.

5.4. Resource Metabolism Modelling and Spatial Modelling in Rural Settlements—Based on the "Organic Waste Self-Consumption" Situation

The study of the resource metabolism in the rural settlements within the Shandong Plain was based on the fundamental data of resource metabolism and considered the current production, living conditions, and resource utilization in these areas. This study established a resource metabolism scenario focused on "organic waste self-consumption",

integrating this with the concepts of resource metabolism and the "Production-Living-Ecology" framework. This scenario allowed for the analysis of resource metabolism flows and the calculation of balanced quantities within the village. By incorporating these concepts, this study analyzed resource metabolism flows and balanced rationing. Subsequently, this study constructed a resource metabolism model and a spatial pattern model from the ground up to optimize and enhance the resource metabolism system in rural settlements, improving its integration with spatial elements.

The framework of "organic waste self-consumption" in resource metabolism was established, ensuring that while meeting the fundamental food needs of the village population and livestock, organic waste such as sewage, feces, and straw generated from human, livestock, and agricultural activities was systematically utilized. This approach addresses the primary issues concerning the ecological improvement in rural environments today. This approach tackles critical issues in rural ecological enhancement, encompassing sewage management and local organic waste resource utilization. It is crucial to note that the aim of resource metabolism equilibrium is to maximize the metabolic cycle and self-sufficiency of resource elements within a system. However, this does not imply a completely closed-loop metabolic system without external inputs. Firstly, the rural resource metabolic system requires the continuous external input of solar energy and water resources, including municipal water sources and natural precipitation, as solar energy is essential for all metabolic activities. Secondly, energy self-sufficiency does not imply 100% self-production and consumption but aims for a quantitative balance between energy production and utilization within the system. Lastly, the fertilizers and elements needed for crop production cannot be entirely self-sufficient and must be supplemented externally.

5.4.1. Accounting for the Resource Metabolism Base Allocation

Basic Resource Requirements: Using the smallest spatial unit—a courtyard with an average of 3.1 persons per household—as the base parameter for resource consumption, Table 5 illustrates the annual consumption of major food and water resources and the production of organic waste at the courtyard (3.1 persons), neighborhood (31 persons), and village (530 persons) scales. The resource metabolism capacities and spatial elements at these three scales, along with appropriate resource metabolism technologies, varied. Consequently, the organic waste produced was not directly proportional across scales. For example, in courtyards, organic waste primarily consisted of human feces, domestic organic waste, domestic sewage, and planting organic waste. Small greenhouses, open-air vegetable gardens, and fish farming ponds could consume some of this waste. At the neighborhood scale, additional fecal organic waste from pig and poultry farming was managed, utilizing household biogas tanks and small-scale artificial ecological wetlands to process animal organic waste, domestic sewage, and rainwater. At the village scale, organic waste increased due to the large-scale breeding of cows and sheep, necessitating medium- and large-sized biogas stations for centralized digestion and treatment.

Table 5. Biomass resource base to be consumed (annual average).

Scale Levels	Human and Animal Waste			Domestic Organic Waste	Water		Crop Straw	Notes
	Human	Pig + Poultry	Cow + Sheep		Domestic Sewage	Rainwater		
Courtyard	509 kg	–	–	566 kg	66 m^3	114 m^3	Calculated on the basis of crops that consumed organic waste	Courtyard:neighborhood:village = 3.1:31:530
Neighborhood	5090 kg	21,705 kg	–	5660 kg	660 m^3	345 m^3		
Village	86,530 kg	–	134,228 kg	96,220 kg	–	–		

5.4.2. Resource Metabolism Modelling

Effective organic waste metabolism and consumption require appropriate transformation and utilization of various biomass resources, following the spatial hierarchy of "courtyard-neighborhood-village" from the bottom up. According to the spatial hierarchy

of "courtyard-neighborhood-village" and the principle of "integrating production and life, metabolizing and consuming locally", it was essential to measure the resources required for metabolizing and transforming organic waste at the courtyard scale, along with the spatial indices of various productive spaces and appropriate resource metabolism technologies.

(1) Courtyard

Courtyard space primarily functions for water storage and managing the output of human excreta and organic waste, which is then transported and distributed to neighborhoods. A total of 114 m^3 of collected rainwater directly supplemented fish pond water, followed by the irrigation for fruits and vegetables in courtyards, with any shortfall made up by municipal pipeline water. Based on a 10-day water exchange frequency for fish farming, an ideal pond area of 6.3 m^2 (with a depth of 0.5 m) could meet the annual demand of 34.7 kg of fish per household. Considering gradient utilization and odor issues, 509 kg of human excreta and 566 kg of domestic organic waste were transferred to neighborhood-scale household biogas facilities for oxidative fermentation, generating 87.14 m^3 of biogas for village cooking energy (fecal biogas: 0.06 m^3/kg × 509 kg = 30.54 m^3; domestic organic waste biogas: 0.1 m^3/kg × 566 kg = 56.6 m^3). This process also produced 198.7 kg of methane and 298 kg of digestate, prioritized for fish farming and crop cultivation. Integrating the courtyard space, fish farming required 35 kg/year of methane liquid. The courtyard could support 24 m^2 of rooftop greenhouse and 30 m^2 of an open-air vegetable garden, needing 3.5 kg/m^2/year of methane liquid and 3 kg/m^2/year of methane residue. Methane liquid was fully utilized for fish farming and garden planting, with some residues used for planting. The remaining 276 kg of residues were exported to the neighboring group space. A 24 m^2 rooftop greenhouse could produce 305 kg of vegetables annually (12.7 kg/m^2 × 24 m^2). The remaining digestate was used in the neighborhood space. The 30 m^2 open-air vegetable garden produced 150 kg annually (5 kg/m^2 × 30 m^2), resulting in a total of 455 kg of vegetables and 65.46 kg of straw per year (1.54 kg/m^2 × 24 m^2 + 0.95 kg/m^2 × 30 m^2 = 65.46 kg). These vegetables met the annual demand of 434 kg per household, achieving a vegetable self-sufficiency rate of 105%. Straw was delivered to the group level to feed livestock (Table 6, Figure 16).

Table 6. Resource metabolism status and metabolic modelling at the courtyard level (3.1 persons/household).

Metabolic State	Resource Type	Indicator (yr)	Clarification
Resource input	Rainwater harvesting	114 m^3	Municipal domestic water supply was not included in the calculation process
	Biogas	264.6 m^3	Biogas was the total amount of biogas from both the neighborhood and village scales, and digestate was the total amount of resources to satisfy the cultivation of fruits and vegetables in gardens
	Biogas slurry	198.7 kg	
	Biogas residue	7.22 kg	
Internal metabolism (biology)	Vegetable growing	455 kg	Yard gardening for self-sufficiency
	Aquaculture	34.7 kg	
Resource output	Human waste	509 kg	Distribution to neighborhood spaces for metabolic treatment use
	Domestic sewage	66 m^3	
	Domestic organic waste	566 kg	
	stalk	65.46 kg	

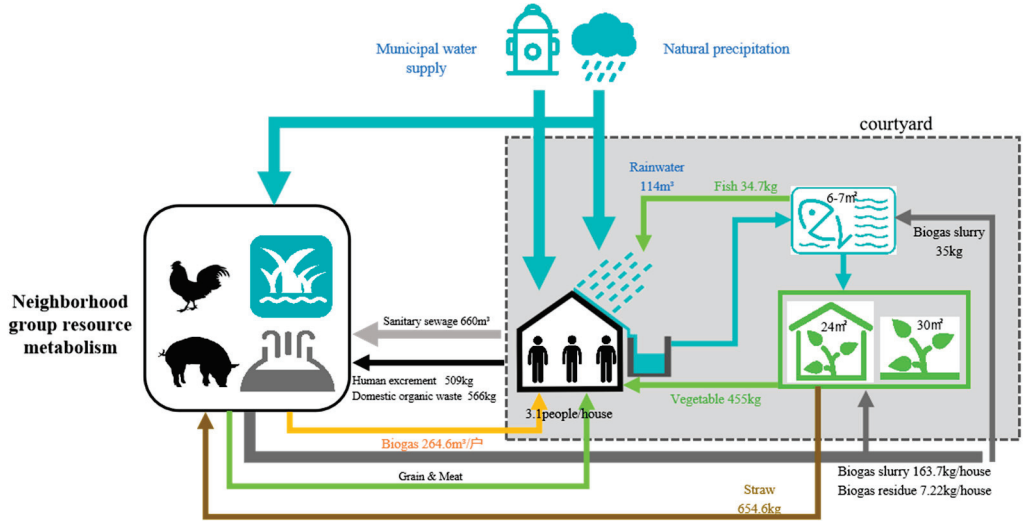


Figure 16. Resource metabolism modelling of courtyards.

(2) Neighborhood

The neighborhood primarily managed livestock manure and domestic sewage in the communal space. With courtyards already meeting vegetable demands, group plantings focused on cereals. To meet the annual meat demand of 10 villagers, 11 pigs and 13 meat birds were raised in the group's communal area, producing sufficient meat and generating 21,705 kg of manure. Approximately 500 m^2 of green space was used for cereal cultivation, yielding 282 kg of cereals annually (28.2 kg per household) and 312 kg of straw. The total straw production from 10 households' vegetable gardens was 967 kg (655 kg from gardens + 312 kg from the cluster), used for livestock breeding. The cluster's household biogas facilities processed 26,795 kg of manure (21,705 kg from livestock + 5090 kg from villagers) and 5660 kg of domestic waste, producing 2173 m^3 of biogas. The biogas residue from 21,705 kg of livestock manure, combined with 2760 kg of residue from 10 village gardens, totaled 7214 kg of biogas residue. The 500 m^2 cereal planting area within the cluster consumed 2969 kg of biogas and 586 kg of digestate. The remaining 6628 kg of digestate was transferred to the village area for centralized agricultural use (Table 7, Figure 17). The resource metabolism flow within the courtyard system boundary is illustrated through a Sankey diagram, reflecting the integration of resource metabolism processes with the spatial morphology of the village, facilitating subsequent spatial metabolism modelling.

Table 7. Resource metabolism status and metabolism models at the neighborhood level (10 households/groups, 31 persons).

Metabolic State	Resource Type	Indicator (yr)	Clarification
Resource input	Rainwater harvesting	412 m^3	Municipal water supply was not included in the calculation process
	Human waste	5090 kg	From the courtyard
	Domestic sewage	660 m^3	
	Domestic organic waste	5660 kg	
	Fruit and vegetable stalks	655 kg	
	Livestock breeding feed	15,568 kg	The amount of external straw feed still needed to be supplied

Table 7. *Cont.*

Metabolic State	Resource Type	Indicator (yr)	Clarification
Internal metabolism (biology)	Grain stalk	312 kg	Group cereal farming
	Animal manure	21,705 kg	–
	Digestate	2969 kg	
	Digestate	586 kg	
Resource export	Cereal cultivation	282 kg	Distribution to courtyards
	Poultry and meat	706 kg	
	Landfill gas	2173 m^3	
	Digestate	1987 kg	
	Digestate	72.2 kg	
		6628 kg	Distribution to villages

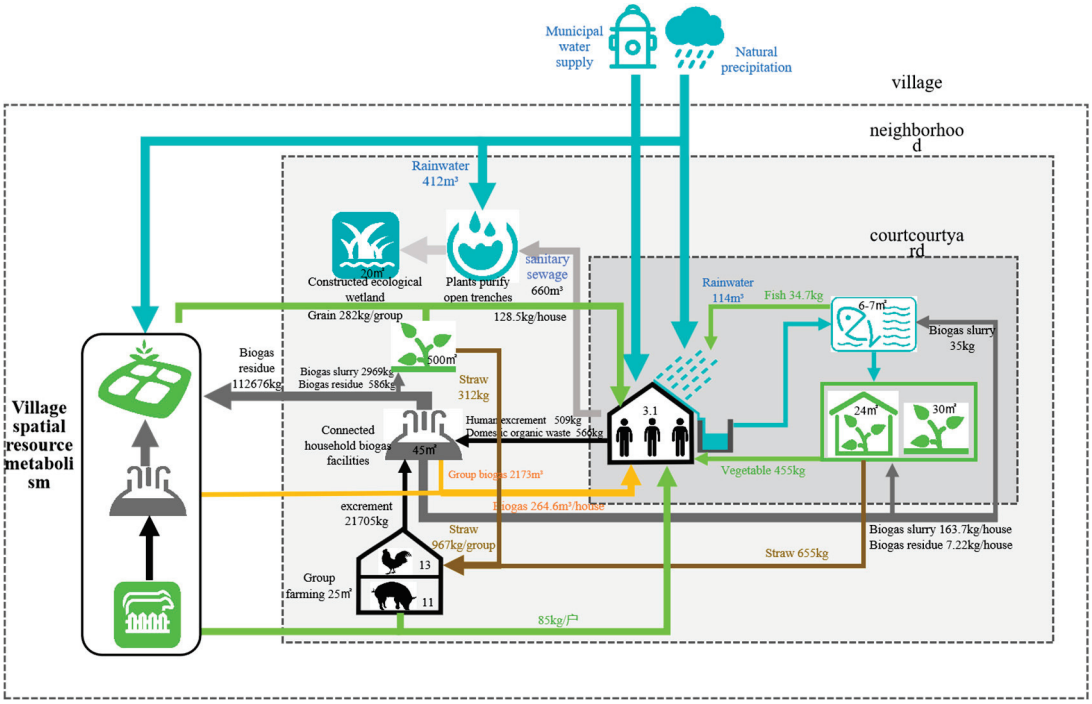


Figure 17. Resource metabolism modelling for neighborhoods.

(3) Whole Village

The metabolic accounting of village resources involved setting up a centralized breeding plant to raise 17 cows and 186 sheep, generating 134,228 kg of manure. A centralized breeding plant for 17 cows and 186 sheep generated 134,228 kg of manure. A centralized biogas station in the breeding space produced 8054 m^3 of biogas, 27,545 kg of biogas residue, and 18,363 kg of biogas slurry. The biogas was distributed to 170 households, each receiving 47.4 m^3, along with 217.3 m^3/household from group biogas plants, totaling 264.7 m^3/household. Each household received 264.7 m^3 of biogas, covering 83.5% of the annual cooking biogas consumption of 317 m^3 per household. The biogas slurry was primarily used for grain cultivation on the village's peripheral arable land. Combining 18,363 kg of biogas residue and 27,545 kg of biogas slurry from the central biogas station with 122,638 kg of biogas residue from 17 clusters provided 140,221 kg of biogas slurry. This mixture could fertilize 41 hectares of grain fields, producing 17,056 kg of grains and 15,416 kg of straw annually. The combined grain output from village farmland and group planting, totaling

21,850 kg, fell short of the annual food demand of 89,252 kg for 530 villagers. Additionally, the straw production was insufficient to meet the feed requirements for cattle and sheep farming (Table 8, Figure 18).

Table 8. Resource metabolism status and metabolic modelling at the village spatial level (530 people).

Metabolic State	Resource Type	Indicator (yr)	Clarification
Resource input	Digestate	112,676 kg	Volume of residual digestate from neighborhoods
	Livestock breeding feed (cattle and sheep)	312,354 kg	The amount of external straw feed still needed to be supplied
Internal metabolism (biology)	Grain stalk	15,416 kg	Cattle and sheep breeding feed
	Animal manure	134,228 kg	Biogas preparation at biogas plants
	Digestate	18,363 kg	Nutrient requirements for supplying cereals for arable cultivation
	Digestate	27,545 kg	
Resource export	Cereal cultivation	17,056 kg	Distribution to courtyards
	Livestock meat (cattle and sheep)	706 kg	
	Landfill gas	8054 m^3	

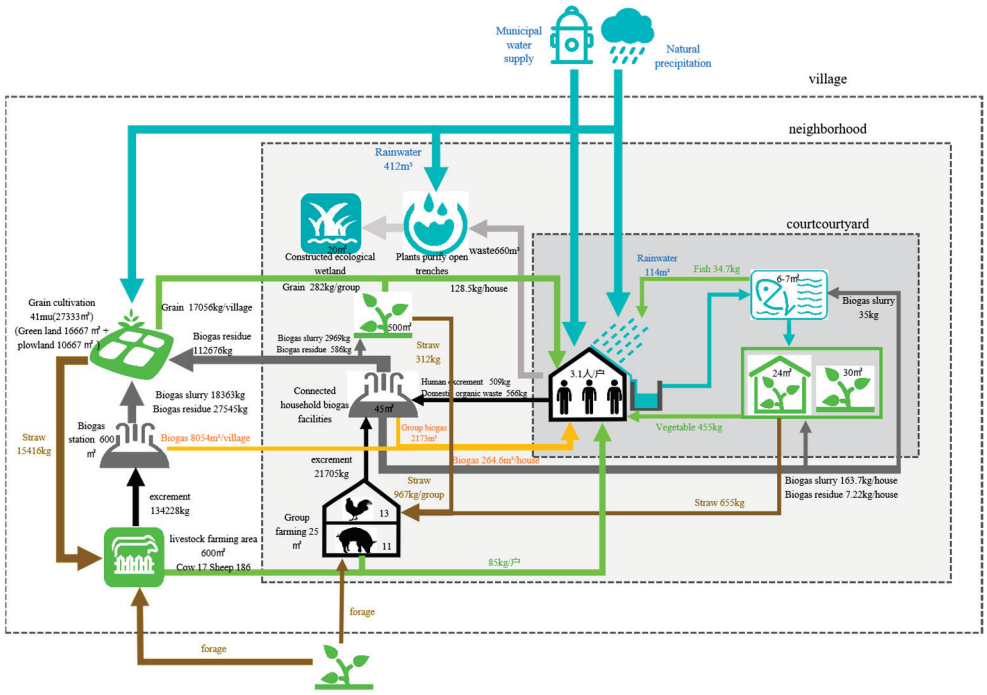


Figure 18. Resource metabolism modelling in the village.

Space allocation for resource metabolism facilities. The breeding area for 17 cows and 186 sheep covered approximately 600 m^2. Adjacent to it, the centralized biogas station, with an annual production capacity of 8054 m^3 of biogas, also occupied 600 m^2. For agricultural cultivation, there were 41 mu of land designated for grains, including 17,000 m^2 of public green space within the village. An additional 16 mu of cultivated land was provided, bringing the total cultivated area of the village to 622 mu.

Analyzing the metabolic flow of various resources at different scales and calculating the self-sufficiency index (SSI) based on the ratio of recycled resources to minimized demand revealed that, under ideal conditions, with 100% self-consumption of organic wastes, the self-sufficiency rate for vegetable cultivation at the yard scale of village residences

was 105%, and for grain cultivation at the neighborhood and village scales, 24.5%. The self-sufficiency rate for straw from fruit, vegetable, and grain cultivation to meet livestock feed demand was 7.3%, and the self-sufficiency rate for cooking energy (biogas) was 83.5% (Table 9, Figure 19). The village had a remaining land area of 622 mu.

Table 9. Statistics on the self-sufficiency of major resources under the situation of organic waste self-consumption.

Resource Type	Quantity Demanded	Supply	Self-Sufficiency Index (SSI)	Metabolic Scale
Landfill gas	317 m^3/household	264.7 m^3/household	83.5%	Neighborhood + village
Fruits	434 kg/household	455 kg/household	105%	Courtyard
Grains	525 kg/household	128.5 kg/household	24.5%	Neighborhood + village
Stalk	465,288 kg/village	33,855 kg/village	7.3%	Courtyard + neighborhood + village

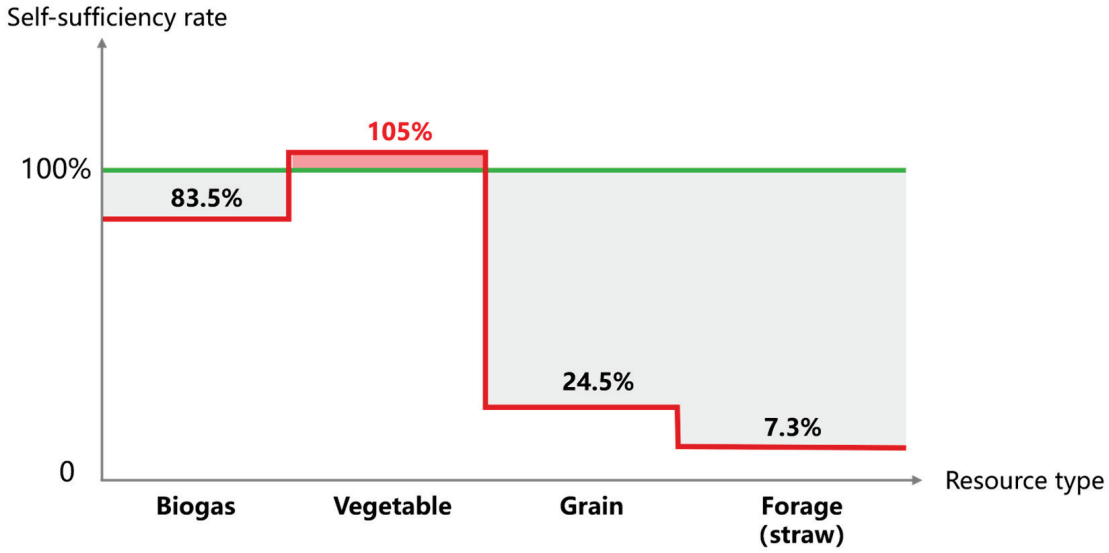


Figure 19. Self-sufficiency rates.

5.4.3. Resource Metabolism Spatial Modelling

The quantitative flow metabolism model and corresponding spatial occupation indices of the main resources for human life and farming production at the three scales—the courtyard, neighborhood, and village—are related from the bottom up. Main resource metabolism elements were allocated reasonably and effectively at each scale, in conjunction with the allocation of basic spatial indices and setting of morphological elements. This approach better adapted to and reflected the spatial layout model of rural settlements under the objective of "organic waste self-consumption". The spatial layout model of rural settlements can better adapt to and reflect the goal of "self-consumption of organic waste".

(1) Spatial Modelling of Courtyards

At the courtyard scale, based on the quantitative measurement of the resource metabolism model, the location and area of various resource metabolism and productive spaces were reasonably allocated (Figure 16). On a 200 m^2 residential base, excluding the village house area of about 90–100 m^2 and courtyard traffic, the remaining 40–50% open space could be used for agricultural cultivation. The roof and ground of a one-story village house provided about 54 m^2 for planting, with 24 m^2 of the roof suitable for a small greenhouse. Vegetable cultivation could assist in heat transfer to neighboring rooms, raising room temperatures in winter. Depending on vegetable yield targets, the courtyard' open vegetable garden could be allocated different areas and locations for resource metabolism and productive spaces (Figures 20 and 21). Depending on vegetable yield

targets, the courtyard open vegetable garden could be converted into a small vegetable greenhouse. Pools of 6–7 m^2 near the courtyard wall could collect precipitation, breed fish, and form an aquaponics system with the planting gallery. Excess water, along with domestic sewage (gray water), could be discharged into the plant purification ditch along the external road, ultimately transferring to the group's small-scale artificial ecological purification wetland system.

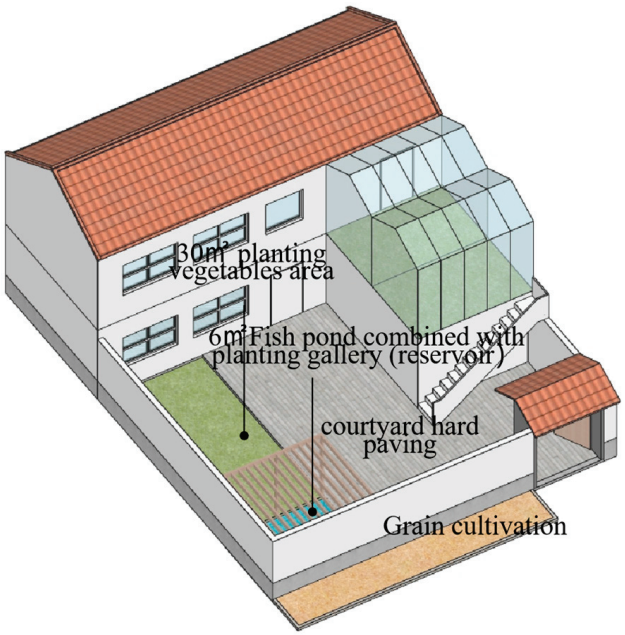


Figure 20. Spatial model of the courtyard.

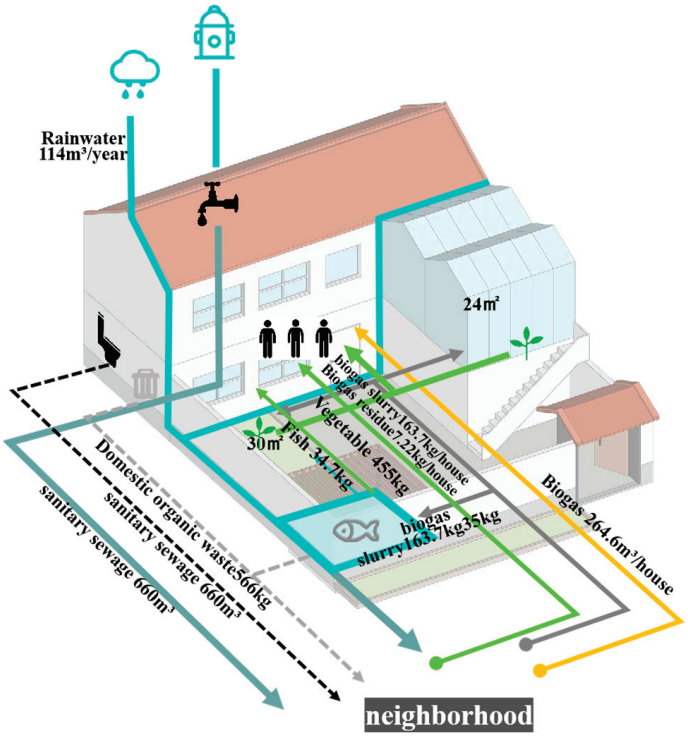


Figure 21. Metabolic spatial model of the courtyard.

(2) Spatial Modelling of Neighborhoods

The neighborhood comprised 10 courtyards responsible for the input, consumption, and distribution of most organic waste resources. Limited open space sites, often unused or abandoned areas, were utilized to integrate various resource-producing and -utilizing technologies and facilities, such as agricultural cultivation spaces, artificial ecological water purification wetlands, and small-scale household biogas digesters. The metabolic space model of the neighborhood was constructed based on the complete recycling and consumption of all types of living and production organic waste by 10 households. The location and area of various facilities, including biogas digesters, were reasonably configured and measured.

Based on the total amount of organic waste at the group scale, it was estimated that a continuous household biogas digester (underground) with an annual biogas production capacity of 2173 m^3 required 45 m^2 of floor space. It is advisable to establish livestock breeding and small-scale greenhouse spaces above it. In the group, 11 pigs and 13 meat birds were raised in a vertical layout. The breeding space was determined to be 25 m^2 based on the number of livestock. The remaining 20 m^2 served as a neighborhood-shared greenhouse. The complementary heat effect of the resource metabolism facilities ensures the underground biogas digester maintains a normal vapor production temperature in winter, while the waste heat from the anaerobic fermentation process insulates the livestock breeding space above. From estimating the artificial ecological wetland area, 10 households in the village produced a total of 660 m^3 of domestic sewage per year. Approximately 580 m^2 of roads and other hard surfaces in the group could collect 412 m^3 of rainwater, totaling 1072 m^3 of gray water. Based on a calculation of 3 m^3/day, the small-scale artificial ecological wetland occupied about 20 m^2 (including 10 m^2 of regulating ponds and 10 m^2 of stabilized ponds combined with lotus root planting, with a water bed depth of 0.7 m). The remaining block vegetable land in front of the house was 140 m^2, and there was 366 m^2 of centralized planting land in the public site, totaling about 500 m^2 mainly used for planting grains. Additionally, a fruit and vegetable planting corridor of about 290 m^2 could be established above the road (Figures 22 and 23). The 10 courtyards in the neighborhood could be flexibly deployed and combined with the open space, integrating suitable resources and metabolic technology facilities to form various group layouts such as enclosed and row types (Figure 24).

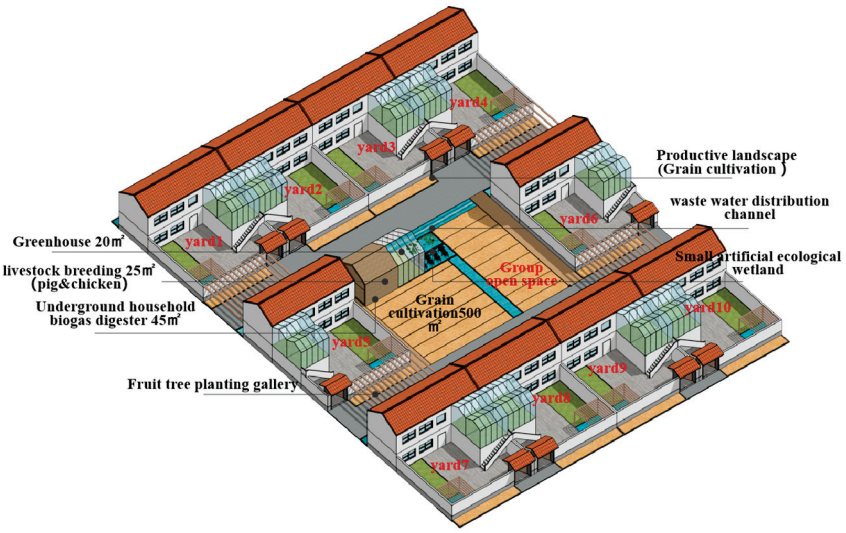


Figure 22. Layout of spatial facilities.

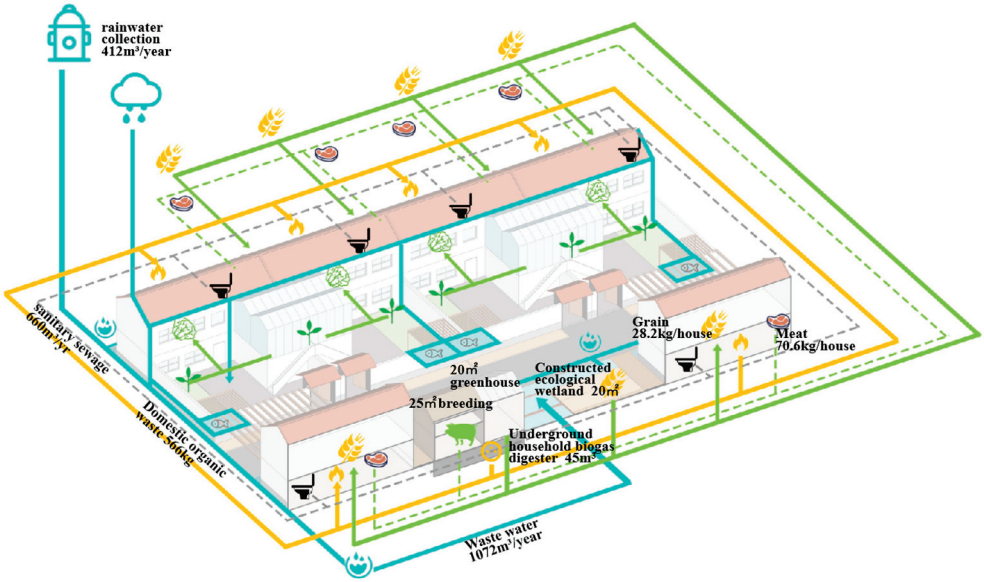


Figure 23. Schematic resource metabolism for the neighborhood spatial model.

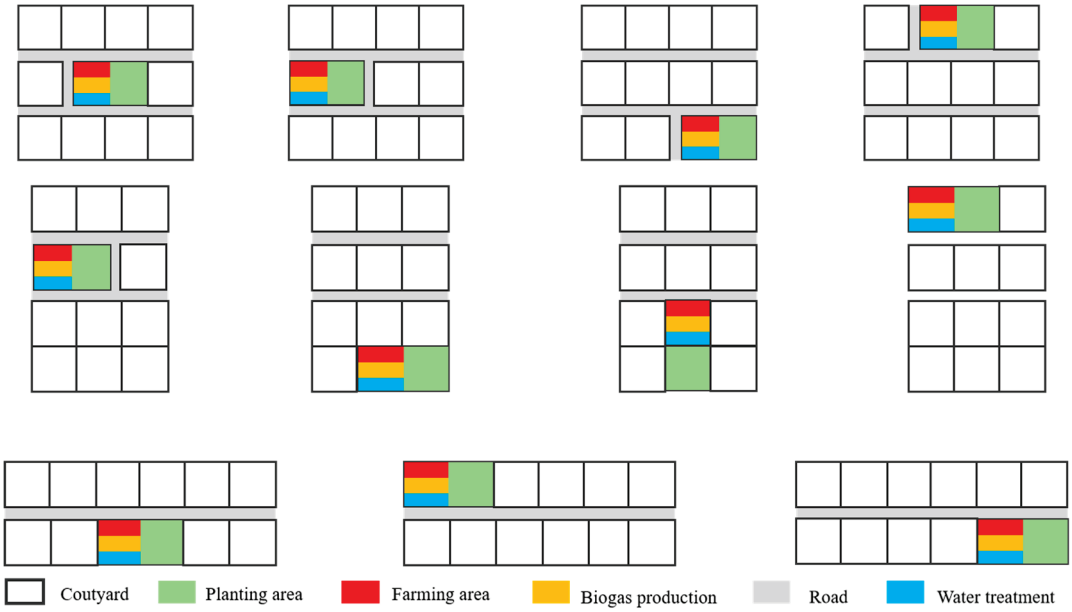


Figure 24. Neighborhood layout.

(3) Village Spatial Modelling

The village, housing 530 residents, covered an area of 766 mu (509,575 m^2). The living area was centralized into 17 neighborhoods, divided by a cross-shaped main road. These clusters were connected through streets and lanes. Land for public buildings (such as the village committee, commerce, health stations, and other public facilities) and green areas were concentrated in the village center. Public green spaces in the village were transformed into productive areas for grain cultivation to meet agricultural production needs and facilitate the consumption of organic waste. The primary resource metabolism facilities were centrally located downwind of the prevailing winds to ensure the efficient metabolism of organic waste and water resources. These facilities were separated from residential areas by green belts to minimize their impact on the living environment (Figure 25).

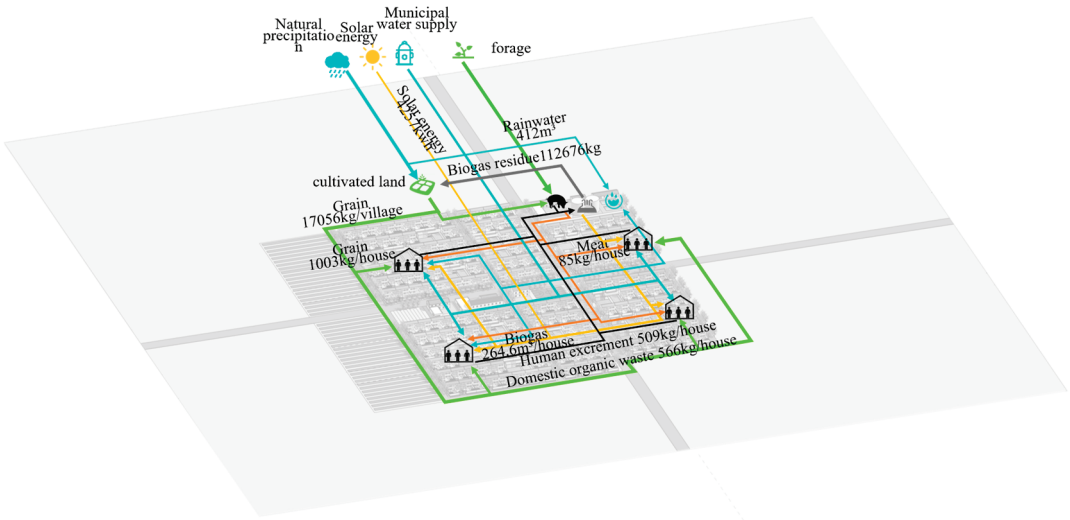


Figure 25. Spatial model of the spatial metabolism in the village area.

6. Conclusions

The resource metabolism modelling process under organic waste self-consumption, utilizing appropriate technologies and integrating spatial elements at different scales, achieved full cyclical metabolism of human and animal organic waste in rural areas. This approach saved significant arable land on the periphery of the village's built-up area. However, it is challenging to achieve self-sufficiency in food resources, necessitating the import of additional nutrients to meet food production needs. The neighborhood scale is crucial in transitioning resource flow and facilitating local transformation. By utilizing public land for livestock breeding, the cultivation of fruits, vegetables, or grains, and water purification and reuse, it is possible to efficiently transform various organic waste resources from village yards. This significantly reduces and decentralizes the burden of constructing and operating resource metabolism facilities at the village scale. This approach also minimizes the distance and process losses associated with resource transmission and distribution. At the courtyard and neighborhood scales, various unused spatial resources are effectively utilized to establish facilities for organic waste resource utilization, achieving the efficient integration of production, living, and ecological spatial elements. While the complete recycling of organic waste from the village population (530 people) and their livestock, meeting nutrient needs for basic food cultivation (especially grains) and cooking energy, remained challenging, modelling the complete consumption of organic waste helped for understanding the dynamic coupling between organic waste consumption and the available space for agricultural support. Modelling organic waste adequacy helps elucidate the dynamic coupling between organic waste consumption and the spatial requirements for agricultural support.

Author Contributions: Conceptualization, M.L. and Z.Z.; methodology, M.L.; software, M.L.; validation, M.L. and Z.Z.; formal analysis, M.L.; investigation, J.Z.; resources, J.Z.; data curation, C.L.; writing—original draft preparation, Z.Z.; writing—review and editing, M.L.; visualization, M.L.; supervision, J.Z.; project administration, C.L.; funding acquisition, Z.Z. All authors have read and agreed to the published version of the manuscript.

Funding: This work was supported by the Natural Science Foundation of Shandong Province of China (General Program) (Grant No. ZR2023ME229) and China. & Shandong Provincial Key R&D Program (Soft Science Project) (No. 2024RKY0604). and "the Case Repository for the Revitalisation and Adaptive Reuse of Industrial Heritage" (Grant No. SDYAL2022157) funded by the Graduate Teaching Case Repository for Professional Degrees in Shandong Province, China.

Data Availability Statement: The data that support the findings of this study are available from the corresponding author [LIU Meng] upon reasonable request.

Conflicts of Interest: ZHOU Zhongkai reports having received financial support provided by the Shandong Provincial Department of Science and Technology, the Natural Science Foundation of Shandong Province of China, and the Graduate Teaching Case Repository for Professional Degrees in Shandong Province. If there are other authors, they declare that they have no known competing financial interests or personal relationships that could have appeared to have influenced the work reported in this paper.

References

1. Wolman, A. The metabolism of cities. *Sci. Am.* **1965**, *213*, 178–193. [CrossRef]
2. Rappaport, R.A. The flow of energy in an agricultural society. *Sci. Am.* **1971**, *224*, 117–133.
3. Ayres, R.U. Industrial metabolism: Theory and policy. In *The Greening of Industrial Ecosystems*; Allenby, B.R., Richards, D.J., Eds.; National Academy Press: Washington, DC, USA, 1994.
4. Alberti, M. Measuring urban sustainability. *Environ. Impact Assess. Rev.* **1996**, *16*, 381424. [CrossRef]
5. Newman, P.W.G. Sustainability and cities: Extending the metabolism modelf1l. *Land Use Urban Plan.* **1999**, *44*, 219–226. [CrossRef]
6. Agudelo-Vera, C.M.; Mels, A.R.; Keesman, K.J.; Rijnaarts, H.H. Resource management as a key factor for sustainable urban planning. *J. Environ. Manag.* **2011**, *92*, 2295–2303. [CrossRef]
7. Girardet, H. The Metabolism of Cities. *Sci. Am.* **1990**, *213*, 179–190.
8. Kennedy, C.; Pincetl, S.; Bunje, P. The study of urban metabolism and its applications to urban planning and design. *Environ. Pollut.* **2011**, *159*, 1965–1973. [CrossRef]
9. Roggema, R. *TransFEWmation: Towards Design-Led Food-Energy-Water Systems for Future Urbanization*; Springer: Cham, Switzerland, 2021.
10. Tillie, N.; Van Den Dobbelsteen, A.; Doepel, D.; Joubert, M.; De Jager, W.; Mayenburg, D. Towards CO_2 Neutral Urban Planning: Presenting the Rotterdam Energy Approach and Planning (REAP). *J. Green Build.* **2009**, *4*, 103–112. [CrossRef]
11. Jan, J.; Nelson, N.; Goosens, F. Recyclicity: A Toolbox for Resource-Based Design. *Archit. Des.* **2011**, *81*, 54–61.
12. Zhao, Q. *A Primer on Urban Efficiency—Research Practices Based on Metabolic Efficiency in Urban Settlements*; Science Press: Beijing, China, 2017; pp. 237–253.
13. Yue, X.; Zhang, Y. The research about concept evolution and development process of ecovillage abroad. *Archit. J.* **2011**, 123–129. Available online: https://xueshu.baidu.com/usercenter/paper/show?paperid=207dc80508da27ffd0c6491915f000a2&site=xueshu_se (accessed on 10 October 2024).
14. Bian, Y. *Reunion Eco-Agricultural Systems*; China Environmental Science Press: Beijing, China, 1988.
15. Weng, B.; Huang, Q.; Chen, J. Construction of Eco-Village-New Development of Sustainable Agriculture. *Yunnan Environ. Sci.* **2000**, *19*, 99–103.
16. Chen, Y.; Yang, Y. Comments and prospects of eco-village construction in China. *North. Environ.* **2011**, *23*, 71–74.
17. Zhao, J.; Zhang, Y. Contemporary Western Experiment on Integration of Urban Agriculture and Urban Space. *New Archit.* **2012**, 27–31. Available online: https://xueshu.baidu.com/usercenter/paper/show?paperid=46b7ec95aee4e9a5e3fb5d696e598357&site=xueshu_se (accessed on 10 October 2024).
18. Baccini, P.; Brunner, P.H. *Metabolism of the Anthroposphere: Analysis, Evaluation, Design*; The MIT Press: Cambridge, MA, USA, 2012.
19. Zhou, Z.; Yang, X.; Zhao, J. The Rural Settlements Design and Practice Under the Resource Metabolism Theory and Its Influence. *Architect* **2021**, 75–83. Available online: http://thearchitect.cabp.com.cn/ch/reader/view_abstract.aspx?file_no=20210508 (accessed on 10 October 2024).
20. Chen, X.; Wu, L.; Dang, Y. The Inherent Mechanism and Enlightenment of Production-Living-ecological Space in Traditional Human Settlement Environment. *Urban Dev. Stud.* **2022**, *29*, 6–11.
21. Chen, X. Spatial Characters and Restructuring Keynotes of the Rural Area in China. *Planners* **2007**, 79–82. Available online: https://xueshu.baidu.com/usercenter/paper/show?paperid=3c439077ab54f58e8485fa1a78cb50dc&site=xueshu_se (accessed on 10 October 2024).
22. Korhonen, J. Two paths to industrial ecology: Applying the product-based and geographical approaches. *J. Environ. Plan. Manag.* **2002**, *45*, 39–57. [CrossRef]
23. Zhou, Z.; Yang, R.; Hao, X.; Zhao, J. Research on the Optimal Design Path and Strategy of Rural Space from the Metabolism Perspective: A Case Study of Xishan Village, Zibo City. *Mod. Urban Res.* **2023**, *8*, 50–58.
24. Forman, R.T. Land mosaics: The ecology of landscapes and regions 1995. In *The Ecological Design and Planning Reader*; Island Press: Washington, DC, USA, 2014; pp. 217–234.
25. Zhou, Z.; Chen, Q.; Zhang, H.; Wu, W. Study on the "Four-in-One" eco-agricultural model. *Renew. Energy Resour.* **2007**, 93–96. Available online: https://xueshu.baidu.com/usercenter/paper/show?paperid=297700d6935bae3ff31930b20406d2a9&site=xueshu_se (accessed on 10 October 2024).
26. Fu, Y. Pleasure of Water Gathered: Restoring the Public Space in Villages Based on Ecological Demonstration on the Design of an Ecological Rainwater Garden in Lianma Village, Guangzhou City. *Archit. J.* **2016**, 101–103. Available online: https://www.gooood.cn/pleasure-of-water-gathered.htm (accessed on 10 October 2024).
27. John, L.; Joshua, B.; Zhang, J. Rural Urban Framework (RUF)/The University of Hong Kong; Jintai Village Reconstruction, Bazhong, China 2017. *World Archit.* **2018**, *36*. Available online: https://www.archdaily.com/882714/jintai-village-reconstruction-rural-urban-framework (accessed on 10 October 2024).

28. Liu, C.; Zhang, Y.; Zhao, J. Research on urban agro-integrated community based on circular metabolism. *City Plan. Rev.* **2018**, *42*, 52–59.
29. Meng, K. Construction of Closed-Loop Model of Material Energy in Tianjin Eco-Village Based on System Dynamics and Research on Spatial Layout. Master's Thesis, Hebei University of Technology, Tianjin, China, 2022. [CrossRef]
30. Yiu, E.C.Y.; Castro Campos, B. *A Novel Planning Model for Approaching a Zero-Food and Zero-Waste Community*; Social Science Electronic Publishing: New York, NY, USA, 2014.
31. Leduc, W.R.W.A.; Rovers, R. Urban Tissue: The representation of the Urban Energy Potential. In Proceedings of the PLEA 2008-25th Conference on Passive and Low Energy Architecture, Dublin, Ireland, 22–24 October 2008.
32. Takeuchi, K.; Namiki, Y.; Tanaka, H. Designing eco-villages for revitalizing Japanese rural area. *Ecol. Eng.* **1998**, *11*, 177–197. [CrossRef]
33. Song, W. Study on the Spatial Form of Traditional Villages in Shandong. Ph.D. Thesis, Dalian University of Technology, Dalian, China, 2021.
34. Shandong Provincial Department of Water Resources. *Shandong Provincial Water Conservancy Yearbook 2012*; Shandong Provincial Map Publishing House: Jinan, China, 2013.
35. Sheng, S.; Wang, Y. Rural Ecological Restoration Strategies in Plain Agricultural Areas Based on the Identification of Ecological Characteristics and Issues through Clustering—A Case Study of Heishan County, Liaoning Province. *Chin. Landsc. Archit.* **2022**, *38*, 20–25.
36. Shandong Provincial Department of Water Resources. *The 13th Five-Year Plan for Water Conservancy Development in Shandong Province Shandong*; Shandong Provincial Department of Water Resources: Jinan, China, 2020.
37. Liu, C.; Zhao, J. *Integrated Community in Cities*; China Architecture & Building Press: Beijing, China, 2016.
38. People's Republic of China Bureau of Statistics. *China Rural Statistical Yearbook*; China Statistics Press: Beijing, China, 2021.
39. Shandong Provincial Bureau of Statistics. *Shandong Statistical Yearbook*; China Statistics Press: Beijing, China, 2021.
40. Shandong Provincial Bureau of Statistics. *Statistical Communiqué on the National Economic and Social Development of Shandong Province in 2022*; China Statistics Press: Beijing, China, 2021.
41. Zhu, J.; Huang, Z.; Zou, C.; Jiang, Y.; Wu, Y. Centralized (Joint Households) Gas Supply Mode of Rural Small-scale Biogas Projects in Ji'an County. *China Biogas* **2008**, *26*, 34–36.
42. A Pattern Language. In *Christopher Alexander*; China Architecture & Building Press: Beijing, China, 1989.
43. Wang, Z.; Fan, L.; Chen, Z. Study on the Pattern of "Eco-habitation" in New Countryside: Case Study of Countryside in Southern Yangtze River Areas of China. *Archit. J.* **2011**, 22–26. Available online: https://xueshu.baidu.com/usercenter/paper/show?paperid=93bf49a58e7dcb0e0133d1e34999f6c9&site=xueshu_se (accessed on 10 October 2024).

Disclaimer/Publisher's Note: The statements, opinions and data contained in all publications are solely those of the individual author(s) and contributor(s) and not of MDPI and/or the editor(s). MDPI and/or the editor(s) disclaim responsibility for any injury to people or property resulting from any ideas, methods, instructions or products referred to in the content.

buildings

MDPI

Article

Examining the Impact of the Built Environment on Multidimensional Urban Vitality: Using Milk Tea Shops and Coffee Shops as New Indicators of Urban Vitality

Ziqi Xu [1], Jiang Chang [1,*], Fangyu Cheng [2], Xiaoyi Liu [1], Tianning Yao [1], Kuntao Hu [1] and Jingyu Sun [3]

[1] School of Architecture and Design, China University of Mining and Technology, Xuzhou 221116, China; ts22190042p31@cumt.edu.cn (Z.X.); ts23190006a31@cumt.edu.cn (X.L.); tianning_yao@cumt.edu.cn (T.Y.); ts22190026p31@cumt.edu.cn (K.H.)
[2] School of Architecture and Design, Harbin Institute of Technology, Harbin 150001, China; fcheng@hit.edu.cn
[3] School of Materials Science and Engineeing, Shanghai University of Engineering Science, Shanghai 201620, China; angjusun@outlook.com
* Correspondence: changjiang@cumt.edu.cn

Abstract: Urban vitality is a critical driver of sustainable urban development, significantly contributing to the enhancement of human well-being. A thorough and multidimensional comprehension of urban vitality is essential for shaping future urban planning and policy-making. This study, focused on Chengdu, proposes a framework for assessing various dimensions of UV through the distribution of milk tea and coffee shops. Using random forest and multi-scale geographically weighted regression models, this study investigates the factors influencing urban vitality from both mathematical thresholds and spatial heterogeneity, and develops spatial maps of future vitality to inform targeted urban strategies. The results show that (1) the milk tea index is effective in capturing population vitality, while the coffee index is more closely associated with economic vitality and urban renewal; (2) office buildings (13.46%) and commercial complexes (13.70%) have the most significant impact on both economic and population vitality, while the importance of transportation factors has notably decreased; (3) the influence of these factors demonstrates spatial heterogeneity and nonlinear relationships, with subway station density of 0.5–0.8 stations per kilometer being optimal for stimulating both types of vitality. The minimum threshold for economic vitality in a given unit is a housing price exceeding 6000 RMB/m^2; (4) the future vitality map suggests that urban planners should pay greater attention to non-central districts with high development potential. Moreover, spontaneous social interactions and consumer behaviors stimulated by various shops are critical components of urban vitality. In designing the physical environment and urban spatial forms, special attention should be given to enhancing the attractiveness of physical spaces and their capacity to accommodate social interaction.

Keywords: urban vitality; milk tea and coffee shops; random forest; MGWR model; nonlinear relationships; social interactions

1. Introduction

The concept of "urban vitality (UV)" originated in the 1960s and has undergone significant evolution and enrichment through the examination of urban morphology and social interactions by Western scholars. Research across diverse disciplines, including geography, sociology, and urban management, has consistently identified UV as a fundamental metric for evaluating urban quality of life [1]. Urban spaces with high vitality are widely regarded as optimal environments for residential, occupational, and recreational purposes, as they foster social cohesion and contribute significantly to the overall well-being of inhabitants. Furthermore, such spaces are instrumental in attracting human capital, stimulating urban innovation, and mobilizing social investment, thereby enhancing urban competitiveness.

Further inquiry into UV must address three core questions: what constitutes UV, how can it be effectively represented, and what factors influence it? Jacobs, who introduced this concept to urban studies, posited that UV emerges from the diversity of life generated by the interweaving of citizen activities and living spaces, with "street life over a 24 h period" being central to the concept of UV [2]. Lynch, from the perspective of spatial morphology, emphasized that the essence of this concept lies in the capacity of settlement morphology to support and accommodate human activities, ecological requirements, and life functions [3]. Meanwhile, Maas deconstructed UV into three essential components: the continuous presence of people in public spaces, their activities, and the environments in which these activities occur [4]. These theoretical perspectives underscore the intricate and complex interactions between human activities and spatial morphology. Kim attempted to conceptualize UV from a more macro-level perspective, extending its theoretical framework to encompass economic, social, and cultural dimensions based on urban sociological theories [5]. The inherent complexity of cities and populations has resulted in an absence of consensus regarding a unified definition of UV; however, the notion that "UV is a multidimensional concept encompassing population, social, economic, and spatial aspects" has gradually gained widespread acceptance [6]. Therefore, this study will primarily focus on the population and economic dimensions, with particular emphasis on how built environment elements facilitate the synergy between dense pedestrian activities and economic consumption.

UV consists primarily of two key aspects: crowd aggregation and place attractiveness. The precise quantification of UV plays a crucial role in objectively assessing the quality of urban development [7]. Traditional methods for measuring human activity, such as field observations, often fell short in effectively capturing large-scale patterns of human movement within urban environments [8,9]. With the development of information technology, large-scale, high spatiotemporal precision "volunteered geographical information" (such as mobile phone signaling data, social media data, and Wi-Fi data) has gradually become a mainstream method for dynamically monitoring and accurately quantifying UV. The advent of large-scale, high-resolution "volunteered geographical information (VGI)"—encompassing mobile location data [10], cell phone signal data [11], social media data [12]—has provided a prominent tool for dynamically monitoring and accurately quantifying UV. Despite these advancements, challenges related to data accessibility have somewhat limited its broader application. Numerous studies have also introduced physical urban elements, such as road intersection density, points of interest (POI) diversity, land-use heterogeneity, and residential price per square meter, as indirect indicators of UV [13–15]. In recent years, night-time light data (NTL), which integrate urban spatial morphology with the intensity of human socio-economic activities, have been widely employed to quantify UV and development, particularly showing strong performance in areas such as urban expansion, economic growth, and energy consumption [16–18]. Nonetheless, it is imperative to account for the intrinsic discrepancies in how different data types capture and represent UV [19]. For instance, university campuses may exhibit high densities of mobile signaling and social media check-ins, yet show relatively low POI distributions, which may lead to potential misinterpretations of vitality in such settings. Therefore, the implementation of a multidimensional analytical framework is essential to ensure a more comprehensive and accurate representation of UV, thereby allowing researchers to derive a deeper and more nuanced understanding of urban dynamics.

Small-scale food venues, such as coffee shops (COSs), beverage outlets, and fast-food restaurants, have recently been recognized as indirect indicators of UV. These venues not only attract crowds but also support diverse economic and social activities within urban streets and communities [20,21]. Their dependence on a stable customer base and sensitivity to environmental changes make them ideal for reflecting the real-time state of UV [22]. Studies conducted in various cities, including the United States [23], Berlin [24], Shenzhen [25], and Beijing [26], have confirmed this observation. COSs are typically located in densely populated and highly walkable areas [27,28], functioning as "third spaces" that

provide platforms for social interaction and co-working [29], while also hosting significant economic activities. Quantitative research by Donner and Guzman has highlighted that communities with Starbucks outlets tend to demonstrate more pronounced economic and innovative development outcomes [30,31]. Glaeser et al. further identified a strong correlation between the presence of Starbucks and key indicators of UV, such as housing prices [32]. Shi et al. employed the "Starbucks Index" calculated based on the number of Starbucks outlets, as a proxy indicator for urban commercial activity and conducted a study that used COSs to represent urban economic vitality [33].

Milk tea, a traditional Chinese beverage [34], has seen rapid global expansion since its rise in popularity around the 2000s [35], with a market size reaching $2.46 billion by 2023 [36]. Despite the growing influence of coffee culture in China [37], consumption data show that tea-based beverages remain dominant [38,39]. With milk tea shops (MTSs) expanding at an annual rate of 15% [40], they have become a notable feature in China's urban landscape. However, most existing research has focused on aspects such as the health impacts of milk tea [35], consumer behavior [41], spatial design [42], and the brand management [43], while little attention has been paid to the relationship between MTSs and UV. It remains unclear whether MTSs, like COSs, can serve as "indicator locations" of UV, and if so, what aspects they might represent. This study, based on a systematic exploration of Chengdu, provides evidence on the potential of MTSs to serve as indicators of UV and explores the aspects they may represent.

In-depth investigation of the spatial drivers behind UV is crucial for formulating targeted policies to promote vitality. Human activities and socio-economic factors are widely recognized as fundamental influences on UV [44,45], while built environment elements—such as facility diversity [46], transportation accessibility [47], mixed land-use [48], urban texture [10], and street color [49]—have also been extensively confirmed to affect the intensity of UV. Adequate infrastructure and well-designed street facades often support more diverse human activities, fostering vibrant streets and communities. Traditional models, such as ordinary least squares (OLS) regression and geographically weighted regression (GWR), have made important contributions to understanding the relationship between the built environment and UV [50,51]. However, the complexity and diversity of urban spatial structures pose challenges for these models in addressing spatial heterogeneity and nonlinear relationships between variables [52]. The fixed bandwidth analysis in GWR models may not fully capture spatial scale differences, and the assumed linear relationship between the built environment and UV has been questioned in the context of rapid urban development [53]. Machine learning (ML) models, which are adept at identifying nonlinear relationships, and multi-scale geographically weighted regression models (MGWR), which account for variations in spatial scales, present new opportunities for advancing our understanding of this relationship [54,55].

In light of the above discussion, this study explores the utility of the "Milk Tea Index (MTI)" and the "Coffee Index (COI)" in representing UV, using Chengdu as a case study. We employ the MGWR model and random forest (RF) to investigate the relationship between built environment factors and UV. Finally, we generate future vitality maps based on the findings to expand the deeper application of these indices. Therefore, this study aims to (1) utilize coffee and milk tea shops to measure different dimensions of UV, compare their similarities and differences, and provide a new methodological reference for the quantitative assessment of UV; (2) explore the relationship between built environment characteristics and UV represented by the MTI and COI while accounting for nonlinear relationships and spatial heterogeneity; (3) propose region-specific strategies to enhance UV based on the findings.

2. Materials and Methods

2.1. Study Area

This study examines 12 administrative districts in Chengdu, each exhibiting distinct levels of development (Figure 1). Historically, Chengdu has been recognized as a highly

livable city with a strong foundation in commerce and trade. Today, it ranks as one of the most economically developed and commercially dynamic regions in western China. Chengdu consistently appears at the top of the "Forbes China Urban Consumption Vitality" index, with its permanent population increasing by nearly 6 million over the past decade. In 2023, Chengdu's food and beverage retail sales accounted for 15.88% of the city's total, significantly surpassing other major cities such as Beijing and Shanghai, positioning Chengdu as the leading city in China for dining expenditures. In the same year, the number of milk tea outlets in Chengdu ranked third nationwide, behind Guangzhou and Shenzhen, while its number of independent coffee shops was second only to Shanghai. Chengdu is emerging as a "beverage capital" of western China [56].

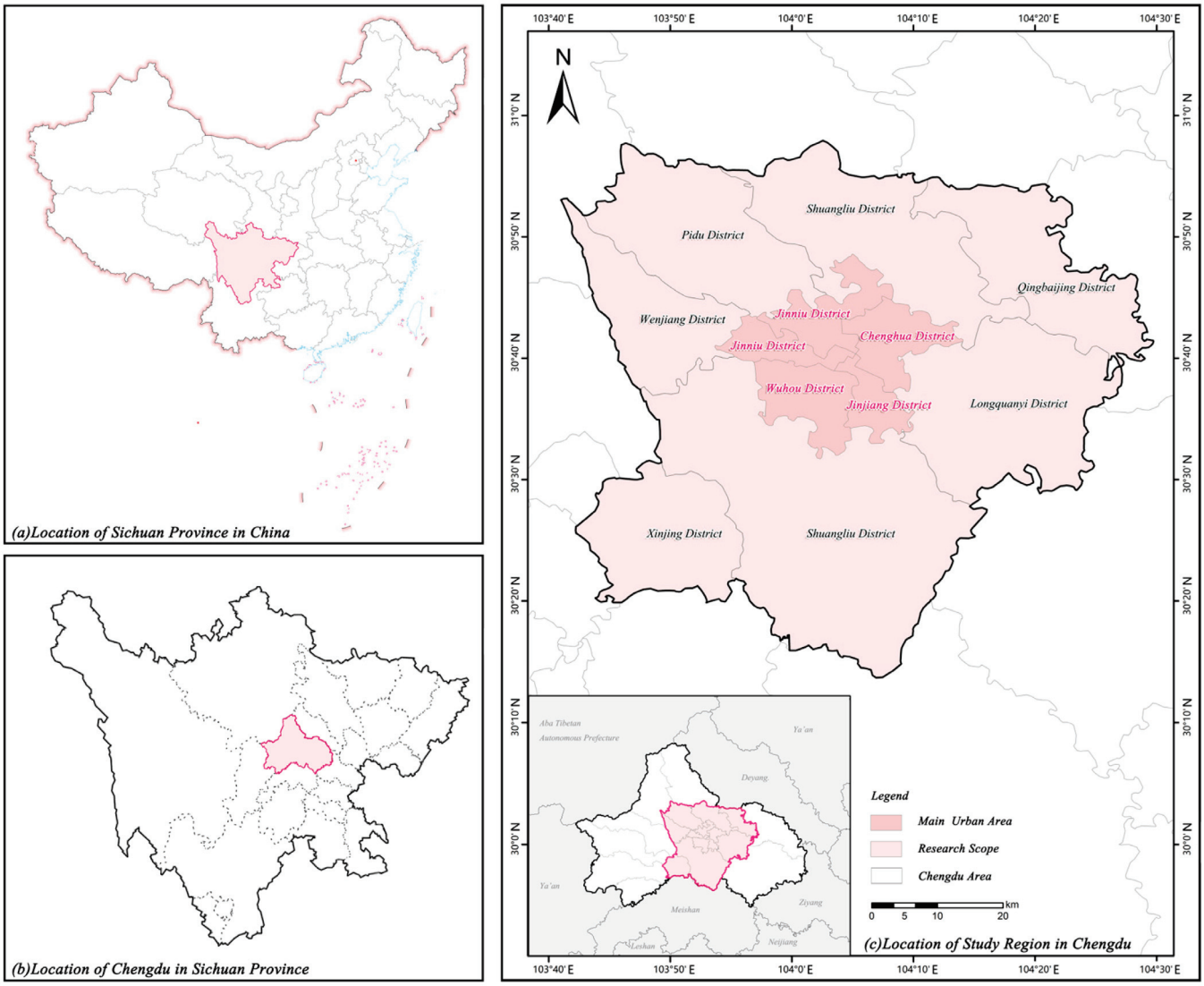


Figure 1. Overview map of the study area((**a**) Location of Sichuan Province in China. (**b**) Location of Chengdu in Sichuan Province. (**c**) The specific composition of the study area).

2.2. Data Sources and Processing

Considering the synthesis of existing research, this paper employs three categories of data: remote sensing imagery, open-source big data, and traditional statistical data. The data type, data source, and acquisition time are shown in Table 1.

Table 1. Data source for this article.

Data Type	Data Name	Data Year	Data Source
Remote sensing imagery	NPP-VIIRS-like NTL Data (NTL)	2012–2023	Yangtze River Delta Science Data Center, National Earth System Science Data Sharing Infrastructure, National Science & Technology Infrastructure of China (http://geodata.nnu.edu.cn/, accessed on 10 July 2024).
	Worldpop Population Data	2000–2020	https://www.worldpop.org/ (accessed on 12 July 2024).
	China GDP Spatial Distribution Kilometer Grid Dataset	2000–2020	Resource and Environmental Science Data Platform (https://www.resdc.cn/DOI/DOI.aspx?DOIID=33, accessed on 15 July 2024)
Open-source big data	POI data	2023	Gaode Map API Data Open Interface (https://lbs.amap.com/, accessed on 18 October 2023)
	Road network data	2023	OpenStreetMap (https://www.openstreetmap.org, accessed on 18 October 2023)
	Housing price data	2023	Lianjia, Beike and other housing sales website (Accessed on 19 October 2023)
Traditional statistical data	Population data	2021	It is compiled from the 7th census data of Chengdu City and the statistical bulletins of various districts and counties. These data were used for precise correction and calibration of population density data.
	Administrative division	2023	National geographic information resources directory service system (https://www.webmap.cn/main.do?method=index, accessed on 23 October 2023)

This study employed an equal grid method to divide the research area, allowing for the aggregation of different data at a unified scale. This method minimizes the errors caused by administrative boundaries, enabling a more refined analysis of UV. Specifically, following the research of Jin et al., the study area was divided into 3977 grids, each measuring 500 m × 500 m [57]. This scale is comparable to the street unit analysis commonly used in planning research and is consistent with the resolution of the night-time light data employed in the study. Additionally, we used data from the Seventh National Census of Chengdu to calibrate the WorldPop population distribution raster data, ensuring the highest possible accuracy. All data were standardized to the Albers_Conic_Equal_Area coordinate system.

2.3. Research Method

The research process of this study is shown in Figure 2 and consists of the following specific steps: (1) constructing UV indicators using POI data from two types of beverage shops; (2) building a built environment dataset by integrating multi-source statistical data, geographic big data, and remote sensing data; (3) applying MGWR and RF models to explore the impact of various factors on UV; (4) predicting the spatial patterns of future UV and proposing planning strategies based on the research findings.

2.3.1. Use Kernel Density Analysis to Construct the MTI and COI

Analogous to the Starbucks Index, this article proposed the MTI and the COI. Considering the differences in commercial composition and scale between Chinese and Western cities, the fact that Starbucks stores account for only 11.38% of all COSs in Chengdu, and the existing conclusion that Starbucks stores and other coffee shops show little difference in their ability to represent UV [58], we selected all types of MTSs and COSs as the focus of this study.

Specifically, based on Gaode Maps' classifications, the study obtained and cleaned POI data for 3880 MTSs and 2513 COSs using Python. Subsequently, kernel density estimation, which effectively visualizes the clustering and dispersion of elements within a region, was

applied to construct both indices. The MTI and COI were defined as the kernel density values of MTSs and COSs POIs within each grid. The relevant calculation formulas are as follows:

$$f(x) = \frac{1}{nh}\sum_{i=1}^{n} k\left(\frac{x - x_i}{h}\right) \quad (1)$$

In the formula, $f(x)$ represents the kernel density function of the observation point, which refers to MTI and COI in each grid; n denotes the number of features (the total count of the two types of stores); h is the search radius; and $x - x_i$ indicates the distance between the estimation point x and the observation point x_i. A higher value of $f(x)$ suggests a greater density of store distribution.

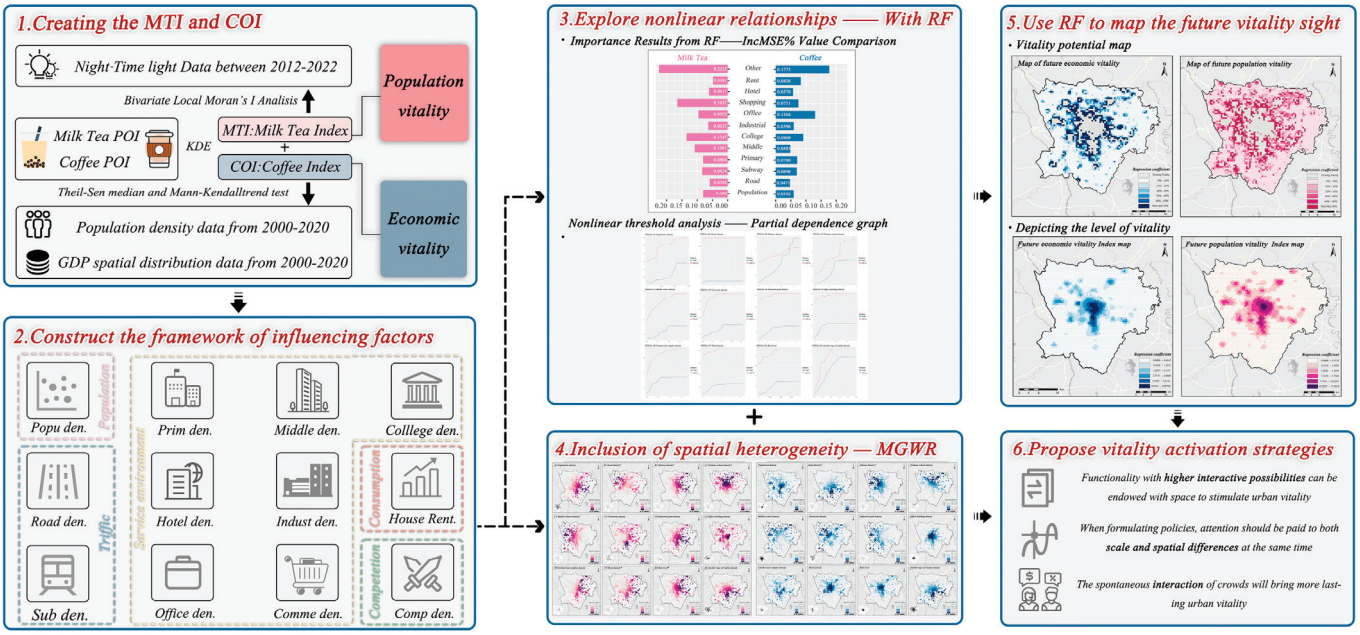


Figure 2. Research framework diagram.

2.3.2. Establish the Relationship Between MTI, COI, and UV

- Select the Indicator for UV

In this paper, NTL was used to represent UV. NTL, which is closely related to urban socio-economic activities such as population migration and regional development, consists of two primary components: the first is derived from static lighting sources, such as street lamps, while the second is related to outdoor human activities, including traffic flow, population mobility, and commercial or recreational activities [59]. Theoretically, this enables a clear distinction between dark, non-urban areas and bright centers of human activity, with variations in brightness indirectly indicating changes in the intensity of human activities [60]. These variations reflect the spatial and temporal distribution and balance of human activity, making NTL a widely used and effective tool for monitoring UV and development [61,62]. Furthermore, Ma et al.'s research confirmed NTL's utility in quantifying regional dynamics over short time scales at provincial, city, county, and pixel levels by examining its relationship with Tencent location big data, which directly reflects human activity, thus enhancing our understanding of human activity patterns [63].

- Validate the Relationship Between the Two Indices and UV Using Spatial Autocorrelation

Spatial autocorrelation was used to determine whether the MTI and COI were statistically and spatially correlated with NTL. Spatial autocorrelation analysis primarily measured the degree of dependency between data points and their neighboring locations [64]. Based on the number of variables, it was divided into univariate Moran's I, which described the overall clustering distribution of data within a region, and Bivariate Local Moran's I, which

revealed whether two elements within the same unit exhibited spatial dependency. The relationship between the attributes of a unit and those of its neighboring units was often characterized by the Local Moran's I (LISA).

In this study, the univariate Moran's I was used to illustrate the overall distribution of each type of store. This index ranges from [−1 to 1], where values > 0 indicate positive spatial autocorrelation, with higher values signifying stronger spatial correlation. The degree of data dispersion is reflected by the Z-score. Bivariate Local Moran's I was employed to establish the spatial coupling relationship between the two indices and UV. Based on the sign of the index, the results are categorized as high-high (both high index and high vitality, H-H) and low-low (both low index and low vitality, L-L), while high-low (H-L) and low-high (L-H) indicate a non-similar relationship between the specific index and vitality within a unit. The H-H in the Local Moran's I indicates that both the area and its neighboring areas have a high concentration of stores. Specifically, the mean values of the two indices and NTL data within each grid were extracted using a grid centroid-based system, and spatial coupling analysis was performed on the vector point attributes. Geoda1.20 software was used to calculate the Moran's I values. Relevant calculation formulas can be found in the reference [65,66].

- Verify the Deeper Meaning of the Indices Through Trend Testing

To enhance our comprehension of the underlying implications of the two types of indices and minimize the element of randomness in this study, this study employed Theil-Sen median analysis and Mann–Kendall significance test, based on the Matlab platform, to spatially quantify the long-term trends in both population and economic development in Chengdu from 2000 to 2020, following the grading and assignment rules outlined in Table 2. Subsequently, the distribution proportions of the two types of stores within units with different development statuses were calculated to verify the validity of the proposed hypotheses. The Sen–MK method does not require the data to have a linear or normal distribution and is insensitive to missing and outlier values in the time series. This method has been widely used for trend detection in long-term time series data [67,68]. A detailed introduction and calculation formula for this method are provided in Supplementary Material S1.

Table 2. Description of each rank.

β	Z	Value	Classification Meaning
β > 0	2.58 < Z	4	Extremely significant increase
	1.96 < Z ≤ 2.58	3	Significant increase
	1.65 < Z ≤ 2.58	2	Slightly significant increase
	Z ≤ 1.65	1	Not significantly increased
β = 0	Z = 0	0	No changes
β < 0	Z ≤ 1.65	−1	Not significantly reduced
	1.65 < Z ≤ 1.96	−2	Slightly significant reduction
	1.96 < Z ≤ 2.58	−3	Significant reduction
	2.58 < Z	−4	Extremely significant reduction

2.3.3. Determine the Impact of Built Environment Factors on UV

This study investigated the influence of various built environment factors on different dimensions of UV, focusing on both statistical thresholds and spatial heterogeneity. RF model was utilized to evaluate the global importance of each factor in shaping UV, comprising three key phases: indicator selection, model development, and result visualization. Additionally, OLS, GWR, and MGWR models were applied to examine whether the effects of these factors on UV exhibit spatial variability.

- Construct the Built Environment Factor Index System

The frequency of visits to urban spaces is determined by two primary factors: the purpose of the visit, and accessibility. As key components of the urban retail sector, the

spatial distribution and location choices of MTSs and COSs represent another crucial factor influencing visitation. Variations in transportation accessibility, population distribution, regional economic conditions, service environments, and competition from similar establishments contribute to spatial differences in the manifestation of UV [69,70]. Therefore this study synthesized built environment factors identified in previous research [71], while incorporating population characteristics, locational conditions, competition, and cost considerations based on retail layout principles [72,73]. Ultimately, 12 indicators representing different dimensions were selected to assess the factors influencing UV.

Human activity plays a crucial role in promoting vitality, and the probability of vitality creation is strongly associated with population density [74]. The level of transportation convenience plays an essential part in influencing the likelihood of people visiting a particular area, and the density of roads acts as a key measure of how easily accessible a region is [75]. The choice of subway stations was determined by Chengdu's significant dependence on its subway system [76]. Regional economic levels are implicitly indicated by the purchasing power and consumption potential of residents, which can be assessed via residential housing prices as a proxy [77,78]. A suitable service environment implies proximity to potential consumers. Considering the different target audiences for the MTs and COs, various types of schools, office buildings, and industrial parks were selected as indicators. Moreover, commercial complexes attract large crowds, and hotels are often located in areas with high tourist and transient populations, making them suitable indicators for evaluating the service environment dimension. Considering spatial agglomeration effects, the density of other similar vitality venues was employed to measure competition intensity [79]. Specific details are provided in Table 3.

- Construct a Machine Learning Analysis Model

RF is a ML model based on classification and regression trees and incorporates the bagging algorithm [80]. Relative to other ML models, the RF minimizes the impact of multicollinearity in data and exhibits robust performance in high-dimensional and nonlinear problems. It also allows for the ranking of predictor importance. The generalizability and robustness of RF significantly reduce the risk of overfitting when processing large datasets, making it a widely adopted and influential analytical method [81].

In this study, we randomly selected 70% of the dataset for model training and reserved the remaining 30% for testing. To enhance the model's generalization ability and determine the optimal parameters, 10-fold cross-validation was employed. The experiment was repeated 50 times, using R^2 and RMSE as metrics to identify two critical parameters: mtry (the number of predictor variables used in each tree) and ntree (the number of decision trees in the forest). For MTSs, mtry was set to 5 and ntree to 150, while for COSs, mtry was set to 4 and ntree to 100. These parameters served as the basis for the subsequent analysis.

- Visualize the Model Results

Variable importance and Partial Dependence Plots (PDPs) were used to elucidate the nonlinear relationships between different factors and UV. Variable importance was measured by IncMSE%, which represents the increase in mean squared error when certain variables are excluded; the higher the value, the more important the variable [82]. PDPs illustrated threshold effects in nonlinear correlations. Detailed calculation formulas and principles are provided in Supplementary Material S2.

- Incorporate Factor Analysis from the Perspective of Spatial Heterogeneity

This study introduced the MGWR model to address biases arising from ignoring spatial heterogeneity in the exploration of influencing factors and to propose spatial strategies for boosting UV. Research indicates that UV exhibits varying gradients and peaks across different spatial scales. The evolution of each phenomenon is often determined by spatial processes operating at multiple scales [7]. Compared to the OLS and GWR models, the MGWR model, proposed by Fotheringham et al., allows for different spatial bandwidths among variables, thereby revealing the underlying implications of spatial heterogeneity at a

finer scale [83]. In this study, we applied OLS, GWR, and MGWR models to investigate the scale effects of different factors influencing UV. The model fitting abilities were evaluated using R^2, AICc, and RSS, which acted as criteria for selecting the optimal model. More comprehensive explanations and mathematical equations can be found in Supplementary Material S3.

Table 3. Description of each impact element.

Variable Type	Factor Index		Definition and Interpretation	Data Dimension
Explanatory variable X	Population characteristics	Population density (PD)	The population density in the street after grid processing	Person/km^2
	Transportation convenience	Road density (RD)	Road density per unit area within the grid	m/km^2
		Subway station density (SSD)	Kernel density data of metro stations per unit area in the grid	per/km^2
	Service environment	Primary school density (PSD)	Kernel density data for primary schools per unit area within the grid	per/km^2
		Middle school density (MSD)	Kernel density data for middle school per unit area within the grid	per/km^2
		University density (UD)	Kernel density data for university per unit area within the grid	per/km^2
		Industrial park density (IPD)	Kernel density data for industrial park per unit area within the grid	per/km^2
		Office building Density (OBD)	Kernel density data for commercial office building per unit area within the grid	per/km^2
		Commercial complex density (CCD)	Kernel density data for commercial complex per unit area within the grid	per/km^2
		Hotel density (HD)	Kernel density data for hotel per unit area within the grid	per/km^2
	Regional economic level	Rent level (RL)	Average selling price of second-hand houses in the street after grid treatment. In this study, the second-hand house price obtained in the grid is used to represent the land rent level in the grid	Yuan
	Competitive influence	Another type of vitality density (ATD)	The numerical value of another index within the grid	per/km^2
Dependent variable Y	MTI or COI			

2.3.4. Utilize Machine Learning to Map Future UV

ML has increasingly become a valuable tool in supporting urban planning decisions. It offers the potential for real-time monitoring of urban changes and predicting trends related to issues such as land-use and environmental pollution [84,85]. Urban spaces should adapt through continuous updates to address rapid development and emerging challenges, making it crucial to accurately determine "where the next step should be."

In current predictive investigations, binary classification models may only ascertain the presence or absence of an event, without considering the fact that events may have varying probabilities of occurrence. Therefore, we opted to integrate both classification and regression models in ML, adopting a soft classification approach that accounts for both the occurrence of the event and its probability. Specifically, we utilized a classification model to estimate the probability of each grid "exhibiting a certain type of vitality" and generate a vitality potential map with values ranging from 0 to 1. Subsequently, a regression model

was employed to predict the vitality levels for grid units with potential exceeding 50%, but currently lacking observed vitality. This process produced two future UV maps, designed to inform the direction of future urban spatial development and improve the precision of planning policies.

3. Results

3.1. Spatial Distribution of UV Represented by NTL

Figure 3 illustrates the changes in NTL for Chengdu from 2012 to 2023, where increasingly red hues indicate higher levels of urban development. Over the past two decades, there has been a sustained increase in UV within Chengdu; however, this growth has not been uniform across the city. The development patterns reveal a concentric expansion from the urban core, with significant growth observed in the southern areas, while the northwest and southeast regions have gradually emerged as pivotal zones for development. Conversely, the northern sector has experienced relatively minimal transformation. The emergence of multiple centers, with district-level cores, has become increasingly evident. This aligns with Chengdu's territorial spatial plan, which follows the differentiated development strategy of "Eastward expansion, Southward extension, Westward control, Northward improvement, and Central optimization". Consequently, the utilization of NTL as a proxy for assessing UV in this research is considered appropriate and valid.

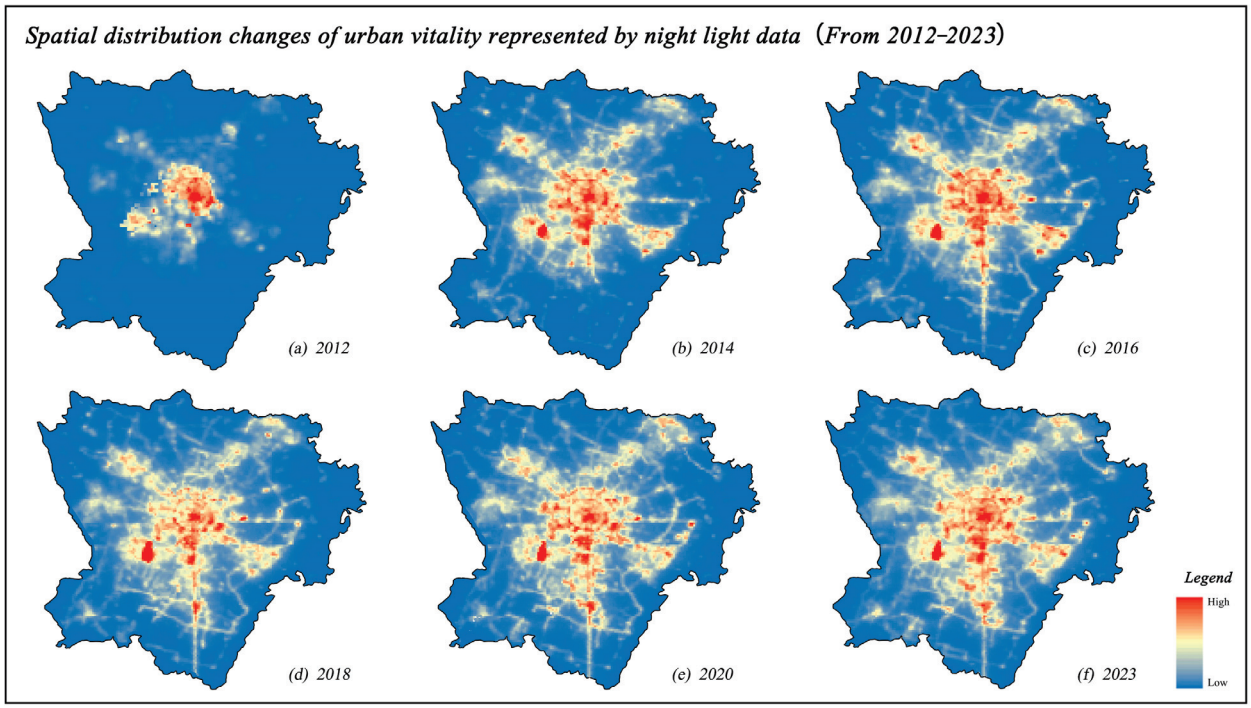


Figure 3. Temporal evolution of NTL in the study area in (**a**) 2012, (**b**) 2014, (**c**) 2016, (**d**) 2018, (**e**) 2020 and (**f**) 2023.

3.2. Relationship Between the MTI and COI with UV

3.2.1. Spatial Patterns of the MTI and COI

Initially, the viability of the MTI and COI was assessed. The spatial distribution of stores serves as the foundation for stimulating UV. The Moran's I for MTSs and COSs are 0.12 and 0.43, with Z-values of 6.54 and 36.52. These findings indicate significant clustering tendencies in the spatial distribution of both shop types at a global scale, with COSs demonstrating a higher degree of clustering compared to MTSs.

The internal correlations of store spatial distribution are illustrated using LISA maps (Figure 4). Employing the natural breaks method, kernel density values are categorized into six levels to depict the spatial patterns of the COI and MTI (Figure 5). COSs exhibit a

significant positive correlation in their spatial distribution, characterized by a "dual-super, dual-core, multi-point" pattern (on the left side of Figure 4). In alignment with the MTI, the H-H regions correspond to the urban core, some historical sites (such as the Shaocheng area and Kuanzhai Alley), and areas that have undergone urban renewal (notably Yulin Community). The "dual-core" are represented by two modern business centers and an innovation hub situated in the southern portion of the city. In non-core areas, the clusters of COSs expand outward from university campuses and specific industrial parks. The L-H regions are relatively sparse and primarily distributed around the periphery of H-H areas. The L-L areas are predominantly located in the northern city areas, where urban development has been relatively slow. The H-L regions are predominantly concentrated in Pidu District, an area in the early stages of economic development.

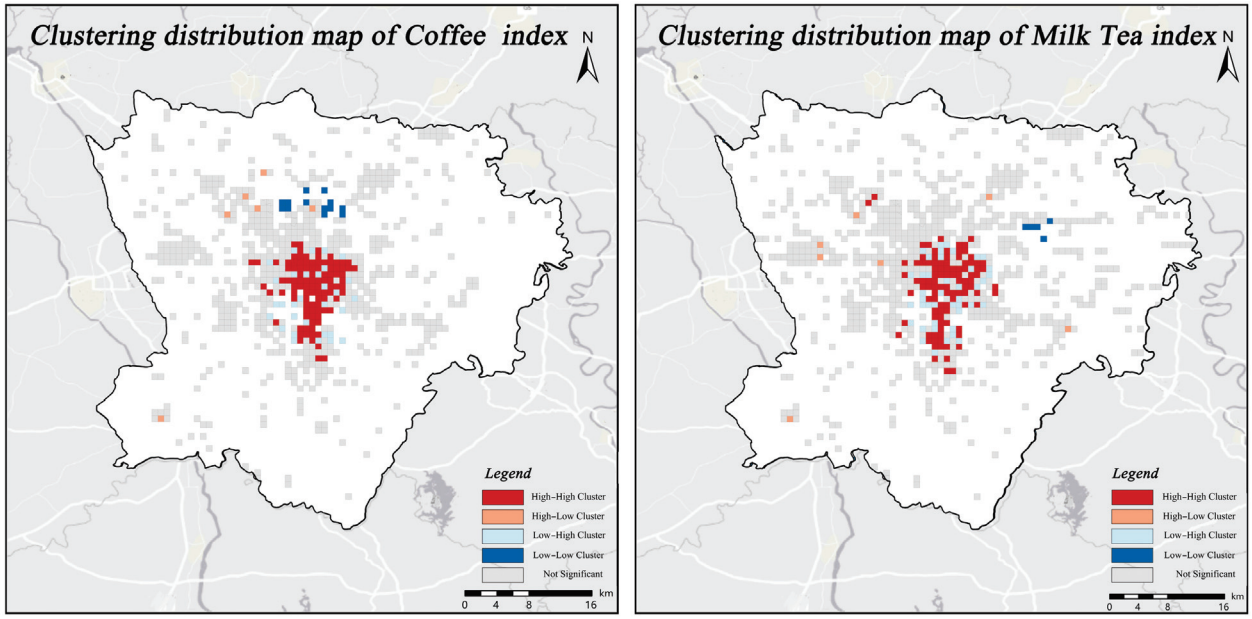


Figure 4. Clustering distribution map of COI and MTI.

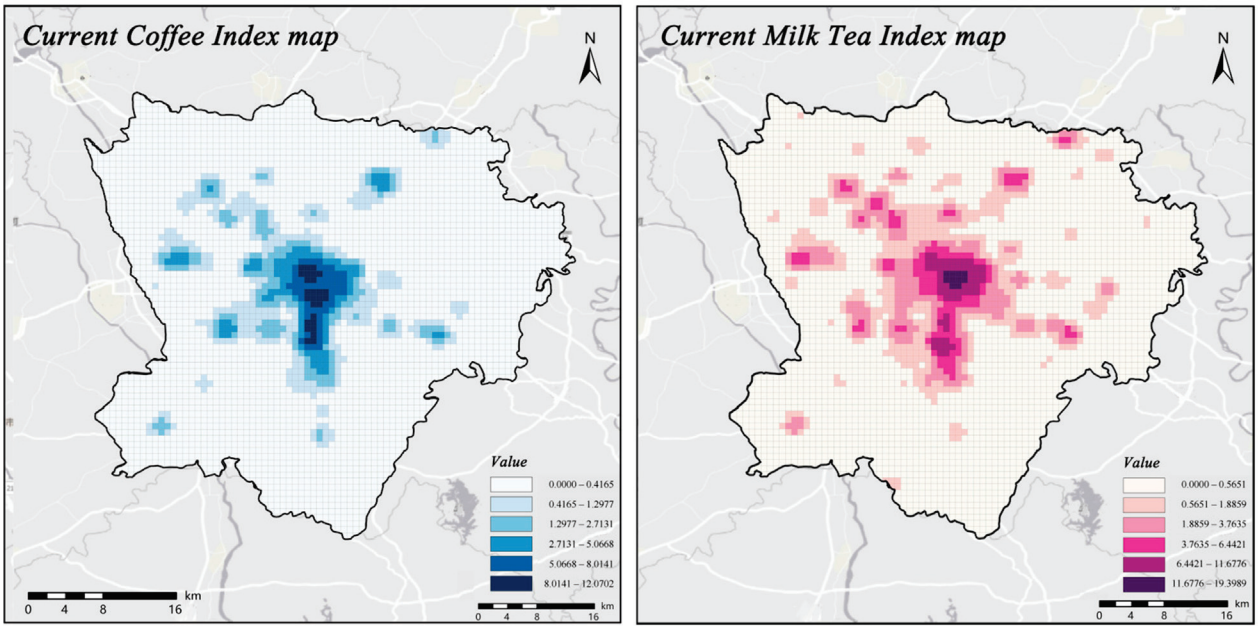


Figure 5. Current COI and MTI map.

The spatial distribution of MTSs shows a pronounced positive correlation, with the H-H regions (indicated in red in the map) closely matching the spatial pattern. A distinct distribution is noted in the northwestern Pidu District, while the L-H regions (shown in light blue) are often mixed with H-H regions or located on their periphery. The phenomena of H-L (shown in orange) and L-L (shown in dark blue) are primarily associated with emerging towns, with H-L regions particularly linked to the newly established industrial city in Wenjiang District. The results indicate that the distribution of MTSs lacks coherence and centrality, exhibiting distinct discrete characteristics. The distribution of MTI is rather heterogeneous, generally displaying an overall pattern characterized by "a single-super core, dual-cores, and multiple-clusters" configuration (on the right side of Figure 4). The "super-core" encompasses the urban core area (Chunxi Road and Tianfu Square) and its surrounding expansion zones (including various key commercial districts and tourist attractions). The "dual-cores" on the southern side consist of a modern business center (Financial City) primarily targeting young populations and an innovation hub (High-tech Development Zone). The "multiple-clusters" dispersed across the city's districts represent high-density clusters centered around universities. In contrast, the high-value clustering of COSs demonstrates stronger coherence than that of MTSs, indicating a more pronounced trend toward centralized spatial distribution.

In general, the spatial distribution of the two types of stores exhibits both similarities and differences. COSs tend to follow a clustered and centralized pattern, whereas MTSs adopt a multi-center layout, with a tendency toward more uniform distribution. Nonetheless, high-density clusters for both types are closely associated with commercial districts and office or innovation hubs. COSs, in particular, appear to be more responsive to advanced technological sectors and innovation-driven activities, indicating that their concentrated distribution may be driven by differing underlying factors.

3.2.2. The Underlying Relationship Between the MTI, COI, and UV

Figure 6 and Table 4 depict the spatial relationship between UV and the distribution of the MTI and COI, as determined by Bivariate Moran's I analysis. The findings confirm that the COI serves as an effective indicator of UV. Should the MTI exhibit a comparable level of performance, it may similarly be regarded as a reliable measure of UV. At the 1% significance level, the analysis shows a Moran's I of 0.356 for the COI, with a Z-value of 58.020, and a Moran's I of 0.417 for the MTI, with a Z-value of 65.835. These results indicate statistically significant spatial autocorrelation between both indices and UV, highlighting the MTI's strong potential as a preliminary indicator of UV.

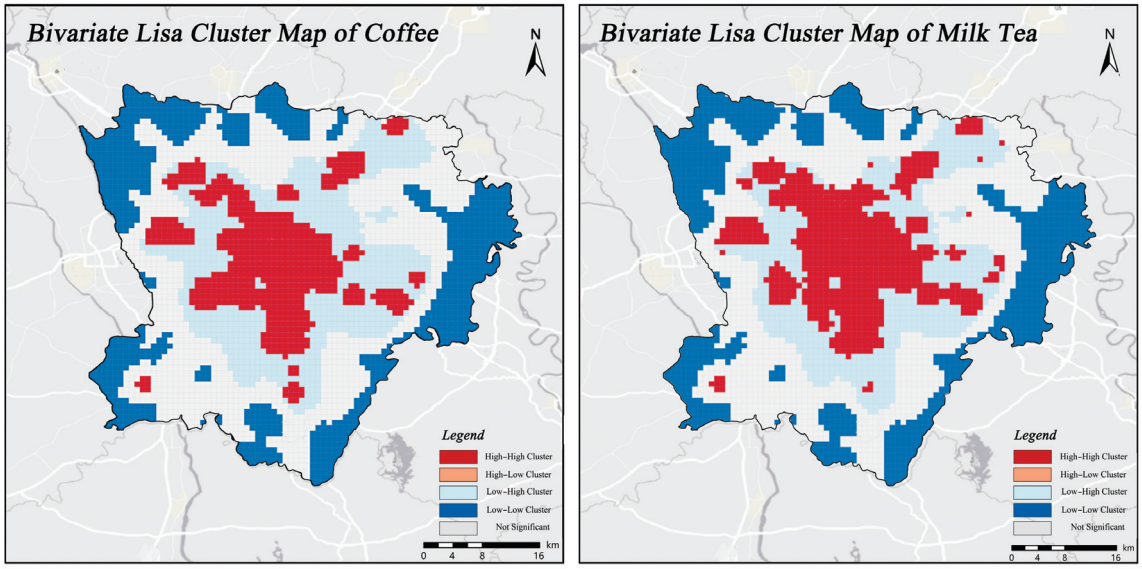


Figure 6. Bivariate cluster analysis of COI, MTI, and UV.

Table 4. Composition of bivariate clustering analysis results.

Store Type	High D—High V	High D—Low V	Low D—High V	Low D—Low V	Not Significant
MT	778 (19.56%)	0 (0.00%)	774 (19.46%)	1085 (27.28%)	1340 (33.69%)
CO	672 (16.89%)	1 (0.00%)	880 (22.13%)	1084 (27.26%)	1340 (33.69%)

Spatially, H-H areas, indicating high index and high UV (represented in red in the figure), are predominantly situated in and around the city's core development zones. These areas exhibit higher vitality values due to the concentration of activities and the diversity of functions, with the distribution of both types of stores predominantly clustered in these locations. The L-L regions are mainly situated at the city's periphery, where lower population density and natural landscapes have limited development. The spatial distribution of H-H and L-L regions aligns with the overall urban development pattern.

The L-H regions, which represent "low density—high vitality," surrounded the H-H regions. This may be attributed to the complexity of the mechanisms that drive UV, suggesting that the overall UV within each grid may not be fully captured by the distribution of these two types of stores. The absence of H-L areas in the results implied that regions with either type of store presence experience varying degrees of socio-economic activity, indirectly corroborating the association between these stores and UV. Furthermore, the number of MTI in H-H areas exceeded that of COI, while the proportion of L-H regions was lower in the MTI compared to the COI. This evidence further reinforces the notion that the MTI can serve as an indicator of UV.

The significant spatial autocorrelation indicates that the MTI has the ability to represent UV. Further comparison of the trend analysis results from grids containing each type of store will help clarify the specific dimensions of vitality that each index captures. The regions with MTSs had average population and economic development index of 2.89 and 2.84, respectively, while the averages for regions with COSs were 2.75 and 2.90. Approximately 66.93% of COSs were located in areas with extremely growing populations (development index > 2), slightly lower than the 70.85% for MTSs. Additionally, 90.5% of COSs were located in areas with an economic development level of 3, whereas MTSs had a little lower percentage of 84.60%. Figure 7 represents the proportion of MTSs and COSs within grids exhibiting same economic and population development trends. COSs have a higher proportion in grids E(2) and E(3), while MTSs dominate in grids where P(>0). Grids P(4) and E(3) are mostly located around core urban commercial districts with rapid economic growth and high population density, resulting in a roughly similar proportion of both types of stores. In grids P(-3) and P(-4), where population decline is significant, COSs hold a higher proportion. This is likely due to these grids being situated near natural landscapes and surrounded by high-end residential areas or urban administrative centers, catering primarily to upper-middle consumers, making them ideal locations for COS serving business purposes.

In summary, grids with a higher proportion of COSs exhibit stronger economic development, supporting the argument that the COI reflects urban economic vitality (EV). In contrast, grids with MTSs show notable population growth, suggesting that the MTI effectively captures population vitality (PV).

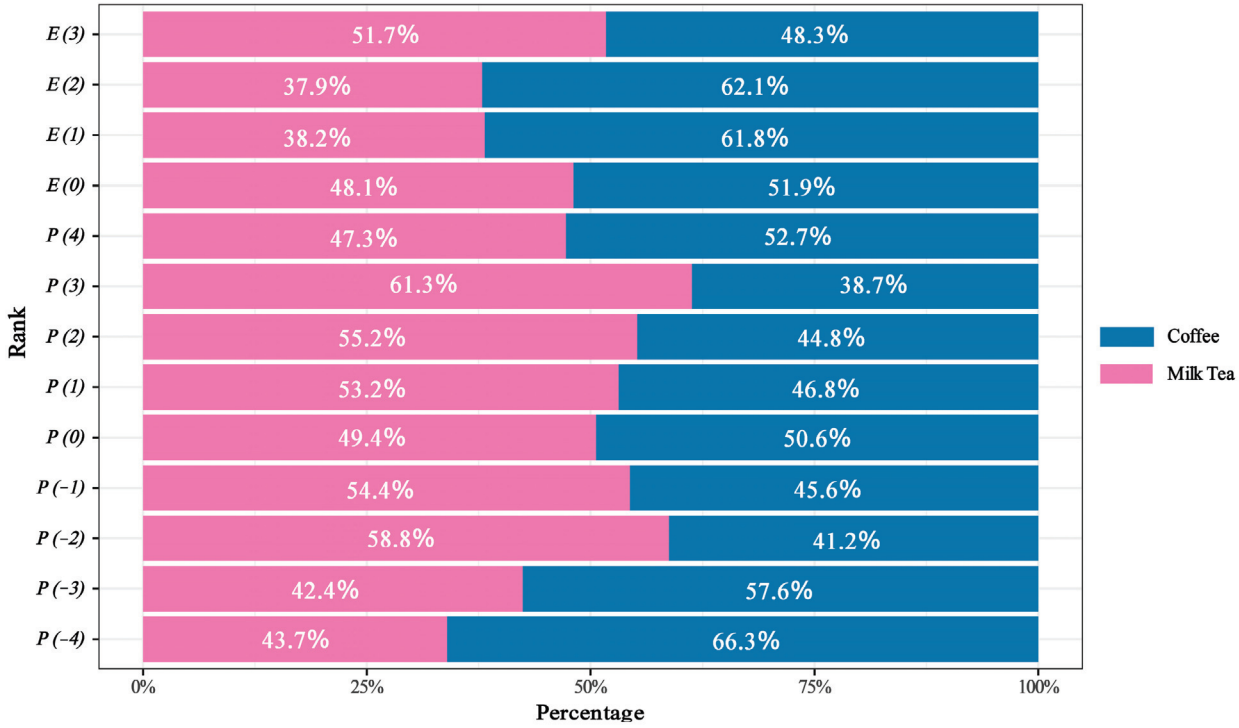


Figure 7. The proportion of each index within different development levels.

3.3. Exploring the Influencing Factors of UV

The RF model discussed in this paper showed excellent performance. The R^2 values for the MTI and COI regression models, respectively, were 0.95 and 0.93, which are near to 1. Additionally, the MSE, MAE, and RMSE values were all small. The regression results of these models are illustrated in Table 5 and Figure 8.

Table 5. Performance evaluation of different models.

Model Type	Store Type	R^2	MSE	MAE	RMSE
RF	MT	0.95	0.14	0.16	0.37
	CO	0.93	0.13	0.15	0.36

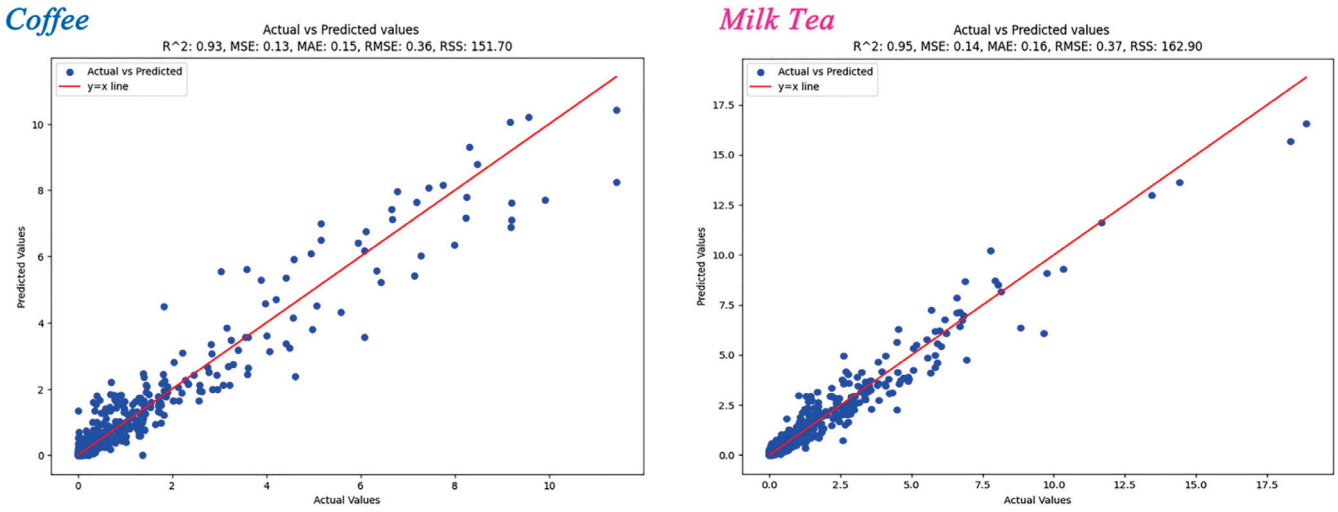


Figure 8. RF model performance evaluation.

3.3.1. Analysis of Importance Results from RF

Figure 9 illustrates the influence of various categories of factors on the vitality represented by two different indices. In general, the interaction between the two types of vitality emerged as the most significant secondary factor. The heterogeneity in the impact of consumption levels was evident, while the density of roads, a transportation element, exerted a relatively minor influence. The influence rankings of other factors did not vary significantly.

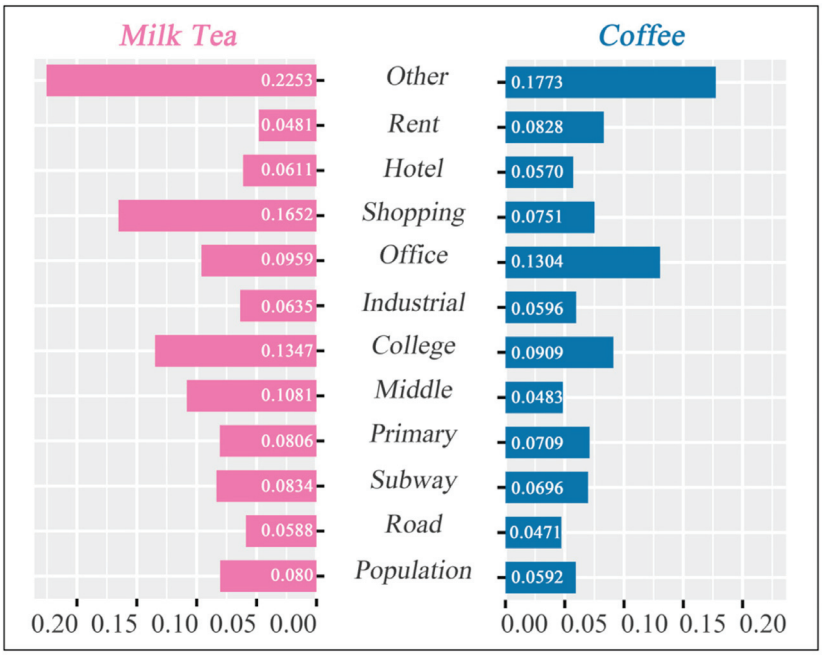


Figure 9. Analysis of the importance of influencing factors.

In terms of PV, service environment factors accounted for the highest proportion at 70.94%. Within this category, the density of commercial establishments, universities, and high schools ranked highest, with values of 0.1652, 0.1347, and 0.1082, respectively. The importance of housing prices, representing consumption levels, was the lowest, contributing only 4.81%, which was less than 7% of the significance of the service environment.

Regarding EV, the distribution of proportions among various factors was relatively balanced. Service environment factors constituted 53.24%, a decrease of 17.70% compared to PV. The density of office buildings, universities, and commercial establishments held the top three positions with influence values of 0.1304, 0.0901, and 0.0751, respectively. The importance of housing prices in terms of consumption levels was 8.29%, ranking fourth among all influencing factors. When comparing the two results, it is clear that the MTI is primarily influenced by aspects relating to population activities, whereas the COI is closely linked to physical elements.

3.3.2. Analysis of Nonlinear Threshold from RF

While relative importance analysis highlights the influence of factors, a deeper understanding of their specific impact on UV is necessary. We used PDPs to describe the baseline and reasonable range of key parameter values for each factor. Figure 10 illustrates the relationship between various factors and the two types of vitality. Overall, the effects are nonlinear, with most factors exhibiting clear threshold effects. Understanding these patterns can guide more effective planning interventions.

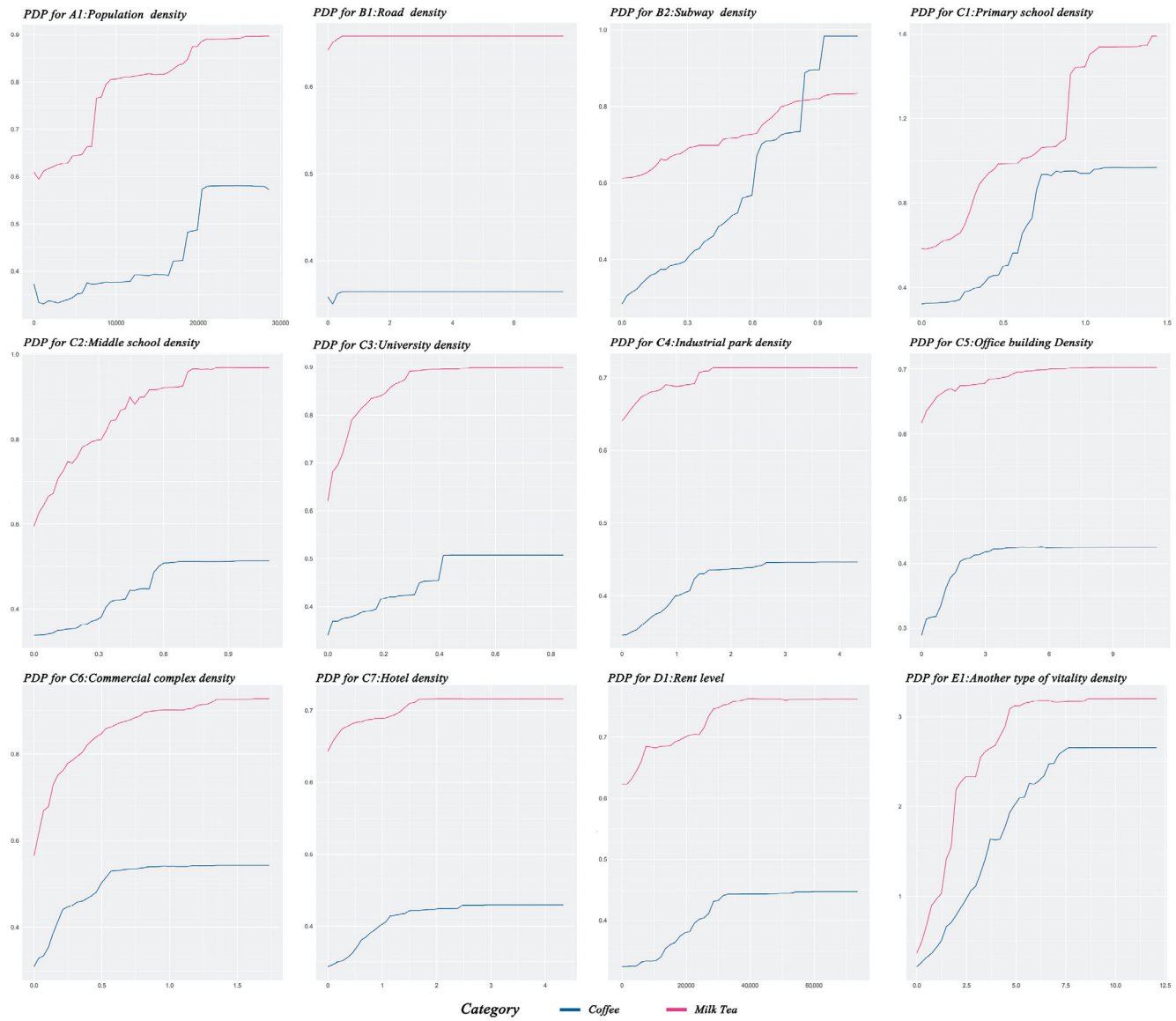


Figure 10. PDP diagram of nonlinear relationship between COI and MTI and various factors.

Population Distribution. The impact of PD on the MTI was positive, increasing progressively with a steady rise in density, peaking significantly at 7500 people/km^2, and then stabilizing. Conversely, for EV, PD within the range of 8000–16,000 people/km^2 did not show a significant enhancement effect; however, beyond 16,000 people/km^2, there was a notable increase, stabilizing around 23,000 people/km^2. A possible explanation was that excessively high PD might have reduced the quality of life for residents, but a larger population base could have increased the number of high-income individuals. This increased consumption capacity might have attracted high-priced coffee shops, highlighting the importance of balancing these factors for urban development.

Transportation Conditions. The increase in SSD effectively enhanced the levels of both types of vitality. Its impact on PV was moderate, whereas the mechanism for enhancing EV was more complex. Three inflection points were identified at 0.5, 0.8, and 1.0 stations/km^2. When the density was less than 0.5 stations/km^2, the role of subway stations in enhancing EV was weak. The density range of 0.5–0.8 stations/km^2 appeared to be the optimal interval, providing numerical reference points for transportation optimization. Both types of vitality seemed insensitive to changes in road density, suggesting that the underlying reasons for this phenomenon warranted further investigation.

Regional Economic Level. Within the RL range of 6000–30,000 RMB/m^2, property prices almost linearly enhanced EV, with 6000 RMB/m^2 serving as the trigger threshold. This phenomenon was consistent with general economic development patterns. For PV, the enhancement effect of housing prices was significant between 1000 and 25,000 RMB/m^2, slowing down beyond this range. This threshold was roughly equivalent to the average housing price in Chengdu.

Service Environment. Factors under this broad category predominantly had a positive effect on both types of vitality. When OBD exceeded 3 buildings/km^2, there was little room for further enhancement of EV, but a significant positive impact on PV was observed, with several value jumps, ultimately reaching a threshold at 8 buildings/km^2. For UD, which was important for both types of vitality, the density threshold and trend were roughly the same, but variations in the y-axis value ranges indicated differing importance. The influence of CCD on EV peaked at around 0.8 complexes/km^2, but it gradually enhanced PV within the range of 0–1.85 complexes/km^2. This might have been due to CO shops often being independently located, while MT shops were more commonly found within commercial complexes. PSD had a similar activation effect on both types of vitality within the range of 0–0.5 schools/km^2, with an optimal configuration of approximately 0.8 schools per kilometer. However, EV was slightly inhibited in the 0.6–0.8 PSD range, and further increases had an insignificant impact. PV continued to rise within this range. An MSD threshold of about 0.7 schools/km^2 significantly enhanced both types of vitality, with increased density leading to resource waste. IPD and RL had less importance for both types of vitality but still exhibited nonlinear effects. An industrial park and hotel density of 2 units/km^2 was favorable for PV, while the thresholds for EV were 2.5 and 3, respectively.

3.4. The Spatial Heterogeneity of Influencing Factors on UV

The assessment of global importance often overlooks spatial heterogeneity introduced by scaling effects. Combining these assessments allowed for a more comprehensive understanding of the local correlations between UV and various factors, thereby enabling the formulation of targeted spatial optimization strategies. Therefore, three regression models, namely OLS, GWR, and MGWR, were developed and their performance disparities are showed in Table 6. The outcomes of the MGWR model were finally utilized to provide strategic recommendations. Prior to running the OLS model, all factors exhibited VIF values below five, indicating the absence of multicollinearity among the variables, allowing them to be included in the subsequent analysis.

Table 6. The regression results of these three models.

Model Element	Milk Tea Shop			Coffee Shop		
	OLS	**GWR**	**MGWR**	**OLS**	**GWR**	**MGWR**
RSS	394.904	334.171	257.154	463.394	254.353	241.195
AICc	1794.432	1744.092	1582.495	1931.177	1832.401	1694.070
R^2	0.532	0.580	0.703	0.450	0.626	0.728

Tables 7 and 8 present the regression findings of bandwidth and regression coefficients. The correlations between several parameters and the two forms of vitality displayed spatial variability, with bandwidth ranges covering local, regional, and global scales. Certain factors showed negligible correlations. A wider bandwidth implies reduced spatial variability, whereas a narrower bandwidth indicates that the independent factors influence the dependent variables only in select regions.

Figure 11 depicts the spatial distribution of the model's R^2 fitting ability, capturing 70.3% of the variance in PV and 72.8% of the variance in EV. The explanatory power for PV increased from southeast to northwest, while EV exhibited better fitting in non-urban core areas. This suggests that the driving mechanisms of vitality near the urban edge are relatively simpler.

Table 7. Model element bandwidth comparison.

Element Type		Milk Tea Shop			Coffee Shop		
		GWR	MGWR	Proportion	GWR	MGWR	Proportion
Population characteristics	Constant	439 (51.35%)	241	28.19%	137 (16.02%)	55	6.43%
	Population density (PD)		853	99.77%		53	6.20%
Transportation convenience	Road density (RD)		786	91.70%		846	98.95%
	Subway station density (SSD)		853	99.77%		853	99.77%
	Primary school density (PSD)		853	99.77%		853	99.77%
Service environment	Middle school density (MSD)		853	99.77%		749	87.60%
	University density (UD)		245	28.65%		143	16.73%
	Industrial park density (IPD)		617	72.16%		853	99.77%
	Office building density (COBD)		76	8.89%		265	30.99%
	Commercial complex density (CCD)		443	51.81%		825	96.49%
	Hotel density (HD)		853	99.77%		55	6.43%
Regional economic level	Rent level (RL)		853	99.77%		162	18.95%
Competitive influence	Another type of vitality density (ATD)		53	6.20%		853	99.77%

Table 8. Regression coefficient of each factor.

Variable	Milk Tea Shop					Coffee Shop				
	Mean	STD	Min	Med	Max	Mean	STD	Min	Med	Max
Constant	0.258	0.172	0.031	0.208	0.667	0.446	0.188	−0.136	0.454	0.862
Population density (PD)	0.099	0.005	0.086	0.1	0.108	0.101	0.259	−0.54	0.073	0.949
Road density (RD)	0.008	0.01	−0.008	0.005	0.035	0.003	0.009	−0.016	0.003	0.025
Subway station density (SSD)	0.03	0.004	0.023	0.03	0.037	0.012	0.004	0.003	0.012	0.018
Primary school density (PSD)	−0.002	0.001	−0.006	−0.002	0	0.043	0.002	0.004	0.043	0.046
Middle school density (MSD)	0.025	0.003	0.018	0.024	0.032	−0.06	0.011	−0.079	−0.061	−0.039
University density (UD)	0.083	0.1	−0.118	0.106	0.264	−0.061	0.19	−0.36	−0.078	0.423
Industrial park density (IPD)	0.028	0.024	−0.029	0.035	0.065	0.035	0.002	0.032	0.034	0.04
Office building density (OBD)	0.272	0.187	−0.062	0.256	0. 918	0.066	0.086	−0.054	0.044	0.273
Commercial complex density (CCDD)	0.019	0.047	0.008	−0.039	0.107	0.189	0.293	−0.507	0.138	1.544
Hotel density (HD)	0.028	0.002	0.024	0.027	0.034	−0.013	0.096	−0.237	0.018	0.222
Rent level (RL)	0.029	0.003	0.022	0.029	0.034	0.061	0. 109	−0.228	0.033	0.464
Another type of vitality density (ATD)	0.539	0.229	−0.046	0.561	1.069	0.1	0.003	0.094	0.1	0.106

The spatial heterogeneity of EV concerning PD was not significant in most areas, with a significant positive correlation only in city centers ($p < 0.05$). At the 10% confidence level, 79.92% of the study area experienced a positive effect of PD. However, PD had a consistently significant positive impact on the MTI, with the degree of impact increasing from southeast to northwest. This indicated that the PD, significantly drives the MTI, it is not a key factor in stimulating EV.

Figures 12 and 13 show the regression results of the MGWR model for the two types of vitality, respectively. The lower left corner depicts the confidence distribution map of the regression results. The regional RL affected only the spatial variation in the COI. The regression coefficients ranged from −0.227 to 0.464, with positive impacts radiating outward from the center of Wuhou District, nearly covering the traditional main urban area of Chengdu. At the 90% confidence level, regions with negative impacts accounted for only 12.02%, mainly concentrated in the southern part of the city, where land prices are higher. This indicated that appropriate land prices could positively stimulate EV.

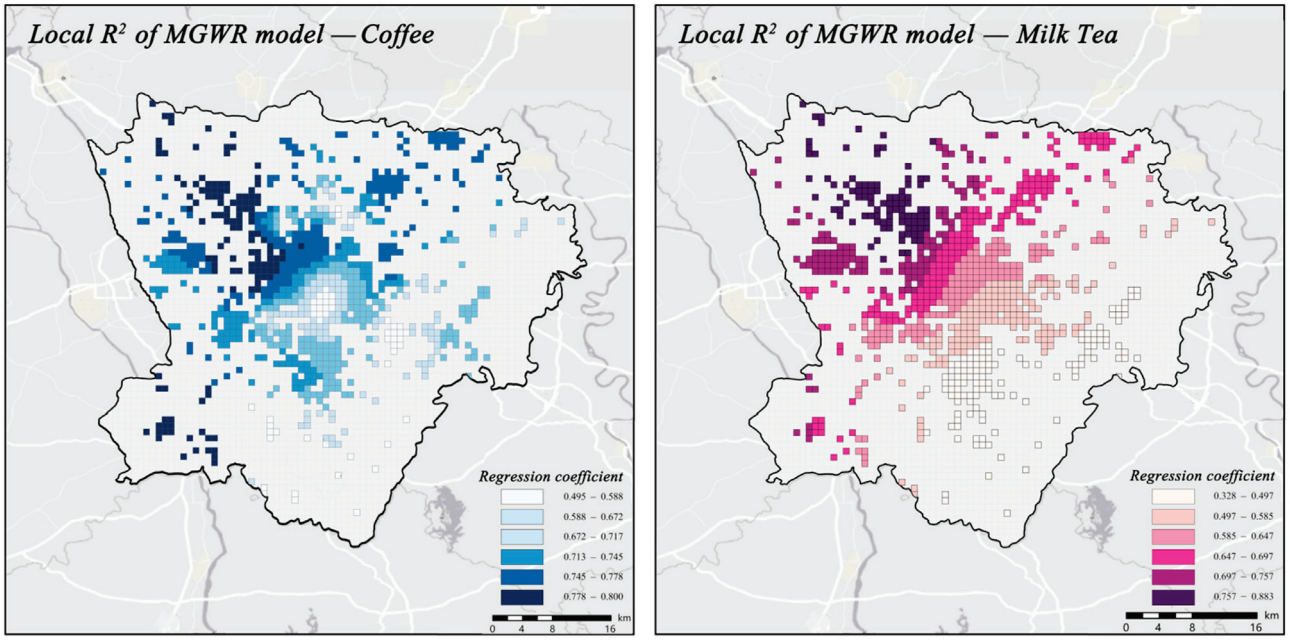


Figure 11. Spatial distribution of regression coefficients in MGWR—R^2.

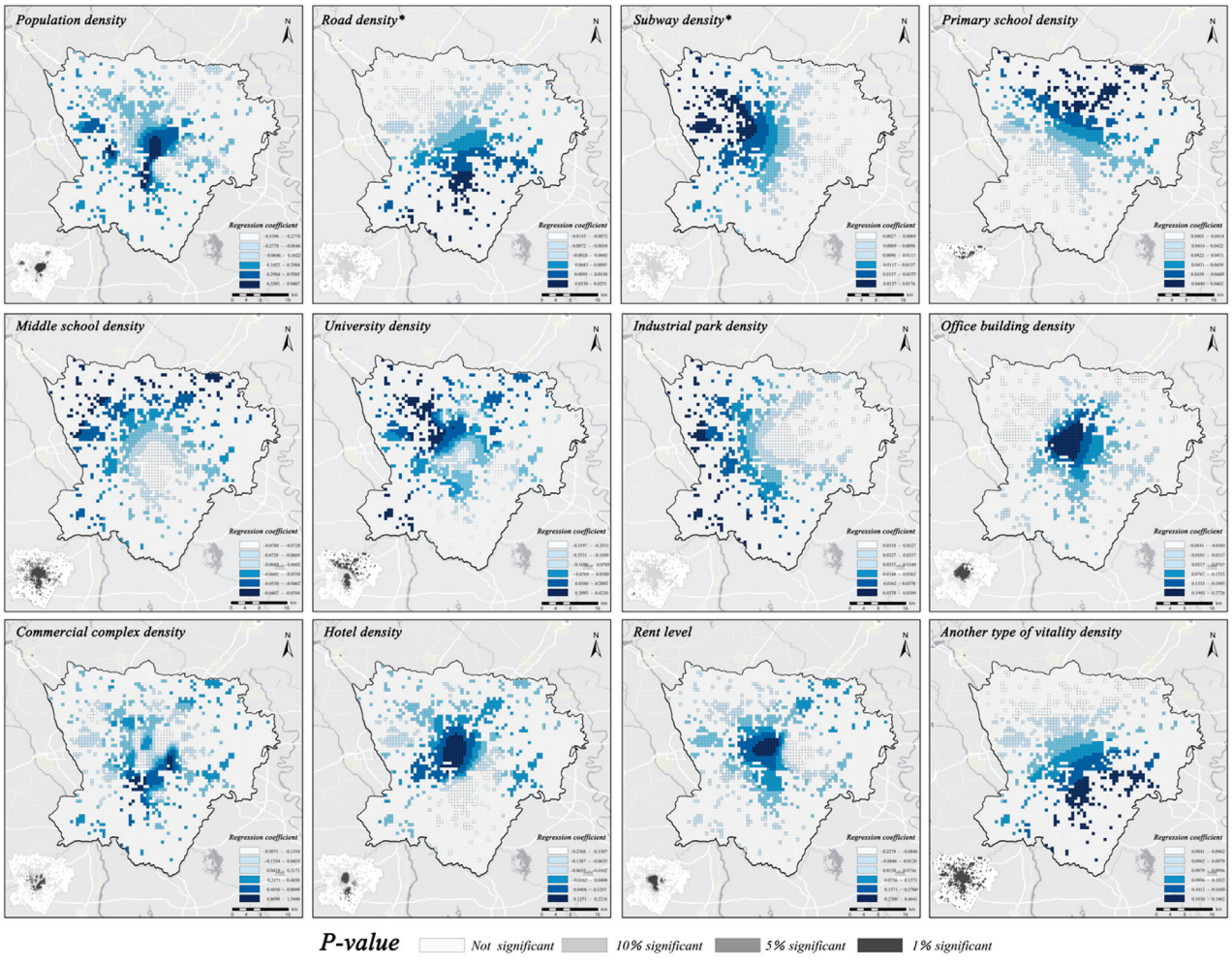


Figure 12. Spatial distribution of regression coefficients in MGWR—COI. (* indicates global insignificance).

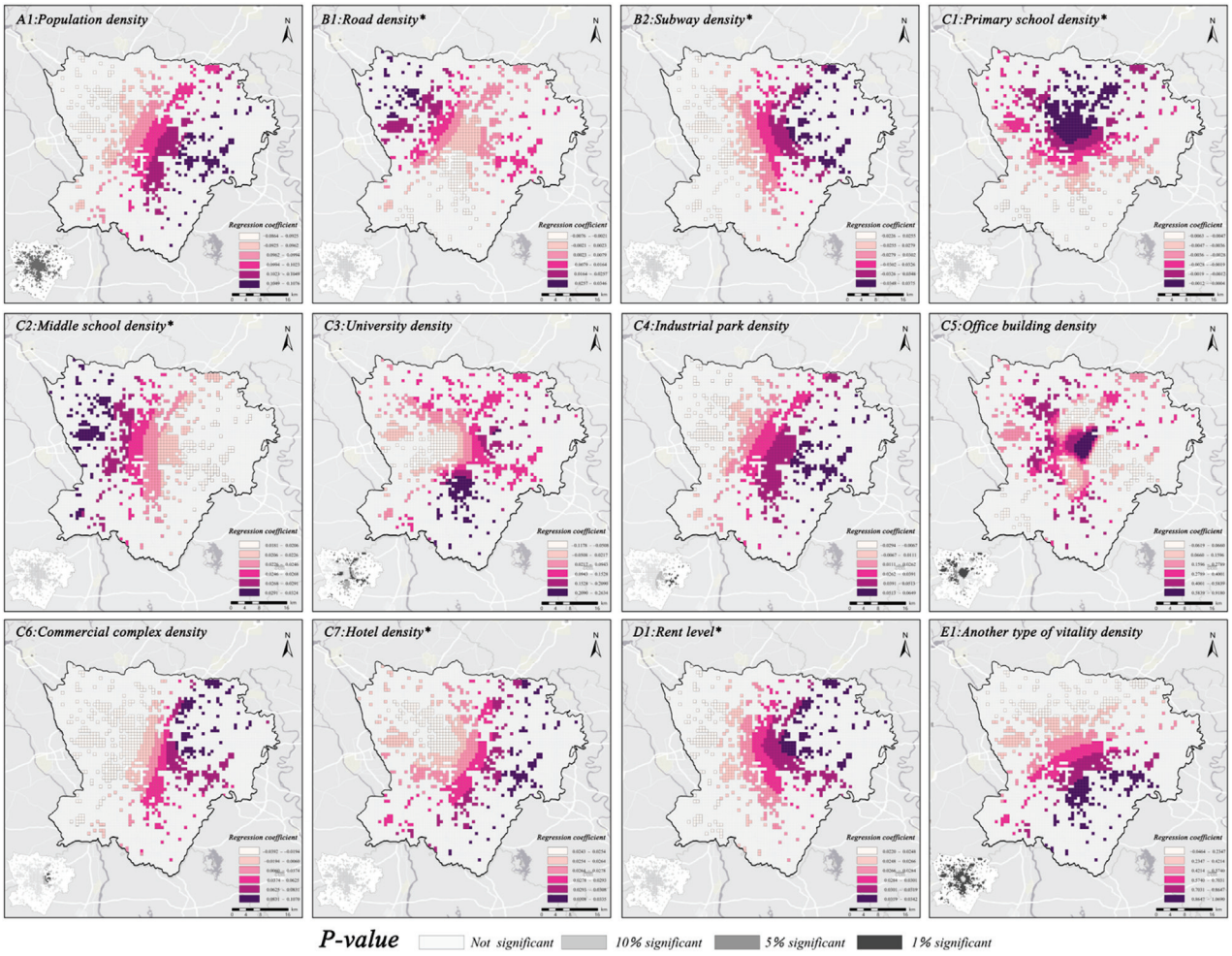


Figure 13. Spatial distribution of regression coefficients in MGWR—MTI. (* indicates global insignificance).

In the service environment, UD, COBD, and CCD significantly influenced both types of vitality. The impact of UD on PV and EV was particularly noticeable in the southern part of the city, while some eastern and northern areas experienced negative effects. The regression coefficients for office buildings were −0.062 to 0.918 for PV and −0.054 to 0.273 for EV. They both showed positive impacts within significant ranges. The promotion of PV by OBD decreased gradually from the city center to the west, while the impact on EV resembled the pattern of RL. CCD slightly enhanced PV in the eastern core area, with significant regression coefficients ranging from 0.080 to 0.107. In the southern, southeastern, and southwestern parts of the city, the coefficients ranged from −0.507 to 1.544 for EV, indicating a strong linkage between EV and CCD in these regions. This alignment reflected the current commercial spatial layout of Chengdu.

The mutual attraction between shops had a positive effect on both PV and EV. EV exhibited regression coefficients ranging from 0.108 to 1.069 with PV, with the effect becoming stronger as the distance from the city center increased. The spread of EV beyond the main urban area significantly enhanced the spatial concentration of PV. The regression coefficients for PV with EV ranged from 0.094 to 0.106, suggesting a somewhat weaker appeal of PV for EV. However, this appeal was stronger in the outskirts of the city.

PD and MD had different impacts on EV. The regression coefficients for MD ranged from −0.079 to −0.039, with a mean of −0.06, indicating that for each additional unit of MD within a grid, EV decreased by 0.06 units. This effect was more pronounced in central urban areas and less so in non-core regions. The increase in PD had a globally positive impact on EV, with coefficients ranging from 0.04 to 0.043, though this effect was only

significant in the northern part of the city. This might be related to the population's age structure in those areas, where higher PD often correlated with a younger demographic.

The regression coefficients for RL ranged from −0.236 to 0.221, with positive impacts concentrated in Qingyang and Wuhou districts, covering most of Chengdu's tourist attractions. These attractions are key areas for external interactions within the city. The presence of coffee shops in these areas may provide meeting spaces for visiting groups, thereby promoting economic cooperation between cities. At the 90% confidence interval, 52.66% of HD contributed to boosting economic prosperity.

However, at the 90% confidence level, most factors did not significantly affect PV. These included RL, RD, SSD, and service environment factors such as HD, PD, and MD. For EV, only transportation conditions (RD, SSD) showed no significant impact at the 90% confidence level.

3.5. Map of Future UV

The previous analysis revealed the spatial characteristics and significant differences between the two types of vitality. Therefore, it is feasible to predict the future spatial vitality pattern of the city based on the current distribution characteristics of the MTI and COI.

First, the accuracy of the prediction model was assessed. Observation of Figure 14 reveals that the ROC curves for the classification predictions of both store types exhibit a pronounced upper-left trajectory, significantly deviating from the ROC curve of a pure random classifier (depicted as a black dashed line in the figure). The AUC (Area Under the Curve) values for these models are 0.987 and 0.984, respectively. The specific data of the confusion matrix in Table 9 also indicate that the models used for classification prediction demonstrate excellent overall performance.

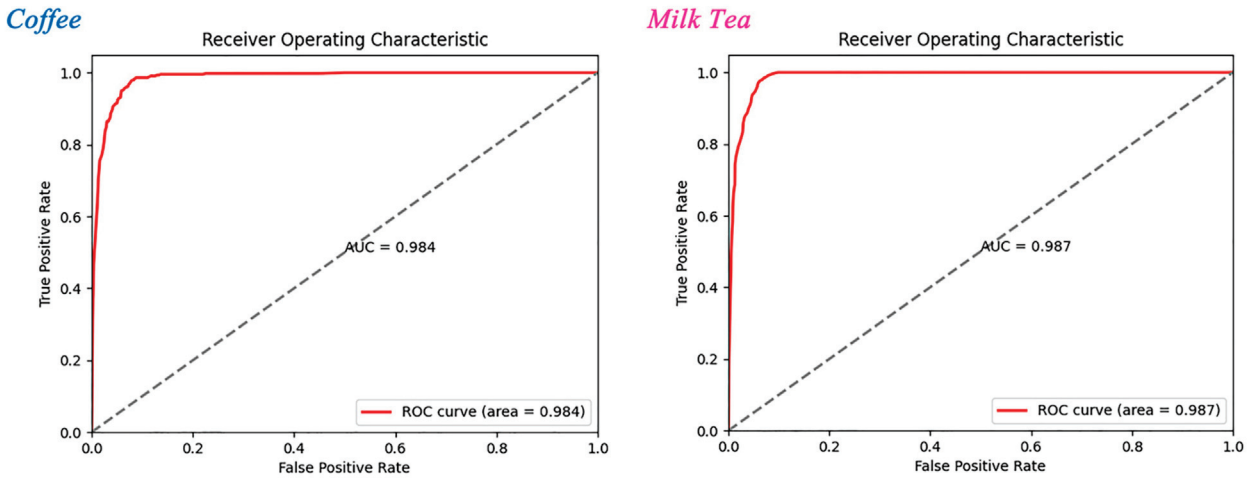


Figure 14. Model fitting ROC curve and AUC area.

Table 9. Two types of store confusion matrix data.

Store Type	Accurarcy	Precision	Recall	F_1
Milk tea shop	0.8648	0.8573	0.8750	0.8652
Coffee shop	0.9043	0.9092	0.9042	0.9056

By overlaying the current vitality map with the prediction map (Figure 15), areas with a high probability of future vitality (where store distribution potential exceeds 50%) but lacking current vitality (non-gray areas) are identified as emerging vitality zones. Overall, future PV is expected to follow a spatial pattern characterized by "high in the center, low on the periphery" with an increasingly balanced distribution. Most of the future vitality will radiate outward from existing high-vitality areas, while high-density population zones are projected to gradually expand southeast, northwest, and southwest, involving regions

such as Chenghua, Jinniu, and Wuhou districts, which are expected to become the city's secondary cores. EV exhibits two distinct trends. One is similar to PV, with high-value areas of economic vitality experiencing relatively little change, mostly characterized by continued strengthening in core areas and slight spillover to surrounding regions, such as Wuhou District in the southwest. This pattern aligns with the siphoning and spillover effects commonly observed in economic development. The other trend, however, is the emergence of new growth points on the eastern and western sides of the city. These potential growth areas can be regarded as key regions for future economic development and should receive additional attention from urban planners.

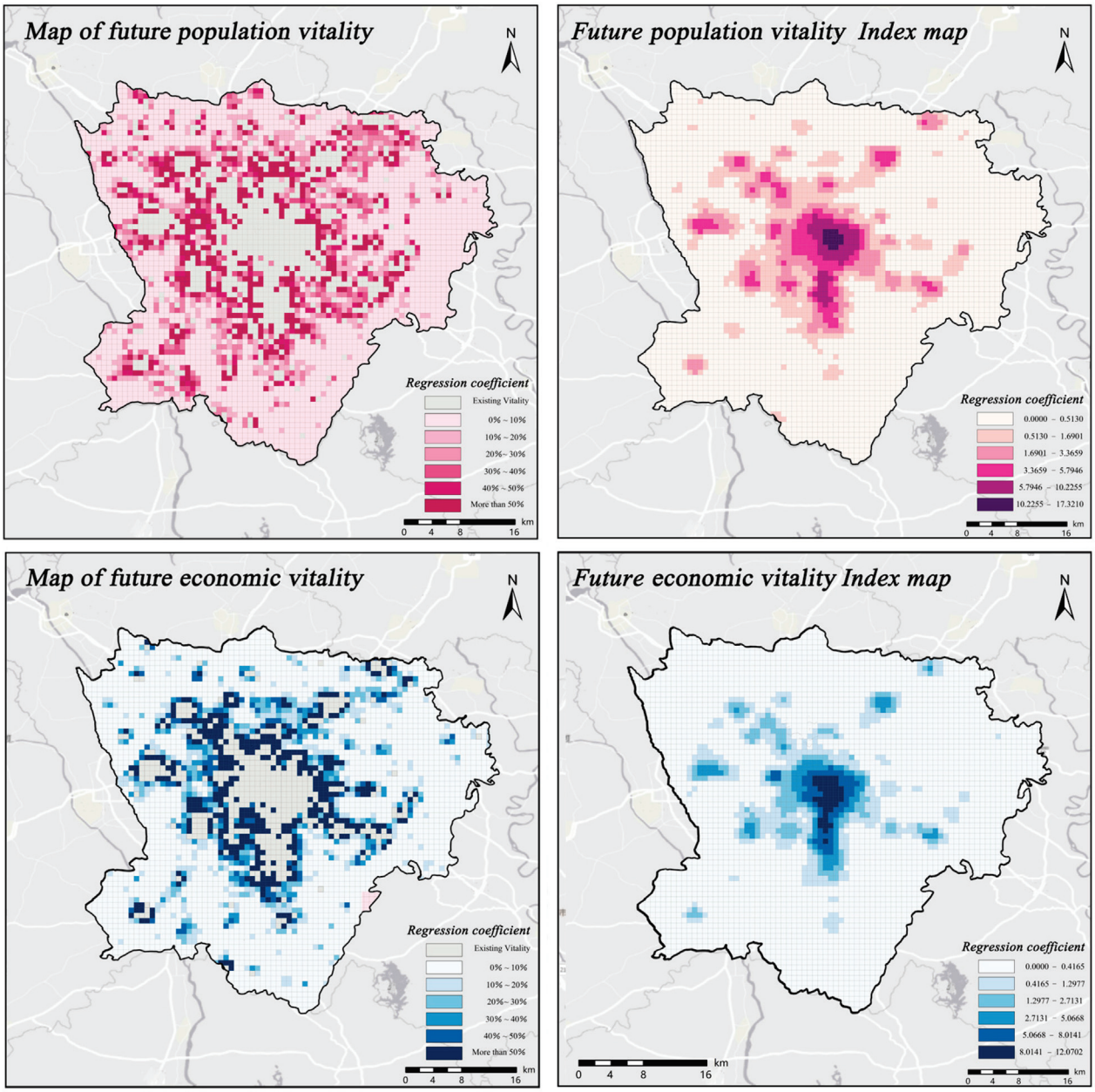


Figure 15. Future UV map (**Left**: probability and **Right**: vitality intensity, the picture is drawn by the author).

4. Discussion

4.1. Coffee and Milk Tea Stimulate UV in Different Ways

The core concept of environmental justice theory is that spaces with certain characteristics often exhibit a disproportionate distribution of environmental "goods" and "bads". Studies in the United States and Australia have shown that unhealthy fast-food outlets tended to be more concentrated in economically disadvantaged areas or regions with racial issues [86], whereas gentrified communities tend to have an increasing number of grocery stores, coffee shops, restaurants, and bars [87]. Previous studies have demonstrated that the spatial distribution of food establishments reflects urban socio-economic development and environmental attributes. This study, based on the context of China, extends existing research by examining COSs and MTSs, confirming that both the COI and MTI could represent certain spatial characteristics of cities. The MTI more effectively captured PV, while the COI better reflected the spatial patterns of urban economic structure. Additionally, the MTI exhibited a stronger correlation with UV than the COI. However, these findings are closely tied to the specific characteristics and development stage of the city, such as dietary habits and leisure activities.

The spatial distribution of MTSs was closely aligned with areas of population concentration, such as urban residential neighborhoods, tourist destinations, and campuses with distinct age demographics. These shops were also found in relatively underdeveloped suburban centers, making them more effective in reflecting PV. In Changsha, a city with an economic profile comparable to Chengdu, the distribution of MTSs exhibits a stronger correlation with EV [88], possibly due to Changsha's traditional preference for spicy cuisine [89], which makes the sweet flavors of MT less appealing to local residents. Consequently, economically prosperous areas tend to attract a larger population of younger, non-local individuals. Chengdu's more diverse culinary traditions, which often incorporate sweet elements, seem to result in greater acceptance of MT among the local population. In contrast, COSs focused more on mapping the city's economic structure onto space, with higher concentrations in areas associated with finance, commerce, and technological research. These included high-tech development zones, financial districts, and industrial parks. Conversely, their presence in economically underdeveloped or rural areas was minimal, which aligns with the findings of Zhao and Shi [90,91].

Notably, our study yielded some intriguing findings. High-value areas of the COI overlapped with areas undergoing or having completed urban renewal, such as the Shaocheng district and Yulin community, which preserved Chengdu's urban fabric and architectural clusters. Under the guidance of urban renewal, the living environments in these areas significantly improved, attracting new industries and high-tech talent, while also increasing land values and driving economic growth. Similarly, in Beijing, COSs were often located in rapidly gentrified hutong areas [37], further reinforcing the connection between COSs and economic development.

Interestingly, in regions such as the UK and the US, where urban development trends differ somewhat from those in China, COSs are also widely distributed in less populated rural areas, often concentrated in village centers and locations rich in natural scenery [27,92]. In South Korea, COSs tend to feature distinctive themed decor, making them more likely to be located in communities near parks and schools. In contrast, the attitude towards COSs in the Netherlands is notably negative. To protect children and adolescents from exposure to drug-related activities, authorities have enforced the closure of COSs within 500 m of schools, as these establishments have frequently been identified in studies as major venues for cannabis transactions [93].

The Bivariate Moran's I analysis for both types of stores confirms that MTI in Chengdu are more effective at capturing UV, a result consistent with findings from Guangzhou and Shenzhen, both cities with large rural populations and migrant workers [94]. In contrast, studies in Beijing have shown that the COI provides a more accurate reflection of UV [95]. These differences can be attributed to various factors, including the cities' different stages of economic development, the composition of their populations, and the history of

commercial transformation. Coffee typically ranges in price from 15 to 35 yuan, while milk tea is generally priced between CN¥ 5 and CN¥ 20, making MTSs a better indicator of UV in economically less developed cities like Chengdu.

4.2. Strategies for Activating Vitality Considering Nonlinear Thresholds and Spatial Heterogeneity

The goal of China's new urbanization is to create human-centered urban spaces, transitioning from "quantitative growth and scale expansion" to "quality improvement and efficiency enhancement". Shaping vibrant, high-quality urban and rural living environments is a key objective for China's sustainable urban development. Changes in the scale of elements can affect the equity of urban spaces, and numerical thresholds can maximize the use of existing resources. Therefore, it is necessary to consider strategies from different perspectives to enhance UV.

From the perspective of factor importance and spatial scale effects, the interaction between the two types of shops emerged as the primary driver of UV, becoming more pronounced with increasing distance from the city center. The expansion of COSs beyond the main urban area attracted MTSs to nearby locations, whereas MTSs did not exert the same influence on COSs. The impact of various transportation modes exhibited significant differences; subway stations had the greatest influence on the COI but minimal effect on PV. This was likely because COSs were often located near convenient transportation in office buildings, while the high housing prices around subway stations imposed greater operational pressure on lower-priced MTSs. The minimal contribution of road density to both types of vitality could be attributed to people prioritizing the practical significance of space over its accessibility. This perspective was also supported by Seung-Chul Noh et al.'s research [96].

In future planning, when aiming to further boost the EV of the high-tech development zone in the south, establishing COSs could be considered as one of the strategies. Detailed surveys of consumption preferences among the populations in universities and research institutions in this area could increase the likelihood of patronage. Only the commercial complexes on the east side of the city center impacted PV; this area is the cultural and entertainment hub of Chengdu. MTSs in this area should adopt differentiated business strategies and consider staggered development with stores within the commercial complexes. For MTSs planning to expand into the southwestern part of the city, attention should be paid to the population density in this area to avoid decision-making errors. When expanding COSs in the city core, additional factors should be incorporated to enhance the explanatory power of the model. Nonlinear threshold relationships indicated that a primary school density of $0.8/km^2$ could maximally stimulate both PV and EV. This value is also similar to the primary school service radius required in the "fifteen-minute living circle residential district" standard in China's current urban residential area planning standards. However, excessively high primary school density suggested that the area is more residential in nature, potentially promoting PV. A reasonable density range could eliminate the strong attribute characteristics of the plots. When the density of COSs exceeded $5/km^2$, they had minimal attraction to MTSs. Conversely, COSs expanded in areas with high densities of MTSs, indicating that COSs enjoyed the spatial location benefits of the MTS cluster. However, due to the mismatch between PV, consumption capacity, and social needs, MTSs could not benefit from this effect. The findings of this study provided new insights and implications for optimizing UV strategies, which are crucial for UV research and fine-grained management.

4.3. The Role of Future Urban Vitality Maps

Glaeser et al. found that Yelp data (restaurant data from the United States) could measure and predict local economic activity in near real-time and at almost any geographic scale, producing more granular and timely socio-economic datasets to aid government decision-making and implementation [97]. Dong et al. demonstrated through case studies of nine cities, including Beijing and Shenzhen, that restaurants have good performance

in predicting urban space and community attributes [22]. Wang et al. also identified that changes in the number of restaurants can serve as an indicator of the effectiveness of poverty alleviation efforts in a region. This finding underscores the powerful role that restaurants played in predicting various aspects of regional development. Based on this, we also mapped the future vitality of Chengdu through COSs and MTSs, also identified potential vitality growth points.

When overlaying the two maps, we found that non-central areas on the west side, such as Wenjiang and Pidu districts, not only have economic development potential but also the possibility of population aggregation. A comparison of the two maps reveals that the gradual expansion of MTSs and the increasing density of COSs align with the growing population concentration and the agglomeration of economic activities. This demonstrated the high credibility of our predictive approach. Urban planners should pay extra attention to areas with anomalies in the future to develop policies that guide the coordinated development of urban–rural integration and industrial economy.

The methodology and evaluation approach used in this study can be directly applied to other cities and different topics. This research expands the utility of restaurant-related POI data in predicting UV, as these data reflect the cumulative results of long-term human activities, enabling large-scale urban dynamic monitoring. Although cities differ in geographic, cultural, and economic conditions, they share many common characteristics in the context of dining, which may reveal hidden regional traits through the study of specific POI spatial distributions. Moreover, combining these data with other sources could provide a more promising method for predicting UV and offer valuable insights for addressing other geographic clustering issues.

4.4. Emphasize the Role of Spatial Social Interaction in Stimulating UV

The rise of the digital era has led individuals to increasingly engage in communication and interaction through virtual environments, posing a significant challenge to the functional value and social attractiveness of physical urban spaces. Urban researchers and designers are thus tasked with enhancing the appeal of physical spaces in cities. Scholars studying UV across different periods have emphasized that the charm of urban spaces largely derives from how the urban landscape is perceived. In designing urban spaces, factors such as historical culture, topography, climate, street scale, building density, land use mix, road network planning, and infrastructure layout should be taken into consideration, as they directly or indirectly impact UV [98].

Although a well-designed physical environment is fundamental to fostering UV, not all cities benefit from favorable resources and rational spatial design. Modifying the built environment to promote UV involves a degree of unpredictability. The essence of vitality lies in social interactions, which is why this study did not use common built environment indicators to explore the factors influencing UV. Geddes argued that space is fundamentally a unique environment where various human activities unfold [99], and Guo et al. further suggested that urban space acts as a carrier of interpersonal relationships, ranging from strong to weak [100]. The core concept of the "social physics" theory is that the "exchange of ideas" formed during social interactions can spread throughout the city via individuals' complex social relationships and spatial mobility, directly influencing urban innovation [58]. This has been well-documented in studies of Shenzhen, China [58]. Interestingly, their research found that high-density urban spaces do not always enhance UV, a view shared by Lan and colleagues [101]. Legeby, in their studies in Sweden [102], and Kang, in their research in Chongqing [103], also emphasized that spaces accommodating various social interactions are highly beneficial to UV. Therefore, promoting interpersonal interactions within spaces should be a key objective in stimulating UV.

Urban spaces facilitate social interactions and stimulate vitality in different ways, with the accumulation of social significance often playing a more substantial role. COSs are frequently regarded as "opportunities themselves" [104], transcending their primary function of beverage consumption. They create spaces where "fluid encounters" can repeat-

edly occur, thereby strengthening weak ties in modern society by promoting interpersonal interactions. This fosters a sense of community and enhances individual belonging, making COSs central to urban life, particularly in Europe and the United States. Additionally, they attract many white-collar workers and young people who use them as co-working spaces. The continuous exchange of information can foster knowledge innovation, which closely links COSs to EV. In contrast, MTSs, characterized by smaller spaces and a focus on takeaway consumption, lack the strong "third place" attribute of COSs. Beyond purchasing beverages, people are often motivated to visit MTSs by the "internet-famous" check-ins [98]. This unique "social symbol" identity brings together individuals with similar perceptions through shared experiences, like queuing, thereby promoting interaction [105]. This method does not rely on specific social classes or occupations, but effectively enhancing PV.

In other words, the different attributes of spaces are essentially various dimensions of vitality itself. COSs, associated with economic or innovation vitality, emphasize knowledge exchange and information flow, while offering comfortable spaces that attract high-tech talent. In contrast, MTSs provide spaces where communities with shared values seek a sense of belonging. Therefore, urban design should not only focus on traditional spatial elements such as spatial form, building scale, land use, and accessibility, but also on social elements such as interpersonal interactions and symbolic meanings. Adjusting inappropriate functions in existing spaces to incorporate features that encourage higher interaction potential can stimulate UV, rather than simply mixing functions. Strategically placing COSs and MTSs with local characteristics could serve as an effective means of revitalizing declining urban areas.

4.5. Limitations of the Study

Our study has several limitations. First, it is important to clarify that the dimensions of UV derived from different types of stores may not align and, in some cases, may even present contradictory interpretations. For example, analyzing UV through the lens of areas with dense microbars would likely focus on a narrow demographic, such as middle-aged white males, while independent bookstores tend to be associated with areas marked by a sense of well-being. Therefore, future research could explore commonalities by overlaying "vitality index maps" from various themes, which suggests a direction for our next steps. Second, while this study established a framework for understanding UV from the perspective of specialized stores, it only used cross-sectional data from Chengdu in 2023 to support the analysis. The NTL used as a proxy for UV also contains some uncertainties. Future research should incorporate longer-term, higher-precision monitoring data to examine the relationship from a spatiotemporal perspective more accurately. Additionally, more advanced GIS analysis techniques and a more diverse set of influencing factor indicators should be employed to further validate the key findings of this study.

5. Conclusions

UV is essential for a city's livability and sustainability. The food and beverage industry, as a central component of urban economies and public life, serves as an effective lens for studying UV. While small-scale food enterprises, such as coffee shops, have been recognized as indicators of economic vitality, the role of milk tea, a distinctly Chinese beverage, has received less attention. This study introduces a novel framework for predicting UV by examining the distribution patterns of coffee and milk tea shops. Using multi-source geospatial data, we constructed the COI and MTI and validated their association with different dimensions of UV. Using RF and the MGWR model, we investigated the factors influencing UV from both mathematical and spatial perspectives, and developed future vitality maps to inform policy decisions for Chengdu.

The findings show that the MTI effectively reflects PV, while the COI is more aligned with EV. Both types of shops are densely concentrated in commercial and office clusters, with COSs often located in areas that have undergone urban renewal. The influence of

transportation on shop distribution has diminished with the rise of food delivery and social functions. Reasonable infrastructure, such as approximately 0.8 primary schools and 0.7 secondary schools per kilometer, may stimulate both EV and PV. The potential maps suggest that population density will gradually expand from the city center, while the eastern and western regions of Chengdu may become key areas for future economic growth, deserving further attention from policymakers. Moreover, this study emphasizes that although the definition of UV continues to evolve, its core remains rooted in social interactions within the city. Therefore, beyond altering the physical urban environment, fostering human interaction should be a key strategy for enhancing UV.

Supplementary Materials: The following supporting information can be downloaded at: https://www.mdpi.com/article/10.3390/buildings14113517/s1. S1: Theil-Sen median analysis and Mann-Kendall trend test (Sen-MK); S2: Random Forest Model (RF) and Result Interpretation Methods; S3: Multivariate geographic regression model (MGWR)

Author Contributions: Conceptualization, Z.X., K.H. and J.C.; Data curation, Z.X., F.C. and X.L.; Formal analysis, K.H. and Z.X.; Funding acquisition, J.C.; Investigation, F.C., T.Y. and Z.X.; Methodology, Z.X. and X.L.; Project administration, J.C.; Resources, J.C.; Supervision, J.C.; Validation, F.C., Z.X. and T.Y.; Visualization, Z.X., X.L., J.S. and K.H.; Writing—original draft, Z.X. and X.L.; Writing—review and editing, Z.X., F.C. and X.L. All authors have read and agreed to the published version of the manuscript.

Funding: This research was Funded by "the Graduate Innovation Program of China University of Mining and Technology (Grant No. 2023WLJCRCZL314)" and "Funded by the Postgraduate Research & Practice Innovation Program of Jiangsu Province (Grant No. SJCX23_1269)".

Data Availability Statement: The original contributions presented in the study are included in the article, further inquiries can be directed to the corresponding author.

Acknowledgments: We would like to thank the editors and reviewers for providing constructive comments on this manuscript.

Conflicts of Interest: The authors declare that they have no known competing financial interest or personal relationships that could have appeared to influence the work reported in this paper.

References

1. Xu, Y.; Belyi, A.; Bojic, I.; Ratti, C. How friends share urban space: An exploratory spatiotemporal analysis using mobile phone data. *Trans. GIS* **2017**, *21*, 468–487. [CrossRef]
2. Jacobs, J. *The Death and Life of Great American Cities*; Knopf Doubleday Publishing Group: New York, NY, USA, 2016.
3. Lynch, K. *Good City Form*; MIT Press: Cambridge, MA, USA, 1984.
4. Maas, P.R. Towards a Theory of Urban Vitality. Ph.D. Thesis, The University of British Columbia, Vancouver, BC, Canada, 1984.
5. Kim, S. Urban Vitality, urban form, and land use: Their relations within a geographical boundary for walkers. *Sustainability* **2020**, *12*, 10633. [CrossRef]
6. Denis, M.; Cysek-Pawlak, M.M.; Krzysztofik, S.; Majewska, A. Sustainable and vibrant cities. Opportunities and threats to the development of Polish cities. *Cities* **2021**, *109*, 103014. [CrossRef]
7. Yue, W.; Chen, Y.; Thy, P.T.M.; Fan, P.; Liu, Y.; Zhang, W. Identifying urban vitality in metropolitan areas of developing countries from a comparative perspective: Ho Chi Minh City versus Shanghai. *Sustain. Cities Soc.* **2021**, *65*, 102609. [CrossRef]
8. Delclòs-Alió, X.; Miralles-Guasch, C. Looking at Barcelona through Jane Jacobs's eyes: Mapping the basic conditions for urban vitality in a Mediterranean conurbation. *Land Use Policy* **2018**, *75*, 505–517. [CrossRef]
9. Filion, P.; Hammond, K. Neighbourhood land use and performance: The evolution of neighbourhood morphology over the 20th century. *Environ. Plan. B Plan. Des.* **2003**, *30*, 271–296. [CrossRef]
10. Wu, J.; Ta, N.; Song, Y.; Lin, J.; Chai, Y. Urban form breeds neighborhood vibrancy: A case study using a GPS-based activity survey in suburban Beijing. *Cities* **2018**, *74*, 100–108. [CrossRef]
11. Jiang, Y.; Han, Y.; Liu, M.; Ye, Y. Street vitality and built environment features: A data-informed approach from fourteen Chinese cities. *Sustain. Cities Soc.* **2022**, *79*, 103724. [CrossRef]
12. Kim, Y.-L. Seoul's Wi-Fi hotspots: Wi-Fi access points as an indicator of urban vitality. *Comput. Environ. Urban Syst.* **2018**, *72*, 13–24. [CrossRef]
13. Ravenscroft, N. The vitality and viability of town centres. *Urban Stud.* **2000**, *37*, 2533–2549. [CrossRef]
14. Jin, X.; Long, Y.; Sun, W.; Lu, Y.; Yang, X.; Tang, J. Evaluating cities' vitality and identifying ghost cities in China with emerging geographical data. *Cities* **2017**, *63*, 98–109. [CrossRef]

15. Oruç, G.D.; Giritlioğlu, C. The evaluation of urban quality and vitality of the Istanbul historical peninsula-Eminönü district. *AZ ITU J. Fac. Archit.* **2008**, *5*, 97–117.
16. Doll, C.N.; Muller, J.-P.; Morley, J.G. Mapping regional economic activity from night-time light satellite imagery. *Ecol. Econ.* **2006**, *57*, 75–92. [CrossRef]
17. Wang, L.; Wang, S.; Zhou, Y.; Liu, W.; Hou, Y.; Zhu, J.; Wang, F. Mapping population density in China between 1990 and 2010 using remote sensing. *Remote Sens. Environ.* **2018**, *210*, 269–281. [CrossRef]
18. Zhang, Y.; Shang, K.; Shi, Z.; Wang, H.; Li, X. Spatial pattern of the vitality of Chinese characteristic towns: A perspective from nighttime lights. *Land* **2022**, *11*, 85. [CrossRef]
19. Tu, W.; Zhu, T.; Xia, J.; Zhou, Y.; Lai, Y.; Jiang, J.; Li, Q. Portraying the spatial dynamics of urban vibrancy using multisource urban big data. *Comput. Environ. Urban Syst.* **2020**, *80*, 101428. [CrossRef]
20. Montgomery, J. Café culture and the city: The role of pavement cafés in urban public social life. *J. Urban Des.* **1997**, *2*, 83–102. [CrossRef]
21. Zukin, S. *Naked City: The Death and Life of Authentic Urban Places*; Oxford University Press: Oxford, UK, 2009.
22. Dong, L.; Ratti, C.; Zheng, S. Predicting neighborhoods' socioeconomic attributes using restaurant data. *Proc. Natl. Acad. Sci. USA* **2019**, *116*, 15447–15452. [CrossRef]
23. Liang, X.; Andris, C. Measuring McCities: Landscapes of chain and independent restaurants in the United States. *Environ. Plan. B Urban Anal. City Sci.* **2022**, *49*, 585–602. [CrossRef]
24. Joosten, V.; Van Nes, A. How block types influences the natural movement economic process: Micro-spatial conditions on the dispersal of shops and Café in Berlin. In Proceedings of the 5th International Space Syntax Symposium, TU Delft, Delft, The Netherlands, 13–17 June 2005; pp. 13–17.
25. Ye, Y.; Li, D.; Liu, X. How block density and typology affect urban vitality: An exploratory analysis in Shenzhen, China. *Urban Geogr.* **2018**, *39*, 631–652. [CrossRef]
26. Xia, C.; Zhang, A.; Yeh, A.G. The varying relationships between multidimensional urban form and urban vitality in Chinese megacities: Insights from a comparative analysis. *Ann. Am. Assoc. Geogr.* **2022**, *112*, 141–166. [CrossRef]
27. Ferreira, J.; Ferreira, C.; Bos, E. Spaces of consumption, connection, and community: Exploring the role of the coffee shop in urban lives. *Geoforum* **2021**, *119*, 21–29. [CrossRef]
28. Hidalgo, C.A.; Castañer, E.; Sevtsuk, A. The amenity mix of urban neighborhoods. *Habitat Int.* **2020**, *106*, 102205. [CrossRef]
29. Pendergrast, M. *Uncommon Grounds: The History of Coffee and How It Transformed Our World*; Basic Books: New York, NY, USA, 2010.
30. Donner, H.; Loh, T.H. Does the Starbucks effect exist? Searching for a relationship between Starbucks and adjacent rents. *Prop. Manag.* **2019**, *37*, 562–578. [CrossRef]
31. Guzman, J. How Starbucks Cafes Can Fuel Startup Growth: The Power of Third Places. Available online: https://business.columbia.edu/research-brief/research-brief/starbucks-startups-third-places (accessed on 15 September 2024).
32. Glaeser, E.L.; Kim, H.; Luca, M. Nowcasting gentrification: Using yelp data to quantify neighborhood change. *AEA Pap. Proc.* **2018**, *108*, 77–82. [CrossRef]
33. Shi, Y.; Liu, D. Relationship between urban new business indexes and the business environment of Chinese cities: A study based on entropy-TOPSIS and a Gaussian process regression model. *Sustainability* **2020**, *12*, 10422. [CrossRef]
34. Hinsch, B. *The Rise of Tea Culture in China: The Invention of the Individual*; Rowman & Littlefield: Lanham, MD, USA, 2015.
35. Min, J.E.; Green, D.B.; Kim, L. Calories and sugars in boba milk tea: Implications for obesity risk in Asian Pacific Islanders. *Food Sci. Nutr.* **2017**, *5*, 38–45. [CrossRef]
36. Insights, F.B. Bubble Tea Market Size, Industry Trends. Available online: https://www.fortunebusinessinsights.com/industry-reports/bubble-tea-market-101564 (accessed on 15 August 2024).
37. Ferreira, J.; Ferreira, C. Challenges and opportunities of new retail horizons in emerging markets: The case of a rising coffee culture in China. *Bus. Horiz.* **2018**, *61*, 783–796. [CrossRef]
38. Ou, X. Total Coffee Consumption Volume in China from Crop Year 2018/19 to 2022/23 with a Forecast for 2023/24 (in 1000 bags). Available online: https://www.statista.com/statistics/1046674/china-coffee-consumption-volume/ (accessed on 5 September 2024).
39. Luo, W. Tea Time Rides Bubbles of New Popularity. Available online: https://www.chinadailyhk.com/hk/article/151386#Tea-time-rides-bubbles-of-new-popularity (accessed on 5 September 2024).
40. Iresearch. Blue Book of China's Catering Business Parameters in 2022. Available online: https://pdf.dfcfw.com/pdf/H3_AP202203141552559209_1.pdf (accessed on 5 September 2024).
41. Ong, A.K.S.; Prasetyo, Y.T.; Libiran, M.; Lontoc, Y.M.A.; Lunaria, J.A.V.; Manalo, A.M.; Miraja, B.A.; Young, M.N.; Chuenyindee, T.; Persada, S.F.; et al. Consumer Preference Analysis on Attributes of Milk Tea: A Conjoint Analysis Approach. *Foods* **2021**, *10*, 1382. [CrossRef]
42. Bu, H.; Yu, Q.; Cao, L. Study on Style Application in Space Design of New-style Tea Drinking Store. *Furnit. Inter. Des.* **2019**, *9*, 114–115.
43. Yan, C. Analysis on the Marketing Strategy of Milk Tea Market Based on Consumption Preference Analysis. *Front. Bus. Econ. Manag.* **2023**, *8*, 47–50. [CrossRef]

44. Zarin, S.Z.; Niroomand, M.; Heidari, A.A. Physical and social aspects of vitality case study: Traditional street and modern street in Tehran. *Procedia-Soc. Behav. Sci.* **2015**, *170*, 659–668. [CrossRef]
45. Malizia, E.; Motoyama, Y. The economic development–vibrant center connection: Tracking high-growth firms in the DC region. *Prof. Geogr.* **2016**, *68*, 349–355. [CrossRef]
46. Li, M.; Liu, J.; Lin, Y.; Xiao, L.; Zhou, J. Revitalizing historic districts: Identifying built environment predictors for street vibrancy based on urban sensor data. *Cities* **2021**, *117*, 103305. [CrossRef]
47. Yang, J.; Cao, J.; Zhou, Y. Elaborating non-linear associations and synergies of subway access and land uses with urban vitality in Shenzhen. *Transp. Res. Part A Policy Pract.* **2021**, *144*, 74–88. [CrossRef]
48. Lopes, M.N.; Camanho, A.S. Public green space use and consequences on urban vitality: An assessment of European cities. *Soc. Indic. Res.* **2013**, *113*, 751–767. [CrossRef]
49. Hu, K.; Xu, Z.; Wang, X.; Wang, Y.; Li, H.; Zhang, Y. Research on street color environment perception based on CEP-KASS framework. *Buildings* **2023**, *13*, 2649. [CrossRef]
50. Long, Y.; Huang, C. Does block size matter? The impact of urban design on economic vitality for Chinese cities. *Environ. Plan. B Urban Anal. City Sci.* **2019**, *46*, 406–422. [CrossRef]
51. Wang, Z.; Wang, X.; Liu, Y.; Zhu, L. Identification of 71 factors influencing urban vitality and examination of their spatial dependence: A comprehensive validation applying multiple machine-learning models. *Sustain. Cities Soc.* **2024**, *108*, 105491. [CrossRef]
52. Cao, X.; Shi, Y.; Zhou, L.; Tao, T.; Yang, Q. Analysis of factors influencing the urban carrying capacity of the shanghai metropolis based on a multiscale geographically weighted regression (mgwr) model. *Land* **2021**, *10*, 578. [CrossRef]
53. Zhou, W.; Liang, Z.; Fan, Z.; Li, Z. Spatio–temporal effects of built environment on running activity based on a random forest approach in nanjing, China. *Health Place* **2024**, *85*, 103176. [CrossRef] [PubMed]
54. Xiao, L.; Lo, S.; Liu, J.; Zhou, J.; Li, Q. Nonlinear and synergistic effects of TOD on urban vibrancy: Applying local explanations for gradient boosting decision tree. *Sustain. Cities Soc.* **2021**, *72*, 103063. [CrossRef]
55. Jiang, Y.; Huang, Z.; Zhou, X.; Chen, X. Evaluating the impact of urban morphology on urban vitality: An exploratory study using big geo-data. *Int. J. Digit. Earth* **2024**, *17*, 2327571. [CrossRef]
56. Tian, L.; Shen, X. Spatial patterns and their influencing factors for China's catering industry. *Humanit. Soc. Sci. Commun.* **2024**, *11*, 1–12. [CrossRef]
57. Jin, A.; Li, G.; Wang, J.; Mehmood Muhammad, S.; Yu, Y.; Lin, Z.-R. Location choice and optimization of development of community-oriented new retail stores: A case study of Freshippo stores in Nanjing City. *Prog. Geogr.* **2020**, *39*, 2013–2027. [CrossRef]
58. Chen, Z.; Dong, B.; Pei, Q.; Zhang, Z. The impacts of urban vitality and urban density on innovation: Evidence from China's Greater Bay Area. *Habitat Int.* **2022**, *119*, 102490. [CrossRef]
59. Li, G.; Gao, J.; Li, L.; Hou, P. Human pressure dynamics in protected areas of China based on nighttime light. *Glob. Ecol. Conserv.* **2020**, *24*, e01222. [CrossRef]
60. Small, C.; Elvidge, C.D. Night on Earth: Mapping decadal changes of anthropogenic night light in Asia. *Int. J. Appl. Earth Obs. Geoinf.* **2013**, *22*, 40–52. [CrossRef]
61. Gao, C.; Li, S.; Sun, M.; Zhao, X.; Liu, D. Exploring the relationship between urban vibrancy and built environment using multi-source data: Case study in Munich. *Remote Sens.* **2024**, *16*, 1107. [CrossRef]
62. Stokes, E.C.; Roman, M.O. Tracking COVID-19 urban activity changes in the Middle East from nighttime lights. *Sci. Rep.* **2022**, *12*, 8096. [CrossRef]
63. Ma, T. Multi-level relationships between satellite-derived nighttime lighting signals and social media–derived human population dynamics. *Remote Sens.* **2018**, *10*, 1128. [CrossRef]
64. Liu, Y.; Wang, J.; Dai, W.; Wang, Z.; Wu, Z. Mapping terrestrial mammals in China based on species richness of functional groups. *Ecol. Indic.* **2024**, *166*, 112401. [CrossRef]
65. Song, W.; Wang, C.; Chen, W.; Zhang, X.; Li, H.; Li, J. Unlocking the spatial heterogeneous relationship between Per Capita GDP and nearby air quality using bivariate local indicator of spatial association. *Resour. Conserv. Recycl.* **2020**, *160*, 104880. [CrossRef]
66. Liu, L.; Li, J.; Wang, J.; Liu, F.; Cole, J.; Sha, J.; Jiao, Y.; Zhou, J. The establishment of an eco-environmental evaluation model for southwest China and eastern South Africa based on the DPSIR framework. *Ecol. Indic.* **2022**, *145*, 109687. [CrossRef]
67. Huang, D.; Cao, S.; Zhao, W.; Zhao, P.; Chen, J.; Yu, M.; Zhu, Z. Urban greening amidst global change: A comparative study of vegetation dynamics in two urban agglomerations in China under climatic and anthropogenic pressures. *Ecol. Indic.* **2024**, *159*, 111739. [CrossRef]
68. Wang, X.; Xiao, J.; Li, X.; Cheng, G.; Ma, M.; Zhu, G.; Altaf Arain, M.; Andrew Black, T.; Jassal, R.S. No trends in spring and autumn phenology during the global warming hiatus. *Nat. Commun.* **2019**, *10*, 2389. [CrossRef]
69. Jung, S.S.; Jang, S.S. To cluster or not to cluster?: Understanding geographic clustering by restaurant segment. *Int. J. Hosp. Manag.* **2019**, *77*, 448–457. [CrossRef]
70. Yang, Y.; Roehl, W.S.; Huang, J.-H. Understanding and projecting the restaurantscape: The influence of neighborhood sociodemographic characteristics on restaurant location. *Int. J. Hosp. Manag.* **2017**, *67*, 33–45. [CrossRef]
71. Ewing, R.; Tian, G.; Goates, J.; Zhang, M.; Greenwald, M.J.; Joyce, A.; Kircher, J.; Greene, W. Varying influences of the built environment on household travel in 15 diverse regions of the United States. *Urban Stud.* **2015**, *52*, 2330–2348. [CrossRef]

72. Teller, C.; Reutterer, T. The evolving concept of retail attractiveness: What makes retail agglomerations attractive when customers shop at them? *J. Retail. Consum. Serv.* **2008**, *15*, 127–143. [CrossRef]
73. Wang, L.; Fan, H.; Wang, Y. Site selection of retail shops based on spatial accessibility and hybrid BP neural network. *ISPRS Int. J. Geo-Inf.* **2018**, *7*, 202. [CrossRef]
74. Ma, D.; Liu, B.; Huang, Q.; Zhang, Q. Evolution Characteristics and Causes—An Analysis of Urban Catering Cluster Spatial Structure. *ISPRS Int. J. Geo-Inf.* **2023**, *12*, 302. [CrossRef]
75. Chen, Y.; Yu, B.; Shu, B.; Yang, L.; Wang, R. Exploring the spatiotemporal patterns and correlates of urban vitality: Temporal and spatial heterogeneity. *Sustain. Cities Soc.* **2023**, *91*, 104440. [CrossRef]
76. Yang, L.; Yu, B.; Liang, Y.; Lu, Y.; Li, W. Time-varying and non-linear associations between metro ridership and the built environment. *Tunn. Undergr. Space Technol.* **2023**, *132*, 104931. [CrossRef]
77. Wang, S.; Wang, J.; Wang, Y. Effect of land prices on the spatial differentiation of housing prices: Evidence from cross-county analyses in China. *J. Geogr. Sci.* **2018**, *28*, 725–740. [CrossRef]
78. Li, H.; Chen, P.; Grant, R. Built environment, special economic zone, and housing prices in Shenzhen, China. *Appl. Geogr.* **2021**, *129*, 102429. [CrossRef]
79. Wu, K.; Wang, Y.; Ye, Y.; Zhang, H.J. A Study on the Influencing Factors and Driving Forces of Spatial Differentiation of Retail Formats in Guangzhou. *J. Geo-Inf. Sci.* **2020**, *22*, 1228.
80. Breiman, L. Random forests. *Mach. Learn.* **2001**, *45*, 5–32. [CrossRef]
81. Liu, Y.; Li, Y.; Yang, W.; Hu, J. Exploring nonlinear effects of built environment on jogging behavior using random forest. *Appl. Geogr.* **2023**, *156*, 102990. [CrossRef]
82. Guo, S.; Li, L.; Wang, S.; Huang, J.; Xie, X.; Wang, Y. What are the dominant drivers and optimal thresholds for a healthy ecosystem in the Yellow River Basin, China? from a perspective of nonlinear nexus. *Ecol. Indic.* **2024**, *162*, 111997. [CrossRef]
83. Fotheringham, A.S.; Yang, W.; Kang, W. Multiscale geographically weighted regression (MGWR). *Ann. Am. Assoc. Geogr.* **2017**, *107*, 1247–1265. [CrossRef]
84. Ma, J.; Cheng, J.C.; Jiang, F.; Chen, W.; Zhang, J. Analyzing driving factors of land values in urban scale based on big data and non-linear machine learning techniques. *Land Use Policy* **2020**, *94*, 104537. [CrossRef]
85. Choung, Y.-J.; Kim, J.-M. Study of the relationship between urban expansion and pm10 concentration using multi-temporal spatial datasets and the machine learning technique: Case study for Daegu, South Korea. *Appl. Sci.* **2019**, *9*, 1098. [CrossRef]
86. Austin, S.B.; Melly, S.J.; Sanchez, B.N.; Patel, A.; Buka, S.; Gortmaker, S.L. Clustering of fast-food restaurants around schools: A novel application of spatial statistics to the study of food environments. *Am. J. Public Health* **2005**, *95*, 1575–1581. [CrossRef]
87. Carroll, G.R.; Torfason, M.T. Restaurant Organizational Forms and Community in the US in 2005. *City Community* **2011**, *10*, 1–24. [CrossRef]
88. Huang, Q.; Yang, B.; Xu, X.; Hao, H.; Liang, L.; Wang, M. Location selection and prediction of Sexy Tea Store in Changsha city based on multi-source spatial data and random forest model. *J. Geo-Inf. Sci* **2022**, *24*, 723–737.
89. Wang, W.; Wang, S.; Chen, H.; Liu, L.; Fu, T.; Yang, Y. Analysis of the characteristics and spatial pattern of the catering industry in the four central cities of the Yangtze River Delta. *ISPRS Int. J. Geo-Inf.* **2022**, *11*, 321. [CrossRef]
90. Zhao, J.; Zong, B.; Wu, L. Site Selection Prediction for Coffee Shops Based on Multi-Source Space Data Using Machine Learning Techniques. *ISPRS Int. J. Geo-Inf.* **2023**, *12*, 329. [CrossRef]
91. Shi, Y.; Yang, F. Features of spatial distribution and impacting factors of Starbucks in Shanghai. *Econ. Geogr.* **2018**, *38*, 126–132.
92. Saey, S.; Foss, K. The Third Place experience in urban and rural coffee shops. *Midwesern J. Under-Grad. Res.* **2016**, *6*, 171–177. Available online: http://research.monm.edu/mjur/files/2019/02/MJUR-i06-2016-8-SaeyFoss.pdf (accessed on 10 July 2024).
93. Langen, M.; Aydin, E.; Eichholtz, P.; Kok, N. Getting high or getting low? the external effects of coffeeshops on house prices. *Real Estate Econ.* **2022**, *50*, 565–592. [CrossRef]
94. Zikirya, B.; He, X.; Li, M.; Zhou, C. Urban food takeaway vitality: A new technique to assess urban vitality. *Int. J. Environ. Res. Public Health* **2021**, *18*, 3578. [CrossRef] [PubMed]
95. Zhou, Y.; He, X.; Zikirya, B. Boba shop, coffee shop, and urban vitality and development—A spatial association and temporal analysis of major cities in China from the standpoint of nighttime light. *Remote Sens.* **2023**, *15*, 903. [CrossRef]
96. Noh, S.-C.; Park, J.-H. Café and restaurant under my home: Predicting urban commercialization through machine learning. *Sustainability* **2021**, *13*, 5699. [CrossRef]
97. Glaeser, E.L.; Kim, H.; Luca, M. *Nowcasting the Local Economy: Using Yelp Data to Measure Economic Activity*; National Bureau of Economic Research: Cambridge, MA, USA, 2017.
98. Yang, F.F.; Lin, G.; Lei, Y.; Wang, Y.; Yi, Z. Understanding Urban Vitality from the Economic and Human Activities Perspective: A Case Study of Chongqing, China. *Chin. Geogr. Sci.* **2024**, *34*, 52–66. [CrossRef]
99. Geddes, P. *Cities in Evolution: An Introduction to the Town Planning Movement and to the Study of Civics*; Williams & Norgate: London, UK, 1915.
100. Jusup, M.; Holme, P.; Kanazawa, K.; Takayasu, M.; Romić, I.; Wang, Z.; Geček, S.; Lipić, T.; Podobnik, B.; Wang, L. Social physics. *Phys. Rep.* **2022**, *948*, 1–148.
101. Lan, F.; Gong, X.; Da, H.; Wen, H. How do population inflow and social infrastructure affect urban vitality? Evidence from 35 large-and medium-sized cities in China. *Cities* **2020**, *100*, 102454. [CrossRef]

102. Legeby, A.; Marcus, L. Does the urban structure of Swedish cities inhibit the sharing of public space? *Built Environ.* **2011**, *37*, 155–169. [CrossRef]
103. Kang, C.; Fan, D.; Jiao, H. Validating activity, time, and space diversity as essential components of urban vitality. *Environ. Plan. B Urban Anal. City Sci.* **2021**, *48*, 1180–1197. [CrossRef]
104. Stenseth, B. Heart of urbanism. The café: A chapter of cultural history. In *Café Society*; Palgrave Macmillan: New York, NY, USA, 2013; pp. 23–42.
105. Yuzheng, Z.; Yan, L.U.; Xiaojian, C. Distribution Characteristics and Influencing Factors of Milk-tea Consumption Space from the Perspective of Scene-Symbol and Physical-Information. *J. Geo-Inf. Sci.* **2023**, *25*, 823–837. [CrossRef]

Disclaimer/Publisher's Note: The statements, opinions and data contained in all publications are solely those of the individual author(s) and contributor(s) and not of MDPI and/or the editor(s). MDPI and/or the editor(s) disclaim responsibility for any injury to people or property resulting from any ideas, methods, instructions or products referred to in the content.

buildings

MDPI

Article

A Pathological Diagnostic Method for Traditional Brick-Masonry Dwellings: A Case Study in Guangfu Ancient City

Qinghong Li [1], Tiejian Zhang [1,*], Yingming Fang [2,3] and Fengzeng Lin [2,4]

[1] School of Architecture and Design, Hebei University of Engineering, Handan 056006, China; liqinghong0016@hotmail.com
[2] School of Architecture and Design, Harbin Institute of Technology, Harbin 150001, China; 23s134159@stu.hit.edu (Y.F.); 22bg34036@stu.hit.edu.cn (F.L.)
[3] School of Civil Engineering, Yancheng Institute of Technology, Yancheng 224051, China
[4] Key Laboratory of Cold Region Urban and Rural Human Settlement Environment Science and Technology, Ministry of Industry and Information Technology, Harbin 150001, China
* Correspondence: zhangtiejianarch@hotmail.com; Tel.: +86-134-7432-6448

Abstract: Many regions of the world have traditional dwellings, which not only represent the main form of residential architecture, but also carry the local vernacular culture, display the region's unique architectural style, materials and technology, and have important historical and cultural value. Due to environmental factors, traditional dwellings often suffer from architectural damage that threatens the stability of their structure and affects their esthetics value, resulting in a significant number of abandoned and demolished houses. In order to scientifically and effectively solve the damage problems of traditional dwellings, based on the theory of architectural pathology, the following diagnostic method for damage manifestation and the characteristics of traditional houses is proposed: "Architectural Pathology Appraisal–Pathological Environment Analysis–Mechanical Properties Testings". The traditional dwellings in the ancient city of Guangfu were used as a case study for the practical application of the methodology for analyzing the main types and causes of the damage of the dwellings by examining the damage information of the dwellings, collecting the environmental data of the damaged walls, and testing the mechanical properties of the damaged walls. The results show that the main damage type in the ancient city dwellings of Guangfu is dampness damage, with corrosion deterioration, wall alkali flooding, and the moisture infiltration phenomenon as the manifested symptoms, and the damage is mainly concentrated in the lower part of the wall. In addition, the humidity and moisture content in the lower part of the wall is higher than that in the upper part of the wall, and the compressive strength of the damaged part of the wall is lower than that of the undamaged part. The humid environment of the old town contributed significantly to the destruction of the dwellings, and water intrusion led to a reduction in the strength of the dwellings' bricks. Through the diagnostic method of building pathology, the causes of Guangfu dwellings' damage are identified, and scientific and targeted damage intervention suggestions are made. This is expected to provide guidance for the treatment and prevention of building pathology in the ancient city of Guangfu and serve as a reference for the diagnosis and treatment of pathology in traditional dwellings in other areas.

Keywords: building pathologies; traditional dwellings; diagnosis; brick walls

1. Introduction

Vernacular architecture is prevalent globally, yet economic and social progress have prompted population migration from rural to urban areas, leading to the extensive abandonment or renovation of rural houses. This has created a dilemma whereby vernacular architecture faces numerous contradictions between its long-term use and conservation

and development efforts [1,2]. Vernacular architecture is not only the embodiment of local traditional ways of life, but also carries deep history and culture. To preserve vernacular architecture, it is essential to restore missing or defective components. Due to factors such as natural and anthropogenic influences, damage and decay are prevalent in local architecture [3–5]. There is no point in restoring and converting a few buildings into a complex. Addressing their deterioration fundamentally requires thorough building examinations to assess their value and issues, along with a comprehensive evaluation of local conditions to formulate precise repair recommendations [6]. Brick-masonry dwellings are the most common form of vernacular architecture in Northern China [7], suffering from inadequate research methodologies and diagnostic approaches for their damage. Thus, developing scientific diagnostic methods is of great research importance for effectively treating building pathology.

The city of Handan, located at the junction of four provinces in China's Hebei Province, has a history spanning over 3000 years. According to the Handan City Government, there are 18 villages in the city with more than 4000 traditional dwellings [8]. Among them, the ancient city of Guangfu in Yongnian County is a famous historical and cultural city in China and the best-preserved of the 11 prefectural cities in Zhili during the Qing Dynasty. At the same time, most residential buildings in the city adopt the brick construction form, preserving the architectural characteristics of traditional residential buildings in Northern China [9]. Therefore, Guangfu dwellings can be viewed as typical representatives of traditional dwellings in the northern region of China. In 2011, the Yongnian District government of Handan City, China, conducted a survey on the ancient city of Guangfu, documenting 173 historical and traditional dwellings. However, field research reveals that many traditional houses have been abandoned or even demolished and rebuilt due to architectural defects. There are now only 63 relatively well-preserved and inhabited traditional dwellings left, and those that remain generally have architectural deficiencies [10]. Building pathologies not only harm the ancient city's historical appearance but also compromise the mechanical properties of building structures and the health of the living environment. However, preserving traditional homes is more difficult than preserving listed buildings [11]. Although some people ultimately continue to live in these dwellings, they can only be roughly repaired using contemporary materials and methods due to a lack of scientific guidance. This type of restoration, rather than addressing the building's underlying problems, results in material and structural incompatibility [12]. Hidden threats to building safety persist, and they exacerbate damage to the appearance of traditional dwellings. Failing to implement maintenance measures and lacking conservation knowledge can lead to severe building pathologies [13], causing the number of traditional dwellings to continue to decline. Therefore, developing science-based, practical solutions to combat building damage is of utmost urgency.

Since the 1950s, scholars in China have been actively studying traditional dwellings [14]. Amid rural revitalization and cultural heritage preservation efforts, traditional dwelling conservation and renewal have yielded substantial outcomes. However, these have primarily focused on interior renewal and style studies, with insufficient research on traditional dwelling pathology [15–18]. Building pathology is in particular caused by poor construction technology, human use, changing environmental conditions at the building's location, and other factors that lead to varying degrees of building damage. Studies on building damage aim not only to repair damaged buildings but also to prevent their occurrence and enhance durability and sustainability. With regard to the investigation of building pathologies, Groak, an expert in the field, first pointed out the importance of preventing building pathologies during planning and construction [19]. With the preservation of historic buildings and urban renewal projects, scientists have gradually placed emphasis on studying building pathologies. When discussing assessment and inspection strategies for older urban buildings, experts underscored the importance of addressing building blight [20]. By examining cracks in building thermal insulation, researchers demonstrate the importance of understanding the causes of building pathologies for effective damage

recovery [21]. Experts specializing in specific building diseases employ sub-wall ventilation technology to tackle moisture transfer issues in historic buildings, underscoring the value of targeted interventions [22]. Furthermore, experts researching damaged buildings have found issues related to moisture, mold, and other pathologies within the structures [23]. Chinese researchers have determined that architectural damage correlates with climatic conditions, building materials, shapes, and other factors during the study of cultural artifact and building preservation [24]. To classify and study building pathologies in various types of heritage buildings, scientists have developed tailored assessment systems and treatment methods [25–27]. Work on field research and testing of the building environment [28,29], and building laboratories or using software to simulate the process of building damage development have been used to further analyze the causes of building damage [30–32]. In order to increase the efficiency and accuracy of diagnosing building damage, some scientists have tried to incorporate machine learning algorithms and laser scanning technology into their research in recent years [33,34]. Scholars have achieved extensive results in the study of architectural pathologies, especially the non-destructive testing methods of architectural pathologies and the actual measurement methods of historical architectural environments, which provide the basis for this paper.

Given the complexity of architectural pathologies, a thorough understanding of the condition of residential buildings and an analysis of the underlying causes of the damage are critical to making decisions about remediation efforts [35]. This study aims to propose and implement a methodology for diagnosing the pathological manifestations of traditional dwellings to assist in identifying conservation solutions. The work encompasses damage investigation, non-destructive testing of mechanical properties, and environmental data analysis. By combining pathological examination with environmental detection, this paper investigates traditional dwellings in Guangfu Ancient City, detects their damage status, and collects pathology environment data. It also proposes appropriate interventions based on specific damage causes, offering guidance for the study of pathologies in traditional housing in other regions.

2. Methods

2.1. Research Framework

The aim of this study is to assess the methods of examining and diagnosing pathological manifestations of traditional dwellings. The following figure shows the contents and steps of this study (Figure 1):

- Collection of basic information: Collect relevant literature and organize information on the number, distribution, types, and construction materials of traditional dwellings.
- Pathological examination of traditional dwellings: The study must use non-destructive tests, which are inspection methods that do not affect or manipulate the physical-mechanical properties of the building, in the context of preserving traditional dwellings. Visual inspection [36], infrared thermography [37], ultrasonic propagation velocity [38], acoustic emission [39], and resistivity [40] are the most commonly used non-destructive testing techniques used to examine historic buildings. Given the large and widespread inventory of traditional Chinese dwellings and the low economic level of the people who primarily use them, low-cost inspection methods that can be used on a large scale should be selected. The research used visual inspections to map damage information and assess the damage status in traditional dwellings [41]. Information includes the type of wall damage, the location of the wall damage, and the extent of damage to the wall.
- Environmental data testing of traditional dwellings: Among the numerous factors that lead to building damage, the influence of the natural environment cannot be overlooked. The study of the effects of the natural environment on damage has become a central issue in the preservation of cultural heritage [42]. In this study, we collected typical annual meteorological data of the region and analyzed the meteorological data to make a preliminary conjecture about the relationship between the architec-

tural pathology of residential buildings and the climatic environment. A sample of residential buildings was then selected for testing building microenvironmental data. The tests measure relative humidity, temperature, wind speed, thermal radiation on the surface of the building walls, and the water content inside the bricks. These parameters are used to draw preliminary conclusions about the pathological environmental properties of the houses, which are then confirmed by macroclimatic environmental data.

- Mechanical performance testing of traditional dwellings and recommendations for intervention: A selection of specific testing tools for testing the mechanical properties of damaged residential buildings and analyzing the causes and severity of residential building damage by combining the results of pathological inspections and pathological environmental tests is carried out. This also produces recommendations for the appropriate damage management measures and interventions based on the pathology.

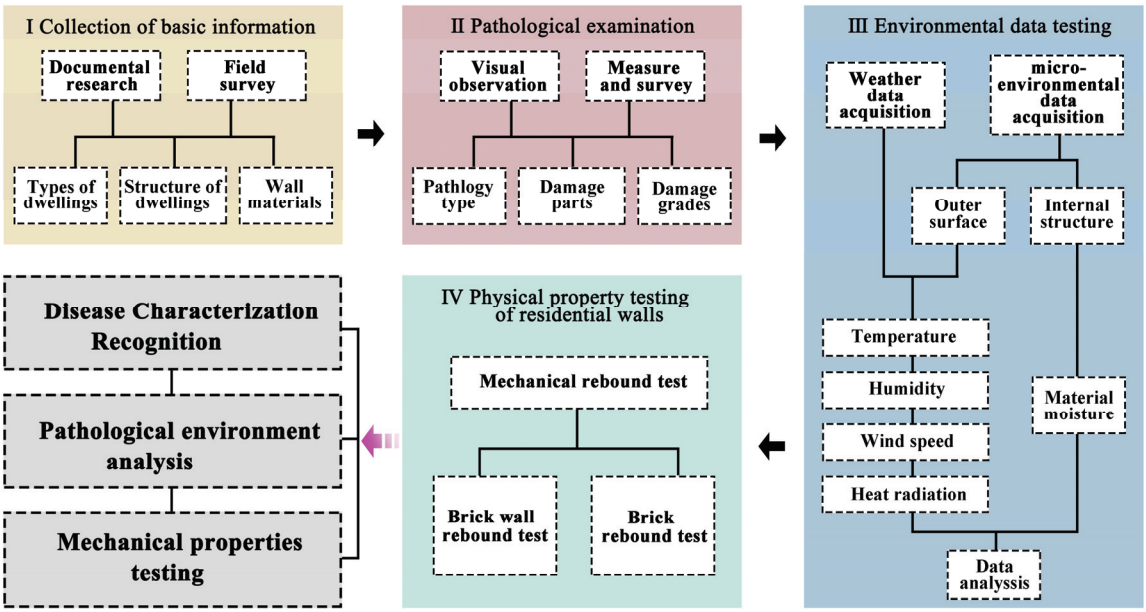


Figure 1. Workflow of holistic approach.

2.2. Current Condition of the Case

The ancient city of Guangfu is located in the southern part of the North China Plain and is surrounded by the Yongnian Depression, a water-rich area. It is located in Yongnian District, Handan City, Hebei Province, China. The ancient city was originally a dryland earth city that was rebuilt as a brick city in the Ming Dynasty [43]. The old town preserves a large number of traditional dwellings. The traditional houses have the characteristic features of courtyard buildings in Northern China, including south-facing courtyards with clearly defined axes. The existing traditional houses in the city are mainly brick houses, with red and blue bricks being the main building materials [44,45]. The main structures within Guangfu Ancient City are single-story brick-masonry buildings. The construction of these buildings can be divided into three parts from bottom to top as follows: the foundation, the walls, and the roof. The predominant types of foundations for residential buildings in the ancient city are rammed earth and brick masonry foundations. The common material used for wall construction within the city is blue brick, with the standard dimensions of 240 × 120 × 55 mm. The roof is typically composed of three layers as follows: the first layer consists of wooden planks or thatch, the second layer is a layer of yellow mud mixed with reed stalks laid over the wooden planks, and the final layer is composed of tiles. In the ancient city of Guangfu, there are primarily two types of architectural structures, namely brick-concrete structures and brick-wood structures. The brick-concrete structures are predominantly utilized in ordinary residential buildings, whereas brick-wood structures

are more common in public buildings and the residences of the nobility. The brick-concrete structures bear load through masonry constructed from bricks or stones, while the brick-wood structures carry loads through a combination of wooden columns and brick walls. Buildings with brick-concrete structures generally have a longer service life compared to those with brick-wood structures, which are more challenging to maintain. Consequently, a greater number of traditional residences with brick-concrete structures are preserved within the city. The investigation found that the damage to traditional houses in the old town is mainly manifested in the walls. Based on the observation and documentation of the brick wall damage phenomena, the following primary building damage problems of the brick wall were identified (Figure 2): moisture infiltration, plastering bulge and rupture, cracks, corrosion and deterioration, wall alkali flooding, plant parasitism, and mold formation.

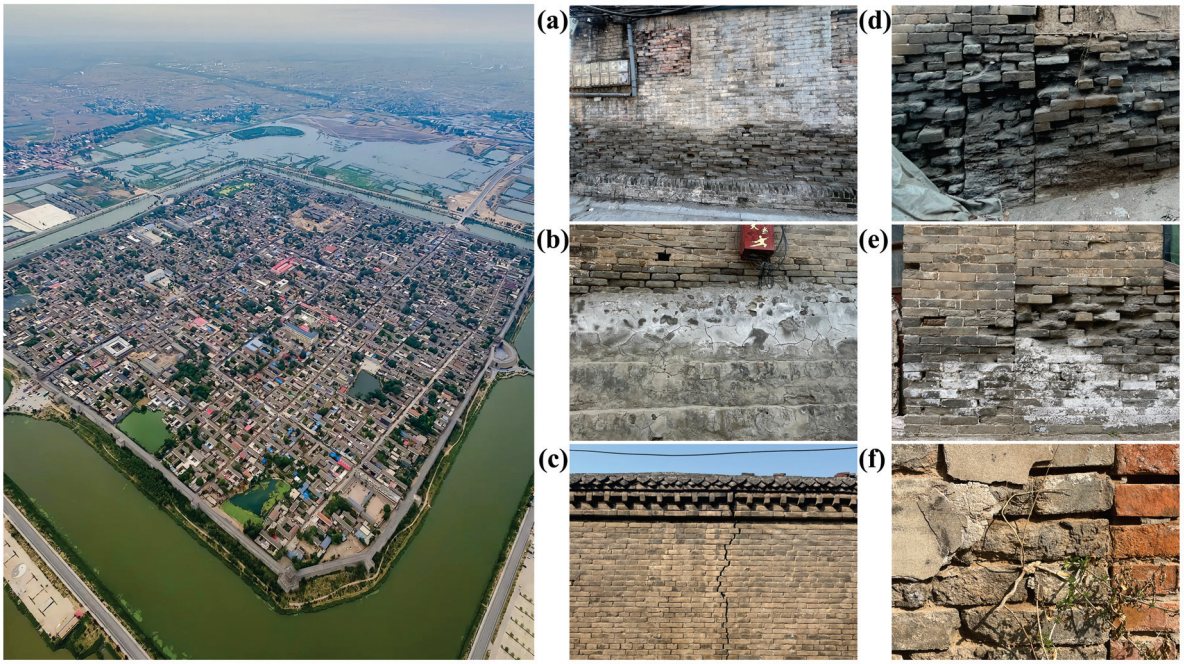


Figure 2. Status of Guangfu Ancient City and damage images of residential dwellings: (**a**) Moisture infiltration; (**b**) Plastering bulge and rupture; (**c**) Cracks; (**d**) Corrosion and deterioration; (**e**) Wall alkali flooding; (**f**) Plant parasitism.

To elucidate the pathology of residential structures, a pre-evaluation of the common damage problems is conducted. For instance, the genesis of cracks in residential brick masonry walls is typically attributed to material properties and environmental factors [46]. Temperature-induced thermal expansion and contraction can initiate the formation of masonry cracks. Additionally, drying shrinkage of brick masonry materials, particularly following the evaporation of water from cement mortar, can precipitate cracking. Environmental factors, such as fluctuations in the water table, uneven foundation settlement, and the influence of corrosive agents, can also induce wall cracks. Cracks can be categorized as structural or non-structural; structural cracks potentially compromise the safety and stability of the building, whereas non-structural cracks primarily impact esthetics and durability [47]. The cracks observed in the old city houses examined in this study are predominantly non-structural. Brick wall efflorescence is primarily associated with brick quality and environmental factors. A humid environment expedites the dissolution and migration of soluble salts, precipitating alkalization [48]. Soluble inorganic salts from groundwater or surface water can infiltrate the brick wall with moisture, leading to alkalization. Variations in environmental water content or temperature fluctuations induce the crystallization and dissolution of salts, resulting in a loose masonry structure, which is also

a major cause of alkalization [49]. Therefore, this study aims to clarify the environmental analysis of the pathological conditions affecting the dwellings.

2.3. Descriptors Used

This study includes numerous parameters. The relevant parameters of the study are defined and explained to make the research content clearer (Table 1). These three "descriptors", essential for the study of the damage, include the following basic parameters: location, type, and degree of wall damage caused by damage [50].

Table 1. Codification and relation of the descriptors used in the research.

Descriptor	Code	Concept	Description
Descriptor 1: Construction units	W1	Upper part of the wall	
	W2	Central part of the wall	
	W3	Lower part of the wall	
	W4	Wall footing	
	W5	Gable wall	
Descriptor 2: Pathology type	P1	Corrosion deterioration	Chipping on the wall surface, damage to the bricks, missing bricks, and chalking.
	P2	Wall alkali flooding	White crystals precipitate inside the wall and adhere to the outside surface of the wall material.
	P3	Moisture infiltration	Water damage to walls, color changes to the material, severe wetting.
	P4	Plastering bulge and rupture	Cracks and bulges in the outer layer of the wall.
	P5	Cracks	Structural cracks in walls with misalignment.
	P6	Mold formation	Parasitic fungi cling to the wall surfaces.
	P7	Plant parasitism	Plants grow up the wall and cause damage to the wall surface.
Descriptor 3: Damage grades		Light damage Moderate damage Severe damage Destruction	

Descriptor 1 is the name of the different parts of the residential wall. Different parts of the wall have different damage states, and to ensure the accuracy and specificity of the study, different parts of the brick walls of the dwellings were defined based on traditional architectural features and divided into five different units (Figure 3). Descriptor 2 refers to the manifestation symptoms of the damage in the dwellings of the ancient city. The seven types of manifestation symptoms of architectural pathology were explained accordingly. Descriptor 3 refers to the extent of the damage. In March 2011, the local government conducted a status quo study on the historical houses in Guangfu Ancient City. The study assessed the current state of building preservation and classified buildings into the following four main categories: better preserved, in need of minor repairs, in need of major repairs, and beyond repair [51]. This study follows the damage classifications of residential buildings according to the classification in the government research report and defines the degree of damage as light damage, moderate damage, severe damage, and destruction.

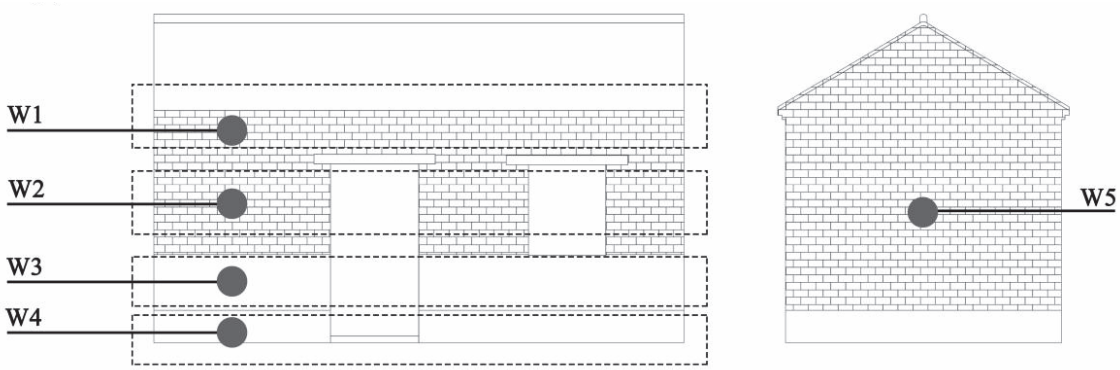


Figure 3. Schematic diagram of the codes for each part of the building wall.

2.4. Field Measurement and Investigation

2.4.1. Methods of Pathological Examination of Traditional Dwellings

In the context of preserving traditional dwellings, this study uses an investigative approach to architectural pathology questions [52]. Exploring the damage information of traditional houses through visual inspection and measurement and mapping the damage and damage information. The damage and damage information map is a graphical tool used for recording the detailed damage and damage status of a building or structure, which typically contains information on the following aspects: the types of damage on living walls, such as cracks and erosion, differentiated according to different symbols or colors on the map (Table 2); the parts of the living wall damage, clearly identifying the specific locations of the damage on the wall, e.g., around the window frames of the wall and in the middle part of the wall; and the extent of the damage to the residential wall. The degree of wall damage is assessed using quantitative indicators such as crack length and damage area, as well as qualitative descriptions such as mild and moderate.

Table 2. Differentiation of surface pathology in residential wall.

Pathology	Identification	Pathology	Identification
P1		P5	
P2		P6	
P3		P7	
P4			

The procedure for image acquisition to capture the current situation of the wall facade of residential buildings is as follows: First, we survey and map the facade of traditional residential buildings to obtain the basic image of the wall frame. Second, we measure and record the contour and location of the damage and take photos to facilitate the positioning of the damage map during the drawing process [53,54]. Using software, we draw pictures of the wall facade of traditional residential buildings (Figure 4). Finally, the image information and associated data are systematically numbered and recorded for each housing unit to facilitate the subsequent quantitative analysis of damage information in traditional dwellings.

2.4.2. Environmental Data Testing Methods for Traditional Dwellings

(1) Climate environment data collection

The environmental climatic data used in this study are TMY (Typical Meteorological Year) data in the Chinese Standard Weather Data (CSWD) format. The data source is the Special Meteorological Dataset for Analysis of the Thermal Environment of Buildings in China, which was developed and published by the Meteorological Data Office of the China

Meteorological Information Center and the Department of Architectural Technology and Science of Tsinghua University [55]. Handan's meteorological data were analyzed using Climate Consultant software and then analyzed and discussed.

(2) Microenvironmental detection methods

From the dwellings where damage symptoms are clearly manifested, three sample groups, each consisting of two sample homes from the same neighborhood, were selected to collect microclimate environmental data. Three groups of building samples or a total of six residential buildings made of brick and concrete were selected for the experiment. The sample groups were, as the figure shows, dispersed as widely as possible, with groups a and b, c and d, and e and f located in different locations within the ancient city and facing different directions. The samples were mainly selected from traditional dwellings of blue brick masonry. The test sites are chosen from the neighborhoods of Yingchun Street, Vulcan Temple Street, and Fuhou Street in the ancient city (Figure 5). The residential data testing will take place between 11 and 15 March 2024. Examination of microclimate data includes examination of relative humidity, wind speed, temperature, and radiation values.

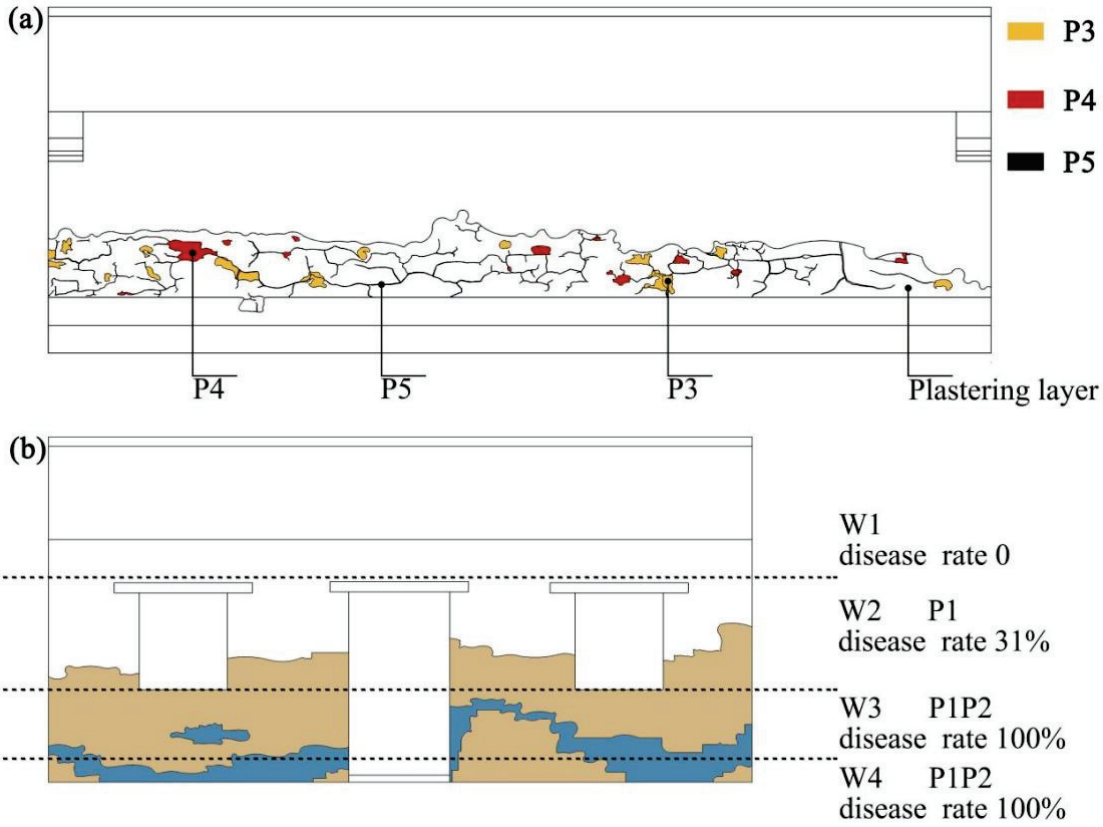


Figure 4. The damage and damage information map. (**a**) Infographic of damage types; (**b**) Infographic on the percentage of damaged area.

The data collection process is essentially divided into two phases; the first involves measuring the physical environmental data of the building at different heights and directions, and the second involves collecting physical environmental data from the damaged areas of the building.The following instruments were selected for microclimate testing. Temperature and humidity are measured with CEM DT-172 temperature and humidity loggers manufactured by Huashengchang Technology Co. Wind speed is detected by Testo 425 anemometer made by German company Testo. Thermal radiation was detected by JTR09 Radiant Thermometer manufactured by Beijing Century Jiantong Technology Co. The moisture content of the bricks was detected by Testo 606-2 Material Moisture Meter made by German company Testo. The test points for microclimate testing were numbered

for each sample during the data testing procedure [56]. The facades of the residential buildings were numbered as ESWN for each of the four directions, and the measurement points were selected for each facade based on the requirements of the actual measurement. For each wall, three lines are constructed at different heights at a distance of 2500, 1200, and 200 mm from the floor, respectively, with an even distribution of detection points along each line (Figure 6). When collecting microclimate data, it is necessary to wait until the instrument data have stabilized before reading. Each measuring point must be measured three times, with the average serving as a record of the measurement results. This ensures that errors due to experimental chance are avoided and the data are reliable and accurate.

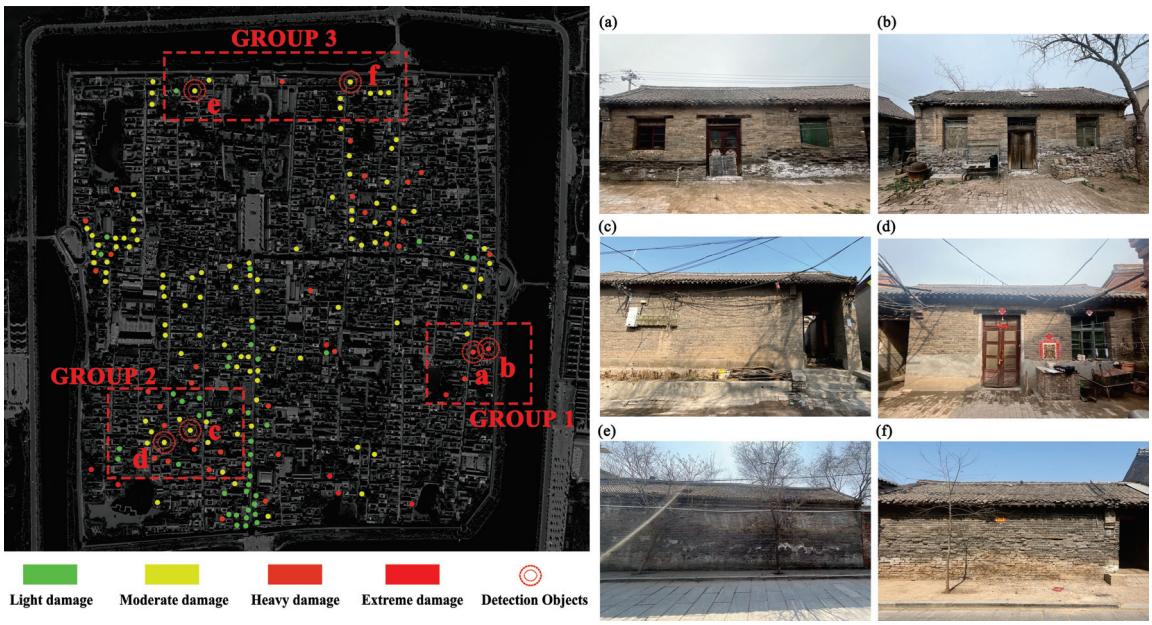


Figure 5. Microenvironmental detection of the current situation of residential houses and their location in the old city. (**a**,**b**) Architectural Status of Selected Residences on Yingchun Street; (**c**,**d**) Architectural Status of Selected Residences on Vulcan Temple Street; (**e**,**f**) Architectural Status of Selected Residences on Fuhou Street.

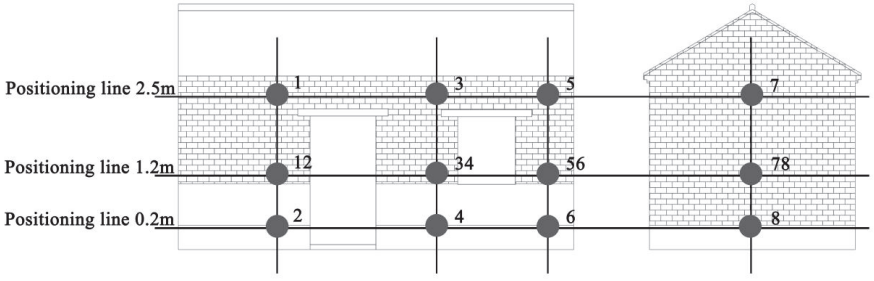


Figure 6. Collection point for microclimate tests.

2.4.3. Mechanical Properties Testing of Residential Brick Walls

(1) Material properties of bricks

Before the invention of concrete, residential buildings were essentially wall structures made of brick materials, which were primarily artificial bricks. Artificial bricks are solid bricks made by firing clay as a raw material [57]. Artificial bricks come in two main varieties, red bricks and blue bricks. Red bricks are created during the firing process when the iron in the clay completely oxidizes, producing iron trioxide red. During the firing process, blue bricks are created when the clay is partially cooled with water. Blue bricks and red bricks have the same raw materials and firing process, only the cooling method

after firing is different; red bricks are naturally cooled, and blue bricks are water-cooled. As for the properties of bricks, blue bricks are fired for a longer period of time and have higher resistance to high temperatures and humidity, while red bricks are fired for a shorter period of time and have a higher compressive strength. However, in terms of the manufacturing process, they are all insufficiently fired bricks (Figure 7). Both have the characteristics of a loose structure, high porosity, and high water absorption. In particular, the expansion stress after water absorption increases the looseness of the brick's microstructure, making it brittle and easy to disintegrate, favoring the development of damage [58].

(2) Mechanical rebound experiments on brick walls

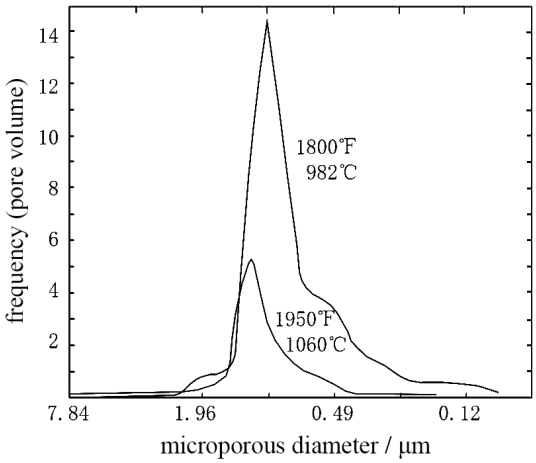


Figure 7. Microporous size distribution of brick products under two temperature conditions: under-firing and normal baking "Adapted with permission from Ref. [59]. 2012, Qingfan Li" [59].

The traditional dwellings in Guangfu Ancient City are brick houses because the brick wall is mainly used to bear pressure. Therefore, the focus of the quality inspection of the wall bricks of the dwellings is on testing their compressive strength, and the index of their strength is directly related to the safety and durability of the structure of the traditional dwellings [60]. The current method for determining the strength of masonry blocks is usually on-site sampling [61]. This provides clear and reliable test results, but it is labor- and time-intensive and can jeopardize the integrity of the masonry itself. This is not suitable for the traditional dwellings in this study, as the appearance of the dwellings needs to be preserved, and the technology can be widely available. Therefore, it is of great importance to study non-destructive testing methods applicable to the strength testing of traditional dwellings. Due to lightweight equipment, easy handling and efficient operation, minimal site requirements, and straightforward data processing, the rebound method is perfect for testing the strength of traditional residential building blocks [62]. In this study, the strength of bricks was determined using the rebound method on residential brick masonry. To indirectly determine the compressive strength of conventional residential bricks, the method relies primarily on the brick rebound value of surface hardness, which is measured using the brick rebound measuring device. Related mechanical parameters such as tensile strength, elastic modulus, and the compressive strength of brick masonry are also calculated, using the correlation of the direct compressive strength of the brick to establish a relationship equation. The parameters of the brick resilience meter are shown in the following table (Table 3).

The tested brick walls were divided into two types of zones, intact and damaged zones. Each type of brick serves as a detection unit and, based on the type of damage present in the brick wall to be tested, the damage zone selects an appropriate number of detection units. In each test unit, 4 measurement areas are randomly selected, the area of each measurement area is no less than 2 square meters, and 20 randomly selected bricks with outward stripes are used as the 20 measurement positions used for rebound testing. The distance between

the selected brick and the edge of the brick wall must be more than 250 mm, and the distance between each measuring area cannot be less than 250 mm. Five impact points are evenly arranged on the measuring surface of each stone. When choosing the impact point, we avoided unevenness in the brick surface. The distance between two adjacent impact points should not be less than 20 mm, and the distance between the impact point and the edge of the brick should not be less than 20 mm, and each impact point can only rebound once. The rebound meter must be horizontal during the test and its axis must be perpendicular to the surface of the brick. The rebound value of a single side position is taken as the average of the rebound values of 5 impact points [63]. There are four villages within the old city: North Village, East Village, South Village, and West Village [47]. The buildings in the South and East Villages have been more extensively restored and preserved due to their high commercial and tourist value. In contrast, the structures in the North and West Villages are comparatively older. Architectural conditions vary among the four villages. Consequently, two brick-masonry dwellings from each village were selected for rebound testing (Figure 8). The resilience test was carried out for each dwelling unit, evaluating the resilience values of bricks within the same wall in various locations.

Table 3. Main indicators of the brick rebound tester.

Main Indicators	Parameter Range
Types of rebounders	HT75-A Brick rebounders
Kinetic energy of an impact	0.735 J
Stretching length of sprung tension springs	75 ± 0.3 mm
Friction on the pointer slider	0.5 ± 0.1 N
Working length of sprung tension springs	61.5 ± 0.3 mm
Spherical radius of the end of the striking rod	25 ± 1 mm
Brick compressive strength conversion formula	$f = 2 \times 10^{-2}R^2 - 0.45R + 1.25$ f: Compressive strength of bricks R: Brick resilience value



Figure 8. Distribution of samples for brick wall rebound testing in the Guangfu Ancient City.

3. Case Study

3.1. Pathological Examination of Residential Brick Walls

Using the number of samples of damaged residential buildings as a quantitative criterion for architectural damage, the information on residential damage in Guangfu Ancient City was summarized and analyzed to draw the following preliminary conclusions (Figure 9):

- The percentage of traditional dwellings with different degrees of damage is as follows (Figure 9a): through the summarization and analysis of the degree of damage to traditional dwellings in the ancient city, it was found that traditional residences in the ancient city generally exhibit varying degrees of damage, with more than half exhibiting moderate damage.
- The number of different building pathology types for brick walls is as follows (Figure 9b): upon summarizing and analyzing the quantities of various architectural pathology types in traditional dwellings of the ancient city, it was determined that the primary pathologies affecting the ancient city are P1 and P3.
- The number of building pathology types in different parts of the brick wall are as follows (Figure 9c): through the summarization and analysis of the quantities of various architectural pathology types in different sections of brick walls in traditional dwellings of the ancient city, it has been determined that the primary pathological types affecting the ancient city are W2, W3, and W4. It can be observed that the architectural pathology phenomena in traditional residences are predominantly concentrated in the middle and lower sections of the walls.

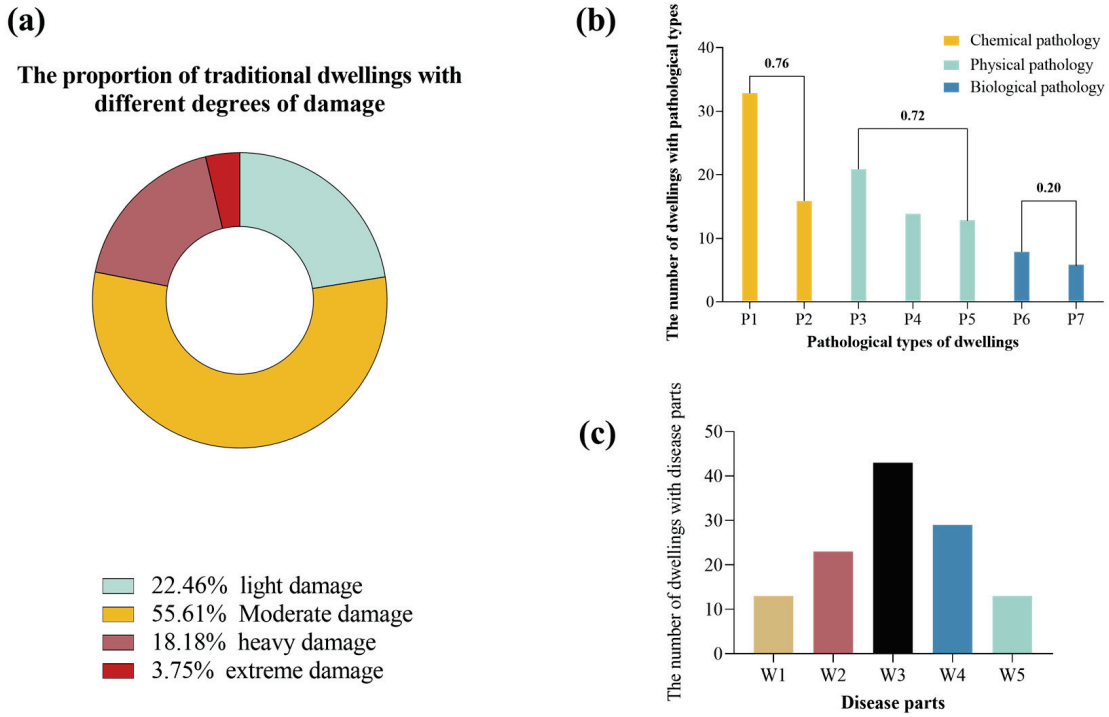


Figure 9. Damage analysis diagram: (**a**) The percentage of traditional dwellings with different degrees of damage; (**b**) The number of different building pathology types for brick walls; (**c**) The number of building pathology types in different parts of the brick wall.

In summary, the damage situation in traditional dwellings in the ancient city is serious, and the number of homes with moderate or higher damage accounts for a relatively large number of homes. There are three types of pathologies that are more pronounced within the walls of ancient city dwellings. Concurrently, the damage information of residential building walls indicates that multiple damage combinations occur on the walls of the same traditional dwelling. For instance, several types of architectural pathologies are observed to co-occur frequently. The types of architectural pathologies that frequently appear also vary across different parts of the building walls. Therefore, there is a certain relationship between the types of architectural pathologies, the wall positions, and among different pathologies themselves. Based on the compilation of residential damage information, this study analyzed the combinations of pathologies in traditional dwellings, the correlations

between different pathologies, and the correlations between different parts of the residential walls and various pathologies (Figure 10).

- Pathological combinations of traditional dwellings (Figure 10a): Through the detection and analysis of brick wall damage in 50 dwellings, a total of 23 combinations of housing damage were identified: Among them, there are three groups of individual pathological combinations; there are eight groups with two pathological combinations; three pathological combinations with ten groups; and four pathological combinations with two groups. Therefore, the residential pathological combinations in the ancient city mainly consist of two and three pathological combinations, and the main pathological combinations are P1P2 and P1P3.
- Pathological correlation of traditional dwellings: As depicted in Figure 10b, the heatmap presents the correlation coefficients between various architectural pathology types. The intensity of the colors indicates the strength of the correlations, with hues closer to red signifying stronger correlations. Through the analysis of the heatmap, we identified several significant clusters of correlations. For instance, positive correlations were observed among the pathologies within the combinations P1P2, P1P3, P3P6, and P4P5. Additionally, some pathological combinations showed weak or non-significant correlations, such as the non-significant correlation between P6P7, suggesting that the occurrence of these combinations may be incidental. Furthermore, we noted some unexpected correlations, such as the negative correlations between P1P7 and P3P5, which may indicate the need to consider the interplay of these pathological causes in future strategies for addressing architectural damage.
- Correlations between pathological parts and pathological types of traditional dwellings (Figure 10c): The heatmap utilizes color intensity to denote the strength of correlations, with hues closer to red signifying stronger associations. Our analysis of the heatmaps revealed several notable clusters of significant correlations. Notably, the darkly colored regions between P1 and W2, W3, and W4 suggest a robust positive correlation, indicating a pronounced relationship. Conversely, the correlation between certain pathologies and wall parts was weak or insignificant, such as the negligible link between P3 and W2, W3, and W5. This may suggest that the occurrence of P3 in these wall parts is somewhat incidental or less predictable. The heatmap reveals that W1 is predominantly affected by pathology P3, while the other four sections, W2, W3, W4, and W5, are primarily affected by P1. Additionally, P1 is observed across all wall parts.

In summary, P1P2P3 architectural pathology was found to occur frequently as a combination of pathologies. These architectural pathologies are mainly symptoms of moisture damage to the brickwork. Natural "defects" occur in the physical and chemical properties of building materials. Brick, one of the oldest building materials, has many internal voids because it is made primarily of fired clay and sand. Through the cavities, moisture is stored inside the building and, together with salts, causes damage to the masonry. Wall dampness-related pathologies, including mold growth and moisture retention, significantly impair indoor air quality and pose health risks to occupants [64]. These conditions can emit mold spores and volatile organic compounds (VOCs) into the indoor environment, thereby degrading air quality. Mold metabolites, such as mycotoxins, can trigger respiratory irritation and allergic responses, with chronic exposure potentially leading to severe health issues such as bronchitis, tonsillitis, rhinitis, and asthma. Individuals with weakened immune systems are at an increased risk of experiencing headaches, fever, and skin or mucous membrane inflammation. Additionally, humid environments facilitate the growth of bacteria and viruses, contributing to respiratory and dermatological health problems [65]. Consequently, dampness-induced wall pathologies exert a profound influence on both indoor air quality and human health, underscoring the need for scientific research and effective preventative measures.

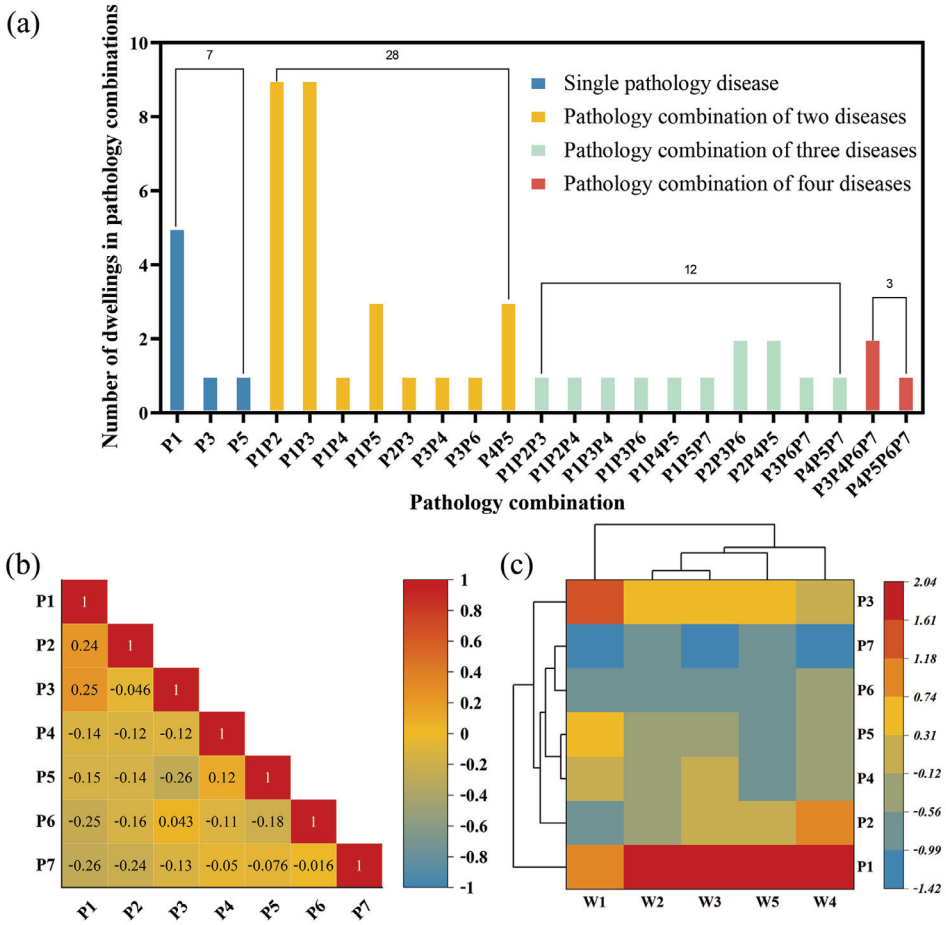


Figure 10. (**a**) Percentage of the number of different pathology combinations of traditional houses in the old city; (**b**) Correlation between the different types of pathologies present in traditional dwellings; (**c**) Heat map of the distribution of different building pathology types in different parts of the wall.

3.2. Analysis of Residential Environment Data

3.2.1. Climatic Environment of Traditional Dwellings

The frequency and severity of extreme weather events has increased dramatically worldwide in recent years, and more extreme weather events are predicted to occur in the future [66]. It is important to study the climatic conditions of traditional dwellings in Guangfu Ancient City because historical structures are particularly susceptible to this unfavorable climate, which leads to the development of architectural pathologies. The findings from the a of the potential impact of macroclimatic environmental factors on masonry wall damage using the Handan climate data (Figure 11) are as follows:

- When the air is saturated with water vapor, the air temperature is equal to the dew point temperature. The difference between dew point and air temperature can therefore indicate how far the water vapor in the air is derived from saturation. From studying Handan's dry bulb and dew point temperatures, buildings that are prone to condensation during the summer months of July and August create a humid environment for the walls.
- When analyzing the wind speeds in Handan, it was found that the maximum wind speeds mainly occur in February, March, and November, and the excessive wind speeds can damage the surface of living walls and cause the phenomenon of wind erosion.

- When analyzing the relative humidity in Handan, it was found that it was significantly above 50%, with the highest relative humidity occurring in July and August in the summer when it was almost 80%. This finding is consistent with the condensation phenomenon discussed in the previous article and can easily occur during these months.
- When analyzing the rainfall in Handan, it was found that July and August are the wettest months in Handan, while rainfall is very uneven throughout the year.

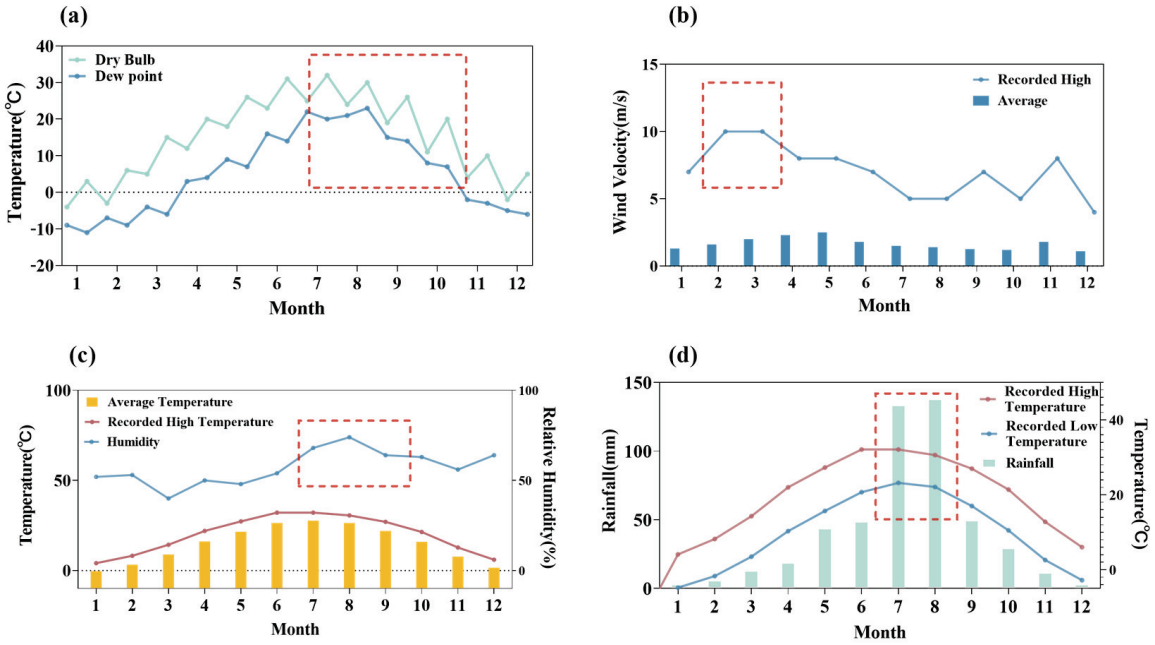


Figure 11. Climate and environmental analysis chart: (**a**) Temperature; (**b**) Wind speed; (**c**) Relative Humidity; (**d**) Precipitation. (The red dotted box shows data for months with significant changes in the climate environment).

In summary, the summer months of July and August are found to be the wettest times of the year in the ancient city of Guangfu. This is also the time when the temperature is closest to the dew point temperature, making buildings vulnerable to condensation. The relative humidity analysis charts also showed that the humidity was higher during this phase, which led to the pathologies. In addition, spring and autumn winds prevailed, exposing the brick walls of the residential buildings to the unfavorable environment of a wet–dry–wet cycle. This resulted in pathologies of varying degrees in the brick residential buildings.

3.2.2. Microenvironmental Analysis of Building Brick Walls

Environmental factors have different effects on building pathology, and buildings and their environments interact and influence each other. The most important climatic elements that make up a building's microclimate are temperature, humidity, wind direction and speed, and solar radiation. These elements also have a significant impact on the overall structure of the building and the comfort of its residents [67,68]. The microclimate data of residential walls were objectively collected in this study, and the test data could accurately reflect the microclimate information on the surface of the brick wall and the degree of environmental influences on it. This allows the investigation of the extent to which microclimate information negatively impacts various brick building components and serves as a basis for further research (Table 4).

Table 4. Study of the residential situation.

Code	Position	Construction	Pathology	Damaged Sections	Damage Grades
a	Yingchun Street	Brick and wood structure	P1P2	W2, W3, W4	c
b		Brick and wood structure	P1P2	W3, W4	c
c	Vulcan Temple Street	Brick and wood structure	P4P5	W4, W5	b
d		Brick and wood structure	P1P3	W5	c
e	Backstreet of the government office	Brick and wood structure	P1P2	W5	b
f		Brick and wood structure	P1P2P3	W5	c

For example, in the case of residential house sample d, the four exposed wall facades of the house are used as measurement points, and each one is selected based on the need for monitoring the surrounding microclimate. Measuring points 1, 3, and 5 are located along the horizontal detection line in the upper part of the wall, 2500 mm above the floor. 12, 34, 56 are distributed along the horizontal detection line in the middle of the wall, 1200 mm above the floor; 2, 4, 6 are distributed along the lower part of the wall, 200 mm above the floor (Figure 12).

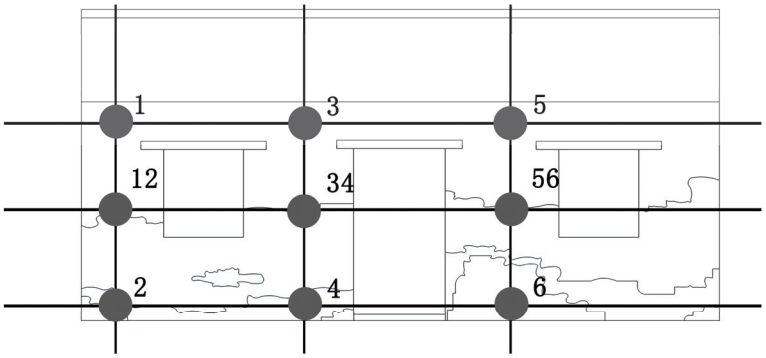


Figure 12. Schematic diagram of microclimate testing points in traditional dwelling d.

As part of the microclimate test, the following variables were measured at each measuring point on the wall surface (Table 5): temperature, humidity, wind speed, solar radiation, and the amount of moisture inside the bricks.

Table 5. Acquisition of microenvironmental data on the north and south walls of sample d.

Detection Point	N-1	N-12	N-2	N-3	N-34	N-4
Temperature (°C)	22	22.1	20.6	20.3	20.2	19.3
Relative humidity (%)	35.6	39.6	40.2	36.4	40.1	40.4
Solar radiation (w\m)	86	142	116	89	130	93
Detection Point	**N-5**	**N-56**	**N-6**	**S-1**	**S-12**	**S-2**
Temperature (°C)	20	19.8	19	18.1	18	18.2
Relative humidity (%)	36.4	37.5	35.2	32.8	33	33.4
Solar radiation (w\m)	134	67	32	43	33	29
Detection Point	**S-3**	**S-34**	**S-4**	**S-5**	**S-56**	**S-6**
Temperature (°C)	18.3	17.9	18.1	20	19	19.2
Relative humidity (%)	33.2	34.4	33.3	32.7	33.5	33.8
Solar radiation (w\m)	46	33	29	49	38	31

The primary physical properties of microenvironmental indicators are temperature, humidity, wind speed, and UV radiation on building surfaces. The damage was mainly caused by the humid environment, according to the research on the pathologies of the walls of ancient houses in Guangfu. This study focused on testing environmental factors, including temperature, wind speed and radiation, as well as the humidity of the wall surface and the moisture content of the bricks. The microenvironments of the walls and different areas of the walls in each orientation of the building vary, influenced by the courtyard-like layout and orientation of the buildings. In this study, the environmental data of differently oriented parts of the sample walls were examined and the following preliminary conclusions were drawn by synthesizing the microenvironmental data of the six samples and analyzing them against the damage data:

- Results from the analysis of the average humidity of the walls in each direction of the sample show that the north and west walls have relatively high humidity, while the south and east walls have relatively low humidity. The north and east walls also experience relatively high temperatures, while the south and east walls experience high temperatures (Figure 13a–c). This suggests that temperature and humidity are correlated; at higher temperatures, water evaporation is easier, and at lower temperatures, humidity increases. Meanwhile, changes in wind speed and radiation intensity have an impact on air humidity, as statistical results from environmental parameter measurements show. The data show that these variables are the highest on the south side of the wall, followed by the east side, and with the lowest values found on the north and west sides of the wall. The data suggest that an increase in wind speed and radiation intensity causes moisture to be more easily removed from the brick material, thereby reducing the humidity within the brick wall.
- There are differences in the microenvironmental parameters in different parts of the wall, and they objectively reflect the physical conditions at the time of damage to the masonry by building pathologies. Therefore, the microenvironmental data from different parts of the brick wall were compared and analyzed with the damage data (Figure 13d–f). The damage and brick moisture comparison of the three sample groups showed that the percentage of damaged wall increased with brick moisture content. According to the measured results, the W4 base area of the wall had a higher probability of damage and a higher moisture content in the brick material.

In summary, in the statistics of the data for all orientations and parts of the brick walls of the residential building, the highest humidity was found on the west side and the highest humidity was found in the base area of the W4 wall. Due to the spatial layout of the ancient urban court residence, the internal wind environment is relatively stable and therefore is more affected by light radiation. It is first concluded that due to the shading of wall foundations and other parts of the wall, these areas are exposed to high humidity, low wind speed, and low intensity of light irradiation, and are in a state of sustained water infiltration and accumulation, making it difficult for water to pass through and reduce the ability of moisture to evaporate evaporation, thus leading to the high and concentrated incidence of the damage.

3.3. Compressive Strength of Residential Brick Walls

Due to the different construction times of the dwellings in the old town, the bricks used were affected by the environment at different periods of time, resulting in different types and severities of damage. As a result, the study was carried out to compare the compressive strengths of different test units in the same dwelling and to analyze the compressive strength results of each dwelling separately. In this study, a total of eight dwellings were tested using the rebound method, with three test units per dwelling, for a total of twenty-four test units. This include eight intact units (640 detection points), six damage units of P1 (480 detection points), one damage unit of P2 (80 detection points), three damage units of P3 (240 detection points), one damage unit of P4 (80 detection points), one damage unit of P5 (80 detection points), two damage units of P6 (160 detection points),

and two damage units of P7 (160 detection points). Average rebound and compressive strength values were calculated for each residential test unit.

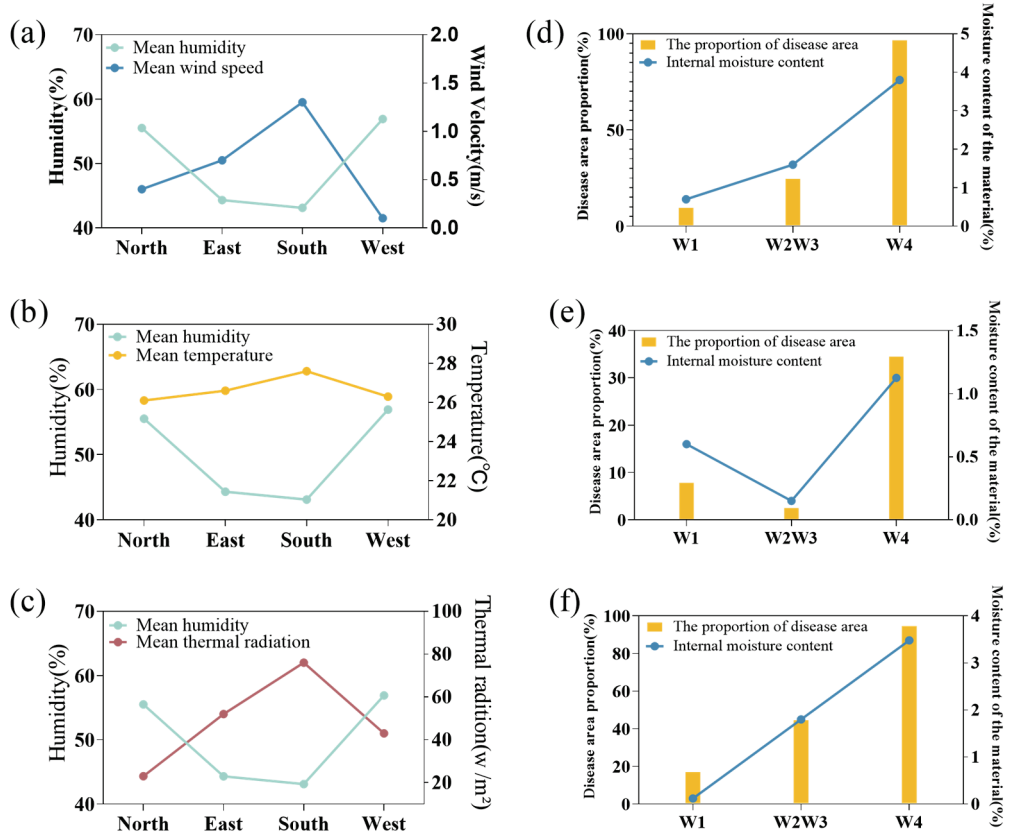


Figure 13. (**a**–**c**) The mean values of humidity, wind speed, temperature, and radiation on the exterior wall surfaces facing various orientations within the same residential structure. (**d**–**f**) The proportion of damage occurrences in various parts of walls and the moisture content of internal materials in different residential buildings.

The findings from the statistics presented in Table 6 are as follows: Within the same dwelling, the compressive strength of the bricks in the damage detection unit was much lower than that of the intact and undamaged detection unit. After combining the eight dwellings for analysis, the bricks of the intact units had an average compressive strength of 13.4 MPa, with the bricks from dwelling no. 2 in the East Village having the highest value at 24.9 MPa and those from dwelling no. 1 in the South Village having the lowest value at 6.1 MPa. The mean value of the compressive strength of the bricks of the damaged units was 5.6 MPa, with the largest compressive strength of the bricks of the P2 unit of the North Village dwelling no. 2 being 11.9 MPa and the smallest of the bricks being 1.6 MPa in the P2 of dwelling no. 2 in the West Village. The 'General Code for Masonry Structures' (GB 55007-2021) stipulates the minimum strength grades for masonry materials [69]. In this study, the urgency of building pathologies is determined by comparing the compressive strength of residential brick materials with the specifications set forth in the code. Meanwhile, the average compressive strength of the housing unit in West Village 2 was the lowest, indicating that the damage posed a major risk to structural safety and there was an urgent need for treatment for the damage.

In summary, the bricks in traditional houses with damaged areas have lower compressive strength than the bricks in the normal, undamaged areas. The compressive strength of bricks is directly related to the structural safety of traditional homes. Therefore, the degree of damage to the structure can be judged by the compressive strength of bricks or brick walls, which determines the method of damage treatment and the degree of urgency for damage treatment.

Table 6. Brick inspection data record sheet.

Detection of Dwellings	Sensor Unit	Average Brick Resilience Value	Brick Compressive Strength/MPa
North Village No. 1	Intact	37.1	12.1
	P1	24.9	2.4
	P3	29.4	5.3
North Village No. 2	Intact	41.8	17.4
	P5	36.9	11.9
	P6	28.2	4.5
East Village No. 1	Intact	34.3	9.3
	P1	26.9	3.6
	P3	27.9	4.3
East Village No. 2	Intact	47.4	24.9
	P1	35.7	10.7
	P7	25.4	2.7
South Village No. 1	Intact	30.4	6.1
	P1	26.7	3.5
	P7	27.6	4.1
South Village No. 2	Intact	35.8	10.8
	P1	28.7	4.8
	P6	34.7	9.7
West Village No. 1	Intact	42.1	17.8
	P1	32.5	7.8
	P4	33.9	9
West Village No. 2	Intact	33.4	8.5
	P3	25.8	3
	P2	23.2	1.6

4. Results and Discussion

4.1. Environmental Influences on the Pathology of Traditional Dwellings

Brick wall dampness damage is influenced by a multitude of factors, leading to variations in the extent of damage manifestation across different environmental samples. In this study, microenvironmental data were collected from six residential buildings within the ancient city. Among them, dwellings a and b were designated as Group 1; dwellings c and d as Group 2; and dwellings e and f as Group 3 (Figure 5). To identify the predominant influencing factors for each sample, we integrated and correlated damage information and environmental data from three groups of residential samples. We then conducted a principal component analysis (PCA) to reduce the dimensionality and compare several variables, utilizing the initial principal components as independent variables in our regression model analysis (Figure 14a). The findings are as follows:

- Figure 14a presents the PCA score plot, illustrating the projection of three groups of residential samples (as shown in Figure 5) onto a new coordinate system defined by the first two principal components. These two principal components account for a combined 62.8% of the total variance in the data, with PC1 explaining 36.8% and PC2 explaining 26.0%. Each point on the score plot represents an individual sample, with its position determined by its scores on PC1 and PC2. The distribution of the sample points reveals their relative positioning along these two principal components, thereby reflecting the similarities and differences among the samples. It is observable from the plot that the samples can be broadly categorized into three distinct clusters, indicating a clear grouping tendency within the data based on the selected principal components. Consequently, there are certain differences between the three sample groups.
- Through principal component analysis (PCA), it has been observed that there are certain distinctions between sample groups. Consequently, an analysis of the principal

component data for humidity and temperature across the three groups of samples has been conducted. The vertical axis of the chart represents relative humidity and wall surface temperature, while the horizontal axis indicates the distance of the wall measurement points from the ground level. Analysis of the temperature and humidity fluctuations depicted in Figure 14b,c reveals a consistent trend across all three sample sets; there is a gradual reduction in wall surface moisture content and a concomitant increase in temperature with increasing height above the ground. This observation suggests that, in addition to climatic and microenvironmental humidity, geographical environmental humidity factors also play a role in the pathology of brick walls in residential structures. For instance, soil moisture can infiltrate the wall through capillary action and then rise along the wall's roots.

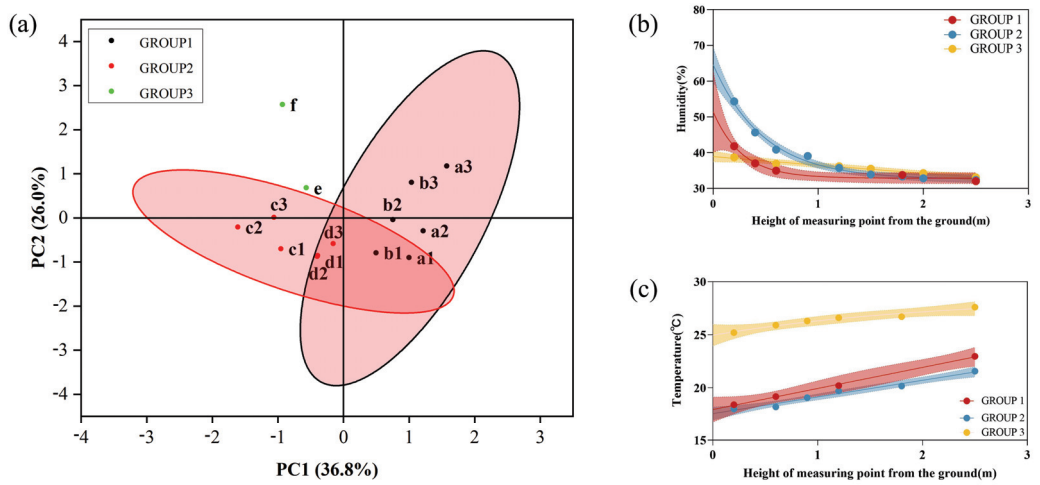


Figure 14. (**a**) Principal component analysis of sample damage environments (In the figure, the letters a, b, . . ., f represent the residences a, b, . . ., f); (**b**) Relationship between sample moisture and distance from the ground; (**c**) Relationship between sample temperature and distance from the ground.

In summary, a variety of factors, including climate, architectural microenvironment, and geographical location, have an impact on residential brick walls. Furthermore, the extent to which these factors influence a given sample varies, suggesting the need for a targeted approach when studying architectural damage [70,71].

4.2. Environmental Effects on the Mechanical Properties of Brick Walls

The primary cause of the damage affecting traditional dwellings in the ancient city of Guangfu is known to be the erosion of the dwellings by water in the surrounding environment, based on an analysis of the pathological environment. In order to schematize the real behavior of the brick in the environmental conditions, quantifying the variability of the performances of building materials in the presence of moisture is essential [72,73]. In this study, the moisture content of brick materials was also tested using a Testo 606-2 material moisture meter during rebound testing of brick walls in traditional dwellings. A correlation analysis was also carried out between the average resilience values and the moisture content of the brick walls. Testing the data for normality revealed that the rebound values followed a normal distribution, but the moisture content did not. Therefore, the choice was made to use Spearman correlation analysis [74].

From the correlation analysis, it can be seen that the correlation coefficient between the rebound value and the moisture content is −0.8017, and the two are negatively correlated with $p < 0.001$, which means that the correlation is statistically significant (Figure 15). Therefore, it is important to analyze the influence of the environment on the mechanical properties of bricks.

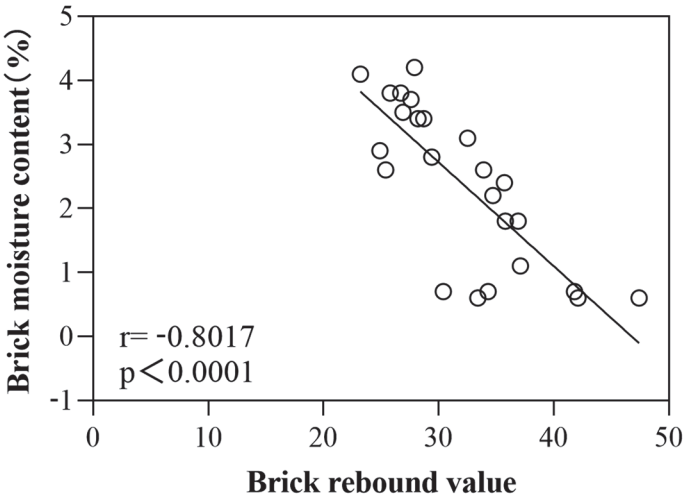


Figure 15. Correlation analysis between resilience values and moisture content of brick walls.

Due to the fact that traditional dwellings are exposed to complex environmental factors over a long period of time, the test results may be subject to some errors. At the same time, the raw material clay used to make bricks varies depending on the local soil composition, resulting in the different properties of the finished bricks. Therefore, in this study, ten traditional residential bricks were selected from the area, including five blue bricks and five red bricks, which were divided into two groups. Each brick was dried and then soaked in a basin so that the bricks had different water content states as follows: dry state, 2% water content, 4% water content, 6% water content, 8% water content, 12% water content and fully saturated. Concurrently, during this process, the moisture content was recorded at hourly intervals to track its variation over time. Brick samples were immediately subjected to a rebound test for each moisture content achieved. After completing the tests, the average of the rebound values at different moisture contents was calculated for each group of brick samples. The influence of moisture content on the elasticity value of brick samples was analyzed by comparing the experimental results of two groups of samples. The test results are listed below (Figure 16a).

From Figure 16a, it can be seen that although the average brick rebound value varies between the two groups of bricks, the values tend to decrease as the moisture content of the bricks increases. At a moisture content from 2% to 6%, the rebound value decreases more significantly, with the maximum decrease being around 3.9. Figure 16b illustrates that the moisture content of the brick material shows an increasing trend during the initial 12 h. Between 12 and 24 h, the moisture content gradually stabilizes, fluctuating within a narrow range. At 21 h, the brick material reaches its peak moisture content. The resilience value of bricks is based on their surface hardness, which is directly impacted by the moisture content of the bricks [75]. Tests have shown that as water erosion of the brick material increases, the mechanical properties of the brick gradually deteriorate. Studies conducted by Lei Z. have reported that moisture infiltration can lead to significant structural damage within a range of specific time periods. Lei Z. conducted an experimental study of moisture in brick masonry in a confined laboratory. The experiment was conducted by placing brick masonry in a pool of water and observing the time of occurrence and distribution of the phenomenon of flooding on the surface of the bricks. During the experiment, the room temperature and humidity were actively regulated by equipment to maintain a stable temperature, humidity, and airflow field. At 168 h, a small number of white crystals began to precipitate on the surface of the brick wall. At 360 h, the alkalized area of the brick wall reached half of the overall area. At 720 h, the brick wall reached the maximum area of alkali [76]. Wall flooding occurs when soluble salts in the water crystallize and precipitate onto the surface of the wall due to evaporation of water inside the wall. When the humidity is high, it dissolves back into the water and returns to the interior of the

material. In this process of repeated dissolution and crystallization, the expansion force of salt crystallization continues to expand the original pores, causing damage to the brick masonry structure [77]. Therefore, wet conditions can adversely affect the mechanical properties of traditional residential brick walls, compromising structural integrity and potentially leading to building damage.

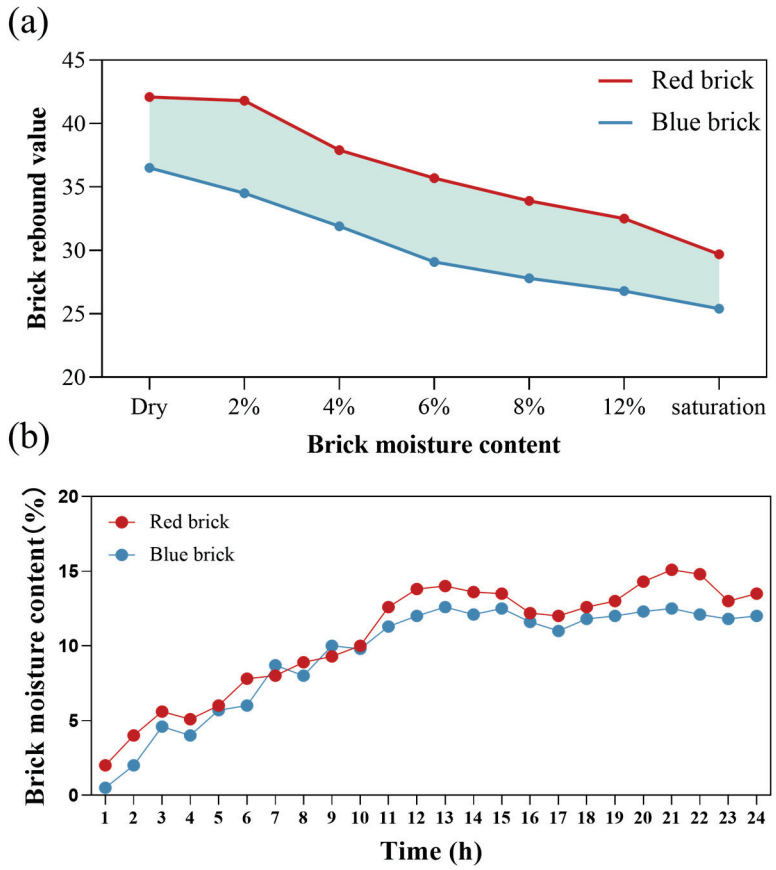


Figure 16. (**a**) Distribution of mean rebound values for each moisture content condition; (**b**) Variation in brick moisture content with time.

4.3. Recommendations for Intervention

The residents of the old city used crude and simple methods to treat the walls of the buildings, such as mixing two types of bricks to fill the missing parts of the walls and applying a layer of veneer directly on the surface of the damaged walls (Figure 17a). The lack of scientific pathological inspection protocols and damage treatment guidance has led residents to take gross measures that not only worsen the damage to the building's historic facade, but also exacerbate the building's ongoing moisture problem [78]. Thus, targeted and scientifically sound strategies need to be developed to address the building's pathologies and extend its service life. On this basis, the following interventions are recommended for the identified construction defects:

(1) Development of an inspection plan

Traditional dwellings should be inspected regularly to maintain their good condition. In addition, scientific pathological investigation methods should be used to deduce causes of damage in traditional residential buildings and identify defects. In this way, data can be obtained to determine preventative measures to preserve these traditional dwellings.

(2) Treatment of building pathologies

Remediation of pathologies should be carried out in such a way that the original appearance of the building is preserved. Suggestions should include targeted repair

measures based on the main pathological symptoms of dwellings. If there are signs of wall alkali flooding and corrosion damage to the wall, it is first recommended to clean the wall surface with TiO_2 in order to further assess the extent of the wall damage. Fonseca et al. used a 1% aqueous solution of distilled anatase water to clean facades [79]. The bricks were then categorized and processed according to the mechanical properties of the wall so that the less damaged bricks could be repaired and reused [80]. As for the severely corroded bricks, the bricks were chiseled away and rebuilt according to the type, size, and style of the original bricks. The masonry was removed and replaced at the same time, with a maximum of 60 cm being replaced at once. If there are cracks in the wall, bonding techniques should first be used to restore the entire wall, by applying cement mortar mixed with 107 glue as an adhesive. The width of the crack dictates the consistency of the mortar. Technical reinforcement measures would then be taken. Since the traditional houses in the old town are single-story brick buildings, brick reinforcement hoops can be used to reinforce the walls [81].

(3) Prevention of building pathologies

In the course of studying building pathologies, it was discovered that some of the traditional local houses have a horizontal waterproof layer in the walls, usually made of materials such as reeds or wooden boards (Figure 17b). Based on the original technology, certain measures can be taken to stop the development of building pathologies. For wall surfaces, silicone coatings can be sprayed evenly onto the brick surface to achieve water and weather resistance. Currently, the following two materials are the best ones for achieving that: sodium methylsilanolate and sodium methylsilicate 3‰ aqueous solution [82]. In addition, chemical injections into the wall can be used to address rising humidity levels inside the wall [83].

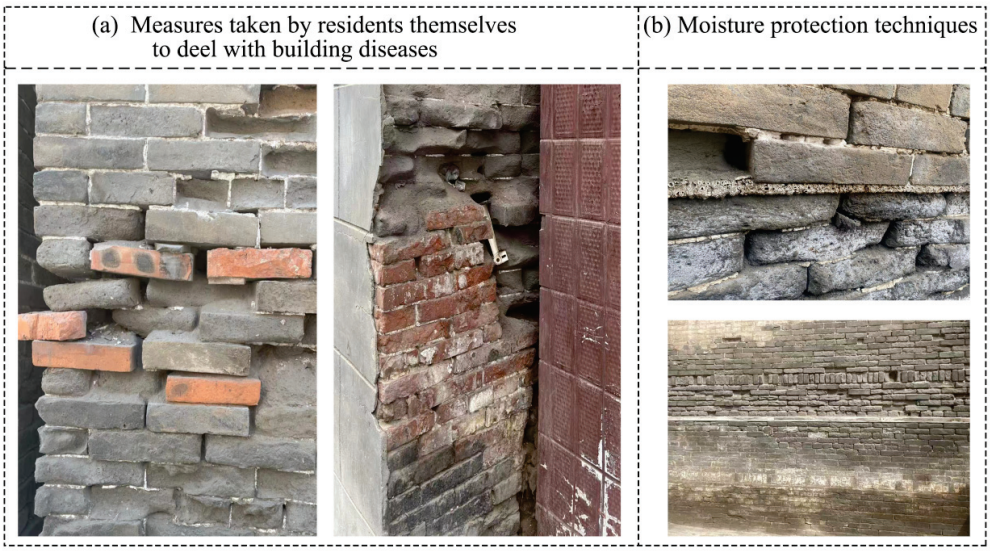


Figure 17. Solutions and preventive measures for existing local construction defects.

5. Conclusions

Traditional brick dwellings are representative vernacular buildings in Northern China, and architectural damage have led to the destruction of their appearance and structure, which has a negative impact on the long-term use and protection of the dwellings. In order to effectively address the damage of dwellings, this article has discussed the process of diagnosing building pathology. The study selected brick houses in the ancient city of Guangfu and examined them using the pathological diagnosis method of "Architectural Pathology Appraisal–Pathological Environment Analysis–Mechanical Properties Testings", proposed in this study. And the symptoms of the ancient city damage, the cause of the damage, and the severity of the damage were derived. The focus of this work is not to

identify the causes of damage to the traditional dwellings of Guangfu Ancient City, but to illustrate the rationality and effectiveness of the proposed damage diagnosis method using the example of Guangfu Ancient City. The conclusions reached by the methodology are discussed below as a whole:

- Architectural Pathology Appraisal: Collecting information on damage in traditional dwellings by means of visual inspection and mapping of damage. For example, the damage in Guangfu Ancient City dwellings is concentrated in the lower part of the wall. The damage mostly occurs in the form of pathological combinations, in which the main performance symptoms are corrosion deterioration, wall alkali flooding, and moisture infiltration. By assessing building pathology, the damage types and damaged parts of dwellings are determined to propose targeted cleaning measures for the lower part of the wall and replacement methods for the damaged bricks.
- Pathological Environment Analysis: The regional climatic environment and the microenvironment of the dwellings were collected and tested, respectively, to analyze the causes of damage in traditional dwellings. For example, the climatic environment data of Handan show that there is heavy rainfall in summer in July and August, and this period is prone to condensation phenomena, resulting in the humid environment in brick walls, thus causing dampness damage. Data from microenvironmental testing show that the lowest part of dwelling walls has the highest humidity because this part of the wall is in the shade, where it is difficult for light and wind to reach, and difficult for moisture to escape. At the same time, the moisture content of the bricks gradually decreases from bottom to top, and the lower bricks are in a permanently a wet state, resulting in higher morbidity. Through the analysis of the pathological environment, it is determined that the damage in residential areas is caused by moisture, so targeted measures should be taken for wall surface and internal moisture protection and water blocking.
- Mechanical Properties Testings: A brick rebound tester was used to test the mechanical properties of the brick walls of the dwellings and determine the extent of the damage to the dwellings. For example, the results of the rebound test indicate that the mechanical properties of the damaged parts of the ancient city dwellings are poor. Meanwhile, results of brick rebound tests show that the degree of water infiltration affects the mechanical strength of the bricks. By testing the mechanical properties, the severity of the damage of various dwellings in the ancient city is determined, so as to judge the order of treatment of the damaged dwellings in the ancient city and the type of reinforcement measures to be taken.

In conclusion, given the large quantity and wide distribution of brick houses, this study proposes a low-tech, low-cost pathological diagnostic approach that is universally applicable. And on the basis of past building damage research and environmental analysis, mechanical property testing was added. Through the three steps of the diagnostic method, we analyze the pathologies of dwellings from the surface to the interior to propose effective scientific management measures. This is expected to provide a reference for the identification and treatment of traditional dwelling pathologies in other areas.

6. Limitations and Further Research

This article presents a diagnostic approach to traditional dwelling pathology by starting with solving traditional dwelling damage and combining them with architectural pathology. This approach includes pathological characterization, etiological analysis, and interventions. The method is also applied and verified using the example of the ancient city of Guangfu, showing that it is useful and effective. However, there are differences between the traditional handmade bricks used in the residential buildings of this study and modern bricks. The walls of traditional residences in ancient cities are generally constructed using traditional craftsmanship, where clay bricks are hand-molded and fired to produce blue bricks [62]. In contrast, modern bricks may incorporate modern industrial raw materials, including quartz sand, white clay, and feldspar. The disparate raw materials and manu-

facturing processes result in different performance characteristics between the two. When calculating compressive strength, this study utilized the strength measurement curve for common modern bricks, which may diverge from the actual compressive strength values. At the same time, the study limited the analysis of the overall performance of the dwellings by focusing only on the bricks of the dwellings after sampling and testing while ignoring the mechanical properties of the mortar. In addition, there is some difficulty in applying the experimental method to simulate the actual environmental conditions and the actual time of occurrence of building damage, and the specific effects of the geographical environment on the residential area are not fully taken into account. For example, the nature of the soil and the water table can influence the level of penetration of wet conditions.

Therefore, subsequent research should involve conducting actual compressive strength tests on local brick materials to verify the accuracy of the rebound method measurements. Additionally, data testing and statistical analysis should be employed to determine the rebound strength curve that aligns with the local brick materials. Moreover, it should investigate and study the soil properties, water table, etc., of the area. Additionally, a multi-parameter, long-time simulation is used to analyze the entire traditional residential house with the aid of simulation software. In our forthcoming research, we will conduct a detailed study on the temporal evolution of various types of structural 'pathologies. We aim to address this issue through the development of models that simulate the moisture force coupling and the migration of moisture and heat within masonry structures, which is crucial for understanding the behavior of brick masonry under different environmental conditions.

Author Contributions: Conceptualization, Q.L. and T.Z.; methodology, Q.L. and T.Z.; software, T.Z.; validation, T.Z. and Y.F.; formal analysis, T.Z.; investigation, T.Z.; resources, F.L.; data curation, T.Z.; writing—original draft preparation, T.Z.; writing—review and editing, Q.L., T.Z., Y.F. and F.L.; visualization, T.Z.; supervision, Q.L. and Y.F.; project administration, Q.L.; funding acquisition, Q.L. All authors have read and agreed to the published version of the manuscript.

Funding: This research was funded by (1) Hebei Provincial Social Science Foundation (HB20SH015); (2) Research Project of Humanities and Social Sciences in Colleges and Universities of Hebei Province (SD2022020).

Data Availability Statement: The original contributions presented in the study are included in the article, further inquiries can be directed to the corresponding author.

Conflicts of Interest: The authors declare no conflicts of interest.

References

1. Tortajada Montalvá, E.; Mileto, C.; Vegas López-Manzanares, F. Assessment Methodology for Physical Vulnerability of Vernacular Architecture in Areas Affected by Depopulation: The Case of Comunidad Valenciana, Spain. *Land* **2024**, *13*, 695. [CrossRef]
2. Rosaleny-Gamón, M.; Cabrera i Fausto, I. Vernacular Architecture Facing a Degrowth Scenario. In *Relevance of Doctoral Research in Architecture*; archiDOCT & Anglia Ruskin University: Cambridge, UK, 2024.
3. Jamil, M.; Shahzad, K.; Mustafa, A. Paradigm Shift of Construction Techniques from Vernacular to Neo—Vernacular in Villages to Sustain Climate Change. *Pak. Soc. Sci. Rev.* **2024**, *8*, 68–81. [CrossRef]
4. Escobar, A.H.; de Miguel, M.L. *Sustainability, Risks and Resilience of Vernacular Heritage*; Taylor & Francis: London, UK, 2024. Available online: https://api.taylorfrancis.com/content/books/mono/download?identifierName=doi&identifierValue=10.4324/9781003475736&type=googlepdf (accessed on 25 June 2024).
5. Xu, H.; Wan, X.; Fan, X. Rethinking the Implementation of Authenticity in Cina's Heritage Conservation—A Case Study of Hongcun Village. *Hum. Geogr.* **2012**, *27*, 107–112. [CrossRef]
6. Korcâk, P. The Goals and Means of Preserving Vernacular Architecture. *ODTÜ Mimar. Fak. Derg.* **1978**, *4*, 139–147. Available online: https://hdl.handle.net/11511/51231 (accessed on 1 July 2024).
7. Wang, D.; Lyu, Q.; Wu, Y.; Fan, Z. The characteristic of regional differentiation and impact mechanism of architecture style of traditional residence. *J. Nat. Resour.* **2019**, *34*, 1864–1885. [CrossRef]
8. Guo, H.; Wang, Y.; Fei, F.; Xu, C. Optimizing and Transforming Measures of Winter Thermal Environment of Guangfu Residence in Handan Guided by Subjective and Objective Evaluation. *J. Tianjin Chengjian Univ.* **2023**, *29*, 108–115. [CrossRef]
9. Li, Q.; Qi, Q. Spatial Form Research of Guangfu Ancient City in Handan. *Archit. Cult.* **2020**, *1*, 242–243. [CrossRef]

10. Xie, K.; Zhao, H.; Yan, J.; Liu, L. Study on the Protection and Utilization of Guangfu Ancient City. *Archit. Cult.* **2021**, 105–106. [CrossRef]
11. Zhu, L. Considerations on Some Questions of Traditional Villages Research. *South Archit.* **2017**, *1*, 4–9. [CrossRef]
12. Mileto, C.; Vegas, F.; García, L.; Pérez, A. Assessment of vulnerability of earthen vernacular architecture in the Iberian Peninsula to natural risks. Generation of an analysis tool. In *Sustainability, Risks and Resilience of Vernacular Heritage*; Taylor & Francis: London, UK, 2024; pp. 69–82.
13. Do Rosário Veiga, M.; Fragata, A.; Velosa, A.L.; Magalhães, A.C.; Margalha, G. Lime-based mortars: Viability for use as substitution renders in historical buildings. *Int. J. Archit. Herit.* **2010**, *4*, 177–195. [CrossRef]
14. Lu, D. 50 Years' Researches on Chinese Folk House. *Archit. J.* **2007**, *11*, 66–69. [CrossRef]
15. Li, Z.; Lv, Y. Several Key Issues in the Study of the Integrity of Southern Vernacular Construction Techniques. *South Archit.* **2018**, *6*, 51–55. [CrossRef]
16. Zhang, D.; Zhang, W.; Chen, D. Analysis and exploration of the concept of traditional settlement protection and development cluster mode in the new period. *Urban Dev. Stud.* **2022**, *29*, 16–21+39. [CrossRef]
17. Porretta, P.; Pallottino, E.; Colafranceschi, E. Minnan and hakka tulou. Functional, typological and construction features of the rammed earth dwellings of Fujian. *Int. J. Archit. Herit.* **2022**, *16*, 899–922. [CrossRef]
18. Lin, Y.; Huang, T.; Yang, W.; Hu, X.; Li, C. A Review on the Impact of Outdoor Environment on Indoor Thermal Environment. *Buildings* **2023**, *13*, 2600. [CrossRef]
19. Groak, S. *The Idea of Building: Thought and Action in the Design and Production of Buildings*; Taylor & Francis: London, UK, 2002.
20. Vicente, R.; Ferreira, T.M.; Da Silva, J.R.M. Supporting urban regeneration and building refurbishment. Strategies for building appraisal and inspection of old building stock in city centres. *J. Cult. Herit.* **2015**, *16*, 1–14. [CrossRef]
21. Freitas, S.S.; de Freitas, V.P. Cracks on ETICS along thermal insulation joints: Case study and a pathology catalogue. *Struct. Surv.* **2016**, *34*, 57–72. [CrossRef]
22. Torres, M.I.M.; de Freitas, V.P. Treatment of rising damp in historical buildings: Wall base ventilation. *Build. Environ.* **2007**, *42*, 424–435. [CrossRef]
23. Singh, J.; Yu, C.W.F.; Kim, J.T. Building pathology, investigation of sick buildings—Toxic moulds. *Indoor Built Environ.* **2010**, *19*, 40–47. [CrossRef]
24. Cheng, S.; Liu, S. Study on the disease characterization and factors of concrete materials of historic architecture in plum rainy climate zone. *Concrete* **2022**, *1*, 79–83+91. [CrossRef]
25. Pan, J.; Lan, J.; Huang, T.; Wang, Y.; Tang, Y. Technical System and Practical Cases of the Plant Disposal on the Top Surface of the Great Wall Heritage Site. *Chin. Landsc. Archit.* **2024**, *40*, 22–27. [CrossRef]
26. Meng, W.; Shang, H.; Gu, L.; Wu, Y.; Hou, G. Study on the Disease Evaluation System of Brick and Wood Structure Historical Buildings in Qingdao Area. *Low Temp. Archit. Technol.* **2024**, *46*, 1–5+11. [CrossRef]
27. Dai, S.; Zhong, Y. Frontier Applied Technologies of Material Pathology Diagnosis, Repair, and Monitor on Historic Building Conservation. *Bull. Chin. Acad. Sci.* **2017**, *32*, 749–756. [CrossRef]
28. Shen, Y.; Liu, S.; Cheng, P. Study on the Pathogenic Environment of Timber Architectural Heritage Along the Southeast Coast of China. *World Archit.* **2023**, *9*, 114–119. [CrossRef]
29. Wang, F. A preliminary survey of the interior temperature and humidity of historic buildings in the Palace Museum. *Sci. Conserv. Archaeol.* **2014**, *26*, 85–93. [CrossRef]
30. Lei, Z.; Zhang, Y.; Wan, L. Forensics, Diagnosis, and Evidence Base: Exploration of the Building Pathology of the Town God's Temple Murals in sTong-vkhor, Qinghai, Under the Influence of Environmental Climate. *South Archit.* **2020**, *5*, 70–77.
31. Sitzia, F.; Lisci, C.; Mirao, J. Building pathology and environment: Weathering and decay of stone construction materials subjected to a Csa mediterranean climate laboratory simulation. *Constr. Build. Mater.* **2021**, *300*, 124311. [CrossRef]
32. Bi, W.; Yan, Z.; Zhang, Z.; Yao, S.; Zhang, J.; Wang, X. Modeling and numerical simulation of heat and mass transfer in the cave wall of the Mogao Grottoes in China. *Build. Environ.* **2021**, *201*, 108003. [CrossRef]
33. Zahs, V.; Anders, K.; Kohns, J.; Stark, A.; Höfle, B. Classification of structural building damage grades from multi-temporal photogrammetric point clouds using a machine learning model trained on virtual laser scanning data. *Int. J. Appl. Earth Obs. Geoinf.* **2023**, *122*, 103406. [CrossRef]
34. Hola, A.; Czarnecki, S. Brick wall moisture evaluation in historic buildings using neural networks. *Autom. Constr.* **2022**, *141*, 104429. [CrossRef]
35. Prieto, A.J.; Silva, A.; De Brito, J.; Macías-Bernal, J.M.; Alejandre, F.J. The Influence of Pathological Situations on Churches' Functionality: An Approach Based on Historical Records. *Int. J. Archit. Herit.* **2017**, *11*, 566–587. [CrossRef]
36. Moropoulou, A.; Labropoulos, K.C.; Delegou, E.T.; Karoglou, M.; Bakolas, A. Non-destructive techniques as a tool for the protection of built cultural heritage. *Constr. Build. Mater.* **2013**, *48*, 1222–1239. [CrossRef]
37. Kordatos, E.Z.; Exarchos, D.A.; Stavrakos, C.; Moropoulou, A.; Matikas, T.E. Infrared thermographic inspection of murals and characterization of degradation in historic monuments. *Constr. Build. Mater.* **2013**, *48*, 1261–1265. [CrossRef]
38. Molero, M.; Segura, I.; Izquierdo MA, G.; Fuente, J.V.; Anaya, J.J. Sand/cement ratio evaluation on mortar using neural networks and ultrasonic transmission inspection. *Ultrasonics* **2009**, *49*, 231–237. [CrossRef]
39. Carpinteri, A.; Lacidogna, G. Damage monitoring of an historical masonry building by the acoustic emission technique. *Mater. Struct.* **2006**, *39*, 161–167. [CrossRef]

40. López-González, L.; Gomez-Heras, M.; de Cosca, R.O.O.; Garcia-Morales, S.; Fort, R. Coupling electrical resistivity methods and GIS to evaluate the effect of historic building features on wetting dynamics during wind-driven rain spells. *J. Cult. Herit.* **2022**, *58*, 209–218. [CrossRef]
41. Bersch, J.D.; Verdum, G.; Lamego Guerra, F.; Falcao Socoloski, R.; Giordani, C.; Zucchetti, L.; Borges Masuero, A. Diagnosis of pathological manifestations and characterization of the mortar coating from the facades of historical buildings in Porto Alegre—Brazil: A Case Study of Chateau and Observatorio Astronomico. *Int. J. Archit. Herit.* **2021**, *15*, 1145–1169. [CrossRef]
42. Shen, Y.; Liu, S. Salt Efflorescence Damage of Architectural Heritage along the Southeast Coast of China Based on Micro-environment Parameters. *Archit. J.* **2022**, *S2*, 61–67.
43. Li, Q.; Zhang, S.; Shen, S. The Study on the Development of Guangfu Ancient City Based on the Influence of Water Environment. *Tradit. Chin. Archit. Gard.* **2024**, *1*, 94–97.
44. Guo, H.; Wang, Y.; Fei, F.; Xu, C.; Wang, L. Research on the Indoor Thermal Environment of Traditional Houses in Handan Guangfu Ancient City in Summer. *Build. Sci.* **2023**, *39*, 90–96+192. [CrossRef]
45. Xie, K.; Zhao, H.; Jin, B.; Lin, X. Study on the Streets, Lanes and Dwellings of Guangfu Ancient City. *Urban. Archit.* **2021**, *18*, 80–82+96. [CrossRef]
46. Wang, Z.; Yang, Z. Cracks in Masonry Houses in Rural Areas and Preventive Treatment Measures. *Agric. Technol. Serv.* **2011**, *28*, 385–386+410. [CrossRef]
47. Wu, C.; Cui, Q.; Lu, Z.; Li, J.; Wu, C. Study on the construction technology for masonry structure reinforcement and renovation. *Archit. Technol.* **2023**, *54*, 1483–1486. [CrossRef]
48. Su, S. Study on the Prevention and Treatment Measures of Alkali Flooding on Clear Water Brick Walls. *Jiangxi Build. Mater.* **2017**, *9*, 129+133. [CrossRef]
49. Feng, N.; Wang, H.; Wang, S.; Song, D.; Zhu, H. Study of efflorescence on the city wall of Xi'an. *Sci. Conserv. Archaeol.* **2012**, *24*, 26–30. [CrossRef]
50. Carretero-Ayuso, M.J.; Rodríguez-Jiménez, C.E.; Bienvenido-Huertas, D.; Moyano, J.J. Interrelations between the types of damages and their original causes in the envelope of buildings. *J. Build. Eng.* **2021**, *39*, 102235. [CrossRef]
51. People's Government of Yongnian County. *Famous Towns of Chinese History and Culture: Guangfu Welcome Materials*; General Office of Handan Municipal People's Government: Handan, China, 2011.
52. Wang, L.; Yao, S. *Building Pathology: Diagnosis and Countermeasures for Common Building Diseases*; China Electric Power Press: Beijing, China, 2002. Available online: http://www.shukui.net/book/1372966.html (accessed on 6 May 2024).
53. Lei, Z.; Sun, Z. Salt Study on Field Survey Methods of Dampness Damage in Buildings: Taking the Taoist Classics Library in Wudang Mountains as an Example. *Archit. J.* **2011**, *S2*, 22–27.
54. Lei, Z.; Wan, L.; Zhang, Y. Investigation, Diagnosis, Assessment and Conservation Strategy for a Wall Painting at Wudang Mountain Taoist Temple Using BIM Technology. *Stud. Conserv.* **2018**, *63* (Suppl. S1), 377–380. [CrossRef]
55. Meteorological Data Room, Meteorological Information Center, China Meteorological Administration. *China Building Thermal Environment Analysis Specialized Meteorological Data Set*; China Construction Industry Press: Beijing, China, 2005.
56. Raposo, P.C.; Correia, J.A.; Sousa, D.; Salavessa, M.E.; Reis, C.; Oaliveira, C.; de Jesus, A. Pathological Inspection of Structural Masonry Walls of a Late-Romantic Historical Building. *Procedia Struct. Integr.* **2017**, *5*, 1102–1107. [CrossRef]
57. Xiao, J.; Liu, W.; Tan, X.; Yang, W. Research on Strength Testing Methods for Bricks of Historically Preserved Buildings. *Eng. Mech.* **2010**, *27* (Suppl. S2), 276–279.
58. Liu, S.; Chen, S. The Impact of Meteorological Parameters on Salt Efflorescence Damage of Historic Architecture in Cold Regions. *Archit. J.* **2017**, *2*, 11–15. [CrossRef]
59. Li, Q. Questions and suggestions on the absence of frost resistance indexes for bricks and blocks in GB 13544-2011. *Brick-Tile* **2012**, *11*, 105–115. [CrossRef]
60. Ding, W. Study on the Strong Measurement Technique of Wall Bricks in Ancient Buildings. *Constr. Qual.* **2019**, *37*, 48–51. [CrossRef]
61. Nunes, C.; Skružná, O.; Válek, J. Study of nitrate contaminated samples from a historic building with the hygroscopic moisture content method: Contribution of laboratory data to interpret results practical significance. *J. Cult. Herit.* **2018**, *30*, 57–69. [CrossRef]
62. Ding, W.; Wang, Z.; Liu, B.; Liu, C.; Li, P. Research on rebound detection technology of ancient city wall bricks. *Build. Struct.* **2014**, *44*, 83–86. [CrossRef]
63. Song, X.; Ou, L. Study on construction of brick rebound strength measurement curve in Qing dynasty imperial tomb city. *Brick-Tile* **2023**, *11*, 23–25. [CrossRef]
64. World Health Organization. WHO Guidelines for Indoor Air Quality: Dampness and Mould. 2009. Available online: https://www.who.int/publications/i/item/9789289041683 (accessed on 16 July 2024).
65. Liu, N.; Liu, W.; Deng, F.; Liu, Y.; Gao, X.; Fang, L.; Chen, Z.; Tang, H.; Hong, S.; Pan, M.; et al. The burden of disease attributable to indoor air pollutants in China from 2000 to 2017. *Lancet Planet. Health* **2023**, *7*, e900–e911. [CrossRef]
66. Urso, A.; Evola, G.; Costanzo, V.; Nocera, F. A critical analysis on the use of different weather datasets to assess moisture-related risks in building components for a Mediterranean location. *J. Build. Eng.* **2023**, *76*, 107177. [CrossRef]
67. Zhu, L.; Liu, S.; Zhu, Y. Influence of Comprehensive Physical Environment Parameters on Wet Diseases of Plastered Cultural Relics in Three Southeastern Coastal Provinces. *Archit. J.* **2022**, *S2*, 68–73.

68. Tang, S.; Liu, S.; Zhu, Y. Research on diseases of brick cultural relics in southeast coastal areas based on microenvironment parameter detection. *Contemp. Archit.* **2023**, *7*, 123–128.
69. *GB 55007-2021*; General Code for Masonry Structure. Standardization Administration of the People's Republic of China: Beijing, China, 2021.
70. de Oliveira, L.M.; Mesquita, E.F.; de Oliveira Freire, F.L.; Bertini, A.A. The influence of the bricks and mortar characteristics, paint, and salts on the rising damp of historic masonries through hygrothermal simulation. *J. Cult. Herit.* **2023**, *64*, 92–101. [CrossRef]
71. Panico, S.; Herrera-Avellanosa, D.; Troi, A. Monitoring rising damp in solid masonry walls: An experimental comparison of five different methods. *J. Build. Eng.* **2023**, *75*, 106999. [CrossRef]
72. Vitiello, V.; Castelluccio, R.; Merino, M.D.R. Experimental research to evaluate the percentage change of thermal and mechanical performances of bricks in historical buildings due to moisture. *Constr. Build. Mater.* **2020**, *244*, 118107. [CrossRef]
73. Hoła, A.; Matkowski, Z.; Hoła, J. Analysis of the moisture content of masonry walls in historical buildings using the basement of a medieval town hall as an example. *Procedia Eng.* **2017**, *172*, 363–368. [CrossRef]
74. Fan, R.; Meng, D.; Xu, D. Survey of Research Process on Statistical Correlation Analysis. *Math. Model. Its Appl.* **2014**, *3*, 1–12. [CrossRef]
75. Li, S. Reuse and Restoration of Green Brick Materials in Lingnan Ancient Buildings. *Cult. Ind.* **2018**, *63* (Suppl. S1), 377–380.
76. Lei, Z.K.; Zheng, J.H.; Zhou, L. Experimental Study of the Characteristics of Damp and Efflorescence Mechanism for Building Brick. *Adv. Mater. Res.* **2012**, *535*, 1697–1701. [CrossRef]
77. Kong, Z.; Li, Y.; Hokoi, S.; Hu, S. The rising damp in two traditional clay-brick masonry walls and influence on heat transfer performance. In *MATEC Web of Conferences, Proceedings of the 4th Central European Symposium on Building Physics (CESBP 2019), Prague, Czech Republic, 2–5 September 2019*; EDP Sciences: Ulis, France, 2019; Volume 282, p. 02097. [CrossRef]
78. Yi, S.; Wang, Z.; Zhang, C.; Li, G. The detection technique for compress strength of sintered clay perforated brick by resilience method. *Brick Tile World* **2006**, *4*, 40–42. [CrossRef]
79. Alfano, F.R.A.; Palella, B.I.; Riccio, G. Moisture in historical buildings from causes to the application of specific diagnostic methodologies. *J. Cult. Herit.* **2023**, *61*, 150–159. [CrossRef]
80. Fonseca, A.J.; Pina, F.; Macedo, M.F.; Leal, N.; Romanowska-Deskins, A.; Laiz, L.; Gómez-Bolea, A.; Saiz-Jimenez, C. Anatase as an alternative application for preventing biodeterioration of mortars: Evaluation and comparison with otherbiocides. *Int. Biodeterior. Biodegrad.* **2010**, *64*, 388–396. [CrossRef]
81. Chen, Y. Construction Technology of Structural Reinforcement and Appearance Restoration of Excellent Historical Buildings. *Build. Constr.* **2024**, *4*, 515–518. [CrossRef]
82. Guo, S. *Conservation and Restoration Engineering of Chinese Heritage Buildings*; Peking University Press: Beijing, China, 2014.
83. van Hees, R.P.; Lubelli, B.; Hacquebord, A. CNew test methods to verify the performance of chemical injections to deal with rising damp. *J. Cult. Herit.* **2018**, *31*, S52–S59. [CrossRef]

Disclaimer/Publisher's Note: The statements, opinions and data contained in all publications are solely those of the individual author(s) and contributor(s) and not of MDPI and/or the editor(s). MDPI and/or the editor(s) disclaim responsibility for any injury to people or property resulting from any ideas, methods, instructions or products referred to in the content.

buildings

MDPI

Article

Optimising Ventilation Strategies Based on Predicted Mean Vote and Indoor CO_2 Concentration: A Case Study of University Teaching Spaces in Cold Region of China

Jiahui Yu [1,2], Hongnan Wang [1,2], Yige Sui [1,2], Yitong Xu [1,2] and Yang Chen [1,2,*]

[1] School of Architecture and Design, Harbin Institute of Technology, Harbin 150006, China; 24b334003@stu.hit.edu.cn (J.Y.); 20s034016@stu.hit.edu.cn (H.W.); 23s134167@stu.hit.edu.cn (Y.S.); 23b334001@stu.hit.edu.cn (Y.X.)

[2] Key Laboratory of Cold Region Urban and Rural Human Settlement Environment Science and Technology, Ministry of Industry and Information Technology, Harbin 150006, China

* Correspondence: chenyang1109@126.com; Tel.: +86-8628-1070

Abstract: Background: Educational spaces, which represent a vital setting for students' learning activities, significantly influence both learning efficiency and physiological health. As university teaching spaces are characterised by high occupancy density and prolonged occupancy, it is vital to address the problem of elevated CO_2 concentrations in these spaces. Although effective ventilation design can improve indoor air quality, the relatively short ventilation periods in cold regions of China, driven by winter insulation requirements, often lead to substandard indoor air quality. Purpose: Based on predicted mean vote (PMV), this study explored the effect of natural ventilation on indoor CO_2 concentration during the transition season in cold regions and proposed reasonable optimization strategies. Method: Through the method of combination of measurement and simulation, an effective design method of doors and Windows and an intermittent ventilation strategy for improving the indoor environment quality of teaching space in universities in cold regions of China are put forward. Result: The results revealed that indoor CO_2 concentrations exceeded the standard limit of 1000 ppm for the majority of the periods studied. Peak indoor CO_2 concentrations reached 1970 ppm, 2751 ppm, and 3200 ppm in large-, medium-, and small-sized classrooms, respectively. The duration of exceeding CO_2 concentration accounted for the highest proportion of class time, which were 89%, 93%, and 88%, respectively. Furthermore, optimisation of door and window design and ventilation methods was carried out for a representative medium-sized classroom. The simulation results indicated that while maintaining indoor comfort ($-0.5 < PMV < 0.5$), peak indoor CO_2 concentrations during class periods decreased from 2551 ppm to 1149 ppm, and the proportion of time for which CO_2 concentrations exceeded standards decreased from 87% to 47%. Conclusions: This study suggests that relevant codes and standards should be refined for the relationship between indoor CO_2 concentration and thermal comfort, and that designers should provide suggestions for suitable door and window design and ventilation strategies to improve indoor air quality in educational spaces in cold regions of China.

Keywords: thermal comfort; CO_2 concentration; teaching space; cold region of China; ventilation optimisation design

1. Introduction

1.1. Impact of Natural Ventilation on Indoor Thermal Comfort and Air Quality

To provide a comfortable indoor thermal environment in cold regions of China, architects often focus on factors such as winter insulation and energy saving for heating [1]. A well-sealed building envelope can effectively reduce indoor heat loss in cold regions, but it may also have a negative impact on indoor air quality [2]. Factors affecting the indoor thermal environment include air quality, acoustics, and lighting, with air quality having the strongest correlation with indoor thermal comfort [3]. In most educational spaces in cold

regions of China, natural ventilation is utilised to improve indoor air quality [4], which is commonly assessed in terms of indoor CO_2 concentration [5,6]. Lei et al. studied the effect of natural ventilation on indoor air quality in dormitories during the winter. The results showed that under similar conditions, without natural ventilation, the indoor CO_2 concentration increased from an initial 2400 ppm to 5000 ppm within 7 h, while with natural ventilation (ventilation opening area of 0.11 m^2), the indoor CO_2 concentration decreased from an initial 2600 ppm to 500 ppm within 7 h [7]. Kuwahara et al. studied the impact of natural ventilation on air quality in air-conditioned rooms, measuring CO_2 concentrations in rooms with different temperature controls. The results showed that natural ventilation provided every 30 min reduced indoor CO_2 concentration by approximately 278 ppm to 325 ppm [8]. Due to variation in seasonal climates, there are significant differences in the frequency and intensity of natural ventilation [9]. Under natural ventilation, indoor temperature and humidity decrease [10], leading to severe indoor heat loss, which directly negatively affects thermal comfort. Deng et al. explored the impact of natural ventilation on indoor thermal comfort in office buildings, and the results showed that, under natural ventilation, when the outdoor air temperature was 20 °C, 60% of the cases could not meet the thermal comfort requirements ($-0.7 < PMVe < 0.7$). When the outdoor temperature was raised to 24 °C, the level of dissatisfaction with indoor thermal comfort decreased by 29% [11]. In cold regions, where there is a large temperature difference between indoor and outdoor environments during winter, balancing indoor air quality and thermal comfort is a pressing task.

Predictive mean vote (PMV) [12] and thermal comfort evaluation indices are commonly used to monitor indoor thermal comfort [13,14]. Research on the indoor thermal environment in buildings in China has often taken indoor air temperature as the primary indicator [15]. In a study by Min et al. of classrooms in a university in Beijing, a neutral temperature of 22.9 °C was found for the indoor thermal environment during winter [16]. In the Mediterranean region, analysis of empirical data and student thermal comfort perceptions revealed that indoor air quality deteriorated with the prolonged closure of doors and windows in winter, emphasising the importance of proper ventilation to balance indoor air quality and thermal comfort [17]. Babich et al. evaluated indoor air quality and thermal comfort based on different standard constraints and proposed optimal design methods [18]. In recent years, there have also been studies on processing data through neural networks [19] and machine learning [20] methods to improve the accuracy of indoor thermal environment prediction.

1.2. Impact of CO_2 Concentration on Productivity Efficiency

High indoor CO_2 concentrations can have direct adverse effects on human physiological health [21–23]. Factors influencing indoor air quality include CO_2 concentration [24], volatile organic compounds, particulate matter, and ventilation system parameters [25]. Apte et al. found that exceeding standard CO_2 concentrations led to adverse symptoms among indoor occupants, such as sore throat, rhinitis, chest tightness, asthma, and decreased attention [26]. Bourbeau et al. found that, after improvements to the ventilation system in office buildings, the prevalence of sick building syndrome among office workers decreased by 40% to 50% [27]. In educational spaces, the rate of emission of indoor pollutants is generally positively correlated with the amount of CO_2 exhaled by humans, and different levels of indoor air quality have varying effects on students' work efficiency [28]. Studies have shown that indoor CO_2 concentrations significantly impact learning efficiency [29,30]. When classroom ventilation efficiency is low [31], students show reduced attention and vigilance. Reasonable classroom ventilation rates can enhance students' attention and classroom productivity. When increasing indoor ventilation rates, it is important to consider the impact of indoor thermal comfort on learning efficiency, especially in cold regions. Xiong et al. investigated the impact of indoor temperature, noise levels, and indoor lighting on performance in different types of tasks. The results indicated that tasks requiring concentration were performed most efficiently in cool indoor temperature

environments, while other types of tasks were better suited to warm and quiet indoor environments [32]. Kaushik et al. found that, when the indoor CO_2 concentration was below 700 ppm and the outdoor temperature was 22–45 °C, production efficiency was high [33]. Franke et al. employed on-site testing and subjective surveys to establish a comprehensive evaluation framework aimed at guiding the optimisation of indoor environmental quality in workspaces through design strategies [31].

China's indoor hygiene standards, established in 1997, and indoor environmental standards, established in 2002, require the daily average indoor CO_2 concentration to be below 1000 ppm. In China's ventilation regulations for educational public buildings, the indoor CO_2 concentration standard was revised from 1500 ppm in 1998 to 1000 ppm in 2017 [34]. Due to high indoor population density and heavy foot traffic, educational spaces often experience elevated CO_2 concentrations, exceeding the standard value of 1000 ppm, in poorly ventilated conditions. When indoor CO_2 concentrations exceed 1000 ppm, students' health and productivity are negatively affected [35]. In cold regions, the phenomenon of elevated CO_2 concentrations in university buildings is even more pronounced. Improving the design of doors and windows in educational spaces and implementing reasonable intermittent ventilation methods can enhance ventilation efficiency, thereby reducing indoor CO_2 concentrations [36,37] and enhancing teaching and learning efficiency [38]. During classes, natural ventilation should be provided to ensure that the PMV value indoors falls within the range of -0.5 to 0.5.

1.3. Literature Gaps and Research Object

Based on the above literature review, the research gaps filled by and innovations of this paper are as follows:

(1) In the severe cold regions of China, there is a significant temperature difference between indoor and outdoor environments during winter, leading to shorter ventilation cycles to reduce indoor heat loss. However, this can result in inadequate indoor air quality. Previous research has rarely focused on the balance between indoor air quality and thermal comfort in these regions, making it necessary to propose reasonable strategies to ensure the health of indoor occupants.

(2) Furthermore, many studies aimed at improving indoor air quality propose optimization strategies focusing on enhancing ventilation systems and spatial layout. However, in the cold regions of China, where teaching spaces primarily rely on natural ventilation, these strategies are not applicable. There is a need to propose indoor ventilation strategies tailored to the specific climatic characteristics of cold regions in China.

This study selects educational spaces in cold regions of China as the research object. Through a combination of measurement and simulation, this study sheds light on the degree to which indoor CO_2 concentration exceeds standards due to poor ventilation. Based on the research results, architectural design optimisation methods and time-based ventilation strategies are proposed, and their effectiveness in resolving the contradiction between indoor thermal comfort and air quality is explored.

2. Methods

This study aimed to determine whether and to what extent indoor CO_2 concentration exceeded standards in a teaching building in a cold region of China through simulation and measurement. First, three types of classrooms (large-, medium-, and small- sized) in a typical teaching building in Harbin were selected as the research subjects, and their indoor CO_2 concentrations were monitored. Based on the measured data, the simulation model was validated, and the indoor air quality was analysed. Second, optimisation designs were proposed in three modes: window opening, entrance, and ventilation modes. The effectiveness of the design strategies in balancing indoor thermal comfort and air quality was verified. The research framework is illustrated in Figure 1.

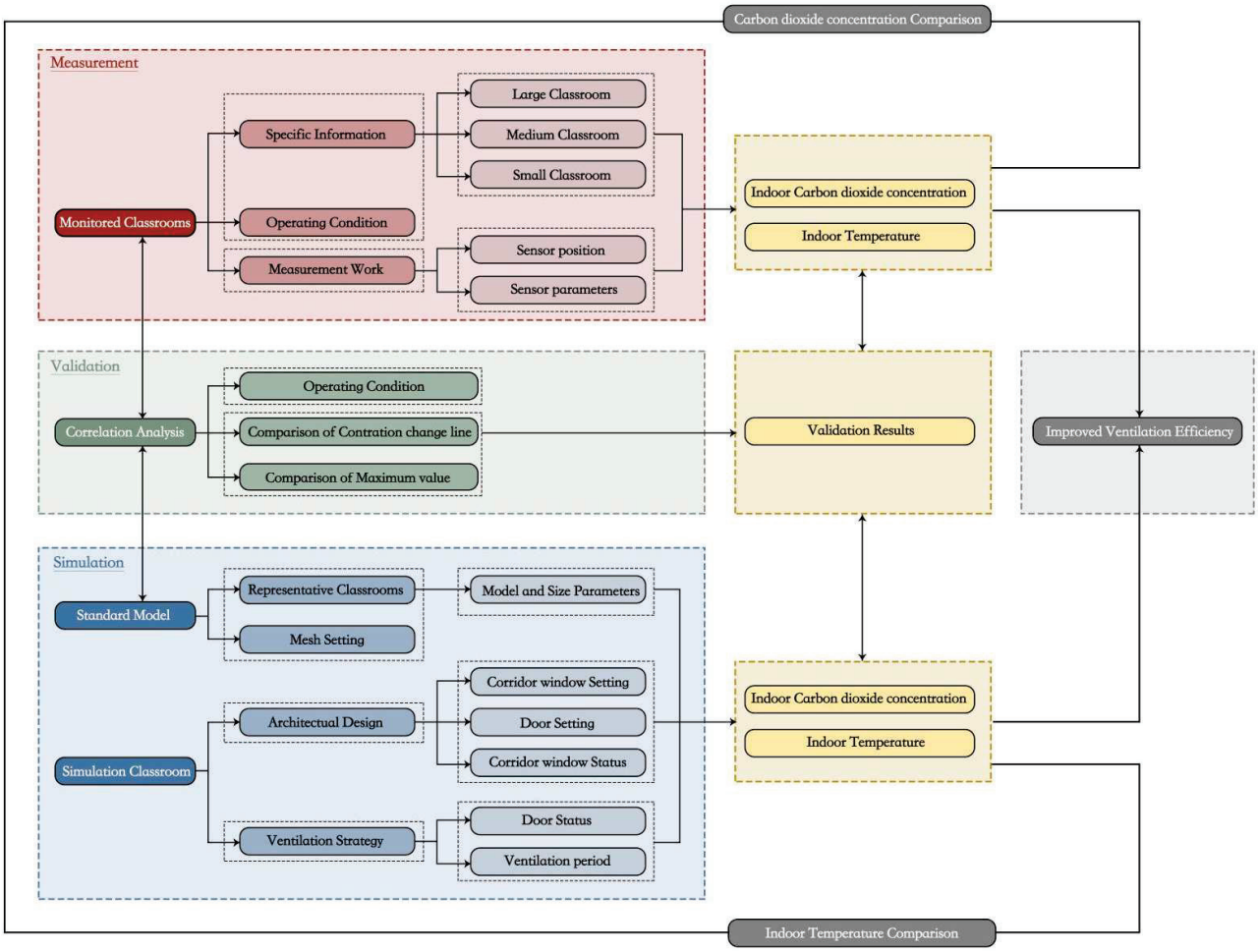


Figure 1. Framework of study.

2.1. Measurement

To reveal the CO_2 concentration situation in naturally ventilated classrooms in cold regions, real-time monitoring of indoor CO_2 concentrations was conducted in three classrooms—small-, medium-, and large-sized—in a university teaching building in Harbin, China, from 24 to 26 April 2023. This period can represent the climatic conditions of the typical transition season in the severely cold region, when the heating has just stopped, but the outdoor temperature is low and the limited natural ventilation time brings potential air quality problems. In order to ensure the comprehensiveness of the monitoring data, the monitoring cycle includes two stages: classroom idle state and class state. This is with the aim of revealing the influence of indoor CO_2 on thermal comfort under different classroom occupancy states. Three types of instructional classroom (Table 1) were selected for real-time monitoring of indoor CO_2 concentrations, with similar occupancy patterns in each classroom during the monitoring period (Table 2). To ensure the accuracy of the measured data, CO_2 concentration was monitored separately in each classroom during unoccupied periods to eliminate the influence of factors such as building orientation and room location on the experimental results. In addition, to ensure that radiator usage and window-opening behaviour did not influence the measured data, CO_2 concentrations during unoccupied class periods were monitored separately in the three classrooms after one week of heating cessation. During the monitoring period, doors and windows were kept closed. As the activity of occupants during class periods had minimal interference with the indoor air environment, it is not discussed in this paper.

Table 1. Classroom-specific information.

Classroom ID	Large Classroom	Medium-Sized Classroom	Small Classroom
Classroom size	13.2 m × 17.3 m × 8.0 m	17.2 m × 6.3 m × 4.0 m	8.1 m × 5.6 m × 4.0 m
Classroom area	221 m^2	107 m^2	45 m^2
Classroom volume	1768 m^2	428 m^2	180 m^2
Maximum personnel capacity	228	70	40
Number and size of windows	16 × 1.52 m × 2.43 m	5 × 1.52 m × 1.82 m	2 × 1.52 m × 1.88 m
Number and size of doors	2 × 2.1 m × 2.9 m	1 × 2.1 m × 2.9 m	1 × 1.4 m × 2.3 m
Ventilation method	Natural ventilation	Natural ventilation	Natural ventilation
Type, quantity, and size of desks	Desk A: 48 × 2.0 m × 0.3 m × 0.9 m Desk B: 12 × 1.6 m × 0.3 m × 0.9 m	Desk A: 10 × 2.1 m × 0.6 m × 0.9 m Desk B: 15 × 1.2 m × 0.6 m × 0.9 m	20 × 1.2 m × 0.5 m × 0.9 m

Table 2. Occupancy status during class periods in different types of classrooms.

Schedule	April 24th			April 25th			April 26th		
	Small Classroom	Medium-Sized Classroom	Large Classroom	Small Classroom	Medium-Sized Classroom	Large Classroom	Small Classroom	Medium-Sized Classroom	Large Classroom
8:00 −9:45	0	0	0	0	35	0	16	0	0
10:00 −11:45	0	0	0	21	36	0	22	11	0
11:45 −13:45	0	0	0	0	0	0	0	0	0
13:45 −15:30	9	19	27	22	38	36	6	43	42
15:45 −17:30	9	19	0	6	38	43	0	0	42
18:30 −20:15	4	25	0	0	0	0	0	0	0
20:15 −21:00	0	0	0	0	0	0	0	0	0

The monitoring equipment selected was sensors with CO_2 probes developed independently by Ubibot (Table 3). The CO_2 monitoring range of the sensors was 0–10,000 ppm, with an accuracy of 30 ppm ±3%. The specific locations of the measurement points are illustrated in Figure 2. To ensure that airflow caused by factors such as infiltration ventilation and temperature differences did not introduce errors into the data, the sensors were placed at a distance from windows, radiators, and electrical appliances. Sensor height should approximate the range of human thermal perception and should not be too close to the ground or significantly higher than the plane of human activity. Therefore, sensors were positioned near the centre of each classroom, at a height of 1.2 m above the ground, and away from where occupants typically breathe.

Table 3. Specifications of sensors.

Schematic Diagram of Sensor	Brand and Model	Measuring Range	Accuracy
	Ubibot-GS1	0–10,000 ppm	30 ppm ± 3%

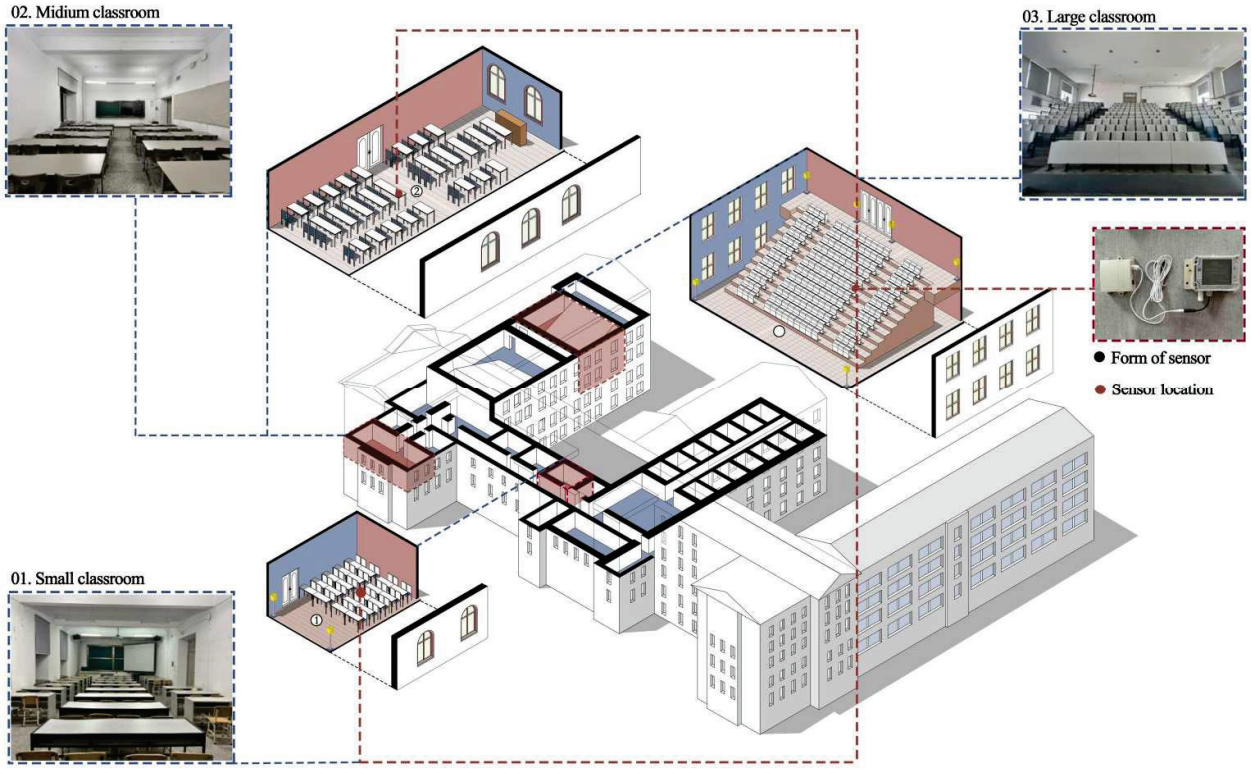


Figure 2. Sensor location information for the three tested classrooms (red-dashed boxes indicate the classroom units selected for data collection).

2.2. Simulation

The study utilised a sub-balanced model for CO_2 in naturally ventilated classrooms as its foundation. It used Airpak3.0 software to establish simulation models, integrating theories of indoor thermal comfort such as the PMV-predicted percentage of dissatisfied model to simulate CO_2 concentration, indoor temperature distribution, and PMV vote distribution within teaching building spaces. The "mesh" function in the Airpak software package was utilised to automatically partition and generate grids in the model, followed by fine-tuning adjustments. Boundary conditions were then set, and the transient simulation results were used to adjust and establish standardised models for subsequent simulations of the classrooms after ventilation design optimisation.

2.2.1. Establishment of Standardised Models

This study used Classroom 218, a medium-sized classroom located on the second floor of the building, which can accommodate up to 72 people, as an example to construct the standardized model. Figure 3 shows the specific details of the classroom selected as a simulation case. As can be seen from Figure 3a, in order to meet the requirements of insulation design in winter, the external walls of the teaching space in cold regions are thicker. Figure 3b shows the details of the layout of the classroom space, which is representative of the typical plan features of the climate zone.

In the field of CFD, common simulation software includes ANSYS Fluent, Airpak, Butterfly, and so on [39]. In this study, Airpak software was used to simulate indoor CO_2 distribution and predict indoor thermal comfort environment. The software is developed by Fluent and is widely used in simulation of indoor ventilation and air conditioning [40]. Figure 4a shows the details of the simulation model. Based on field surveys of teaching spaces in universities in cold regions of China, most classrooms have only one exterior wall, with the remaining three walls being interior walls. Therefore, while keeping the boundary condition parameters constant, this study designated one long side of the classroom as the exterior wall and the other three sides as interior walls. Windows were modelled on the

exterior wall side, with the window opening method and window-to-wall ratio determined based on the measured classroom dimensions. An entrance was positioned in the middle of each interior wall. Four radiator models were placed below the window slit model, each with a constant power of 500 W. Based on the observed indoor occupancy, the model was set to accommodate 35 people, evenly distributed within the classroom. Table 4 presents specific parameters within the classroom module. The quantity in the table is set according to the actual situation of the classroom and the survey results. Personnel sitting size is calculated according to the average height of the investigators, the window seam combined with the survey classroom according to the field measurement and service life reasonable setting, table and chair and podium size according to the field measurement, and CO_2 value is set when sitting human respiration emissions. During the measurement phase, all doors and windows of the classroom were closed. Therefore, in subsequent simulation adjustments, the study simulated the airflow under closed-door and window conditions by setting the gaps in the doors and windows. Additionally, the indoor airflow under open-door and window conditions is illustrated in Figure 4b.

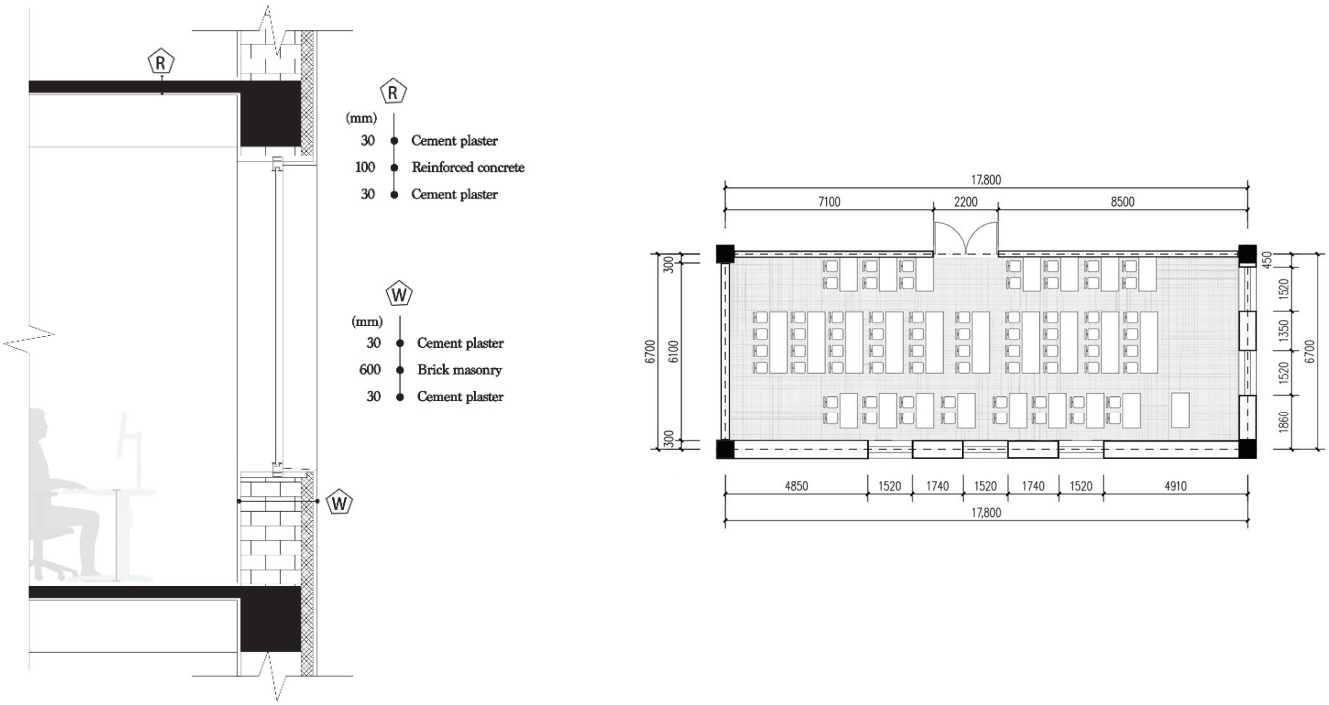


Figure 3. Simulation model envelope structure form and floor plan. (**a**) External wall structure form of simulation model. (**b**) Details of simulation model floor plan.

Table 4. Model and size parameters of each module.

Classroom	Number	Length·Z(m)	Width·Z(m)	Height·Z(m)	Module Type
Personnel (seated position)	35	0.2	0.3	1.73	Person
Outer window seam (north facing)	3	0.015	--	1.5	Opening
Outer window seam (south facing)	2	--	0.015	1.5	Opening
A crack between a door and its frame	1	1.8	--	0.02	Opening
Desk A	15	0.6	0.9	1.2	Block
Desk B	10	0.6	0.9	2.1	Block
Lectern	1	0.8	1.8	1.2	Block
Pollution sources	35	0.04	0.04	0.04	Source

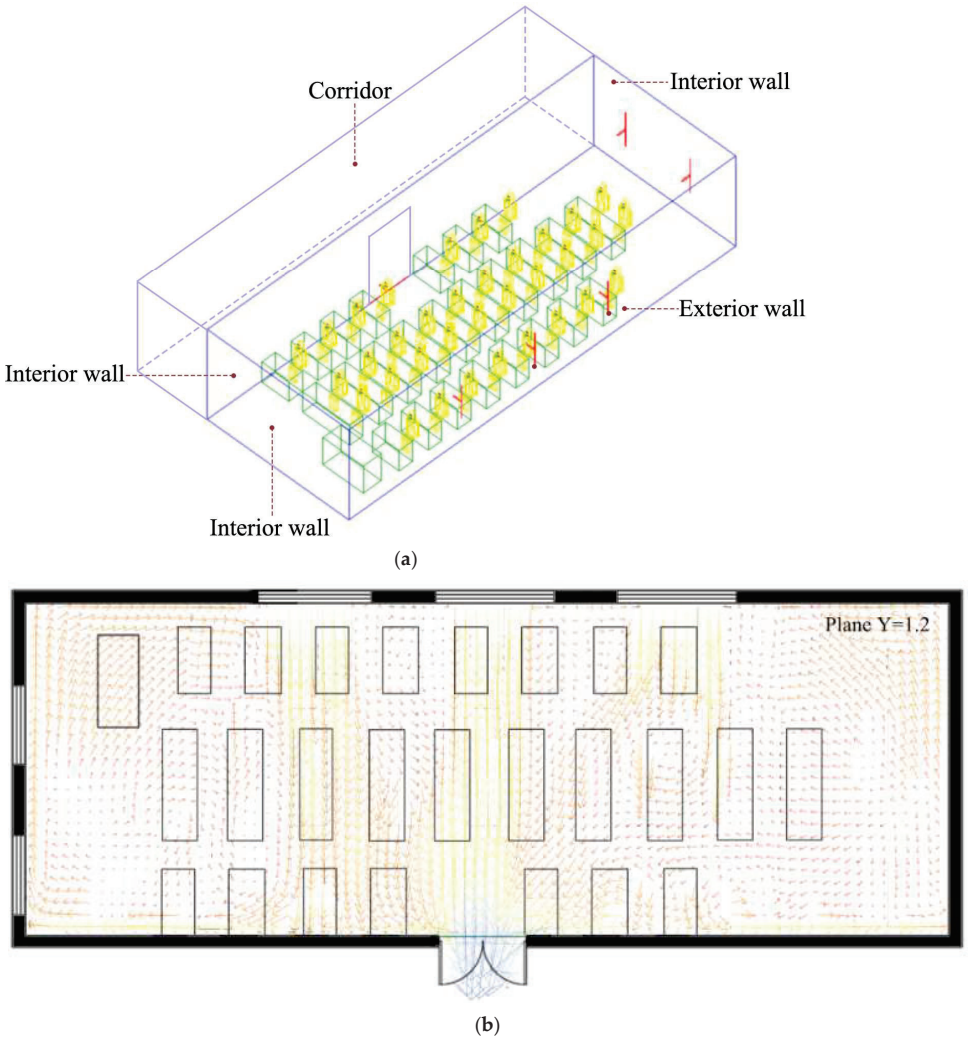


Figure 4. Schematic diagram of standardised model. (**a**) Boundary conditions of the model envelope and schematic layout of tables and chairs. (**b**) Indoor air flow diagram (arrows indicate the direction of air flow).

Figure 5 illustrates the grid division of the standardised model, with (a) showing the cross-section of grid division in the direction of Y = 0.8 m inside the room, and (b) showing the cross-section of grid division in the direction of X = 4.3 m. The maximum grid size in the X, Y, and Z directions was 0.2 m. To enhance simulation accuracy, local refinement was applied at the openings of doors and windows and near human pollution sources, resulting in a total of 892,935 generated grids.

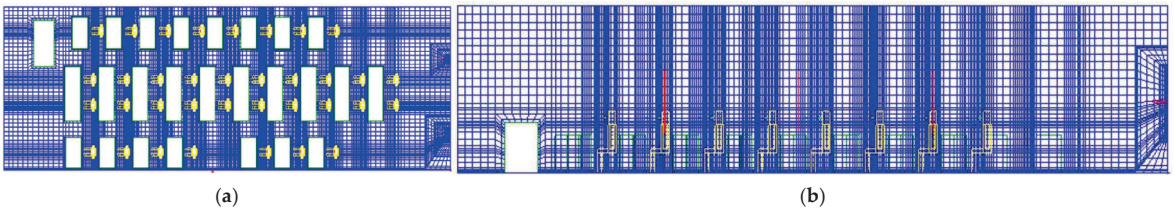


Figure 5. Model mesh division. (**a**) Model mesh division cross-section Y = 0.8. (**b**) Model mesh division cross-section X = 4.3.

2.2.2. Establishment of Different Corridor Windows and Entrance Models

To further explore the impact of different transom window configurations on indoor CO_2 concentration, four models with transom windows of varying heights were established

for comparative study. Due to the low outdoor temperatures and noise levels in cold regions of China during winter, it is difficult to improve indoor air quality by opening exterior windows during class periods. Therefore, it is common for classrooms in cold regions of China to have transom windows installed on interior walls near corridors. When the transom windows are open and doors and exterior windows are closed, according to the principle of thermal buoyancy ventilation, the indoor air environment during class periods is improved. If the transom windows are positioned too low, activities in the corridor and rapid airflow may disturb students during class. Therefore, the bottom height of the transom window in this study was set above the seated and standing eye levels, with the minimum effective opening height being 1.7 m. The indoor ventilation conditions were simulated with four transom window heights: Case 1.1: y = 3.2 m, Case 1.2: y = 2.7 m, Case 1.3: y = 2.2 m, and Case 1.4: y = 1.7 m. Additionally, considering the influence of the positions of entrances on indoor CO_2 concentration, adjustments were made to the number of entrances based on the Case 1.1 model, with front and back entrances set on the long side interior wall of the classroom.

2.2.3. Boundary Condition Setting

This study analysed the distribution of CO_2 during class periods using transient simulation methods. The simulation time step was 2 min, and air environment data, including indoor average CO_2 concentration, were recorded every 4 min. The simulation assumed the incompressible indoor fluid and uniform distribution of CO_2 and temperature field at the initial stage of simulation. The initial CO_2 concentration indoors was set based on test values during unoccupied and occupied class periods in a medium-sized classroom, where the indoor CO_2 concentration reached a steady state of 700 ppm after doors and windows were closed. In this study, the wall with exterior windows is designated as the exterior wall, while the remaining three walls are considered interior walls. In severe cold regions, the significant temperature difference between indoor and outdoor environments leads to heat transfer. The outdoor temperature is set at −10 °C, with a pressure of 100 kPa and a relative humidity (RH) of 70%. The exterior wall is set as a temperature-controlled wall with an initial temperature of 10 °C. The initial indoor temperature is 21 °C with an RH of 50%. The interior walls, ceiling, and floor are specified as insulated boundary conditions since they all face the interior and are expected to have similar temperature conditions to adjacent rooms. Therefore, their initial temperature is set at 18 °C. When doors and windows are closed, indoor air circulation is considered only for infiltration through gaps in the exterior wall windows and interior wall doors. The parameters are set for static pressure ventilation with an infiltration rate of 0.5 h^{-1}. When doors and windows are open, the indoor space is naturally ventilated. During the transitional seasons, the average outdoor wind speed is set at 2 m/s, with a natural ventilation rate of 3 h^{-1}. Additionally, considering the long usage period of the case study building and the presence of significant leaks due to large gaps in doors and windows, the window and door gaps are set to 0.015 m × 1.5 m and 0.015 m × 1.8 m, respectively. The occupants in the classroom were assumed to be seated, with a metabolic heat production of 105 W per person. The lecturer's desk and student desks were simplified as rectangular prisms with insulating physical properties. The power of the radiators was set at 500 W. The pollution source was set as a cube measuring 0.04 m × 0.04 m × 0.04 m, located to the front of the facial model of the occupants. This represented CO_2 release from respiration and was the only modelled source of CO_2 indoors. The release rate of CO_2 was 0.0144 $m^3/(h \cdot p)$, with a temperature of 37 °C. For the PMV calculation, the thermal resistance of clothing for indoor personnel was 1.0 clo for male students and 1.2 clo for female students (typical in spring), and the metabolic rate was set at 1.2 met (sedentary state).

2.2.4. Ventilation in Different Time Periods

To investigate the impact of using transom windows for time-based ventilation on CO_2 concentration, the duration of ventilation was adjusted during class periods to verify its

effectiveness in improving indoor air quality (as shown in Table 5). The exterior windows were set to remain closed throughout the entire period, while the doors and transom windows were opened during break times. The indoor occupancy during class periods was set at 35 people, while during break times it was set at 20 people.

Table 5. Division of indoor ventilation simulation stages.

Stage	Time Period	Number of Indoor Personnel	Door and Window Open Status
Phase one	8:00–8:45	35	External windows and doors closed, corridor windows opened
Phase two	8:45–8:55	20	External windows closed, corridor windows and doors opened
Phase three	8:55–9:40	35	External windows and doors closed, corridor windows opened
Phase four	9:40–10:00	0	External windows closed, corridor windows and doors opened
Phase five	10:00–10:45	35	External windows and doors closed, corridor windows opened
Phase six	10:45–10:55	20	External windows closed, corridor windows and doors opened
Phase seven	10:55–11:40	35	External windows and doors closed, corridor windows opened

2.3. Validation

The study fitted the measured and simulated indoor CO_2 concentration results during class and break periods in the medium-sized classroom separately to verify the accuracy of the simulation model. The accuracy of the model was estimated using Pearson's correlation coefficient (*Pearson's R*). Formula (1) represents the calculation formula for *Pearson's R*. This value indicates the linear correlation between two variables, T_{meas} and T_{sim}, ranging from -1 to 1. When the absolute value approaches 1, the simulation accuracy is higher. This value can be calculated using Formula (1), where T_{meas} represents the measured data and T_{sim} represents the simulated data. To further validate the accuracy of the model, the boundary limits of the coefficient of variation of the (CV(RMSE)) were calculated, which provide insights into the extent of discrepancy between the simulated and measured data. The value can be calculated using Formula (2), where n represents the number of hours during the monitoring period, i represents each hour of the study period, and value of p is suggested to be 1. The acceptable ranges of the CV(RMSE) relative to the hourly calibration data were set at below 30%.

$$Pearson's\ R = \frac{\sum_{y=1}^{n}\left(T_{meas,y}-T_{MRAN}\right)\left(T_{sim,y}-T_{mean}\right)}{\left(\sqrt{\sum_{y=1}^{n}\left(T_{meas,y}-T_{MRAN}\right)^2}\right)\left(\sqrt{\sum_{y=1}^{n}\left(T_{sim,y}-T_{mean}\right)^2}\right)} \quad (1)$$

$$\mathrm{CV(RMSE)} = \frac{1}{\overline{Meas}}\cdot\sqrt{\frac{\sum_{i=1}^{n}(Meas_i - Sim_i)^2}{n-p}} \times 100(\%) \quad (2)$$

2.4. PMV Evaluation Index

Indoor thermal comfort can be measured by the PMV index, which is influenced by six main factors: air temperature, relative humidity, mean radiant temperature, air velocity, clothing insulation, and metabolic rate. Fanger derived mathematical formulas for PMV based on these six factors through extensive experiments [41]. The PMV calculation formula is represented as Equation (3):

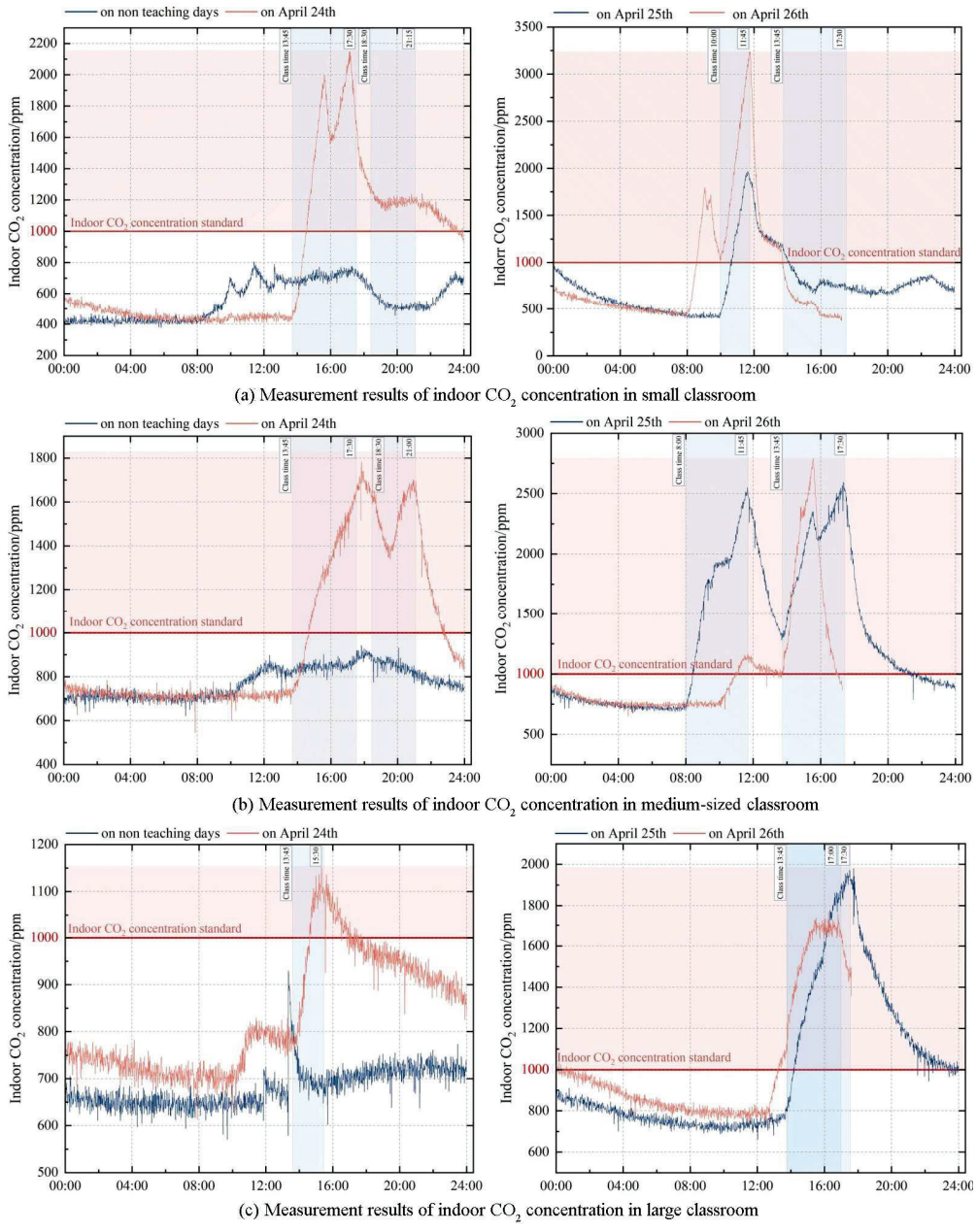
$$\begin{aligned}\mathrm{PMV} = \big((0.303\mathrm{e}^{-0.036\mathrm{M}} &+0.028)\{\mathrm{M}-\mathrm{W}-3.05\times10^{-5}[5733-6.99(\mathrm{M}-\mathrm{W})-\mathrm{P_a}]-0.42[\mathrm{M}-\mathrm{W}-58.15]\\ &-1.7\times10^{-5}\mathrm{M}(5867-\mathrm{P_a})-0.0014\mathrm{M}(34-\mathrm{t_a})-3.96\times10^{-8}\mathrm{f_{cl}}\left[(\mathrm{t_{cl}}+273)^4-(\mathrm{t_r}+273)^4\right]\\ &-\mathrm{f_{cl}}\mathrm{h_c}(\mathrm{t_{cl}}-\mathrm{t_a})\}\big)\end{aligned} \quad (3)$$

where M represents metabolic rate (W/m^3), W represents external work load (W/m^2), P_a represents water vapor pressure (kPa), t_a represents indoor average temperature (°C), tr represents indoor average radiant temperature (°C), f_{cl} represents the garment area coefficient, t_{cl} represents clothing surface temperature (°C), h_c represents the convective heat transfer coefficient between each occupant and the indoor environment ($W/(m^2 \cdot K)$), and v_a represents average air velocity (m/s).

3. Results

3.1. Classroom Monitoring Results

As shown in Figure 6, the CO_2 concentration in all three classrooms, small-, medium-, and large-sized, majorly exceeded the standard during class times. The indoor CO_2 concentration was lower than 1000 ppm on non-school days. During class, when the number of indoor occupants was higher, the CO_2 concentration was significantly higher. As shown in Figure 6a, the rate of accumulation of indoor CO_2 concentration in the small classroom during class was relatively high, and the peak value was large, with the maximum peak value approaching 3200 ppm. This may have been due to the small classroom space, the large number of indoor occupants during the class, and the lack of timely ventilation. In addition, as shown in Figure 6c, because CO_2 accumulated indoors on April 25 and was not removed in a timely manner due to poor ventilation, the indoor CO_2 concentration was still too high during the unoccupied period on April 26.



(a) Measurement results of indoor CO_2 concentration in small classroom

(b) Measurement results of indoor CO_2 concentration in medium-sized classroom

(c) Measurement results of indoor CO_2 concentration in large classroom

Figure 6. CO_2 concentration measurement results.

3.2. Validation Results

To enhance the reliability of the simulation model, Airpak software was used to simulate two scenarios in the medium-sized classroom: occupancy during class and break periods. The measured data were fitted with the simulated data, demonstrating a high level of model credibility. The Pearson's R values for the two scenarios were 0.99066 and 0.98532, both exceeding 0.8. In addition, the study further verified by calculating CV(RMSE) values. It can be seen from the calculation results that the CV(RMSE) values of the two scenarios simulation models are 2.897% and 4.59%, respectively, and the simulation error is far lower than the specified threshold. In Figure 7, the curve of simulated CO_2 concentration over time approximates a linear function graph. However, the slope of the growth rate of CO_2 concentration in the measured data fluctuates significantly. These discrepancies arise from differences in the distribution and activities of teachers and students indoors compared with the simulation conditions. Additionally, variations in the rate of CO_2 release by different individuals disturbed indoor airflow, leading to an unstable increase in indoor CO_2 concentration.

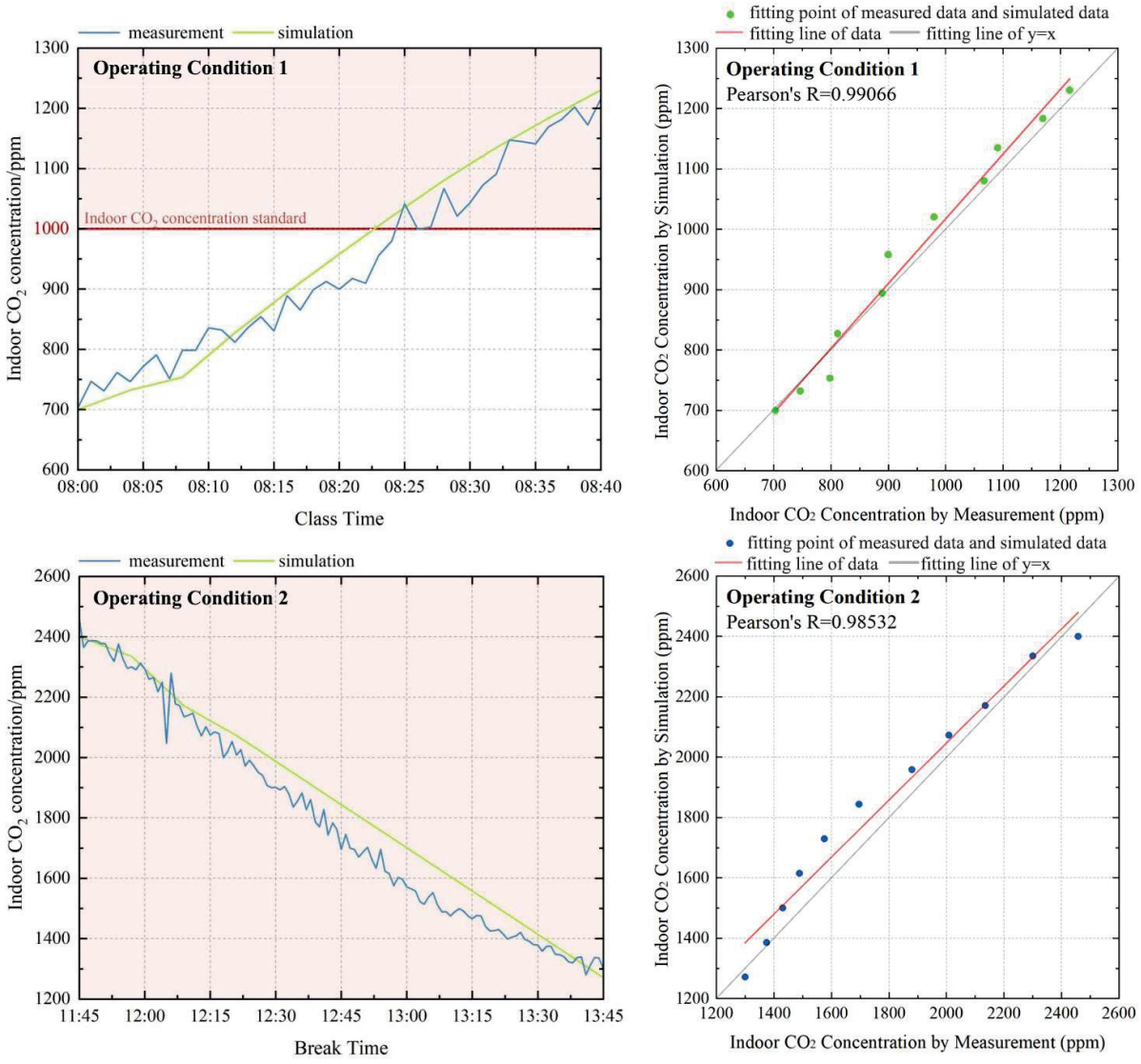


Figure 7. Comparison and validation of simulated data and measured data.

3.3. Simulation Results

3.3.1. Standardised Model Simulation Results

Figure 8 shows that the standardised model with single-side window ventilation exhibited an overall elevated level of indoor average CO_2 concentration. Approximately 12 min after the start of class, the indoor CO_2 value reached the upper limit (1000 ppm). Compared with actual classroom data, this ventilation mode resulted in a higher rate of accumulation of CO_2, with the CO_2 concentration peak rising from 1203 ppm to 1402 ppm (after 40 min of class). Figure 9 illustrates the distribution of CO_2 concentration and temperature within the classroom during a 40 min class period. As seen in (a), the indoor CO_2 concentration increased over time. At a height of Y = 1.2 m (typical breathing height while seated), CO_2 rapidly accumulated in the space farthest from the window, with CO_2 concentration reaching a peak of 1500 ppm after 40 min of class. The temperature distribution cloud map in (b) indicates that after 40 min, the temperature distribution in the horizontal space indoors became more uniform, with the temperature near Y = 1.2 m approaching 26 °C.

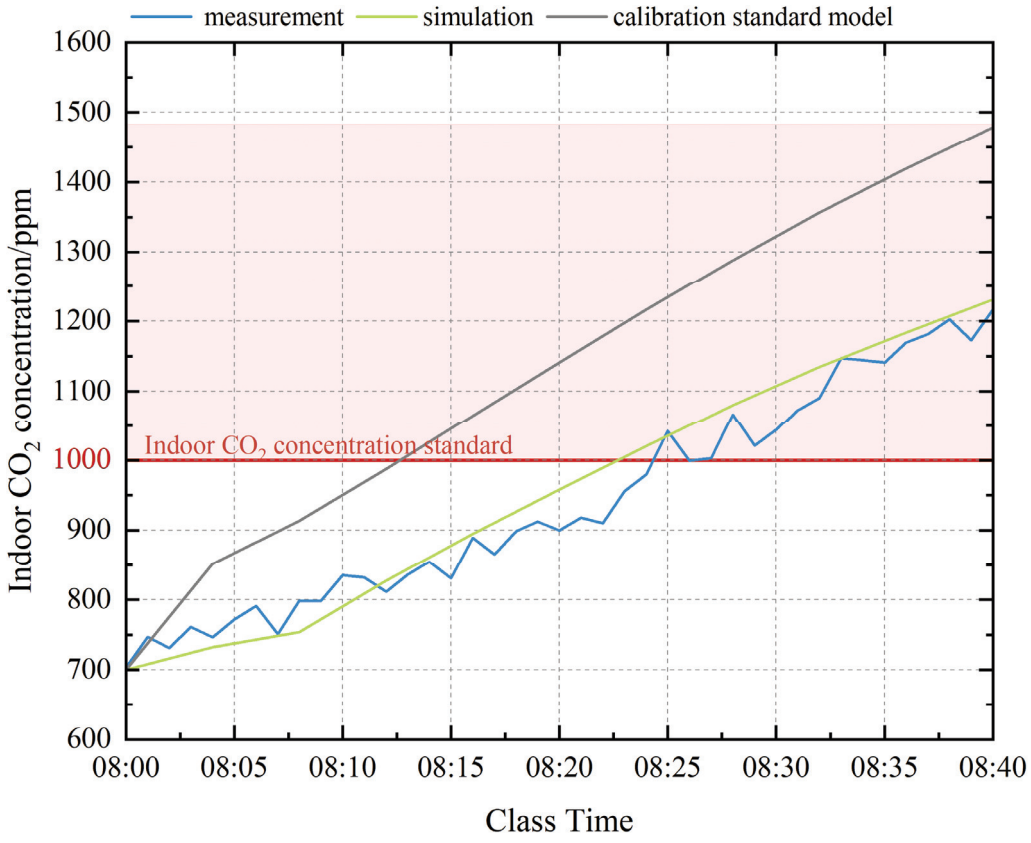


Figure 8. Indoor carbon dioxide concentration changes in corrected, measured, and standardized models.

3.3.2. Simulation Results for Different Corridor Window and Entrance Models

Figure 10a illustrates the varying impacts of four different heights of transom windows on indoor CO_2 concentration. As can be seen from the figure, increasing the height of the transverse window can effectively reduce the CO_2 concentration. Case 1.1 shows a clear improvement, with peak CO_2 concentration reduced by 184 ppm compared to baseline. The trend of curve changes in the graph indicates that, within a 40 min class period, Case 1.1 (window height of 3.2 m) effectively reduced indoor CO_2 concentration. Compared with the standard model, during class time, the Case 1.1 transom window configuration lowered the peak CO_2 concentration from 1402 ppm to 1218 ppm, although this still exceeded the regulatory requirement (1000 ppm). Figure 10b highlights the influence of

entrance numbers, where having two entrances not only delays the exceedance of CO_2 standards but also achieves a lower overall concentration by the end of the class period. The model with two entrances reached a CO_2 concentration of 1000 ppm nearly 10 min earlier than the model with a single entrance. After 40 min, the peak CO_2 concentrations in the two classrooms were 1218 ppm and 1093 ppm, respectively, indicating that appropriately increasing the number of entrances can effectively reduce indoor CO_2 concentration.

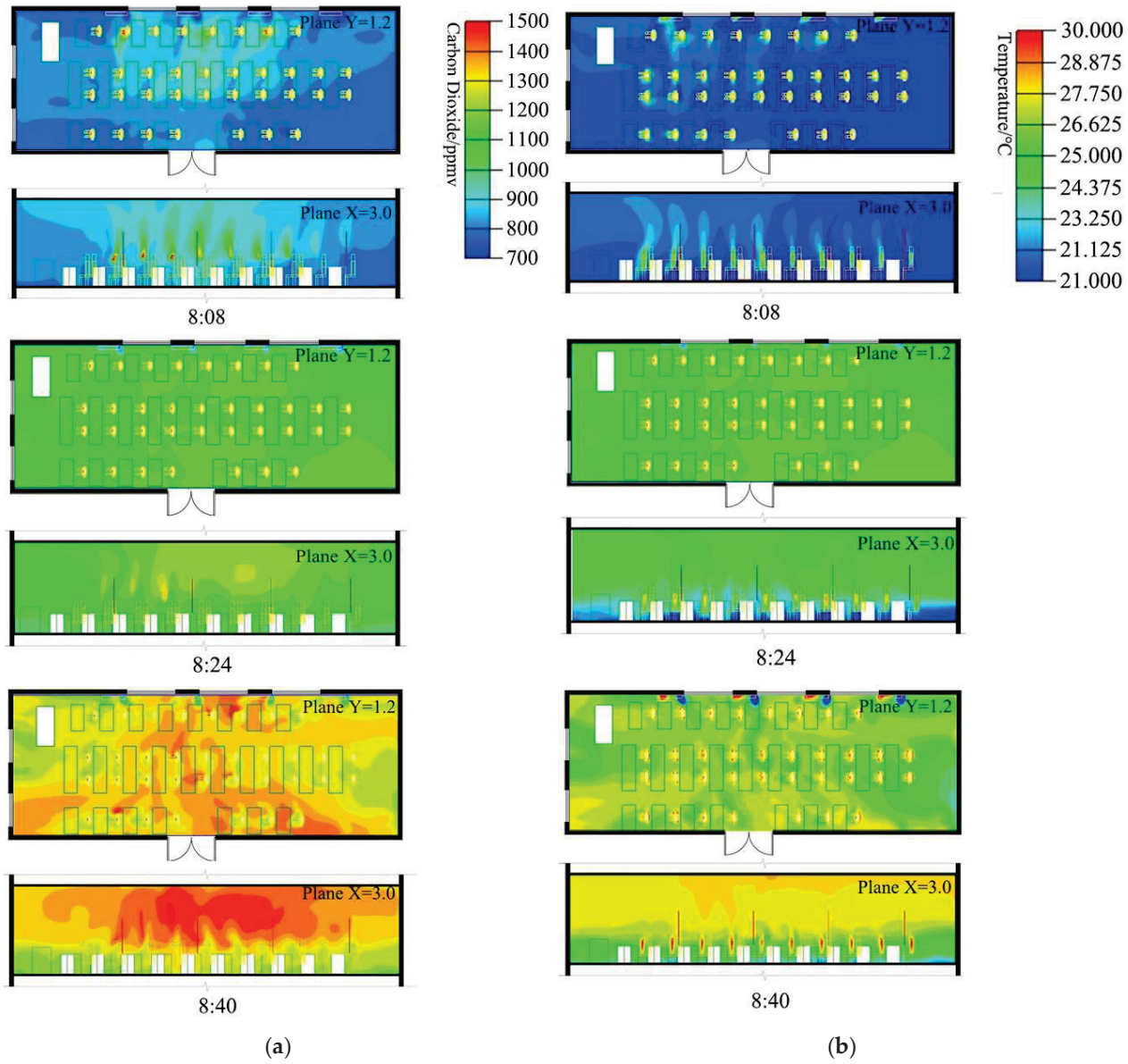


Figure 9. Corrected standardised model of indoor average CO_2 concentration change. (**a**) Simulation results for CO_2 concentration distribution using standardised model. (**b**) Simulation results for indoor temperature field using standardised model.

3.3.3. Minute Ventilation Simulation Results

Figure 11 depicts the variation of CO_2 concentration after the implementation of transom windows and ventilation measures. A comparison of the data in Figure 11 reveals that, during morning class periods in the medium-sized classroom, the observed duration of CO_2 concentration exceeding the standard was 156 min, accounting for 87% of the total class time, with a peak indoor CO_2 concentration of 2551 ppm. After simulation adjustments and adopting segmented ventilation, the duration of CO_2 concentration exceeding the standard during morning class periods was reduced to 84 min, accounting for 47% of

the morning class duration, with an indoor CO_2 peak concentration of 1149 ppm. These findings that combining architectural design adjustments with operational strategies, such as intermittent ventilation, is highly effective in maintaining indoor air quality within acceptable limits while balancing energy efficiency and occupant comfort. Furthermore, this approach highlights the importance of context-specific interventions, as the effectiveness of these strategies may vary depending on factors such as room size, occupancy density, and outdoor environmental conditions.

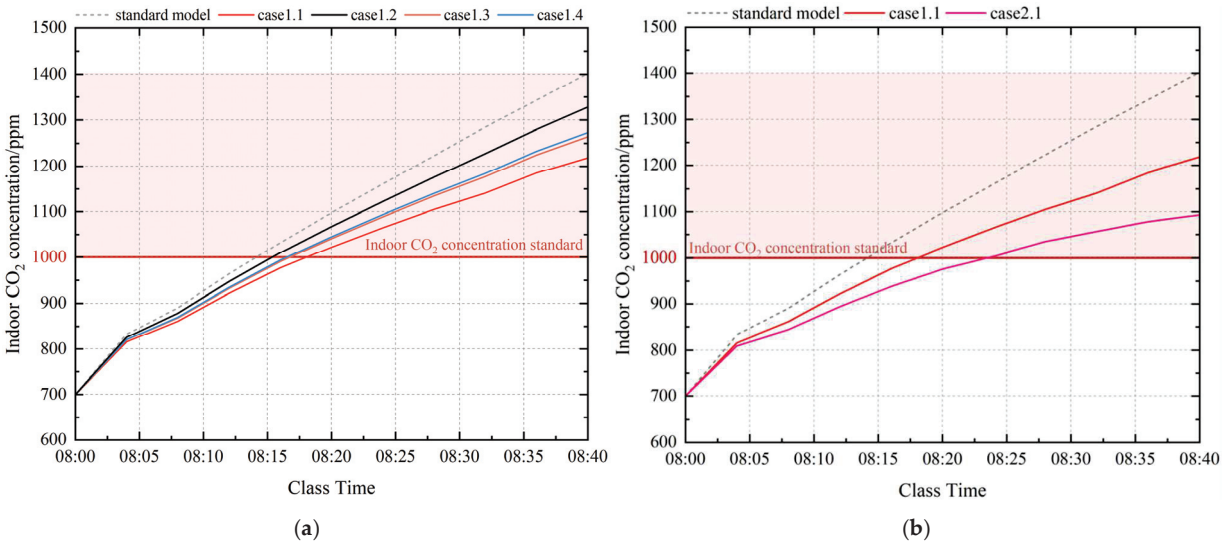


Figure 10. Effects of different door and window designs on indoor CO_2 concentration. (**a**) Effect of different window height on CO_2 concentration (**b**) Effect of the number of entrances on CO_2 concentration.

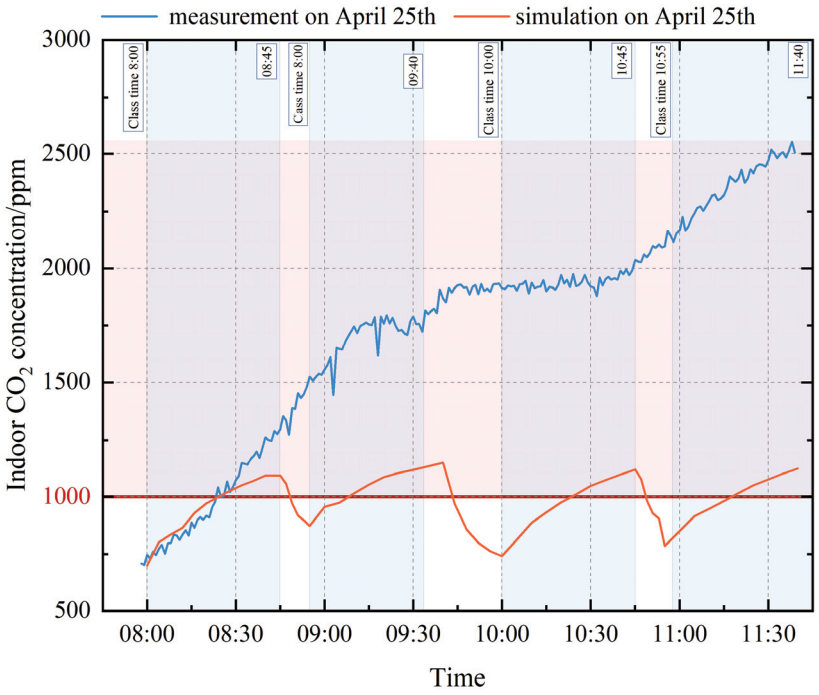


Figure 11. Comparison of the measured data and ventilation design strategy simulation results for the medium-sized classrooms on April 25th.

3.3.4. Indoor Temperature and PMV Simulation Results

Figure 12a shows the simulation results for the indoor temperature field over time in Case 1.1. In the first 40 min of the class, the average indoor temperature increased

from 21 °C to 25.1 °C, and the indoor temperature at the seated level of indoor occupants fluctuated between 24 °C and 26 °C. The average PMV was −0.0791, and the overall indoor thermal comfort was fair. As shown in Figure 12b, 40 min after the class began, the average indoor temperature was 24.2 °C and the overall indoor temperature was relatively low. In addition, compared with the cloud image for Case 1.1, the changes in indoor temperature in the middle area of the classroom and before and after the start of class were obvious. The PMV value was −0.32, and the level of indoor thermal comfort was generally low.

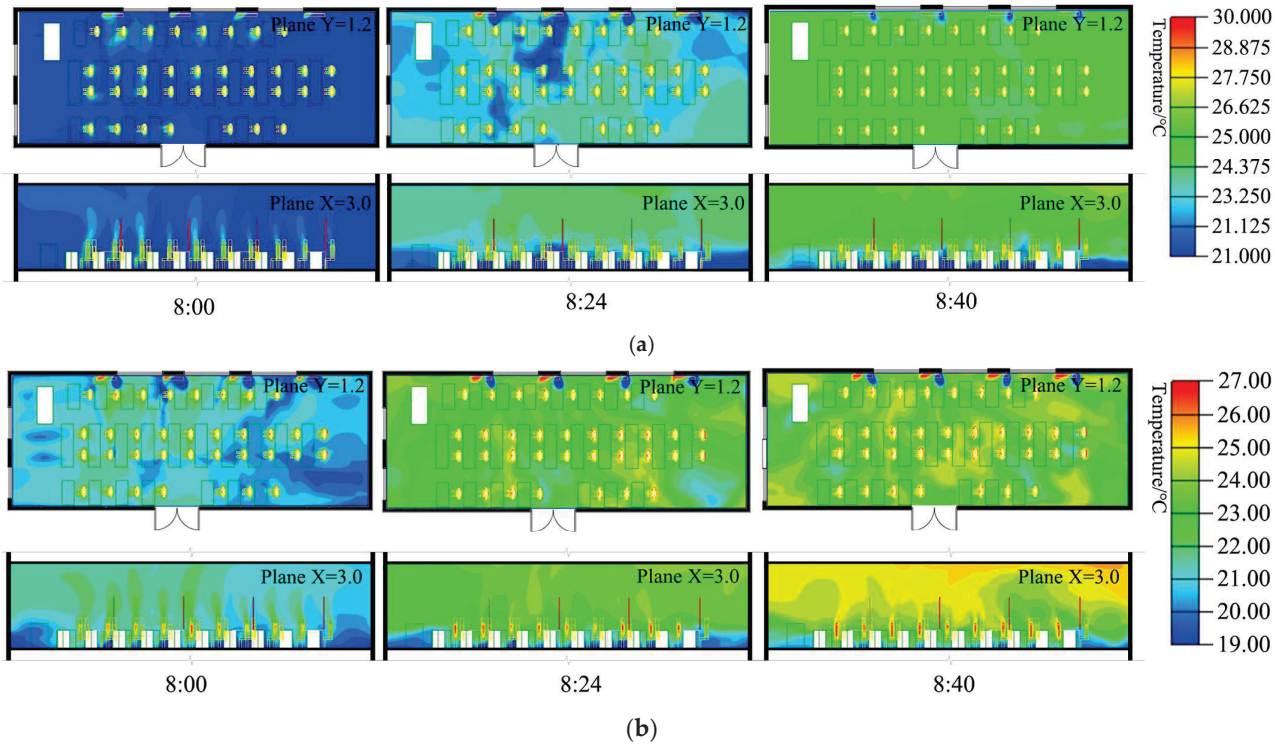


Figure 12. Cloud maps of room temperature changes after 40 min of class. (**a**) Case 1.1: indoor temperature simulation results. (**b**) Case 2.1: indoor temperature simulation results.

4. Discussion

4.1. Effects of Window Height and Number of Entrances and Exits on CO_2 Distribution

The simulation results for adjusting the height of classroom transom windows show that this measure effectively reduced indoor CO_2 concentration. In the design of teaching spaces in cold regions of China, emphasis is placed on cold-proofing and insulation performance, resulting in fewer and smaller openings of doors and windows. However, the efficiency of natural ventilation is often overlooked. According to the simulation data from this study, a transom window height of 3.2 m achieved the best dispersal of indoor CO_2 accumulation. Horizontally, installing transom windows was found to facilitate the discharge of indoor air via infiltration through door and window gaps. Additionally, the study found that selecting an appropriate number of entrances alleviated indoor air quality issues. Figure 13a,b show CO_2 distribution cloud maps for Case 1.1 (one entrance) and Case 2.1 (two entrances), respectively. Compared with that in Case 1.1, the accumulation of CO_2 toward the classroom ceiling was reduced in Case 2.1. The simulation cloud map for Case 2.1 indicates that adding entrances effectively lowered the CO_2 concentration in the horizontal direction of the front and rear spaces of the classroom, but the variation in CO_2 concentration in the middle part of the classroom was relatively small.

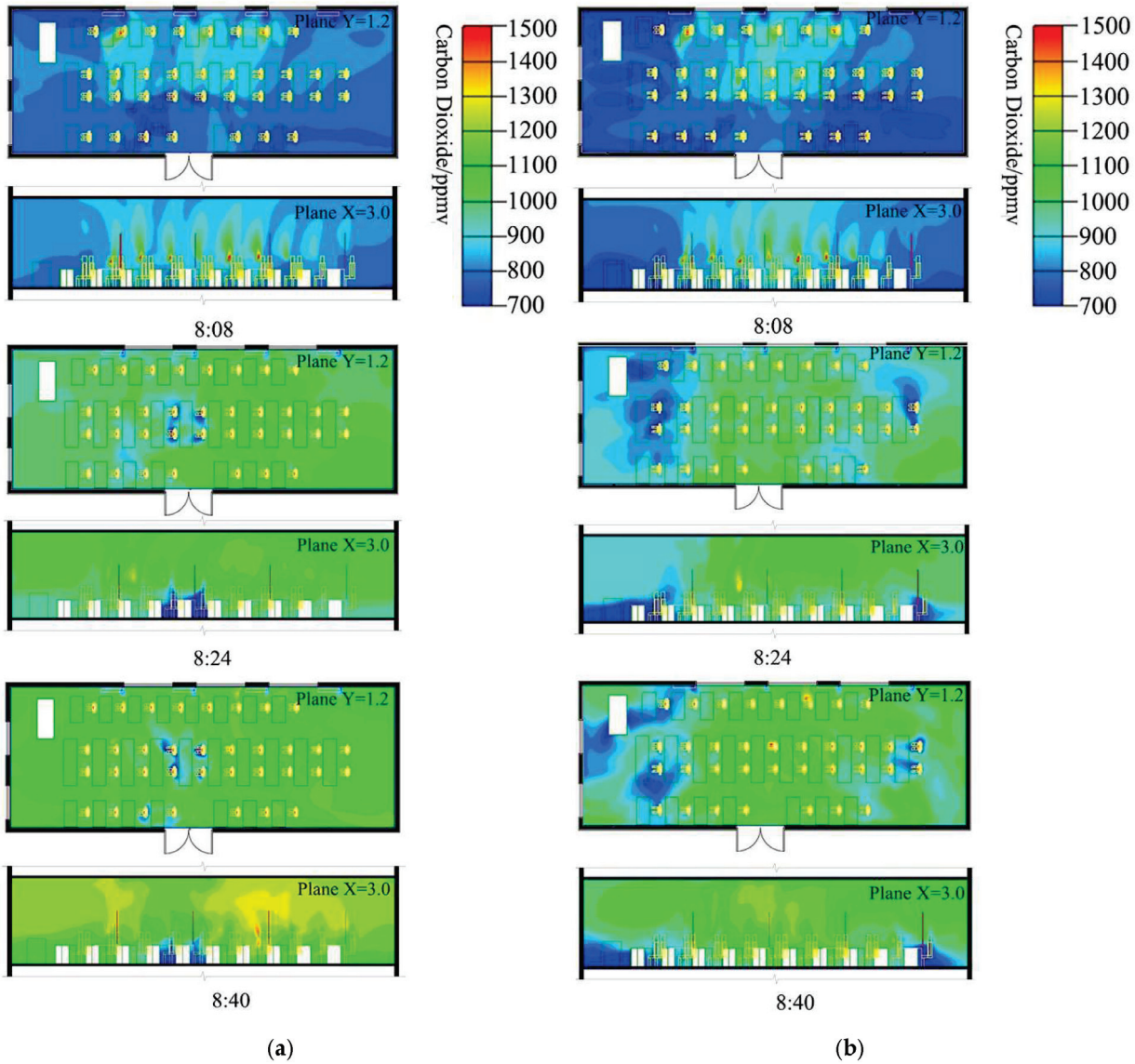


Figure 13. Standardised model of indoor average CO_2 concentration change. (**a**) Case 1.1 (one entrance): simulation results for indoor CO2 concentration. (**b**) Case 2.1 (two entrances): simulation results for indoor CO_2 concentration.

Changes in outdoor climate can significantly affect the effectiveness of ventilation strategies, especially the balance between maintaining thermal comfort and ensuring adequate indoor air quality. Table 6 shows the outdoor temperature data during the monitoring test. It can be seen that the outdoor temperature during this period is low, and the average outdoor temperature is 6.38 °C. It reflects the outdoor climate characteristics in the cold region during the transition season. In cold weather with lower average temperatures (such as April 23 and April 24), natural ventilation from windows and beams may be limited due to heat loss issues, which can lead to higher CO_2 concentrations in the room. On the contrary, in warm weather (such as April 25), the feasibility of extended ventilation increases, thus diluting CO_2 more effectively. These findings highlight the need for adaptive ventilation strategies that take into account real-time meteorological conditions, such as intermittent ventilation plans or dynamic control of window openings based on fluctuations in outdoor temperature.

Table 6. Outdoor temperature during monitoring.

Temperature	Monitoring Date				
	April 22nd	April 23rd	April 24th	April 25th	April 26th
T_{max} (°C)	10.90	10.79	15.71	10.63	13.37
T_{min} (°C)	−1.92	−1.19	−0.90	−0.44	−2.50
$T_{average}$ (°C)	5.00	5.43	8.77	5.60	7.09

During winter, the outdoor temperature in cities in cold regions of China is extremely low, and opening external windows to facilitate natural ventilation to reduce indoor CO_2 concentration is not conducive to indoor thermal insulation. Based on comparative analysis of the simulation results, this study suggests that the number of windows and entrances should be established according to the size of the classroom space. In addition, horizontal windows should be opened during classroom occupancy to improve the natural ventilation efficiency without affecting indoor thermal comfort and slow down the accumulation of indoor CO_2 during class. Therefore, this study proposes the following optimization suggestions to provide guidance for future design practice:

- It is recommended that policymakers revise ventilation standards for education spaces in cold regions to incorporate intermittent ventilation strategies to optimize indoor air quality and thermal comfort during the transition season in the region.
- At the level of architectural design, the air tightness of the building envelope and doors and windows should be reasonably designed, and the relationship between heat preservation and ventilation should be balanced.
- The opening area of the outer window should be reasonably designed for the setting of doors and windows of the teaching space. In addition, considering the addition of the number of classroom entrances and porch windows can effectively help improve the quality of indoor air environment.
- In order to ensure the practical application and effectiveness of the proposed intermittent ventilation strategy, we suggest that coarse filters can be used appropriately to help maintain the CO_2 concentration in the indoor education space below 1000 ppm.
- In order to ensure that the ventilation strategy during teaching space breaks can achieve the plot effect, it is recommended that the ventilation volume value range of large classrooms, middle classrooms and small classrooms be 4 h^{-1} to 6 h^{-1}.

4.2. Balancing Indoor Air Quality and Thermal Comfort

The simulation results for intermittent ventilation show that reasonable natural ventilation effectively reduced indoor CO_2 concentrations and maintained them within the specified range. Figure 14 illustrates temperature contour maps during different ventilation measures, with the PMV values for the three stages being −0.23, −0.09, and −0.6, respectively, indicating good indoor thermal comfort. Compared with natural ventilation during occupied periods, the indoor PMV value of natural ventilation during unoccupied periods was significantly lower, and the rate of decline of CO_2 concentration was accelerated.

University teaching spaces, which are crucial for learning activities among faculty and students, can experience elevated CO_2 concentrations, which negatively impact students' learning efficiency. Some studies have suggested that adequate ventilation can help improve indoor air quality in classrooms, but students' thermal comfort may also be affected to varying degrees [17]. Similarly, Cordero et al. 's study emphasizes the ability of dynamically controlled window opening modes to coordinate air quality and thermal comfort [42]. In addition, Kaushik et al. 's research shows that reasonable door and window area and ventilation volume can effectively balance the relationship between indoor environmental quality and thermal comfort [33]. In order to reduce indoor heat loss and achieve thermal insulation effect, Ai et al. proposed that short-term mechanical ventilation strategies could be used to help indoor environmental quality quickly reach an acceptable level [43]. Therefore, it is essential to design the doors, windows, and other entrances to educational

spaces in cold regions of China to reduce indoor CO_2 concentrations while ensuring indoor thermal comfort during winter. Intermittent ventilation, an effective means of improving indoor air quality, can effectively lower indoor CO_2 concentrations. Based on this study's simulation results, it is advisable to keep corridor windows open during class periods while closing external windows and doors to classrooms. During breaks, classroom front doors should be kept open for ventilation, and after class, corridor windows and front doors should be opened for ventilation while keeping external windows closed.

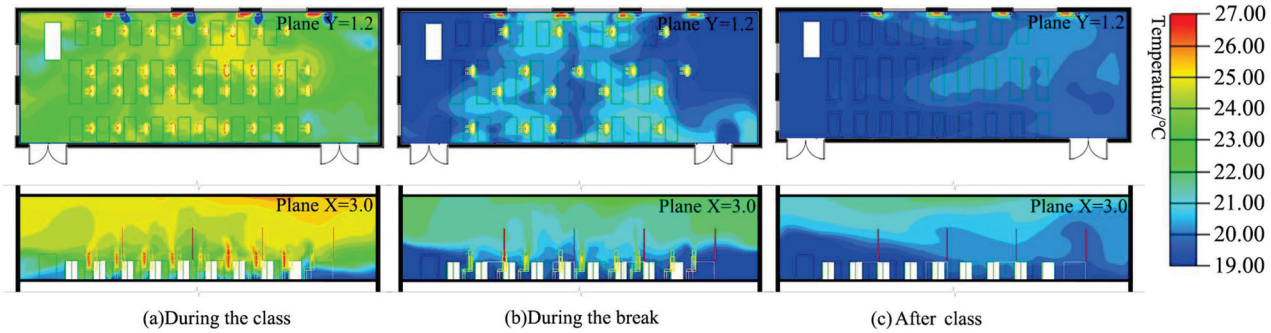


Figure 14. Corrected standardised model of indoor average CO_2 concentration change.

4.3. Limitations

Due to the limitation of experimental conditions, the monitoring time of this study is short, and experimental studies on indoor thermal environment and air quality of teaching space in different seasons should be supplemented in the future. The results of this study highlight the challenges faced by indoor air quality and thermal comfort in teaching spaces in cold regions, but lack a comparative study on the influence of different natural ventilation modes on the results from different seasonal variations. Future studies could expand the monitoring period to capture conditions across different seasons to provide a more comprehensive understanding.

In addition, the limit of indoor CO_2 threshold range (1000 ppm) in this study refers to the Chinese standard, which is different from the international standard. Future research work should emphasize the practicability of different standards to evaluate indoor air quality in teaching spaces in cold regions of China, so as to further promote the construction of healthy indoor environment. Meanwhile, compared with the steady-state ventilation strategy emphasized by CETIAT (France, 2001), this study focuses on exploring the advantages of intermittent ventilation strategy in balancing energy efficiency and thermal comfort.

5. Conclusions

The simulation and monitoring results indicated that indoor CO_2 concentration exceeds the standard in university building teaching spaces in cold regions of China due to poor ventilation. The study also explored methods of effectively improving indoor air quality. The main research findings were as follows:

(1) The measured indoor CO_2 concentration in three classrooms of different volumes during class periods all exceeded the standard requirement (1000 ppm). The peak CO_2 concentrations in the large, medium-sized, and small classrooms reached 1970 ppm, 2751 ppm, and 3200 ppm, respectively. During classroom occupancy, CO_2 concentration exceeding the standard accounted for 89%, 93%, and 88%, respectively, of class time.

(2) Installing transom windows or increasing the number of entrances can effectively reduce indoor CO_2 concentration. The simulation results demonstrated that setting transom windows at a height of 3.2 m indoors reduced the peak CO_2 concentration during class periods from 1402 ppm to 1218 ppm, effectively slowing down the accumulation rate of CO_2. Compared with classrooms with one entrance set in the middle of the interior wall, classrooms with entrances set in both the front and back walls were more conducive to CO_2 reduction. The CO_2 concentrations in classrooms with one entrance and two entrances

were 1218 ppm and 1093 ppm, respectively. It is suggested that the relevant standards for teaching spaces in cold regions can be appropriately added transom windows to solve the problems of indoor air quality and indoor thermal comfort in the transitional season in this area.

(3) Segmental ventilation can effectively reduce indoor CO_2 concentration. In this study, reasonable ventilation strategies were found to reduce the peak indoor CO_2 concentration from 2551 ppm to 1149 ppm, with the proportion of class time for which CO_2 concentration exceeded the standard decreasing from 87% to 47%. Policymakers and architects should improve the design of doors and windows for teaching spaces in cold regions of China and propose reasonable ventilation strategies. On the premise of ensuring thermal comfort, it is recommended to improve indoor air quality through intermittent ventilation.

Author Contributions: J.Y.: writing—original draft and data curation. H.W.: resources, investigation, and data curation. Y.S.: visualization, project administration, methodology, and data curation. Y.X.: visualization, validation, software, and methodology. Y.C.: first draft, conceptualization, and validation. All authors have read and agreed to the published version of the manuscript.

Funding: This research was funded by the National Natural Science Foundation of China, grant number 52078153.

Data Availability Statement: The original contributions presented in the study are included in the article, further inquiries can be directed to the corresponding author.

Conflicts of Interest: The authors declare that they have no known competing financial interests or personal relationships that could have appeared to influence the work reported in this paper.

References

1. Fu, N.; Wei, P.; Jia, Y.; Zheng, X.; Guan, J. Indoor volatile organic compounds in densely occupied education buildings of four universities: Target list, concentration levels and correlation analysis. *Build. Environ.* **2021**, *191*, 107599. [CrossRef]
2. Razali, N.Y.Y.; Latif, M.T.; Dominick, D.; Mohamad, N.; Sulaiman, F.R.; Srithawirat, T. Concentration of particulate matter, CO and CO_2 in selected schools in Malaysia. *Build. Environ.* **2015**, *87*, 108–116. [CrossRef]
3. Chen, Y.; Chen, B.; Deng, J.; Xu, S. The integration model of objective and subjective data of residential indoor environment quality in Northeast China based on structural equation modeling. *Build. Simul.* **2022**, *15*, 741–754. [CrossRef]
4. Ding, E.; Zhang, D.; Bluyssen, P.M. Ventilation regimes of school classrooms against airborne transmission of infectious respiratory droplets: A review. *Build. Environ.* **2022**, *207*, 108484. [CrossRef]
5. Remion, G.; Moujalled, B.; El Mankibi, M. Review of tracer gas-based methods for the characterization of natural ventilation performance: Comparative analysis of their accuracy. *Build. Environ.* **2019**, *160*, 106180. [CrossRef]
6. Huang, K.; Feng, G.; Zhao, L.; Chang, S.; Jiang, M. Survey of Window-Opening Behavior of Severe Cold Area in Winter and Relevant Energy Consumption Analysis. In Proceedings of the 8th International Symposium on Heating, Ventilation and Air Conditioning: Volume 3: Building Simulation and Information Management; Li, A., Zhu, Y., Li, Y., Eds.; Springer: Berlin/Heidelberg, Germany, 2014; pp. 523–533. [CrossRef]
7. Lei, Z.; Liu, C.; Wang, L.; Li, N. Effect of natural ventilation on indoor air quality and thermal comfort in dormitory during winter. *Build. Environ.* **2017**, *125*, 240–247. [CrossRef]
8. Kuwahara, R.; Kim, H. Studying the Indoor Environment and Comfort of a University Laboratory: Air-Conditioning Operation and Natural Ventilation Used as a Countermeasure against COVID-19. *Buildings* **2022**, *12*, 953. [CrossRef]
9. Canha, N.; Almeida, S.M.; Freitas, M.C.; Taubel, M.; Hanninen, O. Winter Ventilation Rates at Primary Schools: Comparison Between Portugal and Finland. *J. Toxicol. Environ. Health* **2013**, *76*, 400–408. [CrossRef]
10. Zhao, Y.; Sun, H.; Tu, D. Effect of mechanical ventilation and natural ventilation on indoor climates in Urumqi residential buildings. *Build. Environ.* **2018**, *144*, 108–118. [CrossRef]
11. Deng, X.; Tan, Z. Numerical analysis of local thermal comfort in a plan office under natural ventilation. *Indoor Built Environ.* **2020**, *29*, 972–986. [CrossRef]
12. Zhang, H.; Liu, Z. Influence of winter natural ventilation on thermal environment of university dormitories under central heating mode in severe cold regions of China. *Archit. Sci. Rev.* **2023**, *66*, 226–241. [CrossRef]
13. Yang, X.; Sun, D.; Zhou, X.; Cai, L.; Ji, Y. Indoor thermal comfort and its effect on building energy consumption. In *Frontiers of Green Building, Materials and Civil Engineering PTS 1-8*; Sun, D., Sung, W.P., Chen, R., Eds.; Trans Tech Publications Ltd.: Stafa-Zurich, Switzerland, 2011; pp. 3516–3519. [CrossRef]
14. Djongyang, N.; Tchinda, R.; Njomo, D. Thermal comfort: A review paper, Renew. *Sustain. Energy Rev.* **2010**, *14*, 2626–2640. [CrossRef]

15. Wong, N.H.; Feriadi, H.; Lim, P.Y.; Tham, K.W.; Sekhar, C.; Cheong, K.W. Thermal comfort evaluation of naturally ventilated public housing in Singapore. *Build. Environ.* **2002**, *37*, 1267–1277. [CrossRef]
16. Jowkar, M.; de Dear, R.; Brusey, J. Influence of long-term thermal history on thermal comfort and preference. *Energy Build.* **2020**, *210*, 109685. [CrossRef]
17. Miao, S.; Gangolells, M.; Tejedor, B. A Comprehensive Assessment of Indoor Air Quality and Thermal Comfort in Educational Buildings in the Mediterranean Climate. *Indoor Air* **2023**, *2023*, 6649829. [CrossRef]
18. Babich, F.; Torriani, G.; Corona, J.; Lara-Ibeas, I. Comparison of indoor air quality and thermal comfort standards and variations in exceedance for school buildings. *J. Build. Eng.* **2023**, *71*, 106405. [CrossRef]
19. Peng, B.; Gao, D.; Wang, M.; Zhang, Y. 3D-STCNN: Spatiotemporal Convolutional Neural Network Based on EEG 3D Features for Detecting Driving Fatigue. *J. Data Sci. Intell. Syst* **2024**, *2*. [CrossRef]
20. Haghirad, M.; Heidari, S.; Hosseini, H. Advancing personal thermal comfort prediction: A data-driven framework integrating environmental and occupant dynamics using machine learning. *Build. Environ.* **2024**, *262*, 111799. [CrossRef]
21. Apte, M.G.; Fisk, W.J.; Daisey, J.M. Associations between indoor CO_2 concentrations and sick building syndrome symptoms in US office buildings: An analysis of the 1994-1996 BASE study data. *Indoor Air-Int. J. Indoor Air Qual. Clim.* **2000**, *10*, 246–257. [CrossRef]
22. Johnson, D.L.; Lynch, R.A.; Floyd, E.L.; Wang, J.; Bartels, J.N. Indoor air quality in classrooms: Environmental measures and effective ventilation rate modeling in urban elementary schools. *Build. Environ.* **2018**, *136*, 185–197. [CrossRef]
23. Geelen, L.M.J.; Huijbregts, M.A.J.; Ragas, A.M.J.; Bretveld, R.W.; Jans, H.W.A.; van Doorn, W.J.; Evertz, S.J.C.J.; van der Zijden, A. Comparing the effectiveness of interventions to improve ventilation behavior in primary schools. *Indoor Air* **2008**, *18*, 416–424. [CrossRef] [PubMed]
24. Chatzidiakou, L.; Mumovic, D.; Summerfield, A. Is CO_2 a good proxy for indoor air quality in classrooms? Part 2: Health outcomes and perceived indoor air quality in relation to classroom exposure and building characteristics. *Build. Serv. Eng. Res. Technol.* **2015**, *36*, 162–181. [CrossRef]
25. Vilcekova, S.; Budaiova, Z. Productivity and Indoor Environmental Quality in Offices. In *Energy Clean Technology*; Stef92 Technology Ltd.: Sofia, Bulgaria, 2015; pp. 993–1000. Available online: https://webofscience.clarivate.cn/wos/alldb/summary/f1c86051-5541-4b05-ad28-ad2a25c6da65-df84e0b0/relevance/1 (accessed on 16 April 2024).
26. Daisey, J.M.; Angell, W.J.; Apte, M.G. Indoor air quality, ventilation and health symptoms in schools: An analysis of existing information. *Indoor Air* **2003**, *13*, 53–64. [CrossRef] [PubMed]
27. Bourbeau, J.; Brisson, C.; Allaire, S. Prevalence of the sick building syndrome symptoms in office workers before and after being exposed to a building with an improved ventilation system. *Occup. Environ. Med.* **1996**, *53*, 204–210. [CrossRef]
28. Petersen, S.; Jensen, K.L.; Pedersen, A.L.S.; Rasmussen, H.S. The effect of increased classroom ventilation rate indicated by reduced CO_2 concentration on the performance of schoolwork by children. *Indoor Air* **2016**, *26*, 366–379. [CrossRef]
29. Bako-Biro, Z.; Clements-Croome, D.J.; Kochhar, N.; Awbi, H.B.; Williams, M.J. Ventilation rates in schools and pupils' performance. *Build. Environ.* **2012**, *48*, 215–223. [CrossRef]
30. Clements-Croome, D.J.; Awbi, H.B.; Bako-Biro, Z.; Kochhar, N.; Williams, M. Ventilation rates in schools. *Build. Environ.* **2008**, *43*, 362–367. [CrossRef]
31. Franke, M.; Nadler, C. Towards a holistic approach for assessing the impact of IEQ on satisfaction, health, and productivity. *Build. Res. Inf.* **2021**, *49*, 417–444. [CrossRef]
32. Xiong, L.; Huang, X.; Li, J.; Mao, P.; Wang, X.; Wang, R.; Tang, M. Impact of Indoor Physical Environment on Learning Efficiency in Different Types of Tasks: A $3 \times 4 \times 3$ Full Factorial Design Analysis. *Int. J. Environ. Res. Public. Health* **2018**, *15*, 1256. [CrossRef]
33. Kaushik, A.; Arif, M.; Tumula, P.; Ebohon, O.J. Effect of thermal comfort on occupant productivity in office buildings: Response surface analysis. *Build. Environ.* **2020**, *180*, 107021. [CrossRef]
34. MOHURD. *Hygienic Requirements for Ventilation in Primary and Secondary School Classrooms*; MOHURD: Beijing, China, 2017.
35. Qabbal, L.; Younsi, Z.; Naji, H. An indoor air quality and thermal comfort appraisal in a retrofitted university building via low-cost smart sensor. *Indoor Built Environ.* **2022**, *31*, 586–606. [CrossRef]
36. Cao, S.-J.; Yu, C.W.; Luo, X. Heating, ventilating and air conditioning system and environmental control for wellbeing. *Indoor Built Environ.* **2020**, *29*, 1191–1194. [CrossRef]
37. Canha, N.; Mandin, C.; Ramalho, O.; Wyart, G.; Riberon, J.; Dassonville, C.; Hanninen, O.; Almeida, S.M.; Derbez, M. Assessment of ventilation and indoor air pollutants in nursery and elementary schools in France. *Indoor Air* **2016**, *26*, 350–365. [CrossRef] [PubMed]
38. Haverinen-Shaughnessy, U.; Moschandreas, D.J.; Shaughnessy, R.J. Association between substandard classroom ventilation rates and students' academic achievement. *Indoor Air* **2011**, *21*, 121–131. [CrossRef]
39. Al Mindeel, T.; Spentzou, E.; Eftekhari, M. Energy, thermal comfort, and indoor air quality: Multi-objective optimization review. *Renew. Sustain. Energy Rev.* **2024**, *202*, 114682. [CrossRef]
40. Chen, S.; Fan, Z.; He, L.; Ma, S.; Liu, J. Ventilation benefit assessment of space organization design for "L" type inner corridor buildings. *Build. Environ.* **2024**, *253*, 111327. [CrossRef]
41. de Dear, R.J.; Akimoto, T.; Arens, E.A.; Brager, G.; Candido, C.; Cheong, K.W.D.; Li, B.; Nishihara, N.; Sekhar, S.C.; Tanabe, S.; et al. Progress in thermal comfort research over the last twenty years. *Indoor Air* **2013**, *23*, 442–461. [CrossRef]

42. Cordero, A.; Melgar, S.; Márquez, J. Validation of Dynamic Natural Ventilation Protocols for Optimal Indoor Air Quality and Thermal Adaptive Comfort during the Winter Season in Subtropical-Climate School Buildings. *Appl. Sci.* **2024**, *14*, 4651. [CrossRef]
43. Ai, Z.; Mak, C.; Cui, D.; Xue, P. Ventilation of air-conditioned residential buildings: A case study in Hong Kong. *Energy Build.* **2016**, *127*, 116–127. [CrossRef]

Disclaimer/Publisher's Note: The statements, opinions and data contained in all publications are solely those of the individual author(s) and contributor(s) and not of MDPI and/or the editor(s). MDPI and/or the editor(s) disclaim responsibility for any injury to people or property resulting from any ideas, methods, instructions or products referred to in the content.

buildings

MDPI

Article

Exploring Optimisation Pathways for Underground Space Quality Under the Synergy of Multidimensional Perception and Environmental Parameters

Tianning Yao [1], Liang Sun [1,*], Lin Geng [2], Yao Xu [3,*], Ziqi Xu [1], Kuntao Hu [1], Xing Chen [1], Pan Liao [1] and Jin Wang [4]

[1] School of Architecture & Design, China University of Mining and Technology, Xuzhou 221116, China; tianning_yao@cumt.edu.cn (T.Y.); ts22190042p31@cumt.edu.cn (Z.X.); ts22190026p31@cumt.edu.cn (K.H.); ts22190020p31@cumt.edu.cn (X.C.); pan.liao@mymail.unisa.edu.au (P.L.)
[2] School of Architecture and Design, Harbin Institute of Technology, Harbin 150001, China; 22b934024@stu.hit.edu.cn
[3] School of Architecture, Southwest Jiaotong University, Chengdu 611756, China
[4] School of Civil Engineering, Yancheng Institute of Technology, Yancheng 224051, China; wangjin@ycit.edu.cn
* Correspondence: sunliang@cumt.edu.cn (L.S.); xuyao@my.swjtu.edu.cn (Y.X.); Tel.: +86-1390520807 (L.S.); +86-18955231912 (Y.X.)

Abstract: With the acceleration of urbanisation and the increased utilisation of underground space, providing a comfortable and healthy environment in public underground areas has emerged as a significant research topic. This study constructs a comprehensive decision-making framework for underground space environments by integrating human perception evaluations with physical environmental parameters. Using Shanghai Wujiaochang as a case study, field data collection and questionnaire surveys were conducted to evaluate key factors such as temperature (22.63 °C–26.39 °C), wind speed (0.26 m/s–0.67 m/s), and sound levels (59.68 dB–61.21 dB) for commercial-oriented spaces, and 63.15 dB–75.45 dB for transport-oriented spaces) to users' perceived experiences. The appropriate ranges for key parameters were identified through single-indicator fitted regression analysis and the XGBoost machine-learning model, revealing the relationship between environmental parameters and human perception. The results indicated significant differences in user needs across various functional spaces, with commercial-oriented areas emphasising environmental attractiveness and comfort, while transport-oriented spaces prioritised access efficiency and safety. This study provided quantitative design benchmarks for underground spaces' dynamic regulation and sustainable management, proposing a precise and adaptive environmental decision-making framework that combines physical parameters with user-perception feedback.

Keywords: underground space; multidimensional perception; environmental regulation; machine learning; suitability parameters

1. Introduction

1.1. Underground Space in the Perspective of Globalisation

With the acceleration of urbanisation, cities worldwide are confronting numerous challenges, including population growth, land resource shortages, and pressures on environmental sustainability. Traditional aboveground spaces fail to meet urbanisation

demands, highlighting the potential of underground spaces to alleviate urban strain. Research indicates that underground space development can effectively increase the liveable area by 25% to 40%, providing enhanced functional support for high-density urban environments [1,2]. Broere et al. have highlighted the unique potential of underground spaces in traffic diversion, commercial development, and emergency evacuation, emphasising that their development is vital for enhancing the overall carrying capacity of cities [3]. Nonetheless, the distinct environmental conditions of underground spaces—such as limited ventilation and inadequate natural light—place significant demands on design and management, which can directly impact user experience and usability [4,5].

In urban spatial-quality research, numerous studies have concentrated on aboveground public spaces, such as parks, streets, and transport hubs. Xu et al. have developed an urban vitality evaluation model utilising Point of Interest (POI) data to investigate the impact of spatial characteristics on urban functions from multiple dimensions [6]. Biljecki and Ito systematically analysed the environmental characteristics of urban streets through streetscape image data, establishing a methodological foundation for urban design and spatial optimisation [7]. Despite the significant advancements in methodology and technology, research on underground spaces remains insufficient, and a unified evaluation framework has yet to be established [8]. Additionally, Yap et al. identified, through international research, that public concern regarding the environmental quality of underground spaces primarily revolves around air quality and health and safety issues, underscoring the importance of environmental regulation in developing underground spaces [9]. The environmental quality of underground spaces impacts user comfort and is closely linked to psychological perception and behavioural patterns. Gao et al. demonstrated the significant influence of building density and functional zoning on psychological perception through quantitative analysis of public perceptions in metro station areas [10]. Sun et al. explored the visual saliency of the guidance system in an underground shopping street using eye movement experiments, emphasising the crucial role of visual elements in environmental design [11,12]. These studies indicate that traditional methods for evaluating physical environments have proven inadequate for comprehensively assessing the environmental quality of underground spaces. Consequently, integrating human perception with environmental regulation has emerged as a vital approach to addressing the complex environmental challenges associated with underground spaces.

1.2. Environmental Decision-Making with a Human Perspective

User-centred evaluation of human perception is a key focus in environmental regulation research. The classical Predicted Mean Vote (PMV) model, introduced by Fanger in 1970, is an assessment method based on physical parameters, including air temperature, relative humidity, radiant temperature, and clothing insulation coefficient, to measure human thermal comfort [13]. The PMV model has been extensively utilised to optimise thermal environments within buildings. For instance, Hong et al. assessed thermal comfort and energy balance in residences using PMV models, and their proposed personalised thermal environment adjustment strategies significantly enhanced the living experience [14]. Additionally, Zhang et al. have improved the PMV model by incorporating metabolic rate adjustments, thereby increasing its adaptability and predictive capability in complex scenarios [15]. The PMV model plays a prominent role in thermal comfort research. However, its focus on single physical dimensions limits its ability to capture users' multidimensional perceptual experiences in complex environments.

To address the limitations of a single-dimensional approach, the Indoor Environment Quality (IEQ) model offers a more comprehensive framework by integrating multidimen-

sional parameters, including air quality, lighting, thermal comfort, and noise, into the assessment [16]. Wong et al. explored the application of the IEQ model within the air-conditioning systems of office spaces, demonstrating its ability to balance user comfort with energy-saving efficiency, thereby providing a valuable reference for environmental regulation [17]. Dunleavy et al. further employed the IEQ model to investigate the psychological impacts of aboveground and underground working environments, revealing the significant influence of underground environmental conditions on users' psychological stress and emphasising the importance of psychological perception in environmental evaluation [18]. However, despite its broad applicability in integrating multidimensional parameters, the IEQ model exhibits limited responsiveness to individual user perceptions in dynamic environments, particularly in confined and complex scenarios such as underground spaces. This limitation indicates a need for further enhancement of the model's systematicity and relevance, as it may impact the accuracy of evaluation results and constrain its practical application in dynamic environment regulation.

In recent years, research methods in multi-sensory integration have opened new avenues for human-centred perception studies. Mittal et al. highlighted the significant role of visual perception in enhancing quality of life and optimising urban spatial environments, underscoring the core importance of the diversity and prominence of visual features in spatial design [19]. Gibson's Sensory Systems Theory further broadens the scope of perception research by advocating for the integrated analysis of multi-sensory data, including vision, hearing, and touch, to capture users' experiences of spatial environments more comprehensively [20,21]. The multi-sensory approach is particularly relevant in the study of underground spaces, where the enclosed nature of these environments often significantly influences users' perception patterns. Yao et al. experimentally categorised space into distinct features and identified substantial differences in perceptual preferences across various spatial orientations. This has provided a quantitative foundation for employing multidimensional perceptual measures in underground space [22]. Despite advancements in human-centred perception research at both theoretical and applied levels, several limitations persist. The interface between theoretical frameworks and practical perception evaluation methods remains imperfect, and the absence of a standardised framework results in inconsistencies between data collection and analysis outcomes. Furthermore, the capacity for real-time capture of subjective perceptual feedback in dynamic environments requires enhancement, particularly in the context of the closed and multifunctional nature of underground spaces, where evaluation results struggle to inform design optimisation directly. In this study, we constructed a framework combining multidimensional perception evaluation and environmental parameter regulation to cope with the above problems and further explore the interaction between user perception and environmental quality.

1.3. Machine Learning Applied to Environmental Evaluation Systems

With the advancement of big data technology, machine learning has emerged as a pivotal tool in environmental evaluation and optimisation research. Unlike traditional statistical methods, machine learning supports perceptual evaluation in dynamic environments through nonlinear modelling and efficient data processing. For instance, Liu et al. have automated the evaluation of large-scale urban environmental quality by analysing street view images using convolutional neural networks (CNNs), significantly enhancing research efficiency [23]. Similarly, Ye et al. have employed the SegNet algorithm to assess the visual quality of streets, further elucidating the potential mechanisms through which environmental design influenced user perceptions [24]. These studies illustrate that

machine learning can uncover latent patterns within complex data, providing a scientific foundation for environmental optimisation.

XGBoost, an integrated learning algorithm based on the Gradient-Boosting Decision Tree framework, has gained widespread application in environmental data modelling due to its high efficiency and predictive capabilities [25]. Tian et al. have utilised XGBoost to analyse psychological assessment data, successfully predicting users' moods in response to specific environmental changes, thereby offering dynamic modelling support for perceptual evaluation [26]. Furthermore, He et al. have integrated XGBoost with SHAP algorithms to examine the exact effects of environmental parameters on user perception, yielding highly accurate and interpretable results for multidimensional data correlation analyses in complex environments [27]. Additionally, Chen et al. have developed a prediction model for air quality in underground spaces using deep multitask learning, which has enhanced pollution monitoring accuracy and facilitated dynamic regulation of the spatial environment with quantitative support [28]. Collectively, these studies have demonstrated the significant technical value of machine learning in optimising underground space environments, providing crucial theoretical support for dynamic perceptual evaluation and design optimisation.

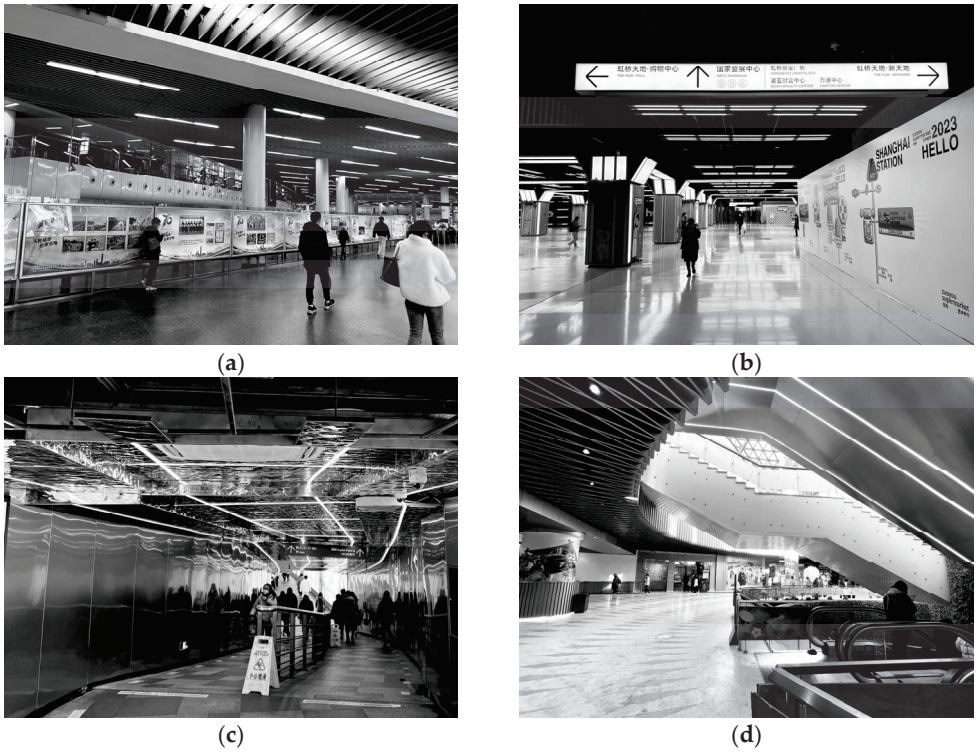
In summary, underground space has emerged as a focal point for research and application due to its potential to alleviate the pressures of urbanisation and enhance the functionality of cities. However, the unique environmental conditions of underground spaces have presented significant challenges for environmental management and user experience. While existing studies have made strides in evaluating single-dimensional physical parameters and multi-sensory fusion, there have remained notable deficiencies in dynamic environmental adaptation, integrating subjective perception with physical parameters, and developing a comprehensive optimisation framework. Furthermore, the techniques for acquiring and analysing perceptual evaluation data are not yet fully developed, complicating efforts to provide adequate guidance for practical environmental optimisation. To address these shortcomings, this paper has integrated human-centred perception with machine-learning techniques to propose a unified framework that explores the intricate relationship between environmental parameters and user perception, aiming to enhance underground spaces' environmental quality. The subsequent method section provides a detailed description of the research design, including data acquisition and processing, the extraction of multidimensional perception indicators, and the application of machine-learning models.

2. Materials and Methods

2.1. Case Study

Shanghai, the economic centre of China, is committed to leveraging urban renewal to enhance urban functions and focuses on urban renewal to improve urban functions, the living environment, and sustainable development. The spatial utilisation of urban underground spaces can effectively address urban challenges such as land shortages and traffic pollution [29]. With the rapid expansion of the metro system, the development of underground spaces in Shanghai has accelerated. Researchers have argued that the underground public spaces in Shanghai serve essential functions and necessitate careful planning and design to optimise their performance [30,31]. For this investigation, the study focused on four specific locations in Shanghai as the case study: (a) the underground space of Shanghai People's Square; (b) the underground space of Hongqiao Hub; (c) the public underground transport space at Jing An Temple; and (d) the underground space at Wujiaochang. The analysis revealed that case (a) was constructed earlier and exhibits

limited commercial activity. Case (b) is still in the early stages of construction, with many facilities yet to become operational. Case (c), primarily serving as a transportation hub, has a relatively singular function. In contrast, case (d) has undergone a reorganisation of spatial resources, possesses diverse functional attributes, and has remained vibrant over time. Consequently, case (d) was selected as the focus of this study, as shown in Figure 1.



(**a**) (**b**) (**c**) (**d**)

Figure 1. Case study of Shanghai: (**a**) the underground space of Shanghai People's Square; (**b**) the underground space of Hongqiao Hub; (**c**) the public underground transport space at Jing An Temple; and (**d**) the underground space at Wujiaochang.

Wujiaochang comprises five distinct roads that collectively delineate five representative commercial areas, as outlined in Table 1. From a human-centred perspective, a walking distance of approximately 500 m is generally acceptable [32]. Consequently, this study concentrates on the underground space of Wujiaochang within a 250 m radius as its primary research area. The autumn season was selected for data collection due to the mild climate conditions in Shanghai during this period, characterised by an average temperature close to the optimal 25 °C for human comfort. This temperature minimised the disparity between indoor and outdoor environments, thereby reducing the temperature-adaptation burden on participants and facilitating the collection of natural and stable environmental perception data.

Table 1. Basic information about the studied site.

No.	Name	Commercial Area × 10,000 m^2	Building Area × 10,000 m^2
A	Wanda Plaza	21	33
B	Bailian Youyicheng Shopping Mall	9	12
C	Heshenghui West Building	16	36
D	Youmai Life Plaza	3	4.5
E	Suning Plaza	1.5	3.5

Initially, spatial data were collected on-site, and the analysis was conducted using Depthmap X for quantification, employing the DBSCAN clustering function to delineate the functional spaces (specific operational processes are detailed in Appendix A) [33–35]. Ultimately, collection points exhibiting distinct functional characteristics were identified, as shown in Table 2. These areas include underground public walkways, commercial walkways, sunken plazas, and other public spaces. The collection points are categorised into commercial-oriented and transport-oriented points, with composite points indicating areas that serve both traffic and commercial functions, as depicted in Figure 2 and Table 2.

Table 2. Number of collection points.

Space Type	Point Number	Questionnaire Number
Commercial point	8	144
Transport point	10	164

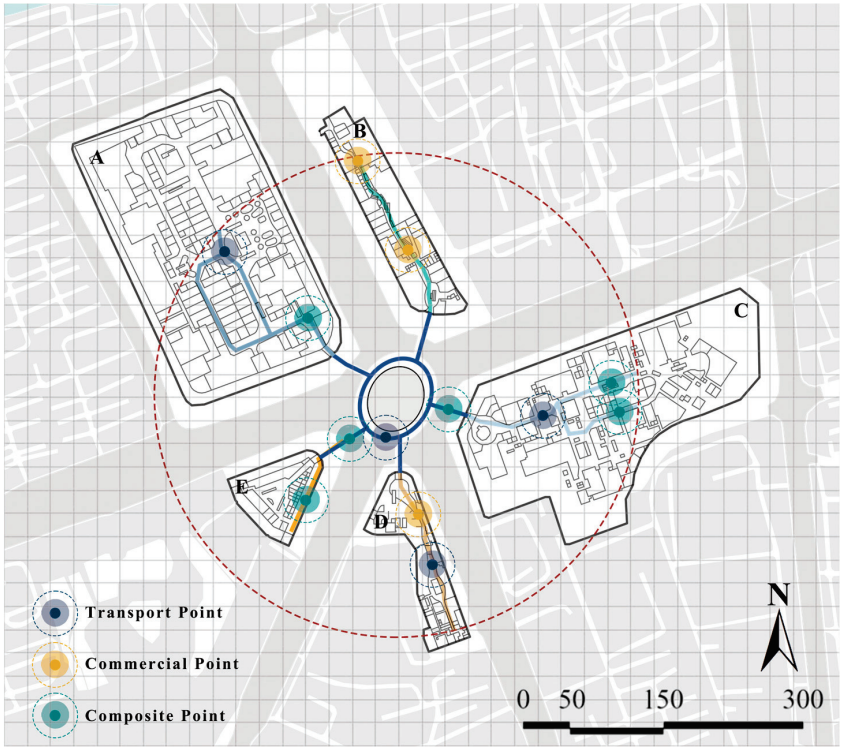


Figure 2. Location of the research object (units in m).

2.2. Research Framework

This study develops a decision-making model for the environmental management of underground public spaces, focusing on human-centred perception. The research is organised into three phases: (i) site selection and research—suitable research subjects are identified and examined through site investigations; (ii) indicator selection and definition—appropriate evaluation and measurement indicators are determined using literature analysis and the Delphi method; (iii) environmental data collection and measurement—on-site measurements emphasise the human-centred collection of spatial perception and physical environment data; and (iv) environmental data processing and analysis—the collected data are processed to identify suitable environmental parameters.

The study investigates the influence of physical environmental factors on users' perceptions of underground spaces and ultimately proposes strategies for regulating the spatial environment. The specific research steps are shown in Figure 3.

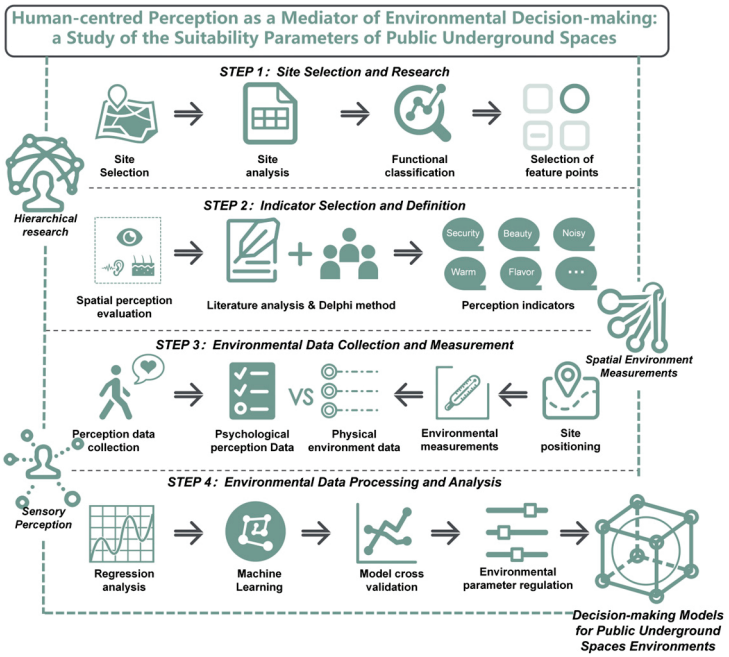


Figure 3. Research framework of the model.

2.3. Research Methodology

2.3.1. Step 1: Site Selection and Research

This research focuses on human interactions and employs the PSPL (Public Space and Public Life Survey) method. This research focuses on human interactions and employs the PSPL method. The PSPL method is frequently used to assess the quality of urban public spaces and remains a vital tool in contemporary studies of urban public spaces (Gehl et al.) [36]. Matan et al. [37] evaluated urban spaces in Australia using the PSPL method and proposed optimisations for these areas. Similarly, Fan and Shi [38] derived recommendations for enhancing urban spaces based on field studies of street-scale façades. A comparative analysis of various underground urban research cases in Shanghai revealed that the underground space in Wujiaochang exhibits a diverse spatial layout and significant pedestrian activity. Moreover, it is characterised by rich spatial functions and extensive traffic coverage. These attributes offer diverse environmental conditions and sufficient experimental samples, making it suitable for underground-space research.

2.3.2. Step 2: Indicator Selection and Definition

The existing research findings were systematically organised using a literature analysis method, identifying indicators of human-centred perception and the physical environment closely related to evaluating spatial quality. This literature analysis method was used to assess the quality and reliability of existing studies while identifying their biases and limitations, and it provided a theoretical basis and reference framework for this study. The Delphi method was then employed to refine the identified indicators.

This study involved a panel comprising five postgraduate students and eleven in-service faculty members, all from related fields, such as architecture and town and country planning. All panel members were required to be researchers in urban and environmental disciplines. Postgraduate members included MSc and PhD students in architecture and environmental studies with strong expertise and research backgrounds. Meanwhile, the in-service faculty members are senior professors and experts in architecture, characterised by their substantial practical experience and teaching history. In the initial consultation

round, the expert group identified pertinent perceptual and environmental indicators based on the existing literature. These indicators included dimensions such as vision [39], auditory [40], olfactory, somatosensory, taste, and other established international research categories. After a thorough screening process, 35 perceptual and 10 environmental indicators were initially recognised. The expert group members reevaluated and classified these preliminary indicators in the second consultation round. After extensive discussions, a refined selection emerged, comprising 22 perceptual and 7 environmental indicators, focusing on security, open, and wind strength. The third consultation round involved gathering anonymous feedback and facilitating targeted discussions based on the input received from the second round, which enabled the expert panellists to reach a consensus. Ultimately, three dimensions were established, consisting of 13 core perceptual indicators and six environmental indicators, which served as the evaluation criteria for assessing sensory perception of spatial quality in this study. Furthermore, a five-level Likert scale was utilised in the questionnaire design, and an additional dimension of 'perception satisfaction' was included as a criterion for evaluating spatial perception suitability, as shown in Table 3. The specialised definitions of each indicator are provided in Appendix B.

Table 3. Spatial-quality sensory-perception evaluation indicators.

Human-Centred Perception Indicator Evaluations						
	Visual-perception evaluation	Strongly disagree	Disagree	Neutral	Agree	Strongly agree
1.	Security	☐1	☐2	☐3	☐4	☐5
2.	Gorgeous	☐1	☐2	☐3	☐4	☐5
3.	Non-repression	☐1	☐2	☐3	☐4	☐5
4.	Beauty	☐1	☐2	☐3	☐4	☐5
5.	Interesting	☐1	☐2	☐3	☐4	☐5
6.	Open	☐1	☐2	☐3	☐4	☐5
7.	Comfortable Lighting	☐1	☐2	☐3	☐4	☐5
8.	Visual perception satisfaction	☐1	☐2	☐3	☐4	☐5
	Auditory perception evaluation	Strongly disagree	Disagree	Neutral	Agree	Strongly agree
9.	Quiet	☐1	☐2	☐3	☐4	☐5
10.	Varied	☐1	☐2	☐3	☐4	☐5
11.	Pleasant	☐1	☐2	☐3	☐4	☐5
12.	Auditory perception satisfaction	☐1	☐2	☐3	☐4	☐5
	Somatosensory perception evaluation	Strongly disagree	Disagree	Neutral	Agree	Strongly agree
13.	Good ventilation	☐1	☐2	☐3	☐4	☐5
14.	Wind strength	☐1	☐2	☐3	☐4	☐5
15.	Warm	☐1	☐2	☐3	☐4	☐5
16.	Somatosensory perception satisfaction	☐1	☐2	☐3	☐4	☐5
Physical environment indicator measurements						
	Measurement indicators	Average value			Unit	
1.	Aspect ratio	-			-	
2.	Humidity	-			Percentage (%)	
3.	Illumination	-			Lux (lx)	
4.	Sound	-			Decibels (dB)	
5.	Temperature	-			Degrees Celsius (°C)	
6.	Wind speed	-			Meters per second (m/s)	

2.3.3. STEP 3: Environmental Data Collection and Measurement

(1) Person-centred perceptual data acquisition

This study used a questionnaire to assess human-centred environmental perception on a defined scale. This approach demonstrated strong efficacy in research concerning urban spatial quality [41]. The study identified 13 locations within the site for evaluating human-centred environmental perception. Questionnaires were administered during three designated periods: 11:00–13:00, 14:00–16:00, and 17:30–19:30. Five architecture and planning students conducted the on-site questionnaires and gathered feedback from respondents. To enhance comprehension, the basic definitions of the indicators were explained to the respondents before the questionnaire. Additionally, respondents were reminded to perform on-site evaluations of their environment to ensure the relevance of their responses. The test subjects primarily consisted of approximately 200 passers-by at the venue, and the random selection of respondents ensured a diverse research sample.

(2) Physical environment data measurements

To assess the physical environmental data within the site, this study conducted several real-time measurements across 13 designated points, focusing on key parameters such as Sound, temperature, illumination, wind speed, and humidity. The measurement equipment included a Kanomax hot-wire anemometer for precise wind speed measurements; a CDT-8820 environmental tester for recording temperature, illuminance, and humidity; and a laser range finder to measure the cross-sectional scale of the site, ensuring accurate recording of physical environmental scales at each point. Data measurements were synchronised with questionnaires to analyse the impact of physical environmental factors on human perceptions. Data were collected from 11 October to 13 October 2023, ensuring continuity and comprehensive coverage.

2.3.4. STEP 4: Environmental Data Processing and Analysis

(1) Determination of indicator weights

This study employed a comprehensive weighting method that integrates the CRITIC and Entropy weight techniques to ascertain the weights of human-centred perception indicators across three dimensions. The Entropy weight method is advantageous, as it quantifies the information entropy of each indicator, enabling the determination of its importance based on the objective variability of the data, free from subjective influences [42]. Meanwhile, the CRITIC weight method ensures that the weight assigned to each indicator accurately reflects its overall impact by analysing the comparison coefficients and the intrinsic correlations among the indicators [43] (The specialised definitions of each weighting method are provided in Appendix C.). Consequently, combining these two methods facilitates a more precise determination of weights within each perceptual dimension, thereby establishing a robust scientific foundation for subsequent analysis.

(2) Correlation analysis

This study employed Kendall's tau-b (τ_b) correlation analysis to identify highly correlated human-centred perception indicators related to physical environment data. Kendall's tau-b (τ_b) is a non-parametric statistical method that effectively measures the correlation between two variables. It is particularly well-suited for analysing hierarchical and non-normally distributed data [44].

(3) Regression analysis

After identifying indicators that exhibit a high correlation with the physical environment data, this study conducted a regression analysis to investigate the relationship

between these perceptual indicators and physical environment variables, such as illuminance. The regression analysis aims to fit curves that clarify this relationship. This method proves effective in the regression analysis of spatial perception [45]. For the scores of the perceptual indicators, this study established a suitability range between 3.5 and 5. Fitting curves inferred the optimal environmental parameters for each perceptual indicator within this range, and the suitability parameters were derived by integrating data from actual measurement points.

3. Results

3.1. Human-Centred Perception Questionnaire Collection

In total, 236 questionnaires were collected during this field study (as detailed in Table 4), with 213 valid responses retained after screening. Among the respondents, 120 were male (56.34%) and 93 were female (43.66%). Regarding age distribution, the 18–29 age group represented the most significant proportion at 49.77%, followed by the 30–39 age group at 19.72%. Respondents under 18 (9.39%) and those over 60 (7.98%) constituted smaller portions of the sample. These results show that young and middle-aged adults, particularly those aged 18–39, form the primary user group of the underground walkway.

Table 4. Collection of Basic Information on the Questionnaire.

	Collection of Basic Information on the Questionnaire		
	Gender	Count	Percentage
1	Male	120	56.34%
2	Female	93	43.66%
	Age group	Count	Percentage
1	Below 18 years	20	9.39%
2	18–29 years	106	49.77%
3	30–39 years	42	19.72%
4	40–60 years	28	13.15%
5	Above 60 years	17	7.98%
	Functional use	Count	Percentage
1	Shopping	94	44.13%
2	Dining	89	41.78%
3	Leisure	87	40.85%
4	Transportation	83	38.97%
5	Walking	64	30.05%
6	Entertainment	62	29.11%
7	Work	35	16.43%
8	Rest	32	15.02%
9	Chatting	22	10.33%
10	Fitness	2	0.94%
11	Others	2	0.94%

The underground space was primarily utilised for commercial and transportation purposes. Specifically, shopping (44.13%), dining (41.78%), and leisure activities (40.85%) represented the main commercial functions, highlighting the space's emphasis on commercial usage. Transportation accounted for 38.97%, further demonstrating the space's dual role in supporting commerce and pedestrian mobility. In contrast, less frequent activities included resting (15.02%), chatting (10.33%), and fitness-related pursuits (0.94%), indicating that the space is more conducive to active, purpose-driven activities rather than passive or social interactions. Consequently, this study seeks to examine the relationship between environmental influences and human-centred perception by focusing on two functionally oriented spaces—commercial and transportation—as the core research contexts.

3.2. Data Standardisation and Empowerment

Table 5 presents the weight relationships among the three dimensions derived using the CRITIC and Entropy weighting methods. The auditory dimension has the highest weight, reaching 36.34%, signifying its dominant role in multidimensional perception. The somatosensory dimension is closely followed by a weight of 32.09%, highlighting the importance of somatosensory factors. In contrast, the visual dimension weighs 31.57%, slightly lower than the first two dimensions.

Table 5. Results of the combined weights method.

	Entropy Weight Method			**CRITIC Weight Method**				
Item	**Information Entropy Value e**	**Information Utility Valued**	**Weight (%)**	**Indicator Variability**	**Indicator Conflict**	**Information Quantity**	**Weight (%)**	**Final Weight (%)**
Visual dimension	0.977	0.023	32.62	1.081	0.646	0.699	30.51	31.57
Auditory dimension	0.974	0.026	37.91	1.094	0.728	0.796	34.77	36.34
Somatosensory dimension	0.980	0.020	29.46	1.049	0.758	0.795	34.72	32.09

3.3. Correlation Analysis of Human-Centred Perception Evaluation and Physical Environment Data

Figure 4 shows that the various space types exhibit distinct correlation patterns. Aspect ratio significantly influenced commercial-oriented spaces, showing a strong positive correlation with wind strength (correlation coefficient = 0.171). Additionally, humidity showed a moderate positive correlation with good ventilation and wind strength, with correlation coefficients of 0.157 and 0.118, respectively. Furthermore, illumination was significantly correlated with comfortable lighting and security, with correlation coefficients of 0.178 and 0.138. Although some correlation trends resemble those in transport-oriented spaces, significant differences exist in commercial-oriented spaces. The correlation between aspect ratio and wind strength remains notable, with a correlation coefficient of 0.140. Illumination plays a more significant role in the transport-oriented space, exhibiting positive correlations with security and openness, with correlation coefficients of 0.185 and 0.160, respectively. Additionally, wind speed emerges as the dominant factor, displaying the highest correlations with good ventilation and wind strength, with correlation coefficients of 0.291 and 0.288.

Nevertheless, certain factors, such as temperature and sound, exhibit weaker correlations in transport-oriented spaces than commercial-oriented spaces. For instance, the correlation between temperature and wind strength is only -0.080, indicating a limited impact on user perception under typical conditions. However, the subtle differences in these correlations across spatial contexts underscore the importance of prioritising key parameters for various functional types of environments.

Through the screening and organisation of the correlation results between human perceptual indicators and physical environment parameters, Table 6 illustrates the relationships between various physical environment data (aspect ratio, humidity, illumination, sound, temperature, and wind speed) and the perceptual dimensions (visual, auditory, and somatosensory). Additionally, it categorises the specific perceptual indicators (e.g., security, comfortable lighting, good ventilation, and wind strength) under the commercial and transport dimensions.

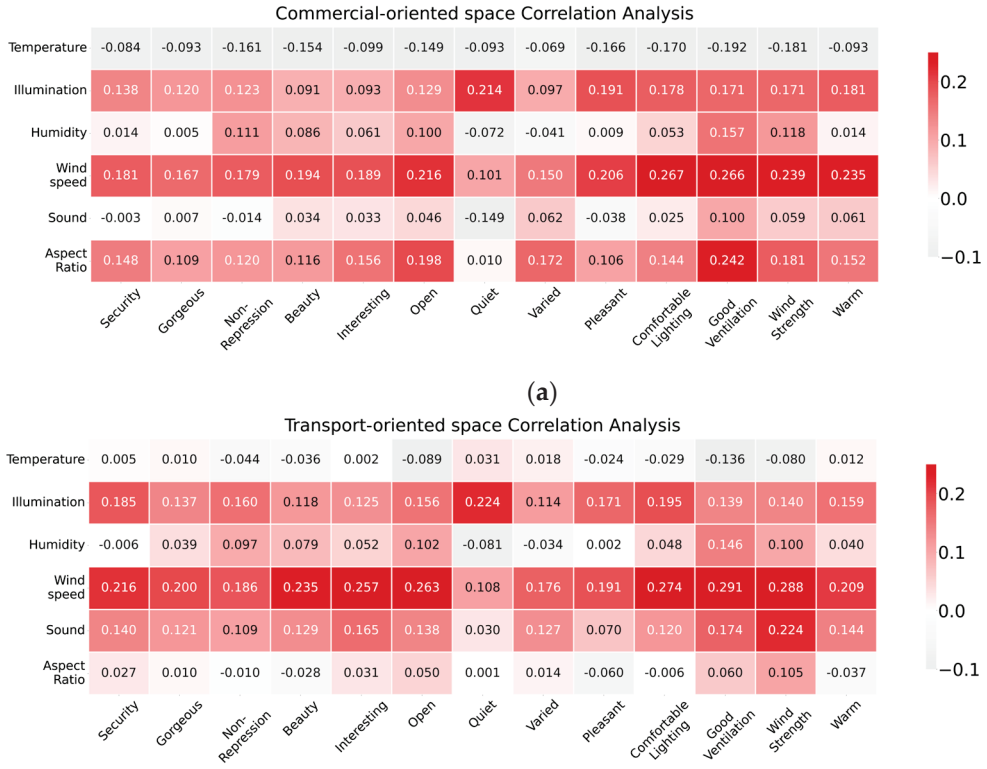


Figure 4. Matrix of correlation coefficients between human-centred perception evaluation and physical environment data: (**a**) matrix of correlation coefficients for spatial sensory indicators of commercial-oriented space; and (**b**) matrix of correlation coefficients for spatial sensory indicators of transport-oriented space.

Table 6. Relevance attributions for the human-centred perception indicators.

Physical Environment Data	Perceptual Dimension	Commercial-Oriented Space's Perceptual Indicators	Transport-Oriented Space's Perceptual Indicators
Aspect ratio	Visual, somatosensory	Security, non-repression, interesting, open, comfortable lighting, good ventilation, wind strength, warm	Wind strength
Humidity	Somatosensory	Good ventilation, wind strength	Good ventilation, wind strength
Illumination	Visual, somatosensory	Security, gorgeous, non-repression, open, comfortable lighting, warm	Security, gorgeous, non-repression, beauty, interesting, open, comfortable lighting, warm
Sound	Auditory	Quiet	Varied
Temperature	Visual, somatosensory	Comfortable lighting, good ventilation, wind strength	Good ventilation
Wind speed	Somatosensory	Good ventilation, wind strength, warm	Good ventilation, wind strength, warm

3.4. Cross-Validation Analysis Based on Traditional Regression and Machine Learning Regression

Through correlation and regression analyses, it is found that different physical environment parameters have significant nonlinear effects on users' perceptual experiences. The physical environment parameters such as aspect ratio, humidity, and illumination significantly increase the satisfaction of perceptual indicators within the appropriate range. Different parameters show differences in the commercial-oriented and transport-oriented spaces. Aspect ratio, humidity, illumination, and other physical environment parameters significantly increase satisfaction in the appropriate range.

3.4.1. Single-Indicator Fitted Regression Analysis

This section integrates single-indicator fitting regression analyses of commercial and transport-oriented spaces. It examines the performance trends of each parameter across different spatial function orientations and refines the recommended ranges.

In the commercial-oriented space (as shown in Figure 5), the aspect ratio is significantly positively correlated with indicators such as wind strength. When the aspect ratio falls between 1.59 and 2.81 or exceeds 3.14, the satisfaction levels of several perception metrics surpass 3.5, particularly wind strength at an aspect ratio of 1.83, which reaches 3.75. This suggests that this ratio optimises users' perception of ventilation within the space. Similarly, humidity significantly enhances the satisfaction of good ventilation and wind strength within the range from 52.31% to 59.22%, with the highest recorded satisfaction at 4.40 occurring at 59.20%. This indicates a strong sensitivity of humidity levels to perceptions of airflow. Illumination levels are notably higher, within the range from 808.11 lx to 1338.24 lx, with a peak satisfaction score of 3.5 for wind strength at an aspect ratio of 1.83, indicating that this ratio also optimises user perceptions of ventilation. Illumination performs best within the 808.11 lx to 1338.24 lx range, as users report significantly greater satisfaction regarding comfort and spatial perception of the lighting, especially for the gorgeous and open metrics, which scored over 4.00. Analysis of sound levels indicates that when the noise level is below 61.21 dB, the satisfaction level for quiet generally exceeds 3.5, particularly at 59.60 dB, where satisfaction reaches 3.00, and at 59.20 dB, where satisfaction increases to 4.40. Regression analysis of temperature indicates that when temperatures range from 22.63 °C to 26.39 °C, the satisfaction levels for good ventilation and wind strength reach 4.50 and 4.00, respectively, underscoring the importance of temperature regulation in enhancing comfort perceptions. Wind speed has a particularly significant impact on user experience, with good ventilation and wind strength scores exceeding 3.5 for wind speeds ranging from 0.26 m/s to 0.67 m/s, further validating the critical role of wind speed in optimising perceptions of ventilation in business-oriented spaces.

In contrast, the transport-oriented space (as shown in Figure 6) exhibits a more refined trend in physical environment parameters. The aspect ratio, ranging from 3.12 to 3.20, significantly correlates with increased user satisfaction regarding wind strength, achieving a peak rating of 4.00. The recommended ranges for humidity and illumination are from 50.09% to 59.20% and from 142.19 lx to 480.03 lx, respectively. Notably, humidity is highly correlated with perceptions of ventilation, while lower illuminance levels (e.g., 158.80 lx and 474.00 lx) align more closely with user preferences for transport spaces. The regression analysis for sound indicates that user satisfaction with quiet is significantly enhanced when noise levels fall between 63.15 dB and 75.45 dB. Temperature is most effective in the range from 21.95 °C to 26.20 °C, optimising perceptions of ventilation and warmth, thereby improving overall satisfaction. Furthermore, wind speed ranging from 0.18 m/s to 0.78 m/s is the most effective in enhancing user satisfaction with good ventilation and warmth. Specifically, wind speed in this range demonstrates a marked increase in ratings for good ventilation and wind strength, with satisfaction peaking at 4.75 for a wind speed of 0.67 m/s.

These results further emphasise the synergies among the parameters and their significant differences across various functionally oriented spaces. Such differences are evident in specific physical environmental parameters and the diverse user needs for different scenarios.

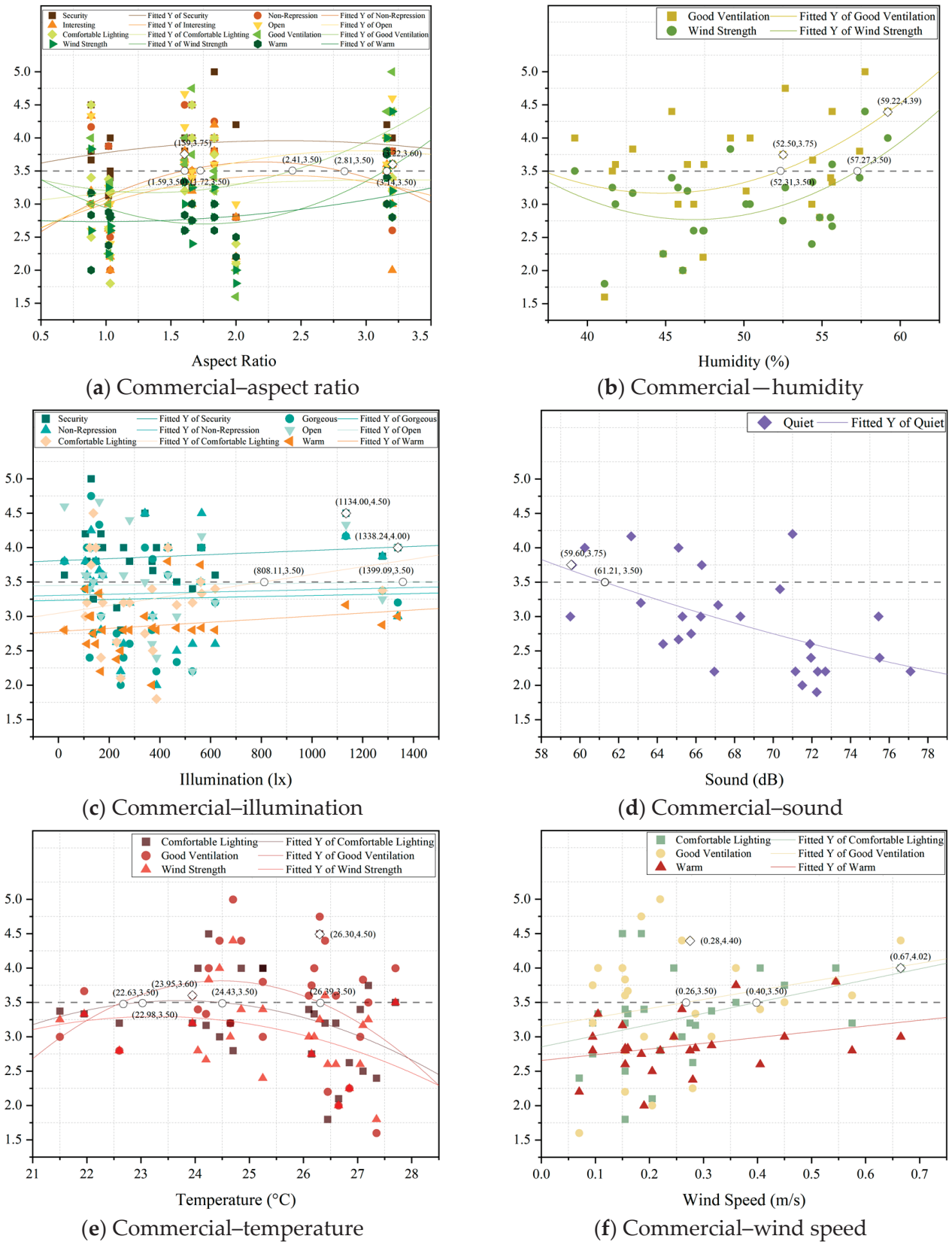


Figure 5. Results of single-indicator fitted regression analyses under commercial-oriented spaces.

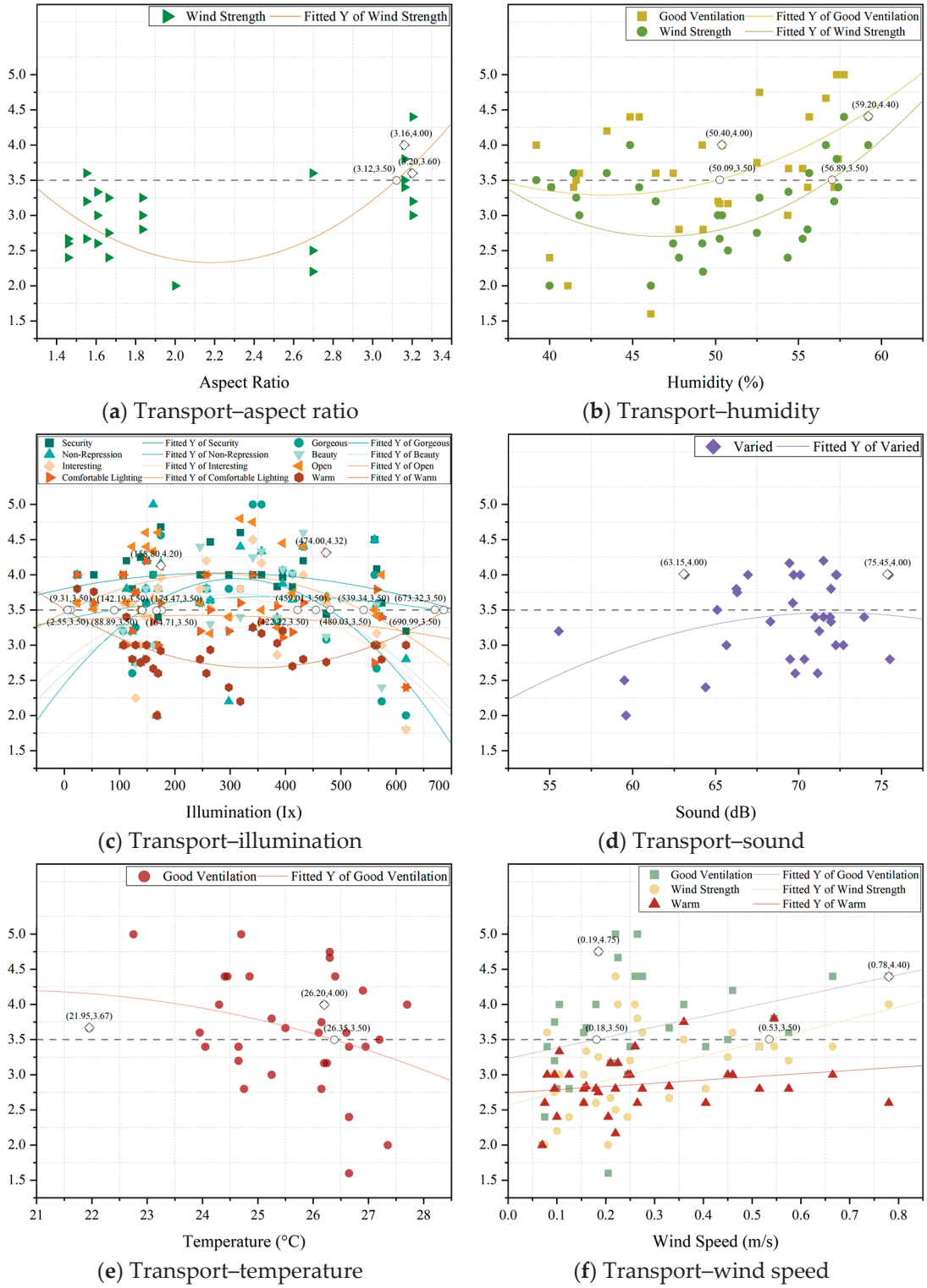


Figure 6. Results of single-indicator fitted regression analyses under transport-oriented space.

3.4.2. Regression Model Analysis Based on XGBoost Algorithm

This study further investigates the nonlinear relationship between physical environmental parameters and human perception indicators, as shown in Figure 7. Although the predictions generated by XGBoost are generally effective, the construction of the model demonstrates a degree of randomness, with R^2 scores proving insufficient in certain instances. The inadequate R^2 scores can be attributed to several factors. (1) Data char-

acteristics: The data distribution in specific dimensions, such as aspect ratio and sound, is more scattered and exhibits more significant variability, complicating the capture of complex relationships. (2) Sample size limitation: The limited number of samples in these dimensions further restricts the model's generalizability and stability. (3) Model-specific limitations: While XGBoost excels in modelling structured data, it is less responsive to weakly correlated features or noisy data, which may account for the model's diminished predictive capability in these dimensions.

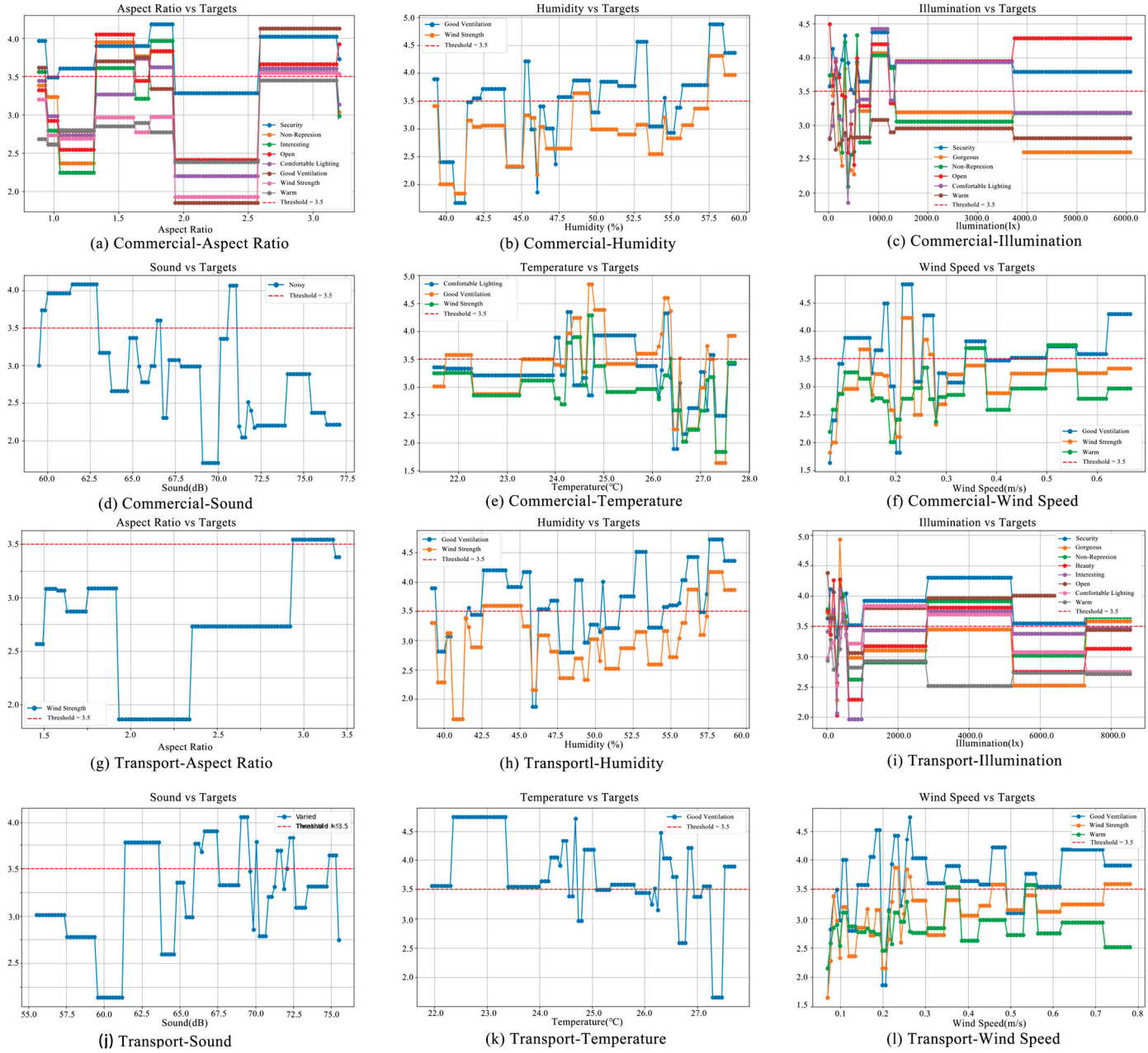


Figure 7. Regression model analyses based on the XGBoost algorithm.

This indicates that result stability needs improvement. Nonetheless, the model shows promise in providing auxiliary references for the future optimisation of environmental parameters. The study specifically selected model results with an R^2 greater than approximately 0.4 and compared these with those observed for single-indicator fits. A detailed analysis of the specific regression results is presented below (as shown in Figure 7).

(1) Aspect Ratio

In the commercial-oriented space, the XGBoost regression model exhibits R^2 values of less than 0.3 for all relevant indicators. This indicates that it does not provide valid predictions and suggests instability within this space. This limitation implies that the XGBoost model struggles to accurately capture the relationship between aspect ratio and human-oriented perception indicators in this context. Consequently, the prediction results for this dimension should be interpreted with caution and regarded as exploratory rather than definitive findings. In the transport-oriented space, the fitted equation for wind strength has an R^2 value of 0.1886, indicating that the model's predictions exhibit insufficient stability to offer informative ranges. As a result, the aspect ratio model prediction results in both spaces lack validity.

(2) Humidity

In the commercial-oriented space, the XGBoost regression model demonstrates that good ventilation's fitted equation has an R^2 value of 0.5212, indicating a good predictive capability, with a recommended humidity range from 39.2000% to 59.2000%. Compared to the recommended humidity range for the single-indicator fit (52.31% to 59.22%), the model extends the range under low-humidity conditions, showcasing greater adaptability. In the transport-oriented space, good ventilation's fitted equation presents an R^2 value of 0.4043, and the model also predicts effectively, recommending a humidity range from 39.2000% to 59.2000%, demonstrating broad applicability under low-humidity conditions.

(3) Illumination

In the commercial-oriented space, the XGBoost regression model demonstrated an R^2 value of 0.4077 for the fitted equation concerning gorgeous, indicating enhanced model prediction capabilities. The recommended illuminance range is between 23.5000 lx and 1184.8990 lx. In contrast, the single-indicator fit suggests a narrower range, from 808.11 lx to 1338.24 lx. The model predicts a lower bound, indicating a more robust user perception under low-illumination conditions. In the transport-oriented space, gorgeous's fitted equation yields an R^2 value of 0.3818, with the model also demonstrating compelling predictions, recommending an illuminance range from 23.5000 lx to 8525.0000 lx. This range is significantly broader than that of the single-indicator fit, which is between 142.19 lx and 480.03 lx, particularly highlighting the model's capability to predict under high-illuminance conditions.

(4) Sound

In the commercial-oriented space, the XGBoost regression model reveals that the fitted equation for noisy has an R^2 value of 0.3654, which is close to the stability threshold but does not meet the desired criteria. The recommended noise range is from 59.68 dB to 71.06 dB, which is broader than the single-indicator fit range, from 59.60 dB to 61.21 dB. This wider prediction range, particularly in high-noise environments, suggests that the machine-learning model is better equipped to handle varying noise conditions. In the transport-oriented space, the fitted equation for varied has an R^2 value of 0.2263, indicating that the model predictions are not sufficiently stable to provide a reliable reference. Given the low R^2 score, the projections for sound should be considered preliminary and indicative of the need for further refinement of the model or additional data collection to improve stability.

(5) Temperature

The results of the XGBoost regression model indicate that the fitted equation for good ventilation in the commercial-oriented space has an R^2 value of 0.5269, predicting a temperature range from 21.75 °C to 27.70 °C. The single-indicator fit predicts a narrower

range, from 22.63 °C to 26.39 °C. This finding suggests that the machine-learning model offers a slightly broader range and encompasses the recommended temperature parameters of the single-indicator fit. This indicates that the model is more flexible and stable in predicting temperature parameters. In the transport dimension, good ventilation's fitted equation has an R^2 value of 0.3602, close to the threshold value, with a recommended temperature range from 21.95 °C to 27.70 °C.

(6) Wind Speed

In the commercial-oriented space, the XGBoost regression model shows that good ventilation's fitted equation has an R^2 value of 0.4828, and the model predicts better, with recommended wind speeds ranging from 0.11 m/s to 0.67 m/s. Compared to the results of the single-indicator fit (0.26 m/s to 0.67 m/s), the model demonstrates higher predictive ability at low wind speeds, indicating that it can accommodate a broader range of environmental conditions. In transport-oriented space, good ventilation's fitted equation has an R^2 value of 0.3681, with a recommended wind speed range from 0.11 m/s to 0.78 m/s, showing a more excellent range of acceptability.

However, the predictive capability is somewhat limited and lacks a high level of stability. This single-indicator fitting regression analysis effectively identified the suitability parameters strongly correlated with the human-oriented perception indicators for each physical environment parameter in commercial-oriented and transportation-oriented spaces. Based on these theoretical calculations and actual data points, the recommended ranges for physical environment parameters are adaptable and serve as a reference for subsequent spatial environment optimisation.

In summary, the XGBoost model demonstrates high stability in predicting humidity, illumination, and other key parameters, with its recommended ranges being more flexible than those derived from single-indicator fitting—particularly in the low and high parameter intervals. Ultimately, this study integrates the results of the single-indicator fitting curves and XGBoost model predictions to create a summary table of the recommended ranges (as shown in Table 7).

Table 7. Summary table of recommended ranges predicted by single-indicator fit curve and XGBoost model.

Commercial-Oriented Space					Transport-Oriented Space				
No.	**Parameter**	**Single-Indicator Recommended Range**	**XGBoost Model Recommended Range**	**Final Recommended Range**	**No.**	**Parameter**	**Single-Indicator Recommended Range**	**XGBoost Model Recommended Range**	**Final Recommended Range**
1	Aspect ratio	1.59–2.81; 3.14–3.22	Not Applicable ($R^2 < 0.3$)	1.59–2.81; 3.14–3.22	1	Aspect Ratio	3.12–3.20	Not Applicable ($R^2 < 0.4$)	3.12–3.20
2	Humidity	52.31%–59.22%	39.20%–59.20%	52.31%–59.20%	2	Humidity	50.09%–59.20%	39.20%–59.20%	50.09%–59.20%
3	Illumination	808.11 lx–1338.24 lx	23.50 lx–1184.90 lx	808.11 lx–1184.90 lx	3	Illumination	142.19 lx–480.03 lx	23.50 lx–8525.00 lx	142.19 lx–480.03 lx
4	Sound	59.60 dB–61.21 dB	59.68 dB–71.06 dB	59.68 dB–61.21 dB	4	Sound	63.15 dB–75.45 dB	Not Applicable ($R^2 < 0.4$)	63.15 dB–75.45 dB
5	Temperature	22.63 °C–26.39 °C	21.75 °C–27.70 °C	22.63 °C–26.39 °C	5	Temperature	21.95 °C–26.20 °C	21.95 °C–27.70 °C	21.95 °C–26.20 °C
6	Wind speed	0.26 m/s–0.67 m/s	0.10 m/s–0.67 m/s	0.26 m/s–0.67 m/s	6	Wind Speed	0.18 m/s–0.78 m/s	0.11 m/s–0.78 m/s	0.18 m/s–0.78 m/s

4. Discussion

4.1. Research Innovation

This study contributes to the literature by addressing gaps in research on the multisensory environmental impacts of underground spaces. It systematically reveals the complex nonlinear relationship between physical parameters and perceptual experiences. Compared with previous studies that mainly focus on the association between behavioural patterns and environmental features, such as Sevtsuk A et al.'s assessment of urban facility construction through pedestrian flow distribution and so on [46,47], and Istrate A's study on the activity of small-scale businesses and buildings along the street [48], the present study introduces a multi-sensory perspective to make up for the lack of research on the

mechanism between physical environmental parameters and perceptual experience. By introducing visual, auditory, and somatosensory dimensions, the study constructed a correlation model between perception and physical environment parameters, providing theoretical support for underground space optimisation.

The results show that physical parameters not only affect a single perceptual index but may also affect multiple perceptual experiences at the same time. For example, humidity significantly increased the satisfaction of good ventilation and wind strength in the range from 52.31% to 59.22% and enhanced overall comfort by modulating the sense of airflow. This finding provides an important basis for fine-tuning the design of physical parameters. This study also found significant differences in lighting and temperature requirements between traffic and commercial spaces. The recommended illuminance range for traffic space is from 142.19 lx to 480.03 lx, while the recommended range for commercial space is from 808.11 lx to 1338.24 lx, which reflects the difference in the light environment demanded by the users in different scenarios in terms of temperature; the results of this study are basically the same as the range of the working environment temperature proposed by Wu and other scholars (from 22.0 °C to 27.3 °C) [49], but the range in this study differs slightly. It is basically consistent with the range proposed by Wu and other scholars (from 22.0 °C to 27.3 °C) [49], but the range of this study is more specific, and it is further found that the commercial space has a higher demand for temperature stability, while the traffic space is more affected by the synergistic factors such as humidity and wind speed.

Compared with traditional indoor space evaluation models that focus on a single physical environment indicator [50], this study systematically introduces a multi-sensory evaluation framework, which strengthens the depth of the 'environment–human' linkage study. Previous studies on underground spaces, such as Meng Q's study, have shown that background music in traffic spaces can mask unwanted noise, and the comfort level is optimal between 65 dB and 70 dB [51], which is consistent with the results of this study, and further reveals that users of commercial spaces are more sensitive to noise than those of traffic spaces.

In summary, this study not only validates the established research results but also presents new contributions at the level of fine-grained understanding of perceptual mechanisms and guidance for optimisation of physical parameters. Through the systematic framework of multi-sensory perception, this study provides a comprehensive and scientific theoretical approach to the design of underground space environments with different functional orientations.

4.2. Limitations and Future Directions

This study explores key issues in the environmental regulation of underground spaces based on human perception evaluation. While the research methodology was effective in achieving the research objectives, the findings also revealed several critical problems in the field that need to be addressed, thus providing important directions for future research.

Firstly, during the data selection process, most of the existing studies have paid relatively more attention to visual perception indicators while covering less of the other perception dimensions, such as visual, auditory and somatosensory. This imbalance limits the comprehensiveness of perception data, as well as the representativeness of the findings. Future research could focus on the balanced collection of multi-sensory data. In addition, environmental indicators do not exist in isolation, and their interactions and their comprehensive influence mechanisms on user perception have not been fully investigated. Future research should focus on the dynamic interactions between these metrics and explore how they synergistically affect the overall user experience.

Second, this study used machine learning to model and analyse environmental data. These results demonstrate the potential of these techniques for modelling environmental perception in underground spaces. However, model stability and generalisation remain limited due to the small size and single source of training data. Therefore, future research should expand the size and diversity of the dataset to cover a wider range of environmental conditions and user perceptions and diversify the data collection channels. Meanwhile, introducing more advanced techniques, such as neural networks or multi-modal fusion approaches, can further improve the adaptability and prediction accuracy of the model in complex environments.

Once again, environmental data collection was focused on specific periods, and this limitation in timeframe may have resulted in differences in seasonal environmental conditions and their impact on user perceptions not being adequately captured. For example, user perceptions of temperature and humidity may be significantly different in winter versus summer, a limitation that may affect the applicability and extrapolation of the study results. For this reason, future studies should conduct long-term and multi-seasonal data collection covering different temporal scenarios to more comprehensively assess the impact of dynamic changes in environmental factors on user perceptions. This broader temporal coverage can provide a more solid foundation for understanding the dynamic relationship between environmental parameters and user perception and enhance the generalisability of the research results.

In addition, the findings suggest that emerging technologies, such as virtual reality (VR) and augmented reality (AR), can be combined in the future to break through the limitations of physical experiments. By simulating multiple physical environment parameters through virtual scenarios, researchers can conduct large-scale experiments more efficiently, collect users' perceptual feedback in multiple scenarios, and enhance the breadth and depth of experimental data. Virtual experiments can not only complement traditional field studies but can also be used to quickly test hypothetical design scenarios and accelerate the design process for underground space optimisation. The rapid development of artificial intelligence (AI) and the Internet of Things (IoT) is driving underground space management towards greater intelligence and adaptability. For example, the combination of intelligent sensor networks and deep-learning algorithms can realise real-time monitoring and adaptive regulation of environmental conditions. Future designs should also achieve a deeper integration between intelligence and sustainability to make underground spaces efficient, adaptable, and environmentally friendly urban infrastructures.

5. Conclusions

Based on the human-centred perception evaluation framework, this study explored the relationship between the physical environment parameters of underground spaces and users' perceptual experiences. It revealed the complex nonlinear effects of different physical environment factors through multidimensional data collection and analysis. Using a combination including a questionnaire survey, correlation analysis, traditional regression analysis, and machine-learning model, we systematically analysed the differentiated performance of visual, auditory and somatosensory dimensions of commercial and transportation functional spaces and their key influencing factors.

The results showed that the role of physical parameters is not a single dimension but affects the user's experience through multidimensional perceptual mechanisms. For example, in the commercial functional space, the aspect ratio significantly enhanced the visual comfort of security and open in a specific range; the appropriate range of humidity and illumination can significantly optimise the user's physical comfort of wind strength,

good ventilation, and so on. In the transportation functional space, the physical parameters are not one-dimensional; instead, work together through multidimensional perceptual mechanisms. However, different results were presented in the transport functional space. The study further validated the suitability ranges of these key parameters through regression and machine-learning modelling and observed significant differences in user needs between commercial and transport spaces regarding temperature, humidity, and illumination.

Additionally, the XGBoost model demonstrated flexibility and adaptability in predicting the impact of humidity, illumination, and temperature, especially at low and high parameter intervals. This provides a more comprehensive theoretical reference for the optimal design of physical environments.

In summary, this study addressed gaps in the environmental perception mechanism of underground spaces and provided a theoretical basis for optimising spaces with different functional orientations. The results not only validate the established theoretical framework; they also further deepen the understanding of the complex interaction between physical environment parameters and perceptual experience, which is of great academic value and practical application significance.

Author Contributions: Conceptualisation, L.S., Y.X. and Z.X.; data curation, Y.X., X.C. and P.L.; formal analysis, L.G. and J.W.; funding acquisition, L.S. and L.G.; investigation, Y.X., Z.X., K.H., X.C. and J.W.; methodology, T.Y. and P.L.; resources, K.H.; software, T.Y. and L.G.; supervision, Z.X.; validation, X.C.; visualisation, T.Y., Y.X. and P.L.; writing—original draft, T.Y.; writing—review and editing, L.S. All authors have read and agreed to the published version of the manuscript.

Funding: This research was funded by the International Science and Technology Cooperation Fund of Jiangsu Collaborative Innovation Center for Building Energy Saving and Construction Technology (Grant No. SJXTGJ2102).

Data Availability Statement: The data presented in this study are available upon request from the corresponding author. Due to privacy concerns, they are not publicly available.

Conflicts of Interest: The authors declare that the research was conducted without any commercial or financial relationships that could be construed as potential conflicts of interest.

Appendix A

In order to more accurately categorise and understand the Pentagon's spatial characteristics and provide methodological support for this study, the diagrams in the study cite parts of the authors' previous study [22]. The aim is to demonstrate the study's basic approach to the classification and distribution of functional characteristics of subsurface space, providing the necessary contextual support for subsequent analyses of the relationship between environmental parameters and perceived quality. It should be noted that although this study shares some of the initial analytical framework and data with the previous study, there are significant differences in the research objectives and methodological presence, among other elements.

(1) Spatial quantification analysis

This study used Depthmap X software to calculate the indicators integration, connectivity, and step depth. These indicators reflect the degrees of spatial integration, transport connectivity, and walking depth, facilitating the distinction between commercial and transport areas. A grid size of 0.8 m $\times$ 0.8 m was adopted as the unit of analysis for constructing view maps. These quantitative methods effectively represent pedestrian access and comprehension within the pedestrianised area, providing insights into the overall structure of the underground space and pedestrian behaviour.

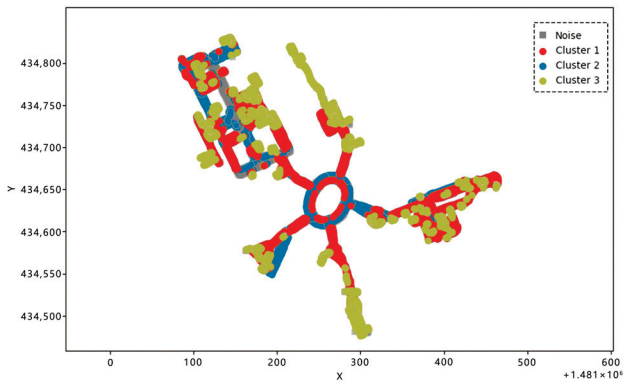
(2) Spatial feature clustering analysis

This study employs the DBSCAN algorithm for cluster analysis by quantifying the spatial data. The algorithm is particularly effective for managing complex spatial datasets and can identify areas with similar spatial features. This study integrates the indicators of integration, connectivity, and step depth for clustering purposes, ultimately revealing two primary functions of spatial characteristics: 'commercial-oriented' and 'transport-oriented'.

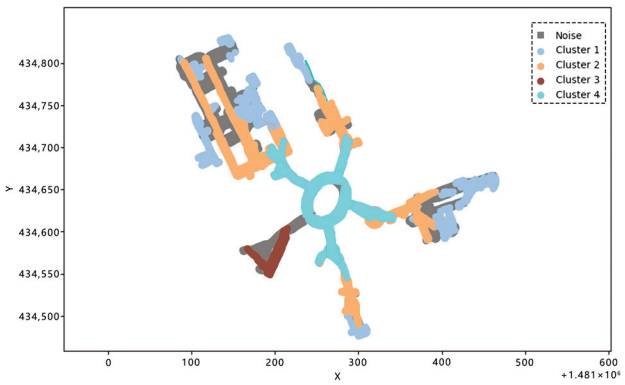
(3) Collection point positioning and feature point selection

By integrating the floor plan results with spatial clustering and combining the functional characteristics of 'commercial-oriented' and 'transport-oriented' spaces, representative feature points are selected within the underground environment. These points primarily concentrate on various functional nodes, including entrances and exits, major commercial zones, and transportation hubs. This approach ensures that the collected data accurately reflects the overall spatial quality characteristics. The specific research steps are shown in Figure A1.

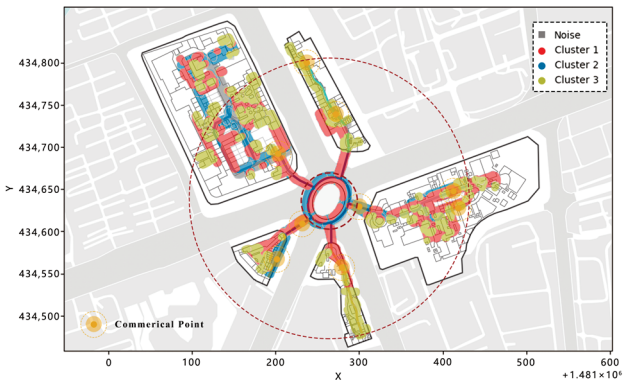
Steps for delineating the subsurface space attributes of the Pentagon site



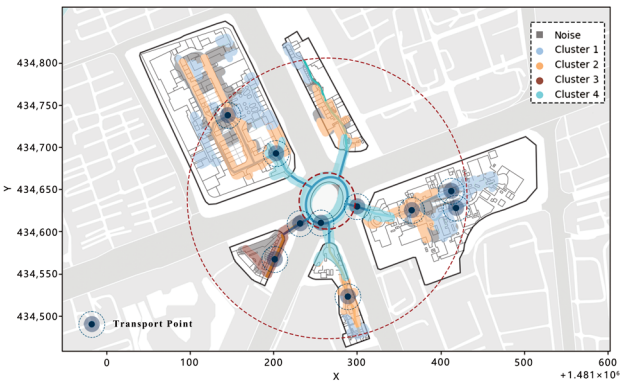
(**a**) Characteristic clustering of commercial-oriented areas



(**b**) Characteristic clustering of transport-oriented areas

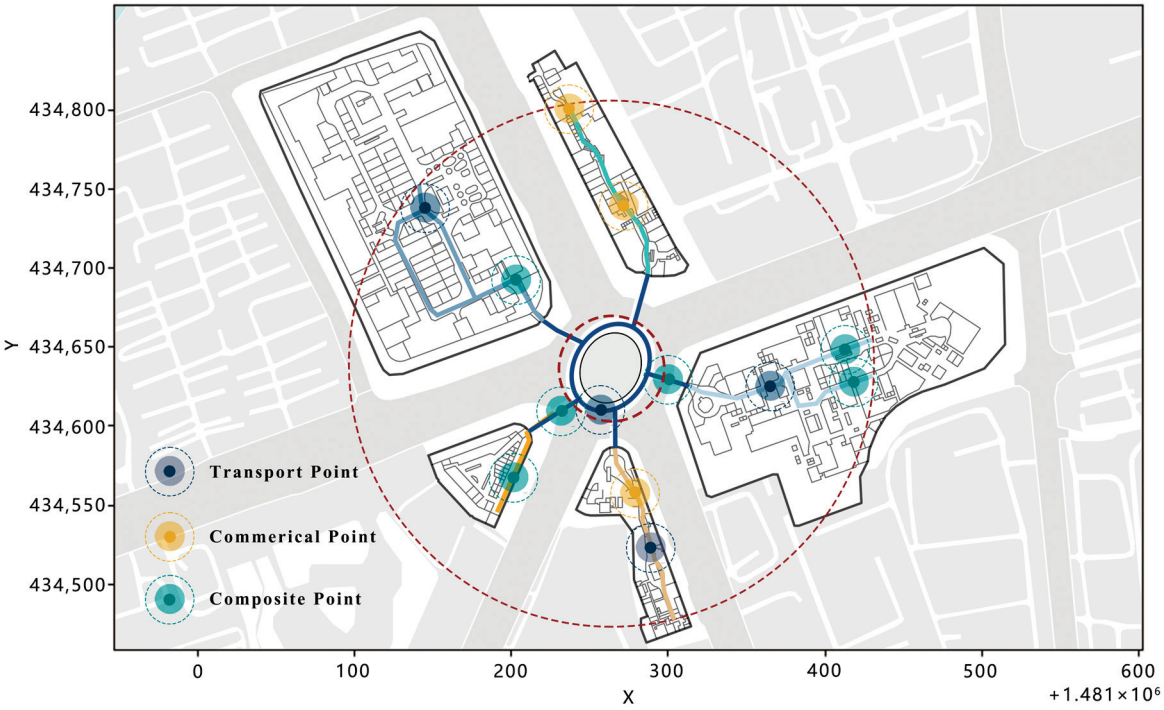


(**c**) Commercial-oriented area character points (after overlay)



(**d**) Transport-oriented area character points (after overlay)

Figure A1. *Cont.*



(**e**) Distribution of feature locations

Figure A1. Steps to classify spatial attributes.

Appendix B

To enhance the scientific rigour and accessibility of the manuscript, particularly for readers outside the specialised field, the study has incorporated a glossary of terms, as shown in Table A1, that elucidates the 13 evaluation indicators related to human-centred perception. This glossary provides precise definitions of the indicators, while explaining them in more accessible language to facilitate broader comprehension. By doing so, the study aims to ensure that readers from diverse backgrounds can effectively understand the key concepts and their relevance to evaluating underground spaces, while maintaining the manuscript's technical accuracy and academic integrity.

Table A1. Glossary of terms.

Number	Human-Centred Perception Indicators Evaluation	Description
1	Security	Represents the level of perceived safety and protection within the underground environment.
2	Gorgeous	Refers to the visual appeal and aesthetic richness of the underground's design and features.
3	Non-repression	Measures openness, avoiding feelings of confinement or claustrophobia in the underground space.
4	Beauty	Reflects the overall attractiveness and harmonious design of the underground.
5	Interesting	Captures the engaging and stimulating qualities of the underground that hold pedestrians' attention.

Table A1. *Cont.*

Number	Human-Centred Perception Indicators Evaluation	Description
6	Open	Describes the spatial experience of openness and freedom, indicating a lack of clutter and barriers.
7	Comfortable lighting	Assesses the adequacy, warmth, and distribution of lighting within the underground, ensuring it supports visibility and comfort.
8	Quiet	Evaluate the noise control level and the absence of disruptive sounds in the underground space.
9	Varied	Describes the presence of a diverse range of sounds, contributing to a dynamic and lively acoustic environment.
10	Pleasant	Reflects the overall enjoyment of the soundscape, with pleasing auditory elements that enhance the underground experience.
11	Good ventilation	Measures the effectiveness of air movement and freshness in the underground, contributing to physical comfort.
12	Wind speed	Assesses the presence and impact of wind within the underground space, considering comfort and usability.
13	Warm	Describes the temperature comfort in the underground, particularly regarding warmth and coziness.

Appendix C

This appendix describes the methodology and specific steps involved in data processing to clarify the processing of survey data and the derivation of weights.

(1) Application of CRITIC and Entropy weight Methods

To objectively determine the weights of each indicator, the study employed a combination of the CRITIC and entropy weight methods. These two approaches effectively assess the importance of each indicator, thereby scientifically reflecting their contributions to the overall evaluation. The CRITIC method calculates weights based on the correlation between indicators and their standard deviations. In contrast, the entropy weight method evaluates the degree of influence of each indicator on the system by computing its information entropy. A lower entropy value indicates greater variability among the indicators in the sample, suggesting a more significant contribution to the comprehensive evaluation.

(2) Specific steps of data processing

The study followed several steps in data processing to ensure the accuracy and validity of the data: (i) data cleaning—the collected questionnaire data underwent preliminary checks to eliminate samples with excessive missing values or irrational responses, thereby ensuring data quality; (ii) data normalisation—to mitigate the influence of different scales, a normalisation process was applied to all indicator data, converting them to a uniform scale range; (iii) weight calculation—by integrating the CRITIC and entropy weight methods, the study calculated the weights of each indicator, ensuring objectivity and rationality in the comprehensive evaluation; and (iv) comprehensive score calculation—utilising the calculated weights, the study weighted and summarised each indicator to derive the final comprehensive score for each sample.

(3) Explanation for the formula of CRITIC and entropy weight method

Integrating the CRITIC and entropy weight methods enhances the ability to capture the variability and complementarity of each indicator accurately. A detailed explanation of the formulas and the procedures for applying these two methods is provided below, as shown in Table A2.

Table A2. Summary of the key algorithms.

Number	Algorithms	Equation	Description
1	Entropy weight	$E_j = -\frac{1}{\ln m}\sum_{i=1}^{m} p_{ij}\ln p_{ij}$ E_j: Entropy value for the jth indicator, p_{ij}: Probability distribution of the ith state for the jth indicator, m: Total number of states.	The entropy weight method is a weight assignment technique grounded in the principles of information entropy. By calculating the information entropy for each indicator, this method evaluates both the uncertainty associated with the indicator and its contribution to the overall information of the system.
2	CRITIC weight	$w_j = \frac{\sigma_j\sum_{i=1}^{m}(1-r_{ij})}{\sum_{j=1}^{m}\sigma_j\sum_{i=1}^{m}(1-r_{ij})}$ w_j: Weight of the jth indicator. σ_j: Standard deviation of the jth indicator. r_{ij}: Correlation between the ith and jth indicators. m: Total number of indicators.	The CRITIC weight method is an objective approach to weight assignment, aiming to allocate higher weights to indicators that exhibit significant variability and low correlation with other indicators. This approach effectively emphasises the indicators that hold greater importance within the system.

References

1. Cellucci, C. Adaptability as a multi-scale strategy for the regeneration of the built environment through circular economy perspective. *AHFE Int.* **2023**, *112*, 45–55.
2. Zhao, J.W.; Peng, F.L.; Wang, T.Q.; Zhang, X.Y.; Jiang, B.N. Advances in master planning of urban underground space (UUS) in China. *Tunn. Undergr. Space Technol.* **2016**, *55*, 290–307. [CrossRef]
3. Broere, W. Urban underground space: Solving the problems of today's cities. *Tunn. Undergr. Space Technol.* **2016**, *55*, 245–248. [CrossRef]
4. Yang, B.; Yao, H.; Wang, F. A review of ventilation and environmental control of underground spaces. *Energies* **2022**, *15*, 409. [CrossRef]
5. Li, X.; Li, L.; Lin, M.; Jim, C.Y. Research on risk and resilience evaluation of urban underground public space. *Int. J. Environ. Res. Public Health* **2022**, *19*, 15897. [CrossRef]
6. Xu, Z.; Chang, J.; Cheng, F.; Liu, X.; Yao, T.; Hu, K.; Sun, J. Examining the impact of the built environment on multidimensional urban vitality: Using milk tea shops and coffee shops as new indicators of urban vitality. *Buildings* **2024**, *14*, 3517. [CrossRef]
7. Biljecki, F.; Ito, K. Street view imagery in urban analytics and GIS: A review. *Landsc. Urban Plan.* **2021**, *215*, 104217. [CrossRef]
8. Tao, H.; Fan, Y.; Li, X.; Zhang, Z.; Hou, W. Investigation of formaldehyde and TVOC in underground malls in Xi'an, China: Concentrations, sources, and affecting factors. *Build. Environ.* **2015**, *85*, 85–93. [CrossRef]
9. Yap, H.S.; Roberts, A.C.; Luo, C.; Tan, Z.; Lee, E.H.; Thach, T.; Kwok, K.W.; Car, J.; Soh, C.; Christopoulos, G. The importance of air quality for underground spaces: An international survey of public attitudes. *Indoor Air* **2021**, *31*, 2239–2251. [CrossRef]
10. Gao, W.; Sun, X.; Zhao, M.; Gao, Y.; Ding, H. Evaluate human perception of the built environment in the metro station area. *Land* **2024**, *13*, 90. [CrossRef]
11. Sun, L.; Xu, Y.; Teng, S.; Wang, B.; Li, M.; Ding, S. Research into the visual saliency of guide signs in an underground commercial street based on an eye-movement experiment. *Sustainability* **2022**, *14*, 16062. [CrossRef]
12. Yao, T.; Ding, S.; Zhang, Y.; Chen, X.; Xu, Y.; Hu, K.; Xu, X.; Sun, L.; Liang, Z.; Huang, Y.; et al. Research on the range of appropriate spatial scale of underground commercial street based on psychological perception evaluation. *Appl. Sci.* **2024**, *14*, 5435. [CrossRef]
13. Fanger, P.O. *Thermal Comfort: Analysis and Applications in Environmental Engineering*; Danish Technical Press: Copenhagen, Denmark, 1970.
14. Hong, S.H.; Lee, J.M.; Moon, J.W.; Lee, K.H. Thermal comfort, energy and cost impacts of PMV control considering individual metabolic rate variations in residential building. *Energies* **2018**, *11*, 1767. [CrossRef]
15. Zhang, S.; Cheng, Y.; Oladokun, M.O.; Wu, Y.; Lin, Z. Improving predicted mean vote with inversely determined metabolic rate. *Sustain. Cities Soc.* **2020**, *53*, 101870. [CrossRef]
16. Wargocki, P.; Frontczak, M.; Schiavon, S.; Goins, J.; Arens, E.; Zhang, H. Satisfaction and self-estimated performance in relation to indoor environmental parameters and building features. In Proceedings of the 10th International Conference on Healthy Buildings, International Society of Indoor Air Quality and Climate, Brisbane, Australia, 8–12 July 2012.

17. Wong, L.T.; Mui, K.W. An energy performance assessment for indoor environmental quality (IEQ) acceptance in air-conditioned offices. *Energy Convers. Manag.* **2009**, *50*, 1362–1367. [CrossRef]
18. Dunleavy, G.; Bajpai, R.; Tonon, A.C.; Cheung, K.L.; Thach, T.-Q.; Rykov, Y.; Soh, C.-K.; de Vries, H.; Car, J.; Christopoulos, G. Prevalence of psychological distress and its association with perceived indoor environmental quality and workplace factors in under and aboveground workplaces. *Build. Environ.* **2020**, *175*, 106799. [CrossRef]
19. Mittal, S.; Sharma, A.K. Quality of life and built environment: Theoretical understanding and research gaps. *Urban India* **2017**, *37*, 37–54.
20. Gibson, J.J. The Senses Are Considered Perceptual Systems. Houghton Mifflin, 1966. Available online: https://psycnet.apa.org/record/1966-35026-000 (accessed on 28 June 2024).
21. Gibson, J.J. *The Ecological Approach to Visual Perception, Classic Edition*; Psychology Press: New York, NY, USA, 2014.
22. Yao, T.; Xu, Y.; Sun, L.; Liao, P.; Wang, J. Application of machine learning and multi-dimensional perception in urban spatial quality evaluation: A case study of Shanghai underground pedestrian street. *Land* **2024**, *13*, 1354. [CrossRef]
23. Liu, L.; Silva, E.A.; Wu, C.; Wang, H. A machine learning-based method for the large-scale evaluation of the qualities of the urban environment. *Comput. Environ. Urban Syst.* **2017**, *65*, 113–125. [CrossRef]
24. Ye, Y.; Zeng, W.; Shen, Q.; Zhang, X.; Lu, Y. The visual quality of streets: A human-centred continuous measurement based on machine learning algorithms and street view images. *Environ. Plan. B Urban Anal. City Sci.* **2019**, *46*, 1439–1457. [CrossRef]
25. Chen, T.; Guestrin, C. XGBoost: A scalable tree boosting system. In Proceedings of the 22nd ACM SIGKDD International Conference on Knowledge Discovery and Data Mining, San Francisco, CA, USA, 13–17 August 2016; pp. 785–794.
26. Tian, Z.; Qu, W.; Zhao, Y.; Zhu, X.; Wang, Z.; Tan, Y.; Jiang, R.; Tan, S. Predicting depression and anxiety of Chinese population during COVID-19 in psychological evaluation data by XGBoost. *J. Affect. Disord.* **2023**, *323*, 417–425. [CrossRef] [PubMed]
27. He, J.; Shi, Y.; Xu, L.; Lu, Z.; Feng, M.; Tang, J.; Guo, X. Exploring the scale effect of urban thermal environment through XGBoost model. *Sustain. Cities Soc.* **2024**, *114*, 105763. [CrossRef]
28. Chen, L.; Ding, Y.; Lyu, D.; Liu, X.; Long, H. Deep multi-task learning based urban air quality indicator modelling. *Proc. ACM Interact. Mob. Wearable Ubiquitous Technol.* **2019**, *3*, 1–17.
29. Cui, J.; Broere, W.; Lin, D. Underground space utilisation for urban renewal. *Tunn. Undergr. Space Technol.* **2021**, *108*, 103726. [CrossRef]
30. Dong, Y.H.; Peng, F.L.; Guo, T.F. Quantitative assessment method on urban vitality of metro-led underground space based on multi-source data: A case study of Shanghai Inner Ring area. *Tunn. Undergr. Space Technol.* **2021**, *116*, 104108. [CrossRef]
31. Ma, C.X.; Peng, F.L.; Zhang, J.B.; Wang, T.-Q. Evaluation of spatial performance of urban underground public space: A case study of Wujiaochang Sub-center in Shanghai. *IOP Conf. Ser. Earth Environ. Sci.* **2021**, *703*, 012013. [CrossRef]
32. Pongprasert, P.; Kubota, H. TOD residents' attitudes toward walking to transit station: A case study of transit-oriented developments (TODs) in Bangkok, Thailand. *J. Mod. Transp.* **2019**, *27*, 39–51. [CrossRef]
33. Hillier, B.; Hanson, J. *The Social Logic of Space*; Cambridge University Press: Cambridge, UK, 1984.
34. Michael, H.; Matthew, P.; Derek, D. Dbscan: Fast density-based clustering with R. *J. Stat. Softw.* **2019**, *91*, 1–30.
35. Chen, Y.; Zhou, L.; Bouguila, N.; Wang, C.; Chen, Y.; Du, J. BLOCK-DBSCAN: Fast clustering for large scale data. *Pattern Recognit.* **2021**, *109*, 107624. [CrossRef]
36. Gehl, J. *Life between Buildings: Using Public Spaces*, 6th ed.; Island Press: Washington, DC, USA, 2011.
37. Matan, A.; Newman, P. Jan Gehl and new visions for walkable Australian cities. *World Transp. Policy Pract.* **2012**, *17*, 30–41.
38. Fan, G.; Shi, Z. Application of PSPL method in urban street public space—An example of Tianlin Road (Guilin Road—Liuzhou Section) in Xuhui District, Shanghai. *IOP Conf. Ser. Earth Environ. Sci.* **2021**, *769*, 022055. [CrossRef]
39. Dubey, A.; Naik, N.; Parikh, D.; Raskar, R.; Hidalgo, C.A. Deep learning the city: Quantifying urban perception at a global scale. In Proceedings of the 14th European Conference on Computer Vision, Amsterdam, The Netherlands, 11–14 October 2016; Part I.. Springer International Publishing: Cham, Switzerland, 2016; pp. 196–212.
40. Axelsson, Ö.; Nilsson, M.E.; Berglund, B. A principal components model of soundscape perception. *J. Acoust. Soc. Am.* **2010**, *128*, 2836–2846. [CrossRef]
41. He, P.; Herthogs, P.; Cinelli, M.; Tomarchio, L.; Tunçer, B. A multi-criteria decision analysis based framework to evaluate public space quality. In *Smart and Sustainable Cities and Buildings*; Springer: Berlin/Heidelberg, Germany, 2020; pp. 271–283.
42. Altin, H. A comparative analysis of CE-Topsis and CE-Maut methods. *Int. J. Strateg. Decis. Sci.* **2020**, *11*, 18–51. [CrossRef]
43. Chen, Q. Application entropy weight and TOPSIS method in English teaching quality evaluation of "Smart Classroom". *EAI Endorsed Trans. Scalable Inf. Syst.* **2023**, *11*. [CrossRef]
44. O'Gorman, T.W.; Woolson, R.F. Using Kendall's τ_b correlations to improve variable selection methods in case-control studies. *Bioindicators* **1995**, *51*, 1451–1460.

45. Wang, J.; Zhao, Y.; Li, W.; Wang, F. Prediction model of multi-channel audio quality based on multiple linear regression. In *Advances in Multimedia Information Processing—PCM 2015, Proceedings of the 16th Pacific-Rim Conference on Multimedia, Gwangju, South Korea, 16–18 September 2015*; Part I.; Springer International Publishing: Berlin/Heidelberg, Germany, 2015; pp. 688–698.
46. Sevtsuk, A. Estimating pedestrian flows on street networks: Revisiting the betweenness indicator. *J. Am. Plan. Assoc.* **2021**, *87*, 512–526. [CrossRef]
47. Lopez Baeza, J.; Carpio-Pinedo, J.; Sievert, J.; Landwehr, A.; Preuner, P.; Borgmann, K.; Avakumović, M.; Weissbach, A.; Bruns-Berentelg, J.; Noennig, J.R. Modeling pedestrian flows: Agent-based simulations of pedestrian activity for land use distributions in urban developments. *Sustainability* **2021**, *13*, 9268. [CrossRef]
48. Istrate, A. Street vitality: What predicts pedestrian flows and stationary activities on predominantly residential Chinese streets, at the mesoscale? *J. Plan. Educ. Res.* **2023**. [CrossRef]
49. Wu, Y.; Chen, X.; Li, H.; Zhang, X.; Yan, X.; Dong, X.; Li, X.; Cao, B. Influence of thermal and lighting factors on human perception and work performance in simulated underground environment. *Sci. Total Environ.* **2022**, *828*, 154455. [CrossRef]
50. Diaz, M.; Piderit, M.B.; Attia, S. Parameters and indicators used in indoor environmental quality (IEQ) studies: A review. *J. Phys. Conf. Ser.* **2021**, *2042*, 012132. [CrossRef]
51. Meng, Q.; Kang, J.; Jin, H. Subjective evaluation of acoustic environment in underground spaces. *Adv. Mater. Res.* **2012**, *450*, 1498–1503.

Disclaimer/Publisher's Note: The statements, opinions and data contained in all publications are solely those of the individual author(s) and contributor(s) and not of MDPI and/or the editor(s). MDPI and/or the editor(s) disclaim responsibility for any injury to people or property resulting from any ideas, methods, instructions or products referred to in the content.

buildings

MDPI

Article

Assessing and Enhancing Green Quantity in the Open Spaces of High-Density Cities: A Comparative Study of the Macau Peninsula and Monaco

Jitai Li [1,†], Fan Lin [2,†], Yile Chen [3,*] and Shuai Yang [4]

[1] School of Landscape Architecture, Guangdong Eco-Engineering Polytechnic, No. 297, Guangshan 1st Road, Tianhe District, Guangzhou 510520, China; jitaili@foxmail.com
[2] Faculty of Business, City University of Macau, Avenida Padre Tomás Pereira, Taipa, Macau 999078, China; b20092100303@cityu.edu.mo
[3] Faculty of Humanities and Arts, Macau University of Science and Technology, Avenida Wai Long, Taipa, Macau 999078, China
[4] School of Art and Archaeology, Hangzhou City University, No. 51 Huzhou Street, Gongshu District, Hangzhou 310015, China; samyang@zju.edu.cn
* Correspondence: 2009853GAT30001@student.must.edu.mo
† These authors contributed equally to this work.

Abstract: Green open space in high-density cities has positive significance in terms of improving the quality of the living environment and solving problems such as "urban diseases". Taking the high-density urban districts of the Macau Peninsula and Monaco as examples, this study divides the planning index of open space green quantity into two dimensions: the blue-green spaces occupancy rate (BGOR) within urban land areas and the blue-green spaces visibility rate (BGVR) of the main streetscape. Using satellite remote-sensing maps, GIS databases, and street-view images, this study evaluates the current green quantity in both regions and compares them to identify best practices. This study aims to assess and enhance the green quantity found in the open spaces of high-density cities, using the Macau Peninsula and Monaco as case studies. The primary research questions are as follows: (1) How can the green quantity in open spaces be effectively measured in high-density urban environments? (2) What planning strategies can be implemented to increase the green quantity and improve the urban living environment in such areas? Therefore, this study proposes planning strategies such as three-dimensional greening, converting grey spaces to green spaces, and implementing policies to encourage public participation in greening efforts. These strategies aim to enhance the green quantity in open spaces, thereby improving the urban living environment in high-density cities like Macau and providing a reference for similar urban areas in the world.

Keywords: high-density urban district; urban open space; green space quantity promotion; planning strategy; blue-green spaces occupancy rate within urban land (BGOR); blue-green spaces visibility rate of the main streetscape (BGVR); Macau; Monaco

1. Introduction

1.1. Research Background

Open space is an important part of urban land use and provides a necessary place for residents to carry out outdoor recreational and leisure activities in their daily lives [1–3]. Macau mainly relies on land reclamation to expand the available land. The total area has

been continuously expanded due to coastal reclamation [4,5] and has gradually expanded from 11.6 square kilometers in 1912 to 29.9 km^2 in 2011. As of 2023, Macau's total land area had reached 33.3 km^2. However, this city accommodates 686,600 people (data as of the third quarter of 2024) [6]. Population density has been increasing. For a high-density city like Macau, how do you enhance the naturalization of urban space under conditions of extremely tight land resource availability? This also brings new challenges and novel approaches to the current urban planning and design industry.

In February 2022, the Macau Special Administrative Region Government approved the implementation of the first-ever "*Macau Urban Master Plan (2020–2040)*", which puts forward "the goal of Macau's urban development and construction as a green, livable, and touristic green, low-carbon, and sustainable city" [7]. It is necessary to form an organically connected blue-green network through the planning of ecological reserves, green areas, or public open spaces, and to link green areas and water nodes such as mountains, water bodies, and parks. Based on Macau's current situation, to achieve this planning goal, it is necessary to significantly increase the level of green space in open spaces in high-density urban areas to realize green development.

1.2. Literature Review: An Evaluation of the Amount of Green Space in International Urban Open Spaces

1.2.1. Indicators for Evaluating Green Space in the Urban Open Space Plan

In addition to the indicators "Green Area Rate" and "Green Coverage", which are commonly used in Chinese domestic technical specifications, other indicators for evaluating the amount of green space in the plane of urban open space mainly include "Green Performance" and "Green Patch Density" [8]. Levant et al. used the green performance evaluation index to make a comprehensive evaluation of green open space in 24 European cities [9]. This index mainly calculates the proportion of green space in urban areas, the proportion of green space per 1000 residents, the existence and planning of regional green space systems, urban green space investment funds, the number of urban green open spaces, green space accessibility, and other influencing factors used in the green performance index to make a comprehensive evaluation of the quality of green open space in urban layout [3,10]. Xiao Xi et al. proposed the evaluation index of "green patch density" for high-density cities, i.e., by mapping the ratio of urban green space surrounding the boundary in satellite remote-sensing images to the total area of the city, combined with influencing factors such as the perimeter of the green space boundary, observing the density of green patches in the urban planar layout, and then evaluating the level of quantity of greenery of the spatial planar green space in high-density cities [11–14]. The level of green space in high-density urban spaces can be evaluated by observing the density of green patches in the urban layout [11,12].

1.2.2. Indicators for Evaluating the Quantity of Greenery in Urban Open Space Façades

Among the evaluation indicators related to the amount of greening of urban open space façades, the most widely used ones are the visible green index and the green view index. These two indexes, both of which essentially reflect an evaluation of the degree of greening of urban space from the visual point of view of human beings, have gradually become the new indexes for measuring the amount of greening of urban space in recent years.

Andrew Larkin et al. used the concept of the "green landscape index" to measure the greenness of urban streetscapes. The specific operation was to use an AI intelligent algorithm model for a large number of low-density residential neighborhoods to calculate,

from a Google panoramic image, the green elements in proportion to the green façade, and then make a comprehensive evaluation of the green visibility of the streetscape [15]. The results of the study show that the AI machine intelligence's computing function has great potential for development and can now be applied to evaluate the green view index of low-density neighborhoods with a relatively simple streetscape element, but the application in more complex neighborhood environments in high-density urban areas is still difficult. Huai Zhen et al., by letting a large number of experimenters watch a panoramic image of green space in urban settlements while wearing a brainwave-measuring instrument, recorded the magnitude of the brainwave changes in each experimenter's brainwave and concluded that a green visibility rate of the panoramic picture in a value interval of 60–80% was the ideal urban living environment conditions measured by the human brain wave; at the same time, they proposed that the green space of the settlements, in the context of guaranteeing the health benefits of a residence, should be 60% [16]. According to Yoji Aoki, a well-known Japanese scholar, the "Visible Green Index" is a useful metric for gauging urban residents' subjective psychological perceptions of the amount of green space in their city [17]. Referring to Natsuki Ogihara's segmented evaluation method of green visibility and the documents of the Japanese Regional Urban Development Bureau and the Ministry of Land, Infrastructure, Transport, and Tourism, when the green visibility rate of urban streetscapes is more than 25%, it reaches an excellent level for the greenness of urban space façades and can be used as the target value of greenness in the planning of the façades of most urban open spaces [18].

1.3. Problem Statement and Objectives

Despite the rich body of research on green area rate, green coverage, green performance, and green patch density, there are significant gaps when applying these findings to high-density cities like Macau. Moreover, the existing literature primarily focuses on two-dimensional assessments of green space quantity, such as the proportion of green space within urban areas and the density of green patches in the urban layout. However, in high-density urban environments, it is equally important to consider the vertical dimension of green space, which is often overlooked. The visual impact of greenery from a street-level perspective, as measured by indicators like the visible green index and the green view index, has gained attention in recent years but is still underutilized in planning practices, especially in complex urban settings like Macau.

Due to the special history of the city and the current governance system of "one country, two systems" [19,20], it is difficult for Macau to copy the practices of Chinese mainland cities in terms of urban planning and construction, and often Macau must learn from the comparative experiences of international cities when formulating its development strategies. At present, there is still no research on a planning strategy for evaluating and enhancing the amount of green space in open spaces in Macau. Referring to the current national standards of Chinese domestic cities, such as the *Urban Green Space Design Code (GB50420-2007)* and *Urban Green Space Planning Standards (GB/T51346-2019)*, the most commonly used indicators for urban green space evaluation and planning include the green space rate, green coverage rate, coverage rate of the service radius of parks and green spaces, the index of parks available to by 10,000 people per capita area of scenic green space in the urban area, etc. [21,22]. However, due to Macau's special urban conditions, it is not possible to assess and improve the current green space planning strategies in Macau. Besides, due to Macau's special municipal conditions, most of these indicators are not applicable and other indicators must be found.

This paper takes the high-density urban areas of the Macau Peninsula and the Principality of Monaco as examples and sets the planning indicators of open space green quantity into two dimensions: the blue-green spaces occupancy rate within urban land and the blue-green spaces visibility rate of the main streetscape; then, it proposes suitable indicators for Macau through an assessment of the current situation and international comparisons. This study also presents a suitable planning strategy for the enhancement of green space in urban open spaces in Macau, so as to provide a reference for the optimization of the human environment in Macau and similar high-density urban areas in China.

2. Study Area and Methods

2.1. Study Area

2.1.1. Macau Special Administrative Region in China

Macau is a port city on the coast of the Pacific Ocean and the South China Sea. It is located on the west bank of the Pearl River Estuary and at a low latitude south of the Tropic of Cancer. It is connected to Gongbei, Zhuhai, Guangdong in the north, Wan Chai and Hengqin across the tributaries of the Xijiang River, the Inner Harbor and the Jiamakou Channel to the west, Lantau Island in Hong Kong to the east across the Lingding Ocean, and the Wanshan Islands to the south [23–25]. The components of Macau include the Macau Peninsula in the north and the outlying islands in the south. The offshore area of Macau refers to the large island, consisting of Taipa, Coloane, and Cotai City [26]. Originally comprising Taipa Island and Coloane Island, after the construction of the Cotai Connecting Highway, reclamation and water flow from the West River brought a large amount of silt, the seabed between the two islands became shallower, and more and more land was formed along the highway. Therefore, the local government started planning for reclamation, and the resulting land became Cotai City (Figure 1), with a total area of about 32.9 km^2. In 2020, the population density of Macau's urban area was about 20,800 people/km^2, which is one of the highest in the world [27]. Among these areas, the urban area of the Macau Peninsula is only 9.3 km^2, and the population density is about 58,300 people/km^2, representing one of the most densely populated cities in the world.



Figure 1. Location of the Macau Peninsula and Macau's outlying islands. The small amount of Chinese text references Zhuhai City, but the area is not within the scope of this study (image source: the author's annotations are based on Google satellite images).

2.1.2. The Principality of Monaco

The Principality of Monaco is located in the south of France. Except for its southern coastline close to the Mediterranean Sea, the entire territory is surrounded by France on three sides to the north, west, and east [28,29]. It is mainly composed of the old city of Monaco and the surrounding areas that were subsequently established, with a land area of about 2.1 km^2 (Figure 2). Monaco had a resident population of about 38,000 in 2019 and a population density of about 18,413/km^2 [28], making it a high-density city. Monaco is a typical "city-state", with a GDP per capita of about USD 170,000 in 2020, ranking it first in the world [30]. Monaco is currently organized into 10 urban districts, 9 administrative districts, and 1 parish. Like Macau, Monaco is one of the few high-density cities in the world with a 100% urbanization level [31]. The problems in the two cities are the same because of the small urban land area and high urban density, and both cities have no surplus land available for the construction of green spaces. In terms of the evolution of the urban form, the size and shape of Monaco's urban area are very similar to those of the Macau Peninsula before reclamation. Except for the newly reclaimed area, the size of Monaco's urban zoning is also similar to that of Macau's, and the scale of the streets is even more similar to that of the streets in the urban area of the Macau Peninsula, which are all characterized by narrow and confined urban spaces. Streets in Monaco's urban areas are mostly one-lane streets with narrow sidewalks that allow only two people to pass sideways; it is only in the newly reclaimed areas that there are more than four lanes in each direction of modern urban traffic. In terms of urban layout, history, and culture, the historic buildings in the urban areas of Monaco and the Macau Peninsula are typically European in style; the establishment of districts in Monaco and the delineation of parishes in Macau are both influenced by the Catholic culture, with churches set up in each district and parish and Catholicism as one of the main religions in the city. In terms of the city's economy and industries, Monaco's mainstay, like Macau's, is tourism and gaming. Monaco and Macau are both developed economies and independent customs territories, and both rank in the top three in the 2019 Global Country/Region GDP per capita rankings. Therefore, Monaco and Macau are highly comparable when examined in terms of urban form, development status, city layout, industrial economy, and standard of living. In particular, most of the zoning areas of the Macau Peninsula are close to those of Monaco, which are both small-scale urban zones. With the exception of some zoning districts where the density of buildings is extremely high, the density of buildings in the urban area of the Macau Peninsula is basically comparable to that of Monaco. In this way, these two specific cities have high comparability. This comparability allows for a more targeted and effective analysis of urban planning strategies, especially in terms of the level of greenery enhancement in high-density urban areas.

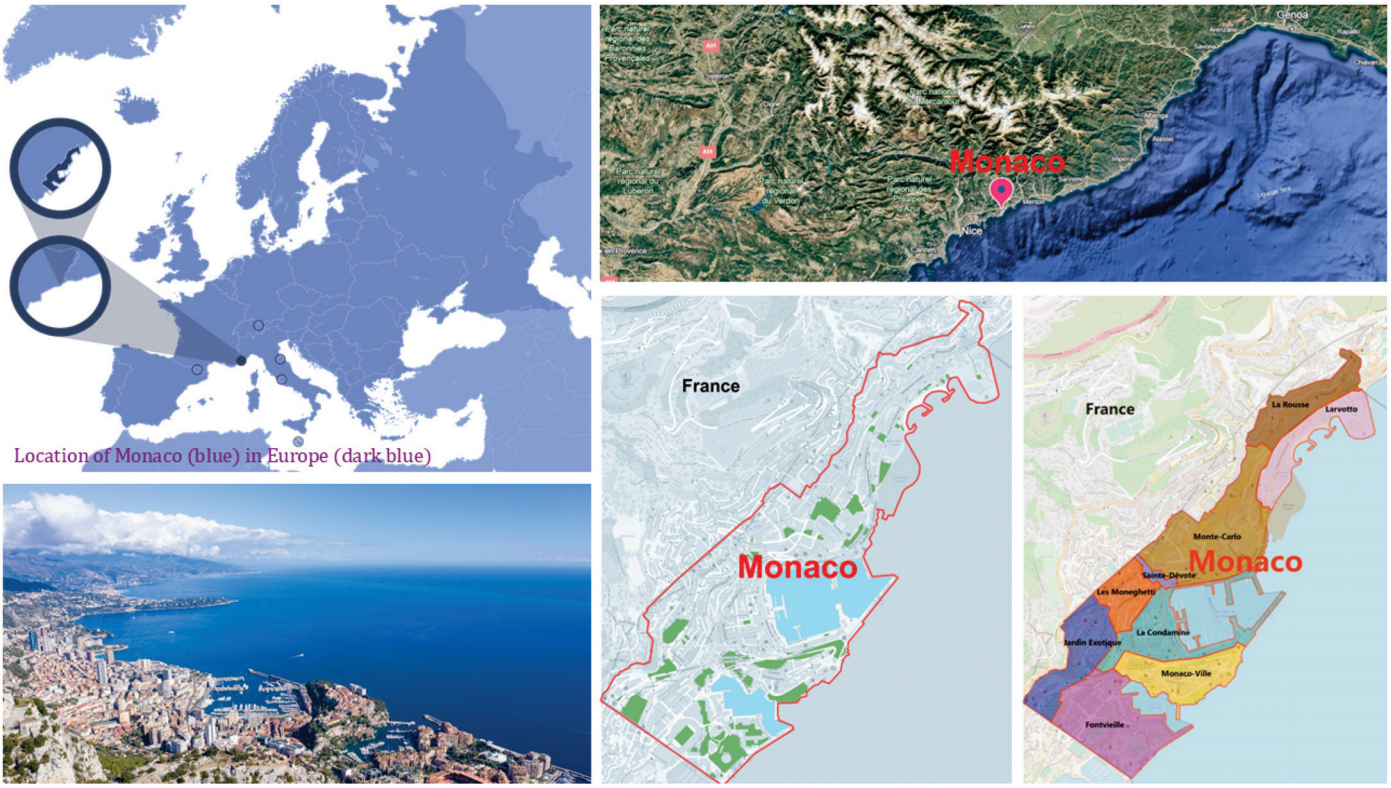


Figure 2. Location of the Principality of Monaco (image source: the author's annotations are based on Google satellite images).

2.2. Data Sources and Methodology

The data used in this paper included the 0.6 m accuracy satellite remote-sensing map of the whole area of Macau (October 2020 version), the 1:10,000 base map of the current status of Macau's urban green space (2020 version), and the 1:1000 AutoCAD map of the whole area of Macau (October 2020 version), as provided by the Macau Cadastral Bureau and the Greening Department of the Municipal Services Department. Other land data and population data were drawn from References [32–39], as a supplement to the above. The study area is 9.3 km^2 of the urban area of the Macau Peninsula (excluding New Town Area A and the artificial island of the Hong Kong-Zhuhai-Macau Bridge, which are under construction by reclamation). Using the 1:1000 AutoCAD map of the whole area of Macau and the 0.6 m precision satellite remote-sensing map, the 1:10,000 base map of the current status of urban green space on the Macau Peninsula in 2020 was checked and updated. After topological proofreading, the green and open spatial data information of the Macau Peninsula, including the urban green space and the natural water bodies, was entered into the ArcGIS geospatial database. Subsequently, after the urban green space information of Macau was counted in the form of a GIS geospatial database, ArcGIS 10.7 software was further used to analyze and evaluate the green open space of the urban area of the Macau Peninsula (Figure 3). The research content is embodied in a set of spatial green quantity evaluation indexes: the blue-green spaces occupancy rate within urban land (BGOR), and the blue-green spaces visibility rate of the main streetscape (BGVR). The specific calculation expression is as follows:

$$BGOR = (GA + NW)/MS \times 100\% \quad (1)$$

where GA is the area of urban green space in the planning area, NW is the area of natural water bodies in the planning area, and MS is the area of urban land. The calculation of the BGOR value for each sub-area of the Macau Peninsula can be quantified by the Macau GIS green open space database:

$$BGVR = (EA + EW)/ES \times 100\% \quad (2)$$

where EA is the visible area of vegetation in the streetscape image, EW is the visible area of natural water bodies in the streetscape image, and ES is the area of the streetscape image's view. The BGVR value is calculated by capturing the city streetscape samples from Baidu/Google Street View maps and entering them into the ArcGIS software for calculation.



Figure 3. Distribution of green open spaces in 17 precincts of the Macau Peninsula (image source: drawn by the author).

The Principality of Monaco currently has eight urban administrative divisions: Fontvieille, Jardin Exotique, Monaco-Ville, La Condamine, Les Moneghetti, Larvotto, Monte-Carlo, La Rousse, and Sainte-Dévote, excluding the new district of Le Portier, which is under construction on reclaimed land. In addition, the study of the statistical area of the Fontvieille and La Condamine districts in Monaco's urban subdistricts includes the natural waters of the two inner city harbors, Port de Fontvieille and Port Hercule de Monaco, respectively (Figure 4).



Figure 4. Distribution of green open spaces in Monaco's urban subdivisions (image source: drawing by the author).

Population data for Monaco's city subdivisions were taken from the 2016 census of the Principality of Monaco. Of these, no permanent population counts are available for Sainte-Dévote. The data sources underlying the BGOR values for the study of Monaco's nine city sub-districts include Open Street Map 50-meter-accuracy multi-layer vector map data (2021 edition), Google Earth satellite image maps with a maximum accuracy of 7.0 m (2018 edition), Monaco city statistics, and Monaco's 2016 city sub-district population census data. The method used for Monaco city map GIS data analysis is to extract the 50-meter-precision Open Street Map urban green open space-related layers and convert them into isometric vectorized map data by scale. Then, the map information data are imported into the ArcGIS spatial database. On this basis, the map information data analysis and statistics function of ArcGIS 10.7 software is used to extract the map information related to green open spaces in the Monaco urban zoning area, further analyze the proportion of green

open space in Monaco city, and conduct a comparative analysis with the urban area of the Macau Peninsula.

Regarding indicators for evaluating the amount of green in the three-dimensional urban façade landscape, the visible green index, i.e., the percentage of green in one's field of vision, is researched more frequently in the academic world at present. In Japan, the green visibility index has been officially used to evaluate the greening level of urban neighborhoods. However, in a waterfront city, the natural elements in the streetscape space are not only green but also include the blue color of the water area. Therefore, this paper proposes to use the BGVR as an indicator for examining the level of naturalization of urban spaces. Referring to the calculation method for the stratified sampling of the green visibility rate, and taking into account the actual situation in Macau, the specific measurement method of BGVR is as follows:

(1) Select six streets with representative landscapes in each of the 17 sub-districts of the Macau Peninsula, with names such as Avenida de, Avenida, Avenue, Largo, and so on. Then, we take one node landscape in each street for measurement purposes; the location of the selected points is shown in Figure 5.



Figure 5. Location of the selected sites for BGVR value measurements for sample streets in the Praia Grande e Penha district (image source: drawing by the author).

(2) Use the Baidu map website's 2019–2020 version of the street view image as a sampling base map, framing the camera installed in the street view, shooting from a car roof at a height of about 2.5 m above the ground, with the lens position along the street center line perspective shift, and framing a time period for sufficient daylight between 8:00 a.m. and 17:00 p.m.

(3) Using ArcMap 10.7 software, the blue and green natural elements in each streetscape image are labeled with blue and green layers, in combination with the semantic segmentation method. The percentage of each blue and green natural spatial element's labeled layer in the streetscape map is calculated one by one. Lastly, the percentage of blue-green layers in each streetscape image in ArcMap is converted isometrically to the BVGR values for streetscape nodes in each neighborhood for statistical purposes (for example, the Barra e Manduco district, Tamagnini Barbosa district, and Guia district).

3. Results

3.1. Evaluation of the Quantity of Green Areas in the Macau Peninsula

3.1.1. Evaluation of Open Space and Green Quantity in the Urban Areas of the Macau Peninsula

By the end of 2020, the area of urban green space on the Macau Peninsula was 1,817,215 m^2, the area of natural water bodies was 550,501 m^2, and the BGOR rate was 24.8%. Through further study of the 17 sub-districts of the Macau Peninsula, it was found that the gap between the green open space indicators of each sub-district was obvious. For example, the difference between the indicators of the Barca and Guia districts was more than 65%, and the polarization of the urban environment was more marked.

As shown in Figure 3 and Table 1, the average value of BGOR for the 17 urban areas in the Macau Peninsula urban area is 18.5%, and there are large gaps among the indicators between the sub-districts. Among them, the north-central regions of the peninsula (the Barca district and Horta e Costa e Ouvidor Arriaga district) have the lowest BGOR values, which are 0.91% and 2.58%, respectively. The central, western, and part of the northern regions (Baixa de Macau district, Doca do Lamau district, Fai Chi Kei district, Areia Preta e Iao Hon districts, Barra e Manduco district, etc.) have a BGOR value of less than 10%; the southeastern, northeastern, and part of the northwestern regions (ZAPE district, NATAP district, and Ilha Verde district) BGOR values are moderate, ranging from 10% to 15%. The southwest and southern regions (Praia Grande e Penha district and NAPE e Aterros da Baía da Praia Grande district) have high levels of BGOR values, ranging from 25% to 43%, and the eastern region (Móng Há e Reservatório district and Guia district) had the highest levels of BGOR values, at 52.95% and 67.49%, respectively.

Table 1. Summary of BGOR volume calculations for 17 sub-districts in the Macau Peninsula.

No.	City Zoning and Numbering	BGOR (%)	No.	City Zoning and Numbering	BGOR (%)
17	9. Barca	0.91	8	10. Patane e São Paulo	13.60
16	8. Horta e Costa e Ouvidor Arriaga	2.58	7	4. NATAP	14.09
15	7. Doca do Lamau	5.34	6	13. ZAPE	14.47
14	16. Barra e Manduco	6.61	5	2. Tamagnini Barbosa	18.72

Table 1. *Cont.*

No.	City Zoning and Numbering	BGOR (%)	No.	City Zoning and Numbering	BGOR (%)
13	15. Baixa de Macau	7.70	4	17. Praia Grande e Penha	25.00
12	3. Areia Preta e Iao Hon	7.74	3	14. NAPE e Aterros da Baía da Praia Grande	42.82
11	6. Fai Chi Kei	10.11	2	5. Móng Há e Reservatório	52.95
10	11. Conselheiro Ferreira de Almeida	11.27	1	12. Guia	67.49
9	1. Ilha Verde	12.84	Area-wide average	Macau Peninsula	24.80

Source: statistics and plotting by the author.

3.1.2. Evaluation of the Green Quantity of Open Space Façades in the Urban Areas of the Macau Peninsula

Evaluations were made by combining an analysis of the BGVR indicator of the major streetscape in the neighborhoods of the Macau Peninsula in Table 1 above and referring to the segmented evaluation method of green visibility rate proposed by the Japanese scholar Natsuki Ogihara. The BGVR indicators of Macau's various neighborhoods can be roughly categorized into three intervals: lower (<15%), medium (15~25%), and higher (>25%), with an average of 18.3% for the whole area of the Macau Peninsula, which is at the medium level. As can be seen from Tables 2 and 3, the distribution of BGVR values in the neighborhoods of the Macau Peninsula is uneven, with higher BGVR values seen mainly in the new reclamation areas, such as the NATAP district, NAPE e Aterros da Baía da Praia Grande district, and ZAPE district. In contrast, the core, old districts of the Peninsula (e.g., Barra e Manduco district, Barca district, and Patane e São Paulo districts) have single-digit BGVR values, indicating a poor level. Overall, among the 17 sub-districts of the Macau Peninsula, there are 6 urban areas with poor BGVR values, 9 urban areas with moderate values, and only 2 urban areas with better values.

Table 2. The Macau Peninsula's 17 sub-district BGVR values, showing measurement illustrations.

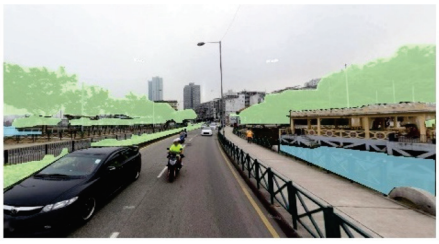
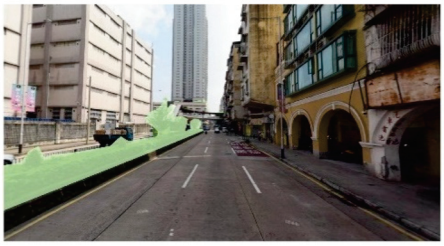
Barra e Manduco BGVR Average = 7.6%		
		
(1) Avenida de Sai Van BGVR = 19.7%	(2) Rua do Almirante Sérgio BGVR = 5.9%	(3) Rua da Praia do Manduco BGVR = 2.0%

Table 2. *Cont.*

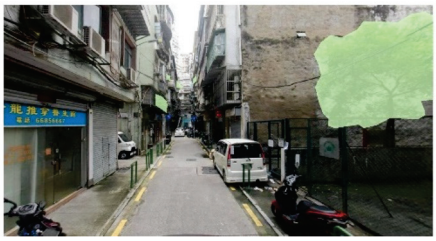
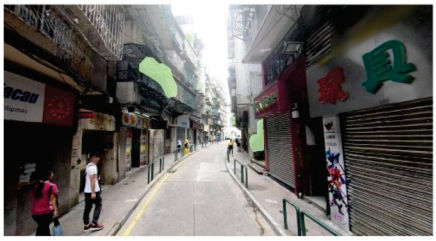
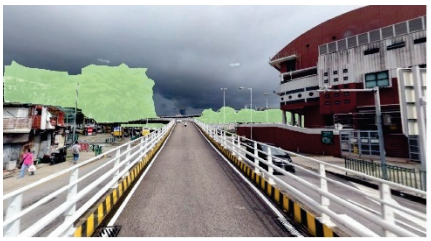
		
(4) Travessa De Chan Loc BGVR = 11.3%	(5) Rua Dos Cules BGVR = 1.2%	(6) Rua das Lorchas BGVR = 5.2%
Tamagnini Barbosa BGVR Average =13.9%		
		
(1) Avenida do Conselheiro BGVR = 15.9%	(2) Rua Central de Toi Sán BGVR = 18.4%	(3) Avenida de la Barbosa BGVR = 33.3%
		
(4) Rua Marginal do Canal das Hortas BGVR = 1.9%	(5) Praça das Portas do Cerco BGVR = 8.1%	(6) Rua Vá Tai BGVR = 5.8%
Guia BGVR Average =23.8%		
		
(1) Avenida de Sidónio Pais BGVR = 31.3%	(2) Estrada Do Engenheiro Trigo BGVR = 47.9%	(3) Estrada da Vitória BGVR = 18.3%

Table 2. *Cont.*

		
(4) Rua da Fonte da Inveja BGVR = 16.8%	(5) Estrada de Cacilhas BGVR = 12.6%	(6) Calçada Da Vitória BGVR = 15.8%

Source: statistics and plotting by the author.

Table 3. Sorting of BGVR values in 17 sub-districts of the Macau Peninsula.

No.	City Zoning and Numbering	BGOR (%)	No.	City Zoning and Numbering	BGOR (%)
17	10. Patane e São Paulo	6.7	8	7. Doca do Lamau	17.9
16	16. Barra e Manduco	7.6	7	14. NAPE e Aterros da Baía da Praia Grande	23.0
15	9. Barca	9.8	6	5. Móng Há e Reservatório	23.0
14	6. Fai Chi Kei	13.8	5	12. Guia	23.8
13	2. Tamagnini Barbosa	13.9	4	13. ZAPE	24.1
12	3. Areia Preta e Iao Hon	14.8	3	1. Ilha Verde	24.7
11	11. Conselheiro Ferreira de Almeida	15.0	2	4. NATAP	26.5
10	8. Horta e Costa e Ouvidor Arriaga	16.8	1	17. Praia Grande e Penha	33.3
9	15. Baixa de Macau	16.9	Area-wide average	Macau Peninsula	Average 18.3

Source: statistics and plotting by the author.

3.2. Empirical Comparison: Evaluation of the Green Quantity of Urban Open Spaces in Monaco

3.2.1. Evaluation of the Greening of Monaco's Urban Open Space Plan

As previously mentioned in the methodology, the researchers utilized ArcGIS 10.7 software for mapping, data analysis, and statistics to extract pertinent information about green open spaces in Monaco's urban districts. They then further analyzed the proportion of green open spaces in Monaco (Table 4) and subsequently compared and analyzed it with the urban areas of the Macau Peninsula (Tables 5 and 6). The specific results are shown below.

Table 4. Measurement of BGOR in Monaco, shown by sub-district.

City Zoning and Numbering	City Zoning Area (m^2)	Area of Green Open Space in the Sub-District (m^2)	Urban Population (People)	Area of Green Open Space per Capita (People/m^2)	BGOR (%)
1. Fontvieille	392,930	125,345	4420	23.8	31.9
2. Jardin Exotique	240,000	41,280	5117	8.1	17.2
3. Monaco-Ville	200,000	45,600	1064	42.9	22.8
4. La Condamine	536,550	260,227	5141	28.3	48.5
5. Les Moneghetti	120,000	87	4195	0.02	0
6. Sainte-Dévote	20,000	2480	-	-	12.4
7. Monte-Carlo	440,000	38,720	8259	4.7	8.8
8. Larvotto	220,000	30,800	2026	15.2	14.0
9. La Rousse	180,000	7020	7087	1.0	3.9
Total	2,349,480	551,559	37,309	Average 14.8	Area-wide average 23.5

Source: statistics and plotting by the author.

Table 5. Comparison of BGOR values between Monaco and the Macau Peninsula, shown by sub-district.

Subdivision of the City of Monaco	BGOR (%)	Macau Peninsula Urban Zoning	BGOR (%)	Macau Peninsula Urban Zoning	BGOR (%)
1. Fontvieille	31.9	1. Ilha Verde	12.84	10. Patane e São Paulo	13.60
2. Jardin Exotique	17.2	2. Tamagnini Barbosa	18.72	11. Conselheiro Ferreira de Almeida	11.27
3. Monaco-Ville	22.8	3. Areia Preta e Iao Hon	7.74	12. Guia	67.49
4. La Condamine	48.5	4. NATAP	14.09	13. ZAPE	14.47
5. Les Moneghetti	0	5. Móng Há e Reservatório	52.95	14. NAPE e Aterros da Baía da Praia Grande	42.82
6. Sainte-Dévote	12.4	6. Fai Chi Kei	10.11	15. Baixa de Macau	7.70
7. Monte-Carlo	8.8	7. Doca do Lamau	5.34	16. Barra e Manduco	6.61
8. Larvotto	14.0	8. Horta e Costa e Ouvidor Arriaga	2.58	17. Praia Grande e Penha	25.00
9. La Rousse	3.9	9. Barca	0.91		

Source: statistics and plotting by the author.

The research data show that the current BGOR value of Monaco is 23.5%, which is closer to the BGOR value of 24.8% for the urban area of the Macau Peninsula. In particular, the per capita green open space area of Monaco's 8 urban administrative sub-districts is close to the per capita value of the 17 sub-districts on the Macau Peninsula. Some urban districts in Monaco (e.g., Monte-Carlo District and Jardin Exotique District) have similar land-use conditions as Ilha Verde District and Baixa de Macau District on the Macau Peninsula, with lower urban green space occupancy, all having single-digit BGOR values,

and urban districts that are extremely lacking in green space. At the same time, both Monaco and the Macau Peninsula also have several urban areas with high urban green space occupancy rates and BGOR values greater than 20%, which support the beautiful landscape of the coastal tourist cities, such as Monaco's Fontvieille district, the Monaco-Ville district, and the Macau Peninsula's Praia Grande e Penha district and NAPE e Aterros da Baía da Praia Grande district.

Table 6. Comparison of urban green space per capita between Monaco and the Macau Peninsula, shown by sub-district.

Subdivision of the City of Monaco	Urban Green Space per Capita (m^2)	Macau Peninsula Urban Zoning	Urban Green Space per Capita (m^2)	Macau Peninsula Urban Zoning	Urban Green Space per Capita (m^2)
1. Fontvieille	23.8	1. Ilha Verde	2.49	10. Patane e São Paulo	13.60
2. Jardin Exotique	8.1	2. Tamagnini Barbosa	2.06	11. Conselheiro Ferreira de Almeida	11.27
3. Monaco-Ville	42.9	3. Areia Preta e Iao Hon	0.45	12. Guia	67.49
4. La Condamine	28.3	4. NATAP	1.19	13. ZAPE	14.47
5. Les Moneghetti	0.02	5.Móng Há e Reservatório	19.25	14. NAPE e Aterros da Baía da Praia Grande	32.98
6. Sainte-Dévote	-	6. Fai Chi Kei	1.07	15. Baixa de Macau	7.70
7. Monte-Carlo	4.7	7. Doca do Lamau	0.35	16. Barra e Manduco	6.61
8. Larvotto	15.2	8. Horta e Costa e Ouvidor Arriaga	0.19	17. Praia Grande e Penha	25.00
9. La Rousse	1.0	9. Barca	0.06		

Source: statistics and plotting by the author.

3.2.2. Evaluation of the Green Quantity of Open Space Façades in the Urban Area of Monaco

This research on the BGVR value of Monaco is consistent with the above research method regarding the neighborhood landscape of Macau. The sampling and quantification research process is as follows:

(1) According to the size of the area of different sub-districts and the number of roads in Monaco, three to six main streets with representative landscapes are selected in each city sub-district for quantification of the BGVR value, including Boulevard, Avenue, Rue, and Quai, using different scales of streets, with each street a node streetscape. Among them, the streets of Boulevard, Avenue, Rue, Quai and others correspond to streets on the same scale in Macau, such as Avenida, Estrada, Rua, Travessa, and so on.

(2) Using the Google Maps Street View image, version 2020–2021, as the sampling base map, the BGVR values of the main streetscapes in each city sub-division of Monaco are calculated (Table 7).

Table 7. Example of the calculation of BGVR values for the Monaco districts of Larvotto and La Rousse.

Larvotto **BGVR average value = 32.6%**		
		
(1) Princess Grace Boulevard BGVR = 29.4%	(2) Larvotto Boulevard BGVR = 35.4%	(3) Princess Grace Street BGVR = 33.1%
La Rousse **BGVR average value = 39.1%**		
		
(4) Father Luis Flora Street BGVR = 44.0%	(5) Turnau Avenue BGVR = 38.9%	(6) Via Italia BGVR = 34.5%

Source: statistics and plotting by the author.

(3) The blue and green natural elements of the street scene images of each city sub-district of Monaco were identified with blue and green layers, using ArcMap 10.7 software, and the percentage of each blue and green natural spatial element identification layer in each street scene map surface was calculated one by one. Then, the blue and green layer percentage of the street scene images was converted isometrically to BVGR values for the nodes of each neighborhood of Monaco using ArcMap software for analysis (Table 8).

Table 8. Comparison of BGVR values between the urban zones of Monaco and the Macau Peninsula.

Subdivision of the City of Monaco	**BGVR (%)**	**Macau Peninsula Urban Zoning**	**BGVR (%)**	**Macau Peninsula Urban Zoning**	**BGVR (%)**
1. Fontvieille	33.1	1. Ilha Verde	24.7	10. Patane e São Paulo	6.7
2. Jardin Exotique	31.5	2. Tamagnini Barbosa	13.9	11. Conselheiro Ferreira de Almeida	15.0
3. Monaco-Ville	65.7	3. Areia Preta e Iao Hon	14.8	12. Guia	23.8
4. La Condamine	17.2	4. NATAP	26.5	13. ZAPE	24.1
5. Les Moneghetti	17.9	5.Móng Há e Reservatório	23.0	14. NAPE e Aterros da Baía da Praia Grande	23.0

Table 8. *Cont.*

Subdivision of the City of Monaco	BGVR (%)	Macau Peninsula Urban Zoning	BGVR (%)	Macau Peninsula Urban Zoning	BGVR (%)
6. Sainte-Dévote	18.5	6. Fai Chi Kei	13.8	15. Baixa de Macau	16.9
7. Monte-Carlo	23.5	7. Doca do Lamau	17.9	16. Barra e Manduco	7.6
8. Larvotto	32.6	8. Horta e Costa e Ouvidor Arriaga	16.8	17. Praia Grande e Penha	33.3
9. La Rousse	39.1	9. Barca	9.8		
Monaco-wide	Average 31.0			Macau Peninsula-wide	Average 18.3

Source: statistics and plotting by the author.

The research showed that although the BGOR values of the urban subzones of Monaco and the Macau Peninsula are comparable, the BGVR values are different. According to the three intervals categorized by the BGVR indicator above, Monaco has no subzones with low BGVR values (<15%) and three subzones with medium levels (15–25%), accounting for 33.3% of the total, with the remaining six subzones with high levels (>25%) accounting for 66.6% of the total (Table 9). The average BGVR value for the whole area of Monaco was 31.0%, which was 12.7% higher than that of 18.3% for the Macau Peninsula, indicating that the naturalized landscape of the façade space in the urban area of Monaco was better and substantially higher than that of the urban area of the Macau Peninsula. If we compare the extreme values of BGOR between the Monaco and Macau Peninsula urban sub-districts, for example, the Les Moneghetti district in Monaco can still achieve a BGVR value of 17.9% for its façade space, although its BGOR value is about 0 and its per capita area of green open space is 0.02 m^2. Comparatively speaking, the BGVR value of the Barca district on the Macau Peninsula, which has a BGOR value of 0.91, is only 9.8, which is substantially lower than that of the Les Moneghetti district. It can be seen that by strengthening the three-dimensional greening of neighborhoods, the level of spatial greening in high-density urban areas can be effectively improved and the level of spatial naturalization enhanced.

Table 9. Summary of information related to green open space in each of Monaco's municipal subdivisions.

City Zoning and Numbering	Area of Zoning (m^2)	Area of Urban Green Open Space (m^2)	Urban Population (People)	Area of Green Open Space per Capita (m^2/People)	BGVR (%)	BGOR (%)
1. Fontvieille	392,930	125,345	4420	23.8	33.1	31.9
2. Jardin Exotique	240,000	41,280	5117	8.1	31.5	17.2
3. Monaco-Ville	200,000	45,600	1064	42.9	65.7	22.8
4. La Condamine	536,550	260,227	5141	28.3	17.2	48.5
5. Les Moneghetti	120,000	87	4195	0.02	17.9	0
6. Sainte-Dévote	20,000	2480	-	-	18.5	12.4
7. Monte-Carlo	440,000	38,720	8259	4.7	23.5	8.8
8. Larvotto	220,000	30,800	2026	15.2	32.6	14.0
9. La Rousse	180,000	7020	7087	1.0	39.1	3.9
Total	2,349,480	551,559	37,308	Area-wide average 14.8	Average 31.0	Area-wide average 23.5

Source: statistics and plotting by the author.

4. Discussion: Planning Strategies for Enhancing Green Space in Open Space on the Macau Peninsula

4.1. Strategies for Enhancing the Quantity of Greenery of Land Use Plans

Unlike the public ownership of land in Chinese mainland cities, the Basic Law of the Macau Special Administrative Region of the People's Republic of China (Lei Básica da Região Administrativa Especial de Macau da República Popular da China) explicitly protects private land and property, and the government does not have the right to build on or remodel privately owned land or properties other than those owned by the government. Therefore, the protection system of land property rights stipulated in the Basic Law of the Macau Special Administrative Region of the People's Republic of China is one of the main factors affecting the difficult operation of Macau's urban master plan and the preparation of plans related to land use in recent years.

The population data of Macau in the past 20 years show that the number of people in Macau has been increasing year by year, and the density of the urban population has also been increasing (Table 10). The population data for Macau in the past 20 years can be used to project that the population of Macau will continue to show an increasing trend in the next 10 years. This means that an increasing urban population needs to be accommodated in the already limited urban green space, resulting in a serious shortage of urban green space per capita. Regarding the current situation of green open space in the urban areas of the Macau Peninsula, some have suggested that residents should be allowed to "see the green seams and build micro-green spaces" within the streets to increase the amount of green space, but the relevant measures can only be implemented with the cooperation of the citizens on their own initiative and on the premise of complying with the Basic Law of Macau. Although the method of "plugging in the green seams" has had some effect on the greening rate of some neighborhoods, it is not enough to substantially solve the actual problems of the Macau Peninsula, such as the low per capita green space rate. Therefore, for the Macau Peninsula, the way to improve the quality of the human environment in high-density urban areas would be to change the nature of the use of some government-controlled land and to adjust the attributes of some urban land through scientific planning.

Table 10. Population statistics of the Macau Special Administrative Region from 2004 to 2024.

Year	Total Population of Macau
2004	465,333
2005	488,144
2006	512,423
2007	538,100
2008	549,200
2009	542,200
2010	552,300
2011	557,400
2012	582,000
2013	607,500
2014	636,200
2015	646,800
2016	644,900

Table 10. *Cont.*

Year	Total Population of Macau
2017	653,100
2018	667,400
2019	679,600
2020	683,100
2021	683,200
2022	672,800
2023	683,700
2024	686,600

Source: statistics data from the Government of Macau Special Administrative Region Statistics and Census Service. The deadline for Macau's demographic statistics in 2024 is the third quarter of 2024.

Among the 18 sub-categories of Macau's current urban green space classification, only 13 are mainly under the management of the Macau Municipal Affairs Bureau, and the rest are mostly privately owned. In the urban area of the Peninsula, managed by the Macau Municipal Affairs Bureau, there is also a large area of urban squares and foregrounds belonging to the "gray open space" category that can be changed in terms of the nature of the land. The degree of greening of these sites is generally low, with a green area ratio of less than 30%, making it impossible to include them in the category of urban green space. They can be upgraded through measures such as expanding the area of green pavement and planting trees to increase the amount of green space, so that they can then be transformed into urban green spaces.

As shown in Table 11, by calculating the potential greenable land in the Macau Peninsula, more than 10 of the 13 urban areas with a current BGOR value in the Macau Peninsula of lower than 20% can be upgraded by changing the land attributes of the urban gray open space (Open Space Reserve Land) and transforming the land attributes into green space through greening, thereby enhancing the BGOR value of the urban zoning. For example, high-density urban areas such as the Ilha Verde district, Tamagnini Barbosa district, and Patane e São Paulo district can directly increase the occupancy rate of urban green open space by more than 1%, which is of practical significance regarding the improvement of the actual quality of the human environment in the Macau Peninsula.

Table 11. Comparison of before and after BGOR value enhancement in 17 sub-districts of the Macau Peninsula.

Macau Peninsula Urban Zoning	Urban Area (km^2)	Gray Open Space Area Available (m^2)	Current Urban Zoning BGOR Values (%)	Upgraded Urban Zoning BGOR (%)
1. Ilha Verde	0.5	3230	12.84	13.49
2. Tamagnini Barbosa	0.4	4216	18.72	19.77
3. Areia Preta e Iao Hon	0.4	797	7.74	7.94
4. NATAP	0.6	639	14.09	14.20
5. Móng Há e Reservatório	1.0	0	52.95	-
6. Fai Chi Kei	0.3	3846	9.90	11.18
7. Doca do Lamau	0.2	2565	5.34	6.62
8. Horta e Costa e Ouvidor Arriaga	0.2	253	2.58	2.71

Table 11. *Cont.*

Macau Peninsula Urban Zoning	Urban Area (km^2)	Gray Open Space Area Available (m^2)	Current Urban Zoning BGOR Values (%)	Upgraded Urban Zoning BGOR (%)
9. Barca	0.3	0	0.91	-
10. Patane e São Paulo	0.4	4911	13.60	14.83
11. Conselheiro Ferreira de Almeida	0.3	743	11.27	11.52
12. Guia	0.3	0	67.49	-
13. ZAPE	0.8	97	14.47	14.48
14. NAPE e Aterros da Baía da Praia Grande	2.1	1569	42.82	42.89
15. Baixa de Macau	0.5	438	7.70	7.79
16. Barra e Manduco	0.5	306	6.61	6.67
17. Praia Grande e Penha	0.4	0	25.00	-

Source: statistics and plotting by the author.

4.2. Strategies for Enhancing the Quantity of Greenery of Neighborhood Landscape Façades

Monaco's experience can provide a reference for Macau's high-density neighborhoods to enhance spatial naturalization. In terms of the planar indicator of the urban green space occupancy rate (BGOR), the urban area of Monaco is slightly lower than that of the Macau Peninsula by 1.3%. However, Monaco's BGVR value is higher than that of the urban area of the Macau Peninsula by 12.7%, indicating the higher level of spatial naturalization of its neighborhood façade. Taking Av. Princess Grace in Monaco as an example, the improvement in BGVR is mainly due to the extensive wall greening of the building façades along the street, using trellis rails combined with climbing plants. These vertical greenings can directly increase the BGVR value of a building façade by 51.9%, and the effect on the BGVR value of the streetscape space is as high as 27.8% (Figures 6 and 7), which is a valuable experience from which Macau can learn.

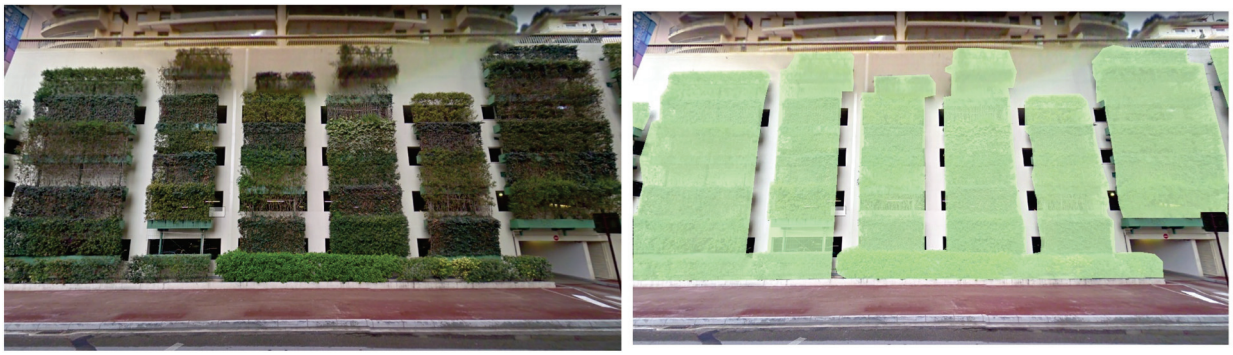


Figure 6. Comparison of greening enhancement: potential values for building façades on Av. Princess Grace, Monaco (image source: photography and drawing by the author).

In some urban areas on the Macau Peninsula with low planar BGOR and façade BGVR values, the walls of buildings along the streets in many neighborhoods are not greened as a façade. Taking Rua dos Hortelãos and Avenida da Praia Grande in Areia Preta e Iao Hon district as examples, after simulating the façade area's share of the building walls along the street and estimating the greenable space of the wall surfaces of the two streets in combination with the ArcGIS software, it was concluded that the BGVR values of the two neighborhoods could be increased by 21.5% and 28.0%, respectively (Figures 8 and 9). If this wall greening is implemented, the neighborhoods with BGVR values that were

originally at the poor level can be improved to a medium-high level. Therefore, in the case of urban land constraints that make it difficult to expand green space construction, the use of three-dimensional greening technology in high-density urban areas of the Macau Peninsula can effectively improve the greening level of the neighborhood's façades, which is a greening pathway worth promoting in urban spaces.



Figure 7. Comparison of three-dimensional greening enhancement: potential values for streetscape spaces on Av. Princess Grace, Monaco (image source: photography and drawing by the author).



Figure 8. Before-and-after comparison of the incremental green space increase at Rua dos Hortelãos, Macau Peninsula (image source: photography and drawing by the author).



Figure 9. Comparison of incremental green space before and after an increase in green space next to Avenida da Racecourse, Macau Peninsula (image source: photography and drawing by the author).

4.3. Policies to Encourage Public Participation in Greening Strategies

Macau has a history of land reclamation to expand the available land. From 11.6 km^2 in 1912 to 33.3 km^2 as of 2023, this city has continuously expanded its land area through

coastal reclamation. During this period, green space development was not a primary focus, leading to a relatively low green space ratio in the first urban areas. The early focus on land reclamation and economic development without sufficient attention being paid to green space planning has left a legacy of low green space coverage in many older urban areas. For example, the central districts of the Macau Peninsula have a green space ratio of less than 10%, with some areas having a BGOR value as low as 0.91%. In the 1990s and early 2000s, there was a gradual shift in urban planning policies toward more sustainable development. The government began to recognize the importance of green spaces for improving the inhabitants' quality of life and started to allocate more land for parks and green areas in the newly planned urban district. However, since the high-density centralized urban area of the Macau Peninsula was already built in the 20th century, the problem of a lack of urban green space in the high-density urban areas of the Macau Peninsula has not been improved.

In high-density cities, one of the greening strategies that can directly increase the amount of greening in urban spaces is to encourage residents to green their balconies, rooftops, and patios. Currently, there are a number of internationally developed city governments that have introduced a series of economic incentive policies to encourage residents to actively participate in urban greening. For example, the Portland Municipal Government of the United States has adopted the Green Roofs policy, which requires that the green roof coverage rate of urban public facilities should reach 70%. As an incentive, developers can receive additional compensation for building plot ratios while reducing some of the stormwater management fees. Commercial and industrial buildings can be subsidized by USD 6.06 per 1000 m^2 [40]. Several German cities have introduced economic incentives since 1983 to continuously encourage residents to implement green roofs, green walls, and green gardens on their own initiative. The Berlin City Council, in order to increase the amount of roof-based green space in the city's high-density neighborhoods by about 65,750 m^2, subsidizes the construction costs of roof greening by EUR 25–60/m^2 for residents of the area. The city of Linz, Austria, has introduced a comprehensive and legally binding greening policy, which stipulates that if a building of more than 100 m^2 with a slope of up to 20° is to be constructed in the city, 12 cm of plant growth medium must be retained on the uppermost surface of the roof structure, and more than 80% of the roof surface must be covered with vegetation. In the case of the construction of underground parking lots and other facilities, more than 30% of the roof surface of the parking lots should be retained as a greening area. In order to encourage the implementation of this statutory policy, the Municipality of Linz has implemented a policy of reimbursing up to 30% of the total cost of the construction, including the cost of construction and design, which is given to the builder as compensation [41].

In contrast, there are no economic incentives to encourage residents to actively participate in the greening of roofs, walls, balconies, and gardens in the urban planning and greening policies of the Macau SAR Government. In the high-density urban areas of the Macau Peninsula, except for some high-class neighborhoods and casinos that have roof gardens, most of the roofs of residential buildings are still in a state of "abandonment" (Figure 10). Compared with the urban governance situation in developed countries, it is not enough for the Macau SAR government to call on citizens to carry out urban greening on their own initiative through publicity. Incentive policies must be put in place to mobilize citizens and enterprises in order to promote spatial greening in the high-density urban areas of Macau.



Figure 10. A large number of the roofs of residential buildings in the high-density urban areas of the Macau Peninsula are still in a state of "abandonment" (image source: photography by the author).

5. Conclusions

The Macau Peninsula is a high-density international city with extremely scarce land resources. Optimizing the use of green open space resources through scientific planning to support the sustainable development of the urban environment in the future is a significant challenge. As Macau's urban industry develops and its population continues to increase, the demand for green open spaces will also rise year by year. It is essential to think long-term and rationally plan the current urban open space resources.

For the high-density urban areas of the Macau Peninsula, the planning strategies for the enhancement of the quantity of greenery in urban open spaces mainly include:

(1) Three-dimensional greening: by all means, vigorously promote the development of three-dimensional greening of building façades and roofs in high-density neighborhoods, so as to effectively enhance the amount of green space.

(2) Turning grey into green: greening part of the existing gray open space (i.e., the current open space reserve land, such as the ungreened Largo and Plaza) and releasing about 23,000 square meters of green space in the central area of the city after reasonable greening of the Largo and Plaza.

(3) Planning for greening: 30% of the land in the new reclamation area A/C/D/E, which is being reclaimed for construction, will be planned as green space, which can increase the area by about 150 hectares of green space.

(4) Policies to pave the way for greening: formulate appropriate greening incentive policies to guide citizens toward actively participating in expanding the open space and the three-dimensional greening of Macau's existing urban neighborhoods, and to expand the blue and green spatial vista of the waterfront shoreline. In addition, the Macau SAR government can transfer part of the permanent population and tourism and other industries to the neighboring Hengqin island in the future, so as to reduce the population density of the urban area of the Macau Peninsula and improve the per capita level of green open space.

In addition to these strategies, it is crucial to monitor and evaluate the effectiveness of these measures over time. This can be achieved through regular assessments of green space quantity and quality, as well as through feedback from the community. Public participation and education are also key components of a successful greening strategy, as they can help to foster a sense of ownership and responsibility among the residents regarding urban green spaces.

Overall, Macau is a high-density international city with extremely scarce land resources, and it is a major challenge to optimize the use of green open space background resources through scientific planning in order to support the sustainable development of the urban environment in the future. As Macau's urban industry develops and its population continues to increase, the demand for green open space will also increase year by year, and it is necessary to think long-term and rationally plan the current urban open space resources. The greening strategy for open space in high-density urban areas of Macau that is proposed in this paper can also provide a reference for the construction of similar high-density urban centers in the world.

Author Contributions: Conceptualization, J.L. and F.L.; methodology, J.L.; software, J.L.; validation, J.L., F.L. and S.Y.; formal analysis, J.L. and Y.C.; investigation, J.L.; resources, J.L.; data curation, J.L.; writing—original draft preparation, J.L. and F.L.; writing—review and editing, J.L. and Y.C.; visualization, S.Y.; supervision, Y.C. and S.Y.; project administration, Y.C.; funding acquisition, Y.C. All authors have read and agreed to the published version of the manuscript.

Funding: This research was funded by the Guangdong Provincial Department of Education's key scientific research platforms and projects for general universities in 2023: Guangdong, Hong Kong, and Macau Cultural Heritage Protection and Innovation Design Team (grant number: 2023WCXTD042). Yile Chen is one of its members. The funders had no role in the study conceptualization, data curation, formal analysis, methodology, software, decision to publish, or preparation of the manuscript. This study received no additional external funding.

Data Availability Statement: Jitai Li organized and participated deeply in the investigation of this study and has all the original data. If you are interested, please contact Jitai Li (jitaili@foxmail.com) for further information.

Conflicts of Interest: The authors declare no conflicts of interest.

References

1. Thompson, C.W. Urban open space in the 21st century. *Landsc. Urban Plan.* **2002**, *60*, 59–72. [CrossRef]
2. Marcus, C.C.; Francis, C. (Eds.) *People Places: Design Guidlines for Urban Open Space*; John Wiley & Sons: Hoboken, NJ, USA, 1997.
3. Burgess, J.; Harrison, C.M.; Limb, M. People, parks and the urban green: A study of popular meanings and values for open spaces in the city. *Urban Stud.* **1988**, *25*, 455–473. [CrossRef]
4. Sheng, N.; Tang, U.W.; Grydehøj, A. Urban morphology and urban fragmentation in Macau, China: Island city development in the Pearl River Delta megacity region. *Isl. Stud. J.* **2017**, *12*, 199–212. [CrossRef]
5. Edmonds, R.L.; Kyle, W.J. Land use in Macau: Changes between 1972 and 1994. *Land Use Policy* **1998**, *15*, 271–292. [CrossRef]
6. Demographic Statistics for the 3rd Quarter of 2024. Macau Special Administrative Region: Statistics and Census Service (DSEC). Available online: https://www.dsec.gov.mo/en-US/Statistic?id=101 (accessed on 13 January 2025).
7. *Government of Macau Special Administrative Region: Draft Consultation Text of the Master Plan of the Macau Special Ad-ministrative Region (2020–2040)*; Land, Public Works and Transport Bureau: Macau, China, 2020.
8. Niu, W.; Shen, Q.; Xu, Z.; Shang, W. Evaluation of the Land Use Benefit of Rapidly Expanding Cities based on Coupling Coordination and a Transfer Matrix. *J. Resour. Ecol.* **2023**, *14*, 542–555. [CrossRef]
9. Levent, T.B.; Vreeker, R.; Nijkamp, P. *Multidimensional Evaluation of Urban Green Spaces: A Comparative Study on European Cities*; VU University Amsterdam, Faculty of Economics, Business Administration and Econometrics: Amsterdam, The Netherlands, 2004. Available online: https://research.vu.nl/en/publications/multidimensional-evaluation-of-urban-green-spaces-a-comparative-s (accessed on 5 December 2024).

10. Dong, Q.; Cai, J.; Chen, S.; He, P.; Chen, X. Spatiotemporal Analysis of Urban Green Spatial Vitality and the Corresponding Influencing Factors: A Case Study of Chengdu, China. *Land* **2022**, *11*, 1820. [CrossRef]
11. Xiao, X.; Li, M. Green Patch Density: Study on the Index for Planning and Layout of Green Space in High-density Cities. *China Landsc. Archit.* **2017**, *33*, 6.
12. Tan, Z.; Lau, K.K.L.; Ng, E. Urban tree design approaches for mitigating daytime urban heat island effects in a high-density urban environment. *Energy Build.* **2016**, *114*, 265–274. [CrossRef]
13. Zhang, Q.; Zhou, D.; Xu, D.; Rogora, A. Correlation between cooling effect of green space and surrounding urban spatial form: Evidence from 36 urban green spaces. *Build. Environ.* **2022**, *222*, 109375. [CrossRef]
14. Samsudin, R.; Yok, T.P.; Chua, V. Social capital formation in high density urban environments: Perceived attributes of neighborhood green space shape social capital more directly than physical ones. *Landsc. Urban Plan.* **2022**, *227*, 104527. [CrossRef]
15. Larkin, A.; Hystad, P. Evaluating street view exposure measures of visible green space for health research. *J. Expo. Sci. Environ. Epidemiol.* **2019**, *29*, 447–456. [CrossRef] [PubMed]
16. Zhu, H.; Yang, F.; Bao, Z.; Nan, X. A study on the impact of Visible Green Index and vegetation structures on brain wave change in residential landscape. *Urban For. Urban Green.* **2021**, *64*, 127299. [CrossRef]
17. Xiao, X.; Li, M. The Method of Measurement and Applications of Visible Green Index in Japan. *Int. Urban Plan.* **2018**, *33*, 6.
18. Ministry of Land Infrastructure Transport and Tourism; Urban and Regional Development Bureau. The Psychological Effect of Urban Greenery on the Landscape to Alleviate the Discomfort of Midsummer Days: A Social Experimental Study of the Correlation Between the Amount of Urban Greenery and the Psychological Effect. 2005. Available online: https://www.mlit.go.jp/kisha/kisha05/04/040812_3/01.pdf (accessed on 20 June 2022).
19. Cai, T.; Tang, R.; Wang, H.; Li, S.D. One country two systems: A comparative study of national identity between Hong Kong and Macau. *Chin. Sociol. Rev.* **2022**, *54*, 107–130. [CrossRef]
20. Chou, K.P. Hong Kong and Macau under one country, two systems. In *Interpreting China's Development*; World Scientific Publishing: Singapore, 2007; pp. 67–71.
21. Zhang, K.; Fan, W.; Shi, J. Recreation suitability evaluation of countryside forests in Shanghai and corresponding developing guidance. *J. Nat. Resour.* **2019**, *34*, 2270–2280. [CrossRef]
22. Guo, Y.; Su, J.G.; Dong, Y.; Wolch, J. Application of land use regression techniques for urban greening: An analysis of Tianjin, China. *Urban For. Urban Green.* **2019**, *38*, 11–21. [CrossRef]
23. Porter, J. *Macau: The Imaginary City*; Routledge: Milton Park, UK, 2018.
24. Wang, L.; Huang, G.; Zhou, W.; Chen, W. Historical change and future scenarios of sea level rise in Macau and adjacent waters. *Adv. Atmos. Sci.* **2016**, *33*, 462–475. [CrossRef]
25. Zhang, J.; Su, F.; Ding, Z. Sea Reclamation Status of Countries around the South China Sea from 1975 to 2010. *Sustainability* **2017**, *9*, 878. [CrossRef]
26. Pinheiro, F.V.; Wan, P. Urban planning practices and scenarios for Macau development. In Proceedings of the 12th Real Estate Society Annual Conference, University of Macau, Macau, China, 9–12 July 2007.
27. Demographia World Urban Areas; 19th Annual Edition: 202308; Winnipeg, Canada. Available online: http://www.demographia.com/db-worldua.pdf (accessed on 18 January 2025).
28. James, G. *Introduction to Monaco*; Gilad James Mystery School: Denver, CO, USA, 2023.
29. d'Hauteserre, A.M. Bridging the culture nature divide in Monaco. *Landsc. Urban Plan.* **2001**, *57*, 209–223. [CrossRef]
30. Monaco | Data. 2020. Available online: https://data.worldbank.org/country/MC (accessed on 26 April 2022).
31. Monaco | History, Map, Flag, Population, Royal Family & Facts. Encyclopedia Britannica. 2021. Available online: https://www.britannica.com/place/Monaco (accessed on 26 April 2022).
32. *Macau Urban Green Space Classification Standard 2015*; Civic and Municipal Affairs Bureau of the Macau Special Administrative Region: Macau, China; South China Agricultural University: Guangdong, China, 2015.
33. Statistics and Census Bureau. *Macau Population Projections 2016–2036*; Macau Special Administrative Region Statistics and Census Service: Macau, China, 2017; pp. 5–10.
34. Census and Statistics Department. *Population Statistics 2020*; Government of Macau Special Administrative Region Statistics and Census Service: Macau, China, 2021; pp. 25–35.
35. Census and Statistics Department. *Population Census*; Government of Macau Special Administrative Region Statistics and Census Service: Macau, China, 2021; pp. 1–4.
36. Census and Statistics Department. *Population Statistics 2021*; Government of Macau Special Administrative Region Statistics and Census Service: Macau, China, 2022; pp. 27–32.

37. Land and Urban Construction Bureau. *Final Report of the Consultation on the Draft Urban Master Plan of the Macau Special Administrative Region (2020–2040)*; Land and Urban Construction Bureau of the Macau Special Administrative Region: Macau, China, 2021; pp. 11–29.
38. Land and Urban Construction Bureau. *Urban Planning Study for New Town Area A*; Land and Urban Construction Bureau of the Macau Special Administrative Region: Macau, China, 2020.
39. Land and Urban Construction Bureau. *New Town District Master Plan Stage 3 Public Consultation Text*; Land and Urban Construction Bureau of the Macau Special Administrative Region: Macau, China, 2015.
40. Ayalon, R. Making Rooftops Bloom: Strategies for Encouraging Rooftop Greening in Montréal. 2006. Available online: https://www.scribd.com/document/487290668/Making-Rooftops-Bloom-Final-Draft (accessed on 26 April 2022).
41. Ngan, G. *Green Roof Policies*; Landscape Architecture Canada Foundation: Kanata, ON, USA, 2004.

Disclaimer/Publisher's Note: The statements, opinions and data contained in all publications are solely those of the individual author(s) and contributor(s) and not of MDPI and/or the editor(s). MDPI and/or the editor(s) disclaim responsibility for any injury to people or property resulting from any ideas, methods, instructions or products referred to in the content.

buildings

MDPI

Article

Operationalizing Sustainability in Old Community Renewal: A Post-Occupancy Evaluation of Resident Satisfaction in Chengdu, China

Qiaoli Ouyang [1], Fengxiang Liu [2] and Yanyu Wang [1,*]

[1] School of Architecture, Southwest Jiaotong University, Chengdu 610097, China; oyql@my.swjtu.edu.cn
[2] No. 32182 Troop of the Chinese People's Liberation Army, Beijing 100043, China; jt253610@gmail.com
* Correspondence: wangyy@swjtu.edu.cn

Abstract: The sustainable renewal of old communities is a key approach to improving residents' quality of life and optimizing urban stock space. However, the research on the effectiveness of renewal initiatives, particularly regarding resident satisfaction, remains insufficient. This study aimed to develop a structured approach by constructing a sustainable development framework with 28 indicators across five aspects—traffic space, leisure space, green space, sense of belonging, and comfort—to evaluate residents' satisfaction with both physical and spiritual dimensions. Utilizing the IPA–Kano method, a revised IPA quadrant diagram was generated to guide optimization efforts. This study conducted an extensive survey across 16 communities in Chengdu, China, to identify key patterns and challenges. Based on these insights, four representative projects were selected as case studies. The study revealed that the 28 evaluation indicators were categorized into 12 necessary needs and 16 expectation needs. Furthermore, the community renewal projects in Chengdu place a notably greater emphasis on the spiritual dimension. Specifically, satisfaction scores for 14 indicators—11 related to the material dimension and 3 related to the spiritual dimension—were found to be below the average score of 3.28. Targeted renewal strategies are proposed for these indicators. This method offers valuable insights and references for future old community renewal designs and contributes to the sustainable transformation of urban stock spaces in China.

Keywords: IPA–Kano method; old community renewal; post-occupancy evaluation; resident satisfaction

1. Introduction

Urban renewal is seen as a complex process. It involves reusing resources and optimizing the environment, allowing for continuous improvements to the economic, social, and environmental conditions of cities. In the face of urban problems such as economic recession, environmental pollution, and land shortages, research on urban renewal has received extensive attention worldwide [1–3]. Since 2021, CNY 13.7 trillion has been invested in China's urban renewal activities, and there have been 154,000 urban renewal projects [4]. As a crucial component in urban renewal, renewal at the community level is believed to possess great potential. In 2024 alone, 56,000 old community renewal projects have been started in China, and it is expected that the renewal tasks in communities built before 2000 will be fully completed in 2025 [5]. The renewal of old communities has emerged as an important means of addressing urban issues. In 1987, the World Commission on Environment

and Development officially defined the concept of sustainable development in the report "Our Common Future", establishing the core principle of "meeting the needs of the present without compromising the ability of future generations to meet their own needs" [6]. In 2015, the United Nations Development Summit adopted the 2030 Agenda for Sustainable Development. Goal 11 focuses on "making cities and human settlements inclusive, safe, resilient, and sustainable", highlighting the importance of sustainable renewal at the community level [7]. As a significant factor affecting the effectiveness of community renewal, resident satisfaction with renewal projects plays a pivotal role in implementing sustainable community renewal. Currently, the governments of various countries typically adopt the top–down planning method. This method often encounters conflicts with residents' demands, thereby triggering problems such as residential segregation [8,9], gentrification [10], and social equity [11,12]. However, for governments and policymakers, during the renewal of old communities, the needs of local residents are difficult to grasp. As the direct subjects in judging the renewal effect in old communities, residents have the most in-depth and comprehensive understanding of the community. Consequently, guiding and encouraging residents to participate in the community's sustainable renewal has become the focus of widespread attention in most countries [13–15].

In recent years, some scholars have delved into the concepts of renewal and development for old communities in terms of renewal mode [16,17], emotional needs [18], and community governance [19]. These studies are not merely confined to improving the building itself and the backward infrastructure [20,21] so as to bring about improvements in the material dimension. The core lies more in the social effects brought about by strengthening social networks [22,23], paying attention to vulnerable groups [24,25], and maintaining fairness and justice [26,27]. This people-orientated renewal concept has enhanced the enthusiasm of residents around participating in community affairs [28]. Gradually, residents have started to participate in aspects such as problem investigation and stating their needs in renewal projects through methods like voting, forums, and meetings [29,30]. However, the participation of residents has not fully permeated throughout the entire project. Especially in terms of research on feedback after the project is completed, the involvement of residents is insufficient, which leads to the renewed communities still facing problems such as similar functions in facility configurations, low utilization rates, and a lack of community identification [31]. Resident feedback, as the final stage of community renewal projects, also forms a foundation for scientifically, rationally, and effectively facilitating the sustainable development of community renewal [32].

Post-occupancy evaluation (POE) originated in European and American countries in the 1960s. It is regarded as a feedback-based environmental evaluation method. POE has been practiced in numerous specific projects and is considered an essential component of the project life cycle. A cyclic pattern of "Programming—Design—Use—Expert Evaluation—Residents' Post–Occupancy Evaluation—Optimization" has been formed (Figure 1). Currently, the POE method is widely researched in fields such as university campuses [33], urban greenways [34], and public buildings [35]. Compared with the above fields, the composition of community environments is relatively complex, and the stakeholders are diverse. Kytta introduced a planning evaluation method from the residents' perspective with the use of GIS [36]. Yin J et al. analyzed three types of communities in Xi'an—urban, suburban, and exurban neighborhoods. By employing the IPA–Kano model, they evaluated these communities and identified the priority factors for improving community residents' satisfaction [14]. Chen J et al. proposed the use of the structural equation model (SEM) to evaluate the factors affecting satisfaction among residents in resettlement communities [37]. Consequently, the majority of the existing literature focuses

on the evaluation of established communities, while the evaluation of older community renewal in current studies is relatively scarce. This imbalance in the field of study leads to an inability to assess whether renewal projects truly meet residents' needs, which is detrimental to the achievement of the Sustainable Development Goals.

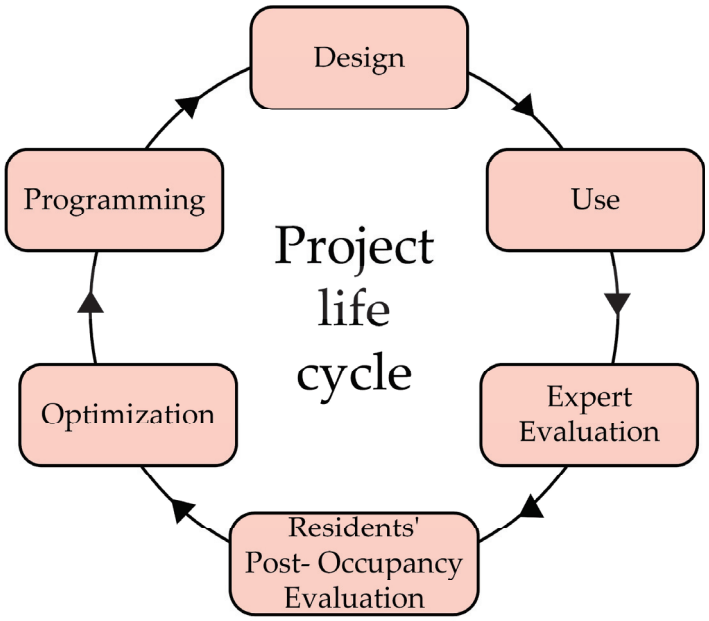


Figure 1. Project life cycle (source: authors).

IPA is a method that reflects users' subjective experiences and psychological feelings. It is mainly used to evaluate the importance and performance of elements and determine the priority of element improvement. However, there is a situation where the perceived performance of elements and the actual performance are non-linear [38]. On the other hand, the Kano model method can classify the elements into necessary needs, expectation needs, and excitement needs according to the impact of the needs on the overall performance. Therefore, scholars have proposed the IPA–Kano method to improve the precision of index element division and prioritization. Wang, M. applied the IPA–Kano model to identify the four building facade design elements that influence tourist travel satisfaction [39]. Yu, P. proposed an optimization design process based on the IPA–Kano model to ascertain the indicators for short-term, medium-term, and long-term updates to urban waterfront spaces [40]. Zhang, Q. applied the IPA–Kano model to the optimization of senior community amenities, thereby enhancing the satisfaction of elderly residents and the development of age-friendly communities [41].

Research on the sustainable evaluation of old community renewal is notably lacking within the Chinese context. Therefore, the research gaps that this paper aims to address are as follows:

(1) Most existing studies have focused on theoretical and practical approaches to early-stage resident participation in renewal projects. However, there is still a noticeable lack of systematic and in-depth assessment regarding residents' feedback on the characteristics and actual effects of updated communities. Analyzing residents' feedback on updated communities is of significant importance in promoting sustainable development in community renewal.
(2) Although post-occupancy evaluation is widely applied in numerous fields, few people utilize the IPA–Kano model to quantitatively analyze residents' satisfaction after the

renewal of old communities. This method can provide data support in identifying the key factors influencing residents' satisfaction.

(3) Most scholars focus on the research of renewal models. However, they fail to use feedback information to dynamically adjust and optimize renewal strategies, which makes it difficult to precisely meet the ever-changing needs of residents. This study will thoroughly explore the feedback data and propose targeted sustainable optimization strategies.

Four typical cases of old community renewal in Chengdu, Sichuan Province, China, are used as examples in this paper. In light of the challenges confronting communities in China, a framework for sustainable development tailored to the renewal of old communities has been established. Combining the advantages of using IPA analysis for judging the renovation priority and the Kano model for determining the intensity of users' demand, the importance score is adjusted according to the demand intensity. Conducting a practical and effective evaluation of the current state of community renewal in Chengdu, key indicators affecting satisfaction are identified. Based on these research findings, we propose targeted improvement strategies to enhance the quality of life and happiness of residents and promote sustainable urban development.

2. Study Areas and Methods

This study employed the IPA–Kano method to conduct a systematic evaluation and analysis of the renewal situation of old communities in Chengdu, China. First, through theoretical research, the study of government documents, and a literature review, an evaluation index set was preliminarily compiled. Then, the index set was revised with the help of field interviews and expert evaluation. Second, the research sample was identified, and an IPA questionnaire was used to collect residents' feedback data. Third, the revised IPA–Kano model was used to calculate the evaluation results, and renewal decisions, and strategies were derived based on the IPA quadrant diagram. The framework presented is shown in Figure 2.

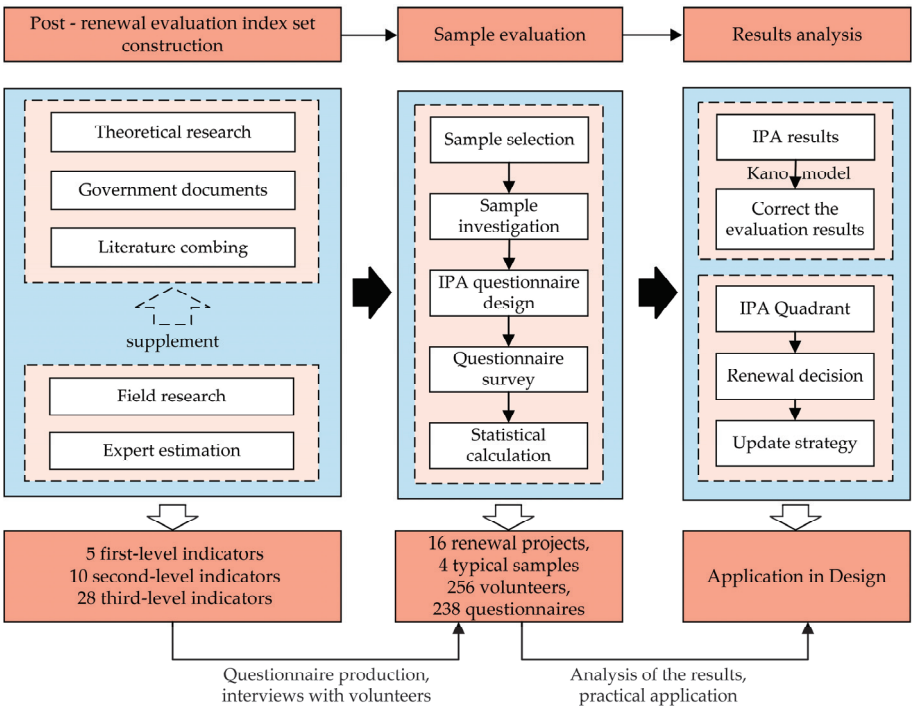


Figure 2. Framework (source: authors).

2.1. Study Areas

Chengdu, a city with a civilization spanning 4500 years and a city-building history of 2300 years, is located in Sichuan Province, China. Moreover, it has long served as the center of Southwest China. As stated in "Chengdu's 14th Five-Year Plan for Urban and Rural Community Development and Governance", Chengdu will carry out the Community Space Quality Improvement Initiative to promote the renewal of old communities. It is planned that by 2025, the renewal projects of 233 old communities will be completed. In this study, we conducted an extensive survey on 16 old community renewal projects in Chengdu, China. Focusing on communities developed before the year 2000 with completed renewal projects, which have been reported by multiple media outlets, we can see that these projects have significant influence (Appendix A).

After an extensive survey, we finally chose excellent cases that have received awards at the city (Chengdu), provincial (Sichuan), or national level in China. These cases represent the overall situation and development trend of old community renewal in Chengdu City. Based on the above requirements, the Southwest Street Area, Ma'an Area, Yulin North Road Community, and Xiajiancao Community were finally selected as the study samples (Figure 3).

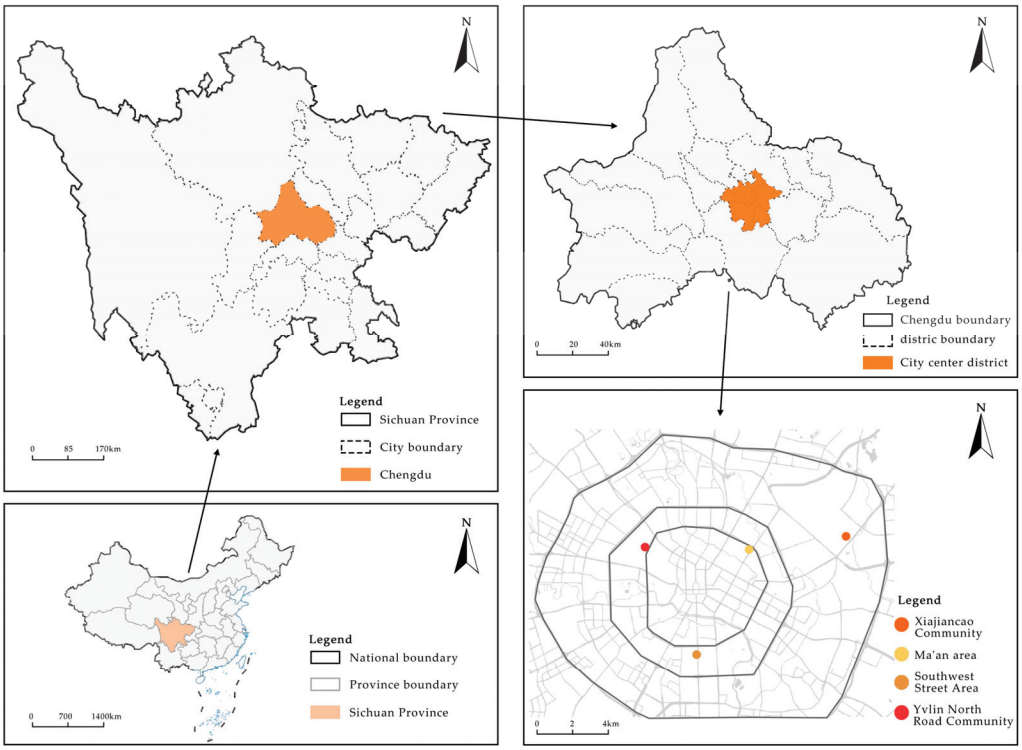


Figure 3. The location of the four samples (source: authors).

The completion years and award information for the four samples are presented in Table 1. The Southwest Street Area Renewal Project is aimed at stimulating community vitality and reshaping the scene of Chengdu's urban life. The renewal of public facilities, such as leisure plazas and fitness centers, is primarily focused in the Ma'an Area. Residents' quality of life and community cohesion are improved by strengthening the social functions of public spaces. The Yulin North Road community renewal is characterized by friendliness, openness, and diversity. The introduction of trendy businesses is focused on, while traditional shops are retained, and a harmonious symbiosis of old and new elements is achieved. The renewal of the Xiajiancao Community integrated 13 courtyards into an

open-style compound; by enhancing the openness and connectivity of the community, a comfortable and convenient living space was created for residents.

Table 1. The completion years and awards of the four example projects.

Sample	Completion Years	Award
Southwest Street Area	2021	Provincial Demonstration Project for the Renovation of Old Urban Communities
Ma'an area	2022	National Exemplary Elderly-Friendly Community
Yulin North Road Community	2021	Chengdu's Outstanding Case of Urban Renewal
Xiajiancao Community	2019	Urban Renewal and Experience Practices for the Renovation of Old Courtyards

2.2. Methods

2.2.1. Construction of the Evaluation Index System

Against the backdrop of sustainable renewal, this paper integrates multi-dimensional evaluation criteria for sustainable buildings, inclusive community facilities and services, livable community landscapes, economic productivity, proud and well-educated communities, and community management, as proposed by the United Nations Sustainable Development Goal 11 [42]. Incorporating Maslow's hierarchy of needs, for this study, we conducted a field survey of 16 old communities in Chengdu, interviewing over 100 local residents. We delve into and summarize the concerns and community issues that matter to the residents. Furthermore, extensive references are made to the relevant literature on community evaluation [43–52], which facilitated the preliminary establishment of an evaluation index for the renewal of old communities.

These indicators have been categorized into two dimensions: material and spiritual. The material dimension refers to the tangible environment, which consists of various objective material renewal elements that can affect residents' daily lives. These aspects include traffic space, leisure space, and green space. The spiritual dimension refers to the intangible environment, which represents the perception of the environment. It includes a sense of belonging and comfort. In addition, we engaged five university professors specializing in urban planning and architecture, three designers with extensive practical experience in urban design and renewal projects, two government administrators responsible for urban construction, and two community leaders and volunteers. Their expertise encompasses work or academic experience related to urban and community renewal planning and sustainable development. Utilizing the Delphi method, a questionnaire survey was conducted to eliminate unreasonable indicators. Through multiple rounds of expert questionnaire surveys, a consensus was reached on the rational establishment of this set of indicators.

Finally, an analytical hierarchy process (AHP) index system of "goal—criterion—indicator" was established. This system consists of 5 first-level indicators, 10 second-level indicators, and 28 third-level indicators (Figure 4).

2.2.2. IPA–Kano Method

The application of the IPA analysis method in this paper can objectively reflect users' perception of the importance and satisfaction regarding the renewal elements of old communities. Based on the data, the importance–performance scores of the renewal indicators

were computed and plotted in four quadrants. The first quadrant represents the "Continued Keep Zone", the second quadrant represents the "Excessive Concern Zone", the third quadrant represents the "Secondary Promotion Zone", and the fourth quadrant represents the "Key Promotion Zone" (Figure 5).

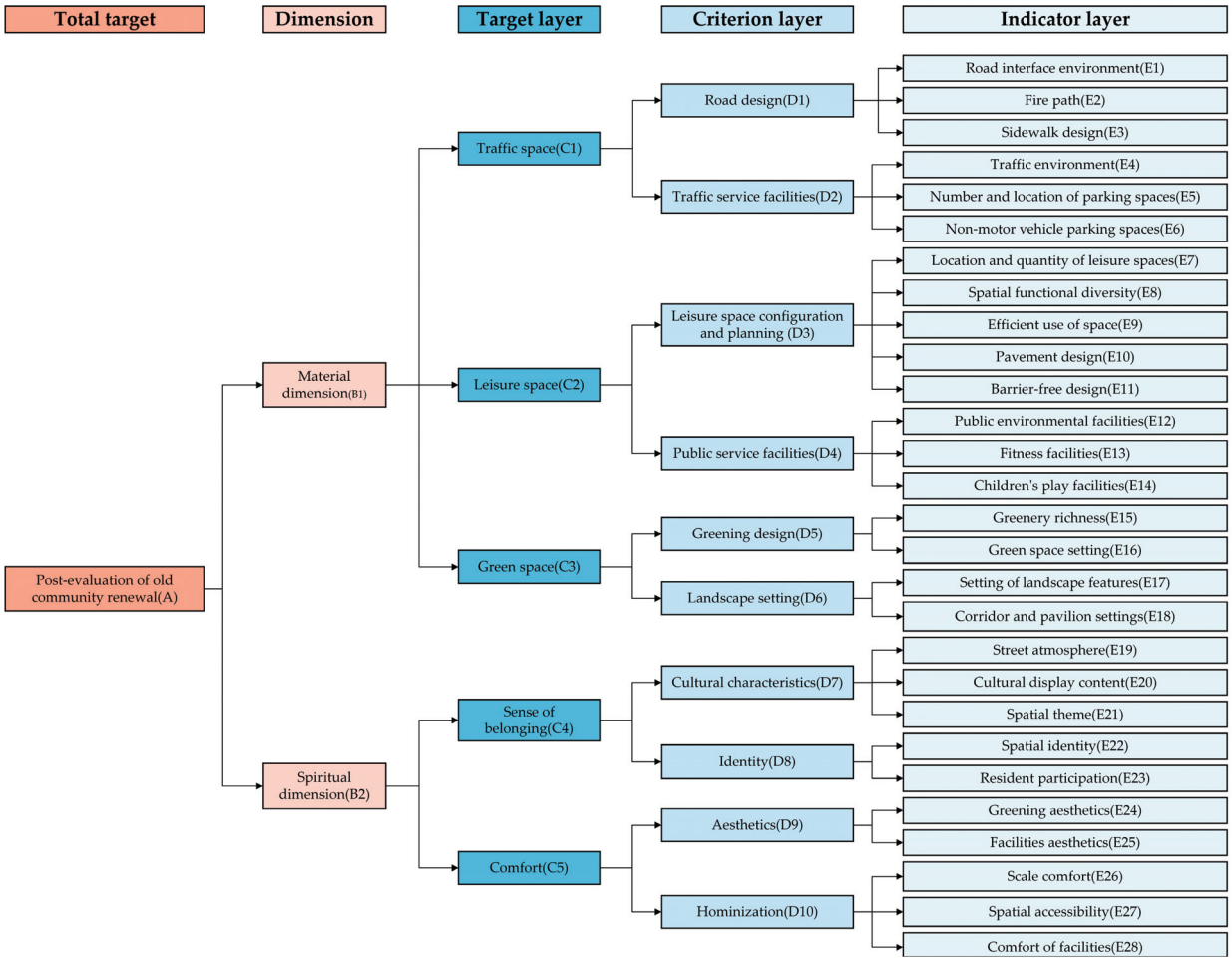


Figure 4. The evaluation index system for old community renewal (source: authors).

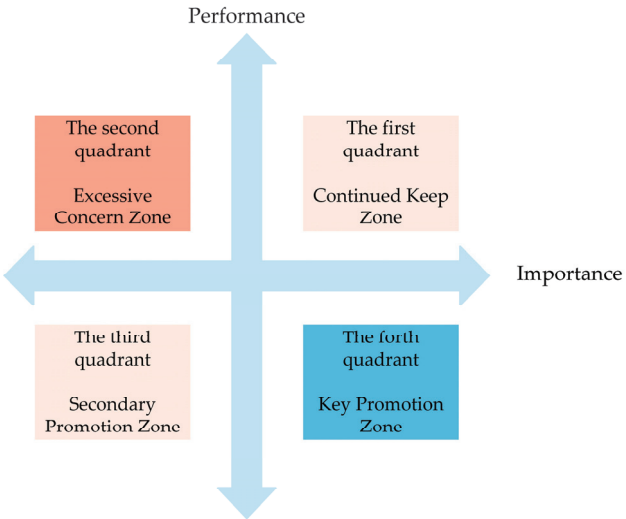


Figure 5. IPA quadrant (source: authors).

The questionnaire scoring is highly dependent on users' subjective judgments and experiences. Specifically, the higher the performance of renewal elements, the higher the satisfaction. It has limited relevance to the current situation in old community renewal. The results are neither objective nor accurate. Consequently, the Kano model is introduced in this paper. The intensity of users' demand is incorporated into the calculation process of the importance score by this model, and then the revised importance score is derived. The intensity of demand can reflect the gap between the actual situation and psychological expectations, thereby providing the basis for revising the importance score. The formula for calculating demand intensity value is as follows:

$$N = q - m \tag{1}$$

In (1), N represents the demand intensity value, q represents the average importance, and m represents the average satisfaction value.

The revised improvement rate is calculated by taking into account the satisfaction target value, the rating value, and the demand intensity. The target value of satisfaction is set according to the type of user demand factor (necessary, expectation, or exciting). The revised coefficient is 0.5 for necessary demands, 1 for expectation demands, and 2 for exciting demands [43]. The calculation method of the revised importance score is as follows:

$$G = \frac{m_a}{m_m} \tag{2}$$

In (2), m_a represents the target satisfaction value; m_m represents the satisfaction rating value; and G represents the revised rate.

$$iG = (G)^{1/k} \tag{3}$$

In (3), k represents the revised coefficient, G represents the revised rate, and iG represents the revised improvement rate.

$$iI = I * iG \tag{4}$$

In (4), I represents the importance rating value, iG represents the revised improvement rate, and iI represents the revised importance score.

2.2.3. Questionnaire Design

The assessment elements of the questionnaire are designed based on the evaluation index set for the renewal of old communities. Subsequently, the score range is determined through the Likert five-point scale method. Five points represent "very important" or "very satisfied", while one point represents "very unimportant" or "very dissatisfied". Prior to the formal survey, a small number of questionnaires were randomly distributed in the study area to ensure that they were easily comprehensible for respondents.

3. Results

3.1. Questionnaire Distribution and Respondent Data

The author conducted the survey in August 2023, selecting 50 to 70 respondents from each chosen sample. In total, 256 questionnaires were distributed, and 238 were retrieved, resulting in a validity rate of 92.9% (Table 2).

The questionnaire was designed to consist of three parts: basic personal information, the evaluation of satisfaction with the old community renewal, and the evaluation of

the importance of the old community renewal. Among the 238 valid samples, there is a balanced proportion of men and women. In terms of age distribution, the number of people over 60 years old is the largest, reflecting the existence of a certain degree of aging in the community. In terms of the duration of residence, the highest number of respondents have lived in the community for over 10 years, indicating a high level of resident stability in this older community. These long-term residents typically exhibit a stronger sense of identity and belonging and are more inclined to participate in community maintenance and renewal activities. The number of respondents who have lived in the community for less than a year is the lowest. However, they have also accumulated a certain level of experience in community living and have formed a certain perception of the community environment during their stay. In terms of household structure, the community comprises both young and elderly individuals living independently and traditional multi-generational family structures. Regarding income, the results suggest that the majority of community residents belong to the middle-income group, with a relatively concentrated income distribution (Table 3).

Table 2. Distribution of questionnaires.

Sample	Number of Valid Questionnaires
Southwest Street Area	63
Ma'an area	52
Yulin North Road Community	67
Xiajiancao Community	56

Table 3. Respondent information statistics.

Characteristic	Category	Number	Proportion
Sex	Male	109	45.80%
	Female	129	54.20%
Age	Under 18 years old	13	5.46%
	18–30 years old	51	21.43%
	30–40 years old	32	13.45%
	40–50 years old	48	20.17%
	50–60 years old	41	17.23%
	Over 60 years old	53	22.27%
Role	Dweller	61	25.63%
	Tourist	27	11.34%
	Worker	67	28.15%
	Other	83	34.87%
Residence time	Under 1 year	23	9.66%
	1–3 years	45	18.91%
	3–10 years	53	22.27%
	Over 10 years	117	49.16%
Household structure	Single-generation living	115	48.32%
	Two-generation living	59	24.79%
	Three-generation living	64	26.89%
Income	0–5000 CNY	32	13.45%
	5000–10,000 CNY	112	47.06%
	10,000–20,000 CNY	75	31.51%
	20,000 CNY	19	8.00%

3.2. Reliability and Validity

To ensure the accuracy of the survey data, the data were tested for reliability. The test results indicate that Cronbach's alpha coefficient for the importance of the total scale is 0.917, and Cronbach's alpha coefficient for satisfaction is 0.926. This suggests that the questionnaire has a high level of reliability (Table 4).

Table 4. Reliability test.

	Number of Indexes	Cronbach's Alpha
Importance	28	0.917
Satisfaction	28	0.926

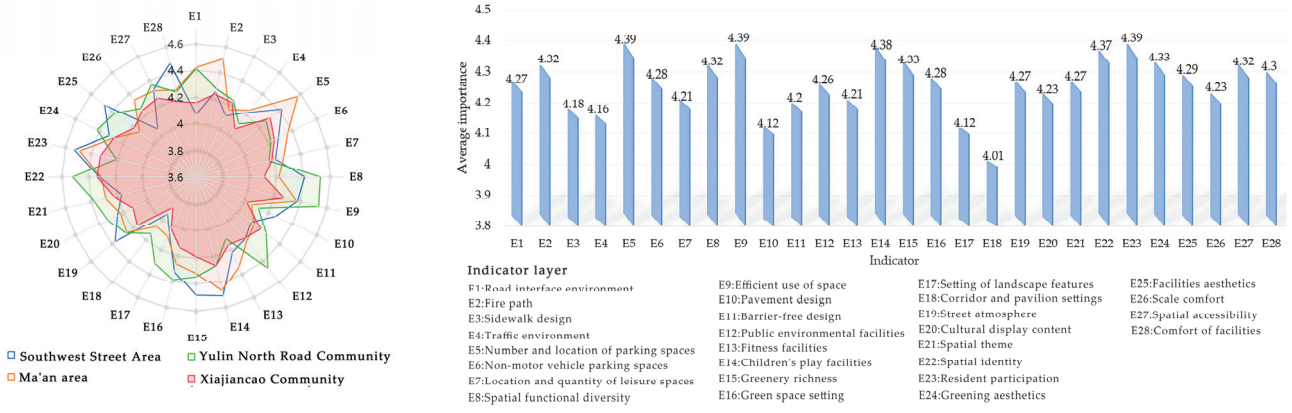
Meanwhile, the validity test was conducted on the sample data. The test results indicated that the KMO value for importance was 0.834, the KMO value for satisfaction was 0.822, and the significant probability of Bartlett's Spherical test statistic value was 0.000, less than 0.01, suggesting a correlation among variables. This suggests that the questionnaire had good validity (Table 5).

Table 5. Validity test.

	KMO	Bartlett's Sphere Test
Importance	0.834	0.000
Satisfaction	0.822	0.000

3.3. IPA Analysis

Based on the importance scores collected, the indicator scores were calculated (Figure 6). The importance scores are indicative of the users' tendency to attach importance to the item. A comparison among the groups indicates that the users exhibit a stronger tendency to attach importance to E5, E9, and E14 and a lower tendency to attach importance to E3, E4, E10, and E18. While the four samples demonstrate a similar tendency to attach importance to some of the updating elements, the tendency to attach importance to E1, E23, E25, and E28 varies considerably.



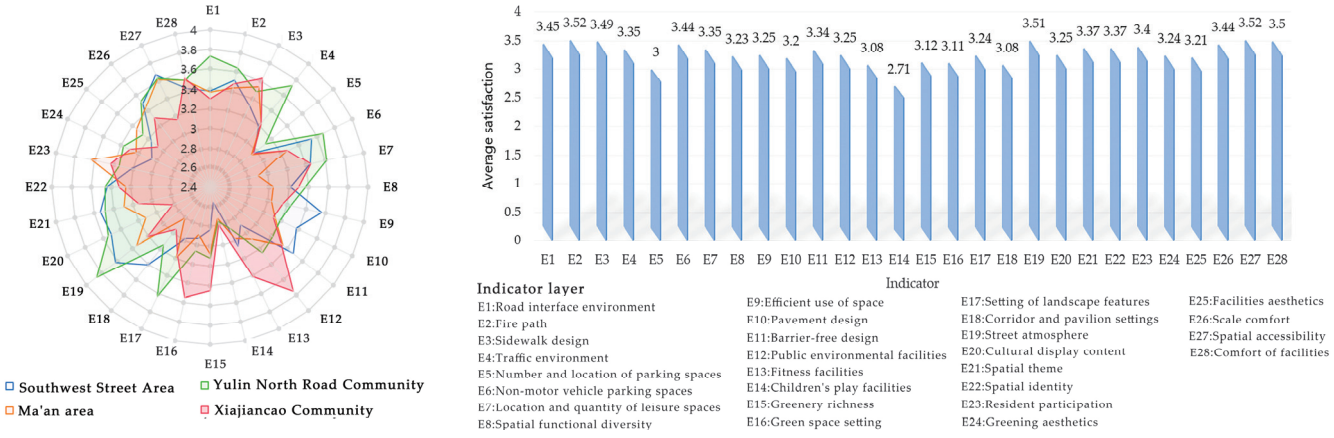
(**a**) (**b**)

Figure 6. (**a**) Index layer importance score; (**b**) average importance (source: authors).

Based on the average importance value, the average values of the indicators for the three aspects of traffic space, sense of belonging, and comfort fall within the range of 4.2 to

4.39, suggesting that users place a high emphasis on these aspects. In contrast, the average values of the indicators for the two aspects of leisure space and green space span from 4.01 to 4.38. This indicates that residents either do not pay much attention to some of these indicators or, due to limited resources, prioritize other, more important indicators. Regarding specific indicators, residents exhibit the lowest tendency to attach importance to the installation of corridor and pavilion settings (E18), with a score of 4.01. Conversely, they demonstrate the highest tendency to attach significance to the number and location of parking spaces (E5), efficient use of space (E9), and resident participation (E23), with a score of 4.39 (Figure 6).

The satisfaction level of each indicator was determined based on the satisfaction scores from the questionnaire (Figure 7). Among these indicators, E2 and E19 exhibit relatively higher satisfaction levels; E5, E14, E18, E24, and E25 show relatively lower satisfaction levels; and the satisfaction performance of E7, E12, E16, E20, and E27 varies significantly across groups.



(**a**) (**b**)

Figure 7. (**a**) Index layer satisfaction score; (**b**) average satisfaction (source: authors).

The average satisfaction values for the four samples are presented in Figure 7. The average satisfaction values for the indicators for the traffic space level range from 3.35 to 3.49, indicating a relatively high score. The average values for the indicators for the leisure space and green space levels ranged, respectively, from 2.71 to 3.35 and from 3.08 to 3.24, suggesting that residents were not satisfied with the renewal elements on both levels. In terms of specific indicators, residents were least satisfied with children's play facilities (E14), with a score of 2.71, and most satisfied with fire paths (E2) and spatial accessibility (E27), with a score of 3.52.

A four-quadrant graph was plotted based on the above results (Table 6). Specifically, the data from Figure 6 were used to represent the importance of the *x*-axis, and the data from Figure 7 were used to represent the satisfaction on the *y*-axis. The average values of the two are taken as the origin. For the indicators in the first and second quadrants, the decision-making result is "Keep", and in terms of priority comparison, the first quadrant > the second quadrant. For the indicators in the third and fourth quadrants, the decision-making result is "Promotion", and in terms of priority comparison, the fourth quadrant > the third quadrant.

Table 6. IPA quadrant.

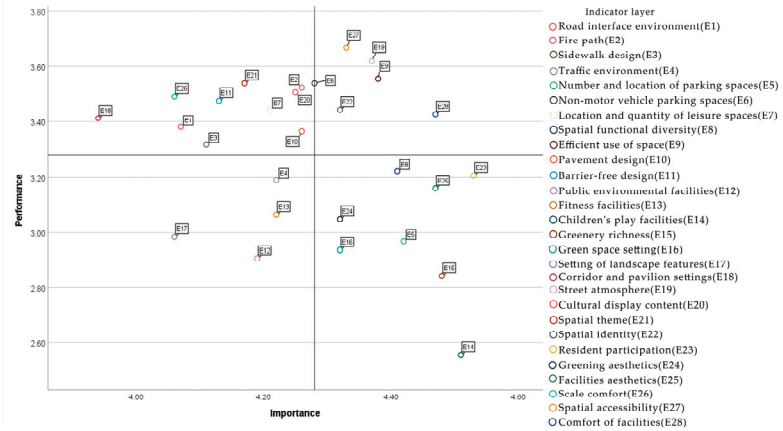
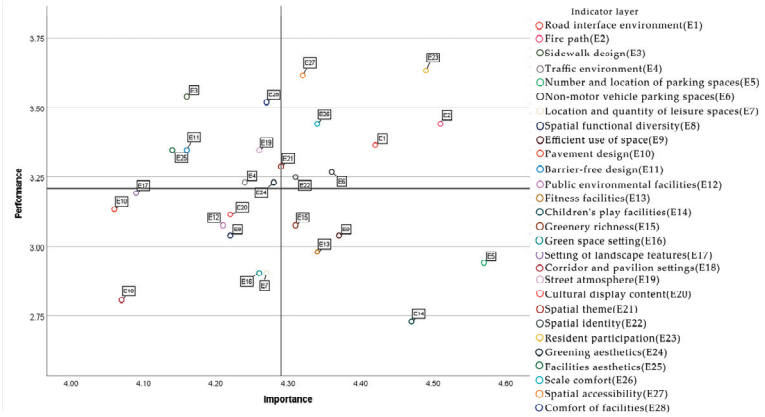
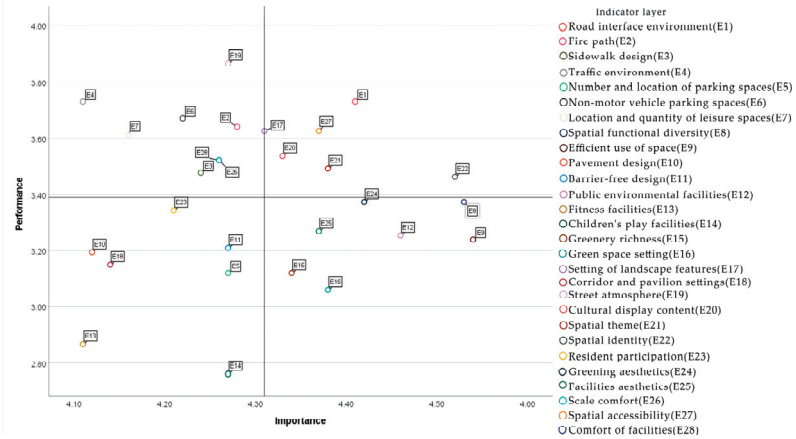
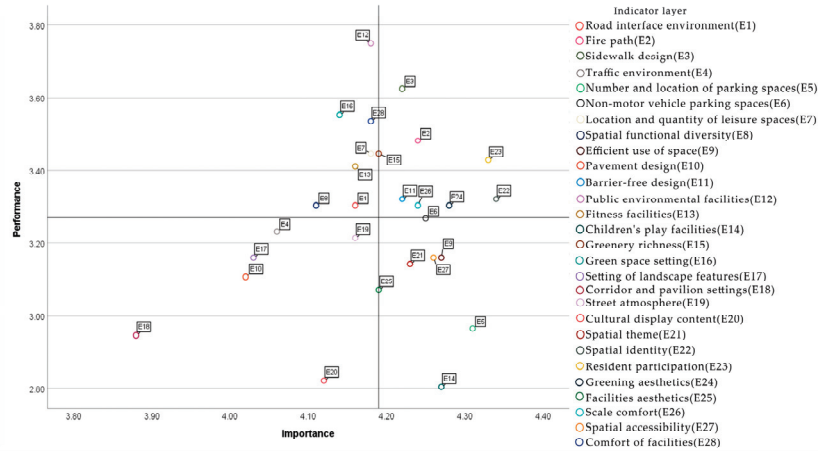
Sample	IPA Quadrant
Southwest Street Area	
Ma'an area	
Yulin North Road Community	

Table 6. *Cont.*

Sample	IPA Quadrant
Xiajiancao Community	

3.4. Calculation of Revised Importance Based on Kano Model

The average importance and average satisfaction of the four samples were used as the comprehensive evaluation results for the renewed old community in Chengdu. To make the results more accurate, the Kano model was introduced to revise the importance scores. Based on the formula, the demand intensity of residents for each level of indicators was calculated (Figure 8).

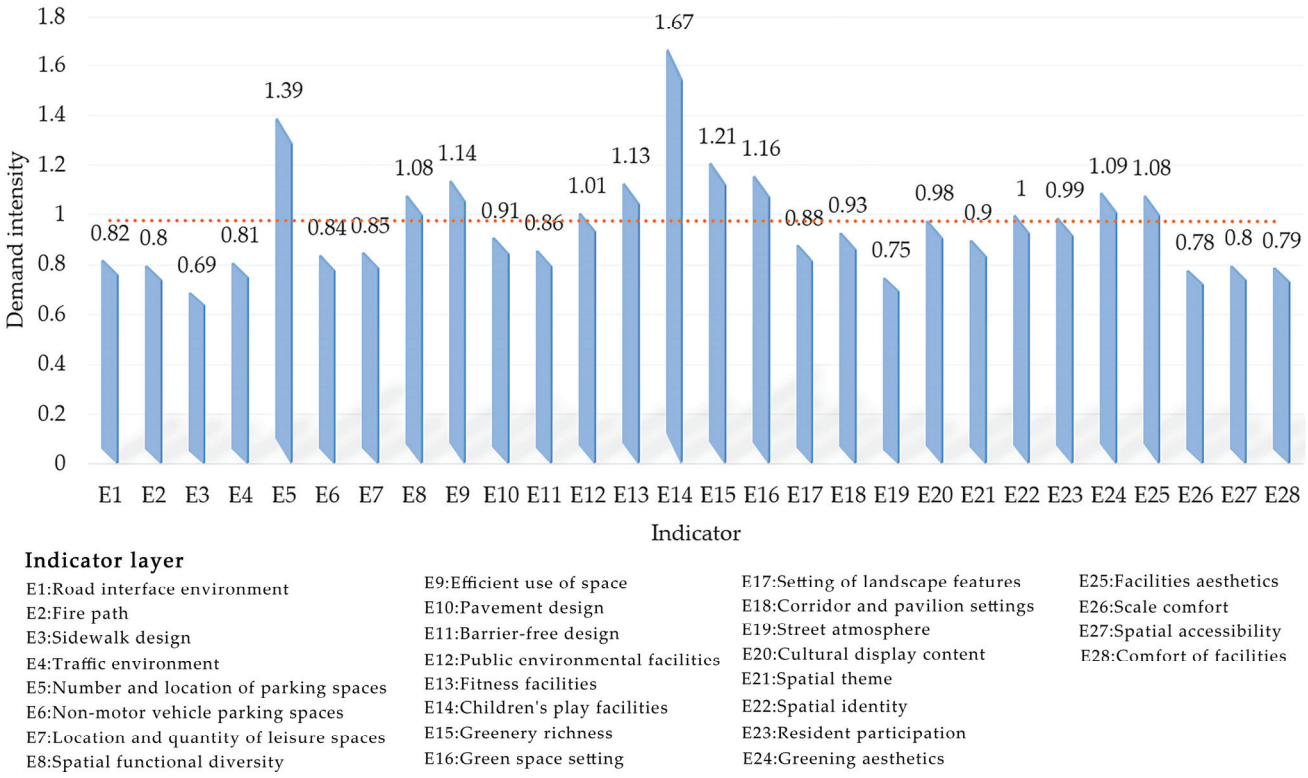


Figure 8. Indicator demand intensity (source: authors).

Combining the research data and the characteristics of the Kano model, the average value for the demand intensity of 0.99 is taken as the critical value for this demand classifi-

cation. Indicators with demand intensity values higher than the critical value are necessary needs, those lower than the critical value are expectation needs, and those with satisfaction higher than the importance are excitement needs. When only must-have indicators are provided, residents' satisfaction does not increase. When desired indicators are provided, residents' satisfaction rises.

Table 7 reflects the classification of the indicators and their corresponding satisfaction target values and calculates the revised importance (Table 8).

Table 7. Satisfaction target value.

Demand Factor	Number	Satisfaction Target Value
Necessary demands	E5 E8 E9 E12 E13 E14 E15 E16 E22 E23 E24 E25	4.0
Expectation demands	E1 E2 E3 E4 E6 E7 E10 E11 E17 E18 E19 E20 E21 E26 E27 E28	3.5

Table 8. Importance of correction.

Number	Satisfaction	Target Value	Revised Rate	Revised Coefficient	Revised Improvement Rate	Original Importance	Revised Importance
E1	3.45	3.5	1.01	1	1.01	4.27	4.33
E2	3.52	3.5	0.99	1	0.99	4.32	4.30
E3	3.49	3.5	1.00	1	1.00	4.18	4.19
E4	3.35	3.5	1.04	1	1.04	4.16	4.35
E5	3	4	1.33	0.5	1.78	4.39	7.80
E6	3.44	3.5	1.02	1	1.02	4.28	4.35
E7	3.35	3.5	1.04	1	1.04	4.21	4.40
E8	3.23	4	1.24	0.5	1.53	4.32	6.63
E9	3.25	4	1.23	0.5	1.51	4.39	6.65
E10	3.2	3.5	1.09	1	1.09	4.12	4.51
E11	3.34	3.5	1.05	1	1.05	4.2	4.40
E12	3.25	4	1.23	0.5	1.51	4.26	6.45
E13	3.08	4	1.30	0.5	1.69	4.21	7.10
E14	2.71	4	1.48	0.5	2.18	4.38	9.54
E15	3.12	4	1.28	0.5	1.64	4.33	7.12
E16	3.11	4	1.29	0.5	1.65	4.28	7.08
E17	3.24	3.5	1.08	1	1.08	4.12	4.45
E18	3.08	3.5	1.14	1	1.14	4.01	4.56
E19	3.51	3.5	1.00	1	1.00	4.27	4.26
E20	3.25	3.5	1.08	1	1.08	4.23	4.56
E21	3.37	3.5	1.04	1	1.04	4.27	4.43
E22	3.37	4	1.19	0.5	1.41	4.37	6.16
E23	3.4	4	1.18	0.5	1.38	4.39	6.08
E24	3.24	4	1.23	0.5	1.52	4.33	6.60
E25	3.21	4	1.25	0.5	1.55	4.29	6.66
E26	3.44	3.5	1.02	1	1.02	4.23	4.30
E27	3.52	3.5	0.99	1	0.99	4.32	4.30
E28	3.5	3.5	1.00	1	1.00	4.3	4.30

Based on the satisfaction and revised importance scores, we created an IPA quadrant map of Chengdu's old community renewal. Then, according to the quadrant map, the need for the renovation and upgrading of the indicators was derived, as shown in Figure 9.

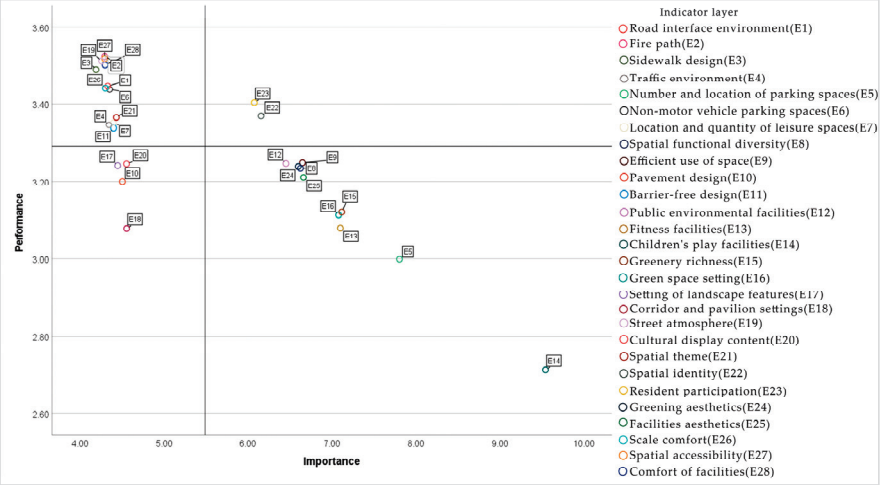


Figure 9. Revised IPA quadrant (source: authors).

4. Discussion

4.1. Analysis of Factors Influencing Residents' Satisfaction

The quality of residents' evaluations of the renewed old communities largely reflects the level of renewal quality and is closely related to residents' perception of physical environment characteristics (Figure 10). Firstly, in contrast to previous studies focusing on the walking potential in community environments, our findings reveal a different reality within China's older communities. The supply–demand gap for parking spaces is widening due to the constraints of past planning in older communities. The evaluation indicates that in the fourth quadrant, resident satisfaction with the number and location of parking spaces is low. Additionally, the demand intensity, at 1.39, is characteristic of necessary needs. Contrasting with the emphasis on walking as a healthy and environmentally friendly mode of transportation in numerous healthy community studies [44–46], Chinese residents, influenced by practical living and working conditions, often prioritize convenience in transportation [47]. Against this backdrop, the number and location of parking spaces become particularly crucial, highlighting the unique needs of residents during the renewal of China's older communities. Secondly, among the eight indicators of the leisure space, six of them are in the third and fourth quadrants and need further improvement. This indicates that residents' demands for leisure spaces are evolving towards diversified and mixed-function scenarios [48]. Among them, the demand intensities of the three indicators, E7, E10, and E11, are all lower than 0.99, belonging to the category of expectation demands. However, the current situation regarding community renewal is not yet able to meet the needs of different demographic groups simultaneously, with the needs of the elderly being particularly underserved. This result is consistent with previous studies. Due to the early construction of older communities, there has been insufficient attention paid to accessibility features and other age-friendly initiatives [49,50]. However, given the high proportion of elderly residents in older communities, living in an age-friendly community equipped with ample resting spaces, high-quality public environmental facilities, and completely barrier-free facilities holds significant positive implications for promoting active aging and creating a safe and healthy community environment [51,52]. The evaluation results for the green space indicators after the renewal show that residents' satisfaction with the richness of greenery and the layout of green spaces is only 3.24 and 3.08, and both of these two indicators belong to the category of expectation demands. Two indicators of residents' physical exercise are mental health [53] and improved cognitive ability [54].

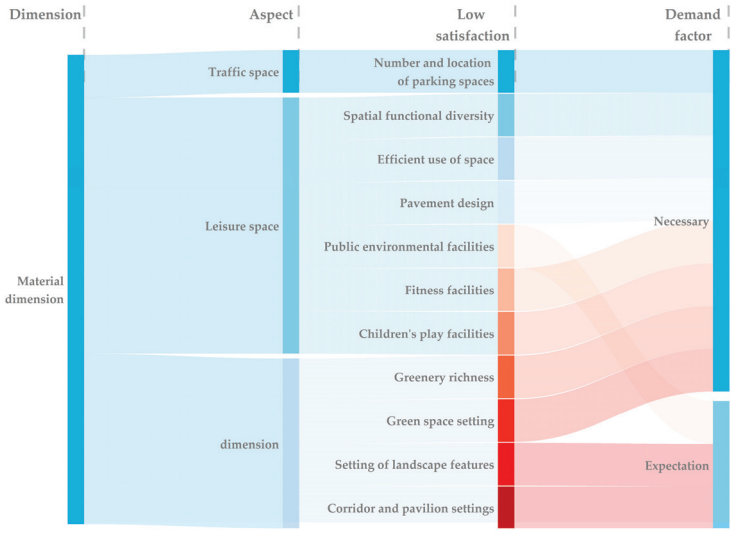


Figure 10. Indicators focused on improvement in the material dimension (source: authors).

This paper responds to the academic topic emphasizing the creation of a spiritual dimension in research. It examines the performance of existing regeneration models in terms of a sense of belonging and comfort [55,56] (Figure 11). The indicators related to residents' sense of belonging and comfort are mostly expectation demands. That is, when the corresponding indicators are met, residents' satisfaction will increase significantly. This is a crucial and prioritized factor in ensuring residents' satisfaction with the regeneration process. This finding differs from existing research. Existing research generally suggests that the lack of attention paid to the spiritual level in community construction leads to problems such as alienation in neighborhood relationships and an insufficient sense of belonging [57,58]. In these studies, the focus is often placed on elucidating the adverse effects and contributing factors, overlooking the spiritual dimension. Our findings diverge from the existing literature due to Chengdu's unique characteristics; compared to other cities, it boasts a relaxed lifestyle and a vibrant civic culture. So, its older community renewal projects highlight humanistic care and emotional support. The community carries the residents' emotions around "home", so finding ways to better focus on community culture and strengthen emotional communication with different residents represents an issue that needs to be further considered and resolved in future regeneration.

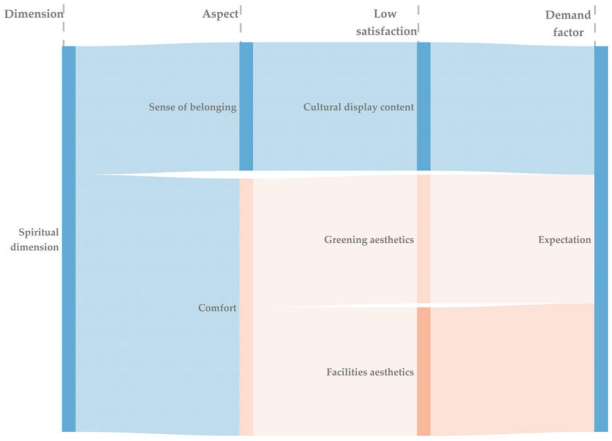


Figure 11. Indicators focused on improvements to the spiritual dimension (source: authors).

4.2. Optimization Strategies

Based on the revised IPA quadrant (Figure 9), this paper proposes optimization strategies in five dimensions: traffic space, leisure space, green space, sense of belonging, and comfort (Table 9).

Table 9. Renewal decision.

	Number	Decision
The first quadrant	E22 E23	Keep
The second quadrant	E1 E2 E3 E4 E6 E7 E11 E19 E21 E26 E27 E28	Keep
The third quadrant	E10 E17 E18 E20	Promotion
The fourth quadrant	E5 E8 E9 E12 E13 E14 E15 E16 E24 E25	Promotion

The overall strategy for traffic space is "Keep", and the number and location of parking spaces need to be optimized and enhanced. Based on the actual situation, the old communities can be subjected to the process of removing walls and combining courtyards. Adjacent courtyards or open spaces can be integrated to serve as parking areas. In addition, night-time parking spaces should be increased appropriately. Also, the space within the community should be made rationally usable according to the time of day through the installation of lifting piles and other movable devices (Figure 12).

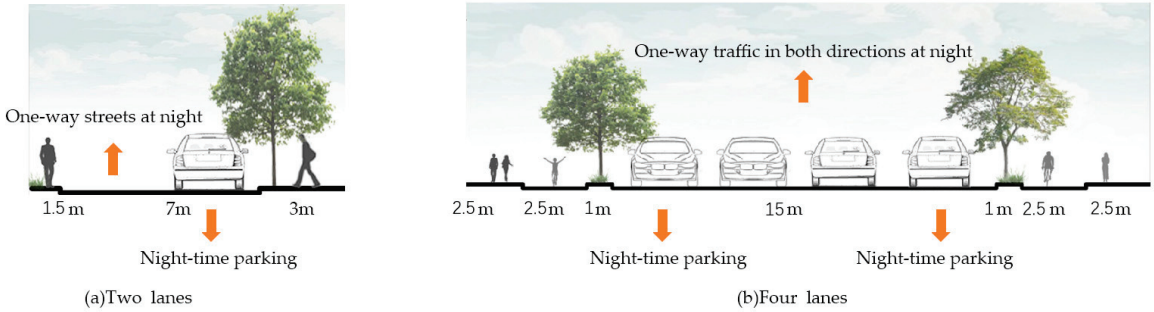


Figure 12. Time-share parking (source: authors).

For leisure space, the overall strategy is "Promotion". The indicators for spatial functional diversity, the efficient use of space, pavement design, public environmental facilities, fitness facilities, and children's play facilities require enhancement. Specifically, designers should make full use of movable facilities and furniture to enhance the versatility of the site and dynamically adjust the function of the site (Figure 13). The esthetics of the paving will be enhanced through color contrast and coordination and by focusing on the enclosure of the boundaries. At the same time, the rational planning of community leisure facilities and improvement of lighting quality will be implemented. Through a layout based on "small concentration and large dispersion", fitness equipment, ping pong tables, and other sports facilities will be added in combination with green spaces and footpaths to meet the needs of residents regarding fitness. In addition, according to the needs of children of different ages, diversified play facilities such as slides, swings, and sandboxes will be provided.



Figure 13. Movable facilities (source: authors).

The overall strategy for the green space is "Promotion", with enhancement indicators including greenery richness, a green space setting, a setting with landscape features, a corridor, and pavilion settings. Fragmented spaces with renewal potential and value are screened. Then, acupuncture-type greening interventions are implemented, through which the overall quality of green spaces will be significantly improved via local modifications. At the same time, the open-space incorporation of fitness, sightseeing, gardening, and other composite functions creates a "pocket space" for residents' daily activities to enhance the quality of green space (Figure 14).

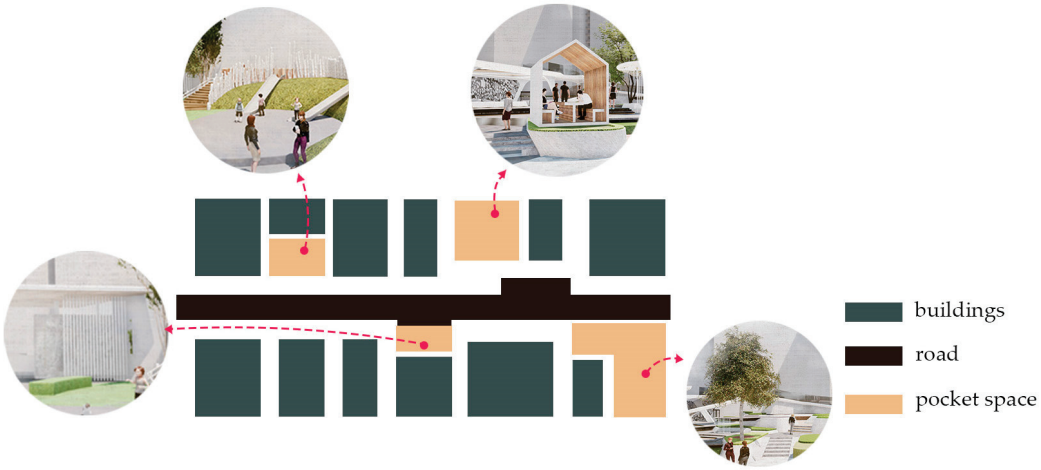


Figure 14. Pocket space (source: authors).

The overall strategy for the sense of belonging is "Keep", with a focus on enhancing the cultural display content. At present, traditional methods such as display boards and slogans are still adopted by the community, and these methods lack community cultural characteristics. Three-dimensional displays can be added to present the cultural content in a more vivid and intuitive form. In addition, the number of small gathering venues should be increased to enhance the radiation effect of gatherings (Figure 15). Community cohesion could be enhanced through the organization of activities like traditional cultural experiences, festivals, and parent–child cultural events.

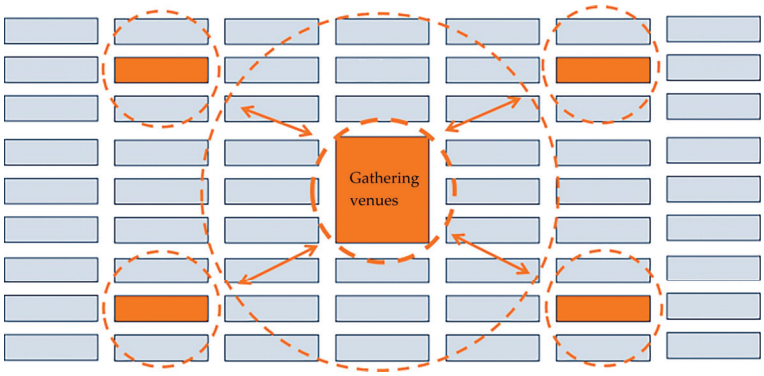


Figure 15. Gathering venues (source: authors).

The overall strategy for comfort is "Keep", mainly to improve greening and facility esthetics. Greater emphasis should be placed on the selection of green plants, color coordination, and seasonal adaptation to achieve a visually appealing effect. Meanwhile, AR, VR, and 3D technologies should be utilized to enhance the artistry and interactivity of main pedestrian paths, nodes, key buildings, and walls.

4.3. Limitations

This paper demonstrates the utility of the IPA–Kano evaluation method. It can identify renewal elements that residents value highly but which are not fully fulfilled, guiding the government in formulating its subsequent renewal program. However, the evaluation process in this paper has some limitations. Although the four samples selected are typical, the time constraints of the study preclude the research and evaluation of more cases. Subsequently, more empirical cases will be incorporated into the study. In addition, the method for determining the evaluation index set in this study still has room for further optimization. In the future, methods such as big data and machine learning will be integrated to capture key information about the community after the renewal via the Internet, and the evaluation indicators will be further adjusted and optimized to improve the accuracy and science of the evaluation index set.

5. Conclusions

As an important part of residents' lives, the community is regarded as the basic unit of production, living, and national governance. At present, some old communities are confronted with problems such as functional degradation, facility decay, and space shortage. Renewal work is regarded as an important task in urban development. Therefore, this paper focused on the current renewal practices of four old communities in Chengdu, Sichuan Province, China. The main findings are as follows:

(1) In this paper, an index set specifically for the post-renewal evaluation of old communities was constructed. The Kano model was utilized to modify the IPA scores, thereby identifying the demand intensity and satisfaction levels for renewal elements. This structured approach fills the gap in the quantitative assessment of the effects of renewal projects in the current research. It contributes to the precise optimization of old communities and the improvement of residents' quality of life and ultimately promotes the sustainable development of communities.

(2) The satisfaction levels for 28 renewal elements were analyzed through the quadrant, and the indicators that needed to be promoted and kept were identified. Specifically, renewal projects in old communities in Chengdu place more emphasis on renewal elements in the spiritual dimension, with only three dissatisfied indicators. At the

same time, there are deficiencies in the improvement of some physical dimensions, where there are 11 dissatisfied indicators, resulting in a relatively low level of resident satisfaction. In fact, with economic development, residents' requirements for the physical environment are no longer limited to the satisfaction of a single function but show a trend of diversification.

(3) Based on the 12 necessary needs and 16 expectation needs identified according to the demand intensity, through mining feedback data, sustainable optimization strategies tailored to the renovation needs of Chinese old communities were proposed in the physical and spiritual dimensions. These strategies focus on the core demands of residents for the renovation of old communities and aim to effectively improve the quality of old communities and residents' life satisfaction. Against the backdrop of China's urban renewal, they provide practical guidance cases and strategic references for the renovation of old communities in various regions, contributing to the achievement of the high-quality development of urban space.

In conclusion, the research results demonstrate the feasibility and adaptability of the post-renewal evaluation method for old communities. It can not only promptly identify blind spots and misunderstandings in the renewal process and ensure that renewal strategies can be dynamically adjusted according to residents' needs but also provide valuable references and inspiration for the government and designers. This method preserves the potential for future improvements, providing scientific support for the development of sustainable community renewal policies. In the future, we intend to refine our evaluation index further. By conducting in-depth case studies on older communities in various regions, we will explore the similarities and differences in residents' satisfaction with community renewal efforts. Our goal is to identify strategies that can be applied more broadly. Additionally, we aim to influence policy by implementing effective feedback mechanisms to create a repository of sustainable community renewal resources. This repository will include case studies that integrate both scientific and practical aspects to improve the efficiency and effectiveness of policies related to sustainable community development. The construction of a lifecycle management system for community renewal based on POE is essential in achieving long-term community stability and advancing sustainable development goals at the urban and national levels.

Author Contributions: Conceptualization, Q.O.; Investigation, F.L.; Methodology, Q.O., F.L. and Y.W.; Software, F.L.; Supervision, Y.W.; Visualization, Q.O.; Writing—original draft, Q.O. and F.L.; Writing—review and editing, Q.O. and Y.W. All authors have read and agreed to the published version of the manuscript.

Funding: This research was funded by the Young Scientists Fund of the National Natural Science Foundation of China (No. 52208035).

Data Availability Statement: The original contributions presented in the study are included in the article; further inquiries can be directed to the corresponding author.

Acknowledgments: The authors would like to thank all project funders, journal editors, and anonymous reviewers for their comments and suggestions.

Conflicts of Interest: The authors declare no conflicts of interest.

Appendix A

Table A1. Overview of the 16 renewal projects.

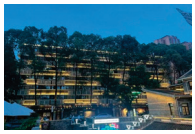
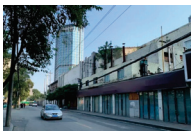
Number	Sample	Era	Area	Sample Range	Before Update	After Update
1	Southwest Street Area	The 1980s–1990s	0.28 km^2			
2	Ma'an area	The 1980s	0.13 km^2			
3	Yulin North Road Community	The 1980s	1.20 km^2			
4	Xiajiancao Community	The 1950s	0.72 km^2			
5	Minebea Community	The 1980s–1990s	0.40 km^2			
6	Caojiaxiang Area	The 1950s–1980s	0.40 km^2			
7	Dongguang Community	The 1980s–1990s	2.60 km^2			
8	Dongmen Shijing Community	The 1990s	0.55 km^2			
9	Fuzijie Area	The 1980s–1990s	0.37 km^2			

Table A1. *Cont.*

Number	Sample	Era	Area	Sample Range	Before Update	After Update
10	Mianjie Area	The 1980s–1990s	0.74 km^2			
11	Qingyang North Road Community	The 1990s	0.44 km^2			
12	Yingui Area	The 1980s	0.11 km^2			
13	Yulin East Road Community	The 1980s	0.45 km^2			
14	Zaozi Lane Area	The 1980s	0.28 km^2			
15	Zhengjie Community	The 1990s	0.25 km^2			
16	Zhonghuan Siyuan Area	The 1990s	0.10 km^2			

References

1. Almeida, C.P.; Ramos, A.F.; Silva, J.M. Sustainability Assessment of Building Rehabilitation Actions in Old Urban Centres. *Sustain. Cities Soc.* **2018**, *36*, 378–385. [CrossRef]
2. Guo, R.; Song, X.; Li, P.; Wu, G.; Guo, Z. Large-Scale and Refined Green Space Identification-Based Sustainable Urban Renewal Mode Assessment. *Math. Probl. Eng.* **2020**, *2020*, 2043019. [CrossRef]
3. Zhang, X.; Du, L.; Song, X. Identification of Urban Renewal Potential Areas and Analysis of Influential Factors from the Perspective of Vitality Enhancement: A Case Study of Harbin City's Core Area. *Land* **2024**, *13*, 1934. [CrossRef]
4. Tencent News. Urban Renewal Focuses on "Three Major Tasks": How Can Trillions of Funds Act as a "Wrench"?_Tencent News. Available online: https://news.qq.com/rain/a/undefined (accessed on 15 January 2025).
5. Economic Information Daily. Promote the Renovation of Old Urban Residential Communities and Blocks: Urban Renewal Picks Up Speed. Available online: https://www.gov.cn/zhengce/202501/content_6996657.htm (accessed on 15 January 2025).
6. Fang, X.; Zhou, B.; Tu, X.; Ma, Q.; Wu, J. "What Kind of a Science Is Sustainability Science?" An Evidence-Based Reexamination. *Sustainability* **2018**, *10*, 1478. [CrossRef]
7. Transforming Our World: The 2030 Agenda for Sustainable Development. Available online: https://digitallibrary.un.org/record/3923923?v=pdf (accessed on 16 February 2025).
8. Liu, Y.; Dijst, M.; Geertman, S. Residential Segregation and Well-Being Inequality between Local and Migrant Elderly in Shanghai. *Habitat Int.* **2014**, *42*, 175–185. [CrossRef]

9. Cao, K.; Harris, R.; Liu, S.; Deng, Y. How Does Urban Renewal Affect Residential Segregation in Shenzhen, China? A Multi-Scale Study. *Sustain. Cities Soc.* **2024**, *102*, 105228. [CrossRef]
10. Breton-Carbonneau, A.C.; Anguelovski, I.; O'Brien, K.; Echevarría-Ramos, M.; Fina, N.; Genty, J.; Seeder, A.; Binet, A.; Williams, P.C.; Cole, H.V.S.; et al. Exploring Ownership of Change and Health Equity Implications in Neighborhood Change Processes: A Community-Led Approach to Enhancing Just Climate Resilience in Everett, MA. *Health Place* **2024**, *89*, 103294. [CrossRef] [PubMed]
11. Wang, Q.-C.; Liu, X.; Jian, I.Y.; Zhang, E.-J.; Hou, Y.-T.; Siu, K.W.M.; Li, Y.-B. Community Resilience in City Emergency: Exploring the Roles of Environmental Perception, Social Justice and Community Attachment in Subjective Well-Being of Vulnerable Residents. *Sustain. Cities Soc.* **2023**, *97*, 104745. [CrossRef]
12. Nikuze, A.; Sliuzas, R.; Flacke, J. From Closed to Claimed Spaces for Participation: Contestation in Urban Redevelopment Induced-Displacements and Resettlement in Kigali, Rwanda. *Land* **2020**, *9*, 212. [CrossRef]
13. Li, Y.; Zhang, S.; Zhu, D. Co-Creation of Community Micro-Renewals: Model Analysis and Case Studies in Shanghai, China. *Habitat Int.* **2023**, *142*, 102951. [CrossRef]
14. Yin, J.; Cao, X.; Huang, X.; Cao, X. Applying the IPA–Kano Model to Examine Environmental Correlates of Residential Satisfaction: A Case Study of Xi'an. *Habitat Int.* **2016**, *53*, 461–472. [CrossRef]
15. Du, T.; Zeng, N.; Huang, Y.; Vejre, H. Relationship between the Dynamics of Social Capital and the Dynamics of Residential Satisfaction under the Impact of Urban Renewal. *Cities* **2020**, *107*, 102933. [CrossRef]
16. Tang, D.; Gong, X.; Liu, M. Residents' Behavioral Intention to Participate in Neighborhood Micro-Renewal Based on an Extended Theory of Planned Behavior: A Case Study in Shanghai, China. *Habitat Int.* **2022**, *129*, 102672. [CrossRef]
17. Wang, D.; Li, S. Social Conflicts and Their Resolution Paths in the Commercialized Renewal of Old Urban Communities in China under the Perspective of Public Value. *J. Urban Manag.* **2024**. [CrossRef]
18. Gao, Q.; Yin, D.; Zhu, H. Urban Regeneration and Emotional Politics of Place in Liede Village, Guangzhou, China. *Habitat Int.* **2020**, *103*, 102199. [CrossRef]
19. Huang, R.; Liu, G.; Li, K.; Shrestha, A.; Fu, X.; You, K.; Deng, X. How to Utilize Neighborship: The Role of Residents' Social Capital in the Neighborhood Renewal in China. *Environ. Impact Assess. Rev.* **2023**, *103*, 107273. [CrossRef]
20. Hassan, G.F. Regeneration as an Approach for the Development of Informal Settlements in Cairo Metropolitan. *Alex. Eng. J.* **2012**, *51*, 229–239. [CrossRef]
21. Li, Z.; Wu, F. Residential Satisfaction in China's Informal Settlements: A Case Study of Beijing, Shanghai, and Guangzhou. *Urban Geogr.* **2013**, *34*, 923–949. [CrossRef]
22. Deakin, M. The Case for Socially Inclusive Visioning in the Community-Based Approach to Sustainable Urban Regeneration. *Sustain. Cities Soc.* **2012**, *3*, 13–23. [CrossRef]
23. Mousavinia, S.F.; Pourdeihimi, S.; Madani, R. Housing Layout, Perceived Density and Social Interactions in Gated Communities: Mediational Role of Territoriality. *Sustain. Cities Soc.* **2019**, *51*, 101699. [CrossRef]
24. Zhang, M.; Wu, W.; Zhong, W.; Zeng, G.; Wang, S. The Reshaping of Social Relations: Resettled Rural Residents in Zhenjiang, China. *Cities* **2017**, *60*, 495–503. [CrossRef]
25. Ji, Q.; Yin, M.; Li, Y.; Zhou, X. Exploring the Influence Path of High-Rise Residential Environment on the Mental Health of the Elderly. *Sustain. Cities Soc.* **2023**, *98*, 104808. [CrossRef]
26. Chao, R.; Xue, D.; Wang, B. Evaluating Human Needs: A Study on the Spatial Justice of Medical Facility Services in Social Housing Communities in Guangzhou. *Land* **2024**, *13*, 1109. [CrossRef]
27. Zhang, Y.; Wu, Q.; Wu, L.; Li, Y. Measuring Community Green Inequity: A Fine-Scale Assessment of Beijing Urban Area. *Land* **2021**, *10*, 1197. [CrossRef]
28. Lin, S.-M.; Lee, H.-Y.; Hu, H.-L.; Chien, K.-H. To Join the Rebuild or Not? An Exploration of the Factors Influencing the Public's Intention to Participate in Urban Renewal. *Sci. Prog.* **2022**, *105*, 368504221140273. [CrossRef] [PubMed]
29. Liu, G.; Zhang, Y.; Zhuang, T.; Yi, H.; Cao, Z.; Wu, H.; Fu, X. Deciphering Trust in Grassroots Government for Vibrant Resident Participation in Neighborhood Regeneration: An Empirical Study in China's Top-down Governance System. *Cities* **2024**, *152*, 105244. [CrossRef]
30. Hui, E.C.; Chen, T.; Lang, W.; Ou, Y. Urban Community Regeneration and Community Vitality Revitalization through Participatory Planning in China. *Cities* **2021**, *110*, 103072. [CrossRef]
31. Zhang, C.; Lu, B. Residential Satisfaction in Traditional and Redeveloped Inner City Neighborhood: A Tale of Two Neighborhoods in Beijing. *Travel Behav. Soc.* **2016**, *5*, 23–36. [CrossRef]
32. Peng, Y.; Lai, Y.; Li, X.; Zhang, X. An Alternative Model for Measuring the Sustainability of Urban Regeneration: The Way Forward. *J. Clean. Prod.* **2015**, *109*, 76–83. [CrossRef]
33. Sigurðardóttir, A.K.; Hjartarson, T.; Snorrason, A. Pedagogical Walks through Open and Sheltered Spaces: A Post-Occupancy Evaluation of an Innovative Learning Environment. *Buildings* **2021**, *11*, 503. [CrossRef]

34. Qi, Z.; Jin, X.; Liang, X.; Han, B.; Zhou, Y. A New Framework for Dynamic Visual Landscape Quality Evaluation of Greenways Based on Perceived Sensory Dimensions: A Case Study of Chengdu Urban Greenway. *J. Environ. Manag.* **2024**, *370*, 122950. [CrossRef]
35. Zhu, Y.; Huang, W.; Hu, L. Research on a Commercial Building Space Traffic Flow Design Based on Post-Occupancy Evaluation. *Buildings* **2022**, *12*, 838. [CrossRef]
36. Hull, A.; Alexander, E.R.; Khakee, A.; Woltjer, J. *Evaluation for Sustainability and Participation in Planning*; Routledge: London, UK, 2011.
37. Chen, J.; Pellegrini, P.; Xu, Y.; Ma, G.; Wang, H.; An, Y.; Shi, Y.; Feng, X. Evaluating Residents' Satisfaction before and after Regeneration. The Case of a High-Density Resettlement Neighbourhood in Suzhou, China. *Cogent Soc. Sci.* **2022**, *8*, 2144137. [CrossRef]
38. Tontini, G.; Silveira, A. Identification of Satisfaction Attributes Using Competitive Analysis of the Improvement Gap. *Int. J. Oper. Prod. Manag.* **2007**, *27*, 482–500. [CrossRef]
39. Wang, M.; Jia, Z. Investigating the Correlation between Building Façade Design Elements and Tourist Satisfaction—Cases Study of Italy and the Netherlands. *Habitat Int.* **2024**, *144*, 103001. [CrossRef]
40. Yu, P.; Zhang, Y. A Satisfaction Study of Waterfront Public Spaces in Winter Cities from a Demand Perspective: A KANO-IPA Model Analysis Based on Northeastern China. *Land* **2025**, *14*, 92. [CrossRef]
41. Zhang, Q.; Zheng, Z.; Kang, D.; Zhou, Y.; Zhang, Y.; Zhang, X. Prioritizing Neighbourhood Amenities to Enhance Neighbourhood Satisfaction: A Case Study in Wuhan, China. *Int. J. Environ. Res. Public Health* **2023**, *20*, 3528. [CrossRef] [PubMed]
42. SUC Standard—SUC Sustainable Cities and Communities Project. Available online: http://www.suc2030.org.cn/bzzn/ (accessed on 16 February 2025).
43. Liu, T.; He, M.; Wang, Y.X.; Yan, Y.Q. Comprehensive Evaluation of Satisfaction of Tianjin Water Park Based on AHP and Kano Model Analysis. *J. Shandong Agric. Univ. (Nat. Sci. Ed.)* **2016**, *47*, 417–424.
44. Zuniga-Teran, A.A.; Orr, B.J.; Gimblett, R.H.; Chalfoun, N.V.; Marsh, S.E.; Guertin, D.P.; Going, S.B. Designing Healthy Communities: Testing the Walkability Model. *Front. Archit. Res.* **2017**, *6*, 63–73. [CrossRef]
45. Jiang, Z.; Wu, C.; Chung, H. The 15-Minute Community Life Circle for Older People: Walkability Measurement Based on Service Accessibility and Street-Level Built Environment—A Case Study of Suzhou, China. *Cities* **2025**, *157*, 105587. [CrossRef]
46. Wedyan, M.; Saeidi-Rizi, F. Assessing the Impact of Walkability Indicators on Health Outcomes Using Machine Learning Algorithms: A Case Study of Michigan. *Travel Behav. Soc.* **2025**, *39*, 100983. [CrossRef]
47. Xie, H.; Yan, P.; Bai, M.; Chen, Z. An Efficient Parking-Sharing Program through Owner Cooperation with Robust Slot Assignment and Incentive Revenue Distribution. *Transp. Res. Part E Logist. Transp. Rev.* **2024**, *191*, 103697. [CrossRef]
48. Mu, S. Community Building in Social-Mix Public Housing: Participatory Planning of Ankang Redevelopment Plan. *Procedia—Soc. Behav. Sci.* **2016**, *222*, 755–762. [CrossRef]
49. Yung, E.H.K.; Conejos, S.; Chan, E.H.W. Public Open Spaces Planning for the Elderly: The Case of Dense Urban Renewal Districts in Hong Kong. *Land Use Policy* **2016**, *59*, 1–11. [CrossRef]
50. Subramanian, D.; Jana, A. Assessing Urban Recreational Open Spaces for the Elderly: A Case of Three Indian Cities. *Urban For. Urban Green.* **2018**, *35*, 115–128. [CrossRef]
51. Zhao, J.; Peng, Z.; Liu, L.; Yu, Y.; Yu, Y. Evaluation on the Internal Public Space Quality in Affordable Housing Based on Multi-Source Data and IPA Analysis. *Land* **2021**, *10*, 1000. [CrossRef]
52. Zhang, J.; Cai, J.; Zhang, X.; Zhang, W. The Spatiotemporal Organizational Order of Living Circle Units Based on the Law of Walking Time-Distance Distributions. *Land* **2024**, *13*, 2105. [CrossRef]
53. Liu, Y.; Wang, R.; Grekousis, G.; Liu, Y.; Yuan, Y.; Li, Z. Neighbourhood Greenness and Mental Wellbeing in Guangzhou, China: What Are the Pathways? *Landsc. Urban Plan.* **2019**, *190*, 103602. [CrossRef]
54. Helbich, M.; Yao, Y.; Liu, Y.; Zhang, J.; Liu, P.; Wang, R. Using Deep Learning to Examine Street View Green and Blue Spaces and Their Associations with Geriatric Depression in Beijing, China. *Environ. Int.* **2019**, *126*, 107–117. [CrossRef] [PubMed]
55. Huang, T.; Lyu, H.; Chen, X.; Ren, J. The Relationship between Sense of Community and General Well-Being of Chinese Older Adults: A Moderated Mediation Model. *Front. Psychol.* **2023**, *13*, 1082399. [CrossRef]
56. Lu, T.; Zhang, F.; Wu, F. Place Attachment in Gated Neighbourhoods in China: Evidence from Wenzhou. *Geoforum* **2018**, *92*, 144–151. [CrossRef]
57. Liu, S.; Zhang, F.; Wu, F. Contrasting Migrants' Sense of Belonging to the City in Selected Peri-Urban Neighbourhoods in Beijing. *Cities* **2022**, *120*, 103499. [CrossRef]
58. Xu, Y.; Wu, D.; Chen, N. Here I Belong!: Understanding Immigrant Descendants' Place Attachment and Its Impact on Their Community Citizenship Behaviors in China. *J. Environ. Psychol.* **2022**, *79*, 101743. [CrossRef]

Disclaimer/Publisher's Note: The statements, opinions and data contained in all publications are solely those of the individual author(s) and contributor(s) and not of MDPI and/or the editor(s). MDPI and/or the editor(s) disclaim responsibility for any injury to people or property resulting from any ideas, methods, instructions or products referred to in the content.

buildings

MDPI

Article

Research on the Dynamic Defensive Efficiency of Traditional Military Settlements in the Ming Dynasty: A Case Study of Ningbo Coastal Defense, China

Lingxin Meng [1], Ziyao Yang [1], Lifeng Tan [2], Shulong Yan [2,*], Yukun Zhang [1] and Xuan Wang [1]

[1] School of Architecture, Tianjin University, Tianjin 300072, China; menglingxin1997@163.com
[2] International School of Engineering, Tianjin Chengjian University, Tianjin 300384, China; tanlf_arch@163.com
* Correspondence: yanshulong_arch@163.com; Tel.: +86-17-7677-31117

Abstract: Defensiveness is a pivotal characteristic of traditional military settlements in ancient China, influenced by various factors linked to settlement construction and the occurrence of battles. Previous studies have typically focused on specific periods or moments, overlooking the dynamic interrelationships that evolve over time. The study proposes the concept of 'defensive efficiency' as a specific indicator for measuring the level of military defense system construction. Meanwhile, the analytic hierarchy process (AHP) was introduced to decompose the complex defense efficiency indicators into a quantitative system consisting of four levels of evaluation factors, analyse and statistically analyse the individual evaluation factors, and finally integrate and visualise the comparison of the data over multiple periods of time with the help of a geographic information system (GIS). The results of the study show that the changes in defensive efficiency in the four periods reflected the four stages of coastal defense construction in Ningbo during the Ming Dynasty: the preliminary construction period, the full construction period after repeated Wokou infestations, the basic completion period, and the period when Wokou encroachments were reduced and the point of attack was relocated to the south. While the spatial distribution of battles drove the continuous construction and improvement of coastal defense settlements, the improvement of the coastal defense system had an obvious effect on resisting Wokou intrusion. The study enriches the understanding of the cultural significance of traditional Chinese military settlement systems, emphasises the importance of tailor-made strategies appropriate to different historical periods and regional contexts, and provides a basis for the sustainable conservation of extant remains.

Keywords: the Ming coastal defense military system; defensive efficiency; spatial database; GIS; traditional military settlement

1. Introduction

Defensiveness is one of the key characteristics of traditional military settlements in ancient China [1], ancient Rome [2], and many different civilizations [3,4]. During the long and turbulent dynastic changes in Chinese history, traditional settlements, in addition to their basic functions of production, living, religion, and economy, also developed the important characteristic of defensiveness [5]. This characteristic was not only reflected in actions such as building walls and setting up patrols but also in deeper issues of state institutions such as the military system. The defense of borders was of the utmost importance,

which led to the formation of traditional military settlements in ancient China that were particularly defensive in nature.

Under the strict Du-Si-Wei-Suo military and political system of the Ming Dynasty, two lines of defense were formed: the military system of the Great Wall in the north and the military system of coastal defenses in the east—they were one of the most complex and complete systems of defense for military settlements in ancient China. These military settlements, spread along China's coasts, were built to defend against invasions by sea pirates (Wokou) from eastern China. With a total length of over 3000 km from the Liaodong Peninsula in the north to Hainan Island in the south, they have left behind a diverse cultural heritage [6]. However, compared to the visible architectural representations of the Great Wall, which is a UNESCO World Heritage site, the Ming Dynasty coastal defense system has not attracted much attention due to the lack of a tangible material carrier [7]. Its strategic military value and cultural heritage have not yet attracted much attention, and the historical remains and conservation status are lagging behind.

Given the extensive coastline and complex terrain, military settlements needed to possess robust defensive capabilities. In the existing research on ancient Chinese traditional military settlements, there has been a substantial focus on the defensive construction of these settlements [8–10]. Qualitative studies have meticulously documented the construction history and spatial layout, discussing various defensive structures within the settlements, such as walls, fortresses, and watchtowers [11,12]. Throughout this process, the improvement of information collection methods such as GIS and GS has provided more possibilities for quantitative research [13–16]. Researchers have often explored the correlation between settlement locations and the natural environment, as well as the accessibility and defensive reach of these military settlements [17,18]. Then, an increasing number of quantitative research models have been applied, including the use of one or more methods such as AHP [19], CIRTIC [20], and PCA [21] for goal decomposition and the analysis of the internal influencing mechanisms of these settlements. The main reason for choosing AHP in this study is that, compared to objective assignment methods such as PCA, AHP allows for the adjustment of criterion weights through expert judgment, which is more in line with the decision-making logic of ancient military construction. However, most of these studies tend to concentrate on the spatial characteristics or construction features of military settlements at a specific point in time or within a particular region after they were established [22–24]. They often overlook the fact that, due to the ever-changing frontier conditions during the Ming Dynasty, the construction of military settlements was in a state of continuous evolution. The focal points of defense and the defensive structures themselves were constantly being adapted and modified. Thus, there remains a significant gap in the research concerning the dynamic changes in the defensive capabilities of military settlements over a given period.

In general, the level of goal achievement can be evaluated using the concept of "efficiency". Efficiency refers to the ratio of the output of labour to the input of labour, or the amount of work completed per unit of time. "Defensive efficiency", on the other hand, is a measure of the defensive capability of a military settlement system within a specific context [25]. For instance, constructing a highly defensible military settlement in an area with no conflict or building a weakly defensible settlement in a frequently contested stronghold are both examples of inefficiency. The defensive efficiency of a military settlement system is a complex composite index, including factors such as accessibility and the settlement's construction quality, and is influenced by constraints like funding, resources, and policies. In response to previous research focusing on static situations in a certain time slice, this study further deepens the concept of defensive efficiency into dynamic defensive efficiency.

Instead of moment-by-moment fluid dynamic monitoring, it emphasises adaptive adjustments and their efficacy transitions within the framework of a continuum of historical developmental stages.

The study attempts to quantify the dynamic changes in the defense construction of military settlements within a certain range by establishing the concept of 'defensive efficiency' and analysing the internal causes of these changes. This approach not only aids in a deeper understanding of the cultural significance of traditional Chinese military settlements and provides theoretical support for heritage protection and presentation but also offers insights into sustainable construction practices today.

2. Study Area

Because of its developed economy and abundant products, Ningbo became the primary target of Wokou's covetous plundering, while its long coastline and complex and convenient water network made Ningbo a springboard for pirates to invade the mainland, leading to the unrest of the coastal people's lives. As a countermeasure, the Ming government began to actively lay out the coastal defense line; coastal defense military settlement construction officially kicked off. The Ningbo area is one of the important main positions of the Ming Dynasty coastal defense system, and there are three reasons for choosing the Ningbo area as the research object:

(1) Zhejiang defense area has always been the focus of the Ming government coastal defense construction, and Ningbo with the geographical characteristics of the Zhejiang coastal defense gateway (Figure 1) also naturally became the top priority of the Ming and Qing dynasty coastal defense deployment; the construction of coastal defense military colony has a high quantity and quality. Therefore, the coastal defense military colony system in Ningbo during the Ming Dynasty is very representative, and the quantitative analysis of the defensive efficiency of the Ningbo can reflect the construction law of the national coastal defense military colony system.

(2) The comprehensive deployment and construction of coastal defense in Ningbo began during the Hongwu period of the Ming Dynasty. According to local historical records, the Ningbo area experienced 53 years of large-scale invasion during the Ming Dynasty. Therefore, the coastal defense of Ningbo has been in the process of dynamic improvement, with obvious dynamic and sustainable characteristics, which can reflect the ideas and strategies of resisting Wokou in different periods of the Ming Dynasty and can provide references for the study of other military settlements.

(3) Due to Ningbo's special position in China's Ming Dynasty coastal defense system, a wealth of information has been left behind, laying the foundation for the defensive efficiency study.

2.1. Three Major Defense Areas of Ningbo Traditional Military Settlements

The Ningbo coastal defense system can be divided into three major areas according to the spatial relationship between the north, east, and south: First, the north is the Linguan defense area, which is dominated by Linshan Wei and Guanhai Wei. The second is the Dinghai defense area in the east, dominated by Dinghai Wei. The third is the Changguo defense area in the south, dominated by Changguo Wei [2]. The three major areas are delineated according to geographic units, and the layout of the military settlement system within each area also shows certain characteristics. As a relatively independent military region, the defense area has a complete combat system and can organise battles independently. At the same time, the defense areas are also closely linked and cooperate with each other to form a strict coastal defense line.

2.2. Ming Dynasty Ningbo Coastal Defense Battle Overview for Four Periods

During the Ming Dynasty, the intrusion of Wokou occurred almost constantly. In Ningbo, the main times of coastal defense are concentrated in the period from the Hongwu years to the Yongle years in the early Ming Dynasty, from the Zhengtong years to the Chenghua years and during the Jiajing years. The battles in different periods have different laws, and the defensive efficiency of military settlements also changed. Therefore, the division of the time periods is conducive to the comparison of defensive efficiency. The Ming Dynasty is divided into four periods of coastal defense with reference to the Mingdai Wokou Shilue. All the battles and their results recorded in the local records within the four periods were statistically and visually analysed and represented in the Ningbo coastal defense historical information map (Figure 2).



Figure 1. Location of Zhejiang defense zone and Ningbo defense zone.

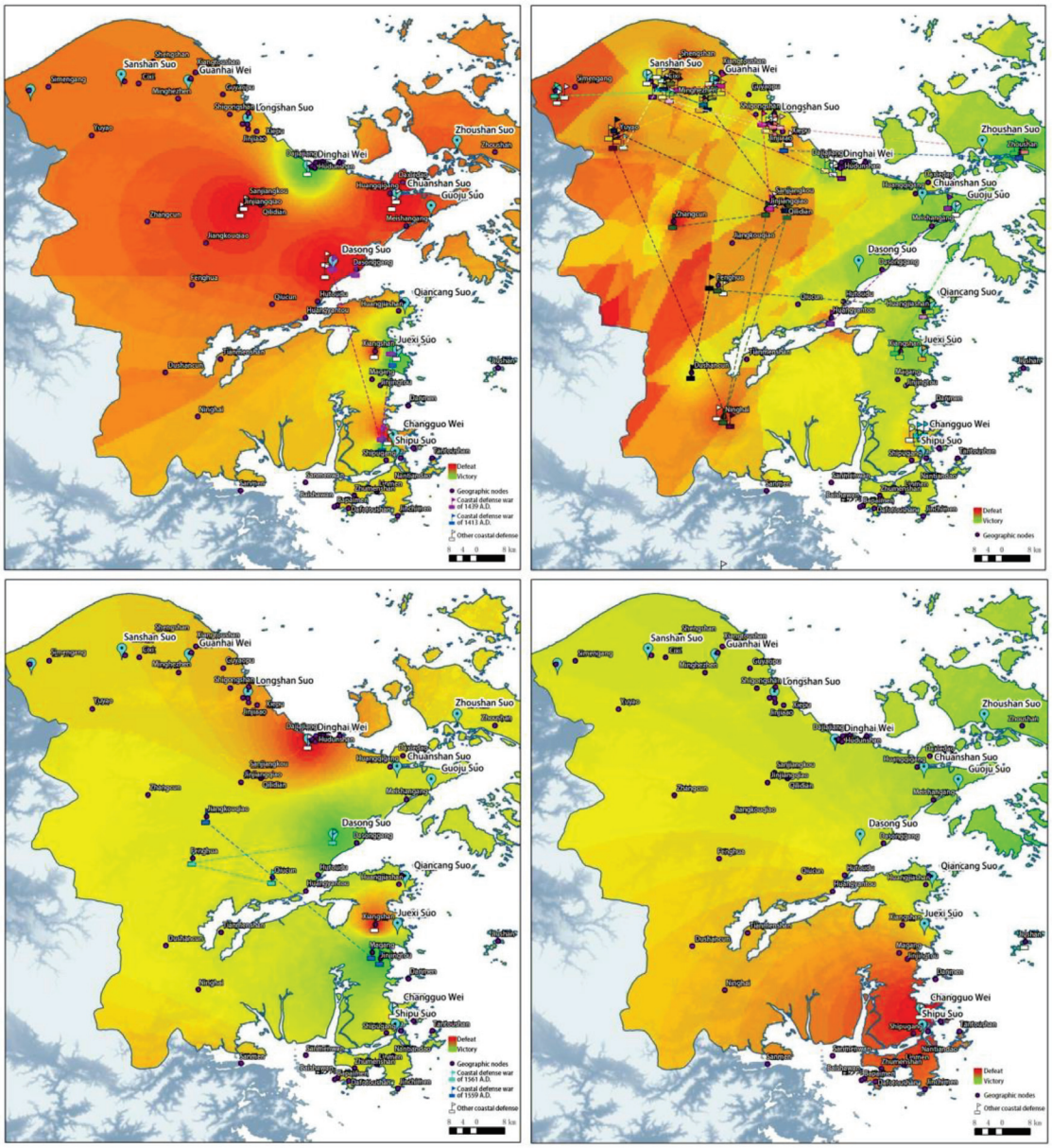


Figure 2. Historical information map of Ningbo coastal defense battles.

a. The first period (1368–1521) is the period from Hongwu to Zhengde. As the Ming regime had not yet stabilised, Wokou invaded the southeast coast. Ming Taizu thus strengthened the maritime and land forces and established a solid coastal defense system. The coastal defense settlements—Weisuo forts in Ningbo—were established during this time. Marking the routes of the Wokou invasions, it can be seen that the two Wokou invasion raids in 1413 and 1439 had a large area of influence, even across war areas. It can be seen that the construction of the coastal defense system as a countermeasure must have a holistic mindset to achieve victory through the concerted defense between the war areas.

b. The second period (1522–1557) is the middle and early period of Jiajing and the period of most concentrated Wokou aggression throughout the Ming dynasty. Compared with the early Ming period, the Jiajing period saw complex and significant changes in defense strategies. Therefore, the Jiajing Period is divided into two sections for comparative analysis. After the Hongwu Period, the peaceful marine environment

led to a series of declining coastal defense constructions. In the early Jiajing Period, the coastal defense of Zhejiang and Fujian had been abandoned for a long time. The two coastal invasions in 1522 and 1523 forced the government to tighten the sea ban policy, but contrary to expectations, this triggered large-scale invasions in Wokou in the middle of the Jiajing period, characterised by a large number of times, long time, large scale, wide area, and repeated and winding routes. The defeat rate of the Lin Guan war area is significantly higher than the other two war areas; the scope of Wokou's invasion even expanded into the interior, and the coastal defense system was significantly damaged. It can be seen that at this period, the expansion of Wokou's power often made it impossible for a single coastal defensive Wei Suo fort to intercept and destroy them in time, and it was necessary for multiple coastal defense forts to work together.

c. The third period (1558–1566) is the late Jiajing Period. In response to the Wokou Invasion, the Ming Dynasty began to take measures to strengthen the coastal defense forces. In particular, the defense systems of Zhejiang and Nanzhili were more complete. Both naval and land forces were stronger than before, and military settlements were repaired. Wokou's power was also weakened. Coastal defense battles in Ningbo and the whole Zhejiang Province were significantly reduced.

d. The fourth period (1567–1644) is the period from Longqing to Chongzhen. The force that remained in Wokou was no longer large, and the damage was relatively light. There were several attacks on the southern coast of Ningbo, which no longer poses a threat. By the end of the Ming Dynasty, Wokou was basically nonexistent near China's coastal areas.

3. Methodology

The main methodology of this study is that after completing the establishment of the defensive efficiency evaluation system for the coastal defense of Ningbo in the Ming Dynasty, the defensive efficiency scores are compared with the historical facts, and in this way the evaluation system is verified to be reasonable and effective (Figure 3). Specific methodologies are described below.

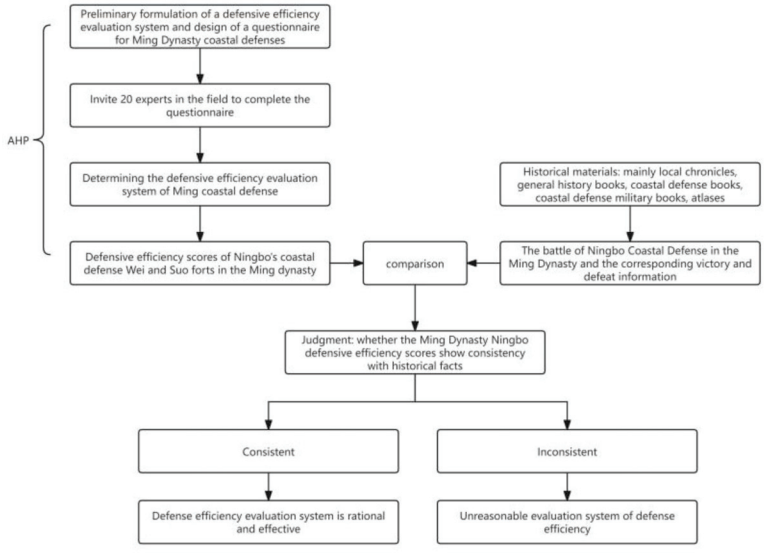


Figure 3. Methodology flowchart.

3.1. Materials

The information on the Ming Dynasty coastal defense military settlements in the Ningbo region discussed in this article primarily comes from three sources. The first is the site information published online by the Ningbo Municipal Government based on China's Third National Cultural Relics Census (available on the Ningbo and Zhejiang Cultural Heritage Protection website [26–28]) and related specialised publications. The second source is the comprehensive field surveys conducted by our research team over the past 15 years and the continually updated database on Ming Dynasty military settlements, including geographic and historical information. The dataset encompasses information on 12 large military settlements within four major defense zones in the Ningbo area, including 4 Wei forts (such as Linshan Wei Fort) and 8 Suo forts (such as Sanshan Suo Fort). The third category is related historical information. It is possible to collect not only settlement-related content but also information about the victories and defeats of battles. Relevant historical information includes local chronicles, coastal defense canonical books, general historical canonical books, coastal defense military books, atlases, and also coastal defense-related chapters extracted from the literature reflecting the life of the people in the Ming Dynasty. The specific bibliography can be found in the table in Appendix A.

3.2. GIS Analysis

In the 1980s, spatial analysis supported by GIS and computer technology began to be applied in archaeological research in western regions such as North America and Europe. Since the 1990s, it has been applied to the field of archaeology, including the traditional settlements research. This study mainly applies ArcGIS 10.8, using kernel density, cost distance, inverse distance weighted neighbourhood, viewshed analysis, etc., to obtain the contribution value of the defensive efficiency impact factors and to evaluate the scores.

3.3. Analytic Hierarchy Process (AHP)

Analytic hierarchy process (AHP) was first proposed by Professor T.L. Saaty of the University of Pittsburgh [29]. It is specifically designed to address decision-making problems involving multiple objectives, multiple criteria, and complex forms. AHP is a scientific research method for quantitatively determining the importance of each influencing factor. This method is widely used in planning and design, especially in situations requiring comprehensive evaluation to reach reasonable decisions [30,31]. The coastal defense military settlement system is a multi-variable system. Defensive efficiency, as a composite index reflecting both speed and capability, also requires separate analysis through layering and classification. AHP can effectively handle the multi-factor, multi-level problems in the quantitative analysis of defensive efficiency by scientifically calculating weight values [32]. Based on long-term research on the factors related to coastal defense military settlements, we attempted to comprehensively collect evaluation indicators that affect the defensive efficiency of military settlements. Using this method, an evaluation system was established based on AHP, with the defensive efficiency of the coastal defense military settlement system as the target layer (A) and the final score being determined by the intermediate layer (B) and the constraint layer (C) (Figure 3).

① A_n: The overall objective of this study—the defensive efficiency of the coastal defense military settlements in Ningbo (A).

② B_n: The overall objective is further divided into two intermediate indicators: the ability for mutual support among settlements (accessibility, B_1) and the military strength of each individual settlement (settlement forces, B_2).

③ C_n: This level further breaks down the intermediate indicators.

Accessibility (B_1) consists of three components: settlement accessibility (C_1), information accessibility (C_2), and postal delivery system accessibility (C_3), which examines the interconnectedness of the military settlement system, it can also be interpreted as the coverage of defense works and the speed of war response. As a systematic whole, the construction of coastal defense military settlements forms a networked layout, where the accessibility of each node in the network is key to the system's rapid operation. The accessibility of core Wei-Suo forts (C_1) determines the ability of nearby Wei-Suo forts to provide support during warfare. Information accessibility (C_2), primarily through beacon towers, represents the early warning capability against pirate invasions. Additionally, the accessibility of the postal delivery system (C_3) reflects the efficiency of material transportation.

Settlement forces (B_2) examines the defensive constructions within the settlements themselves, divided into army power (C_4), which centres on the number of troops, and settlement construction (C_5), which focuses on the fortifications. Unlike the relatively static accessibility indicators, C4 has fluctuated significantly with changes in historical context and must be examined as a dynamic indicator according to historical timelines. This will be statistically analysed according to the four periods of Ningbo's coastal defense previously mentioned.

④ D_n: At the C_n level, some factors can be directly quantified, while others need further breakdown. Information accessibility (C_2) includes the number of beacon towers (D_1) and the visual field of beacon towers (D_2). Settlement forces (C_5) include perimeter (D_3), wall thickness (D_4), wall height (D_5), land gates (D_6), water gates (D_7), watchtowers (D_8), Wopu (D_9, small huts built on top of the wall's horse face for soldiers to shelter from the weather and store weapons), and moats (D_{10}).

3.3.1. Weight Calculate

Based on the established evaluation system, 20 experts in Ming Dynasty military settlements were invited to assess the importance of each layer's evaluation criteria. Part of them are professors and associate professors who are deeply involved in the field and come from Chinese universities, totalling 10. Another part is the frontline staff of cultural relics protection departments in Ningbo and Zhejiang Province, totalling 10. During the preliminary fieldwork of this study, we contacted and cooperated with these frontline staff members, who were invited to fill out the AHP questionnaire. The evaluation scale is divided into five levels (Table 1). By comparing the importance of the evaluation criteria, a judgment matrix was constructed to derive the weight values.

Table 1. Rating scale for the importance of evaluation factors in the judgment matrix [33].

Rating Scale	Importance
1	Of equal importance
2	Slightly more important
3	Significantly more important
4	Strongly more important
5	Extremely more important

Based on the expert scoring results, there are no significant weight differences among the elements in the A, B, and C levels. The changes in weights appear in the D_3–D_{10} elements under C_5. For the time being, the other elements with no differences are equally weighted, and the weight judgment matrix for the D_3–D_{10} evaluation indicators under C_5 is shown in Table 2.

Table 2. D_3–D_{10} layer judgment matrix.

	D_3	**D_4**	**D_5**	**D_6**	**D_7**	**D_8**	**D_9**	**D_{10}**	**W_i**
D_3	1	2	2	3	2	5	4	3	0.249
D_4	1/2	1	1/2	2	2	4	4	3	0.164
D_5	1/2	2	1	2	2	4	4	3	0.194
D_6	1/3	1/2	1/2	1	1/3	4	3	2	0.099
D_7	1/2	1/2	1/2	3	1	4	3	2	0.136
D_8	1/5	1/4	1/4	1/4	1/4	1	1/2	1/5	0.033
D_9	1/4	1/4	1/4	1/3	1/3	2	1	1/2	0.046
D_{10}	1/3	1/3	1/3	1/2	1/2	5	2	1	0.080

3.3.2. Consistency Test

The weight judgment matrix needs to undergo a consistency test. Let λmax be the largest eigenvalue of the judgment matrix, with its corresponding eigenvector being W_i.

$$\lambda max = \frac{\sum(C_5W)_i}{nW_i} \tag{1}$$

Consistency Index: *CI*

$$CI = \frac{\lambda max - n}{n - 1} \tag{2}$$

Consistency Ratio: *CR*

$$CR = \frac{CI}{RI} \tag{3}$$

Random Index: *RI* (Table 3). The evaluation method is as follows: if $CR < 0.1$, it indicates satisfactory consistency; otherwise, the judgment matrix values need to be adjusted to achieve consistency. According to the calculation, the maximum eigenvalue of the matrix is $\lambda max = 8.43$, and the consistency index $CI = 0.062$. Given n = 8, the table shows $RI = 1.41$. $CR = 0.044 < 0.1$ indicates that the results are consistent and the weight values are valid [34].

Table 3. Average random consistency indicator [33].

n	**1**	**2**	**3**	**4**	**5**	**6**	**7**	**8**	**9**
RI	0	0	0.58	0.90	1.12	1.24	1.32	1.41	1.45

The weights of each layer are summarised and compiled to obtain Table 4 for the defensive efficiency of coastal military settlements.

3.3.3. Normalization

To standardise the scoring, we quantify the scores of each one into a percentage scale, $0 \leq F \leq 100$. If the attribute is directly proportional to the score, the calculation is as follows:

$$F = \frac{C_n(fi)}{C_n(fmax)} \times 100 \tag{4}$$

F is the quantified score after scoring; $C_n(fi)$ or $D_n(fi)$ is the attribute value of the settlement under the evaluation criterion; and $C_n(fmax)$ or $D_n(fmax)$ is the maximum value.

If the attribute value is inversely proportional to the score, the calculation is as follows:

$$F = \frac{C_n(fmin)}{C_n(fi)} \times 100 \tag{5}$$

And $C_n(fmin)$ or $D_n(fmin)$ is the minimum value.

Table 4. Weights of defensive efficiency evaluation system.

A	B	W_{Bi}	C	W_{Ci}	D	W_{Di}	W_i
A	**B_1**	0.5	**C_1**	0.33	-	-	0.167
			C_2	0.33	**D_1**	0.5	0.083
					D_2	0.5	0.083
			C_3	0.33	-	-	0.167
	B_2	0.5	**C_4**	0.50	-	-	0.250
			C_5	0.50	D_3	0.249	0.062
					D_4	0.164	0.041
					D_5	0.194	0.049
					D_6	0.099	0.025
					D_7	0.136	0.034
					D_8	0.033	0.008
					D_9	0.046	0.012
					D_{10}	0.080	0.020

4. Results

4.1. Accessibility (B_1)

4.1.1. Settlement Accessibility (C_1)

The coastal defense fortifications were primarily established to protect against pirate invasions, with their locations strategically chosen to ensure interconnectedness, forming a robust defense system along the coast. Settlement Accessibility (C_1) measures the minimum distance between these settlements, which can be determined using the minimum cost distance analysis-based DEM in ArcGIS [35]. Table 5 shows the cost distances between adjacent military settlements, from north (Linshan Wei) to south (Shipu Suo). Shorter distances result in higher contributions to defensive efficiency, thereby increasing the last score.

Table 5. Average minimum distance of Ningbo coastal defense settlements.

Defense Area	Military Settlement	Adjacent Settlement Cost Distance (km)	F_1
Linguan	Linshan Wei	23.89	18
	Sanshan Suo	20.70	21
	Guanhai Wei	17.88	24
	Longshan Suo	19.12	23
Dinghai	Dinghai Wei	22.07	20
	Chuanshan Suo	16.84	26
	Guoju Suo	19.35	22
	Dasong Suo	25.46	17
Changguo	Qiancang Suo	17.09	25
	Juexi Suo	17.22	25
	Changguo Wei	13.17	33
	Shipu Suo	4.34	100

4.1.2. Information Accessibility (C_2)

As an important carrier of information, the layout of beacon towers is a key factor affecting the defensive efficiency, judged by the number of beacon towers (D_1) and the visibility (D_2).

For D_1, the beacon towers are marked and analysed by GIS density analysis to produce a kernel density map (Figure 4) to illustrate the spatial distribution pattern of the beacon towers. The beacon towers in the three main defense zones clearly form three clusters, with each cluster organised around its geographical centre as the core of its defense. The defensive layout of the beacon towers in the Linguan defense area is relatively compact along the coastline, while in the Dinghai and Changguo, the beacon towers are built along the mountains, tightly securing the coastline. The scores for D_1 are shown in Table 6.

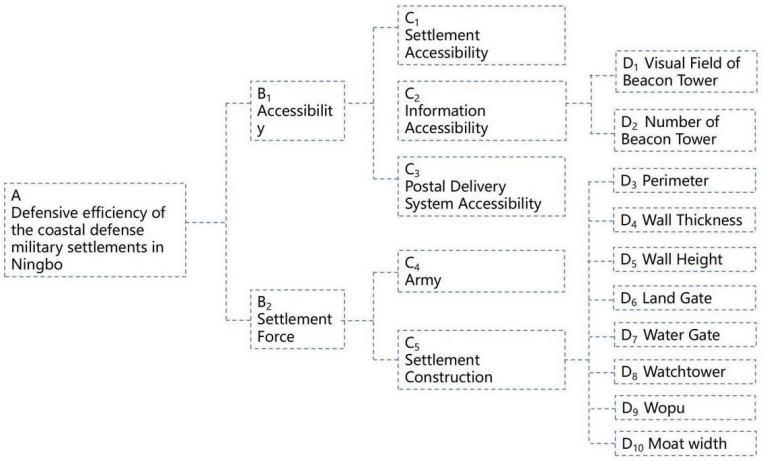


Figure 4. Hierarchy evaluation model of the defensive efficiency.

Table 6. Beacon towers of Ningbo coastal defense settlements (the information for the beacon towers are sourced from reference [36]).

Defense Area	Military Settlement	Beacon Towers	Number of Beacon Tower	$F_{2\text{-}1}$
Linguan	Linshan Wei	Fang (jia)lu Beacon Tower, Daotang Beacon Tower, Zhoujialu Beacon Tower, Wupen Beacon Tower, Miaoshan Beacon Tower, Luojiashan Beacon Tower, Simen Beacon Tower, Zhaogang Beacon Tower, Xigaishan Beacon Tower, Hehuachi Beacon Tower	10	77
	Sanshan Suo	Xujialu Beacon Tower, Lishan Beacon Tower, Meishan Beacon Tower, Xushan Beacon Tower, Cuoyu Beacon Tower, Caishan Beacon Tower, Wujiashan Beacon Tower	7	54
	Guanhai Wei	Xiangtou Beacon Tower, Guashizhai Beacon Tower, Xilongshan Beacon Tower, Xinpu Beacon Tower, Guyao Beacon Tower, Xilongwei Beacon Tower	6	46
	Longshan Suo	Longshan Observatory, Shigongshan Beacon Tower, Longtou Beacon Tower, Longwei Beacon Tower, Shitangshan Beacon Tower, Qingxi Beacon Tower	6	46
Dinghai	Dinghai Wei	Gaoshan Beacon Tower, Zhushan Beacon Tower, Xiaoshan Beacon Tower, Luci Beacon Tower, Zhaobaoshan Beacon Tower, Dagushan Beacon Tower, Zhangshipu Beacon Tower, Dajiangang Beacon Tower, Dayuwan Beacon Tower, Changshanshan Beacon Tower, Zheng (gui) yu Beacon Tower, Lujuan Beacon Tower, Wangjialu Beacon Tower	13	100
	Chuanshan Suo	Qitou Beacon Tower, Suohou Beacon Tower, Baifeng Beacon Tower, Xishan Beacon Tower	4	31
	Guoju Suo	Santashan Observatory, Shengao Beacon Tower, Gaoshan Beacon Tower, Meishan Beacon Tower, Guanshan Beacon Tower, Xiakang Beacon Tower	6	46
	Dasong Suo	Daqian Beacon Tower, Kunting Beacon Tower, Hengshan Beacon Tower, Huangyan Beacon Tower, Citun Beacon Tower, Geao Beacon Tower, Jianqi Beacon Tower, Gangkou Beacon Tower	8	62

Table 6. *Cont.*

Defense Area	Military Settlement	Beacon Towers	Number of Beacon Tower	$F_{2\text{-}1}$
Changguo	Qiancang Suo	Qinglei Beacon Tower, Pumenling Beacon Tower, Dongmenling Beacon Tower, Zhongbao Beacon Tower, Qianshan Beacon Tower, Tuci Beacon Tower, Shanmu (yang) Beacon Tower	7	54
	Juexi Suo	Gongyu (Gongao) Beacon Tower, Banling Beacon Tower, Zhaoao Beacon Tower, Shatou (Shaling) Beacon Tower, Pingfeng Beacon Tower, Yuquan Beacon Tower, Wailing Beacon Tower	7	54
	Changguo Wei	Huangsha Beacon Tower, Songao Beacon Tower, Renyi Beacon Tower, Hejialan Beacon Tower, Houshan Beacon Tower, Qitou Beacon Tower, Wushi Beacon Tower, Qianshan Beacon Tower, Chikan Beacon Tower	9	69
	Shipu Suo	Houshan Beacon Tower, Qianshan Beacon Tower, Dajinshan Beacon Tower, Tuwan Beacon Tower, Songao Beacon Tower, Xiaao Beacon Tower, Fengjiashan Beacon Tower	7	54

For D_2, a larger viewshed of existing beacon towers indicates a stronger capacity for alerting against invasions. The placement of beacon towers must ensure a coherent flow of information within the effective range of visual or audible signals to effectively warn of enemy presence. D_2 serves as a visual evaluation index, representing the ability of beacon towers to communicate with each other and detect nearby enemies. By utilising the Viewshed tool in ArcGIS spatial analysis and loading the corresponding DEM elevation data [37], the viewshed range of the beacon towers can be determined (Figure 5).

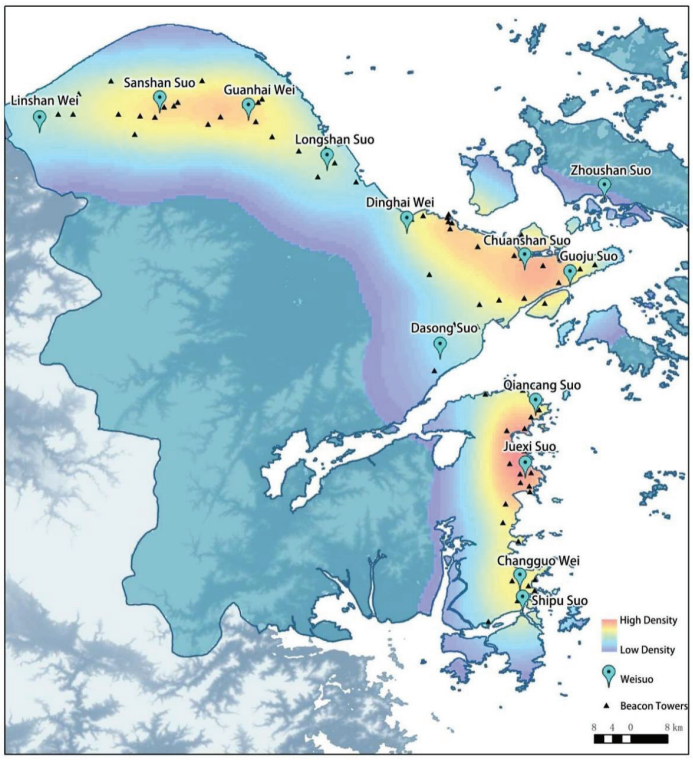


Figure 5. Kernel density map of beacon towers.

In Figure 5, the green areas represent the visible range. The viewshed range of Linguan is the largest. Although the beacon towers defense layout in the Linguan region is farther from the coastline compared to other regions, the lower and relatively flat terrain

of northern Ningbo still allows for full coverage of the coastline. In contrast, the Dinghai and Changguo regions are affected by mountainous terrain, requiring a higher density of beacon towers and optimised placement to meet visibility requirements. By calculating the visual field, the final D_2 scores are shown in Table 7.

Table 7. Beacon tower visual index (D_2) of the coastal defense system.

Defense Area	Military Settlement	Visual Field (km^2)	$F_{2\text{-}2}$
Linguan	Linshan Wei	1070.33	22
	Sanshan Suo	2125.20	44
	Guanhai Wei	1661.19	34
	Longshan Suo	2932.95	61
Dinghai	Dinghai Wei	2446.91	51
	Chuanshan Suo	1730.92	36
	Guoju Suo	4838.76	100
	Dasong Suo	3764.12	78
Changguo	Qiancang Suo	748.32	15
	Juexi Suo	4137.89	85
	Changguo Wei	4000.91	83
	Shipu suo	371.80	8

4.1.3. Postal Delivery System Accessibility (C_3)

In the postal delivery system, the post road is the path of information flow, and the post station is the hub of the entire system. There are six post stations in Ningbo, namely Yaojiang Post Station, Chejiu Post Station, Siming Post Station, Lianshan Post Station, Baiqiao Post Station and Sangzhou Post Station. Since ancient postal route relics can no longer be traced, we first used the cost distance analysis to reconstruct the postal route network in Ningbo (Figure 6). Because material transport requires not only choosing relatively short routes but also avoiding difficult mountain paths and other challenging terrains, the cost distance calculation takes into account these terrain factors. This makes it more suitable for calculating the accessibility of the postal delivery system compared to straight-line distances.

The reconstructed postal routes avoid high elevations and generally run parallel to mountainous terrain. We select the cost distance from each military settlement to the nearest post station as the criterion for evaluating accessibility between each military settlement and its closest post station. Shorter distances indicate better accessibility and higher scores (Table 8). The results indicate that due to terrain influences, the military settlements in the northern Linguan sector are closer to the post stations, resulting in higher postal delivery system accessibility. In contrast, the Changguo sector shows a distinct disadvantage in postal delivery system accessibility.

Table 8. Cost distance of postal delivery system.

Defense Area	Military Settlement	Cost Distance of Post Roads (km)	F_3
Linguan	Linshan Wei	23.31	72
	Sanshan Suo	21.52	78
	Guanhai Wei	34.92	48
	Longshan Suo	21.86	76
Dinghai	Dinghai Wei	16.68	100
	Chuanshan Suo	44.11	38
	Guoju Suo	55.54	30
	Dasong Suo	36.41	46
Changguo	Qiancang Suo	78.31	21
	Juexi Suo	71.05	23
	Changguo Wei	65.33	26
	Shipu suo	71.89	23

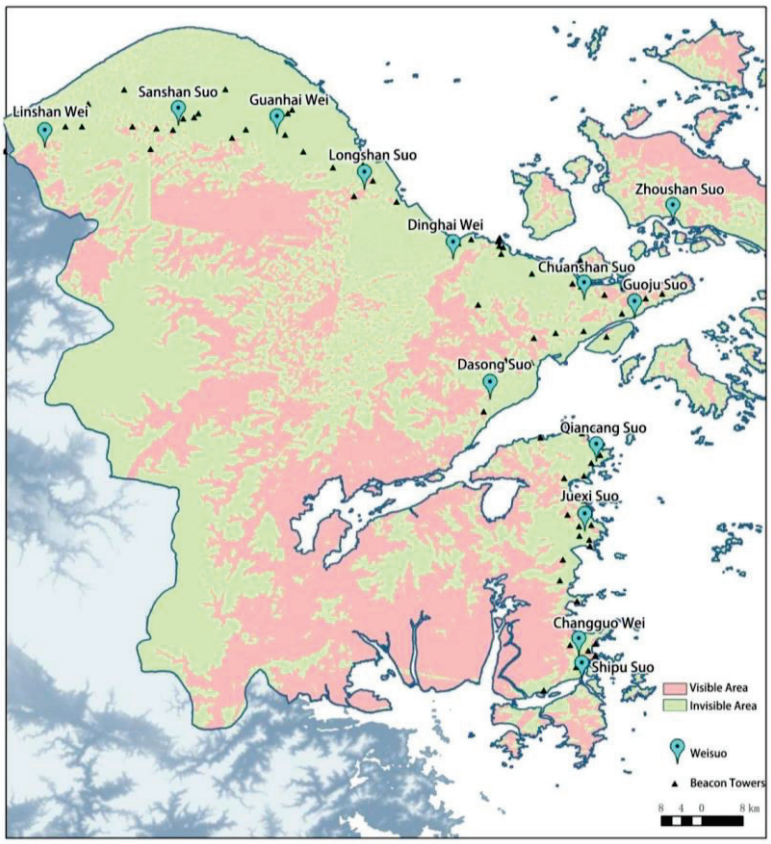


Figure 6. Viewshed of beacon towers.

4.2. Settlement Forces (B_2)

4.2.1. Army Power (C_4)

During the Ming Dynasty, the army power of coastal military settlements fluctuated over different periods. As shown in Table 9, in the first period, during the initial construction of each military settlement, every settlement had a designated troop amount. The designated troop strength for a Wei fort was 5600 soldiers, typically overseeing five subordinate Suo forts. Some Wei forts, like Changguo Wei, only commanded four Suo forts; thus, their designated troop was lower than others. Generally, each Suo fort had a designated strength of 1120 soldiers. For example, Shipu Suo, which combined two Suo, had doubled the troops.

In the second period compared to the first, due to frequent conflicts, troop amounts in each military settlement were greatly reduced. By the second period, the troop strength at Lingshan Wei was no longer recorded, while Juexi Suo was the only one to see an increase in troop numbers.

In the third and fourth periods, there were changes in the Ming court's military system. Troop numbers in each settlement were no longer fixed but fluctuated according to changes in military conflicts. Therefore, troop statistics were no longer recorded separately for each military settlement but aggregated by defense areas. This change in military structure somewhat improved operational efficiency and helped in containing invasions. However, Lingshan and Dinghai defense areas still suffered significant troop losses during conflicts. As conflicts moved southward, the naval construction in the Changguo defense area during the Wanli period led to a significant increase in troops.

Table 9. Number of troops in four periods.

Defense Area	Military Settlement	Army Power							
		1st Period	F_{4-1}	2nd Period	F_{4-2}	3rd Period	F_{4-3}	4th Period	F_{4-4}
Linguan	Linshan Wei	5600	100	-	-	2445	30	1876	56
	Sanshan Suo	1120	20	535	16				
	Guanhai Wei	5600	100	1283	39				
	Longshan Suo	1120	20	531	16				
Dinghai	Dinghai Wei	5600	100	3323	100	8040	100	3292	98
	Chuanshan Suo	1120	20	222	7				
	Guoju Suo	1120	20	468	14				
	Dasong Suo	1141	20	413	12				
Changguo	Qiancang Suo	1120	20	925	28	2560	32	3344	100
	Juexi Suo	1120	20	1437	43				
	Changguo Wei	4480	80	2808	85				
	Shipu suo	2240	40	1445	43				

4.2.2. Settlement Construction (C_5)

As the backbone of military defense, the various components of military settlements must coordinate closely to maximise their defensive capabilities. However, the construction of a fort was not accomplished in a single effort; it often required multiple phases of construction and partial repairs over several dynasties. This necessitates a phased analysis of C_5. Among the 12 Wei and Suo forts, the construction times, gate repair times, and wall repair times are all recorded in local chronicles. These repair records are concentrated in the first two periods of Ningbo's coastal defense settlement construction, with minimal changes in the third and fourth periods. Yang provided a detailed overview of this in reference [25]. After multiple repairs, the construction status of these defensive settlements in the mid to late Ming period is shown in Table 10. Based on the weights of D_3–D_{10} obtained from expert ratings in Table 4, we calculate the scores of these influencing factors and the final scores of the C_5, as shown in Table 11.

To better illustrate the changes in the C_5' scores of military settlements at each stage, we have plotted the variations in F5 based on the time points of each record (Figure 7). The results indicate that in the first stage, the basic construction of the forts in various Wei and Suo was generally completed during the Hongwu period. In the second stage, there was a concentrated repair effort during the Yongle period, resulting in a significant increase. A minor scale of repairs was conducted again in the mid-Jiajing period. Entering the third stage, F5 remained relatively stable by the end of the Jiajing period. We can also clearly observe that the defensive scores of Wei forts improved more significantly, particularly for Guanhai Wei and Linshan Wei. By the 44th year of Jiajing (1565), the defensive performance of the Wei forts had comprehensively surpassed that of the Suo forts.

Table 10. Impact factors of settlement construction (C_5).

	D_3 (m)	D_4 (m)	D_5 (m)	D_6	D_7	D_8	D_9	D_{10} (m)
Dinghai Wei	4204.0	3.3	7.8	6	10	39	2185	3153.0
Chuanshan Suo	2421.9	3.3	6.9	4	12	12	1604	4357.4
Guoju Suo	1592.8	3.3	6.2	3	9	13	920	2859.3
Dasong Suo	2415.4	3.9	5.5	4	20	25	775	1083.6
Linshan Wei	2987.5	14.7	8.2	4	31	42	1142	2767.9
Sanshan Suo	1972	14.7	6.2	4	4	6	699	2154.2
Guanhai Wei	2399.8	9.8	7.8	4	28	36	1370	2983.3
Longshan Suo	1844.7	6.5	7.8	3	15	10	568	3368.4
Juexi Suo	1763.1	9.8	9.1	3	11	23	803	1044.5
Qiancang Suo	1763.1	4.2	8.5	4	12	20	1200	1958.4
Changguo Wei	4113.9	3.3	7.5	4	36	73	1914	705.0
Shipu Suo	1981.2	2.0	7.5	3	13	29	1906	359.0

Table 11. The score of settlement construction (C_5).

	F_{5-3}	F_{5-4}	F_{5-5}	F_{5-6}	F_{5-7}	F_{5-8}	F_{5-9}	F_{5-10}	Final Score
Weight	**0.062**	**0.041**	**0.049**	**0.025**	**0.034**	**0.008**	**0.012**	**0.02**	
Dinghai Wei	100	22	86	80	28	100	100	72	17.71
Chuanshan Suo	46	22	76	90	33	15	73	100	13.85
Guoju Suo	30	22	68	90	25	16	42	66	11.15
Dasong Suo	46	27	60	90	56	32	35	25	12.23
Linshan Wei	56	100	90	80	86	53	52	64	19.23
Sanshan Suo	37	100	68	90	11	8	32	49	13.78
Guanhai Wei	45	67	86	100	78	46	63	68	17.39
Longshan Suo	35	44	86	100	42	13	26	77	14.07
Juexi Suo	33	67	100	90	31	29	37	24	14.15
Qiancang Suo	33	29	93	70	33	25	55	45	12.42
Changguo Wei	78	22	82	80	100	92	88	16	17.27
Shipu Suo	37	14	82	80	36	37	87	8	11.61



Figure 7. Restoration map of Ningbo postal delivery system.

4.3. Final Score

After obtaining the F for each impact factor, we calculate the scores by overlaying them with the weights and then compile the statistics according to the four periods of coastal defense in Ningbo. The results are shown in Table 12. Then, we obtain the final defensive efficiency score for each military settlement in each period.

Table 12. Final defensive efficiency score.

Defense Area	Military Settlement	1st Period	2nd Period	3rd Period	4th Period
Dinghai	**Dinghai Wei**	76.2	76.3	76.3	75.8
	Chuanshan Suo	43.4	42.4	45.9	52.4
	Guoju Suo	61.1	45.9	43.7	50.2
	Dasong Suo	44.5	43.5	47.0	53.5
Linhai	**Linshan Wei**	37.2	35.7	57.2	56.7
	Sanshan Suo	35.1	31.8	55.1	54.6
	Guanhai Wei	65.4	58.4	50.2	56.7
	Longshan Suo	39.4	37.4	59.4	58.9
Changguo	**Juexi Suo**	32.0	34.6	35.6	52.6
	Qiancang Suo	39.9	46.3	43.6	60.6
	Changguo Wei	60.4	61.6	48.4	65.4

To more intuitively compare the differences in defensive efficiency of Ningbo's coastal defenses across different regions and periods, we use the Inverse Distance Weighted (IDW) interpolation method in ArcGIS [38] to project the total defense scores of the coastal settlements in four periods onto a geographic coordinate system (Figure 8). The results indicate that Dinghai Wei in central Ningbo has consistently maintained the highest defense levels, while the defensive efficiency of other regions has shown significant variations over time.

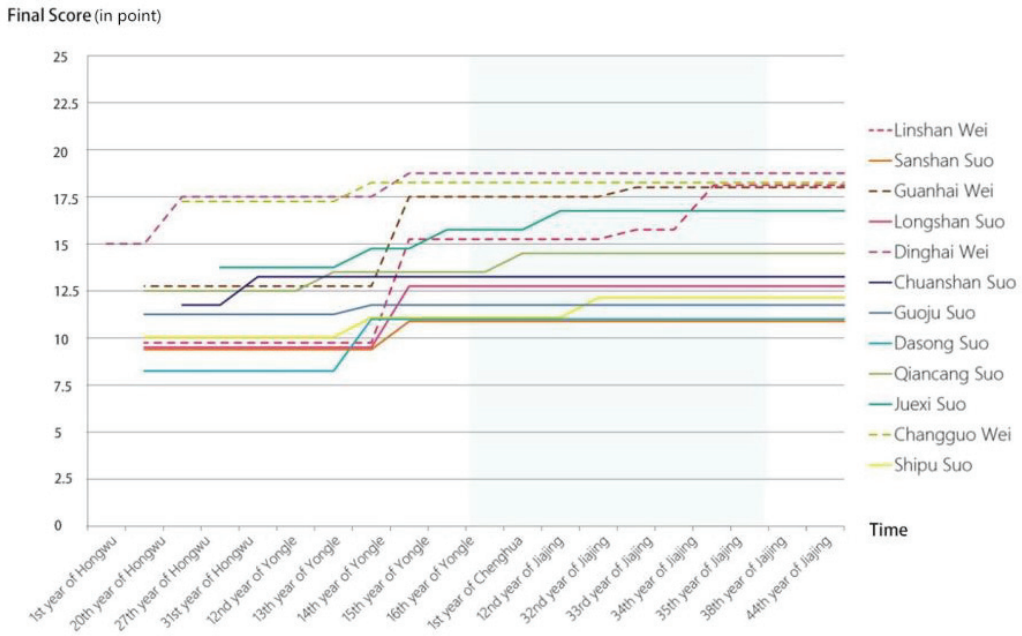


Figure 8. The change of settlement construction (C_5) over time.

By comparing Figure 9 with the historical map of Ningbo coastal defense battles (Figure 2), we can summarise the patterns and characteristics of the changes in the defensive efficiency of Ningbo's coastal military settlements under different historical contexts.

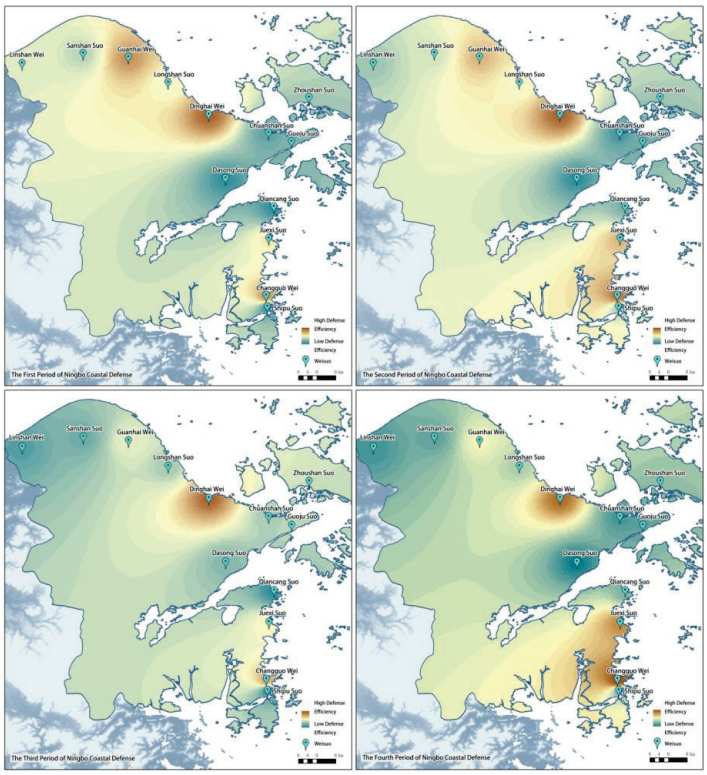


Figure 9. Spatial analysis of the defensive efficiency score.

In the first period, overall, the Dinghai defense area had the highest defensive efficiency, followed by the Linhai defense area and the Changguo defense area. Within the Dinghai defense area, Dinghai Wei had the highest score of 76.2 for defensive efficiency. Comparing the battle victories and defeats collated in Figure 2, Dinghai Wei has a higher probability of victory in this period. In addition, the imbalance within the Dinghai defense area is reflected in both the level of battle victories and defeats and the defensive efficiency. In this period, the defensive efficiency scores of Guanhai Wei, Dinghai Wei, and Changguo Wei were significantly higher than those of other regions; the defensive efficiency of Wei forts within each theatre was higher than that of Suo forts, and the difference in the scores was obvious, reflecting the idea of layered and obvious placement of military forces and accessibility under the hierarchical military defense system of Du-Si-Wei-Suo.

In the second period, the agglomeration within each defense area decreased, showing a more homogeneous development. This corresponds to a turbulent period when Wokou attacks and aggression were most concentrated, and the Chinese Ming government responded to this by beginning a comprehensive and intensive deployment of defenses, and the construction of more citadels began.

In the third phase, both the defensive focus and the centre of the battles were concentrated on Dinghai Wei. At this point, the differences in defensive efficiency scores within each defense area are shrinking, meaning that construction is almost complete.

Comparing the fourth period with the first three periods, it can be found that the defensive efficiency of Linhai defense area was gradually weakened while that of Changguo defense area was strengthened, indicating that the place where the battle took place moved from the north to the south, which is in line with the historical facts.

Through the comparison of the defensive efficiency scores of the four stages with the historical facts compiled in 2.2, it shows that the military settlement defensive efficiency

scores can basically correspond to the historical facts, which verifies the validity of the method.

5. Conclusions

This study introduces the concept of "dynamic defensive efficiency", establishes the evaluation system of China's Ming Dynasty coastal defense military with AHP, takes Ningbo, China as the research object, and forms the dynamic research methodology of China's Ming Dynasty coastal defense military settlement system, and obtains the following conclusions:

(1) For AHP: Under the AHP system, the two factors, accessibility (B_1) and settlement force (B_2), are equally important in the defense efficiency according to the opinions of the interviewed experts. The more obvious difference in weight is the eight factors included in Settlement Construction (C_5), of which the highest weighted factors are Perimeter (D_3) and Wall Height (D_5), and the lowest weighted are Watchtower (D_8) and Wopu (D_9).

(2) For the efficiency of China's Ming Dynasty coastal defense: the changes in defensive efficiency in four periods reflect the four phases of the construction of China's Ningbo coastal defense in the Ming Dynasty, the period of preliminary construction, the period of full-scale construction after repeated Wokou invasions, the period of basic completion, and the period in which Wokou invasions were reduced in large quantities and the point of attack was relocated to the south. Therefore, it can also be seen that, on the one hand, the construction of coastal defense in Ningbo, China during the Ming Dynasty was closely associated with Wokou invasions, and the spatial distribution of battles drove the continuous construction and improvement of coastal defense settlements, and that the Ming Dynasty was an important construction period for coastal defense in ancient China; on the other hand, the improvement of the coastal defense system had an obvious effect on the defense against Wokou invasions.

(3) For the proposed methodology: the validity of the evaluation system is verified through the comparison between the AHP scoring results and the real battle victory and defeat situations in history, forming a reproducible set of quantitative methodology for the defensive efficiency of the Ming Dynasty coastal defense in China.

6. Discussion

The study focuses on the holistic and systematic characteristics of China's Ming Dynasty coastal defenses and thus pays less attention to the specific roles of key defenses such as city walls, fortresses, and water systems. However, the various types of defense facilities of ancient Chinese coastal defense also have considerable traditional wisdom, which is worth expanding in detail and can be explored in depth as a future research direction.

At the level of heritage protection, the data collection and modelling in this study will be used to establish a more comprehensive heritage database, which will provide an important reference for subsequent heritage protection, restoration, display and sustainable development. At the same time, the parallel strategy of "digital twin + physical protection" is proposed to realise the visualisation of the defense scenarios through the construction of a digital twin system, which provides decision support for heritage protection and interpretation of heritage value. In terms of protection ideas, the systematic characteristics of the Ming Dynasty coastal defense suggest that in practice, it is necessary to break through the thinking of monolithic protection and instead establish an overall protection mechanism based on the cluster of settlements. Different specific protection strategies

should be formed for different periods of Ming Dynasty coastal defense characteristics and military settlement remains. At the same time, it is suggested that the defensive efficiency should be incorporated into the value assessment system of military heritage, forming a dynamic protection path of "efficiency analysis—value determination—graded intervention", and promoting the paradigm transformation of cultural relics protection standard from static value determination to dynamic efficiency assessment.

Author Contributions: Writing—original draft, L.M.; data curation, Z.Y.; methodology, L.T.; project administration, S.Y.; conceptualization, Y.Z.; visualization, X.W. All authors have read and agreed to the published version of the manuscript.

Funding: This research was funded by the Ministry of Education's Humanities and Social Sciences Research Project (grant number 23YJC760115) and the Tianjin Art Science Planning Project (grant number A24011).

Data Availability Statement: The original contributions presented in the study are included in the article, further inquiries can be directed to the corresponding author.

Conflicts of Interest: The authors declare no conflicts of interest.

Appendix A

Table A1. Ming Dynasty Ningbo coastal defense historical materials collation.

Category	Specific Materials
Local Chronicles	**Song Dynasty**: Luo Jun, *Baoqing Siming Zhi* (Annals of Siming in the Baoqing Era), 2nd year of Baoqing (1226); Mei Yingfa and Liu Xi, *Kaiqing Siming Xu Zhi* (Continuation of Siming Annals in the Kaiqing Era), 1st year of Kaiqing (1259)
	Ming Dynasty: Hu Zongxian (compiler), Xue Yingqi (editor), *Jiajing Zhejiang Tong Zhi* (General Gazetteer of Zhejiang in the Jiajing Era), 40th year of Jiajing (1561); Yang Shi (compiler), *Ningbo Jun Zhi* (Gazetteer of Ningbo Prefecture), 4th year of Chenghua (1468); Zhou Xizhe and Guan Jian (compilers), Zhang Shiche (editor), *Ningbo Fu Zhi* (Gazetteer of Ningbo Prefecture), 39th year of Jiajing (1560); Huang Runyu, *Ningbo Fu Jianyao Zhi* (Concise Gazetteer of Ningbo Prefecture), Chenghua period (1465–1487); Geng Zongdao et al., *Linshan Wei Zhi* (Gazetteer of Linshan Garrison), Jiajing period (1522–1566); Zhou Li (compiler), *Guanhai Wei Zhi* (Gazetteer of Guanhai Garrison), 41st year of Jiajing (1562); Zhang Shiche et al., *Dinghai Xian Zhi* (Gazetteer of Dinghai County), 42nd year of Jiajing (1563); Yao Zongwen (compiler), *Cixi Xian Zhi* (Gazetteer of Cixi County), 4th year of Tianqi (1624); Mao Dejing and Wang Xiangtong (compilers), Yang Minyi and Zhou Maobo (editors), *Xiangshan Xian Zhi* (Gazetteer of Xiangshan County), 35th year of Jiajing (1556)
	Qing Dynasty: Yu Wanchuan (compiler), Yu Yue (editor), *Zhenhai Xian Zhi* (Gazetteer of Zhenhai County), 5th year of Guangxu (1879); *Hushan Zhi* (Gazetteer of Hushan), 11th year of Daoguang (1831); Wen Xingdao (chief editor), *Kangxi Yin Xian Zhi* (Gazetteer of Yin County in the Kangxi Era), 24th year of Kangxi (1685); Zhang Xian (compiler), Zhou Daozun et al. (editors), *Xianfeng Yin Xian Zhi* (Gazetteer of Yin County in the Xianfeng Era), 6th year of Xianfeng (1856)
	Modern Period: Yang Jifang (chief editor), *Yuyao Liu Cang Zhi* (Gazetteer of Six Granaries in Yuyao), 9th year of the Republic of China (1920); Chen Zhongqi and Yan Xing, *Zhejiang Sheng Yuyao Shi Diming Zhi* (Gazetteer of Place Names in Yuyao City, Zhejiang Province) (1987)
Coastal Defense Canonical Books	**Ming Dynasty**: Zheng Ruozeng, *Chou Hai Tu Bian* (Illustrated Compendium on Coastal Defense), 41st year of Jiajing (1562); Zheng Ruozeng, *Jiangnan Jing Lue* (Military Strategies of Jiangnan), 45th year of Jiajing (1566); Liu Jiansong, *Liang Zhe Hai Fang Lei Kao* (Classified Studies on Coastal Defense in Zhejiang), 3rd year of Wanli (1575); Fan Lai, *Liang Zhe Hai Fang Lei Kao Xu Bian* (Continuation of Classified Studies on Coastal Defense in Zhejiang), 30th year of Wanli (1602); Cai Jiude, *Wo Bian Shi Lue* (Brief Account of Japanese Pirate Incidents), 37th year of Jiajing (1558); Bu Datong (compiler), *Bei Wo Ji* (Records of Japanese Pirate Defense), Wanli period (1573–1620); Zheng Shungong, *Riben Yi Jian* (A Mirror of Japan), 44th year of Jiajing (1565); Xie Jie, *Qian Tai Wo Zuan* (Compilation on Japanese Pirate Defense in Qianzhou), 23rd year of Wanli (1595)
	Qing Dynasty: Xue Fucheng, *Zhe Dong Chou Fang Lu* (Records of Coastal Defense Preparations in Eastern Zhejiang), 13th year of Guangxu (1887); Du Zhen, *Hai Fang Shu Lue* (Summary of Coastal Defense); Zhu Zhengyuan (compiler), *Zhejiang Yan Hai Tu Shuo* (Illustrated Account of Zhejiang's Coast), 25th year of Guangxu (1899)

Table A1. *Cont.*

Category	Specific Materials
General Historical Canonical Books	**Ming Dynasty**: Official Ming court compilations, *Ming Shi Lu* (Veritable Records of the Ming Dynasty); Zhang Juzheng, *Da Ming Hui Dian* (Collected Statutes of the Ming Dynasty), 15th year of Wanli (1587); Li Xian and Peng Shi (chief editors), *Da Ming Yi Tong Zhi* (Comprehensive Gazetteer of the Ming Empire), 5th year of Tianshun (1461)
	Qing Dynasty: Zhang Tingyu, *Ming Shi* (History of the Ming Dynasty), 4th year of Qianlong (1739); Gu Zuyu, *Du Shi Fang Yu Ji Yao* (Essentials of Historical Geography), 31st year of Kangxi (1692); Gu Yanwu, *Tian Xia Jun Guo Li Bing Shu* (Treatise on the Benefits and Flaws of [Governance in] the Empire's Regions), 1st year of Kangxi (1662); Gu Yingtai, *Ming Shi Ji Shi Ben Mo* (Historical Events of the Ming Dynasty from Beginning to End), 15th year of Shunzhi (1658)
Coastal Defense Military Books	**Ming Dynasty**: Mao Yuanyi (compiler), *Wu Bei Zhi* (Treatise on Military Preparedness), 1st year of Tianqi (1621); Hou Jigao, *Quan Zhe Bing Zhi Kao* (Study on Military Systems of Zhejiang), 20th year of Wanli (1592)
	Qing Dynasty: Zhu Lu, *Fang Shou Ji Cheng* (Compendium on Defense), 4th year of Xianfeng (1854)
Literary Works	**Ming Dynasty**: *Hu Zongzhi Qiao Yong Hua Diqing*, Wang Cuiqiao Si Bao Xu Mingshan (Governor Hu's Clever Use of Hua Diqing, Wang Cuiqiao's Death in Repayment to Xu Mingshan), from Lu Renlong's *Zhengxiao Guan Pingding Tongsu Yanyi Xing Shi Yan* (Popular Romance of the World's Heroes), Chapter 7 (Chongzhen period); Zhou Ji, *Hu Shaobao Ping Wo Zhan Gong* (Hu Shaobao's Meritorious Deeds in Suppressing Japanese Pirates), from *Xi Hu Er Ji* (Two Collections of West Lake Stories), Volume 34 (circa Chongzhen period); *Da Guan Jie Sheng Si Jie Yuan Jia*, Zuo Ren Qing Shi Zhong Quan Fo Fa (Bribes Lead to Life-and-Death Feuds, Human Favors Uphold Buddhist Law), from Hua Yang Sanren (editor), *Shi Er Lou Xin Duan Xiu Xiang Xiao Shuo Yuan Yang Zhen* (Newly Engraved Embroidered Novels: Mandarin Ducks Needle), Volume 1 (late Ming/early Qing)
	Qing Dynasty: Xiaoxiang Mi Jindu Zhe (editor), *Mei Chanjuan* (Charming Beauty), from *Bi Li Yuan* (Garden of Brush and Pear), Book 2 (Qing); Cui Xiangchuan, *Yu Chan Ji* (Jade Toad Chronicle), 1st year of Guangxu (1875); Chen Lang, *Xue Yue Mei* (Snow, Moon, and Plum Blossoms), 40th year of Qianlong (1775); Li Baichuan, *Lu Ye Xian Zong* (Legends of the Green Wilds), 28th year of Qianlong (1763); Li Lüyuan, *Qi Lu Deng* (Lamp at the Crossroads), 42nd year of Qianlong (1777)
Atlases	*Guang Yu Tu* (Comprehensive Atlas of the Realm); Xu Bida, *Qian Kun Yi Tong Hai Fang Quan Tu* (Complete Coastal Defense Map of the Unified Realm); Guo Ren, *Liang Zhe Hai Bian Tu* (Coastal Map of Zhejiang); Zhou Lun, *Zhe Dong Hai Bian Tu* (Coastal Map of Eastern Zhejiang); Chen Xi, *Su Song Hai Bian Tu* (Coastal Map of Suzhou and Songjiang); Lu Zhong, *Zhe Jiang Tu* (Map of Zhejiang); Cai Fengshi, *Wen Chu Hai Fang Tu Bei* (Prepared Coastal Defense Maps of Wenzhou and Chuzhou); Li Ruhua, *Wen Chu Hai Fang Tu Lue* (Summary of Coastal Defense Maps of Wenzhou and Chuzhou); Tan Qixiang, *Zhong Guo Li Shi Di Tu Ji* (The Historical Atlas of China)

References

1. Chen, H.; Dong, Y. *Chronicles of the Great Wall of China*; Jiangsu Phoenix Science and Technology Press: Nanjing, China, 2015.
2. Casas, J.; Nolla, M.; Grimal, L.P.; Vivó, D.; Fusté, V.S. Mas Gusó: Un establecimiento militar de época romana en el suburbium ampuritano. *Archivo Espanol De Arqueologia* **2016**, *89*, 117–132. [CrossRef]
3. Löcker, K.; Gallistl, J.; Gugl, C.; Hinterleitner, A.; Schiel, H.; Schlögel, I.; Wallner, M.; Totschnig, R.; Trausmuth, T.; Trinks, I.; et al. *Protected by Shooting at It—The Öde Kloster and an Associated Roman Settlement Within the Military Training Area Bruckneudorf, Austria*; Universitätsverlag Kiel | Kiel University Publishing eBooks: Kiel, Germany, 2023; pp. 183–186.
4. Williams, D. Land Assessment and Military Organisation in the Norse Settlements in Scotland, c900-1266 ad. Doctoral Dissertation, University of St. Andrews, St. Andrews, UK, 1997.
5. Zhang, Y.; Wu, B.; Tan, L.; Liu, J. Information visualization analysis based on historical data. *Multimed. Tools Appl.* **2021**, *81*, 4735–4751. [CrossRef]
6. Tan, L.; Zhou, J.; Zhang, Y.; Liu, J.; Liu, H. Correlation between the Construction of Zhejiang Coastal Military Settlements in the Ming Dynasty and the Natural Terrain. *J. Coast. Res.* **2020**, *106*, 381. [CrossRef]
7. Su, Y. *Study on Coastal Defense in Eastern Zhejiang in Ming Dynasty*; Zhejiang University Press: Hangzhou, China, 2014; pp. 78–85.
8. Yin, Z. Studies on the Coastal Defense Forts System of the Ming Dynasty. Doctoral Dissertation, Tianjin University, Tianjin, China, 2015.
9. Schottenhammer, A. The "China Seas" in world history: A general outline of the role of Chinese and East Asian maritime space from its origins to c. 1800. *J. Mar. Isl. Cult. [Internet]* **2012**, *1*, 63–86. [CrossRef]
10. Wang, C.; Ducruet, C. Regional Resilience and Spatial Cycles: Long-Term Evolution of the Chinese Port System (221bc-2010ad). *Tijdschrift Voor Economische en Sociale Geografie* **2013**, *104*, 521–538. [CrossRef]
11. Cao, Y.; Zhang, Y. Efficient space and resource planning strategies: Treelike fractal traffic networks of the Ming Great Wall Military Defence System. *Ann. GIS* **2018**, *24*, 47–58. [CrossRef]

12. Zhang, Y.; Wu, B.; Tan, L.; Liu, J. Quantitative research on the efficiency of ancient information transmission system: A case study of Wenzhou in the Ming Dynasty. *PLoS ONE* **2021**, *16*, e0250622. [CrossRef] [PubMed]
13. Wheatley, D.; Gillings, M. *Spatial Technology and Archaeology The Archaeological Applications of GIS*; London CRC Press: London, UK, 2013.
14. Wescott, K.L.; Brandon, R.J. *Practical Applications of GIS for Archaeologists*; CRC Press: Boca Raton, FL, USA, 2003.
15. D'Urso, M.G.; Corsi, E.; Nemeti, S.; Germani, M. From excavations to web: A GIS for archaeology. *Int. Arch. Photogramm. Remote Sens. Spat. Inf. Sci.* **2017**, *42*, 219–226. [CrossRef]
16. Cheol, B.S.; Taek, K.H. A Prediction of Long-Term Settlement in Large Reclamated Sites Using Laboratory Consolidation Tests and GIS Techniques. *J. Korean Geoenviron. Soc.* **2006**, *7*, 5–19.
17. Rozenstein, O.; Karnieli, A. Comparison of methods for land-use classification incorporating remote sensing and GIS inputs. *Appl. Geogr.* **2011**, *31*, 533–544. [CrossRef]
18. Du, Y.; Chen, W.; Cui, K.; Guo, Z.; Wu, G.; Ren, X. An exploration of the military defense system of the Ming Great Wall in Qinghai Province from the perspective of castle-based military settlements. *Archaeol. Anthropol. Sci.* **2021**, *13*, 46. [CrossRef]
19. Fan, X.; Wang, Z.; Li, S. Value evaluation model (VEM) of ancient Chinese military settlement heritage: A case study of Liaoxi Corridor in the Ming Dynasty. *Herit. Sci.* **2024**, *12*, 97. [CrossRef]
20. Tan, L.; Liu, H.; Liu, J.; Zhou, J.; Zhao, P.; Zhang, Y.; Zhao, S.; Shen, S.; Li, T.; Wang, Y.; et al. Influence of Environmental Factors on the Site Selection and Layout of Ancient Military Towns (Zhejiang Region). *Sustainability* **2022**, *14*, 2572. [CrossRef]
21. Zhou, J.; Jiang, Y.; Liu, J.; Tan, L.; Meng, L. Evaluation of Chinese traditional military settlements' defensive capabilities via principal component analysis (PCA): A case study of coastal Wei forts in the Ming dynasty. *Herit. Sci.* **2024**, *12*, 100. [CrossRef]
22. Hen, W.; Du, Y.; Cui, K.; Fu, X.; Gong, S. Architectural forms and distribution characteristics of beacon towers of the Ming Great Wall in Qinghai Province. *Asian Archit. Build. Eng.* **2017**, *16*, 503–510. [CrossRef]
23. Du, Y.; Chen, W.; Cui, K.; Zhang, K. Study on Damage Assessment of Earthen Sites of the Ming Great Wall in Qinghai Province Based on Fuzzy-AHP and AHP-TOPSIS. *Int. J. Archit. Herit.* **2019**, *14*, 903–916. [CrossRef]
24. Xu, H.; Chen, F.; Zhou, W. A comparative case study of MTInSAR approaches for deformation monitoring of the cultural landscape of the Shanhaiguan section of the Great Wall. *Herit. Sci.* **2021**, *9*, 71. [CrossRef]
25. Yang, Z. Study on the Defense Efficiency of the Coastal Defense Military Settlements in Ningbo in the Ming Dynasty. Master's Dissertation, Tianjin University, Tianjin, China, 2020.
26. Zhejiang Provincial Government. Zhejiang Provincial Department of Culture Radio Television and Tourism. Available online: https://ct.zj.gov.cn/ (accessed on 9 July 2024).
27. Ningbo Municipal Government. Ningbo Cultural Heritage Protection Website. Available online: https://wglyj.ningbo.gov.cn/index.html (accessed on 9 July 2024).
28. Zhejiang Provincial Government. Zhejiang Provincial Cultural Relics Bureau. Available online: http://wwj.zj.gov.cn/ (accessed on 9 July 2024).
29. Ohta, R. Selection of industrial maintenance strategy: Classical ahp and fuzzy ahp applications. *Int. J. Anal. Hierarchy Process* **2018**, *10*. [CrossRef]
30. Green, J.; Whitton, E. AHP/AHP Pages. *Self Soc.* **1997**, *25*, 51–52. [CrossRef]
31. Ramesh, G. Comparison among Original AHP, Ideal AHP and Moderate AHP Models. *Int. Res. J. Eng. IT Sci. Res.* **2016**, *2*, 40. [CrossRef]
32. Kajita, Y. Proposals of AHP-Type of Disaggregate Logit Model and Improved AHP Model in Modal Choice. *Appl. Mech. Mater.* **2013**, *409–410*, 1166–1172. [CrossRef]
33. Suganthi, L. Multi expert and multi criteria evaluation of sectoral investments for sustainable development: An integrated fuzzy AHP, VIKOR/DEA methodology. *Sustain. Forts Soc.* **2018**, *43*, 144–156. [CrossRef]
34. Sendelj, R.; Ognjanovic, I. Personalized recommendation strategies for elearning: An AHP approach. *Appl. Technol. Innov.* **2014**, *10*, 147–153. [CrossRef]
35. Becker, D.; de Andrés-Herrero, M.; Willmes, C.; Weniger, G.-C.; Bareth, G. Investigating the Influence of Different DEMs on GIS-Based Cost Distance Modeling for Site Catchment Analysis of Prehistoric Sites in Andalusia. *ISPRS Int. J. Geo-Inf.* **2017**, *6*, 36. [CrossRef]
36. Zhang, Y.; Xu, J. *Ningbo Ming-Qing Haifang Yanjiu*; Ningbo Publishing House: Ningbo, China, 2012; pp. 260–275.
37. Cimburova, Z.; Blumentrath, S. Viewshed-based modelling of visual exposure to urban greenery: An efficient GIS tool for practical planning applications. *Landsc. Urban Plan.* **2022**, *222*, 104395. [CrossRef]
38. Khouni, I.; Louhichi, G.; Ghrabi, A. Use of GIS based Inverse Distance Weighted interpolation to assess surface water quality: Case of Wadi El Bey, Tunisia. *Environ. Technol. Innov.* **2021**, *24*, 101892. [CrossRef]

Disclaimer/Publisher's Note: The statements, opinions and data contained in all publications are solely those of the individual author(s) and contributor(s) and not of MDPI and/or the editor(s). MDPI and/or the editor(s) disclaim responsibility for any injury to people or property resulting from any ideas, methods, instructions or products referred to in the content.

buildings

MDPI

Article

Research on the Evolution Characteristics of Building Space in the Central Urban Area of Tianjin Based on Multi-Source Data Collaboration: 2021–2024

Yicheng Zhang [1], Guorui Chen [2] and Xue Yang [3,*]

[1] School of Architecture, Tianjin University, Tianjin 300072, China; urd@tju.edu.cn
[2] College of Architecture and Art, North China University of Technology, Beijing 100144, China; chenguorui@tju.edu.cn
[3] Institute for Urban Regeneration and Development, Tianjin University, Tianjin 300072, China
* Correspondence: yang_xue@tju.edu.cn

Abstract: Urban renewal faces critical challenges in balancing heritage protection and functional upgrades, particularly in dual-attribute cities like Tianjin that preserve industrial legacy while cultivating emerging functions. Existing studies exhibit three gaps: geographical bias toward megacities, fragmented analysis of functional–morphological interactions, and inadequate quantification of "protection-development" tensions. This study addresses these gaps through an integrated framework combining point-of-interest kernel density analysis and satellite imagery segmentation (2021–2024 data). The methodological innovations include: (1) Analysis of urban function changes based on Point of Interest density; (2) Analysis of urban spatial morphology changes based on the texture of buildings within plots; (3) Spatiotemporal coupling analysis of data. Key findings reveal: (a) The overall Point of Interest density in Tianjin increased by 127.2%, achieving further prosperity and development of the city; (b) The renewal of the central urban area exhibits characteristics of "edge aggregation and gradient diffusion"; (c) The historic urban area has reshaped its functional layout through micro-renewal and the relocation of industrial spaces, effectively balancing the conflict between preservation and development. This study systematically summarizes the experiences in resolving the conflict between preservation and development in the urban renewal of Tianjin, providing a reference case for cities undergoing similar dual-attribute renewal.

Keywords: urban renewal; building space; function–form; spatiotemporal evolution; multi-source data

1. Introduction

As a strategic engine for addressing land scarcity, revitalizing aging infrastructure, and reconciling heritage preservation with modern development demands, urban renewal has emerged as a cornerstone of sustainable urbanization in the post-industrial era [1]. China's "14th Five-Year Plan" (2021–2025) [2] elevates urban renewal to a national strategic level, aiming to address multiple challenges such as urbanization transformation, economic quality and efficiency improvement, enhancement of people's well-being, ecological governance, and cultural heritage through systematic solutions. The core of this strategy is to shift the urban development model from "scale expansion" to "connotative development". By optimizing urban spatial structure, improving public service facilities, protecting

historical context, and promoting green and low-carbon development, it seeks to achieve a coordinated enhancement of economic, social, and ecological benefits. This marks a new development stage in China's urbanization process, emphasizing both quality and efficiency [3–5].

By the end of 2024, it will have been four years since the comprehensive implementation of urban renewal initiatives, making it necessary to summarize the experiences and provide a theoretical basis for policy adjustments in the final year of the 14th Five-Year Plan. However, previous urban renewal studies still exhibit deficiencies in the following two aspects:

On the one hand, previous studies have been highly concentrated on the core urban areas of international metropolises such as Beijing, Shanghai, and Shenzhen [6–11], forming a case study paradigm characterized by "high-density built environments". However, there has been insufficient attention to cities like Tianjin, which possess the dual attributes of "historical industrial heritage preservation" and "construction of emerging functional zones". This has resulted in a gap in the explanatory power of theoretical models when addressing the synergistic mechanisms of "incremental renewal" (e.g., the revitalization of the Haihe Economic Belt) and "leapfrog development" (e.g., the construction of the Binhai New Area).

On the other hand, there is data fragmentation: a lack of a collaborative analysis framework for multi-source spatiotemporal data. Although POI (point of interest) data and satellite imagery have been used separately for urban function quantification and morphological analysis, their collaborative application is still in its infancy. In terms of functionality, while POI kernel density analysis [12–14] can depict the spatial clustering characteristics of commercial facilities, it is difficult to reveal the feedback effects of functional mixing on spatial morphology (such as gentrification triggered by excessive commercial expansion in historical districts). In terms of morphology, deep learning-driven interpretation of satellite and aerial imagery [15–17] can precisely identify changes in building textures but has not established dynamic association models with the evolution of POI functions. More critically, existing studies often adopt "static data slices" (such as matching POI and imagery from a single year) [18,19], lacking the capture of the "temporal response chain" in urban renewal processes. For example, although multi-agent models [20–22] can simulate the impact of traffic interventions on resident behavior, they have not integrated POI function evolution data to verify the spatiotemporal effects of business adjustments. Meanwhile, streaming POI-LSTM networks [23–25] achieve dynamic predictions for commercial site selection but do not couple spatial constraints from satellite imagery analysis. This data fragmentation resulted in a "black box" phenomenon [26] in the study of the linkage mechanisms between morphological reconstruction and functional regeneration.

This study aims to address two critical research gaps in dual-attribute cities like Tianjin: (1) How to quantitatively characterize the 'function-form' co-evolution mechanisms under the dual constraints of industrial heritage protection and emerging functional cultivation; and (2) How to integrate multi-source spatiotemporal data (POI and satellite imagery) for dynamic monitoring of urban renewal processes. As the 14th Five-Year Plan enters its final year (2024), this study provides evidence-based indicators to directly support Tianjin's future policy adjustments to optimize the allocation of urban renewal financial resources.

2. Overview of Tianjin's History and Cultural Heritage Protection

2.1. The Historical Context of Urban Development

Tianjin, as an important port city in northern China, has a history of architectural development that can be traced back to the Ming Dynasty's establishment of defenses in 1404.

It has undergone three major phases: the Ming and Qing dynasties' canal transportation hub, the development of concessions in the modern era, and contemporary urbanization, forming a unique urban fabric that blends Chinese and Western styles and merges the ancient with the modern. It is known as the "Museum of World Architecture". In terms of spatial distribution, the old city retains traditional Chinese architectural complexes represented by the Wen Miao (Confucian Temple, originally built in the 1430s) and the Tianhou Temple (originally built in the 1320s), whose wooden framework system and axial layout reflect the regulatory features of northern official architecture (Figure 1). After the port opened in 1860, the nine-nation concession area (which, at its peak, covered more than 15 square kilometers) displayed a distinct Western architectural style, exemplified by buildings such as the HSBC Building (constructed in the 1920s) and the former site of the Astor Hotel (constructed in the 1860s) (Figure 2). Currently, Tianjin has successfully transformed into a modern international port city with the Binhai New Area as its engine, and the skyline of Tianjin is continuously being updated. Modern buildings such as the Tianjin Eye (the only Ferris wheel in the world built on a bridge) and the Jin Tower have become new landmarks of Tianjin (Figure 3).



(**a**) (**b**)

Figure 1. Traditional Chinese architectural representatives: (**a**) Confucian Temple; (**b**) Tianhou Palace.



(**a**) (**b**)

Figure 2. Western-style architectural representatives: (**a**) HSBC Building; (**b**) former site of the Astor Hotel building.

2.2. Cultural Heritage Protection System

The cultural heritage protection system in Tianjin has established a heritage management model that is both systematic and innovative through a multi-level institutional framework and practical approaches. As of 2024, Tianjin has designated 33 National Key Cultural Relics Protection Units and has implemented a three-tiered classification protection

(special, key, and general) for 877 historical buildings, covering the diverse characteristics of architectural heritage. Additionally, through spatial planning integration, 14 historical and cultural districts, including Wudadao and Jiefangbei Road, have been incorporated into a holistic protection framework, while 58 buildings such as the Quanyechang and Guangdong Guild Hall have been selected for the "List of 20th Century Architectural Heritage in China", highlighting their significance in the history of modern architecture. In terms of international heritage certification, the Tianjin section of the Grand Canal (from Sanchakou to Yangliuqing), as a crucial part of the Grand Canal of China, was inscribed on the World Heritage List in 2014. Its heritage elements include hydraulic facilities, dock sites, and historical districts along the route.



(**a**) (**b**)

Figure 3. Contemporary architectural representatives: (**a**) Tianjin Eye; (**b**) Jin Tower.

The architectural history of Tianjin encapsulates China's transition from a traditional agrarian civilization to a modern industrial civilization. Through systematic protection and innovative utilization, Tianjin has maintained its urban characteristic of "coexistence of the ancient and the modern" during the modernization process, providing a model for the historical and cultural inheritance of port cities worldwide.

3. Materials and Methods

In response to the aforementioned issues, this study proposes a dual-dimension analytical framework (Figure 4) for decoding the "function-form" co-evolution mechanism in urban renewal, integrating multi-source spatiotemporal data through three methodological pillars:

- Functional dimension: A diachronic POI density analysis [27] path is constructed using kernel density estimation to quantify the spatial fission (e.g., commercial expansion) and aggregation (e.g., industrial relocation) of urban functions.
- Morphological dimension: Building texture changes are extracted using U-Net (Convolutional Networks for Biomedical Image Segmentation) [28] semantic segmentation, classifying plots into retained, demolished, and newly added types.
- Spatiotemporal coupling: By overlaying changes in POI density with spatial morphological changes, dynamic monitoring of the impact of renewal is achieved. This framework advances previous unidimensional methods by addressing the issue of data fragmentation in urban renewal analysis.

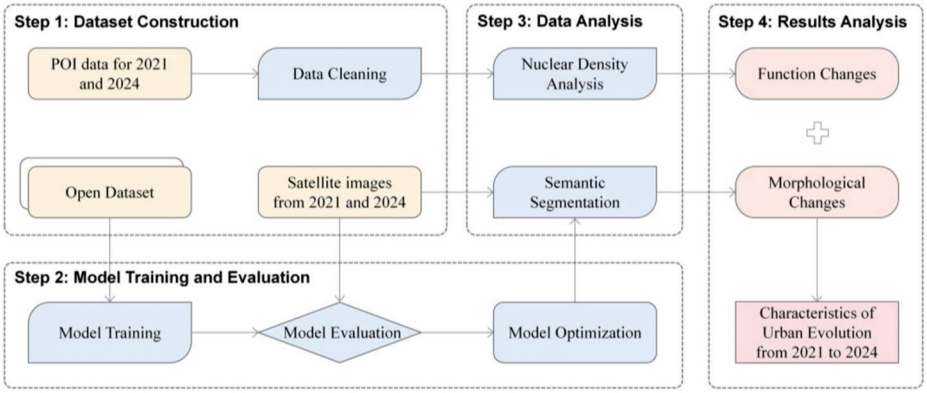


Figure 4. A dual-dimensional analytical framework for urban renewal based on multi-source data collaboration.

3.1. Research Scope and Datasets

3.1.1. Research Area and Phase

Since 2021, Tianjin has actively responded to the national urban renewal strategy by successively introducing the "Implementation Plan for the Renovation and Upgrade of Old Houses and Old Residential Communities and Urban Renewal in Tianjin" [29] and the "Tianjin Urban Renewal Action Plan (2022–2025)" [30]. Relying on the rich historical and cultural resources of the central urban area, Tianjin has successively undertaken representative urban renewal projects such as the Quanyechang Shopping Mall and the Second Workers' Sanatorium, providing important references for renewal practices in other cities across the country.

Choosing Tianjin as the research subject has triple typicality: the parallel regeneration of the Haihe industrial heritage belt and the construction of the Binhai New Area provides a natural laboratory to test the "stock renewal-incremental development" collaborative mechanism [31,32]; the 2021–2024 time-series data cover the main phases of the "14th Five-Year Plan" policy implementation (2021–2024), allowing clear capture of the function–form collaborative evolution path; the gentrification effects in micro-renewals within historic urban areas and the concentrated spatial planning outside these areas reflect the conflict and integration between historical preservation and development.

The study selects the central urban area within the outer ring road of Tianjin as the research scope, based on the following four considerations:

- Typicality: As an important economic center and port city in northern China [33], Tianjin has experienced a rapid urbanization process and has now entered the stock adjustment stage, providing a rich basis of cases and data for urban renewal research.
- Functional Diversity: The central urban area encompasses a variety of functional spaces including residential, commercial, industrial, and public services [34]. The renewal needs of different functional areas vary significantly, making it suitable for multidimensional comparative analysis.
- Data Accessibility: The central urban area boasts abundant and easily accessible POI data and satellite imagery [35], providing reliable data support and enhancing the feasibility and scientific nature of the research.
- Policy Support: Tianjin's policy practices in the field of urban renewal are pioneering and exemplary [29,30], providing a favorable policy environment for the study of the central urban area.

This study focuses on the urban renewal process in the central urban area of Tianjin from 2021 to 2024. The reason is that Tianjin began to fully implement urban renewal in

2021, and the summary of experiences over these four years will help in adjusting the direction of subsequent urban renewal policies, theories, and practices.

3.1.2. Dataset Construction

1. POI Data

POI data, as an important component of geographic information, hold significant value in fields such as urban planning, business analysis, and tourism recommendations. This study obtained POI data for Tianjin through the Amap API, which offers advantages such as rich data, real-time updates, and easy access. Using Python programming (PyCharm Community Edition, Version 2024.3; Python 3.13.2), the study completed steps including coordinate picking, POI data retrieval, format conversion, and coordinate transformation to ensure data accuracy and consistency. To meet the research needs, the POI data were reclassified into 10 subcategories based on functionality (Table 1).

Table 1. Tianjin POI data statistics table.

Category	Quantity		Growth Rate
	2021	**2024**	
urban residential area	11,437	10,864	−5.0%
industrial facilities	5578	4262	−23.6%
commercial facilities	95,611	353,776	270.0%
business facilities	46,605	60,238	29.3%
logistics and warehousing facilities	80	267	233.8%
public service facilities	49,146	70,318	43.1%
utilities	5138	4521	−12.0%
transportation facilities	27,847	42,722	53.4%
green space	173	281	62.4%
square and street space	481	2715	464.4%
total	**242,096**	**549,964**	**127.2%**

2. Satellite Imagery Data

Satellite imagery provides high-resolution information on topography, urban texture, and historical evolution for urban renewal research. There are various satellite remote sensing data products available globally, such as Google Earth, Planet Labs, and Maxar Technologies. Based on the research needs, including high resolution, extensive data coverage, rich historical information, and lower data acquisition costs, this study uses Google Earth historical satellite imagery as the data source. Since Google Earth does not support direct downloading of images for specific areas or selecting resolution levels, this study employs Python to download image tiles from the Google Earth web platform and stitch them together to generate high-resolution satellite imagery of the central urban area of Tianjin for the years 2021 and 2024.

3.2. Model Training and Evaluation

3.2.1. Overview of the Model

U-Net is a convolutional neural network (CNN) architecture widely used for image segmentation tasks, proposed by Ronneberger et al. in 2015 [36]. Inspired by the Fully Convolutional Network (FCN), it adopts a unique U-shaped structure, consisting of a contracting path (encoder) and a symmetric expanding path (decoder). The contracting path captures the contextual information of the image through successive convolutional layers and pooling layers, while the expanding path gradually restores the spatial resolution

of the image through upsampling and convolutional layers. A core feature of U-Net is the "skip connections", which connect feature maps from the encoder with corresponding layers in the decoder, thus preserving more positional information and details during the segmentation process. This architecture enables U-Net to perform exceptionally well when processing images with complex boundaries and details, and it is widely applied in fields such as medical image analysis, architectural structure monitoring, and remote sensing image processing [37].

3.2.2. Training Process

The prediction of buildings is a binary classification problem, where all parts of the dataset, except the target, are labeled as background. The training process included the following steps:

1. Data Processing

Use the os and shutil libraries in Python to clean and format the training and test data, standardizing it into a VOC format dataset.

2. Image Cropping

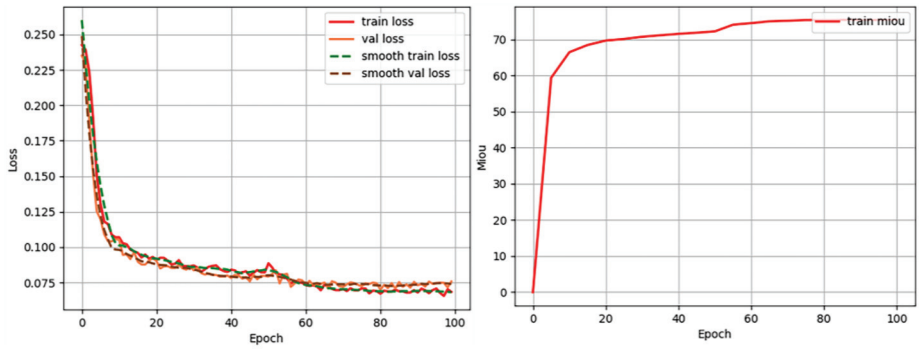
To facilitate model inference, crop large remote sensing images into smaller images of 512 × 512 pixels using the PIL library for cropping operations.

3. Model Training

Train the model based on public datasets to ensure the model's generalization ability.

4. Model Optimization

Use the remote sensing images of Tianjin's central urban area from 2021 and 2024 to test the model. If the prediction accuracy does not meet the requirements, optimize it by changing the dataset or adjusting parameters until the model's performance satisfies the research needs. The final model's mIoU (mean Intersection over Union) reaches 70–80, indicating that the model is well-trained, as shown in Figure 5.



(**a**) (**b**)

Figure 5. Model optimization results: (**a**) The loss curve; (**b**) The mIoU curve.

3.3. Data Analysis

3.3.1. POI Data Analysis

This study utilizes the kernel density analysis tool in ArcGIS 10.8 to systematically analyze POI data in Tianjin, aiming to reveal the characteristics of functional evolution in the central urban area. Kernel density analysis effectively reflects the spatial aggregation degree of different types of points of interest by calculating the distribution density of POIs within a specific region. By setting appropriate search radius and weight parameters,

density maps for various types of POIs are generated, thereby identifying their spatial distribution patterns. By comparing the density distribution of different categories of POIs, a deeper understanding of the macro layout of functional spaces in Tianjin and their impact on urban development can be achieved.

3.3.2. Satellite Imagery Data Analysis

1. Morphological Prediction

Use the optimized U-Net model to perform semantic segmentation on remote sensing images of the central urban area of Tianjin in 2021 and 2024, extracting building contour information.

2. Morphological Comparison

Using the PIL library to compare the building prediction results of 2021 and 2024 on a pixel-by-pixel basis, the changes are categorized into three classes:

- Retained: Building footprints that persist from 2021 to 2024;
- Demolished: Building footprints that disappear from 2021 to 2024;
- Added: Building footprints that are newly added from 2021 to 2024.

3. Image Fusion

Use the PIL library to stitch the cropped smaller images by rows and columns, restoring them to a large image with dimensions consistent with the original image.

4. Data Post-Processing

To optimize the segmentation results considering potential errors caused by factors such as image quality, building shadows, seasonal changes, and the complexity of ground objects, the plots with texture variation (referred to as "updated plots") are categorized into three types based on research needs (Figure 6):

- Texture Change: The existing building footprints within the plots change from 2021 to 2024 but do not completely disappear;
- Texture Disappear: The existing building footprints within the plots completely disappear from 2021 to 2024;
- Texture Appear: New building footprints appear within vacant plots from 2021 to 2024.

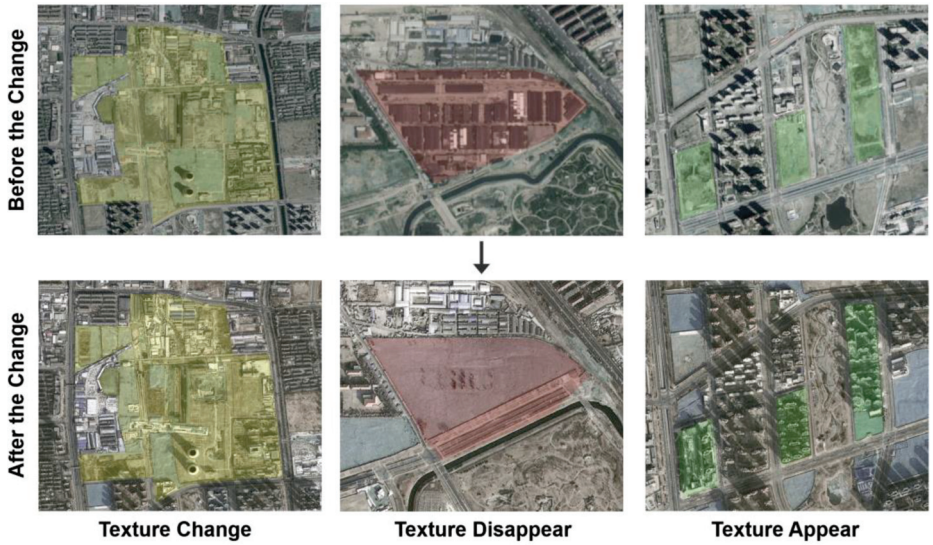


Figure 6. Rules for identifying types of plots involved in urban renewal activities in Tianjin from 2021 to 2024.

4. Results

4.1. Characteristics of Urban Functions Evolution

4.1.1. Characteristics of Spatial Differentiation in Synchrony

Based on the spatial differentiation characteristics of comprehensive kernel density analysis (Figure 7), the POI distribution in Tianjin from 2021 to 2024 exhibits a significant "one core dominance, secondary core support, and multi-point coordination" radiation development model. The overall POI density reaches 799.1 points/km^2, among which:

- The core area (central urban area), as a traditional city center, carries the dual mission of historical and cultural preservation and functional renewal. The POI density gradient shows a characteristic of "dense inside, sparse outside", with commercial facility POIs having the highest proportion and an average density of 529.6 points/km^2 and the core's highest density reaching approximately 2000 points/km^2.
- The secondary core area (Binhai New Area) is primarily driven by industrial functions, forming a "large-scale, cluster-style" renewal model by leveraging the advantages of national-level new area policies. The POI for logistics and warehouse facilities has grown rapidly, with an overall density increase of 226.1% compared to 2021, creating a "mutual nourishment of twin cities" effect with the central urban area.
- The multi-point areas (such as Wuqing and Baodi, which are remote suburban areas) exhibit a "patchy" distribution characteristic, with a significant increase in green space POI density (Δ = 364.6%), reflecting the development philosophy that "lucid waters and lush mountains are invaluable assets".

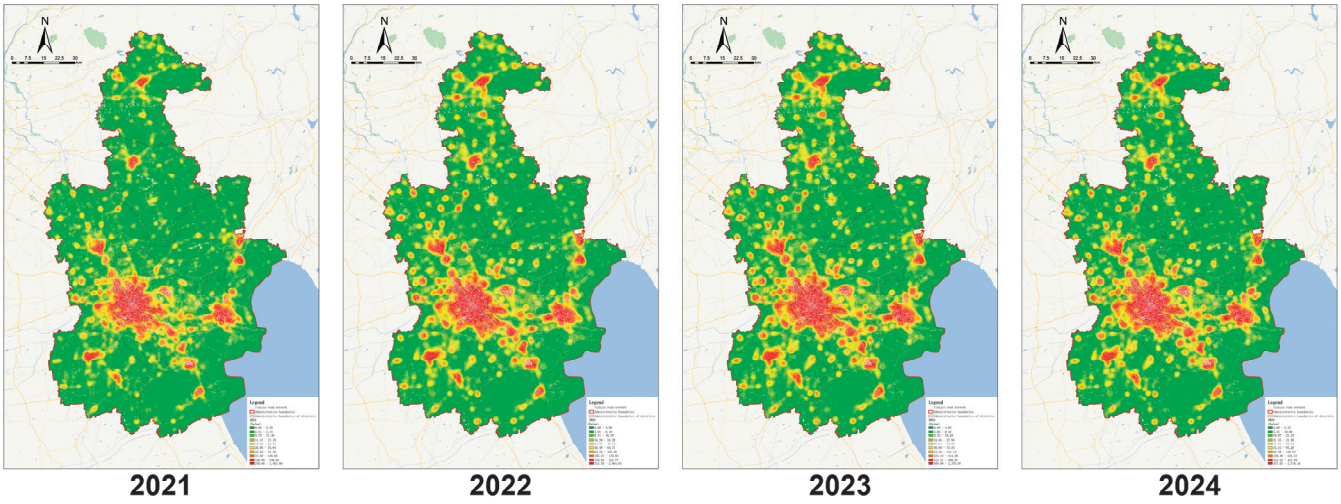


Figure 7. The 2021–2024 Tianjin POI comprehensive kernel density analysis map: The highest density of the main core has increased by 99.7%, and the characteristics of "one core dominance, secondary core support, and multi-point coordination" have become more evident.

4.1.2. Evolutionary Patterns of Temporal Functionality

Between 2021 and 2024, the overall POI density in the central urban area increased by 84.3%. Through the analysis of kernel density of different functional types of POIs (Figure 8), it was found that some functional types showed distinct evolutionary paths:

- Public space fission: The POI density of green space increased by 762.7%, forming a "Haihe Green Corridor + Community Park" nested structure; the POI density of plaza and street space increased by 116.7%, reflecting the Tianjin municipal government's absolute emphasis on environmental protection and the livelihood sector during the "14th Five-Year Plan" period.

- Improvement of public services: Benefiting from the continuous investment of special funds for the renovation of old residential areas, the POI density of public service facilities increased by 15.9% on the basis of 62.6 points/km^2 in 2021, and the POI density of public utilities also increased by 30.9%. The construction effectiveness of "complete communities" was quite significant.
- Industrial space restructuring: Industrial facilities were relocated from the central urban area, resulting in a 44.3% decrease in POI density, while a dual-core cluster formed in the Binhai New Area, and the Xiqing-Wuqing industrial corridor began to take shape. The POI density of commercial facilities increased by 193.3%, with significant growth in both the density and area of core commercial districts. This corroborated the "dual-city multi-node" urban functional spatial pattern established by Tianjin's "14th Five-Year Plan", as well as the land-use planning and control measures guiding industrial relocation and service sector agglomeration.

4.2. Characteristics of Urban Morphology Evolution

In November 2022, the Tianjin Municipal Planning and Natural Resources Bureau announced the "Tianjin Historical and Cultural City Protection Plan (2021–2035)", which clearly delineated the scope of the historical urban area of Tianjin. As a city recognized for its historical and cultural significance in China, the renewal and development of Tianjin's central urban area are influenced by multiple factors, with distinct differences observed inside and outside the historical urban area.

4.2.1. Typological Characteristics of Spatial Texture

The "Tianjin Historical and Cultural City Protection Plan (2021–2035)" [38] delineates the historical district with reference to the built-up area of the city in 1949, covering an area of approximately 54 square kilometers. This district includes the old city, nine foreign concessions, and contemporary business districts, highlighting the more pronounced contradiction between protection and development. This study analyzes the urban fabric from the "inner-outer" dimensions of the historical district (Figure 9):

1. Inside the Historical District

In terms of texture types, traditional hutongs, Western-style blocks, and modern high-rise clusters coexist along the banks of the Haihe River, forming a composite structure of "Haihe Axis + Grid Units". Regarding functional distribution, residential areas (40.8%), public services (30.4%), and commercial areas (14.5%) create a "residential-dominated, service-supported" functional ratio, with industrial land accounting for only 1.4%. Additionally, the historical district retains a large number of historical buildings and cultural sites, which not only enrich the city's cultural heritage but also provide residents with ample cultural activities and leisure spaces. In terms of spatial utilization, the historical district exhibits high density and compactness, with high land use efficiency. Moreover, due to the well-developed transportation network and comprehensive public transportation facilities within the historical district, residents enjoy convenient travel, further promoting the region's economic development and population concentration.

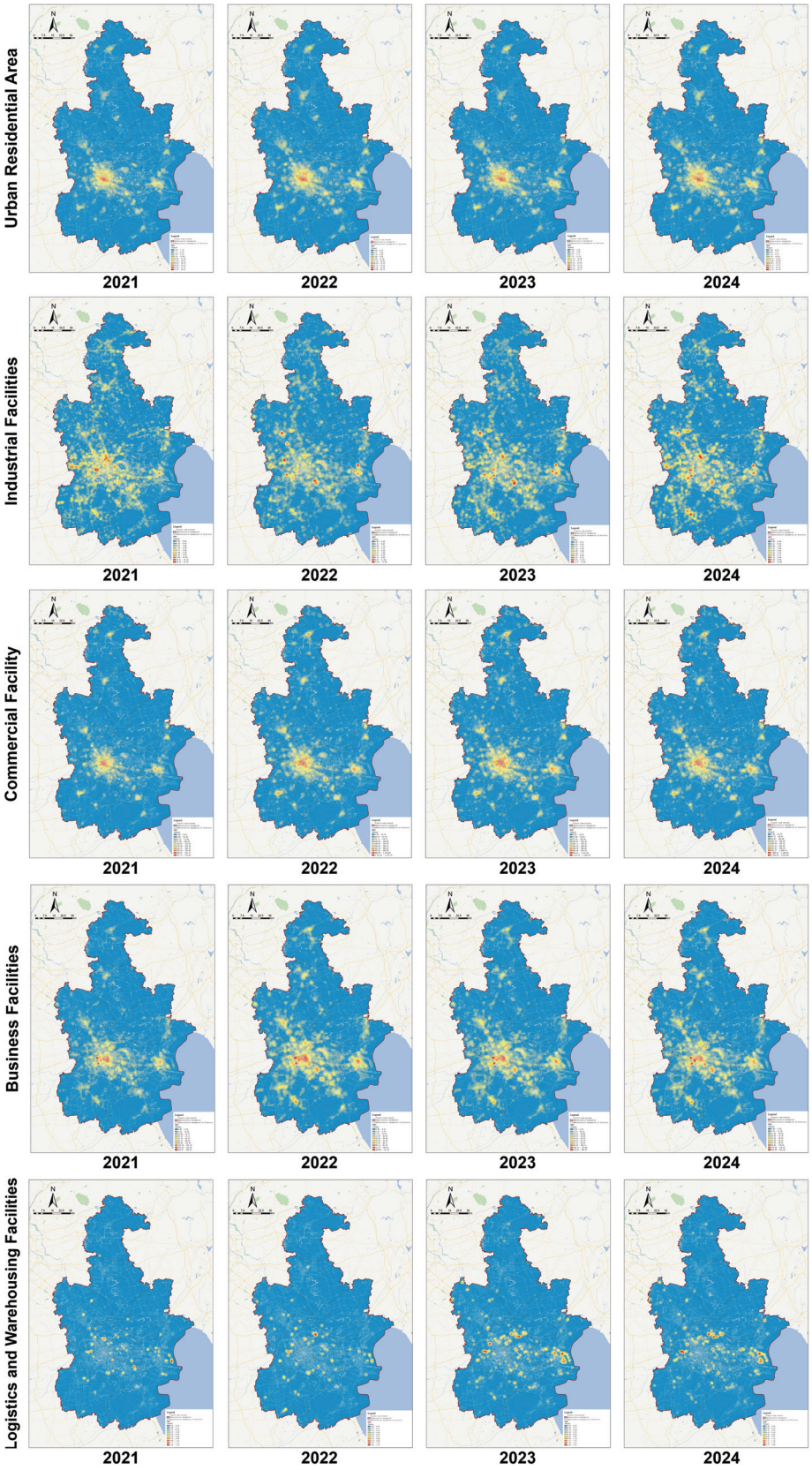


Figure 8. *Cont*.

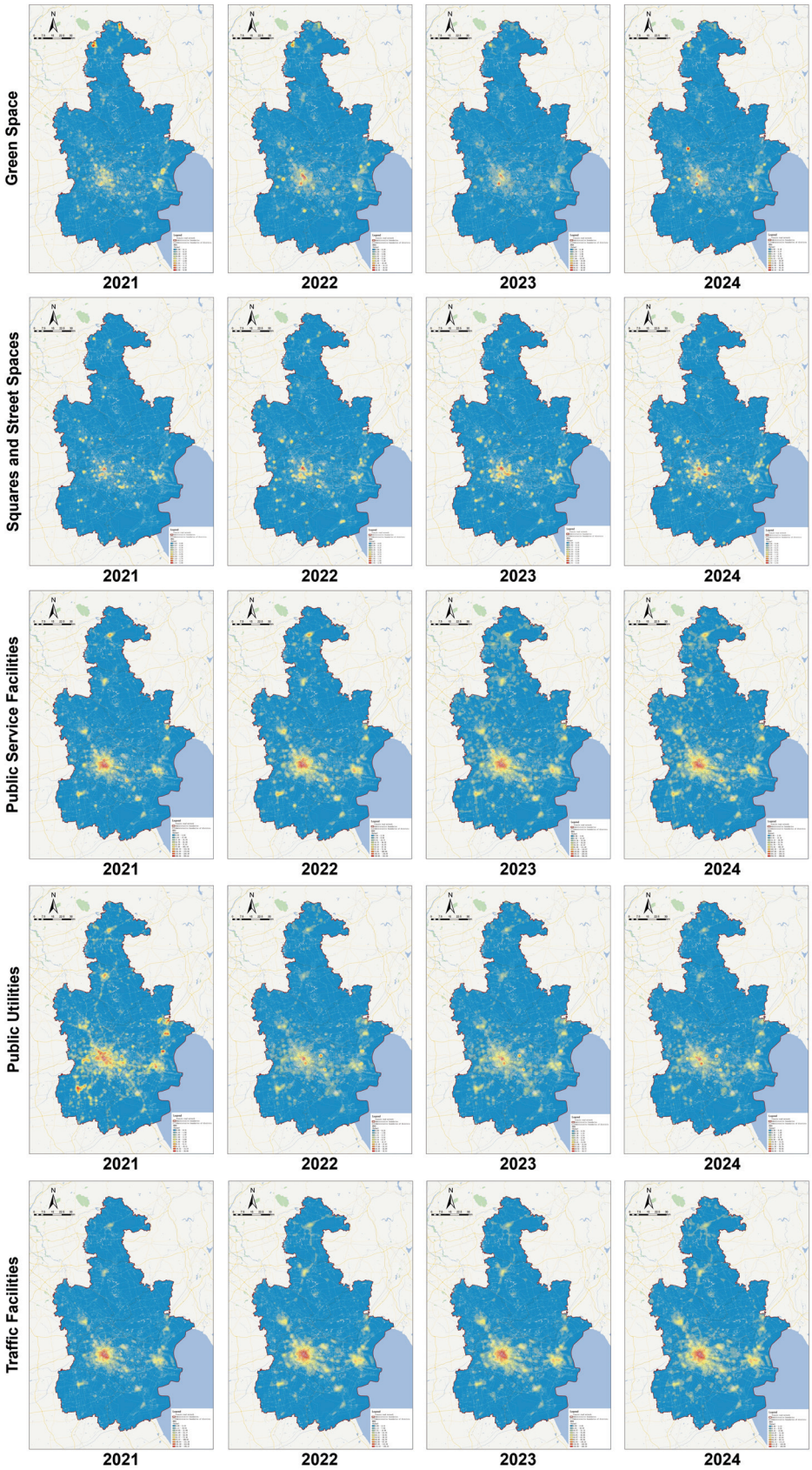
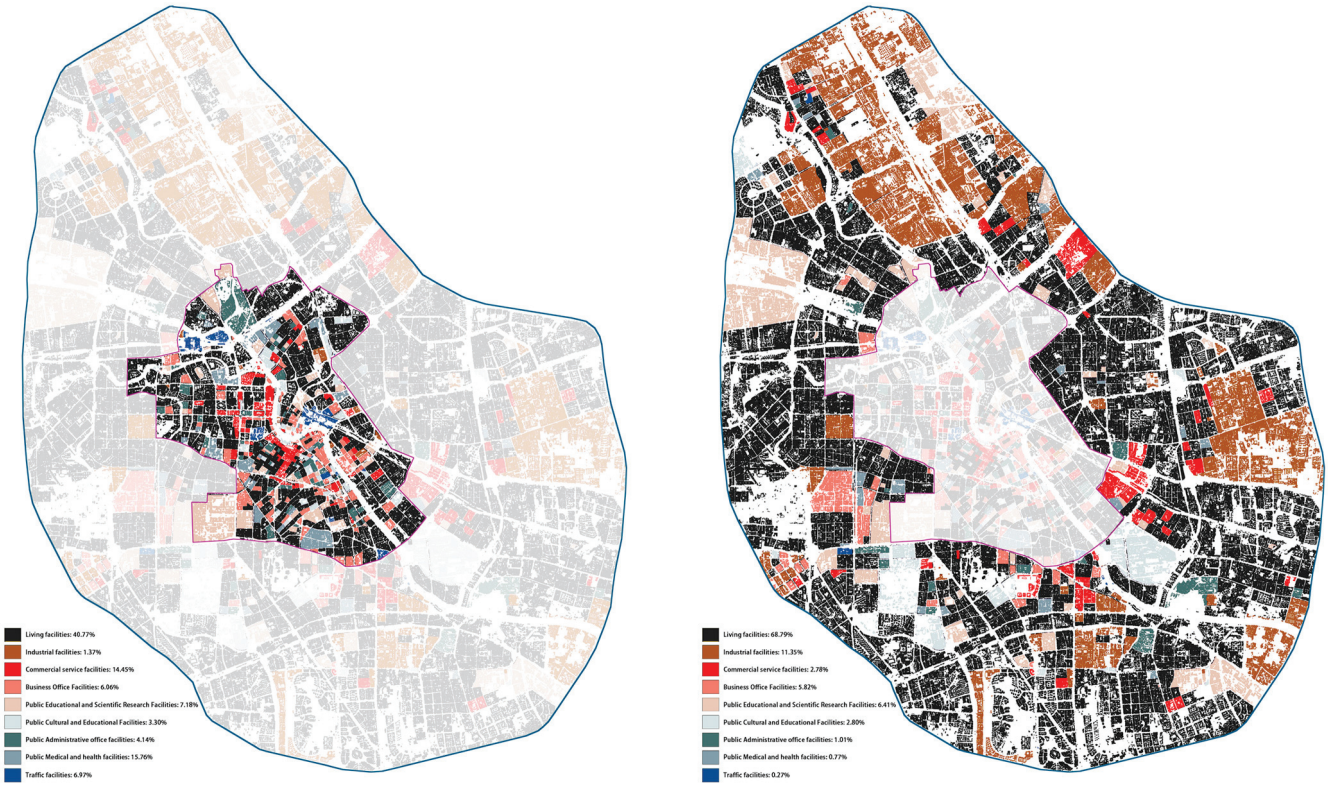


Figure 8. The 2021–2024 Tianjin kernel density analysis map of POIs with different functional types: Shows a clear trend of public space fission, improvement of public services, and industrial space restructuring.



(**a**) (**b**)

Figure 9. Spatial texture and functional zoning of Tianjin central urban area: (**a**) Historical district; (**b**) Outside the historical district.

2. Outside the Historical District

In terms of texture type, a "layered radiation" structure is presented, with residential clusters on the inside and industrial parks on the outside. In terms of functional composition, residential areas (68.8%) and industrial areas (11.4%) dominate, while public service facilities account for 10.9%, reflecting the characteristics of industry–city integration. Additionally, outside the historical district, the texture shows a clear trend towards modernization, with high-rise residential areas and emerging industrial parks gradually rising, bringing new vitality and economic growth points to the city. In the spatial layout, the area outside the historical district exhibits low-density, decentralized characteristics, with relatively flexible land use, which is conducive to urban expansion and renewal. It is noteworthy that the transportation network outside the historical district is also continuously improving, with the construction of highways, subways, and other modern transportation facilities further enhancing the area's convenience and attractiveness. Meanwhile, with the advancement of urbanization, a number of commercial streets and cultural venues with local characteristics have emerged outside the historical district, providing residents with diverse options for consumption and entertainment. These emerging commercial and cultural venues not only enrich the city's cultural connotations but also promote interaction and integration between the historical district and external areas.

4.2.2. Spatiotemporal Differentiation of the Update Process

Through the detection of changes in architectural texture (Figure 10), it was found that the renewal intensity of the central urban area presents a characteristic of "edge aggregation and gradient diffusion":

1. Overall Renewal Characteristics (2021–2024):

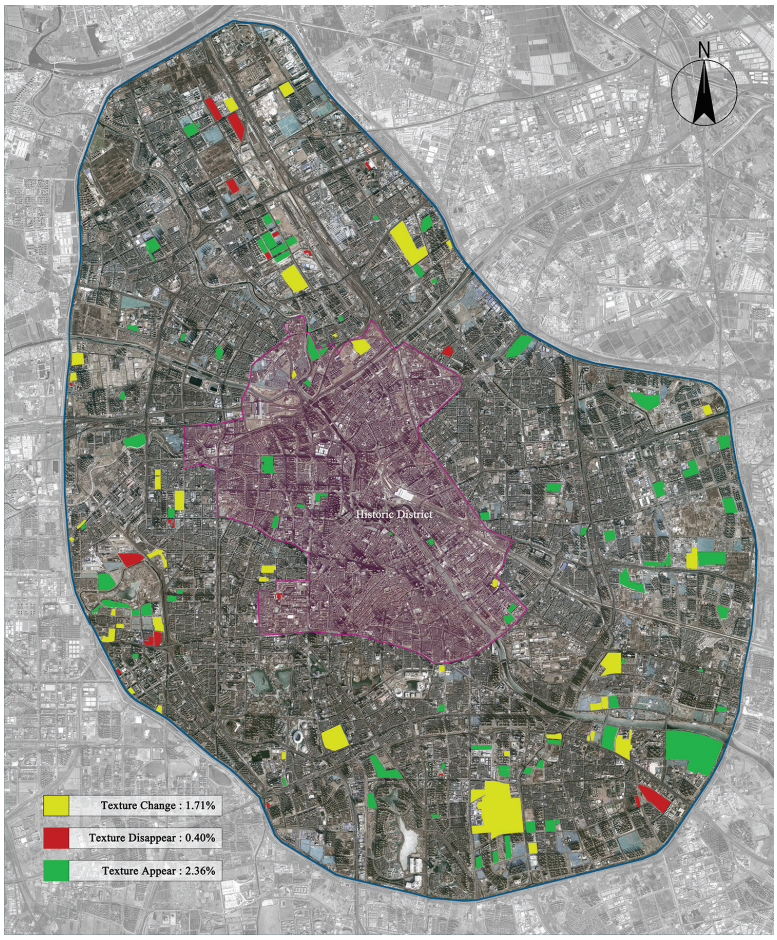


Figure 10. Detection of urban texture changes in Tianjin's central urban area.

The renewal plots in the central urban area account for 4.47% of the total area, mainly concentrated in the edge regions. These edge regions often have significant land development potential and policy support, thus becoming key areas for urban renewal projects. This helps to alleviate spatial pressure within the central urban area while promoting rational urban spatial layout and functional optimization. Among them, renovation-type renewal plots (1.71%) mainly involve the renovation of industrial facilities, public facilities, and public service facilities, aiming to enhance the efficiency of existing infrastructure and promote the optimal allocation and sustainable use of resources. Demolition-type renewal plots (0.40%) mainly target old industrial facilities and shantytowns, reflecting the urban renewal policies of old city renovation and shantytown redevelopment, aiming to improve residents' living environment and enhance the overall image of the city. New construction-type renewal plots (2.36%) involve the addition of residential, commercial, and public service facilities, reflecting the response to new functional demands and the expansion of spatial layout in the process of urban development.

2. Specificity of Historical Urban Area Renewal:

In order to protect historical buildings and cultural heritage, the renewal of historical urban areas is strictly restricted, requiring a balance between preservation and development. Moreover, the historical urban area is primarily positioned for residential, commercial, and public service functions, with renewal projects focusing more on enhancing the efficiency

and quality of existing functions rather than large-scale structural changes. Between 2021 and 2024, renewal plots within the historical urban area accounted for only 1.51%, with the renovation-type mainly involving the activation of inefficient public spaces (0.37%), demolition-type for shantytown redevelopment (0.05%), and new construction-type mainly focusing on public service and transportation facilities (1.09%). Given limited resources, the government may prioritize allocating more renewal resources to the external areas of the central urban area to promote balanced development of the entire city.

4.3. Feature Summary

The evolution of the functions and forms of the central urban area of Tianjin exhibits a complex characteristic of parallel protection and development. Functionally, the core area has established a spatial pattern centered on historical and cultural preservation dominated by modern service functions by relocating industrial facilities and enhancing the concentration of commerce and services. It also builds a "residence-service-ecology" nested system by relying on the fission of public spaces and the improvement of public services. The morphological evolution presents a gradient differentiation characteristic: within the historical city, a composite structure of traditional texture and modern high-rises is maintained, and inefficient spaces are revitalized through micro-updates, with strict restrictions on large-scale development. The external areas promote industrial–urban integration through a concentric expansion model, achieving industrial relocation and a residential–industry cluster layout through concentrated renewal of peripheral areas, forming a coordinated development path of "core conservation-outer expansion". This spatial restructuring not only maintains the spatial genes of a historical and cultural city but also responds to the needs of sustainable urban development through functional replacement and gradient development, providing a valuable experience and reference for the renewal and development of other cities.

5. Discussion

This study, through the integration and analysis of data from multiple sources, successfully reveals the synergistic evolution patterns between function and form in the urban renewal process of Tianjin. The research results indicate that urban renewal is not merely a transformation of physical space but a process of mutual interaction and promotion between function and form. However, despite achieving certain research findings, there is still room for optimization in terms of the breadth and depth of data collection, the accuracy and efficiency of data cleaning, and the precision and applicability of algorithms. These issues may potentially affect the accuracy and reliability of the research results. Therefore, to further enhance the quality and depth of the research, it is necessary to delve into these potential impacts and find corresponding improvement paths. These include, but are not limited to, optimizing data collection methods, increasing the automation and intelligence level of data cleaning, and improving and innovating algorithms to adapt to the complex and ever-changing scenarios of urban renewal.

5.1. The Temporal and Spatial Limitations of Data Collection

In terms of data collection, the resolution of Google Earth imagery (0.5–1 m) makes it difficult to accurately identify small building modifications (such as illegal shacks and temporary structures), resulting in a potential 15–20% miss rate for plots requiring demolition updates. This particularly affects the spatial recognition accuracy of micro-renewal projects in historic urban areas (e.g., renovation projects of less than 50 m^2 within courtyard alleys may not be effectively captured). Moreover, information on the renovation

of building facades, municipal pipelines, and other such details is also difficult to obtain through satellite imagery. Additionally, the POI update cycle for Amap is approximately 3–6 months, leading to a data lag for new facilities (for example, the POI annotation for a new community service center in 2024 may be delayed), and its classification system does not reflect the contribution values of new hybrid functional spaces such as "industrial heritage revitalization" and "shared offices". Improvement directions include integrating drone oblique photography (0.1 m resolution) and nighttime light data (NPP/VIIRS) to build a multi-scale spatial perception system, as well as introducing crowdsourced geographic data (such as consumer review site merchant tags) and planning approval data to construct a multi-source database for urban function perception. Moreover, considering the impact of different seasons and weather conditions on satellite image quality, it is necessary to develop targeted image screening standards to reduce interference with data collection accuracy caused by cloud cover, shadow casting, and other factors. Furthermore, to address the lag in POI data, establishing a real-time data-sharing mechanism with local government planning departments can be considered to ensure the timely inclusion and classification update of new facilities, thereby improving data timeliness and accuracy. These improvement measures are expected to further enhance the spatial recognition accuracy and functional analysis depth of urban renewal projects.

5.2. Challenges of Data Cleaning Complexity

In terms of data cleaning, the U-Net model has a misclassification rate of up to 12.3% for building shadows in high-density urban areas (as shown in Figure 11), with some contiguous shadows being mistakenly identified as demolition-type plots. This leads to a potential overestimation error of 5–8% in the demolition-type update area (0.40%) in central urban areas. Additionally, some POI (point of interest) labels (such as "community convenience store") exhibit functional alienation (actually also serving as parcel collection points, community canteens, etc.), leading to a deviation of up to ± 0.05 in the functional mix index of kernel density analysis, affecting the accuracy of public service facility density assessment. Improvement methods include integrating multi-temporal imagery and LiDAR point cloud data, verifying segmentation results through three-dimensional geometric features, and employing the BERT model to perform semantic parsing on POI names and user reviews, thereby constructing a fine-grained functional label system. Furthermore, in low-density residential and industrial areas at the urban fringe, due to the scattered distribution of buildings and high vegetation coverage, the U-Net model may experience breaks and misalignments in identifying building outlines, resulting in biased estimates of building density and floor area ratio in these areas. To address this issue, super-resolution reconstruction technology from deep learning can be introduced to enhance the detailed features of images, thereby improving the accuracy of building identification. Additionally, combining field surveys and drone aerial data can facilitate manual verification and correction of the model's output to ensure the quality and accuracy of data cleaning.



Figure 11. Example of partial shadow occlusion in satellite images. (Image source: https://earth.google.com (accessed on 2 October 2024)).

Moreover, due to the diversity and complexity of urban renewal projects, the renewal models and functional orientations of different areas vary, posing higher demands on data cleaning. Therefore, during the data cleaning process, it is essential to fully consider the characteristics and needs of urban renewal and develop targeted cleaning strategies and methods to ensure data accuracy and usability. For example, for renewal projects in historical urban areas, emphasis should be placed on the protection and inheritance of architectural styles, as well as the excavation and display of historical culture. In contrast, in emerging industrial clusters, attention should be given to the aggregation and allocation of innovative elements, as well as the construction and optimization of the industrial ecosystem.

5.3. Spatial Heterogeneity of Algorithm Accuracy

In terms of algorithm accuracy, the U-Net model shows a significant performance difference between historical urban areas (mIoU = 78.2%) and industrial parks (mIoU = 65.4%), with the segmentation accuracy for industrial factory sloped roofs being 17.6 percentage points lower than that for residential buildings. This may lead to conclusions about changes in the POI density of industrial facilities in the Binhai New Area being affected by shape misdetection. Additionally, the time reference inconsistency between POI data (updated quarterly) and satellite imagery (updated annually) results in a 3–6-month lag effect in function–morphology correlation analysis, reducing the confidence in causality inference regarding the growth in logistics and warehousing facilities' density and spatial expansion. Improvement directions include introducing the Transformer architecture to enhance feature extraction capabilities, adding prior knowledge of building roof types (such as sloped roof and flat roof classifiers) and constructing a Space-Time Cube model for sliding window matching on a monthly basis. To further reduce the impact of spatial heterogeneity on algorithm accuracy, a multi-scale fusion strategy could be adopted by integrating satellite imagery data of different resolutions to capture multi-level information from local details to the overall layout. Additionally, considering that varying seasonal lighting conditions and environmental changes may affect image quality, exploring seasonal adaptive algorithms that automatically adjust model parameters according to seasonal changes could improve segmentation accuracy across different seasons. Finally, to more comprehensively evaluate the algorithm's performance, more evaluation metrics such as Precision, Recall, and F1 Score could be introduced to comprehensively assess the model's performance in different scenarios.

6. Conclusions

This study employs an analytical approach that combines POI data with satellite imagery to deeply explore and reveal the spatiotemporal patterns of the collaborative evolution of functionality and form in the central urban area of Tianjin:

- In terms of functionality, this study finds that the concentration of commercial activities and the dispersed reorganization of industrial activities have reshaped the urban spatial structure, forming a new pattern of "dual-city with multiple nodes". At the same time, the fission of public spaces and the improvement in infrastructure quality have strongly supported the construction of "complete communities".
- In terms of form, this study points out the gradient differences between the concentrated renewal of peripheral areas and the micro-renewal of historical urban areas, reflecting the sustainable development path the city has taken in "core conservation and peripheral expansion".
- Methodologically, this study combines POI kernel density analysis with U-Net architectural texture detection technology to build an integrated framework, providing a new technical paradigm for dynamic monitoring of urban renewal.

Nevertheless, this study also highlights the limitations of the current data resolution and the inadequacies of algorithms in addressing spatial heterogeneity, issues that require further optimization through the integration of multi-source data. Looking forward, the research can be further expanded to assess the functional mix of industrial heritage and simulate renewal policies, aiming to provide more systematic and comprehensive decision support for high-quality urban development. Additionally, there is a need for ongoing collaboration between researchers, policymakers, and stakeholders to ensure that the insights gained from this study are effectively translated into actionable strategies. By fostering interdisciplinary dialogue, we can better understand the complex interplay between industrial heritage, urban renewal, and sustainable development.

Author Contributions: Conceptualization, Y.Z. and X.Y.; methodology, G.C.; software, Y.Z.; validation, Y.Z. and X.Y.; formal analysis, G.C.; investigation, Y.Z.; resources, X.Y.; data curation, Y.Z.; writing—original draft preparation, Y.Z.; writing—review and editing, Y.Z.; visualization, G.C.; supervision, X.Y.; project administration, X.Y.; funding acquisition, X.Y. All authors have read and agreed to the published version of the manuscript.

Funding: This research was funded by the 14th Five-Year National Key Research and Development Program of the Ministry of Science and Technology of the People's Republic of China, "Construction of Urban Renewal Typology and Renewal Methods for Typical Types" (2022YFC3800303).

Data Availability Statement: The datasets presented in this article are not readily available because the data are part of an ongoing study.

Acknowledgments: In addition, the authors would like to thank Kun Song for his guidance on the research direction and Wanqi Jing and Zehao Liu for their assistance with the specific work.

Conflicts of Interest: The authors declare no conflicts of interest. The funders had no role in the design of the study; in the collection, analyses, or interpretation of data; in the writing of the manuscript; or in the decision to publish the results.

References

1. Bi, C.; Little, J.C. Integrated assessment across building and urban scales: A review and proposal for a more holistic, multi-scale, system-of-systems approach. *Sustain. Cities Soc.* **2022**, *82*, 103915. [CrossRef]

2. Outline of the 14th Five-Year Plan for National Economic and Social Development of the People's Republic of China and the Long-Range Objectives Through the Year 2035. Available online: https://www.gov.cn/xinwen/2021-03/13/content_5592681.htm (accessed on 20 March 2025).
3. Zhang, J.; Wang, G.; Xiong, L. Using a Data Mining Method to Explore Strategies for Improving the Social Interaction Environment Quality of Urban Neighborhood Open Spaces. *Architecture* **2023**, *3*, 128–136. [CrossRef]
4. Sun, J.; Li, H.; Xiao, R.; Yao, G.; Zou, F. Dynamics of Heat Island Intensity in a Rapidly Urbanizing Area and the Cooling Effect of Ecological Land: A Case Study in Suzhou, Yangtze River Delta. *Sustainability* **2024**, *16*, 4422. [CrossRef]
5. Ouyang, Y.; Bai, X.; Wang, X.; Chen, Y.; Huang, G.; Xie, D. Case Study on Cultural Industry Empowerment in Urban Renewal: A Focus on Guangzhou, China. *Sustainability* **2025**, *17*, 439. [CrossRef]
6. Li, Q.; Lv, S.; Cui, J.; Zhang, J.; Liu, Y. Environmental Perception about Pedestrian Environment on Cultural Visitation Roads. *Sustainability* **2024**, *16*, 7097. [CrossRef]
7. Zhang, Z.; Sun, Q. Integrated Design Methods for Sustainable Public Seating in Urban Communities—A Shanghai Case Study. *Sustainability* **2024**, *16*, 9096. [CrossRef]
8. Zhang, P.; Zhang, T.; Fukuda, H.; Ma, M. Evidence of Multi-Source Data Fusion on the Relationship between the Specific Urban Built Environment and Urban Vitality in Shenzhen. *Sustainability* **2023**, *15*, 6869. [CrossRef]
9. Zhang, W.; Xin, J. Green Spaces and the Spontaneous Renewal of Historic Neighborhoods: A Case Study of Beijing's Dashilar Community. *Sustainability* **2023**, *15*, 16566. [CrossRef]
10. Jiang, C.; Huang, R.; Huang, S.; Shen, T. Unveiling Sustainable Co-Creation Patterns in Entrepreneurial Ecosystems of Shanghai's High-Density Urban Communities. *Sustainability* **2024**, *16*, 10642. [CrossRef]
11. Lee, C.-C.; Wang, Y.; Tang, C.; Li, X.; Yin, J. A Visual Preference Analysis of Building Façades in Street View Images: A Case Study of Nanshan District, Shenzhen. *Buildings* **2025**, *15*, 611. [CrossRef]
12. Šoltésová, M.; Iannaccone, B.; Štrba, Ľ.; Sidor, C. Application of GIS Technologies in Tourism Planning and Sustainable Development: A Case Study of Gelnica. *ISPRS Int. J. Geo-Inf.* **2025**, *14*, 120. [CrossRef]
13. Yao, C.; Li, G.; Yan, S. Design Strategies to Improve Metro Transit Station Walking Environments: Five Stations in Chongqing, China. *Buildings* **2024**, *14*, 1025. [CrossRef]
14. Guo, X.; Cui, X. GIS-Based Study on the Suitability of Site Selection for Community Complexes in Old Residential Areas in Xi'an, China. *Buildings* **2025**, *15*, 551. [CrossRef]
15. Agustiyara, A.; Mutiarin, D.; Nurmandi, A.; Kasiwi, A.N.; Ikhwali, M.F. Mapping Urban Green Spaces in Indonesian Cities Using Remote Sensing Analysis. *Urban Sci.* **2025**, *9*, 23. [CrossRef]
16. Zhang, W.; Yu, M.; Chen, X.; Zhou, F.; Ren, J.; Xu, H.; Xu, S. Combining Deep Fully Convolutional Network and Graph Convolutional Neural Network for the Extraction of Buildings from Aerial Images. *Buildings* **2022**, *12*, 2233. [CrossRef]
17. Fu, X.; Wu, M.; Ponnarasu, S.; Zhang, L. A Hybrid Deep Learning Approach for Real-Time Estimation of Passenger Traffic Flow in Urban Railway Systems. *Buildings* **2023**, *13*, 1514. [CrossRef]
18. Li, J.; Chen, Y.; Zhao, D.; Zhai, J. The Impact of Built Environment on Mixed Land Use: Evidence from Xi'an. *Land* **2024**, *13*, 2214. [CrossRef]
19. Zhu, D.; Dang, X.; Shi, W.; Chen, Y.; Li, W. Urban Functional Zone Mapping by Integrating Multi-Source Data and Spatial Relationship Characteristics. *Proceedings* **2024**, *110*, 17. [CrossRef]
20. Pan, L.; Yang, N.; Zhang, L.; Zhang, R.; Xie, B.; Yan, H. Assessment of the Impact of Multi-Agent Model-Based Traffic Optimization Interventions on Urban Travel Behavior. *Electronics* **2025**, *14*, 13. [CrossRef]
21. Kalyuzhnaya, A.; Mityagin, S.; Lutsenko, E.; Getmanov, A.; Aksenkin, Y.; Fatkhiev, K.; Fedorin, K.; Nikitin, N.O.; Chichkova, N.; Vorona, V.; et al. LLM Agents for Smart City Management: Enhancing Decision Support Through Multi-Agent AI Systems. *Smart Cities* **2025**, *8*, 19. [CrossRef]
22. Liang, Z.; Várady, G.; Zagorácz, M.B. Sustainable Application of Automatically Generated Multi-Agent System Model in Urban Renewal. *Sustainability* **2023**, *15*, 7308. [CrossRef]
23. Zou, J.; Zhang, X.; Cong, Y.; Gao, Z.; Shi, J. Research and Modeling of Commercial Location Selection Based on Geographic Big Data and Mobile Signaling Data—A Case Study of the Central Urban Area of Beijing. *ISPRS Int. J. Geo-Inf.* **2024**, *13*, 432. [CrossRef]
24. Li, Y.; Huang, Y.; Liu, Z.; Zhang, B. A Distributed Scheme for the Taxi Cruising Route Recommendation Problem Using a Graph Neural Network. *Electronics* **2024**, *13*, 574. [CrossRef]
25. Chen, J.; Feng, Q.; Fan, D. Vehicle Trajectory Prediction Based on Local Dynamic Graph Spatiotemporal–Long Short-Term Memory Model. *World Electr. Veh. J.* **2024**, *15*, 28. [CrossRef]
26. Roodenrijs, J.C.M.; Hegger, D.L.T.; Mees, H.L.P.; Driessen, P. Opening up the Black Box of Group Decision-Making on Solar Energy: The Case of Strata Buildings in Amsterdam, the Netherlands. *Sustainability* **2020**, *12*, 2097. [CrossRef]

27. Zhang, T.; Zhu, X.; Liu, Y.; Jia, C.; Bai, H. Research on the Spatial Structure of the Beijing–Tianjin–Hebei Urban Agglomeration Based on POI and Impervious Surface Coverage. *Buildings* **2024**, *14*, 1793. [CrossRef]
28. Tyvoniuk, V.; Trach, R.; Trach, Y. Integration of Probability Maps into Machine Learning Models for Enhanced Crack Segmentation in Concrete Bridges. *Appl. Sci.* **2025**, *15*, 3201. [CrossRef]
29. Notice from the General Office of the Tianjin Municipal People's Government on Issuing the Implementation Plan for the Renovation and Upgrade of Old Residential Buildings and Neighborhoods and Urban Renewal in Tianjin. Available online: https://www.tj.gov.cn/zwgk/szfwj/tjsrmzfbgt/202106/t20210624_5486108.html (accessed on 20 March 2025).
30. "Tianjin City Renewal Action Plan (2022–2025)" Open for Public Comments. Available online: https://www.tj.gov.cn/zmhd/dczj/ptwz/202206/t20220609_5900229.html (accessed on 20 March 2025).
31. Fang, Y.-N.; Zeng, J.; Namaiti, A. Landscape Visual Sensitivity Assessment of Historic Districts—A Case Study of Wudadao Historic District in Tianjin, China. *ISPRS Int. J. Geo-Inf.* **2021**, *10*, 175. [CrossRef]
32. Wang, Q.; Sun, X.; Wang, R.; Zhou, L.; Zhou, H.; Di, Y.; Li, Y.; Zhang, Q. Research on Urban Energy Sustainable Plan under the Background of Low-Carbon Development. *Sustainability* **2023**, *15*, 14206. [CrossRef]
33. Qu, T.; Zhang, L.; Wu, Z. City Spatial Structure Evolution Affected by Special Events in Different Historical Periods: A Case Study of Tianjin. *Sci. Geogr. Sin.* **2014**, *34*, 656.
34. Liu, W.; Yan, J.; Sun, X.; Song, R. Research on "Identification–Cognition–Perception" of the Pedestrian Spaces Around Subway Stations near Popular Tourist Attractions from the Tourists' Perspective: A Case Study of Tianjin. *Land* **2025**, *14*, 145. [CrossRef]
35. Zhang, D.; Song, K.; Zhao, D. Leveraging Multi-Source Data for the Trustworthy Evaluation of the Vibrancy of Child-Friendly Cities: A Case Study of Tianjin, China. *Electronics* **2024**, *13*, 4564. [CrossRef]
36. Ronneberger, O.; Fischer, P.; Brox, T. U-Net: Convolutional Networks for Biomedical Image Segmentation. In Proceedings of the 2015 Medical Image Computing and Computer-Assisted Intervention, Munich, Germany, 5–9 October 2015.
37. Dong, X.; Liu, Y.; Dai, J. Recognition of Concrete Surface Cracks Based on Improved TransUNet. *Buildings* **2025**, *15*, 541. [CrossRef]
38. Draft of the Protection Plan for the Historical and Cultural City of Tianjin (2021–2035) Public Notice. Available online: https://ghhzrzy.tj.gov.cn/ywpd/cxgh_43015/ghgs/202211/t20221102_6024105.html (accessed on 20 March 2025).

Disclaimer/Publisher's Note: The statements, opinions and data contained in all publications are solely those of the individual author(s) and contributor(s) and not of MDPI and/or the editor(s). MDPI and/or the editor(s) disclaim responsibility for any injury to people or property resulting from any ideas, methods, instructions or products referred to in the content.

buildings

MDPI

Article

Spatiotemporal Dynamics and Driving Factors of Urban Green Space in Texas (2001–2021): A Multi-Source Geospatial Analysis

Tengfei Ma [1,†], Huakai Ye [1,†], Yujing Lai [1,2], Haoying Han [1], Yangguang Song [1] and Yile Chen [3,*]

[1] Faculty of Innovation and Design, City University of Macau, Avenida Padre Tomás Pereira, Taipa, Macau 999078, China; u23092120302@cityu.edu.mo (T.M.); u23091120171@cityu.edu.mo (H.Y.); u23092120433@cityu.edu.mo (Y.L.); hanhaoying@gmail.com (H.H.); u23091120642@cityu.edu.mo (Y.S.)
[2] Department of Architecture and Urban Planning, Shandong Urban Construction Vocational College, Jinan 250014, China
[3] Faculty of Humanities and Arts, Macau University of Science and Technology, Avenida Wai Long, Tapai, Macau 999078, China
* Correspondence: chenyile@must.edu.mo
† These authors contributed equally to this work.

Abstract: This study investigates the changes in urban green space coverage across 254 counties of varying types in Texas from 2001 to 2021, aiming to explore the spatial patterns of green space transformation and its socioeconomic driving factors. By analyzing Landsat remote sensing data and building type datasets, combined with land use transition matrices, GIS spatial statistics tools, and regression analysis of population and GDP data, this study comprehensively examines the green space change patterns of different urban types. The results indicated significant differences in green space changes across different types of cities: (1) Urban areas with higher populations and rankings, as well as their surrounding regions, show a more pronounced trend of green space converting into built-up urban areas, particularly the expansion of medium and low-density areas. (2) In contrast, green space changes in smaller cities and rural areas occur at a slower pace. Further analysis reveals that the transformation of green spaces is primarily driven by residential land development, with about 39% of green space in high-density urban areas and over 65% in medium and low-density areas being replaced by residential land. (3) The regression analysis results indicate that population growth and GDP growth are the main driving factors for green space changes, explaining up to 86% and 84% of the green space changes, respectively. These findings provide important theoretical support and practical guidelines for urban green space conservation, planning, and sustainable development policies.

Keywords: urban green space; spatiotemporal evolution; influencing factors; GIS spatial statistics; regression analysis

1. Introduction

Urban green space typically refers to open and undeveloped land within urban areas that contains green vegetation, such as parks, gardens, street plants, lawns, green roofs, and forests [1]. It can also be defined as urban land fully covered by living green vegetation, including areas like woodlands, grasslands, and shrublands [2,3]. Urban green space is considered one of the most important elements of people's living environments. With the ongoing process of urbanization, changes in the quantity and quality of urban green

spaces have attracted widespread attention in recent years [4–6]. Urban green spaces are not only vital sources of ecosystem services, such as air purification, climate regulation, and biodiversity conservation, but also play a crucial role in improving living environments, providing spaces for recreation and psychological health support, and enhancing residents' overall well-being [7]. Changes in urban green spaces have profound impacts on the health of urban ecosystems and the quality of residents' lives, directly reflecting shifts in land use. The primary characteristics of these changes include the replacement of green spaces with buildings and impermeable surfaces such as roads and parking lots [8], alterations in ecological functions such as mitigating the urban heat island effect and improving air quality [9], and socioeconomic inequalities emerging over time in the spatial distribution of green spaces [10].

As one of the largest states in the U.S. by land area, Texas has experienced significant population and economic growth over the past two decades, with strong urban expansion dynamics. Its 254 counties exhibit substantial variation in urban classification, economic structure, and natural conditions, making it an ideal case region for observing changes in green space coverage and their main influencing factors [11]. In the state, reports of green space being overtaken by urban land often trigger public concern about ecological environment and quality of life, while government agencies continuously explore legislative and planning strategies to balance development and conservation. This context underscores the necessity and urgency of studying the occupation and transformation of green spaces in Texas.

The launch of the Landsat satellite series has provided researchers with abundant data sources, enabling systematic monitoring of land cover changes [12]. In recent years, machine learning and deep learning methods have been employed for the automated processing of Land Use/Land Cover data (LULC), significantly improving the accuracy and efficiency of land use classification [13]. Based on satellite remote sensing imagery (such as Landsat), the Normalized Difference Vegetation Index (NDVI), and land use/cover data, scholars have described the spatiotemporal patterns of urban green space changes at a macro level, exploring their relationships with socioeconomic, policy, and environmental variables [14–16]. For example, Heo et al. examined the link between green space coverage and population health indicators, noting that increased green space significantly improved the physical and mental health of residents [7]. Xing et al. analyzed the imbalance between the supply and demand of green spaces across 102 cities in Hunan Province, China, and applied spatial regression models to assess the impact of economic development on green space distribution [17]. Kitch through a long-term data analysis of 260 U.S. cities, found that high-density built-up areas often face severe green space shortages and emphasized the negative health impacts of green space deficiency on low-income populations [18]. Additionally, Chen revealed significant disparities in accessibility to outdoor green spaces among urban populations in the Global South and North by utilizing high-resolution population distribution and green space data [14]. In the field of environmental and social equity research, an increasing number of studies have focused on the impact of green space on social equity [6,14]. Some scholars point out that the equitable distribution of green space is not only related to environmental protection but also directly influences the quality-of-life differences between social classes [19]. Methodologically, recent studies on urban green space changes and their driving factors have widely utilized remote sensing data analysis, land use modeling, spatial statistical techniques, and regression analysis. For example, Seto et al. employed MODIS imagery to study global urban expansion, emphasizing the extensive impacts of urban growth on ecosystems [20]. Zhu et al. using Landsat data combined with NDVI indices, analyzed green space changes in Guangzhou,

China, highlighting uneven distributions of urban green spaces [21]. Additionally, Schinasi et al. applied spatial regression models to explore the influence of socioeconomic variables on green space reduction [22], while Ducey et al. utilized regression analysis to assess the role of population density and GDP on green space dynamics [23]. However, these studies still face certain methodological limitations. Firstly, most research has concentrated on large cities or metropolitan areas [20], lacking systematic comparative analyses across cities of varying sizes. Secondly, quantitative assessments of socioeconomic drivers remain relatively limited, with some studies primarily relying on descriptive analyses [22]. Furthermore, the impacts of medium and low-density urban expansion on green spaces have not been fully explored; many studies mainly focus on high-density urban core areas, neglecting the long-term effects of suburban and low-density expansions on green space [21].

However, existing studies have mainly focused on the "overall change in green space" or "the impact of green space on health and equity", with less emphasis on the "differentiated processes and uses of green space when it is transformed into various density urban built-up areas". This research gap somewhat limits our understanding of the mechanisms behind green space transformation, especially since the process and reasons for green space conversion may vary significantly in different types of urban built-up areas [6]. Especially in regions like Texas, which have a vast geographical area and highly heterogeneous internal structures, existing research has mainly focused on macro-level analyses, lacking classification and quantitative analyses of the green space transformation process at the micro level [24,25]. Exploring the relationship between green space occupation and socioeconomic factors, particularly the spatial differences among different urban types, remains a research direction worth investigating. Recent studies have made significant progress in analyzing urban green space changes. For example, Wang et al. used machine learning methods to predict green space changes in the Tokyo metropolitan area, significantly improving the accuracy of data analysis [26]. Haaland and van den Bosch, in their research on European cities, emphasized the importance of green space conservation policies, highlighting the key role of government interventions in mitigating green space conversion [27]. However, these studies still have limitations. For instance, machine learning methods generally exhibit lower interpretability when explaining socioeconomic driving factors [26], and policy-oriented research often lacks specific spatial data support [27].

However, in large-scale rapidly urbanizing areas, there has been a lack of systematic quantitative research on how green spaces are encroached upon by different density urban land uses and the underlying mechanisms involved. Based on the aforementioned research background and literature review, the following key questions can be summarized:

(1) How does urban expansion affect green space resources in terms of spatial differentiation and use transformation across large geographical regions?
(2) Do different types of cities exhibit consistent spatiotemporal distribution patterns when green spaces are replaced by low, medium, or high-density urban areas?
(3) What are the differences in the driving effects of socioeconomic factors (such as population, GDP) and policy orientation on green space occupation and changes across the 254 counties of Texas?

To achieve the stated objectives, this study integrates multi-source data (Landsat remote sensing, building typology, and land use transition matrices) and GIS-based spatial statistical methods. Regression analysis quantifies the contributions of population and GDP growth to green space changes, bridging research gaps across different city types. Additionally, this research focuses not only on large cities but also includes medium-sized, small, and rural areas, aiming to provide tailored policy recommendations for green

space planning and protection that align with diverse urban contexts, thereby fostering sustainable urban development.

2. Materials and Methods

2.1. Study Area: Texas in the Directly Reflecting Shifts in Land Use U.S.

Texas is located in the south-central United States, bordering Louisiana to the east, Arkansas to the northeast, Oklahoma to the north, and New Mexico to the west. It also shares borders with the Mexican states of Chihuahua, Coahuila, Nuevo León, and Tamaulipas and has a Gulf of Mexico coastline in the southeast (Figure 1). The region selected for this study is the entire state of Texas, with the administrative boundaries of its 254 counties serving as the analysis units.

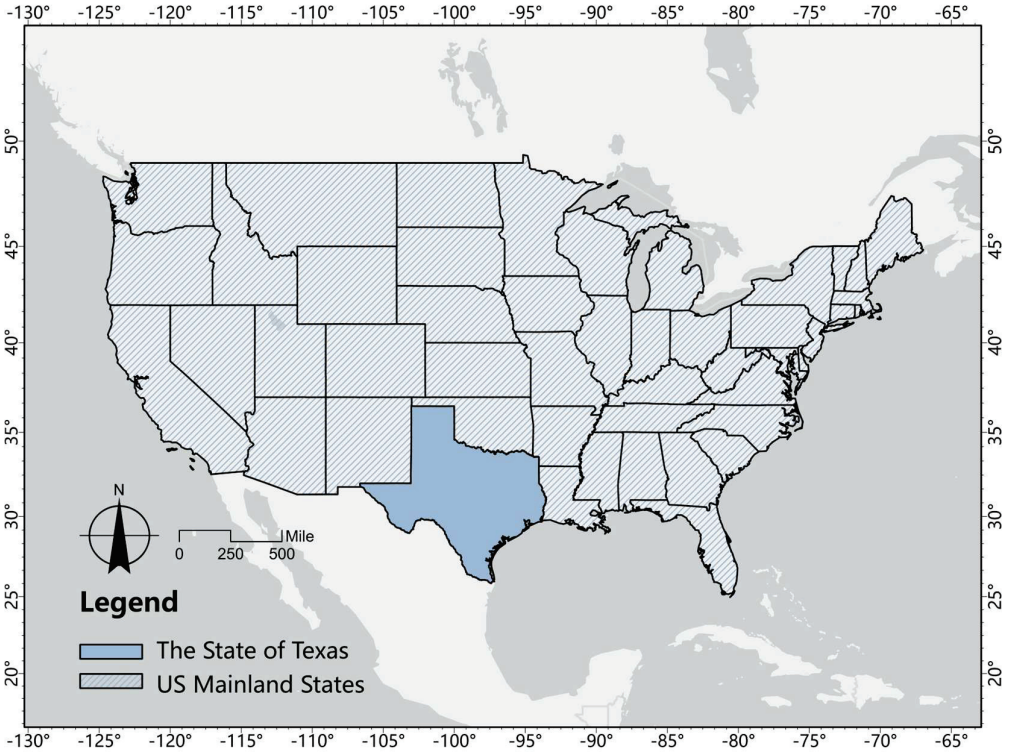


Figure 1. Regional map of Texas (Base on WGS 1984).

Texas is geographically diverse, with climates ranging from humid subtropical in the east to semi-arid and arid regions in the west. Annual precipitation decreases from over 1200 mm in the east to below 500 mm in the west, while vegetation coverage transitions from dense forests to savannas and desert shrublands [28]. Annual average temperatures range from approximately 10 °C in the north to 27 °C in the south, with summer temperatures exceeding 40 °C in some areas. Extreme weather events, such as droughts, heat waves, and hurricanes, pose challenges to green space changes and urban expansion [3].

As one of the fastest-growing regions in the United States, Texas has experienced nearly 43% population growth since 2000, with an increase of approximately 470,000 residents in 2022 alone [29]. This rapid population growth has driven urban expansion, while relatively permissive land use policies have exacerbated suburban sprawl, increasing infrastructure pressures and significantly impacting the conversion of green spaces [21]. Since the 1980s, a pro-business environment led by the Republican Party has attracted many companies to move in, boosting urban economic prosperity. However, relatively relaxed land use policies have also triggered disorganized suburban sprawl, increasing pressure on

infrastructure and public services and significantly influencing the transformation of green spaces [30–32].

Therefore, this study focuses on the dynamic transformation of green spaces at the county scale across the entire state of Texas, conducting a systematic analysis based on administrative divisions and related data. The boundary vector files of Texas as a whole and its 254 counties were obtained from the GADM (Database of Global Administrative Areas, https://gadm.org, accessed on 12 January 2025).

2.2. Data Source

2.2.1. Land Use Dataset

Landsat satellite data, characterized by long-term continuity, multispectral capabilities, medium spatial resolution, and free and open access, are widely used in land use/cover research to reveal environmental trends over decades. Specifically, Landsat-8 satellite data utilize the 2–7 spectral bands provided by the Operational Land Imager (OLI) to effectively identify and monitor surface features such as vegetation, water bodies, soil, and buildings (https://www.usgs.gov/landsat-missions/landsat-8, accessed on 12 January 2025). To obtain land use information for different periods in Texas, this study integrated the NLCD 2021 and NLCD 2019 datasets from the USGS National Land Cover Database developed using Landsat-8 satellite data. These datasets use a unified classification scheme for land cover categories and are accessible through Google Earth Engine (GEE).

In the data preprocessing stage, the classification results were merged into 11 major categories for consistent comparative analysis. Finally, TIF format observation data for five periods—2001, 2006, 2011, 2016, and 2021—were selected for the subsequent spatiotemporal change study.

2.2.2. Encroachment Intensity (EI)

To better measure the conversion patterns of green space into urban built-up areas, this study defines the "Encroachment Intensity (EI)" as the degree to which green space is converted to built-up areas, specifically referring to the area of green space converted into built-up land.

Over a five-year scale:

$$EI = \sum_{n} - \sum_{n-5}$$

Over a twenty-year scale:

$$EI = \sum_{n} - \sum_{n-20}$$

where "n = 254" represents the sample size of the 254 counties. By calculating both the five-year and twenty-year spans, the study can clearly reveal the phased and long-term impacts of urban expansion on green space.

2.2.3. Urban–Rural Classification

To distinguish between different levels of urban areas, this study adopts the Urban–Rural Classification Scheme for Counties proposed by the National Center for Health Statistics (NCHS) (the related report can be downloaded from https://www.cdc.gov/nchs, accessed on 13 January 2025). This standard divides counties across the country into six categories: large central metro (counties in MSAs of 1 million or more population), large fringe metro (counties in MSAs of 1 million or more population that did not qualify as large central metro counties), medium metro (counties in MSAs of populations of 250,000 to 999,999), small metro (counties in MSAs of populations less than 250,000), micropolitan (counties in micropolitan statistical areas), and noncore (nonmetropolitan counties that did

not qualify as micropolitan), which will help identify differences in urbanization levels and green space conversion within Texas in the subsequent analysis.

2.2.4. Population and GDP Data

The population and GDP data for this study primarily come from the United States Census Bureau and the Texas State Library and Archives Commission (available at https://www.tsl.texas.gov/, accessed on 16 January 2025). The population data are derived from both the Population Census and the Population Estimates Program, with key time points including 2000, 2005, 2010, 2020, and 2021. The GDP data are sourced from the U.S. Bureau of Economic Analysis (https://apps.bea.gov/histdatacore/Regional_Accounts_new.html, accessed on 14 January 2025), corresponding to the same time periods as the population data.

2.2.5. Texas Building Typology Dataset

Additionally, to gain a deeper understanding of the detailed functions and expansion processes of urban built-up areas, this study collected building type datasets for Texas. These datasets include information on building types, construction years, and building areas, with each building represented as a polygon (available at https://disasters.geoplatform.gov/USA_Structures/, accessed on 12 January 2025). This data will be integrated with the previously mentioned land use classification to facilitate a more thorough analysis of urban expansion and green space conversion patterns.

2.3. Methods

2.3.1. Methodology

This study systematically analyzed the spatiotemporal dynamics and driving factors of urban green spaces in Texas from 2001 to 2021. The process was as follows (Figure 2): first, multi-source data on land use, encroachment intensity, urban–rural classification, population, and GDP were collected; then, a land use transition matrix was built to quantify the transition relationships between different land use types, and a Sankey diagram was used to visually present the evolution patterns; next, the average annual change rates of different land use types were calculated to assess the impact of human activities; then, counties were classified from three dimensions: MSA list, level of urbanization, and geographic location characteristics, to test the spatial differences in the conversion of green spaces to built-up areas; subsequently, in the GIS, the green space change layer was filtered and overlaid with the building dataset to determine the main types of buildings converted from green spaces to built-up areas and to compare their scales and distribution patterns; finally, bivariate mapping and linear regression models were combined to investigate the impact of population and GDP growth on green space encroachment, and the spatial coupling relationships and quantitative relationships were visualized and analyzed to determine whether areas with rapid population and economic growth showed a more significant trend of green space conversion to built-up areas.

2.3.2. Land Use Transition Matrix

The land use transition matrix is a typical application of the Markov model in the quantitative study of land use change. It is used to represent the transition relationships between different land use types at different time periods within a study area. This matrix is widely applied in fields such as land resource management, urban–rural planning, and environmental protection. Typically, the rows of the land use transition matrix represent the land use types at the initial time period (T1), the columns represent the land use types

at the subsequent time period (T2), and the matrix elements P_{ij} represent the total area of land type *i* converted to type *j* during the T1–T2 period.

In this study, we combined Landsat data with a resolution of 30 m × 30 m from 2001 to 2021. Using ArcMap software (version 10.8.2) developed by the Environmental Systems Research Institute (ESRI), we employed the raster calculator in the map algebra tool to extract land use type changes for the same pixels across different years (values ranging from 0 to 10, representing different types). From this, we constructed the land use transition matrix. Additionally, to visually present the transitions between land use types, a Sankey diagram was used, providing a more intuitive way to identify and understand the land use evolution patterns across different periods in Texas.

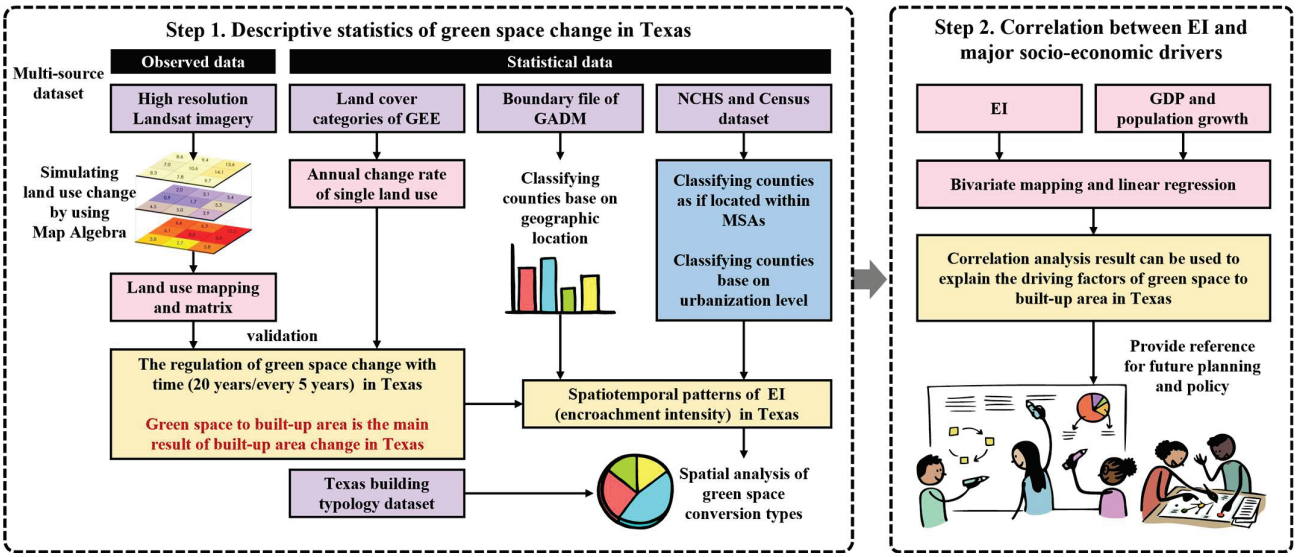


Figure 2. Study flow chart.

2.3.3. Annual Change Rate of Individual Land Use

To explore the evolution trends of various land use types from 2001 to 2021 (with each phase being 5 years), this study adopts the average annual change rate of a single land use type as a measure of this change. The calculation formula is as follows:

$$\text{Average Annual Change Rate} = \frac{\text{Change in Area of a Single Type}}{\text{Starting Area of the Type} \times \text{Year Interval of the Study Period Change in Area of a Single Type}} \times 100\%$$

where Change in Area refers to the increase or decrease in the area of the land type between the current and previous time periods. Starting Area refers to the area of the land type in the previous time period.

This indicator can be used to assess the extent to which human activities have impacted and altered different land use types during various stages, particularly in the context of rapid urbanization, revealing the dynamic changes in land use across different time periods.

2.3.4. Spatial Statistics on Different Types of Urban Green Space Change

To examine the differences in land use change due to urbanization, this study classifies the 254 counties in Texas from three dimensions:

(1) MSA vs. Non-MSA: According to the U.S. government's definition of Metropolitan Statistical Areas (MSAs), counties within an MSA are categorized as one group, while the remaining counties are classified as another. Numerous studies have shown that MSA regions typically exhibit more prominent urbanization, higher population

growth, and greater economic development, all of which have a more pronounced impact on land use change, especially green space conversion.

(2) Different Urbanization Levels: This study adopts a county classification method currently used by the American Cancer Society (ACS). When conducting cancer screening and differential reporting across the United States, the American Cancer Society uses this classification and naming approach. Based on this, counties are classified into different levels of urbanization, such as large metropolitan counties, small-to-medium metropolitan counties, and nonmetropolitan counties [33].

(3) Geographic Location Characteristics: The 254 counties are divided into three categories based on geographic characteristics as follows: coastal counties (those bordering the Gulf of Mexico), inland border counties (those bordering the Mexican border), and other inland counties.

This classification is used to investigate the differences in green space conversion patterns under different geographical conditions. For both of these classification variables, the study tests whether there are significant spatial differences in the conversion of green spaces to built-up areas.

2.3.5. GIS-Based Spatial Analysis of Green Space Conversion Types

Using GIS analysis tools, the green space change layer was first filtered. This layer was then overlaid with the Texas building dataset to determine the main building types converted from green space to built-up areas using the "building centroid localization" method. The process involves the following steps:

(1) Calculating the geometric centroid of each building using ArcGIS 10.8.

(2) Applying the "Select by Location" tool with the spatial relationship set to "Center within features," where features in the input layer are selected if their centers fall within a chosen feature (for polygons and multipoints: geometric centroid is used; for line inputs: midpoint of the geometry is used).

This method establishes the spatial relationship between building centroids and built-up areas. By avoiding traditional polygon intersections, it eliminates issues like duplicate classification and attribution ambiguity, ensuring each building is uniquely associated with one built-up area density attribute. This significantly enhances the accuracy of spatial analysis and classification results.

Based on this, the study further compares the scale and distribution patterns of green space conversion to "high, medium, and low-density" built-up areas (three density classes of built-up areas are extracted from NLCD based on impervious surface coverage; however, the specific parameters are not publicly available), quantifying the changes in land use structure in Texas under the backdrop of rapid urbanization.

2.3.6. Bivariate Mapping and Linear Regression

To further explore the impact of population and GDP growth on green space encroachment by built-up areas, this study combines bivariate mapping and linear regression models. The bivariate mapping tool in ArcGIS Pro was used to visualize the spatial coupling relationships between population growth, GDP growth, and green space encroachment intensity at the county-level scale. By overlaying color gradients, this method identifies spatial consistency between high-growth and high-encroachment areas. Population growth and GDP growth are continuous variables, while green space encroachment intensity is also a quantitative indicator, making them suitable for linear regression analysis based on variable type requirements. Additionally, when constructing linear regression models for population growth, GDP growth, and the intensity of green space encroachment, respec-

tively, several observed outliers were excluded. These outliers might be due to potential data collection errors or the occurrence of extreme events. Eventually, the sample sizes were n = 253 and n = 251, respectively (the original sample size was n = 254). A linear regression model is applied for statistical testing to determine whether areas with rapid population and economic growth show a more significant conversion of green space to built-up areas and to investigate the underlying mechanisms.

3. Results

3.1. Transitions Between Green Space and Built-Up Areas

In 2021, of the approximately 24,957 km^2 of built-up land in Texas, about 18,618 km^2 was existing built-up area, while approximately 4085 km^2 came from the conversion of previous green spaces, becoming the main source of green space change (Figure 3). A comparison of remote sensing images from 2001, 2006, 2011, 2016, and 2021 reveals the significant expansion of built-up areas around major cities such as Dallas, Houston, and Austin. This expansion is accompanied by a noticeable reduction and fragmentation of green spaces, particularly around the urban core areas.

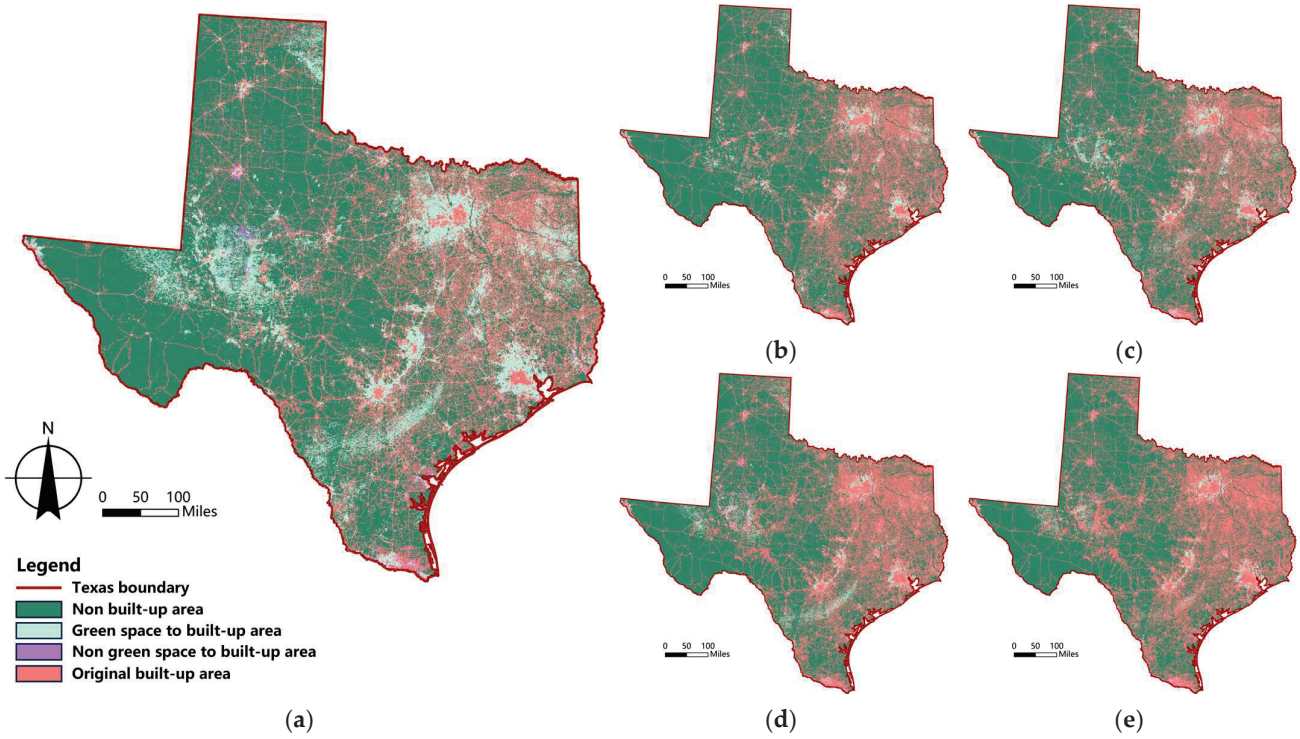


Figure 3. Visualization of the land use transition matrix results for Texas at the global level: (**a**) 2001–2021; (**b**) 2001–2006; (**c**) 2006–2011; (**d**) 2011–2016; (**e**) 2016–2021 (image source: drawn by the authors).

The results of the period-based statistical analysis are as follows:

(1) 2001–2006: Built-up areas increased slightly, with major expansion occurring around large cities.
(2) 2006–2011: The expansion rate accelerated, with surrounding green spaces and agricultural land being significantly occupied.
(3) 2011–2016: The urban boundary continued to expand, and the reduction of green spaces persisted.

(4) 2016–2021: The urbanization process intensified, and the newly added built-up areas continued to occupy green and agricultural land at a high intensity.

The flow chart (Figure 4) based on data from different time periods shows the conversion of green spaces and agricultural land into urban built-up areas, reflecting the profound impact of urbanization on land use patterns. Notably, the flow of green space into urban land is significantly wider than other conversion paths, indicating a larger scale of occupation. In certain areas, there is also some degree of mutual conversion between different types of green spaces (such as grasslands, shrublands, and forests); however, the overall scale is relatively small and not as prominent compared to the trend of green space reduction driven by urban expansion.

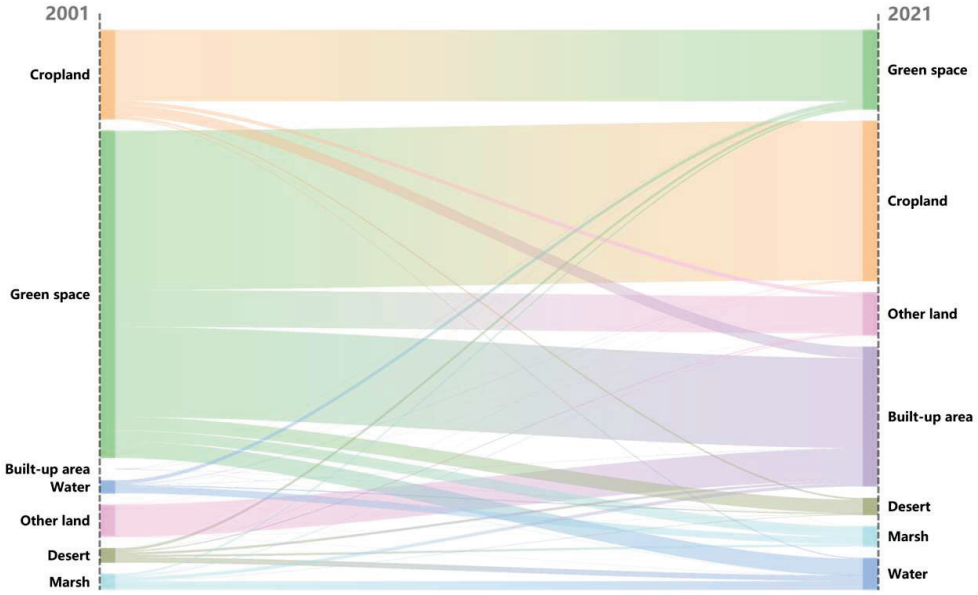


Figure 4. Sankey diagram visualizing the land use transition matrix results for Texas at the global level (image source: drawn by the authors).

From the statistical results of changes in a single land use (2001–2021) shown in Figure 5, it can be observed that, after 2016, certain types of green space may show a slight increase in localized areas. However, overall, the decreasing trend remains. The change rate over five-year intervals also indicates that, in the later periods, fluctuations in the increase and decrease in green space became more pronounced in some regions.

3.2. The Encroachment of Green Space in Different County Classifications

3.2.1. Classification of Counties by MSA List

After classifying counties into metropolitan and nonmetropolitan categories based on the Metropolitan Statistical Area (MSA) list, it was found that green space encroachment was more pronounced in metropolitan areas, which appeared as darker fill colors in multi-layer overlay analysis maps (Figure 6). Additionally, built-up area increases in some counties were concentrated in former green spaces (Table 1).

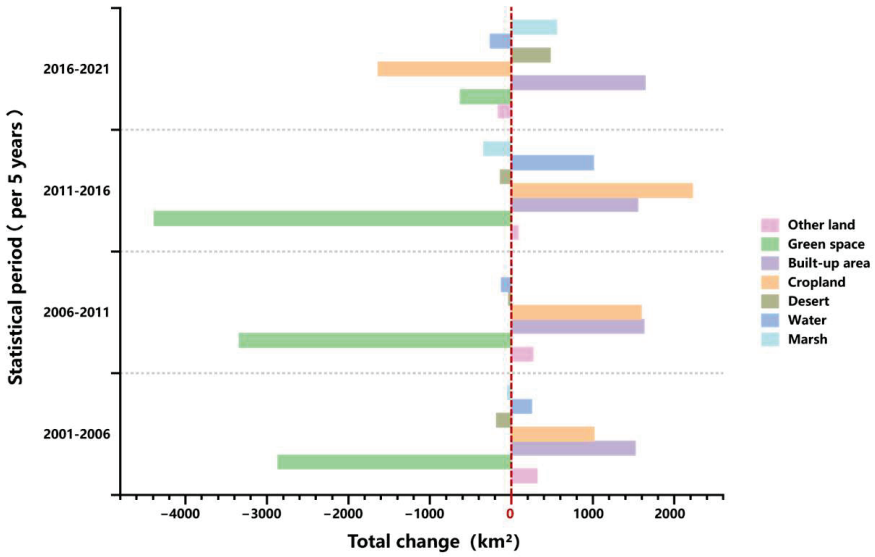
3.2.2. Classification of Counties by Urbanization Level

After classifying counties into large metropolitan counties (populations over 1 million), small-to-medium metropolitan counties, and nonmetropolitan counties by urbanization level, it was found that green space encroachment was more pronounced in metropolitan areas, which appeared as darker fill colors in multi-layer overlay analysis maps (Figure 7).

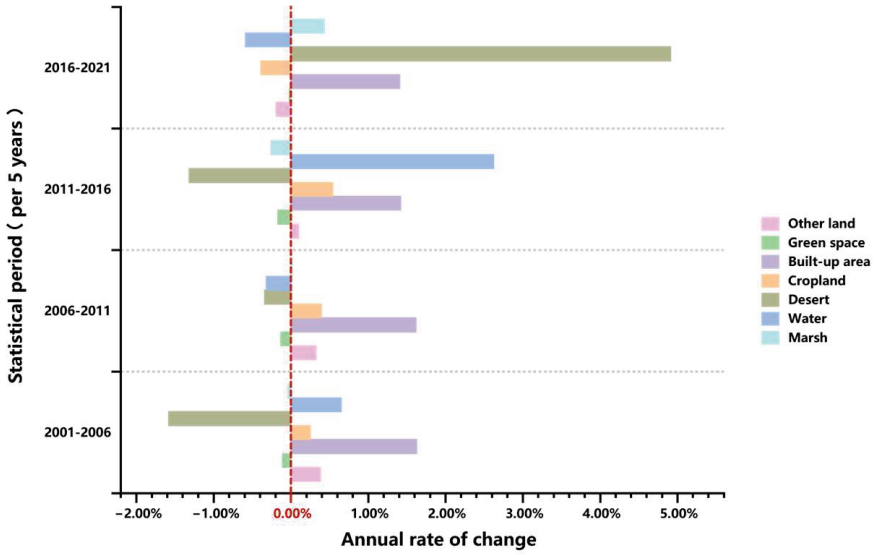
Additionally, it was observed that built-up area increases in some counties were concentrated in former green spaces (Table 2).

3.2.3. Classification of Counties by Geographic Location

After classifying the 254 counties in the state into coastal counties, inland border counties, and other inland counties, the area of green space converted into built-up areas showed a certain degree of accumulation. Among the three types of counties, some counties had more than 10 km^2 of green space occupied by built-up areas; however, overall, no particularly significant differences were observed (Figure 8). Coastal counties exhibited a slightly more concentrated distribution for this indicator, and the other two types of counties also showed similar trends (Table 3).



(**a**)



(**b**)

Figure 5. Changes in a single land use (2001–2021): (**a**) total change in a single land use every five years; (**b**) annual change rate of a single land use every five years (image source: drawn by the authors).

Table 1. Intensity of green space to built-up area in the classification of the MSA list of counties.

		Metropolitan Counties	Nonmetropolitan Counties
Descriptive statistics	Classification rules	Counties situated within MSAs	Counties outside of MSAs
	Number of counties	134	120
	Total land (km^2)	341,039	345,174
	Total change (km^2)	3385	706
	Intensity of changes	1.0%	0.2%
Differentiation analysis	Mann–Whitney test	p value < 0.001	

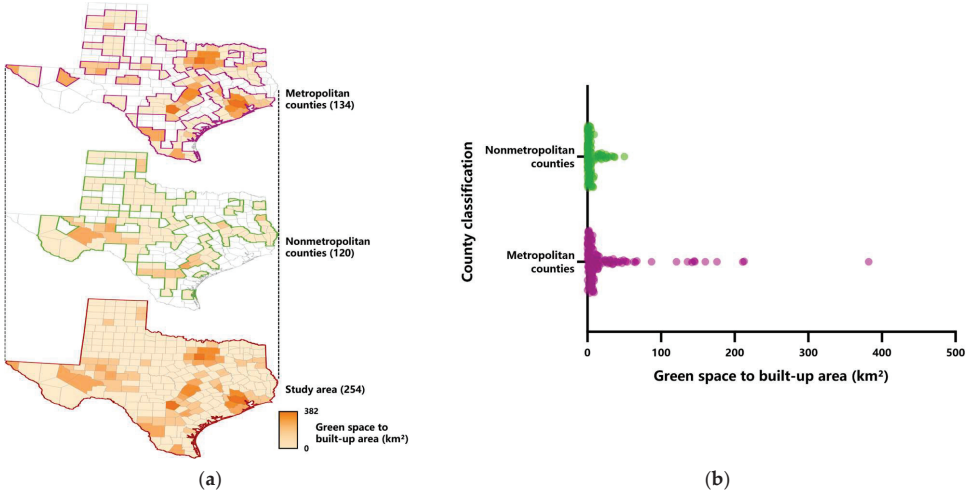


Figure 6. Conversion of green space to built-up areas in metropolitan counties and nonmetropolitan counties (20-Year change): (**a**) multi-layer overlay analysis map depicting the spatial variation in the intensity of green space encroachment by built-up areas across different counties; (**b**) scatter plot of spatial differences in the intensity of green space encroachment by built-up areas in different counties.

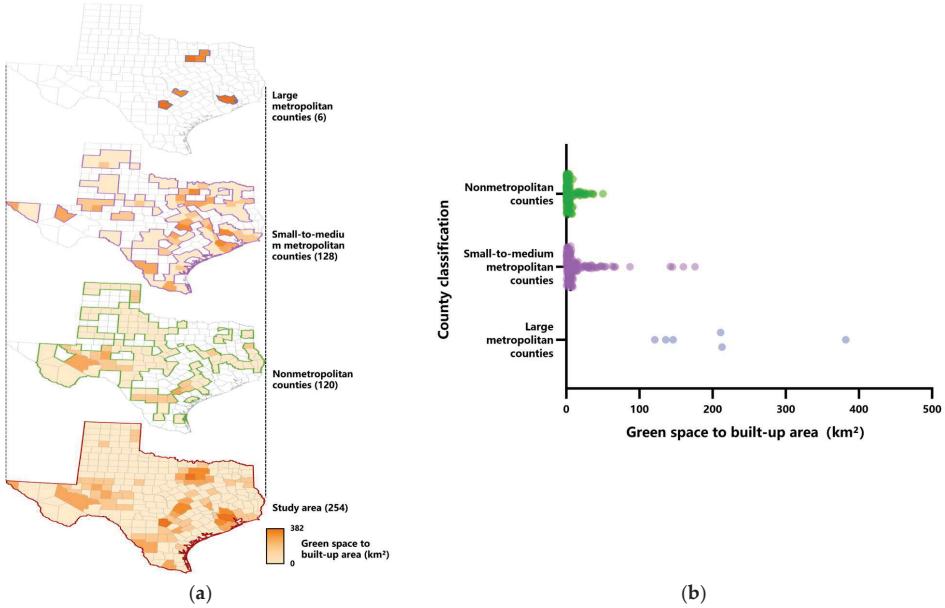
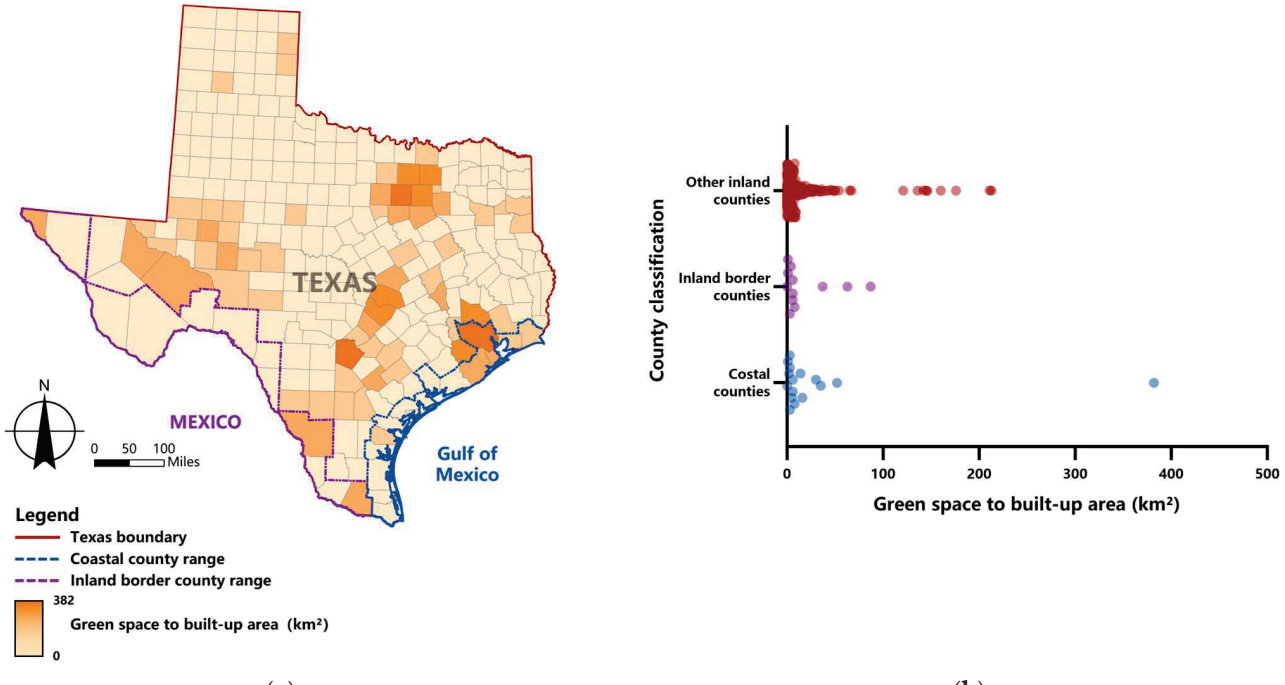


Figure 7. Conversion of green space to built-up areas in counties with different urbanization levels (20-Year change): (**a**) multi-layer overlay analysis map depicting the spatial variation in the intensity of green space encroachment by built-up areas across different counties; (**b**) scatter plot of spatial differences in the intensity of green space encroachment by built-up areas in different counties.

Table 2. Intensity of green space to built-up area in the classification of the urbanization level of counties.

		Large Metropolitan Counties	Small-to-Medium Metropolitan Counties	Nonmetropolitan Counties
Descriptive statistics	Classification rules	Counties situated within MSAs with populations exceeding one million	Counties situated within MSAs with populations below one million	Counties outside of MSAs
	Number of counties	6	128	120
	Total land (km^2)	17,452	323,587	345,174
	Total change (km^2)	1209	2175	701
	Intensity of changes	6.9%	0.7%	0.2%
Differentiation analysis	Kruskal–Wallis test		p value < 0.001	



(**a**) (**b**)

Figure 8. Conversion of green space to built-up areas in counties with different geographical regions (20-Year change): (**a**) map of spatial differences in the intensity of green space encroachment by built-up areas in different counties; (**b**) scatter plot of spatial differences in the intensity of green space encroachment by built-up areas in different counties.

3.3. Types of Green Space Occupied by Urban Built-Up Areas

Statistics on land use conversion of green space over the past 20 years show that residential land has the highest proportion of occupation in medium and low-density built-up areas, making it the primary direction of green space occupation in urban expansion. In high-density built-up areas, both commercial and residential land contribute to the reduction of green spaces, indicating that the development of high-density areas often involves buildings with mixed functions (Figure 9).

Table 3. Intensity of green space to built-up area in the classification of the location of counties.

		Coastal Counties	**Inland Border Counties**	**Inland Counties**
Descriptive statistics	Classification rules	Counties located along the coastline	Counties located inland and along the U.S.-Mexico border	Counties located inland but not along the U.S.–Mexico border
	Number of counties	16	12	226
	Total land (km^2)	37,258	80,674	568,281
	Total change (km^2)	564	221	3300
	Intensity of changes	1.5%	0.3%	0.6%
Differentiation analysis	Kruskal–Wallis test		p value = 0.2592	

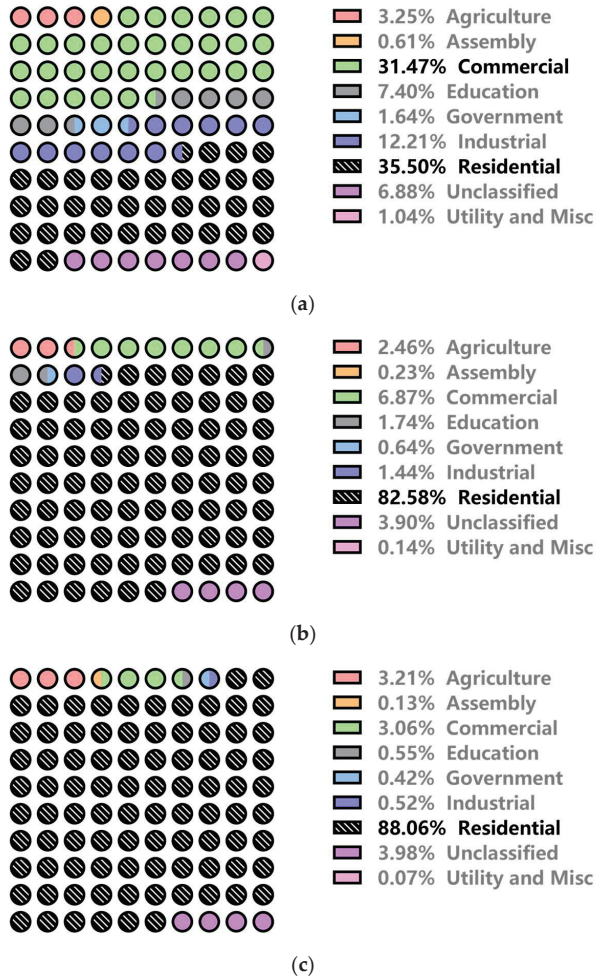
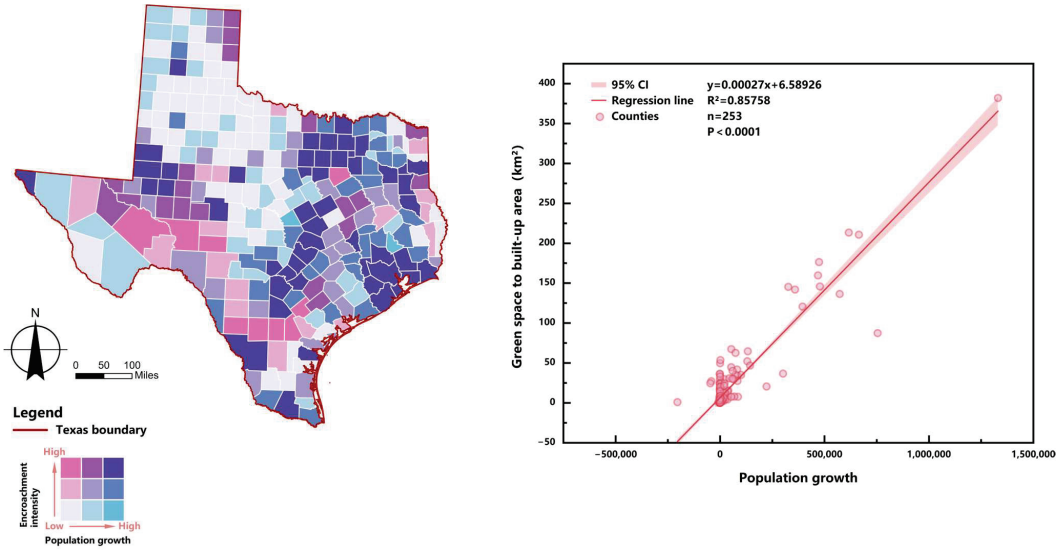


Figure 9. Proportions of different types of buildings in the built-up areas converted from green space in Texas (2001–2021): (**a**) high-density built-up areas; (**b**) medium-density built-up areas; (**c**) low-density built-up areas.

3.4. Bivariate Choropleth Map and Linear Regression

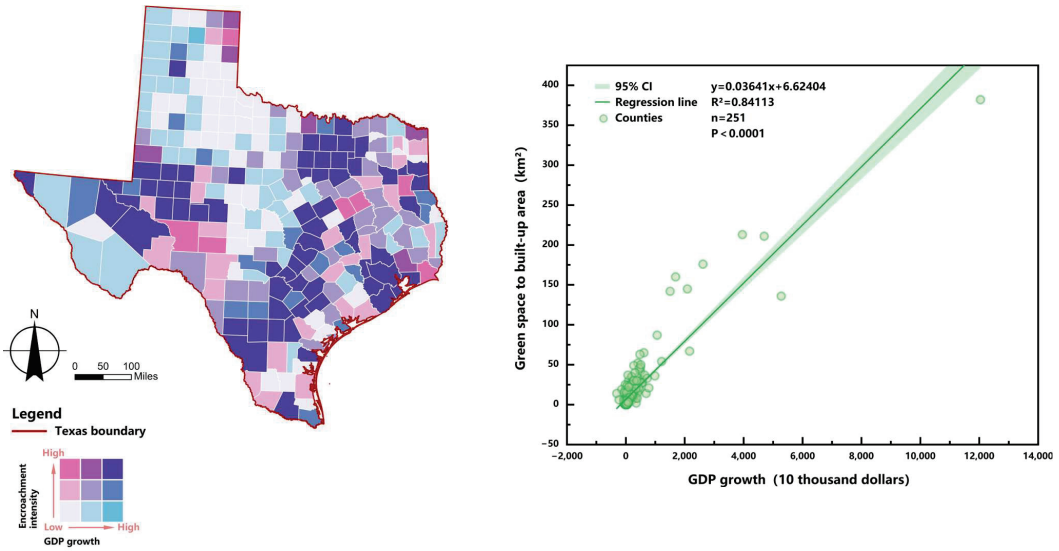
In the bivariate mapping, population/GDP changes in county-level regions show a positive correlation with green space reduction. Areas shown as high–high in the color overlay gradient classification are primarily concentrated in counties of metropolitan areas such as Dallas, Houston, and Austin. Linear regression analyses of population

change vs. green space reduction ($R^2 \approx 0.86$, $p < 0.001$) and GDP change vs. green space reduction ($R^2 \approx 0.84$ $p < 0.001$) both demonstrated high goodness-of-fit, indicating that population/GDP growth in most counties can effectively explain the increased intensity of green space encroachment by built-up areas. There are a few outliers in the scatter distribution of counties, indicating that the situation in these counties deviates from the overall trend. The extent of green space conversion or the rates of population and economic growth in these regions do not align completely with other areas (Figures 10 and 11).



(**a**) (**b**)

Figure 10. Correlation between population growth and the intensity of green space encroachment by built-up areas: (**a**) bivariate mapping map of population growth and the intensity of green space encroachment by built-up areas; (**b**) linear regression of population growth and the intensity of green space encroachment by built-up areas.



(**a**) (**b**)

Figure 11. Correlation between GDP growth and the intensity of green space encroachment by built-up areas: (**a**) bivariate mapping map of GDP growth and the intensity of green space encroachment by built-up areas; (**b**) linear regression of GDP growth and the intensity of green space encroachment by built-up areas.

Outliers:

(1) Population Change vs. Green Space Change
Some counties exhibit "rapid population growth but insignificant green space reduction" or "population decrease but significant green space reduction".

(2) GDP Change vs. Green Space Change
Some counties show "GDP growth but insignificant green space reduction" or "GDP decline but significant green space reduction".

4. Discussion

4.1. Spatiotemporal Patterns of Green Space Changes in Different Types of Cities

This study shows that urban expansion in Texas over the past two decades has been concentrated mainly around large cities and their surrounding areas, with a particularly significant occupation of green spaces. The conversion of green space to built-up areas is most commonly observed around major cities such as Dallas, Houston, and Austin. This phenomenon corresponds to previous studies focusing on green space changes in large cities or metropolitan areas:

For example, Ref. [15] explored urban green space changes in the cities of Kolkata and Howrah, West Bengal, India. Scholar Chen, B. conducted a quantitative analysis of green space changes in 98 large cities with populations over 1 million in 2007 [34]. Schinasi, L. H. estimated the correlation between green space and gentrification in 43 of the largest Metropolitan Statistical Areas (MSAs) in the U.S. [35]. Qing Wang completed a 25-year tracking study of green space changes in the Tokyo metropolitan area [26]. Kitch, J. C. analyzed the dynamics of green space growth in the top 20% of census tracts in U.S. cities from 2001 to 2019 [18]. Zhu, Z. pointed out the imbalanced urbanization levels in different regions of Guangzhou and their significant spatiotemporal differences in watershed land use and landscape patterns [21].

These studies all highlight that those large cities, due to the high concentration of industry and population, tend to have more green space encroachment. The results of this study similarly show that the scale of green space conversion to built-up areas is most prominent around Texas's three major cities and the transportation corridors linking them. This confirms the common pattern of "urban expansion encroaching on green space" in rapid urbanization. The ongoing concentration of population and economic activities [36], as well as the increase in the non-agricultural population and industrial transformation [21], have further strengthened this trend.

4.2. Socioeconomic Drivers of Green Space Change

Through model analysis and geographic information visualization methods, this study examined the extent to which population, GDP, urban rank, and geographic location influence green space changes. The results show that the population variable has a more significant relationship with green space conversion than GDP. The influx and growth of population often directly trigger the expansion of housing and infrastructure, further encroaching on green space. This aligns with Ducey, M. J. [37] and others' assertion that "population is more critical than other factors in predicting urban land use change models" and echoes [14], who found a significant positive correlation ($R = 0.11$, $p < 0.001$) between population variables and urban green space change in large cities.

GDP changes also promote the occupation of green space by urban built-up areas; however, the correlation is slightly lower than that of population. Regarding urban geographic location (coastal counties, inland border counties, etc.), the study shows that this

factor does not produce a significant difference in green space change. This suggests that across Texas, whether coastal or near the border, green spaces are similarly under pressure from urban expansion. In contrast, urban rank and the extent of population change are more central drivers in determining the outcome of green space conversion.

Notably, other studies have also highlighted the role of various socioeconomic factors in the process of green space change. For instance, Seto et al. in their global analysis of urban expansion, found that the impact of economic growth on green space encroachment varies significantly across different city types [20]. Urban expansion in developing countries relies more on newly developed land, whereas cities in developed countries depend more on urban renewal and redevelopment. In their research on East Asian urban systems, they noted that variations in land finance policies have led to uneven implementation of urban green space protection measures. Cities heavily dependent on land-transfer revenues are more prone to sacrificing green spaces for real estate development. Additionally, Haaland and van den Bosch demonstrated that European cities typically adopt stricter green space preservation policies [27], emphasizing the optimization of ecosystem services to mitigate green space loss caused by urban expansion [21]. In contrast, the urban expansion pattern in Texas aligns more closely with the characteristics of rapidly growing metropolitan areas, characterized by significant green space conversion driven by rapid population growth and economic development within a short timeframe, coupled with relatively weaker policy controls.

In the regression analysis of population and GDP with green space change, several county data points significantly deviated from the overall trend, forming outliers, which may reflect the following certain special regions or policy factors:

(1) Population Growth but Insignificant Green Space Reduction: This may occur in regions where, despite rapid urbanization, well-established green space protection or land use planning policies were implemented. Alternatively, changes in agricultural land or other land types may have interfered with the green space data, making it appear that green space has not been significantly occupied.
(2) Population Decrease but Significant Green Space Reduction: This could be related to economic recession, weak government oversight, or outdated urban planning. Green space may have been destroyed due to lack of maintenance or illegal development. During industrial shifts, some regions may have been influenced by external investments or short-term development activities, leading to the one-time occupation of green space without a population return.
(3) GDP Growth but Insignificant Green Space Reduction: Some regions may have simultaneously advanced economic development and ecological construction, such as implementing ecological compensation or vertical greening and public green space renovation in built-up areas, thus slowing actual encroachment on green space. If GDP growth in the area mainly relies on sectors with relatively small spatial demands, such as non-manufacturing or information industries, the actual expansion of land use may not be significant.
(4) GDP Decline but Significant Green Space Reduction: This could be due to a lack of effective management during economic contraction, with green spaces facing random development or improper land reuse. In cases of fiscal stress and planning defects, green spaces are vulnerable to being sold off or repurposed for other uses, accelerating their degradation.

The presence of these outliers further illustrates that green space changes are not solely influenced by macro variables such as population or GDP. They are also affected by complex socioeconomic policies, planning management approaches, and industrial

structures. Therefore, more in-depth analysis involving qualitative research and field surveys is needed to fully understand the underlying causes.

4.3. Green Space Occupation

In the green space conversion patterns over the past two decades, most green spaces have been occupied by residential land uses, with this trend being particularly strong in medium and low-density urban areas. Texas experienced an increase of approximately 9 million residents between 2000 and 2022, with a growth rate of nearly 43% [29]. Such a significant population increase has inevitably led to strong demand for urban land. During urban expansion, to meet the demands for housing, commerce, and public services, cities often prioritize converting green spaces with favorable locations or development potential [38]. High-density built-up areas show a characteristic of both residential and commercial land encroaching on green spaces, driven by the need for commercial facilities and comprehensive services in central urban areas, which further intensifies the occupation of green spaces.

This phenomenon is not limited to Texas; global studies also indicate that urban expansion encroaching on green spaces is a widespread trend. For instance, Seto et al. in their global study of urban expansion, noted that rapid urbanization often occurs at the expense of green spaces, particularly in densely populated and economically fast-growing regions [20]. Additionally, Zhu et al. in their research on urban expansion in Guangzhou, found that increased population influx and infrastructure development continually replaced green spaces with residential and commercial uses, especially in suburban areas [39]. Haaland and van den Bosch further emphasized that the reduction in green spaces during urbanization not only affects ecosystems but also potentially exacerbates social inequalities, as low-income groups often face difficulties accessing sufficient public green spaces [27].

Meanwhile, some cities have implemented stricter green space protection measures to mitigate the negative ecological impacts of urban expansion. For example, many European cities have effectively managed the rate of green space conversion through adopting a "compact city" development model and rigorous land use planning [40]. In contrast, cities in the United States typically experience more pronounced trends of green space encroachment due to less stringent land use regulations. Particularly in Texas, rapid urban expansion poses greater challenges to implementing effective green space protection policies [41].

4.4. Limitations of the Study

Despite the implementation and analysis in this study, there are still several limitations, as follows:

(1) Satellite Data Accuracy and Recognition Limitations: The identification of low-density and medium-density built-up areas still mainly relies on the coverage percentage of impervious surfaces in satellite products. Different levels of urban built-up areas may suffer from ambiguous identification and errors in actual statistical results. Higher-resolution imagery or ground survey data are needed for further correction.

(2) Limited Types of Driving Factors: This study primarily focuses on population, GDP, urban rank, and geographic location, exploring their correlations with green space changes without conducting an in-depth analysis of climatic and environmental factors. This decision was based on several considerations: first, urban expansion and the reduction of green spaces are predominantly driven directly by socioeconomic factors, while the impact of climate change tends to be relatively indirect [21]; second, numerous studies have already examined the effects of climatic factors on ecosys-

tems, and the current study aims to complement this by focusing specifically on anthropogenic factors [27]; additionally, due to constraints in data availability and methodological approaches, this research is better suited to examining the role of socioeconomic variables in green space conversion rather than the effects of long-term climate trends [3]. Future research could further integrate climate change data to investigate the long-term impacts of extreme weather events on green space protection and urban planning.

(3) Lack of Policy Factors: The success of green space protection in some exceptional areas is closely linked to the active intervention of local policies. Including policy dimensions in the research would help to better understand the role and influence mechanisms of local governments in regulating urban land expansion.

5. Conclusions

This study used 30-m resolution Landsat remote sensing data and land use transition matrices to quantitatively analyze the changes in green space across 254 counties in Texas from 2001 to 2021. By integrating the NCHS urban ranking classification and U.S. building datasets, the study explored the spatiotemporal evolution patterns of green spaces in different types of cities. Additionally, regression models incorporating socioeconomic factors such as population and GDP were used to identify their driving effects on green space changes. The results show that the rate of green space change slowed down over the five years after 2016; however, the overall trend remained one of contraction. Spatially, the reduction in green space was most significant in large cities and their surrounding areas, and the converted green spaces were mainly used to meet the demand for low, medium, and high-density housing. Regression analysis revealed that, compared to other factors, population change was the primary driver of green space change, with a correlation of 86%. Moreover, economically developed areas tended to have a higher concentration of green space occupation. It is important to note that this study did not incorporate detailed policy factors and community-level social attributes, which may have a greater impact in certain areas. Furthermore, higher-resolution remote sensing imagery and multi-level analytical methods could deepen the understanding of green space evolution mechanisms. This study provides an empirical case for green space dynamics in U.S. cities, offering valuable insights for policymakers in urban planning, green space management, and monitoring, supporting the development of more sustainable urban development strategies.

Author Contributions: Conceptualization, T.M. and Y.L.; methodology, H.Y.; software, H.Y. and Y.S.; validation, T.M. and H.Y.; formal analysis, T.M. and Y.L.; data curation, T.M.; writing—original draft preparation, T.M. and Y.L.; writing—review and editing, H.H. and Y.C.; visualization, H.Y.; supervision, H.H. and Y.C. All authors have read and agreed to the published version of the manuscript.

Funding: This research received no external funding.

Data Availability Statement: The dataset supporting the findings of this study has not been publicly uploaded. However, it is available from the corresponding author upon reasonable request.

Acknowledgments: The authors would like to express their gratitude to the City University of Macau for its support throughout this research. We also sincerely appreciate the valuable guidance and assistance provided by Haoying Han, whose insights and expertise contributed significantly to the completion of this study.

Conflicts of Interest: The authors declare no conflicts of interest.

References

1. Mitchell, R.; Popham, F. Effect of exposure to natural environment on health inequalities: An observational population study. *Lancet* **2008**, *372*, 1655–1660. [CrossRef] [PubMed]
2. Zhao, J.; Chen, S.; Jiang, B.; Ren, Y.; Wang, H.; Vause, J.; Yu, H. Temporal trend of green space coverage in China and its relationship with urbanization over the last two decades. *Sci. Total Environ.* **2013**, *442*, 455–465. [PubMed]
3. Smith, J.; Brown, K.; Thompson, R. The impact of extreme climate events on land use change in Texas. *J. Clim. Adapt.* **2022**, *15*, 221–234.
4. Teeuwen, R.; Milias, V.; Bozzon, A.; Psyllidis, A. How well do NDVI and OpenStreetMap data capture people's visual perceptions of urban greenspace? *Landsc. Urban Plan.* **2024**, *245*, 105009. [CrossRef]
5. Dallimer, M.; Tang, Z.; Bibby, P.R.; Brindley, P.; Gaston, K.J.; Davies, Z.G. Temporal changes in greenspace in a highly urbanized region. *Biol. Lett.* **2011**, *7*, 763–766. [CrossRef]
6. Liu, S.; Zhang, X.; Feng, Y.; Xie, H.; Jiang, L.; Lei, Z. Spatiotemporal dynamics of urban green space influenced by rapid urbanization and land use policies in Shanghai. *Forests* **2021**, *12*, 476. [CrossRef]
7. Heo, S.; Bell, M.L. Investigation on urban greenspace in relation to sociodemographic factors and health inequity based on different greenspace metrics in 3 US urban communities. *J. Expo. Sci. Environ. Epidemiol.* **2023**, *33*, 218–228. [CrossRef]
8. Dinda, S.; Das, P.; Dutta, D. Assessing the impact of urban land-use dynamics on the ecological vulnerability of Kolkata Municipal Corporation (KMC), India. In *Urbanization and Regional Sustainability in South Asia: Socio-Economic Drivers and Environmental Concerns*; Mandal, D., Dutta, D., Mukhopadhyay, A., Eds.; Springer: Cham, Switzerland, 2021; pp. 495–512. [CrossRef]
9. Hunter, R.F.; Cleland, C.; Cleary, A.; Droomers, M.; Wheeler, B.W.; Sinnett, D.; Nieuwenhuijsen, M.; Braubach, M. Environmental, health, wellbeing, social and equity effects of urban green space interventions: A meta-narrative evidence synthesis. *Environ. Int.* **2019**, *130*, 104923. [CrossRef]
10. Kabisch, N.; Korn, H.; Stadler, J.; Bonn, A. (Eds.) *Nature-Based Solutions to Climate Change Adaptation in Urban Areas: Linkages Between Science, Policy and Practice*; Springer: Cham, Switzerland, 2017. [CrossRef]
11. Texas Land and Resource Management Act. *Texas Land and Resource Management Act 2019*; Texas State Legislature: Austin, TX, USA, 2019.
12. Wulder, M.A.; White, J.C.; Loveland, T.R.; Woodcock, C.E.; Belward, A.S.; Cohen, W.B.; Fosnight, E.A.; Shaw, J.; Masek, J.G.; Roy, D.P. The global Landsat archive: Status, consolidation, and direction. *Remote Sens. Environ.* **2018**, *185*, 271–283. [CrossRef]
13. Zhu, X.; Tuia, D.; Mou, L.; Xia, G.S.; Zhang, L.; Xu, F.; Fraundorfer, F. Deep learning in remote sensing: A comprehensive review and list of resources. *IEEE Geosci. Remote Sens. Mag.* **2017**, *5*, 8–36. [CrossRef]
14. Chen, B.; Wu, S.; Song, Y.; Webster, C.; Xu, B.; Gong, P. Contrasting inequality in human exposure to greenspace between cities of Global North and Global South. *Nat. Commun.* **2022**, *13*, 4636. [CrossRef]
15. Halder, B.; Bandyopadhyay, J.; Al-Hilali, A.A.; Ahmed, A.M.; Falah, M.W.; Abed, S.A.; Yaseen, Z.M. Assessment of urban green space dynamics influencing the surface urban heat stress using advanced geospatial techniques. *Agronomy* **2022**, *12*, 2129. [CrossRef]
16. Ali, G.; Pumijumnong, N.; Cui, S. Valuation and validation of carbon sources and sinks through land cover/use change analysis: The case of Bangkok metropolitan area. *Land Use Policy* **2018**, *70*, 471–478. [CrossRef]
17. Xing, Z.; Zhao, S.; Li, K. Evolution pattern and spatial mismatch of urban greenspace and its impact mechanism: Evidence from parkland of Hunan Province. *Land* **2023**, *12*, 2071. [CrossRef]
18. Kitch, J.C.; Nguyen, T.T.; Nguyen, Q.C.; Hswen, Y. Changes in the relationship between Index of Concentration at the Extremes and US urban greenspace: A longitudinal analysis from 2001–2019. *Humanit. Soc. Sci. Commun.* **2023**, *10*, 862. [CrossRef]
19. Prăvălie, R.; Borrelli, P.; Panagos, P.; Ballabio, C.; Lugato, E.; Chappell, A.; Birsan, M.V. A unifying modelling of multiple land degradation pathways in Europe. *Nat. Commun.* **2024**, *15*, 3862. [CrossRef]
20. Seto, K.C.; Güneralp, B.; Hutyra, L.R. Global urban land expansion and its effects on biodiversity. *Proc. Natl. Acad. Sci. USA* **2011**, *108*, 7687–7692.
21. Zhu, Z.; Liu, B.; Wang, H.; Hu, M. Analysis of the spatiotemporal changes in watershed landscape pattern and its influencing factors in rapidly urbanizing areas using satellite data. *Remote Sens.* **2021**, *13*, 1168. [CrossRef]
22. Schinasi, L.H. Green space and gentrification in 43 US metropolitan areas. *Environ. Res.* **2021**, *200*, 111751.
23. Ducey, M.J.; Johnson, K.M.; Belair, E.P.; Cook, B.D. The influence of human demography on land cover change in the Great Lakes States, USA. *Environ. Manag.* **2018**, *62*, 1089–1107. [CrossRef]
24. Zhou, W.; Wang, J.; Qian, Y.; Pickett, S.T.; Li, W.; Han, L. The rapid but "invisible" changes in urban greenspace: A comparative study of nine Chinese cities. *Sci. Total Environ.* **2018**, *627*, 1572–1584. [PubMed]
25. Song, Y.; Chen, B.; Kwan, M.P. How does urban expansion impact people's exposure to green environments? A comparative study of 290 Chinese cities. *J. Clean. Prod.* **2020**, *246*, 119018.

26. Wang, Q.; Takatori, C.; Chen, Z. Urban dynamics and their implication on greenness trends: A 25-year retrospective study of the changing face of Tokyo metropolitan area. *Environ. Sustain. Indic.* **2024**, *23*, 100427. [CrossRef]
27. Haaland, C.; van den Bosch, C.K. Challenges and strategies for urban green-space planning in cities undergoing densification. *Urban For. Urban Green.* **2015**, *14*, 760–771.
28. National Centers for Environmental Information (NCEI). *Climate Data Summary for Texas*; National Oceanic and Atmospheric Administration (NOAA): Silver Spring, MD, USA, 2023.
29. US Census Bureau. *Texas Population Passes the 30-Million Mark in 2022*; U.S. Census Bureau: Washington, DC, USA, 2023.
30. Zhang, L.; Li, M. Urban sprawl and green space loss in Texas: A case study. *J. Urban Plan.* **2021**, *39*, 112–130.
31. Liu, X.; Wang, Y.; Chen, Z. The impact of population growth on land use and infrastructure development in Texas. *Urban Dev. Rev.* **2019**, *27*, 85–102.
32. Johnson, R.; Smith, M. Economic growth and land use policies: Implications for urban green space in Texas. *J. Environ. Manag.* **2022**, *58*, 54–70.
33. Islami, F.; Baeker Bispo, J.; Lee, H.; Wiese, D.; Yabroff, K.R.; Bandi, P.; Sloan, K.; Patel, A.V.; Daniels, E.C.; Kamal, A.H.; et al. American Cancer Society's report on the status of cancer disparities in the United States, 2023. *CA Cancer J. Clin.* **2024**, *74*, 136–166.
34. Chen, B.; Nie, Z.; Chen, Z.; Xu, B. Quantitative estimation of 21st-century urban greenspace changes in Chinese populous cities. *Sci. Total Environ.* **2017**, *609*, 956–965. [CrossRef]
35. Schinasi, L.H.; Cole, H.V.; Hirsch, J.A.; Hamra, G.B.; Gullon, P.; Bayer, F.; Lovasi, G.S. Associations between greenspace and gentrification-related sociodemographic and housing cost changes in major metropolitan areas across the United States. *Int. J. Environ. Res. Public Health* **2021**, *18*, 3315. [CrossRef]
36. Balland, P.A.; Jara-Figueroa, C.; Petralia, S.G.; Steijn, M.P.; Rigby, D.L.; Hidalgo, C.A. Complex economic activities concentrate in large cities. *Nat. Hum. Behav.* **2020**, *4*, 248–254. [CrossRef] [PubMed]
37. Ducey, M.J. Modeling urban land use change. *Landsc. Urban Plan.* **2018**, *177*, 47–56.
38. Wolch, J.R.; Wilson, J.P.; Fehrenbach, J. The role of green spaces in urban environments and the socio-economic implications of their development. *Urban Stud.* **2014**, *41*, 241–258.
39. Zhu, Z.; Zhang, Y.; Chen, X. Urbanization and green space dynamics in China: Evidence from Guangzhou. *J. Environ. Manag.* **2021**, *289*, 112478.
40. Jim, C.Y. Sustainable urban green spaces in high-density cities. *Landsc. Urban Plan.* **2013**, *126*, 104–112.
41. Zhao, P.; Lü, B.; Woltjer, J. Urban expansion and green space loss in China: A global perspective. *Habitat Int.* **2020**, *96*, 102124.

Disclaimer/Publisher's Note: The statements, opinions and data contained in all publications are solely those of the individual author(s) and contributor(s) and not of MDPI and/or the editor(s). MDPI and/or the editor(s) disclaim responsibility for any injury to people or property resulting from any ideas, methods, instructions or products referred to in the content.

buildings

MDPI

Review

Promoting Circular Economy of the Building Industry by the Use of Straw Bales: A Review

An Li [1,2], Chong Guo [3,4], Jian Gu [3,4], Yanyuan Hu [3,4], Zhaoyang Luo [3,4,*] and Xunzhi Yin [5,*]

[1] School of Social Sciences, Faculty of Humanities and Social Sciences, Harbin Institute of Technology, Harbin 150001, China; anli@hit.edu.cn
[2] School of Management, Harbin Institute of Technology, Harbin 150001, China
[3] School of Architecture and Design, Harbin Institute of Technology, Harbin 150001, China
[4] Key Laboratory of Cold Region Urban and Rural Human Settlement Environment Science and Technology, Ministry of Industry and Information Technology, Harbin 150001, China
[5] College of Civil Engineering and Architecture, Zhejiang University, Hangzhou 310058, China
* Correspondence: luozhaoyang@hit.edu.cn (Z.L.); x.yin@zju.edu.cn (X.Y.)

Abstract: Over the past decade, the concept of a circular economy has increasingly gained attention as a framework for guiding businesses and policymakers. Given its significant environmental impact, the building industry plays a pivotal role in the transition toward a circular economy. To address this, our review proposes a bio-based building material, specifically straw bale, which elaborates on the circularity of bio-based buildings based on the 3R principles of a circular economy: reduce, reuse, and recycle. In terms of the "reduce" principle, straw-bale buildings can reduce construction waste, the environmental impact, energy requirements, and carbon emissions. Regarding the "reuse" principle, straw-bale buildings utilize agricultural waste resources and are easily disassembled due to their prefabrication. As for the "recycle" principle, straw-bale buildings can undergo physical, biological, and biochemical conversion processes (thermochemical conversion), yielding both wooden composite boards and potential biogas and biomass fuels for electricity and heating. This study evaluates the contribution of straw packaging construction and the use of straw as a raw material, using the 3R principles to determine future research opportunities for the construction industry to achieve a circular economy. The results of this study offer circular economy solutions and interdisciplinary research insights for researchers and practitioners interested in the building environment.

Keywords: circular economy; construction industry; bio-based buildings; straw bales; 3R principles (reduce, reuse, recycle); sustainable development

1. Introduction

The building industry is a highly active industry in both developed and developing countries [1]. Its practices wield significant influences on the sustainable development of society, the environment, the economy, etc. Additionally, the building industry stands as one of the primary sectors that consumes resources and generates waste within economic activities. It takes the lead as the top consumer of resources globally. The waste generated during construction-related production, operation and demolition is also a main factor in greenhouse gas emission, posing a challenge to the goal of achieving global peak carbon emissions [2]. Nowadays, the building industry still complies with the linear "procure–produce–process" economic model, which features a high consumption of natural resources and a low recycling ratio. The adoption of such a development model results in high waste production and poor sustainability as well as serious negative effects on the environment [3]. Thus, it is crucial to make efforts to boost efficiency in the use of construction resources for the global sustainable development of the building industry [4,5].

In recent years, attention toward the circular economy (CE) has significantly increased. Serving as an alternative to the traditional linear economic model, the CE holds the potential to offer a new solution for enhancing the sustainability of the building industry and

is regarded as a novel approach to achieving its sustainable development [6,7]. The CE system returns materials and products to the supply chain as resources, with a focus on the decoupling of economic growth from environmental damage through the establishment of a regeneration system [8]. By maximizing the reuse and recycling of materials and components, the CE minimizes the primary resource consumption and waste production [9–11] while maintaining high efficiency and adding value to the products and materials [12,13]. The waste-to-resources model can effectively enhance the efficiency of the use of resources, and it is an important part in the closed-loop of the CE [14].

As depicted in Figure 1, the circular economy (CE) framework employs "reduce, reuse, and recycle (3R)" as guiding principles to establish a foundation for recycled waste management and the recycling of materials [8,15]. The first principle, "reduce", embraces the idea of "reducing from the source": minimizing the use of disposable resources, raw materials and waste from the source [16] while reducing or eliminating the production of pollutants [17], thus mitigating environmental damage [18]. "Reuse" refers to maximizing the utilization of products by maintaining and recycling them, extending their life span. Products or components that are not considered waste are reused and continue to function as before. Compared with the production of new products from raw materials, the concept of "reuse" may be an efficient alternative for managing waste because it can utilize resources more efficiently and significantly reduce environmental damage, i.e., the impact on the environment is minimal [19]. The principle of "recycle" proposes processing renewable materials into new products to minimize the consumption of raw materials.

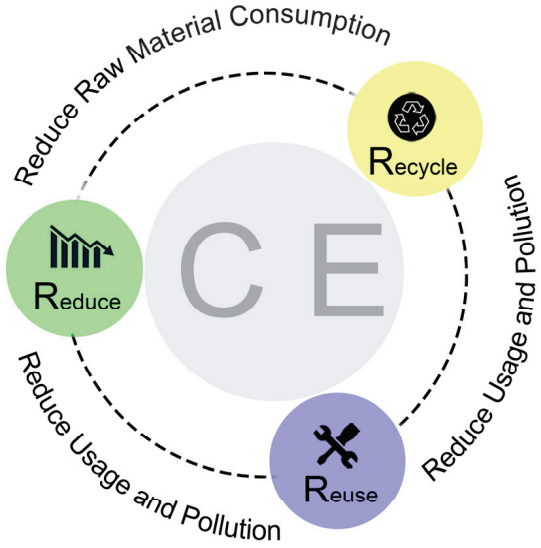


Figure 1. CE-3R model diagram.

The 3R principles have established the groundwork for global waste management and offer a solution for addressing global warming. The 3R principles have become a universally acknowledged concept embraced both in theory and in practical applications. However, recently, emphasis has been put on a more delicate tiered structure, with other choices for recycling such as "redesign", "renew", and "reuse". In this way, the maximum value of the resources can be preserved and reach a high level of circularity during the lifespan of multiple products [20]. Although the term "circular economy" may not have a universally agreed-upon definition, it generally encompasses the principles of reducing investment and reusing and recycling waste [15,21]. The CE model focuses on efficiently managing resources by minimizing consumption, and it substitutes the concept of "scrap" with the reuse, recycling, and renewal of materials and components [15,22].

The CE model has the potential to address the shortcomings of the linear economic model adopted by the building industry, resolving the tension between economic prosperity and environmental protection inherent in the linear economic model. However,

the application of the CE concept remains at an early stage [22]. To sustain the cyclical nature of architecture engineering, it is of great importance to integrate the environmental and economic impacts of construction impacts into structural design. Relying solely on green construction during the operational phase is not enough to reduce its environmental effects [22]. A critical issue in this aspect is the selection of building materials, which urgently requires alternative developmental paths or the procurement of building materials from different sources [23]. Research has pointed out that one possible strategy to balance efficiency and to curb climate change is to choose low-energy building materials. Utilizing renewable materials and transitioning from a disposable linear economy to the CE are two approaches to addressing resource scarcity. From this perspective, natural materials stand out as favorable options due to their low energy requirements and minimal embedded energy [24]. However, traditional buildings carry significant carbon footprints and contribute to environmental degradation [25,26].

The inception of bio-based materials began in France in the 2000s, while the concept was formally introduced in a decree issued on 19 December 2012. The content and attribution conditions relating to the label "bio-based buildings" are in line with EU Regulation No. 305/2011. Thus, bio-based materials are defined as "materials produced by plant or animal biomass that can be used as raw materials for building and decorative products, fixed furniture and building materials in buildings". Bio-based construction products consist of cellulosic biomass, which is mainly made up of the material straw, which forms the bulk of the volume, and also contains binders (synthetic or mineral) and additives (organic or inorganic). The latter is added to improve the performance, thus enhancing the durability, efficiency, and performance of building materials. They have many uses, such as as flame retardants (FR), water repellents, and fungicides or fungicides. The use of additives must be in accordance with EU regulations such as the Registration, Evaluation, Authorization and Restriction of Chemicals (REACH) regulation to avoid threatening human health or the environment.

Bio-based building materials appear to offer significant promise in advancing the sustainable development of the building industry. Firstly, buildings made of wood, straw, hemp or cork themselves have low environmental impacts. Bio-based materials, from their initial growth phase to their utilization, dismantling, and eventual recycling as building materials, form an entirely closed-loop system provided that the emissions related to the processes are disregarded [27]. Thus, the green construction technology represented by the use of bio-based materials, can contribute largely to the goal of lowering 50% of the global energy and materials consumption [28]. Secondly, with appropriate construction design, bio-based buildings' thermal capacity can match or even surpass the buildings using traditional petrochemicals as thermal materials [29]. Bio-based materials are also promising and effective building materials thanks to their carbon isolation effects, which can effectively reduce the carbon footprint of the construction industry [29].

This study explores the applicability of straw-bale building as a major bio-building type within the framework of the circular economy's 3R principles—reduce, reuse, recycle. By analyzing existing research on circular economy and bio-based construction, it aims to assess its feasibility and the potential of straw-bale building in promoting the circular economy, thereby offering an innovative approach to sustainable development.

2. Existing Research on the Circular Economy and Straw-Bale Buildings

2.1. Data Collection

For the literature reviews, we initially conducted a comprehensive literature examination across three domains, namely, the circular economy, its manifestations in the construction sector, and straw-bale construction. The Web of Science Core Collection's SCIE and SSCI databases were chosen for this research. While reviewing research on the circular economy, the term "circular economy" was used as the main search topic within the database, with the search duration set to "all" and the language filter for English. This yielded a total of 19,809 articles. In reviewing research on the manifestation of the circular

economy in the construction sector, both "circular economy" and "construction" were used as search topics in the database. The search duration remained set to "all", with the language filter set for English, resulting in 1624 articles. Subsequently, in reviewing research on straw-bale construction, the term "straw-bale construction" was searched for, with the search duration once again set to "all" and the language filter for English. This yielded 2409 articles.

2.2. Bibliometric Visualization Analysis

Using the visualization analysis tool provided by Web of Science, research trends over the years for both the circular economy and its manifestation in construction were acquired. From Figure 2, it can be concluded that the development trend of the circular economy and its application within construction are in synchrony, ascending concurrently. This proves that circular economy implementation within the construction sector positively correlates with and significantly contributes to the advancement of the overall circular economy.

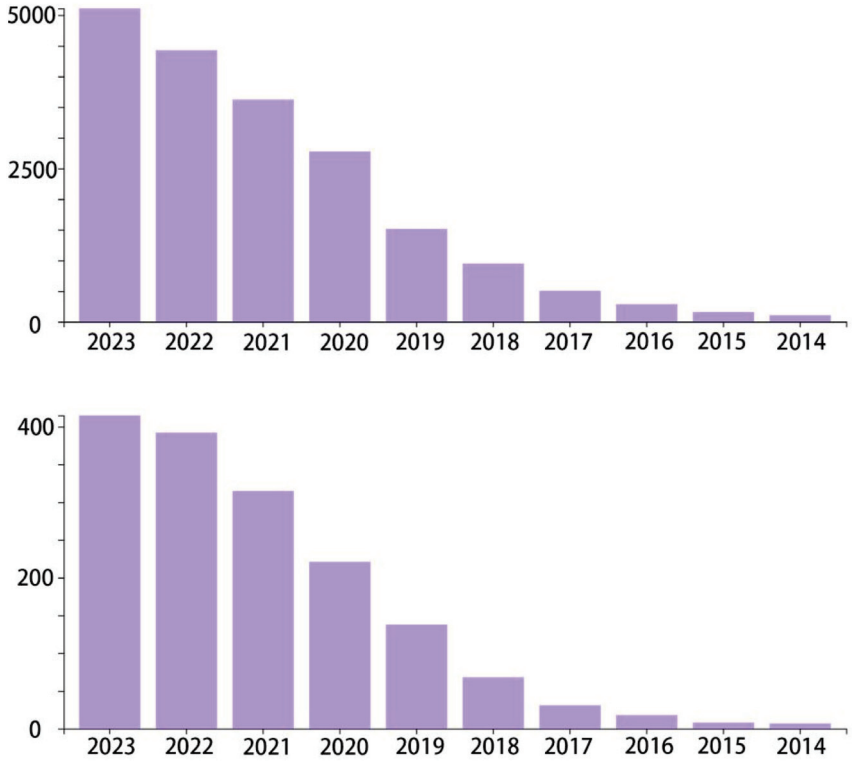


Figure 2. Annual publication trend of research articles on the circular economy (**above**) and its manifestation in the construction sector (**below**).

Using the Citespace tool, both sets of literature were subjected to visual analysis, encompassing keyword co-occurrence, clustering, and emergence to explore their content. As shown in Appendix A (Figures 1 and 2), the research found that the top ten keywords in the study of the circular economy in the construction field are "life cycle assessment", "management", "construction", "performance", "design", "energy", "system", "sustainability", "economy", and "waste" (Tables 1 and 2). The keywords "life cycle assessment" and "energy" highlight the importance of evaluating the environmental impacts and energy efficiency of construction materials such as straw bales. Straw-bale construction, which demonstrates a low energy consumption and high calorific value, becomes a viable, energy-efficient choice for the construction industry, aligning with the circular economy's focus on reducing energy use. Keywords including "management" and "system" emphasize the importance of structured approaches to recycling and resource management, indicating that systematic processes are crucial for enhancing sustainability in construction. The combination of "sustainability" and "waste" in research suggests an increasing trend

of using agricultural residues such as straw for construction purposes, promoting the transformation of waste into valuable resources. Discussions in the construction industry about "economy" and "waste management" show a shift toward a circular economic model where materials are reused to minimize waste. The construction industry's interest in straw-bale buildings, as an effective waste management and resource recycling strategy, reflects its commitment to the principles of a circular economy. The significant presence of keywords related to post-treatment processes like "combustion" and "anaerobic digestion" in straw-bale building research indicates potential areas for cross-industry dialogue within the circular economy framework, focusing on the downstream impacts and energy potential of recycled materials.

As shown in Appendix A (Figures 3 and 4), the research found that the top ten keywords in the literature on straw-bale buildings are "wheat straw", "straw", "performance", "rice straw", "behavior", "biomass", "mechanical property", "pretreatment", "enzymatic hydrolysis", and "waste" (Tables 3 and 4). These keywords cover various important aspects of straw-bale construction, from the basic characteristics of the materials to the application of processing technologies. The keywords "mechanical property" and "performance" point to the research focus on the mechanical and functional assessment of construction materials such as straw bricks, ensuring that these natural materials meet the structural and durability requirements for building applications. The keywords "enzymatic hydrolysis" and "pretreatment" highlight the technological processes for the effective transformation of biomass materials, steps that are crucial for enhancing the usability and performance of the materials. "biomass" and "behavior" may relate to how biomass materials react and interact in different environments, which are essential for understanding how materials perform under various conditions. The keyword "waste" reflects a core concept in the circular economy; namely, how to convert discarded agricultural residues into useful building and energy materials, thus achieving waste reduction and efficient resource utilization.

Table 1. Top 20 keywords in the circular economy literature.

Keywords	Frequency	Centrality	Year
life cycle assessment	218	0.06	2016
management	179	0.05	2017
construction	169	0.12	2016
performance	160	0	2018
design	143	0.23	2015
energy	131	0.22	2007
system	124	0.01	2016
sustainability	123	0.13	2011
economy	113	0	2007
waste	112	0	2018
framework	93	0.14	2014
impact	93	0.02	2014
demolition waste	87	0.04	2019
model	85	0.07	2018
barrier	83	0	2010
waste management	80	0.03	2018
concrete	78	0	2015
strategy	72	0.04	2018
built environment	71	0.01	2017
building material	70	0.02	2015

Table 2. Keyword clusters in the circular economy literature.

Number	Category
0	urban mining
1	circular economy
2	barriers
3	metabolic engineering
4	construction and demolition waste
5	carbon dioxide
6	industrial symbiosis
7	solid waste management
8	circular supply chain
9	renewable energy
10	smart city
11	urban agriculture
12	industry 4

Table 3. Top 20 keywords in the straw building literature.

Keywords	Frequency	Centrality	Year
wheat straw	313	0.15	1991
straw	243	0.1	1991
performance	171	0.03	2002
rice straw	168	0.15	2003
behavior	159	0.33	1992
biomass	150	0.38	1991
mechanical property	141	0.04	2008
pretreatment	86	0.23	2002
enzymatic hydrolysis	86	0.02	2004
waste	85	0.03	2002
lignocellulosic biomass	82	0	2013
soil	78	0.07	1995
concrete	78	0.05	2013
fiber	78	0.04	2000
wood	70	0.06	2001
carbon	69	0.23	1994
nitrogen	69	0.03	1991
energy	69	0.03	2007
impact	69	0	2012
lignin	66	0.09	1993

Table 4. Keyword clusters in the straw building literature.

Number	Category
0	thermal conductivity
1	organic matter
2	nest building
3	wheat straw
4	agricultural residues
5	solid convectivity
6	enzymatic hydrolysis
7	steam explosion
8	tandem mass
9	compressive strength
10	hemp concrete
11	anaerobic digestion
12	combustion

Based on the keywords and focal areas of the two research domains, it is evident that straw-bale buildings play a crucial role in achieving a circular economy in the construction field. Therefore, straw-bale buildings hold feasibility in realizing the circular economy in the construction field, showcasing considerable adaptability in certain aspects. Utilizing bio-based materials and agricultural residues to produce straw bricks can achieve resource recycling while offering energy-saving, low-carbon, and eco-friendly construction material options.

3. Achieving the "Reduce" Principle of the Circular Economy

The building industry stands as one of the foremost contributors to global waste generation, consuming vast quantities of natural resources and generating significant waste during construction and demolition processes. Thus, in order to minimize or eliminate this waste, advancements in technologies and methodologies are imperative [30]. Most of the construction activities still rely on labor-intensive on-site building methods, which, due to their high pollution levels, do not comply with sustainable development objectives. Moreover, these methods often lack stringent quality control due to site-specific conditions. Such activities also contribute to a lot of construction waste, which constitutes a significant challenge in waste management and disposal [31]. Meanwhile, building energy consumption is projected to rise steadily as a result of the increasing population and people's increasing demand for household appliances and indoor comfort [5]. Thus, the evaluation in the current study of buildings' energy consumption is of vital importance [32]. The focus on green construction, alongside its energy conservation implications has drawn more and more attention worldwide [33].

3.1. Reducing Construction Waste and the Environmental Impact

Bio-based fibers possess numerous advantageous properties, with straw being a notable example due to its renewability, biodegradability, and environmentally friendly production process [34]. Straw is a major bio-based chemical fiber derived from nature, and it is used as a building material after processing [35]. The method of deconstructing waste at the end of a building material's life cycle is very important. Figure 3 demonstrates how the prefabrication of bio-based materials in the construction process can diminish construction waste and the environmental impact. Straw naturally degrades in the soil and participates in the natural system, and thus no construction waste is produced. Moreover, finely crushed straw significantly shortens the broken length and increases the contact area of

straw stems with the external environment, thereby accelerating the decomposition rate of the straw [36]. Straw residues are potential sources of organic carbon and plant nutrients to improve soil organic matter dynamics, nutrient cycling, and the soil's physical environment. Compared with burning, cutting the straw and sending it back to the fields directly can avoid environmental pollution [37]. Meanwhile, all nutrients contained in the straw can be sent back to the soil in this way. Thus, the utility of the soil organic carbon and nutrients is promoted and the physical, chemical, and biological characteristics [38–40] of the soil are improved, facilitating nutrient recycling, averting nitrogen loss, and strengthening the soil's structure [41,42]. The cut straw can provide significant nutrients to increase crops' productivity as well.

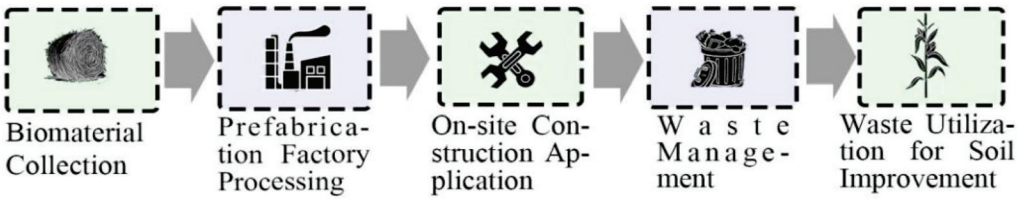


Figure 3. Prefabrication of bio-based materials in the construction process.

Meanwhile, the prefabrication of straw-bale buildings also plays a crucial role in determining the incidence of waste. With a prefabricated low-carbon modular construction system and the "design for disassembly" principle, straw-bale buildings stand the chance of avoiding waste and reducing greenhouse gas emissions [43]. The building type is built in a temporary "flying factory" near the construction site, mostly using local labor and straw. This process, besides reducing the waste produced during the pre-cutting of engineered timber, can utilize most of the materials with near-zero processing waste [44]. Recent research analyzed the impacts of the greenhouse gas produced in the buildings' life cycles and the life cycle of the prefabricated modular straw buildings by using the "cradle to demolishment" and "cradle to the grave" approaches [45,46]. The modular buildings perform better than conventional buildings, especially in their potential in decelerating global warming. Through the prefabrication mode, straw-bale buildings made in the planning and designing stages have reduced more waste in the construction sector than in on-site construction practice [47]. Furthermore, standardization, modularization, and prefabrication methods contribute to cost reduction in building construction. Compared with traditional construction methods, on-site prefabricated construction significantly minimizes construction waste, waste water, noise, toxic gases, and dust [48]. The potential for achieving zero-waste production through the recycling of prefabricated straw-bale buildings exemplifies the principle of green construction. It emphasizes waste reduction and building flexibility in the construction sector and thus mitigates the environmental impacts associated with building and demolition activities, which aligns closely with the concept of a circular economy (CE) [35,49].

3.2. Reducing the Energy Requirement

The embodied energy of bio-based materials are notably lower than that of fossil-based materials [50]. Therefore, recycling rich and renewable local biological resources in construction can significantly reduce energy consumption in the industry. Globally, industries are increasingly turning to manufacturing processes as they consume approximately 13% less energy than the electrical energy consumed in on-site construction. Meanwhile, the manufacturing processes of prefabricated construction consume around 28% less fuel than those of on-site construction [51].

As the main source of bio-based building materials, agricultural residues such as wheat, corn, and rice straw have long been utilized in building insulation due to their hollow structures, low cost, low density and thermal conductivity [5]. The thermal conductivity of ecological materials falls within a range of 0.035 to 0.051 W/(m.K), which is

similar to that of traditional insulation materials (0.030 and 0.042 W/(m.K)) [52]. Compared with the system of conventional buildings, straw-bale buildings are cost-effective and achieve high thermal performance [53]. This allows them enhance the thermal capacity of the buildings, improving insulation performance, reducing heat loss, and preventing overheating in summer [54].

Using straw bales as thermal insulation material not only saves energy [5] but also lowers the buildings' heating energy consumption and greatly reduces the need for heating and air conditioning, ensuring occupants' comfort [55]. Therefore, straw-bale buildings are commonly deemed suitable for regions with high heating needs. Wall et al. (2012) demonstrated through testing that prefabricated innovative low-carbon building prototypes using straw-bale plates exhibit excellent thermal performance [44].

The UK's Low Impact Affordable Communities for Living (LILAC) project highlights the benefits of using straw bales to improve the thermal envelope of buildings, resulting in reduced operational energy consumption. The project shows that typical apartments have a thermal energy usage of 35.73 kWh/m^2/year. By employing the ModCell straw-bale wall system, the energy efficiency ratio is 25% higher than that of the buildings built in accordance with the 2010 Building Code. This improvement is particularly advantageous given the average space heating demand of 140 kWh/m^2/year for existing housing stocks in the UK [56]. Furthermore, Yin et al. (2020) proposed an evaluation of energy sustainability of the buildings with straw-bale walls in China's rural areas, and the results showed that applying such structures can lower thermal consumption by 45.82–204.07 kWh/m^2/year and reduce coal consumption by over 40% (Figure 4) [37].

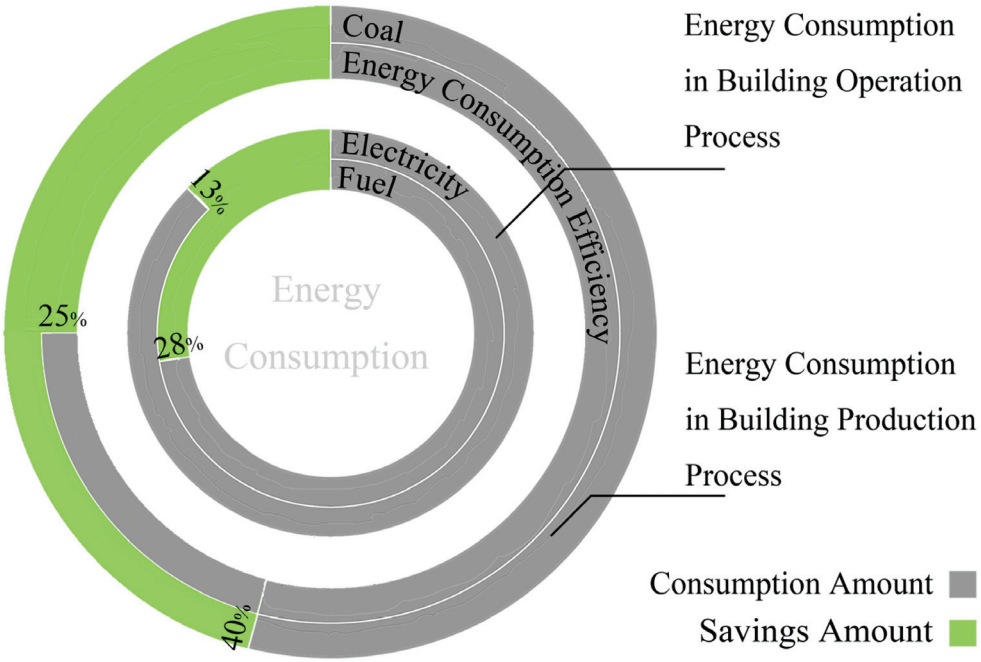


Figure 4. Energy consumption in building production process.

3.3. Reducing Carbon Emissions

Conventional construction materials including steel and cement have a significant impact on the environment. Cement, in particular, is a crucial building material but also contributes to approximately 5% of total man-made carbon dioxide emissions. This makes the cement industry a key sector for decelerating the emission of carbon dioxide [57]. With the increasing demand to reduce carbon emissions in the building industry, there is a growing need for low-embodied-carbon buildings. Globally, numerous initiatives are underway to reduce the carbon footprint of the building industry. Using bio-based building materials including straw bales can be an efficient method to achieve a low carbon footprint

for buildings [58]. Compared with concrete and other conventional building materials, straw bales are fully renewable and sequester carbon throughout their life cycle, effectively locking carbon within the plant-based building materials [32,59]. The proper treatment of bio-carbon storage is critical to quantifying greenhouse gas emissions from bio-based materials. Additionally, the production of bio-based materials results in lower carbon emissions and embodied energy compared with that of petrochemical materials [60]. The use of straw bales can greatly reduce carbon emissions and embodied energy compared with conventional materials, including fired brick and cement blocks [61].

Recently, scholars have researched the refinement of bio-based building materials, including straw bales [62]. Based on the research, quick-growing bio-materials show greater potential as carbon sinks due to their shorter rotation period, offering a greater capacity for carbon sequestration (Figure 5) [63]. Crop cycles of wheat and rice span less than a year, making them promising bio-based building materials. Wheat straw bales often absorb around 1.35 kg of carbon dioxide per kg of body weight [64]. According to the GWPbio figures, each kind of raw material and biological carbon repository can be used to quantify the effects of the carbon cycle [65]. Yin et al. suggested expanding the use of straw bales in future architectural designs in Northern China. They advocate incorporating straw bales into mainstream mid-rise structures to lower embodied carbon and operational carbon as well as to eliminate major pollution sources [53].

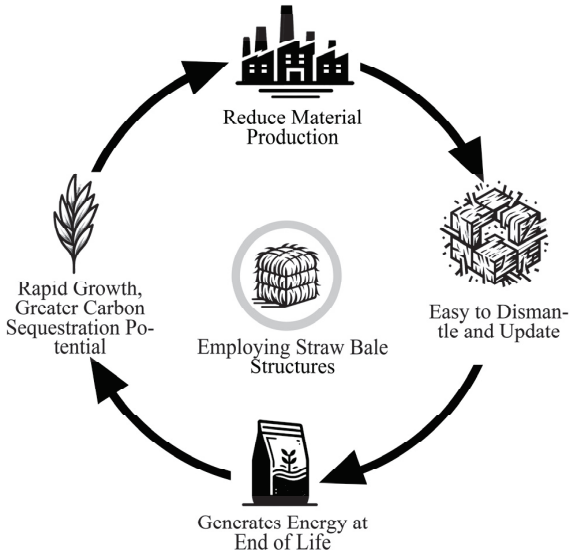


Figure 5. Carbon-reduction process for straw bales.

To understand the impact of biological carbon storage on climate change, researchers have evaluated the entire life cycle of products [66], including the initial stage (production, transportation to the construction site, and construction), the usage stage (maintenance, repair, and energy loss during transmission), and finally, the end of life (EOL) stage (demolishment, transportation, and EOL processing) [60]. Boyd et al. estimates that recycling and renewing can significantly reduce greenhouse gas emissions by over 50% compared with emissions from demolition alone, thus aiding the mitigation of global warming [67]. In addition, recycling replaces the preliminary production of new products and relieves the EOL burden on deserted buildings. Recycled materials can be reused in new buildings, building repairs, or renovation, thereby averting energy consumption and greenhouse gas emissions throughout the entire process from the raw material extraction to the final production. Cornaro et al. conducted an comparative life-cycle assessment of straw-bale walls and conventional fired-brick walls with the same thermal conductivity in the experimental building. The results indicate that during the production and construction stages, the equivalent carbon dioxide emissions and the embodied energy of the straw wall are 50% lower than those of the traditional wall [68].

Therefore, using straw-bale structures to replace conventional building envelopes serves a dual purpose: storing carbon and making contributions to global carbon-reduction targets by lowering carbon dioxide emissions. This occurs during both the construction stage and the demolition stage. Figure 5 illustrates the entire carbon-reduction process associated with straw-bale construction. Considering the carbon-sequestration function of bio-based materials comprehensively, the initial construction emits zero carbon. It is proved that the benefits of the carbon dioxide contained in bio-materials has the potential to significantly decelerate global warming. If these bio-materials are used to generate energy at the end of their life, carbon emissions can be further reduced [69]. In summary, compared with traditional construction materials, the use of bio-based building materials has significant potential to reduce carbon dioxide emissions in the building industry. Straw bales, as a kind of bio-based building material, have a notable advantage in carbon sequestration throughout the building life cycle compared with traditional materials. This advantage will lower the carbon footprint associated with the building industry. Additionally, this type of bio-based material plays a positive role in enhancing the soil quality and increasing crop yields as well. Therefore, the promotion of bio-based building materials such as straw bales will have a positive impact in mitigating global warming. It can help the construction industry achieve low-carbon goals and promote the effective use of agricultural waste at the same time. Moreover, the end-of-life conversion of bio-based building materials into energy could further reduce carbon emissions, underscoring the vital role of the circular economy and green building in achieving environmental sustainability.

4. Achieving the "Reuse" Principle of the Circular Economy

Biomass derived from agricultural waste is abundant on Earth. Agricultural waste, including wheat straw and straw, are often either used for animal feed or burned in the fields, which not only adds negative economic value [70] but also contributes to serious air pollution [71]. Addressing this issue demands environmentally friendly disposal solutions for straw rather than the current practice of field burning. Embracing sustainable approaches to utilizing crop stubble can notably mitigate air pollution arising from open burning [72]. Some countries have implemented agricultural production policies to prohibit the burning of primary resources in situ. Therefore, agricultural residues have become abundant, requiring new markets and appropriate applications. To meet the reuse principle of CE, straw-bale buildings offer a dual benefit: the reuse of agricultural byproducts and the ability to be disassembled through prefabrication.

4.1. Reuse of Agricultural Waste Resources

As a kind of solid waste, straw used in building materials has been widely discussed for reuse worldwide. Straw, being one of the most abundant lignocellulosic agricultural residues globally, represents a crucial natural resource. In China, for instance, the substantial amount of recycled straw residue in the field and the portion that can be collected and utilized by direct repair amount to approximately 616,000 tons, accounting for about three-quarters of the total straw production [73]. This serves as a powerful driving force for expanding the use of straw in the building industry. Agricultural straw, due to its hollow structure, low thermal conductivity, low density, and low cost [74], is considered to be a better building material compared with conventional construction materials. The use of straw bales in the building industry will facilitate the disposal of straw and will provide an energy-efficient alternative to current building types. Straw bales, typically sourced from wheat, oats, or other types of straw, are utilized to create building envelopes. The UK Lilac Garden community adopted straw and wood as a source of materials for bio-based buildings due to their suitability for community-built elements and their potential to bolster local supply chains. In the UK alone, 2.37 million tonnes of waste straw are returned into farmland annually, enabling 423,000 houses to be built [56], underscoring the significant potential for straw reuse in the building industry.

Platt et al. investigated the novel production of oriented prototype straw bales with the specific objective of their application in the construction sector [75]. Their innovative approach involves repurposing straw originally sourced from agricultural bales (Figure 6). The reconfiguration of the baling process is aimed at orienting the straw fibers in a preferential manner to substantially enhance both thermal resistance and mechanical performance. In this process, the loose straw is manually loaded into a compaction chamber and subsequently compressed utilizing a hydraulic jack. This re-baling process yields significant improvements in thermal resistance, with a reduction of approximately 28% in the required insulation thickness.



Figure 6. Production of oriented prototype straw bales.

Therefore, bio-based architecture stands out for its utilization of abundant available agricultural waste resources that are all derived from recycled products, thereby fostering a circular economy. Leveraging agricultural waste as an alternative to conventional building materials and integrating recycling into production processes can significantly mitigate environmental impacts. This approach represents a prime CE strategy for reducing environmental impacts while adding more value to the product [76].

4.2. Ability to Disassemble Achieved by Prefabrication

The average composition of building demolition waste in Europe shows that up to 85% of waste is stone waste [77], such as end-of-life (EOL) concrete. At present, the recycling of waste mainly focuses on scrap metal and steel products with higher value added. Most of the waste is exposed to the open air or deposited in landfills without any treatment, which not only leads to substantial waste removal expenses but also occupies land, and the accumulation of untreated waste poses a significant risk of environmental pollution.

Recent prefabrication innovations have revolutionized the new building industry, accelerating the prefabrication of buildings. Prefabrication of frames, in particular, is gaining traction as a viable alternative to traditional demolition and recycling methods [78]. Prefabricated straw-bale buildings adopt the general project contracting mode, which firstly optimizes the architectural design and material selection and assembly based on the technical characteristics of straw-bale buildings. This system includes the design of basic living units that can be superficially grown, the design of invisible variable nodes that are convenient for disassembly and assembly, and the architectural responsibility system based on the general contract management mode of EPC projects. It is often suggested that deconstruction, demolition design, and reuse design need to be incorporated into the design phase, which is crucial for reducing the generation of construction waste [30]. To get rid of landfills, products should prioritize their reconfigurability and detachability, making them easy to dismantle or recycle during their usage stage.

As shown in Figure 7, the prefabrication of straw-bale buildings has defined the organization of routine procedures and operating procedures [79], making the disassembly and deconstruction of building structures more convenient. This approach promotes the design of the life cycle and ensures the material uniformity of buildings with extensive service

lives [79]. The premise of deconstruction lies in the design of prefabricated, preassembled, and modular structures and the simplification and standardization of connecting details, along with designs that accommodate deconstructed logistics, the reuse of materials and the realization of a closed-loop cycle building materials [80]. Due to efficient manufacturing, prefabricated timber structure construction activities reduce wood waste to almost zero [81], thus making it easier to reuse and recycle building components and materials after the end of the structure's life [31,82]. Overall, prefabricated bio-based building materials are easy to be recycled in two aspects. Firstly, waste minimization during the design phase involves the design of structures and goods with an extended service life, making them easy to repair, upgrade, or use in different ways in future cycles. This approach is supplemented by avoiding errors and by guiding construction activities while taking into account waste minimization [3]. Secondly, the prefabrication of bio-based buildings adopts the off-site construction mode, which helps to reduce the wasting of resources and which makes it possible to disassemble and reuse building components in other places. There are four main scenarios for the reuse of bio-based building materials after deconstruction, such as (1) the relocation of buildings; (2) the reuse of components; (3) the reprocessing of materials; and (4) the recycling of materials. Of the four cases, reuse is preferred over reprocessing or recycling because it requires no additional energy, whereas reprocessing or recycling involves degradation and a limited contribution to new products. Through prefabrication and a modular design, bio-based building materials can achieve higher resource efficiency and environmental friendliness throughout the building life cycle. Prefabrication not only reduces material waste during construction but also simplifies the process of material recovery and reuse during the demolition phase. This approach not only enhances the overall sustainability of building materials but also provides the construction industry with a practical pathway to transition toward a circular economy. By optimizing design and construction processes, material utilization can be significantly improved, reducing the environmental impact.

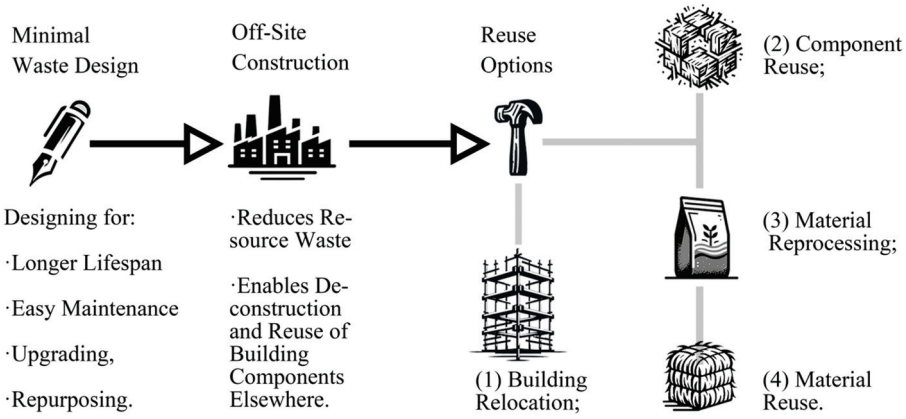


Figure 7. Advantages of prefabrication in straw-bale buildings.

In addition to the process, the most common way to recycle concrete from traditional buildings is to simply break it and then use it as a foundation for road construction, which is considered to be a low-grade or low-value-added route. For high-grade concrete recycling, the wet process is typically utilized. However, this method necessitates large washing equipment, which can be prohibitively expensive [83], so the recycling of ordinary (normal weight) concrete waste is not yet popular in the EU. Conversely, prefabricated straw-bale buildings are based on modular products which are constructed off-site. Compared with reinforced concrete, they can be easily dismantled for reuse or used as energy sources at the end of the building life span.

Shea et al. introduced the ModCell prefabricated straw-bale panel system [84]. This innovative panel is assembled by using straw bales to fill a supporting framework measuring a dimension of 3.19 m in width, 2.66 m in height, and 0.49 m in thickness (Figure 8).

Typically, the framework is made from engineered glue- or cross-laminated timber. The internal arrangement of straw bales adheres to a traditional brick-wall masonry pattern, with alternating stacking and secure fastening accomplished using timber dowels. Additionally, stainless steel reinforcements are incorporated as corner braces and vertical strapping is used to reinforce the structure. Both faces of these panels are meticulously coated with lime render in three layers. Notably, this panel system has demonstrated its practicality and effectiveness through its successful implementation in the construction of a prototype building located at the University of Bath, known as the BaleHaus at Bath.



Figure 8. ModCell panel (**left**) and the complete prototype house at the University of Bath campus (**right**).

5. Achieving the "Recycle" Principle of the Circular Economy

Solid-waste management is a challenge for urban authorities in developing countries. The main reason is that the increased waste production has burdened municipal budgets with high management costs. Thus, using sustainable technologies to decelerate climate change and to provide continuous energy is vital for realizing a CE [85]. As the fourth-largest energy source in the world, biomass can be transformed into new energy products like electric power, molded fuel, methane, liquid fuel, etc., which is rather important not only for tackling global climate change and the contradiction between power supply and demand but also for ecological and environmental protection [86]. Crops used as bio-based construction materials, such as agricultural and forestry residues, can be recycled and re-enter the circulatory system after reprocessing. This transmission be achieved in three major ways: physical treatment, involving the use of grass clippings as pressure plates; biochemical (physical) treatment, which involves gas by fermentation; and (thermal) chemical treatment, which provides energy for heat, steam, electricity and biological fuel by methods like direct combustion [87–89].

5.1. Recycling through Physical Treatment Processes

Wood waste such as wooden floors, ceilings, and ornaments from construction and demolition sites accounts for 10% of the total amount of waste, surpassing only concrete waste. The wood waste generated in construction and demolition sites is usually not included in any recycling list and ends up in combustion facilities or landfills [90]. In the face of worldwide shortages of forest resources, there is growing interest in producing particleboards with agricultural residues [91]. Wood has always been the main source of raw materials for particleboards and fiberboards, while wood biomass is the most traditionally used raw material in the lignocellulosic biocomposite industry [92]. The topic of how to recycle construction wood residues into useful products has been studied for decades [93], and the most common method of reusing them is to manufacture particleboards from wood waste recycled from construction.

Yet recently, rice–wheat straw (RWS) has drawn more attention from researchers. Wheat straw contains large amounts of fiber. Particleboards with densities ranging from 0.59 to 0.8 g/cm^3 are named medium-density particleboards. Straw particleboards, due

to their rigidity, strength, and low cost, are applied widely [94] and have the potential to replace wood in particleboard manufacturing [95]. Therefore, it is possible to use straw brick-wall envelopes as raw materials for making particleboards, which will alleviate the huge demand for wood. By grinding the recycled straw bales into fibrous particles [96] and using phenolic resin as the adhesive, it is possible to produce polymer composite particleboards [97] with low formaldehyde content [98].

Among many products, the recommended properties of wood particle composite boards are that they are able to absorb noise, maintain the temperature of the indoor living space, and partially or completely substitute for timber particleboards and heat shields [99]. The straw–wood particle composite boards adopt the approach taken in the man-made board sector to produce insulation boards. Agricultural lignocellulose fibers such as rice and wheat straw can easily break into fragments or granules, similar to wood particles or fibers (Figure 9). Straw is also chosen as a raw material because of its usability [99]. We can use straw–wood particle composite materials both as insulation materials and as insulation boards. Insulation boards can be used for a variety of purposes, including for roof and wall sheathing, subfloors, the interior surfaces of walls, and ceilings.



(**a**) (**b**)

Figure 9. (**a**) Solid-wood particle board; (**b**) and straw–wood particle board.

5.2. Recycling through Physical Biological Processes

Biological energy is the main domestic energy for rural families in developing countries, because it is cheap and readily available. Using biological energy productively is a major strategy not only for rural families to raise their salaries but also for improving their health, living environment, etc. [100]. Wheat straw waste used in bio-based buildings has great potential for anaerobic digestion [101], which, if transformed appropriately and biologically into methane, can be a potential source of energy [101,102].

The anaerobic biological treatment of agricultural solid waste has become more and more important in recent years. As shown in Figure 10, the technology to transform agricultural biomass waste into bioenergy is environmentally friendly and sustainable. Anaerobic digestion, a biological process facilitated by various types of microbes, decomposes biomass waste into energy. The process occurs in an anaerobic environment, utilizing macrobes that can decompose organic ingredients into biogas to produce methane [103]. How much methane can be produced during the anaerobic digestion of biodegradable organic matter depends on the amount and type of material added to the system [101]. After being preprocessed at 180 °C, wheat straw produces 53% more biogas [104], which can be used to power EDM or turbines.

In addition, there is a growing interest in transforming manure-crop residue mixtures into methane for its clear benefits. Firstly, when crop residues are mixed with manure, more methane can be generated, as the annual amount of corn stalks and wheat straw is about four times that of manure [105]. Secondly, such a mixture can improve the nutritional compatibility of high-nitrogen fertilizers and produce crop residues with high carbon content but deficient in nitrogen. Research indicated that mixing pig manure and corn stalks can generate fertilizers. Methane yields from manure–straw mixtures are significantly higher than those from pig manure or straw alone, which is attributed to a more favorable carbon–oxygen ratio [106,107]. Adding straw to pig manure enhances the

biogas yield in thermophilic anaerobic digestion, with over 50% of the carbon in straw converted into gas. Moreover, bio-based products deprived of additives can be recycled or reused for composting or biodegradation. They can also be transformed into energy or sent to landfills. Unlike polyurethanes, straw can be composted simply after selective deconstruction. The composition or chemical properties of carbohydrates (such as lignin, cellulose, hemicellulose content) and the density of other nutrients they contain are related to all sorts of domestic and industrial applications [73].

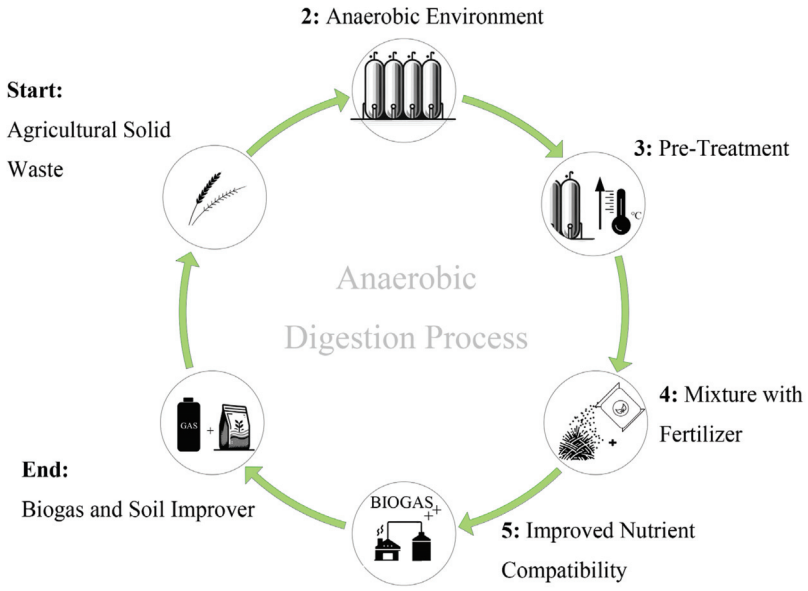


Figure 10. Anaerobic digestion process.

5.3. Recycling through Biochemical Conversion (Thermochemical Conversion)

Rising energy prices and environmental demands have rekindled people's interest in harnessing crop residues for energy production. Biomass energy is the richest and most versatile renewable energy in the world [108], with the potential to significantly contribute to the renewable energy supply by producing useful and valuable bio-fuels [109]. Crop residues such as grain and corn stalk residues can be transformed into liquid or gaseous bio-fuels through thermochemical or biotechnological processes, representing a promising resource for bio-energy development [110]. Transforming agricultural residues into biomass feedstocks for power generation and district heating is becoming increasingly common [111], particularly in rural areas of developing countries [112], where the potential of crop residues for bio-energy is gaining more and more attention [113].

Straw stubble used in bio-based buildings, such as cellulose and lignin, contains large amounts of biochemical energy. This kind of biomass can be partly acquired in a sustainable way. If combusted at the end of its service life, it can be converted into bioenergy generating heat and/or electricity [87] to offset the consumption of fossil fuels [114], effectively recycling its energy [115]. Pulverized biomass fuels burn much faster than coal and can produce flames similar to oil or gas fuels, delivering the same high-power output [116]. Due to the more efficient processing and combustion, the energy cost in upgrading is fully compensated. As with the energy balance, production costs are recovered from combustion, ensuring a balanced energy budget. Additionally, a higher combustion efficiency can also lower the consumption of fuels [116].

Meanwhile, different residues from crop production hold potential for meeting renewable energy targets. Applying biomass to transporting fuels can increase the use of heat and electricity production significantly [117]. Specific regulations on how to improve and ensure the productive utilization of bioenergy are also needed [100]. The new emerging concept of integrated waste bio-refinery fosters the circular bio-economy and addresses current waste issues [52]. It involves the integration of several biochemical or thermochem-

ical transformations to produce value-added products, essential for achieving a circular economy in developing countries [118]. Rabbat et al. [52] proposed a waste management strategy pertaining to bio-based building products that focuses on waste-to-energy (WTE) routes. In cases of non-recyclable wastes, this strategy diverges from traditional landfill disposal methods. Instead, it entails the conversion of bio-based construction waste into thermal energy, electricity, and alternative fuels to cater to market demands, yielding substantial financial gains. It is projected to mitigate around 315,000 tons of CO_2 emissions and conserve 75,000 tons of fossil fuels per tonnage of waste valorized, amounting to an estimated economic benefit of 78.9 million euros. Furthermore, the recovered energy can be seamlessly integrated into an integrated biorefinery system, allowing for the production of value-added products such as bioenergy, biochemicals, and biofuels. Consequently, this comprehensive strategy not only contributes significantly to environmental preservation but also generates substantial economic profits.

As the global demand for sustainable buildings grows, it is expected that more projects will adopt bio-based materials in the future. These materials not only help reduce construction waste and carbon emissions but also significantly enhance the overall environmental performance of buildings through their recyclability and reusability features. Moving forward, policymakers and the construction industry should focus more on integrating circular economy principles into building design and construction. This may include promoting the use of environmentally friendly building materials through legislation and regulations, as well as supporting the research and development of new material technologies to enhance efficiency and sustainability. Additionally, public awareness and consumer demand for eco-friendly buildings will continue to drive the market toward these solutions. Therefore, the construction industry is likely to undergo a significant transformation by using bio-based materials and circular economy approaches, addressing environmental issues while also driving technological innovation and economic growth.

6. Conclusions

In conclusion, this review proposes a bio-based building material solution that elaborates the circularity of straw-bale buildings from the basic dimensions of the 3R principles of the circular economy. It evaluates the contribution of straw-bale buildings and the use of straw as a raw material within the context of CE principles, identifying future research opportunities for achieving a circular economy in the building industry.

The research underscores several environmental benefits of the transition from bio-based buildings to a circular built environment:

"Reduce" principles: (1) Reduce the construction waste and environmental impact; (2) Lower the energy requirement; (3) Minimize carbon emissions;

"Reuse" principles: (1) Reuse agricultural waste resources; (2) Enable disassembly through prefabrication;

"Recycle" principles: (1) Utilize physical treatment processes for recycling; (2) Employ biological processes for recycling; (3) Explore biochemical conversion (thermochemical conversion) for recycling. This approach can not only facilitate the production of wooden composite boards but also offers the potential for converting waste into biogas and biomass fuels for electricity and heating purposes.

Properly transforming and utilizing straw in straw-bale construction can effectively reduce the pollution caused by straw burning while also providing additional policy compensation to villagers. The results of this study offer valuable insights into circular economy solutions and interdisciplinary research for the building industry, serving as a resource for both researchers and practitioners interested in the CE and the building environment. This study utilizes years of experience gained in policies and industry and explores how to fully utilize bio-based buildings from a CE perspective, which may be the key to achieving a circular building industry.

An important aspect of future work is to make necessary adjustments to the current building design standards in order to incorporate them into the circular strategy of this

study. In addition, future research may explore in more detail the connection between circular construction technology and social challenges in order to find more scientifically reasonable solutions. For example, material costs are integral to overall construction expenses and can influence the selection of bio-based building materials. Even though bio-based buildings have a better CO_2 balance, in most cases, they are not necessarily a cost-effective option for reducing emissions in the long run. For this reason, a more detailed cost analysis should be done before policymakers begin to design and promote policies on bio-based buildings. Establishing cost-effective solutions could significantly enhance the closed loop of these emerging materials and bolster the circularity of the built environment.

Author Contributions: Conceptualization, X.Y.; methodology, A.L. and X.Y.; writing—original draft preparation, A.L., C.G. and J.G.; writing—review and editing, X.Y. and Y.H.; visualization, C.G. and J.G.; supervision, Z.L.; project administration, Z.L.; funding acquisition, A.L. All authors have read and agreed to the published version of the manuscript.

Funding: This work research was funded by the National Natural Science Foundation of China (Grant No: 52008127) and the Annual Project of Philosophy and Social Science Research Planning of Heilongjiang Province (Grant No: 22JYC328).

Data Availability Statement: No new datasets were created or analyzed during this study. Data sharing is not applicable to this article as no datasets were generated or analyzed.

Conflicts of Interest: The authors declare no conflicts of interest.

Appendix A

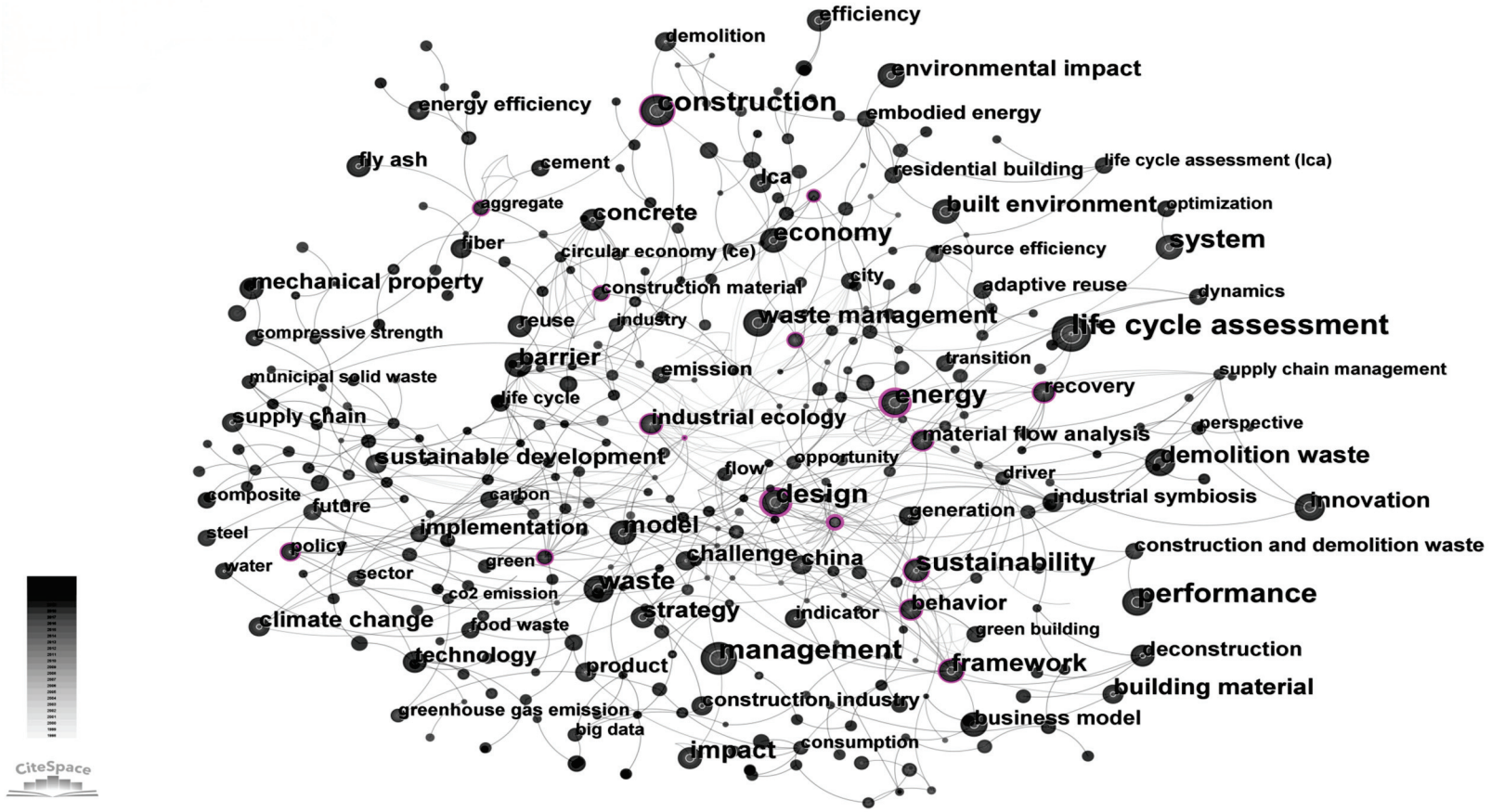


Figure 1. Keyword co-occurrence in the literature search on the circular economy in the construction field (Purple edges indicate high centrality of keywords).

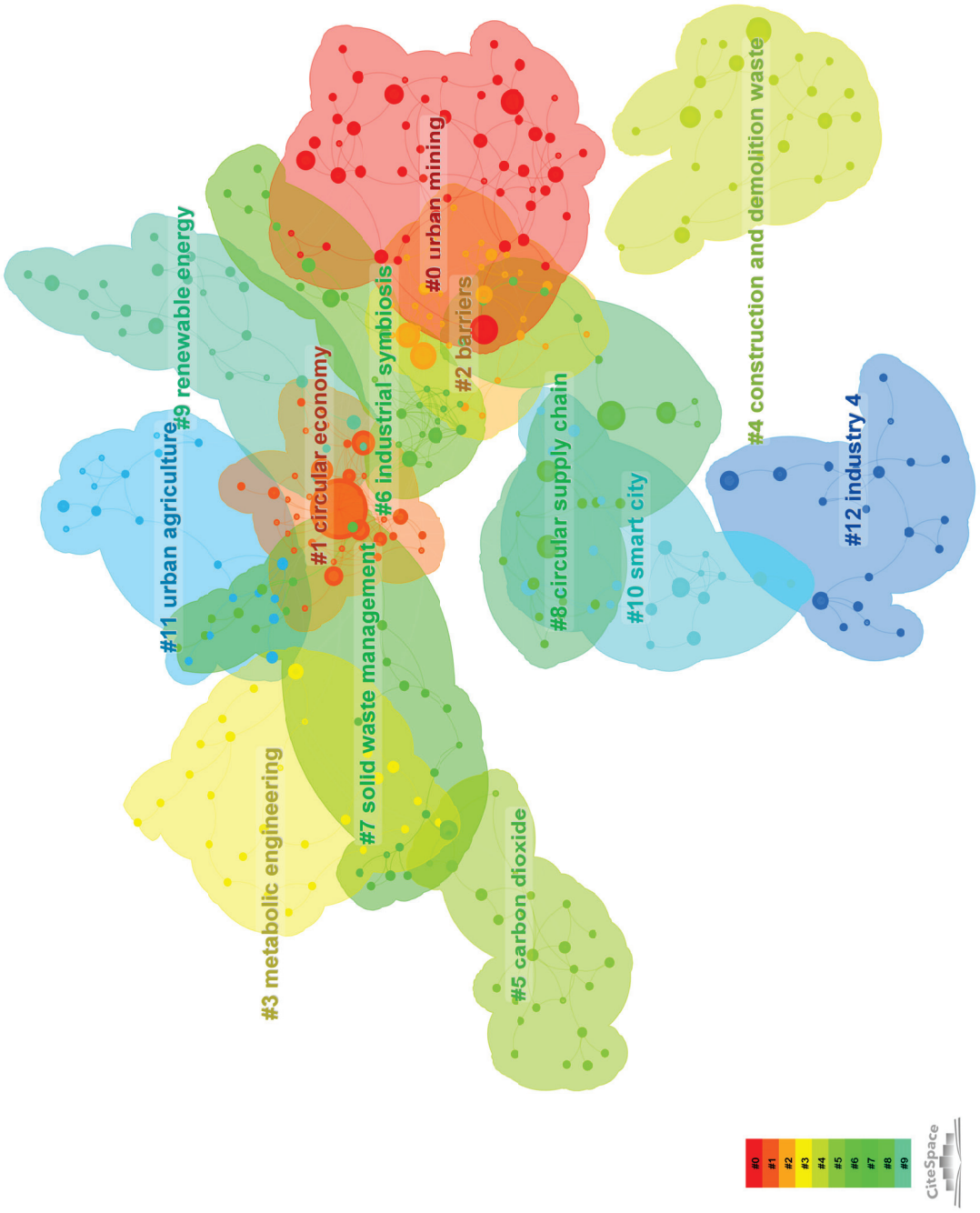


Figure 2. Keyword clustering in the literature search on the circular economy in the building industry.

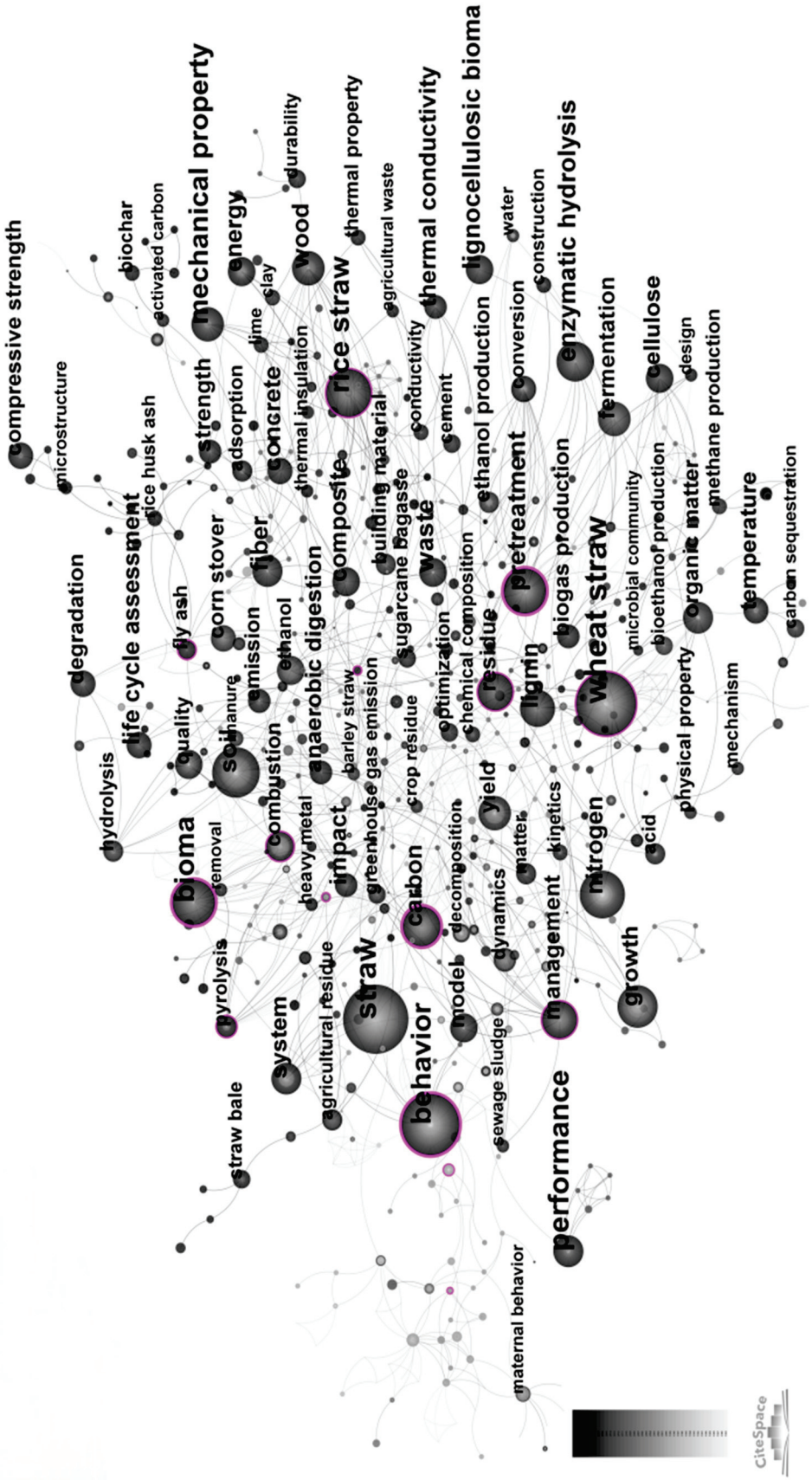


Figure 3. Keyword co-occurrence in the literature search on straw-bale construction (Purple edges indicate high centrality of keywords).



Figure 4. Keyword clustering in the literature search on straw-bale construction.

References

1. Lima, L.; Trindade, E.; Alencar, L.; Alencar, M.; Silva, L. Sustainability in the construction industry: A systematic review of the literature. *J. Clean. Prod.* **2021**, *289*, 125730. [CrossRef]
2. Reis, G.S.d.; Quattrone, M.; Ambrós, W.M.; Cazacliu, B.G.; Sampaio, C.H. Current applications of recycled aggregates from construction and demolition: A review. *Materials* **2021**, *14*, 1700. [CrossRef] [PubMed]
3. Shooshtarian, S.; Maqsood, T.; Caldera, S.; Ryley, T. Transformation towards a circular economy in the Australian construction and demolition waste management system. *Sustain. Prod. Consum.* **2022**, *30*, 89–106. [CrossRef]
4. Arora, N. Environmental Sustainability-necessary for survival. *Environ. Sustain.* **2018**, *1*, 1–2. [CrossRef]
5. Liu, L.; Li, H.; Lazzaretto, A.; Manente, G.; Tong, C.; Liu, Q.; Li, N. The development history and prospects of biomass-based insulation materials for buildings. *Renew. Sustain. Energy Rev.* **2017**, *69*, 912–932. [CrossRef]
6. Pieroni, M.P.P.; McAloone, T.C.; Pigosso, D.C.A. Business model innovation for circular economy and sustainability: A review of approaches. *J. Clean. Prod.* **2019**, *215*, 198–216. [CrossRef]
7. Jesus, A.D.; Mendonça, S. Lost in transition? Drivers and barriers in the eco-innovation road to the circular economy. *Ecol. Econ.* **2018**, *145*, 75–89. [CrossRef]
8. Ghisellini, P.; Cialani, C.; Ulgiati, S. A review on circular economy: The expected transition to a balanced interplay of environmental and economic systems. *J. Clean. Prod.* **2016**, *114*, 11–32. [CrossRef]
9. Ghisellini, P.; Ripa, M.; Ulgiati, S. Exploring environmental and economic costs and benefits of a circular economy approach to the construction and demolition sector. A literature review. *J. Clean. Prod.* **2018**, *178*, 618–643. [CrossRef]
10. Charef, R.; Morel, J.C.; Rakhshan, K. Barriers to implementing the circular economy in the construction industry: A critical review. *Sustainability* **2021**, *13*, 12989. [CrossRef]
11. Wübbeke, J.; Heroth, T. Challenges and political solutions for steel recycling in China. *Resour. Conserv. Recycl.* **2014**, *87*, 1–7. [CrossRef]
12. Bocken, N.M.P.; Olivetti, E.A.; Cullen, J.M.; Potting, J.; Lifset, R. Taking the circularity to the next level: A special issue on the circular economy. *J. Ind. Ecol.* **2017**, *21*, 476–482. [CrossRef]
13. Pauliuk, S. Critical appraisal of the circular economy standard BS 8001:2017 and a dashboard of quantitative system indicators for its implementation in organizations. *Resour. Conserv. Recycl.* **2018**, *129*, 81–92. [CrossRef]
14. Jiménez Rivero, A.; Sathre, R.; García Navarro, J. Life cycle energy and material flow implications of gypsum plasterboard recycling in the European Union. *Resour. Conserv. Recycl.* **2016**, *108*, 171–181. [CrossRef]
15. Kirchherr, J.; Reike, D.; Hekkert, M. Conceptualizing the circular economy: An analysis of 114 definitions. *Resour. Conserv. Recycl.* **2017**, *127*, 221–232. [CrossRef]
16. Pesce, M.; Tamai, I.; Guo, D.Y.; Critto, A.; Brombal, D.; Wang, X.H.; Cheng, H.G.; Marcomini, A. Circular economy in China: Translating principles into practice. *Sustainability* **2020**, *12*, 832. [CrossRef]
17. Cagno, E.; Trucco, P.; Tardini, L. Cleaner production and profitability: Analysis of 134 industrial pollution prevention (P2) project reports. *J. Clean. Prod.* **2005**, *13*, 593–605. [CrossRef]
18. Figge, F.; Young, W.; Barkemeyer, R. Sufficiency or efficiency to achieve lower resource consumption and emissions? The role of the rebound effect. *J. Clean. Prod.* **2014**, *69*, 216–224. [CrossRef]
19. Jayawardana, J.; Sandanayake, M.; Kulatunga, A.K.; Jayasinghe, J.A.S.C.; Zhang, G.M.; Osadith, S.A.U. Evaluating the circular economy potential of modular construction in developing economies—A life cycle assessment. *Sustainability* **2023**, *15*, 16336. [CrossRef]
20. Reike, D.; Vermeulen, W.J.V.; Witjes, S. The circular economy: New or refurbished as CE 3.0?—Exploring controversies in the conceptualization of the circular economy through a focus on history and resource value retention options. *Resour. Conserv. Recycl.* **2018**, *135*, 246–264. [CrossRef]
21. Homrich, A.S.; Galvão, G.; Abadia, L.G.; Carvalho, M.M. The circular economy umbrella: Trends and gaps on integrating pathways. *J. Clean. Prod.* **2018**, *175*, 525–543. [CrossRef]
22. Andersen, S.C.; Birgisdottir, H.; Birkved, M. Life cycle assessments of circular economy in the built environment—A scoping review. *Sustainability* **2022**, *14*, 6887. [CrossRef]
23. Smol, M.; Kulczycka, J.; Henclik, A.; Gorazda, K.; Wzorek, Z. The possible use of sewage sludge ash (SSA) in the construction industry as a way towards a circular economy. *J. Clean. Prod.* **2015**, *95*, 45–54. [CrossRef]
24. Melià, P.; Ruggieri, G.; Sabbadini, S.; Dotelli, G. Environmental impacts of natural and conventional building materials: A case study on earth plasters. *J. Clean. Prod.* **2014**, *80*, 179–186. [CrossRef]
25. Pomponi, F.; Moncaster, A. Embodied carbon mitigation and reduction in the built environment—What does the evidence say? *J. Environ. Manag.* **2016**, *181*, 687–700. [CrossRef] [PubMed]
26. Allwood, J.M.; Ashby, M.F.; Gutowski, T.G.; Worrell, E. Material efficiency: A white paper. *Resour. Conserv. Recycl.* **2011**, *55*, 362–381. [CrossRef]
27. Kromoser, B.; Reichenbach, S.; Hellmayr, R.; Myna, R.; Wimmer, R. Circular economy in wood construction—Additive manufacturing of fully recyclable walls made from renewables: Proof of concept and preliminary data. *Constr. Build. Mater.* **2022**, *344*, 128219. [CrossRef]
28. Çetin, S.; De Wolf, C.; Bocken, N. Circular digital built environment: An emerging framework. *Sustainability* **2021**, *13*, 6348. [CrossRef]

29. Bo, R.; Zhang, H.R.; Ma, Z.X.; Yin, R.Y.; Li, A.; Yin, X.Z. Straw bale construction towards nearly-zero energy building design with low carbon emission in northern China. *Energy Build.* **2023**, *298*, 113555. [CrossRef]
30. Udawatta, N.; Zuo, J.; Chiveralls, K.; Zillante, G. Improving waste management in construction projects: An Australian study. *Resour. Conserv. Recycl.* **2015**, *101*, 73–83. [CrossRef]
31. Jaillon, L.; Poon, C.S. Life cycle design and prefabrication in buildings: A review and case studies in Hong Kong. *Autom. Constr.* **2014**, *39*, 195–202. [CrossRef]
32. Nässén, J.; Hedenus, F.; Karlsson, S.; Holmberg, J. Concrete vs. wood in buildings—An energy system approach. *Build. Environ.* **2012**, *51*, 361–369. [CrossRef]
33. Zairul, M. The recent trends on prefabricated buildings with circular economy (CE) approach. *Clean. Eng. Technol.* **2021**, *4*, 100239. [CrossRef]
34. Li, Z. Development and perspective of bio-based chemical fiber industry. *Chin. J. Biotechnol.* **2016**, *32*, 775–785.
35. Purchase, C.; Zulayq, D.; O'Brien, B.; Kowalewski, M.; Berenjian, A.; Tarighaleslami, A.H.; Seifan, M. Circular economy of construction and demolition waste: A literature review on lessons, challenges, and benefits. *Materials* **2021**, *15*, 76. [CrossRef]
36. Prats, S.A.; Merino, A.; Gonzalez-Perez, J.A.; Verheijen, F.G.A.; De la Rosa, J.M. Can straw-biochar mulching mitigate erosion of wildfire-degraded soils under extreme rainfall? *Sci. Total Environ.* **2021**, *761*, 143219. [CrossRef]
37. Yin, X.Z.; Yu, J.Q.; Dong, Q.; Jia, Y.H.; Sun, C. Energy sustainability of rural residential buildings with bio-based building fabric in northeast China. *Energies* **2020**, *13*, 5806. [CrossRef]
38. Mandal, K.G.; Misra, A.; Hati, K.; Bandyopadhyay, K.; Ghosh, P.; Mohanty, M. Rice residue-management options and effects on soil properties and crop productivity. *Food Agric. Environ.* **2004**, *22*, 224–231.
39. Tirol-Padre, A.; Tsuchiya, K.; Inubushi, K.; Ladha, J.K. Enhancing soil quality through residue management in a rice-wheat system in fukuoka, Japan. *Soil Sci. Plant Nutr.* **2005**, *51*, 849–860. [CrossRef]
40. Singh, Y.-S.; Gupta, R.; Singh, G.; Singh, J.; Sidhu, H.; Singh, B. Nitrogen and residue management effects on agronomic productivity and nitrogen use efficiency in rice—Wheat system in Indian Punjab. *Nutr. Cycl. Agroecosyst.* **2009**, *84*, 141–154. [CrossRef]
41. Odogwu, J.A.; Atere, C.T.; Olayinka, A.; Adegbite, M.O. Microbial respiration and nitrogen and phosphorus mineralization in cow dung—Amended soils depending on moisture contents: A microcosm study. *J. Soil Sci. Plant Nutr.* **2022**, *22*, 1044–1051. [CrossRef]
42. Abera, G.; Wolde-meskel, E.; Bakken, L.R. Carbon and nitrogen mineralization dynamics in different soils of the tropics amended with legume residues and contrasting soil moisture contents. *Biol. Fertil. Soils* **2012**, *48*, 51–66. [CrossRef]
43. Lehmann, S. Low carbon construction systems using prefabricated engineered solid wood panels for urban infill to significantly reduce greenhouse gas emissions. *Sustain. Cities Soc.* **2013**, *6*, 57–67. [CrossRef]
44. Wall, K.; Walker, P.; Gross, C.; White, C.; Mander, T. Development and testing of a prototype straw bale house. *Proc. Inst. Civ. Eng. Constr. Mater.* **2012**, *165*, 377–384. [CrossRef]
45. Li, Z.; Shen, G.Q.; Alshawi, M. Measuring the impact of prefabrication on construction waste reduction: An empirical study in China. *Resour. Conserv. Recycl.* **2014**, *91*, 27–39. [CrossRef]
46. Perez-Garcia, J.; Lippke, B.; Comnick, J.; Manriquez, C. An assessment of carbon pools, storage, and wood products market substitution using life-cycle analysis results. *Wood Fiber Sci.* **2005**, *37*, 140–148.
47. Newaz, M.T.; Davis, P.; Sher, W.; Simon, L. Factors affecting construction waste management streams in Australia. *Int. J. Constr. Manag.* **2020**, *22*, 2625–2633. [CrossRef]
48. Sun, S.; Ma, D.; Zhou, G. Applications and analysis of the composite wall on construction in Heilongjiang Province. *Procedia Eng.* **2015**, *118*, 160–168. [CrossRef]
49. Cavalliere, C.; Dell'Osso, G.R.; Favia, F.; Lovicario, M. BIM-based assessment metrics for the functional flexibility of building designs. *Autom. Constr.* **2019**, *107*, 102925. [CrossRef]
50. Pittau, F.; Krause, F.; Lumia, G.; Habert, G. Fast-growing bio-based materials as an opportunity for storing carbon in exterior walls. *Build. Environ.* **2018**, *129*, 117–129. [CrossRef]
51. Ali, M.B.; Saidur, R.; Hossain, M.S. A review on emission analysis in cement industries. *Renew. Sustain. Energy Rev.* **2011**, *15*, 2252–2261. [CrossRef]
52. Rabbat, C.; Awad, S.; Villot, A.; Rollet, D.; Andrès, Y. Sustainability of biomass-based insulation materials in buildings: Current status in France, end-of-life projections and energy recovery potentials. *Renew. Sustain. Energy Rev.* **2022**, *156*, 111962. [CrossRef]
53. Yin, X.; Lawrence, M.; Maskell, D. Straw bale construction in northern China—Analysis of existing practices and recommendations for future development. *J. Build. Eng.* **2018**, *18*, 408–417. [CrossRef]
54. Tran Le, A.D.; Maalouf, C.; Mai, T.H.; Wurtz, E.; Collet, F. Transient hygrothermal behaviour of a hemp concrete building envelope. *Energy Build.* **2010**, *42*, 1797–1806. [CrossRef]
55. Webb, M. Biomimetic building facades demonstrate potential to reduce energy consumption for different building typologies in different climate zones. *Clean Technol. Environ. Policy* **2022**, *24*, 493–518. [CrossRef]
56. Chatterton, P. Towards an agenda for post-carbon cities: Lessons from Lilac, the UK's first ecological, affordable cohousing community. *Int. J. Urban Reg. Res.* **2013**, *37*, 1654–1674. [CrossRef]
57. Worrell, E.; Price, L.; Martin, N.; Hendriks, C.; Meida, L.O. Carbon dioxide emissions from the global cement industry. *Annu. Rev. Energy Environ.* **2001**, *26*, 303–329. [CrossRef]
58. Maskell, D.; Gross, C.; Thomson, A.; Wall, K.; Walker, P.; Mander, T. Structural development and testing of a prototype house using timber and straw bales. *Proc. Inst. Civ. Eng.—Struct. Build.* **2015**, *168*, 67–75. [CrossRef]

59. Galimshina, A.; Moustapha, M.; Hollberg, A.; Padey, P.; Lasvaux, S.; Sudret, B.; Habert, G. Bio-based materials as a robust solution for building renovation: A case study. *Appl. Energy* **2022**, *316*, 119102. [CrossRef]
60. Wijnants, L.; Allacker, K.; De Troyer, F. Life-cycle assessment of timber frame constructions—The case of rooftop extensions. *J. Clean. Prod.* **2019**, *216*, 333–345. [CrossRef]
61. Zhou, Y.; Trabelsi, A.; El Mankibi, M. A review on the properties of straw insulation for buildings. *Constr. Build. Mater.* **2022**, *330*, 127215. [CrossRef]
62. Torres-Rivas, A.; Palumbo, M.; Haddad, A.; Cabeza, L.F.; Jiménez, L.; Boer, D. Multi-objective optimisation of bio-based thermal insulation materials in building envelopes considering condensation risk. *Appl. Energy* **2018**, *224*, 602–614. [CrossRef]
63. Ahmad, H.; Chhipi-Shrestha, G.; Hewage, K.; Sadiq, R. A comprehensive review on construction applications and life cycle sustainability of natural fiber biocomposites. *Sustainability* **2022**, *14*, 15905. [CrossRef]
64. Sodagar, B.; Rai, D.; Jones, B.; Wihan, J.; Fieldson, R. The carbon-reduction potential of straw-bale housing. *Build. Res. Inf.* **2011**, *39*, 51–65. [CrossRef]
65. Breton, C.; Blanchet, P.; Amor, B.; Beauregard, R.; Chang, W.S. Assessing the climate change impacts of biogenic carbon in buildings: A critical review of two main dynamic approaches. *Sustainability* **2018**, *10*, 2020. [CrossRef]
66. Arehart, J.H.; Hart, J.; Pomponi, F.; D'Amico, B. Carbon sequestration and storage in the built environment. *Sustain. Prod. Consum.* **2021**, *27*, 1047–1063. [CrossRef]
67. Bertino, G.; Kisser, J.; Zeilinger, J.; Langergraber, G.; Fischer, T.; Österreicher, D. Fundamentals of building deconstruction as a circular economy strategy for the reuse of construction materials. *Appl. Sci.* **2021**, *11*, 939. [CrossRef]
68. Cornaro, C.; Zanella, V.; Robazza, P.; Belloni, E.; Buratti, C. An innovative straw bale wall package for sustainable buildings: Experimental characterization, energy and environmental performance assessment. *Energy Build.* **2020**, *208*, 109636. [CrossRef]
69. Crafford, P.L.; Blumentritt, M.; Wessels, C.B. The potential of South African timber products to reduce the environmental impact of buildings. *South Afr. J. Sci.* **2017**, *113*, 56–63. [CrossRef]
70. Ram, M.; Mondal, M.K. Comparative study of native and impregnated coconut husk with pulp and paper industry waste water for fuel gas production. *Energy* **2018**, *156*, 122–131. [CrossRef]
71. Li, L.; Wang, Y.; Zhang, Q.; Li, J.; Yang, X.; Jin, J. Wheat straw burning and its associated impacts on Beijing air quality. *Sci. China Ser. D Earth Sci.* **2008**, *51*, 403–414. [CrossRef]
72. Hou, L.; Chen, X.; Kuhn, L.; Huang, J. The effectiveness of regulations and technologies on sustainable use of crop residue in Northeast China. *Energy Econ.* **2019**, *81*, 519–527. [CrossRef]
73. Wang, Y.J.; Bi, Y.Y.; Gao, C.Y. The assessment and utilization of straw resources in China. *Agric. Sci. China* **2010**, *9*, 1807–1815. [CrossRef]
74. Hajj, N.E.; Mboumba-Mamboundou, B.; Dheilly, R.M.; Aboura, Z.; Benzeggagh, M.; Queneudec, M. Development of thermal insulating and sound absorbing agro-sourced materials from auto linked flax-tows. *Ind. Crops Prod.* **2011**, *34*, 921–928. [CrossRef]
75. Platt, S.; Maskell, D.; Walker, P.; Laborel-Preneron, A. Manufacture and characterisation of prototype straw bale insulation products. *Constr. Build. Mater.* **2020**, *262*, 120035. [CrossRef]
76. Uemura Silva, V.; Nascimento, M.F.; Resende Oliveira, P.; Panzera, T.H.; Rezende, M.O.; Silva, D.A.L.; Borges de Moura Aquino, V.; Rocco Lahr, F.A.; Christoforo, A.L. Circular vs. linear economy of building materials: A case study for particleboards made of recycled wood and biopolymer vs. conventional particleboards. *Constr. Build. Mater.* **2021**, *285*, 122906. [CrossRef]
77. Gálvez-Martos, J.L.; Styles, D.; Schoenberger, H.; Zeschmar-Lahl, B. Construction and demolition waste best management practice in Europe. *Resour. Conserv. Recycl.* **2018**, *136*, 166–178. [CrossRef]
78. Diyamandoglu, V.; Fortuna, L.M. Deconstruction of wood-framed houses: Material recovery and environmental impact. *Resour. Conserv. Recycl.* **2015**, *100*, 21–30. [CrossRef]
79. Tam, V.W.Y.; Le, K.N.; Wang, J.Y.; Illankoon, I.M.C.S. Practitioners recycling attitude and behaviour in the Australian construction industry. *Sustainability* **2018**, *10*, 1212. [CrossRef]
80. Pulaski, M.; Hewitt, C.; Horman, M.; Guy, B. Design for deconstruction. *Mod. Steel Constr.* **2004**, *44*, 33–37.
81. Quale, J.; Eckelman, M.; Williams, K.; Sloditskie, G.; Zimmerman, J. Construction matters: Comparing environmental impacts of building modular and conventional homes in the United States. *J. Ind. Ecol.* **2012**, *16*, 243–253. [CrossRef]
82. Islam, H.; Zhang, G.; Setunge, S.; Bhuiyan, M.A. Life cycle assessment of shipping container home: A sustainable construction. *Energy Build.* **2016**, *128*, 673–685. [CrossRef]
83. Zhang, C.; Hu, M.; Dong, L.; Gebremariam, A.; Miranda-Xicotencatl, B.; Di Maio, F.; Tukker, A. Eco-efficiency assessment of technological innovations in high-grade concrete recycling. *Resour. Conserv. Recycl.* **2019**, *149*, 649–663. [CrossRef]
84. Sun, C.; Gu, J.; Dong, Q.; Qu, D.G.; Chang, W.S.; Yin, X.Z. Are straw bales better insulation materials for constructions? A review. *Dev. Built Environ.* **2023**, *15*, 100209. [CrossRef]
85. Guerrero, L.A.; Maas, G.; Hogland, W. Solid waste management challenges for cities in developing countries. *Waste Manag.* **2013**, *33*, 220–232. [CrossRef]
86. Muscolo, A.; Settineri, G.; Papalia, T.; Attinà, E.; Basile, C.; Panuccio, M.R. Anaerobic co-digestion of recalcitrant agricultural wastes: Characterizing of biochemical parameters of digestate and its impacts on soil ecosystem. *Sci. Total Environ.* **2017**, *586*, 746–752. [CrossRef]
87. Van de Kaa, G.; Kamp, L.; Rezaei, J. Selection of biomass thermochemical conversion technology in the Netherlands: A best worst method approach. *J. Clean. Prod.* **2017**, *166*, 32–39. [CrossRef]

88. Gupta, G.K.; Mondal, M.K. Bio-energy generation from sagwan sawdust via pyrolysis: Product distributions, characterizations and optimization using response surface methodology. *Energy* **2019**, *170*, 423–437. [CrossRef]
89. Lora, E.S.; Andrade, R.V. Biomass as energy source in Brazil. *Renew. Sustain. Energy Rev.* **2009**, *13*, 777–788. [CrossRef]
90. Yang, T.H.; Lin, C.J.; Wang, S.Y.; Tsai, M.J. Characteristics of particleboard made from recycled wood-waste chips impregnated with phenol formaldehyde resin. *Build. Environ.* **2007**, *42*, 189–195. [CrossRef]
91. Sampathrajan, A.; Vijayaraghavan, N.C.; Swaminathan, K.R. Mechanical and thermal properties of particleboards made from farm residues. *Bioresour. Technol.* **1992**, *40*, 249–251. [CrossRef]
92. Chaturvedi, V.; Verma, P. An overview of key pretreatment processes employed for bioconversion of lignocellulosic biomass into biofuels and value added products. *3 Biotech* **2013**, *3*, 415–431. [CrossRef]
93. Clausen, C. CCA removal from treated wood using a dual remediation process. *Waste Manag. Res.* **2000**, *18*, 485–488. [CrossRef]
94. Parker, P. A summary report on building materials produced from wheat straw. *Inorg.-Bond. Wood Fiber Compos. Mater.* **1997**, *5*, 47–48.
95. Mo, X.; Cheng, E.; Wang, D.; Sun, X.S. Physical properties of medium-density wheat straw particleboard using different adhesives. *Ind. Crops Prod.* **2003**, *18*, 47–53. [CrossRef]
96. Wang, D.; Sun, X.S. Low density particleboard from wheat straw and corn pith. *Ind. Crops Prod.* **2002**, *15*, 43–50. [CrossRef]
97. Sahin, A.; Tasdemir, H.M.; Karabulut, A.; Gürü, M. Mechanical and thermal properties of particleboard manufactured from waste peachnut shell with glass powder. *Arab. J. Sci. Eng.* **2017**, *42*, 1559–1568. [CrossRef]
98. Wang, S.Y.; Yang, T.H.; Lin, L.T.; Lin, C.J.; Tsai, M.J. Properties of low-formaldehyde-emission particleboard made from recycled wood-waste chips sprayed with PMDI/PF resin. *Build. Environ.* **2007**, *42*, 2472–2479. [CrossRef]
99. Yang, H.S.; Kim, D.J.; Kim, H.J. Rice straw-wood particle composite for sound absorbing wooden construction materials. *Bioresour. Technol.* **2003**, *86*, 117–121. [CrossRef]
100. Feng, T.; Cheng, S.; Min, Q.; Li, W. Productive use of bioenergy for rural household in ecological fragile area, Panam County, Tibet in China: The case of the residential biogas model. *Renew. Sustain. Energy Rev.* **2009**, *13*, 2070–2078. [CrossRef]
101. Demirbaş, A.; Pehlivan, E.; Altun, T. Potential evolution of Turkish agricultural residues as bio-gas, bio-char and bio-oil sources. *Int. J. Hydrogen Energy* **2006**, *31*, 613–620. [CrossRef]
102. Demirbas, A. Combustion characteristics of different biomass fuels. *Prog. Energy Combust. Sci.* **2004**, *30*, 219–230. [CrossRef]
103. Marty, D.; Bonin, P.; Michotey, V.; Bianchi, M. Bacterial biogas production in coastal systems affected by freshwater inputs. *Cont. Shelf Res.* **2001**, *21*, 2105–2115. [CrossRef]
104. Rajput, A.A.; Zeshan; Visvanathan, C. Effect of thermal pretreatment on chemical composition, physical structure and biogas production kinetics of wheat straw. *J. Environ. Manag.* **2018**, *221*, 45–52. [CrossRef]
105. Varel, V.; Hashimoto, A.; Chen, Y. Effect of temperature and retention time on methane production from beef cattle waste. *Appl. Environ. Microbiol.* **1980**, *40*, 217–222. [CrossRef]
106. Fujita, M.; Scharer, J.M.; Moo-Young, M. Effect of corn stover addition on the anaerobic digestion of swine manure. *Agric. Wastes* **1980**, *2*, 177–184. [CrossRef]
107. Hashimoto, A.G. Conversion of straw—Manure mixtures to methane at mesophilic and thermophilic temperatures. *Biotechnol. Bioeng.* **1983**, *25*, 185–200. [CrossRef]
108. Valdez-Vazquez, I.; Acevedo-Benítez, J.A.; Hernández-Santiago, C. Distribution and potential of bioenergy resources from agricultural activities in Mexico. *Renew. Sustain. Energy Rev.* **2010**, *14*, 2147–2153. [CrossRef]
109. Bridgewater, A. Biomass fast pyrolysis. *Therm. Sci.* **2004**, *8*, 21–50. [CrossRef]
110. Elmore, A.J.; Shi, X.; Gorence, N.J.; Li, X.; Jin, H.; Wang, F.; Zhang, X. Spatial distribution of agricultural residue from rice for potential biofuel production in China. *Biomass Bioenergy* **2008**, *32*, 22–27. [CrossRef]
111. Dam, J.V.; Junginger, M. Striving to further harmonization of sustainability criteria for bioenergy in Europe: Recommendations from a stakeholder questionnaire. *Energy Policy* **2011**, *39*, 4051–4066.
112. Dendukuri, G.; Mittal, J.P. Household energy needs of a village in the Rayalaseema area of Andhra Pradesh, India. *Energy Convers. Manag.* **1993**, *34*, 1273–1286. [CrossRef]
113. Xu, X.; Fu, Y.; Li, S. Spatiotemporal changes in crop residues with potential for bioenergy use in China from 1990 to 2010. *Energies* **2013**, *6*, 6153–6169. [CrossRef]
114. Gregoire, K.P.; Becker, J.G. Design and characterization of a microbial fuel cell for the conversion of a lignocellulosic crop residue to electricity. *Bioresour. Technol.* **2012**, *119*, 208–215. [CrossRef]
115. Werner, F.; Taverna, R.; Hofer, P.; Richter, K. Carbon pool and substitution effects of an increased use of wood in buildings in Switzerland: First estimates. *Ann. For. Sci.* **2005**, *62*, 889–902. [CrossRef]
116. Marks, J. Wood powder: An upgraded wood fuel. *For. Prod. J.* **1992**, *42*, 52–56.
117. Scarlat, N.; Martinov, M.; Dallemand, J.F. Assessment of the availability of agricultural crop residues in the European Union: Potential and limitations for bioenergy use. *Waste Manag.* **2010**, *30*, 1889–1897. [CrossRef]
118. Nizami, A.S.; Rehan, M.; Waqas, M.; Naqvi, M.; Ouda, O.K.M.; Shahzad, K.; Miandad, R.; Khan, M.Z.; Syamsiro, M.; Ismail, I.M.I.; et al. Waste biorefineries: Enabling circular economies in developing countries. *Bioresour. Technol.* **2017**, *241*, 1101–1117. [CrossRef]

Disclaimer/Publisher's Note: The statements, opinions and data contained in all publications are solely those of the individual author(s) and contributor(s) and not of MDPI and/or the editor(s). MDPI and/or the editor(s) disclaim responsibility for any injury to people or property resulting from any ideas, methods, instructions or products referred to in the content.

buildings

MDPI

Review

Historic District Conservation: A Critical Review of Global Trends, Development in the 21st Century, and Challenges Through CiteSpace Analysis

Lin Geng [1], Minghui Xue [1], Jia Li [2,*] and Jiaoguo Ma [3]

[1] School of Architecture and Design, Harbin Institute of Technology, Harbin 150001, China
[2] College of Art, Northeast Agricultural University, Harbin 150030, China
[3] Jinan Urban and Rural Planning Compilation and Research Center, Jinan 250013, China
* Correspondence: li_jia@neau.edu.cn

Abstract: This study reviews the global trends, developments, and challenges in the conservation of historic districts through CiteSpace analysis. Since the dawn of the 21st century, research on historic districts has witnessed rapid growth. The research mainly focuses on fields such as urban studies, heritage conservation, and sustainable development. Although the concept of the Historic Urban Landscape has emerged, its local application remains challenging. Research findings on economic impacts are complex, and resilience assessment and community participation have become important topics. However, issues like inconsistent definitions and low community participation still exist. Future research should focus on narrowing the gap between theory and practice to better protect cultural heritage in the context of urban development.

Keywords: CiteSpace analysis; historic areas; historic conservation area; historic district; historic urban landscape; sustainable development

1. Introduction

The study of historic districts represents a complex and multifaceted area of research, situated at the intersection of urban planning, architectural heritage, and cultural studies. These districts, often referred to by various terms such as "Historic Landscape", "Historic Urban Area", "Historic Conservation Area", "Historic Area", and "Historic City Center", are spaces that bridge the gap between individual historic buildings and entire cities. This semantic ambiguity complicates comparative analysis and policy implementation. It is rooted in divergent legal frameworks, cultural contexts, and disciplinary perspectives. For instance, UNESCO's Historic Urban Landscape (HUL) paradigm (2011) [1] attempted to reconcile these terms but coexists with persistent localized definitions like the U.S.-centric "historic district" [2] and France's Secteur Sauvegardé under the Malraux Law (1962) [3]. The overlapping nature of these concepts and the diverse terminologies used to describe them highlight the need for a comprehensive review and synthesis of the existing literature. This complexity is further compounded by the rapid increase in research output since the 21 century, which has led to a fragmented understanding of the field. Therefore, a systematic review using tools like CiteSpace is essential to analyze the development and trends in this area of study.

Historic districts have evolved significantly over the past century, influenced by seminal documents and international charters. The conceptualization of historic districts

has undergone profound shifts since the early 20th century [4]. The first period was from 1900 to 1930. It emerged as a reaction to modernist urbanism, and foundational texts like the Athens Charter (1933) advocated for heritage protection beyond individual monuments [5]. After WWII, critiques of modernist planning (e.g., Jane Jacobs' The Death and Life of Great American Cities) catalyzed interdisciplinary approaches to urban conservation [6]. This period saw a shift from focusing solely on individual monuments to recognizing the value of entire historic urban cores. Subsequent milestones, including the Venice Charter (1964) [7], the Amsterdam Declaration (1975) [8], the Nairobi Recommendation (1976) [9], and the Washington Charter (1987) [10], further expanded the scope and principles of conservation. In the late 20th century, the international framework expanded conservation principles. These included authenticity (Nara Document, 1994) [11] and adaptive reuse (Burra Charter, 1999) [12]. In the 21st Century, the HUL framework (UNESCO, 2011) redefined historic areas as layered socio-ecological systems [13], while recent ICOMOS initiatives (2022) integrate resilience into conservation agendas [14] (Figure 1).

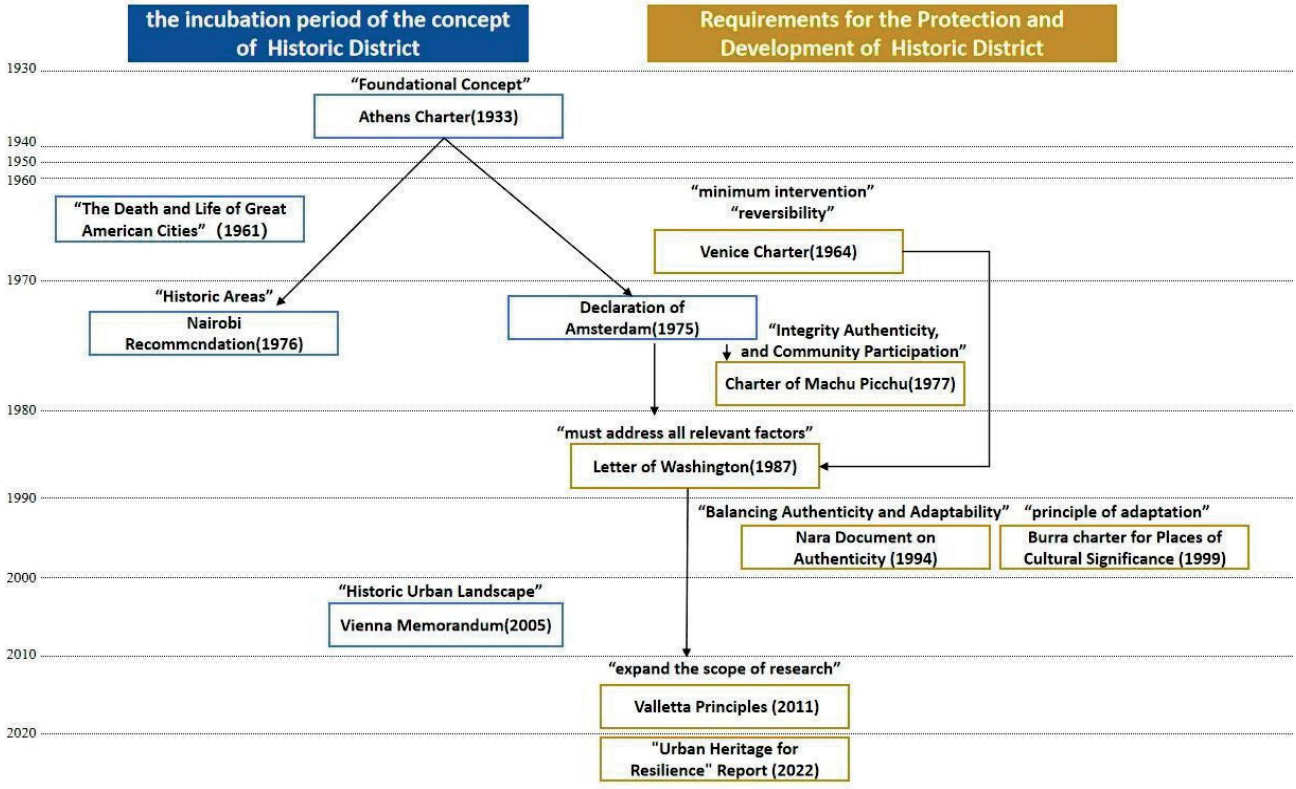


Figure 1. The concept of historical district developmental processes in historical documents.

The transformation of conservation frameworks from CIAM's modernist urbanism to UNESCO's holistic HUL approach mirrors a paradigmatic shift towards interdisciplinary collaboration. Early charters such as the Athens Charter (1933) placed a premium on functional zoning and monument preservation. In contrast, contemporary frameworks accentuate integrated social systems [5,15]. This transition reflects broader trends within heritage studies, where disciplines spanning from urban planning to environmental science now converge to grapple with intricate conservation challenges [16]. Paradoxically, however, this interdisciplinary expansion has blurred the conceptual boundaries of historic districts. Terms like "Historic Urban Landscape" and "Historic Conservation Area" now encapsulate a wide spectrum, ranging from architectural heritage to socioeconomic dynamics, thus complicating policy implementation across culturally diverse regions [13].

The emergence of localized conservation models further accentuates the tension between universal principles and contextual particularities. While UNESCO's HUL framework endeavors to standardize practices, countries like China and France have maintained distinct definitions firmly rooted in their national legal systems [3,17]. For instance, China's recent emphasis on "adaptive reuse" exemplifies its unique equilibrium between economic development and heritage preservation [18], while European models frequently prioritize community-led revitalization [8]. This divergence underscores a crucial gap: global frameworks encounter difficulties in catering to the diverse needs of historic districts shaped by different political economies and cultural values [19].

Since the dawn of the 21st century, an exponential growth in localized case studies has further fragmented the field. Although these studies offer granular insights into specific contexts, they often lack comparative analysis, rendering it arduous to derive generalizable strategies. A comprehensive review is thus essential to synthesize these localized findings and identify overarching trends. Notably, there is a conspicuous dearth of reviews that comprehensively examine the development of research papers on this subject, discuss the primary methods employed in these studies, and explore future directions. Significantly, no review has hitherto utilized CiteSpace to analyze the literature on historic districts, visualize the knowledge landscape, or take research clusters as focal points for abstraction and analysis. Considering the ongoing debates regarding historical documents and their impact on research development over the past two decades, this gap is of great significance. To bridge this gap, our study aims to systematically review the development of research on historic districts since 2001, predict future trends, and provide a comprehensive understanding of this field. Consequently, this paper takes 'Historic district' as its central focus and employs CiteSpace to offer a comprehensive review of the field's recent developments, summarize overall trends since the beginning of the 21st century, and construct a cognitive map of research evolution in this area.

2. Research Materials, Methods and Process

2.1. Materials

To ensure the academic quality and relevance of the literature reviewed, we focused on the core collection of the Web of Science database, encompassing the Science Citation Index (SCI), Social Science Citation Index (SSCI), and Arts & Humanities Citation Index (A&HCI), as well as the Scopus database. We utilized the "Topic" search function to scan the titles, abstracts, and author keywords of articles within these databases. Given that the term "historic district" is frequently interchanged with related expressions such as "historic landscape", "historic urban landscape", and "historic urban area", we incorporated these alternative terms into our search strategy to capture a comprehensive range of relevant studies. The Web of Science and Scopus databases were selected mainly because they have comprehensive subject coverage and complementary literature resources, which can meet the multidisciplinary research needs of historic district conservation. They have high academic authority and timely data updates, facilitating access to cutting-edge research findings. These two databases contain a wealth of international research and are equipped with powerful retrieval and analysis tools. However, they also have limitations. For example, they mainly include English-language research, and some professional and regional studies are not included. Other databases were not included due to limited resources and energy. Moreover, this study focuses on international mainstream research trends. These two databases can meet the core research requirements, while other databases are less relevant to the research focus.

Given that our research focuses on the research trends of the 21st century, the time range was set from 2001 to 2024, and the search was conducted on 7 March 2025. To ensure the accuracy and completeness of the study, we excluded articles that focused on individual buildings, complete historic cities, standalone historic gardens, or forests, as these were not relevant to our research objectives. As a result, 438 articles were selected for analysis (Figure 2). The data used in this study does not include early research because there are significant differences in theory and methods between early and modern research. Early research has fewer documents and less mature research methods, which may interfere with the analysis of current research hotspots and emerging fields. The time range of 2001–2024 was chosen because significant changes have occurred in the field of historic district conservation since the 21st century. The research focus has shifted to areas such as sustainable development. During this period, the quantity and quality of research in the database are more guaranteed, and there have been many technological innovations in related fields. This is conducive to studying the impact of new technologies on historic district conservation.



Figure 2. Literature screening process.

2.2. Methods

Knowledge mapping, an advanced bibliometric and scientometric method, enables the visual representation of quantitative subject knowledge analysis. Widely adopted tools for such analysis include HistCite, Sci2, VOSviewer, and CiteSpace [20]. To achieve distinguishable knowledge mapping results, we tested CiteSpace's default clustering algorithm methods. Evaluation criteria included cluster clarity and alignment with historic district research domains, consistent with Chen's (2016) findings on cluster validation in bibliometric analysis [21]. The findings showed that CiteSpace's default algorithm generated sharper thematic clusters that were better aligned with domain knowledge. In this study, we employ CiteSpace V 6.4.R1 (64-bit), a software tool developed by Chaomei Chen, to identify trends, visualize citation networks, and explore dynamic patterns within research [22]. Utilizing clustering algorithms at its core, CiteSpace generates multi-perspective visualizations of co-citation networks, enhancing the interpretability of author and document co-citation analyses [23]. This tool facilitates the classification, co-occurrence, and collaborative network analysis of database studies, offering intuitive insights into evolutionary trends, knowledge linkages, and research frontiers. Its applications span over 60 disciplines, including computer science, information science, medicine, engineering, and economics [21].

When conducting the analysis using CiteSpace, to more scientifically evaluate the robustness and distinctiveness of the identified research clusters, we calculated and analyzed key cluster validation metrics. Among them, Modularity Q is used to measure the network modularity. The higher this value is, the more significant the cluster structure is, and the better the clustering effect. Silhouette scores, on the other hand, are used to assess the internal consistency of the clusters. The closer the score is to 1, the better the compactness and separation of the clusters, indicating a higher clustering quality. In this study, after calculation, the Modularity Q of the data sample in this paper ranges from 0.6 to 0.8, and the silhouette scores are around 0.91. This indicates that the research clusters

we identified have good robustness and high clustering quality, providing a reliable basis for subsequent research [21].

When processing data to construct the knowledge graph, we selected the Pathfinder pruning method. Among the numerous methods available for data screening and network simplification, the Pathfinder pruning method has unique advantages. The literature data in the field of historic district research is voluminous and complex in relationships. The Pathfinder pruning optimizes based on the global structure of the network, enabling it to precisely screen out paths of key significance and remove redundant connections. This characteristic makes it possible to highlight the associations between core research themes more effectively when visualizing the literature network, clearly presenting the key context of the research field. For example, when analyzing the keyword co-occurrence network, Pathfinder pruning can retain those connections that play a crucial role in connecting different research themes and transmitting important information, avoiding the network from becoming too complex to interpret due to too many unimportant connections. Compared with other pruning methods, it can better balance the relationship between information retention and network simplification. At the same time, considering that this study aims to comprehensively determine the development context, hotspots, and trends in the field of historic district research, the advantages of the Pathfinder pruning method are highly consistent with the research objectives. Therefore, we only use the Pathfinder pruning method in this study to ensure that we can accurately and effectively excavate and present the key information in the data [21].

2.3. Research Process

In the research process, we adopted co-citation hybrid analysis, a framework pioneered by Small [24], which posits that two papers form a co-citation relationship if jointly cited by a third paper. The analytical process adheres to the following algorithmic principle [25]: Format the collected data and use CiteSpace's deduplication function to remove duplicate literature. Set the time slice to one year to establish a temporal dimension foundation for subsequent analysis.

Time zone segmentation is a crucial feature of CiteSpace software. Users need to conduct time zone segmentation (Time Slicing) to set the length of each time slice. This helps capture the knowledge domain at different times. Then, by combining these time-related pictures, researchers can investigate them from a diachronic perspective [26]. Afterwards, one should format the collected data, use CiteSpace's deduplication function to remove duplicate studies, and set the time slice to one year to establish a temporal dimension foundation for subsequent analysis.

CiteSpace's network scaling technique trims redundant links while preserving critical connections, ensuring clarity in visualizing disciplinary frontiers. To enhance cluster interpretability, noun phrases from document titles were extracted using the log-likelihood ratio (LLR) algorithm, enabling precise labeling of research themes [27]. Parameters such as node frequency and betweenness centrality reflect the scholarly impact of publications, while clustering outcomes delineate the conceptual framework of historic district research, offering a foundation for future inquiries [25]. Network Construction and Analysis encompasses several key steps: first, building citation or co-citation networks by selecting node types (such as authors, institutions, keywords) and link types to map the associative structure of the research field; next, applying centrality analysis using betweenness centrality to gauge nodes' bridging roles in network connectivity (where higher values signify greater impact on connectivity) and eigenvector centrality to evaluate a node's influence via its connections to high-impact nodes; and finally, performing cluster analysis with the LLR

(log-likelihood ratio) algorithm [28]. This algorithm statistically identifies significant term co-occurrences to extract cluster labels, uncovering the field's knowledge structure and research dynamics by clustering studies under shared themes. The process is illustrated in Figure 3.

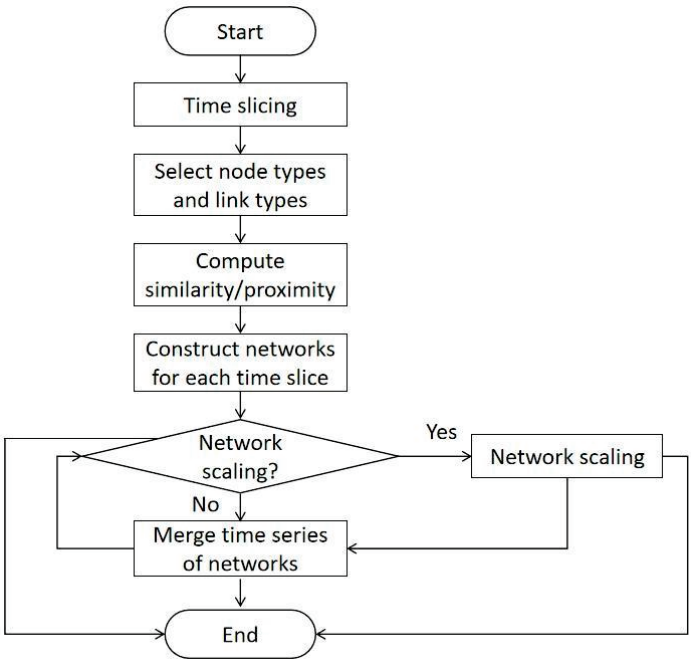


Figure 3. CiteSpace's analysis flow chart.

3. Results

3.1. Data Analysis

3.1.1. Publication Trends

The number of publications is a significant indicator of the research development trend in the field of historic districts. The annual distribution and cumulative number of articles are shown in Figure 4. The overall trend indicates exponential growth, with a notable increase after 2013. The most significant surge occurred in 2021, likely driven by public health issues in historic urban areas during the COVID-19 pandemic [29]. Since 2015, the number of publications has shown substantial and rapid growth, with an average annual increase of 36.57%. This suggests that, although the concept of this field has been around for decades and there has been a long period of inactivity in terms of academic paper publications, it was not until the second decade of the 21st century that this field received extensive attention in academic circles.

The rapid growth of research during this period may be attributed to multiple factors. For instance, after China implemented the "Regulations on the Protection of Famous Historical and Cultural Cities, Towns, and Villages" in 2008, there was a surge in research output (165 articles, accounting for 37.67%) [17]. Concurrently, following the release of UNESCO's "Historic Urban Landscape (HUL)" framework in 2011, related studies grew starting from 2014. A citation burst for the keyword "historic urban landscape" occurred between 2019 and 2020 (burst strength: 2.76), indicating the guiding role of international policies in shaping research directions [13]. The peak publication volume in 2021 (77 articles) was directly related to the increased focus on the resilience of historic urban areas during the COVID-19 pandemic, with "resilience" emerging as a key keyword that year (burst strength: 2.63). For example, researchers noted that the layout of historic

districts aids in pandemic isolation and enhances urban resilience [30]. Additionally, research on "heritage tourism" has grown since 2015 (keyword frequency: 23), aligning with the global demand for exploring the economic value of cultural heritage.

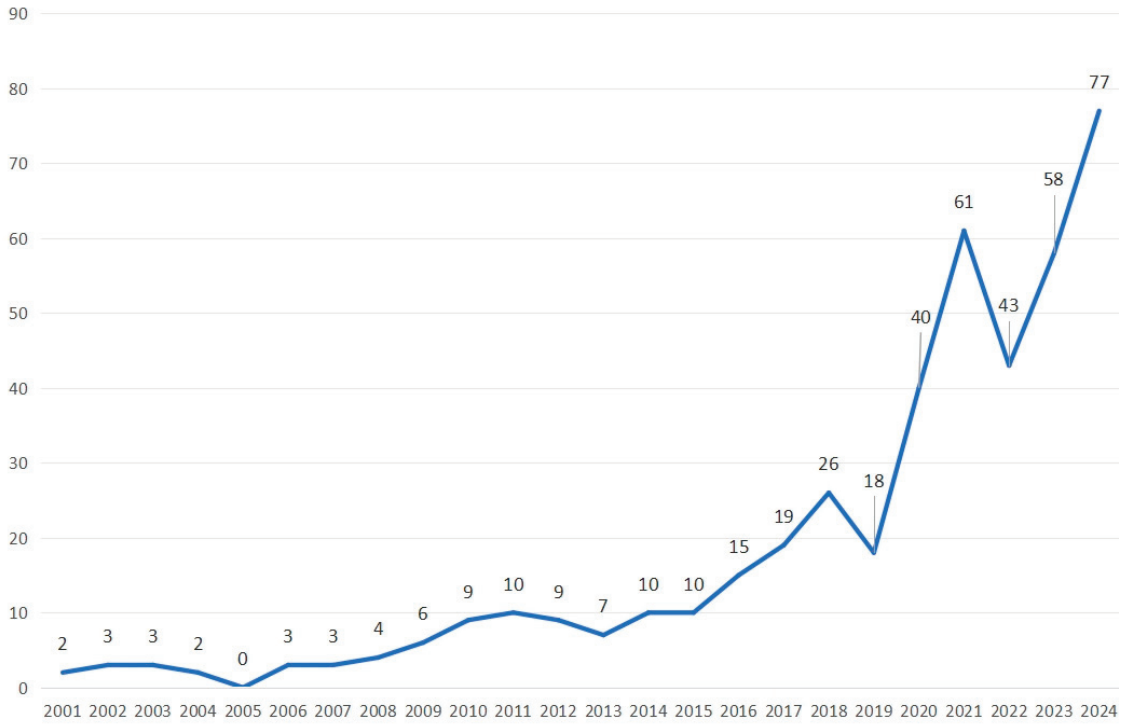


Figure 4. Annual publications from 2001 to 2024.

3.1.2. Geographical Distribution

To understand the global participation in this field, we analyzed the geographical distribution of research contributions. The node type was set to cited journal and the time slice was set to 1 year to generate a co-citation map of journals. By setting the node type to country and using the Pathfinder pruning method, we generated a time zone map of contributing countries and regions, as shown in Figure 5. A total of 59 nodes and 115 lines were obtained, showing that 59 countries carried out relevant research in this field and 115 cooperative relationships were produced. Under the current settings, the silhouette score is 0.9155 and the Modularity Q value is 0.8018. Both of these values fall within the reasonable ranges [21].

China leads in the number of publications (165), followed by the USA (46) and Italy (37). The countries with the greatest academic influence are China (0.41), the UK (0.17), the USA (0.14), and Spain (0.14), as shown in Table 1. China's dominant role, which began explosively after 2008, is directly related to policy changes and the significant economic benefits associated with historic districts [31]. China's dominance (163 publications) stems from policy initiatives. Even prior to that, scholars had major concerns about the detrimental effects of China's rapid urban development on historical and cultural heritage [32]. After the 2008 implementation of the Regulations on the Protection of Famous Historical and Cultural Cities, Towns, and Villages, Chinese governments at all levels formulated a plethora of new laws and regulations [17]. The inscription of a site on the World Heritage List has also made the authorities pay more attention to China's heritage protection and has clearly defined the key objects of protection [33]. Consequently, historic districts attracted heightened attention. These endeavors encompassed both the direct renovation of historic

districts and the provision of direct financial support for related research. Under the direct impetus of the government, a series of heritage conservation projects and management systems, with the application of digital technologies included, were put into practice for protective purposes [34].

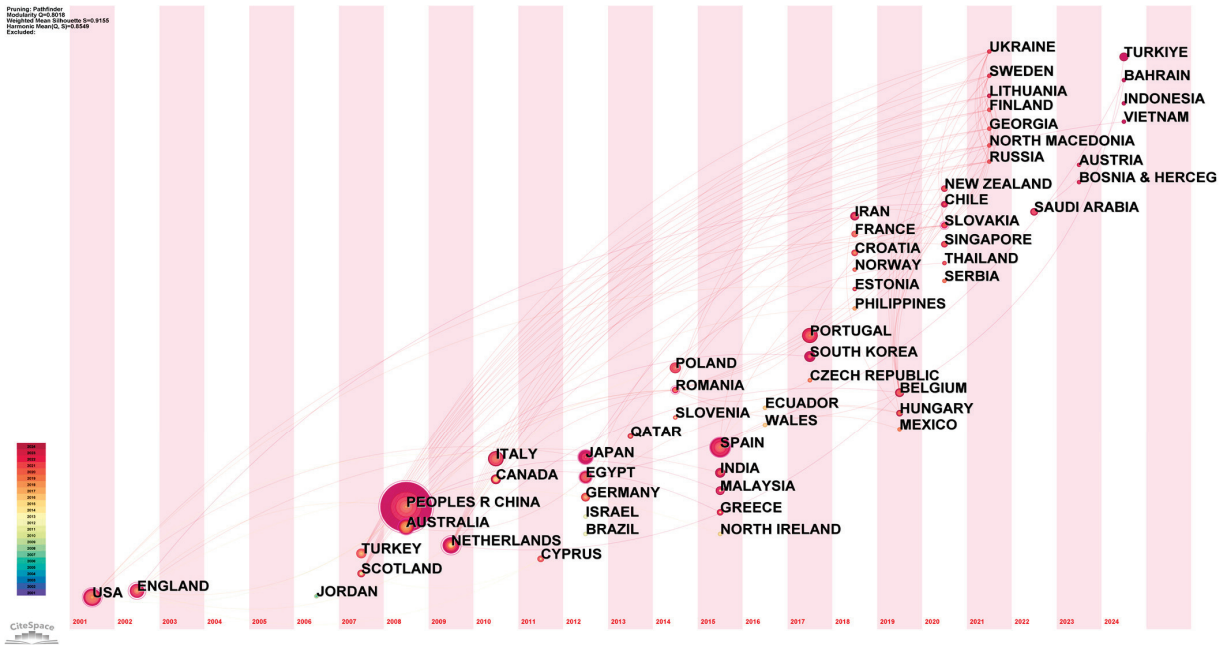


Figure 5. Time zone distribution of research contributions (Node size: publication count; node color: research start year; cooperation network pruned via Pathfinder).

Table 1. List of contributing countries and number of records contributed.

No.	Frequency	Country	Centrality
1	165	China	0.41
2	46	USA	0.14
3	37	England	0.17
4	31	Spain	0.14
5	27	Italy	0.03
6	21	Turkey	0.00
7	20	Japan	0.13
8	15	Netherlands	0.06
9	14	Portugal	0.08
10	14	Australia	0.18

Collaboration patterns differ regionally: China (centrality 0.40) emphasizes domestic teams focusing on technical applications (GIS, space syntax), while Europe (e.g., UK, Italy) fosters transdisciplinary projects via EU frameworks (e.g., Horizon 2020), prioritizing HUL theoretical innovation [35].

3.1.3. Cited Journals

To identify the key journals in this field, we analyzed the co-citation network of journals. Setting the node type to cited journals with the Pathfinder pruning method, we generated a list of contributing journals and the number of records contributed, as shown in Table 2. The top three journals by citation frequency are *Sustainability*, *Cities*, and *Landscape and Urban Planning*. The journals with the highest betweenness centrality are *Landscape*

and Urban Planning, *Cities*, and *Habitat International*, indicating their significant role in connecting different research areas. The top 10 journals primarily focus on urban studies, architecture, environment, energy, landscape, urban planning, and sustainable society, reflecting the main research directions in this field. High centrality scores for *Sustainability* (0.05) and *Landscape and Urban Planning* (0.21) reflect disciplinary shifts. *Sustainability* serves as a multidisciplinary platform integrating environmental science, sociology, and engineering, aligning with HUL's holistic approach. *Landscape and Urban Planning* drives spatial analysis methods, bridging heritage conservation and urban planning.

Table 2. List of contributing Journals and number of records contributed.

No.	Freq	Centrality	Cited Journal	Quartile Rank
1	159	0.05	*Sustainability*	Q1
2	157	0.16	*Cities*	Q1
3	130	0.21	*Landscape and Urban Planning*	Q1
4	94	0.14	*Habitat International*	Q1
5	82	0.07	*Urban Studies*	Q1
6	81	0.03	*International Journal of Heritage Studies*	Q1
7	75	0.02	*Land Use Policy*	Q1
8	69	0.04	*Journal of Cultural Heritage*	Q1
9	69	0.03	*Sustainable Cities and Society*	Q1
10	61	0.03	*Land*	Q1

3.1.4. Research Subjects

To identify the main research subjects, we generated a co-occurrence map of subject categories: the co-occurrence network of research subjects in Figure 6. By setting the node type to country and using the Pathfinder pruning method, a total of 70 nodes and 185 lines were obtained, showing that 70 subjects carried out relevant research in this field and 185 subjects relationships were produced. Under the current settings, the silhouette score is 0.8263 and the Modularity Q value is 0.6059. Both of these values fall within the reasonable ranges [21]. We generated a list of research subjects and the number of records contributed, as shown in Table 3.

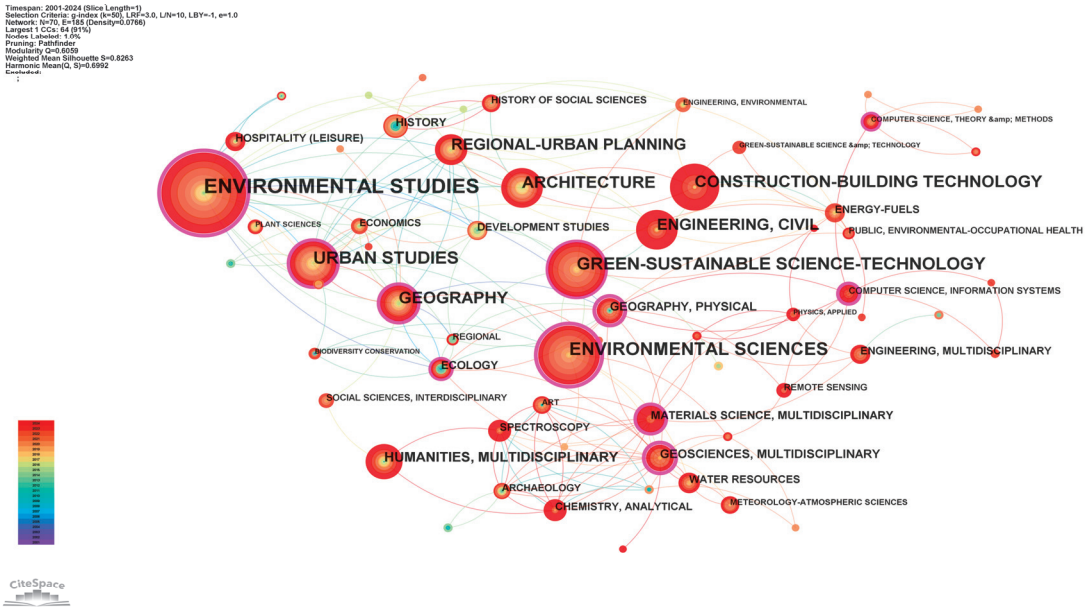


Figure 6. Research subject co-occurrence network (nodes represent academic disciplines; edges indicate interdisciplinary linkages; Pathfinder algorithm used for pruning).

Table 3. List of major research subjects and number of records.

No.	Freq	Centrality	Subjects
1	155	0.38	Environmental Studies
2	90	0.42	Environmental Sciences
3	73	0.14	Green/Sustainable Science/Technology
4	72	0.24	Urban Studies
5	53	0.04	Construction/Building Technology
6	51	0.26	Geography
7	51	0.03	Architecture
8	43	0.01	Regional/Urban Planning
9	43	0.02	Engineering, Civil
10	24	0.03	Humanities, Multidisciplinary

Based on the co-occurrence network of research subjects and relevant data, environmental studies, environmental science, and green and sustainable science and technology hold significant sway in the realm of historic district research. This trend underscores the fact that in the contemporary era, the exploration of historic districts extends far beyond the confines of mere architecture and culture. Instead, there is a growing and intense focus on the surrounding environment. Urban studies, too, have a pivotal role to play in the research of historic districts. This clearly demonstrates that the connection between historic districts and the overall development of cities has captured extensive attention. The involvement of the geography discipline in historic district research signals a heightened emphasis on the spatial distribution, geographical environmental features, and regional disparities of these districts.

3.2. Academic Groupings and Research Focus

To clarify specific research topics in historic district research, this article analyzes from multiple aspects. First, a keyword co-occurrence map shows keyword frequencies and changes over time for identifying hotspots and trends. In Section 3.2.1, by setting "keyword" as the node type and using the Pathfinder pruning method, core keywords are found. Burst detection and timeline analysis are performed, and the research's current state and direction are analyzed from aspects like scope, methods, strategies, and emerging trends. In Section 3.2.2, co-citation clustering analysis identifies 10 effective clusters across various fields, verifying their validity and showing topic diversity and relevance. In Section 3.2.3, a co-occurrence map of landmark references clarifies key references, reflecting the complexity and multi-dimensionality of current research.

3.2.1. Keyword Research Areas

In our analysis, we selected "keyword" as the node type and employed Pathfinder as the pruning method. As a result, a network composed of 438 nodes and 709 lines was generated. Here, each node represents a keyword, so there were 438 distinct keywords identified, and the 709 lines signify the connections between these keywords, as shown in Figure 7. The centrality value serves as an indicator of the academic influence of each keyword. To showcase the most prominent ones, we have listed the top 20 keywords in Table 4. Subsequently, we carried out a burst detection analysis on these 446 keywords. The Kleinberg algorithm [36] was employed for this purpose, with the aim of identifying the keywords that underwent sudden and substantial changes in their usage patterns over time.

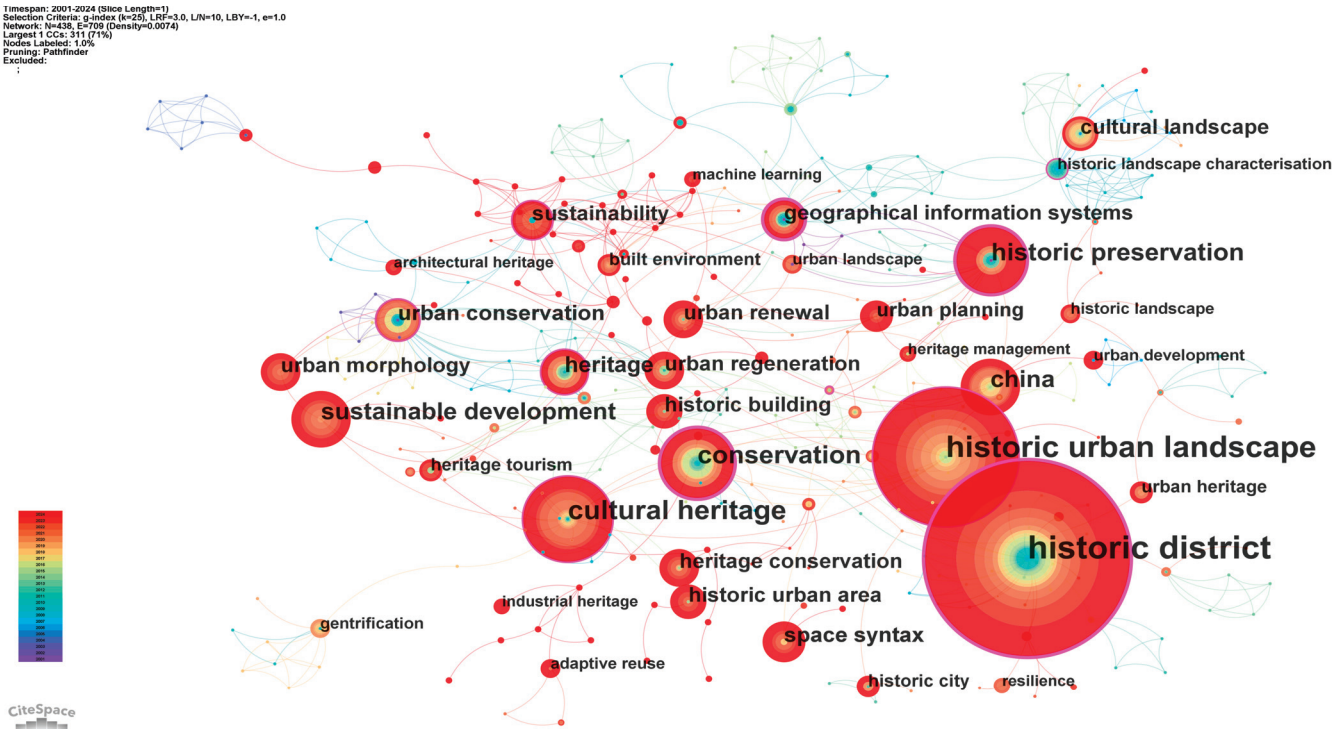


Figure 7. Keyword co-occurrence network map (node size indicates keyword frequency; edge thickness represents co-occurrence strength; network pruned using Pathfinder algorithm).

Table 4. List of contributing keywords and number of records contributed.

No.	Freq	Centrality	Keywords	Year
1	62	0.32	historic district	2008
2	44	0.18	historic urban landscape	2014
3	27	0.14	cultural heritage	2008
4	22	0.29	conservation	2008
5	21	0.25	historic preservation	2001
6	18	0.1	sustainable development	2020
7	18	0.05	China	2015
8	14	0.19	heritage	2009
9	13	0.01	space syntax	2018
10	13	0.14	urban conservation	2003
11	12	0.06	urban renewal	2013
12	12	0.01	urban morphology	2021
13	12	0.18	sustainability	2009
14	12	0.24	geographical information systems	2001
15	12	0.08	urban regeneration	2011
16	12	0.01	heritage conservation	2015
17	11	0.01	historic urban area	2015
18	11	0.01	historic building	2014
19	11	0.03	cultural landscape	2006
20	10	0.04	urban planning	2022
21	7	0.02	urban heritage	2020
22	7	0.05	built environment	2019
23	7	0.06	heritage tourism	2015
24	7	0.02	historic city	2012
25	6	0.02	urban development	2006

In the burst detection analysis using CiteSpace, the γ parameter is a crucial factor that significantly affects the sensitivity of identifying emerging trends. In this study, we set the γ parameter to 0.2, which was based on comprehensive considerations. Prior to setting this parameter, we conducted multiple tests with different γ values. When the γ value was set too low (e.g., 0.1), it generated an excessive number of detection results that included many minor fluctuations. These fluctuations might not represent truly meaningful changes in research trends and instead could interfere with the judgment of core trends. On the other hand, when the γ value was set too high (e.g., 0.5), some trends that changed moderately but were of great significance might be excluded from the analysis. In the field of historic district research, we aim to capture trends that are both significant and can reflect the real dynamic changes in the field. Through repeated tests and careful analysis of the results, we found that when the γ value is 0.2, it can retain key trend information while effectively filtering out unnecessary noise data. This setting allows the burst detection results to focus on the key factors that have a major impact during the development of the research and drive the transformation of research directions, which is consistent with the goal of this study to sort out the development context, hotspots, and trends in the field of historic district research. The results are presented in Figure 8. In order to study the development and changes of keywords, we have generated a keyword timeline chart. Using the Pathfinder pruning method, the analysis yielded a Modularity Q of 0.7705 and a silhouette S of 0.9111, as shown in Figure 9.

Keywords	Year	Strength	Begin	End	2001 - 2024
sustainability	2009	**3.51**	2022	2024	
cultural heritage	2008	**3.13**	2021	2022	
historic landscape characterisation	2006	**3.11**	2006	2013	
sustainable development	2020	**2.95**	2020	2022	
historic urban landscape	2014	**2.76**	2019	2020	
gentrification	2010	**2.73**	2018	2020	
resilience	2021	**2.63**	2021	2022	
urban morphology	2021	**2.43**	2021	2024	
urban planning	2022	**2.39**	2022	2024	
cultural landscape	2006	**2.27**	2015	2019	

Figure 8. Keyword bursts (burst detection using Kleinberg's algorithm) from 2001 to 2024.

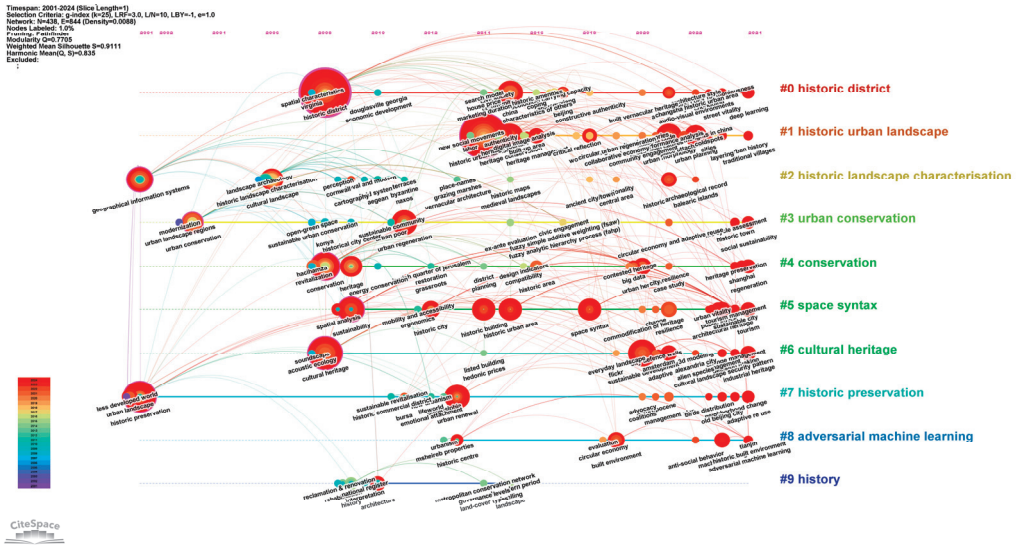


Figure 9. Keyword timeline chart using the Pathfinder pruning method.

- Research Scope

The research scope of historic districts mainly focuses on the intersection of urban and regional studies. Keywords such as "historic district", "historic urban landscape", and "historic urban area" indicate that this field has always revolved around understanding the spatial and functional dynamic relationships between cities and their historic core areas. In addition, words like "sustainable development", "heritage", "conservation", and "urban renewal" show that the research goals are extensive, covering multiple aspects from heritage conservation to adaptive renewal and sustainable urban planning.

- Research Methods and Research Strategy

Commonly used research methods in this field include the application of models and spatial analysis tools. Keywords such as "urban morphology", "geographical information systems", and "space syntax" highlight the reliance on analytical frameworks. These methods are crucial for studying the spatial and environmental characteristics of historic districts and help to deeply understand the complex interactions among urban form, heritage conservation, and contemporary urban needs. In addition, with the passage of time, continuous learning has also become an important development direction.

The analysis also reveals a significant focus on mitigation strategies and their impact on historic districts. Keywords like "conservation", "preservation", and "cultural heritage" indicate that research often explores the effects of urban development, tourism, and conservation efforts on historic areas. This includes studies on the protection of existing districts, the design of new interventions, and the evaluation of energy efficiency in built environments. The research aims to balance the need for preservation with the demands of modern urban life, ensuring that historic districts remain vibrant and sustainable.

- Emerging Trends

In the comprehensive consideration of frequency and centrality (calculated by multiplying frequency by centrality), "historic district" and "historic urban landscape" perform most prominently, indicating that the main research areas still revolve around these two aspects. At the same time, international historical documents such as the 2022 ICOMOS "Urban Heritage for Resilience" Report show that the frequency of the keyword "Resilience" surged in 2022, presenting a consistent change trend. Research trends also demonstrate an increasingly deep cross-integration among various research clusters. For example, when studying the sustainable development of historic districts, it is crucial to integrate research findings from multiple fields. The high attention given to the "HUL" (Historic Urban Landscape) concept in the 2005 Vienna Memorandum aligns with the research directions of various clusters, which also reflects this trend of cross-integration. This further indicates that an integrated research approach that combines aspects of urban studies, environmental science, heritage conservation, and sustainable development is becoming increasingly important in the research of historic districts.

In addition to these existing research areas, several emerging trends are gradually emerging. The increasing frequency of terms such as "sustainable" and "cultural heritage" suggests a growing interest in holistic approaches to heritage conservation. This holistic approach includes integrating environmental, social, and economic factors into the planning and management of historic districts. Furthermore, the emergence of keywords like "gentrification" and "resilience" implies a shift towards more people-centered research, reflecting the impact of global challenges on the research of historic districts.

3.2.2. Clustering Analysis of Keywords

We conducted co-citation clustering analysis to identify the main research topics. By setting the node type to co-cited documents and using a 10% threshold, we obtained 438 nodes and 844 links. The analysis identified 10 effective clusters, as shown in Figure 10. The clusters cover a wide range of topics, including urban studies, environmental sciences, heritage conservation, and sustainable development. Cluster labels were extracted via the log-likelihood ratio (LLR) algorithm, and the validity of the 10 generated clusters was verified using Modularity Q and silhouette scores. We conducted comparative tests on the Mutual Information, Latent Semantic Indexing (LSI), and log-likelihood ratio (LLR) algorithms. Mutual Information clusters items based on statistical associations. In this study, it led to incoherent clustering concepts, making it difficult to reflect the uniqueness of historic district research. LSI had difficulty capturing the subtle relationships in the literature. It often merged different research fields, obscuring the research focus. In contrast, LLR can accurately identify term co-occurrences, effectively distinguish different research themes in historic district research, and better meets the research requirements. Using the Pathfinder pruning method, a Modularity Q value of 0.7705 was obtained, demonstrating significant modularity, as well as a Silhouette Score of 0.9111, indicating high internal consistency. These metrics confirm the robustness of the thematic groupings [21].

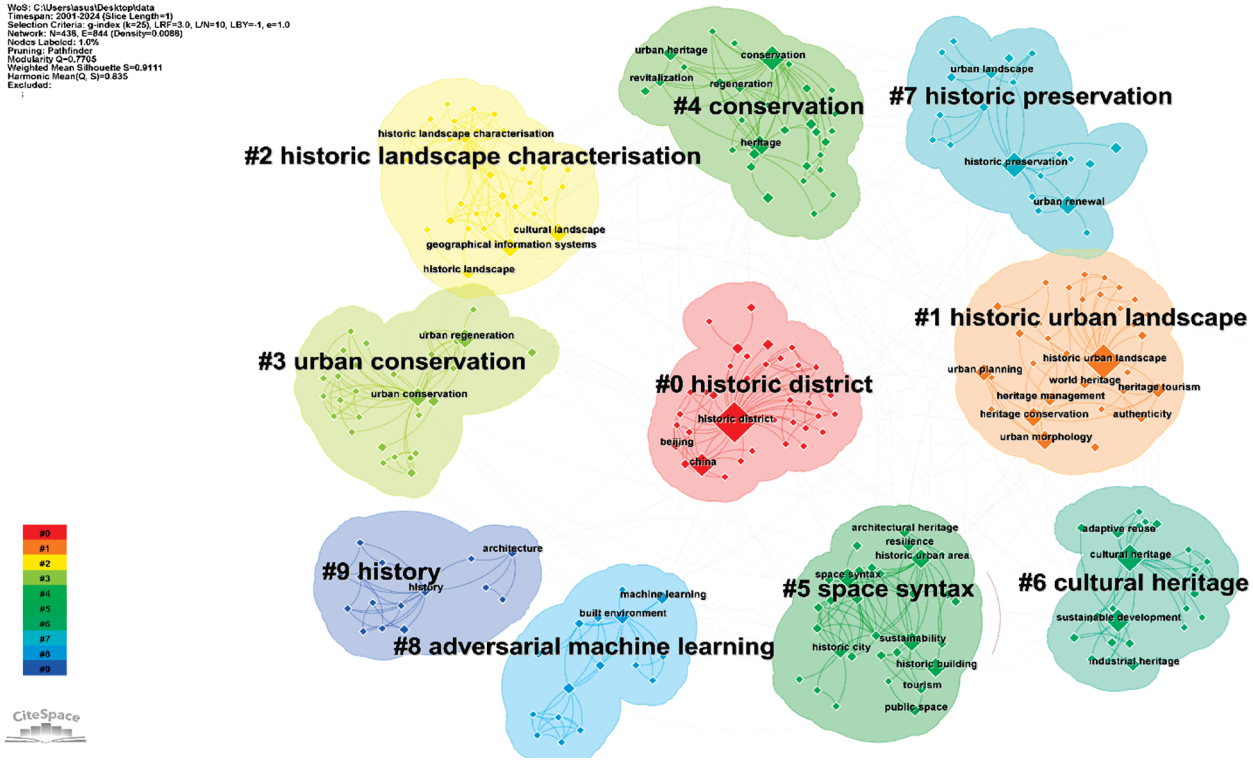


Figure 10. Keyword co-occurrence clustering map (cluster labels extracted via log-likelihood ratio (LLR) algorithm, depicting 10 core research themes).

Clusters in urban research focus on the relationship between historic districts and overall urban development, offering a theoretical basis for urban planning and district positioning. Environmental science-related clusters center on the ecological environment of historic districts, crucial for their green and sustainable development. Heritage conservation clusters revolve around protecting cultural heritage in these districts, involving conservation techniques and cultural inheritance. Sustainable development clusters consider multiple factors to explore paths for the sustainable development of historic districts.

Research trends show a growing cross-integration of these clusters. For instance, when studying the sustainable development of historic districts, it is essential to integrate the findings of multiple fields.

3.2.3. Landmark References

To identify the research topics in this field, we conducted a landmark reference co-occurrence map to display the frequency of co-occurrences among different references in Figure 11. We identified the top 10 landmark references based on citation frequency, as presented in Table 5. Using the Pathfinder pruning method, a Modularity Q value of 0.8018 was obtained, demonstrating significant modularity, as well as a Silhouette Score of 0.9155, indicating high internal consistency.

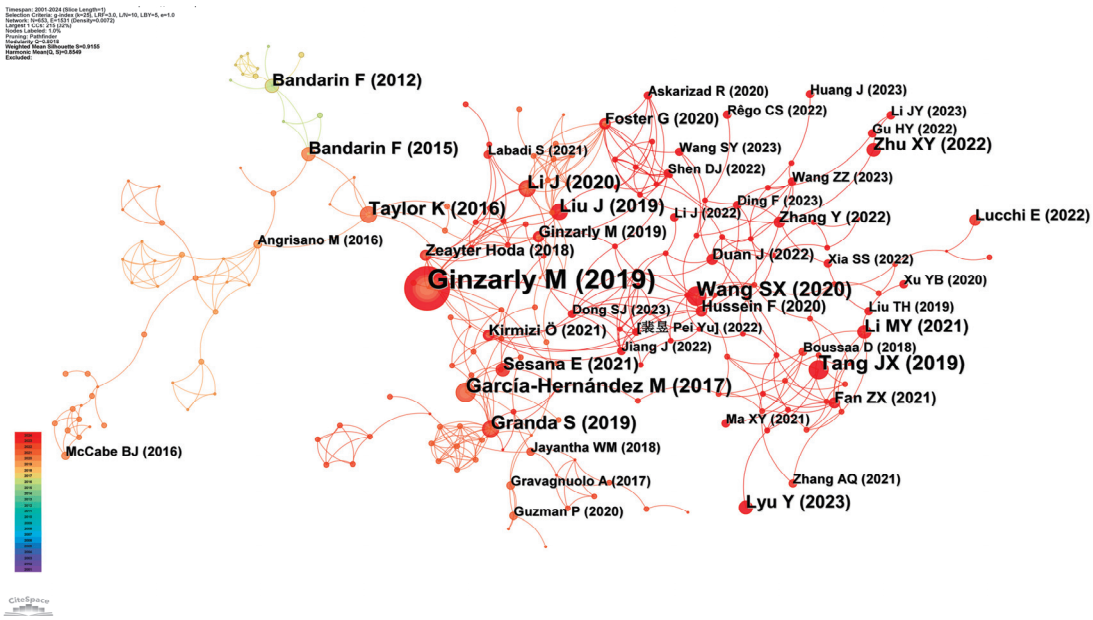


Figure 11. Landmark reference co-occurrence map.

Table 5. List of landmark references based on citation frequency.

NO.	Count	Year	Method	Cited Reference
1	16	2019	Desk work	The Historic Urban Landscape approach to urban management: a systematic review [35].
2	7	2017	Territorial paradigm	Cultural Heritage and Urban Tourism: Historic City Centres under Pressure [37].
3	7	2019	Visual measuring	Measuring visual quality of street space and its temporal variation: Methodology and its application in the Hutong area in Beijing [38].
4	7	2020	Morphological investigation	Pingyao: The historic urban landscape and planning for heritage-led urban changes.
5	6	2019	Fire Risk Index Method	Assessing Vulnerability and Fire Risk in Old Urban Areas: Application to the Historical Centre of Guimarães [39].
6	6	2020	Desk work	Community participation in cultural heritage management: A systematic literature review comparing Chinese and international practices [40].

Table 5. *Cont.*

NO.	Count	Year	Method	Cited Reference
7	6	2019	Field research and structural equation modeling	Effects of soundscape perception on visiting experience in a renovated historical block [41].
8	6	2016	Desk work	The Historic Urban Landscape paradigm and cities as cultural landscapes. Challenging orthodoxy in urban conservation [42].
9	5	2021	Urban sensor data	Revitalizing historic districts: Identifying built environment predictors for street vibrancy based on urban sensor data [43].
10	5	2015	Questionnaire surveys and partial least squares structural equation modeling	A Study on the Sustainable Development of Historic District Landscapes Based on Place Attachment among Tourists: A Case Study of Taiping Old Street, Taiwan [44].

We constructed a co-occurrence map of landmark references, which form the theoretical and methodological foundation of historic district research. Methodologically, these references integrate multidisciplinary approaches: desk work (40%) dominates, followed by spatial analysis (e.g., space syntax) and empirical investigations (questionnaires, field measurements). Notably, the temporal distribution of landmark references exhibits distinct phases: post-2019 studies account for 60%, indicating accelerated methodological innovation in recent years. For instance, Lyu et al. [45] used deep learning to evaluate street vitality, while Zhang et al. [46] applied social network analysis to community participation mechanisms, reflecting a technology-driven shift. Collectively, the landmark references reveal three research trajectories: theoretical evolution and practical challenges of the Historic Urban Landscape (HUL) framework; sustainable development-oriented technological applications; and the dynamic balance between community participation and tourism impacts.

4. Key Issues in the Research of Historic Districts

Based on the previous analysis, since the beginning of the 21st century, significant progress has been made in the research of historic districts in many aspects. It also faces complex problems in terms of concepts, conservation and development, sustainable development, urban renewal strategies, and community participation (Figure 12).

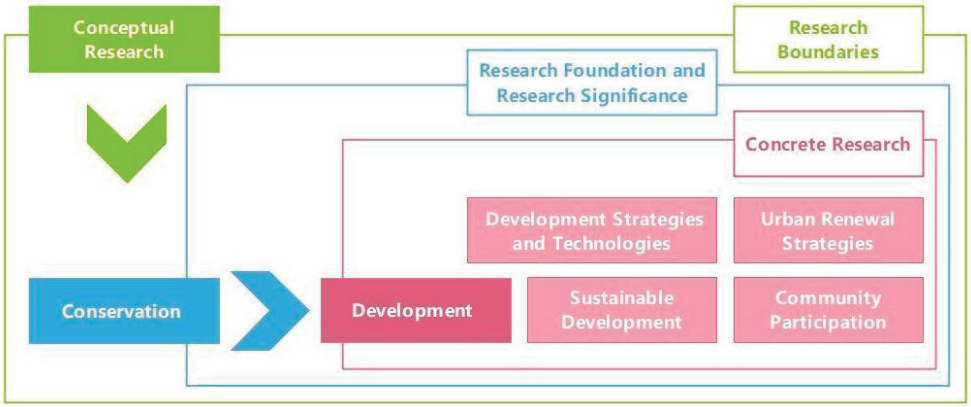


Figure 12. Key issues in the research of historic districts.

4.1. Conceptual Research

In recent years, research on historic areas has made significant progress in multiple directions. First, conceptual studies on historic areas have deepened, especially the concepts of "Historic District" and "Historic Urban Landscape" (HUL) [42]. The emergence of the HUL concept is considered an important development direction for regional heritage research and has gained particular attention in Europe, likely due to the influence of UNESCO and the European tradition in heritage studies. However, applying HUL principles at the local level remains a challenge, and researchers have proposed six steps as guidelines for local governments [35]. The expansion of the HUL concept goes beyond traditional district studies, emphasizing the multi-dimensional characteristics of the urban environment, including topography, geomorphology, hydrology, historical and modern architectural environments, open spaces, land use patterns, socio-cultural practices, economic processes, etc. [16]. As China integrates into the global system, the HUL concept is also gradually being incorporated into related research in China [17].

Although the HUL concept is of great significance, it faces numerous difficulties in practical applications due to differences in regional laws, cultures, and academic disciplines. Existing studies interpret it in a scattered manner, lacking a unified standard and thus making it difficult to guide practice. Future research should clarify its core elements, take into account regional differences, and establish a unified framework to enhance its applicability in different contexts.

4.2. Conservation

In the field of historic district conservation, value analysis is a fundamental and crucial aspect. Many studies have been dedicated to exploring effective value analysis methods, among which the Analytic Hierarchy Process (AHP) is widely applied [47], where authors have conducted analyses by combining AHP with Data Envelopment Analysis (DEA), providing a more comprehensive perspective for the value assessment of historic districts. Wang, Jin et al. [48] considered the dual nature of historic districts as both cultural heritage and living communities. Kou, Zhou et al. proposed using a combination of qualitative and quantitative methods with weighted averages. This approach is applicable to various historic districts and regions, offering a scientific method for conservation practice [49]. Some scholars have also attempted to conduct comprehensive restoration of historical areas based on the achievements of academic research [50].

While various value analysis methods are being explored and historical texts play a crucial role in historic district conservation, it is essential to note that these two aspects do not operate in isolation. In fact, they are intricately connected. The value analysis methods rely on historical texts to a great extent, as the information within these texts can significantly enrich the value assessment process. They are not only important bases for conservation work but also the foundation for formulating conservation strategies. In the cultural research of historical areas, numerous cases around the world offer rich research materials. Akbar, Iqbal et al. focused on the protection strategies of British-era heritage in Saddar Bazar, Karachi, through literature reviews and field investigations [51]. Despite abundant regulations on historical area conservation, the literature review reveals issues. Anderheggen pointed out that many historic districts overly emphasize aesthetic values at the expense of context values, causing local practices to ignore the significance of local historical and cultural resources [52]. Moreover, literature reviews can provide an assessment basis for restoring damaged historic districts, as shown in the study by Beeson, Lombardi et al. [53]. Value analysis methods in conservation face issues. They cannot fully account for historic districts' complex values. Research on historical documents is lacking,

and conservation often over-focuses on aesthetics, separating theory from practice. Future work should optimize these methods, dig deeper into historical documents, and bridge the theory–practice gap to safeguard districts' comprehensive values.

4.3. Development Strategies and Technologies

The development strategies and technologies of historic districts are multifaceted. In perception research, Septianto et al. classified districts as vibrant, relaxing, or dull based on public views, highlighting the importance of human sensory experiences [54]. This classification offers a new perspective for urban planners to design more appealing historic areas. Some scholars also focus on the consumers' intention to revisit historical blocks in order to find the key elements for the development of historical blocks [55].

Zhang and Xu explored users' humanistic needs from a cognitive psychology angle, aiming to create more user-friendly renovated spaces [18]. Regarding conservation, Zhang et al. proposed a 3D diagnostic framework for historic cultural areas, which can precisely analyze current conditions for better preservation [56]. Leng et al. and Li and Wang emphasized cultural continuity for authenticity [57,58]. Big data has become a key research tool; Lyu et al. used it to analyze the urban morphology of Yushan Historic District, uncovering its spatial development secrets [45,59]. Gao et al. pointed out Wi-Fi data's potential to understand people's movement patterns [60]. Xie et al. studied the auditory and visual environments of historic areas [61]. Pan et al. incorporated cultural ecosystem services into research, promoting ecological and cultural balance [62]. In China, historic area conservation research combines methods like GIS and space syntax [38,63,64]; urban regeneration research has gained attention, such as assessing the visual quality of street spaces and their changes using computer vision and deep learning technologies [38]. In addition, neural networks have also been applied to the research of historical areas [65].

For spatial structure, research has been carried out by using relatively traditional surveying and mapping methods [66]. Liang et al. analyzed the spatial structure of a historic district based on human behavior, revealing its social and functional attributes [67]. Zhu et al. put forward public-space-based optimization strategies for historic districts, enhancing their functionality and attractiveness [68]. Research in this area is plentiful but fragmented. New technologies' applications do not suit historic districts well. To improve, research directions need integration, and the fit between technologies and practical needs must be enhanced to better guide practice.

4.4. Sustainable Development

In the field of research on the sustainable development of historic districts, numerous achievements have provided key insights into different aspects of this complex topic. It mainly includes two strategic directions: low-carbon development and resilience (Figure 13).

Yang developed a method for detecting the surface temperature of historic districts, laying the foundation for subsequent low-carbon research and facilitating a deeper understanding of their energy-related characteristics [69]. Fan and Li paid attention to the changes in the microclimate of courtyards in historic districts, including issues related to thermal, lighting, solar, and wind environments [70]. Volkova, Krupenski et al. proposed that the adoption of district heating can significantly reduce carbon emissions in historic districts, providing a practical solution to address environmental sustainability issues [71]. Zhu and Chiou found that place attachment can positively influence tourists' pro-tourism and pro-environmental behaviors, providing a new perspective for the landscape planning of historic districts [44]. Dai, Xu et al. improved the ecological footprint model by using

component analysis and considering the main characteristics of historic districts, revealing that the ecological footprint of tourists is higher than that of residents [72].

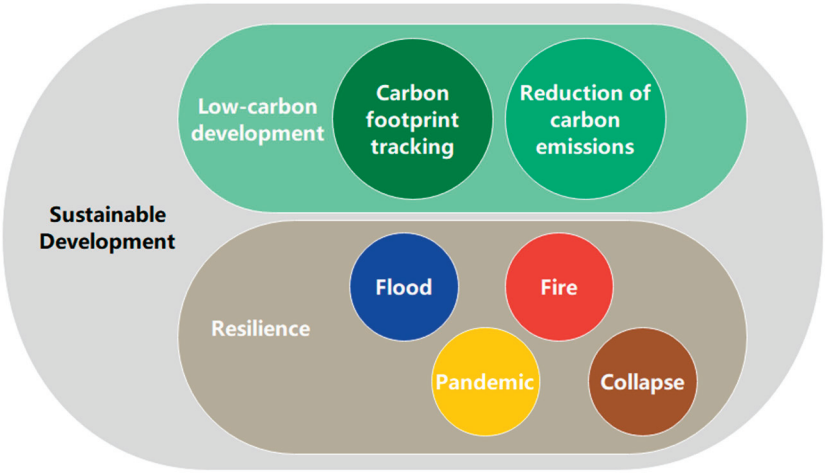


Figure 13. Sustainable development factors.

The relevant initiatives of the European Union regard historic districts as socio-ecological–technical systems, emphasizing the connection between resilience, disaster risk management, and climate change adaptation [73]. Granda and Ferreira combined the spatial structure with tourist behavior to conduct a fire resilience assessment of historic districts [39]. Bologna Pavlik and Zhou pointed out the role of historic districts in urban resilience, especially during the pandemic. Their layout is conducive to isolation and can slow down the spread of diseases [30]. Si, Li et al. proposed a hierarchical construction of the waterlogging prevention and control system for historic districts, making it consistent with historical features and coordinating with flood prevention systems. They also use intelligent platforms to strengthen supervision [74]. Tahoon, Abdel-Fattah et al. pointed out that social factors are often ignored in heritage risk assessment and clarified the predictive relationship between human-made disasters and the socioeconomic vulnerabilities of historic districts, providing a basis for preventing human-made disasters [75].

In the field of research on the sustainable development of historic districts, although there are achievements, such as progress in low-carbon and resilience research, there are also many limitations. Most of the research results in low-carbon development are theoretical and difficult to apply in practice. The method of detecting the surface temperature of historic districts only provides a theoretical basis and cannot contribute to practical energy optimization, thus failing to solve the problem of energy utilization. The assessment models and strategies in resilience research do not fully consider the actual situation of historic districts. When assessing risks like fires and floods, they overlook the complex social and economic structures and unique cultural backgrounds of these districts. As a result, the assessment results deviate from reality, and the strategies are difficult to use to deal with risks. At the same time, there is insufficient integration of multiple disciplines. The research results of various disciplines are isolated from each other, lacking a synergistic effect. Moreover, the research often ignores the uniqueness of historic districts. When pursuing sustainable development, it is easy to damage their original cultural and social values.

4.5. Urban Renewal Strategies

In urban renewal strategies for historic districts, a diverse range of concepts exist (Figure 14). The planning of historic districts is the primary concern for their development,

and different research studies focus on various aspects in specific design strategies. Zhao and Lou elaborated in detail on the revival ideas for historic districts from aspects such as cultural connotations, commercial atmosphere, traditional charm, living conditions, and implementation strategies. In the context of rapid urban construction, historic districts face issues like insufficient feature protection and landscape damage [76]. However, traditional urban design has drawbacks, including incomplete feature research, an imperfect work process, and a disconnection between design and implementation, mainly due to a mismatch between goals and implementation. Wang proposed a new action-oriented urban design approach that divides the work process into four stages, design preparation, planning, implementation, and evaluation, constructing a practical framework that is of great significance for the protection of historic districts [77]. Historic area regeneration strategies often emphasize their uniqueness and local characteristics through urban design to address historical, cultural, economic, or environmental values [41,78]. However, Nasser criticized these strategies for potentially leading to gentrification [79].



Figure 14. Historic district renewal strategies.

The concept of "creative city" has also influenced the design of historic districts. Chen studied creative clusters in media art, literature, etc., and presented findings to aid old-street renovation and Taiwan's historic district development [80]. In fact, during the development of historic districts, there is often potential space for new buildings. Embedded design is a common technique used in the design of historic districts, as noted by Shi, Hu et al. and Ochsner [81,82]. Li included street landscape elements like tree shade in the design [83]. Diversity and accessibility are considered to be important design objectives for vitality [84].

Some scholars suggest applying the Transit-Oriented Development (TOD) model to historical blocks [85]. Zhang proposed a Slow Traffic System to boost historic district vitality, as non-motorized transport can ease traffic congestion [86]. Deng and Chen found residents' emotional experiences are linked to their assessments of walking, public, landscape, and green areas, guiding quality-of-life improvements [87]. Sun and Chen categorized non-motorized lanes for better cycling environments [88]. Oba and Iseki noted that proper surface parking planning can safeguard urban landscapes [89]. Wen et al. used multi-source data to quantify factors affecting street-corner vitality [90]. Chen, Shu et al. introduced IT to simplify historic district design, and Ren, Wu et al. proposed sustainable

design strategies [91,92]. However, current design strategies have unclear concepts and implementation issues, lack unified evaluation, and often neglect residents' needs and district features. Future research should clarify concepts and establish a scientific evaluation system for balanced conservation and development.

Current research on historical blocks' impact on property values lacks a consistent conclusion, yet progress has been made on general influencing factors. Designating historic districts usually boosts property values, with premiums affected by heritage status and conservation regulations [93–95]. Zahirovic—Herbert and Gibler pointed out that these premiums are related to the historical reputation of the district [96]. However, like Heintzelman and Altieri, they argued that heritage conservation might have a negative impact, suggesting that other factors cause the supposed positive effects [97]. Nevertheless, Leichenko showed an undeniable link between historic areas and the economy [98]. Zhou proposed that this implies that the economic elements of historic districts are significantly influenced by political–economic factors [19]. Winson—Geideman, Jourdan et al. found that historic properties' value is affected by age, with increasing depreciation, and that inter-district price differences related to historic designation are at least partly due to investment disparities [99].

The impact of tourism on historic districts is complex. Initially, it is often considered negative for long-term residents. Shen et al. noted issues like property dispossession and cultural loss. Since the 1990s in China, heritage tourism has been seen as a way to revitalize historic districts [100]. Liu emphasized that this form of tourism focuses on providing tourists with nostalgic, cultural, and educational experiences [101]. European research, as García—Hernández, De la Calle—Vaquero et al. pointed out, shows tourism-induced morphological and functional changes in historic centers [37]. However, some scholars hold a different view. Xie, Li et al. argued that tourism can have positive impacts [102]. Luo and Chiou proposed a framework considering physical and cultural–natural environments for district management [103]. The study by Araya, Naoi et al. showed the importance of tourist attraction features for foreign tourists [104]. Current research is controversial due to single-perspective studies, lacking coverage of economic, cultural, and social impacts and balance mechanism research. Broader perspectives, integrated methods, and win–win solutions are needed.

4.6. Community Participation

In the realm of community participation, local communities, being both custodians and users of cultural heritage, are recognized as crucial stakeholders [105]. In many cases, residents have restricted opportunities to engage in conservation and regeneration strategies. The decision-making power is predominantly held by governments, as noted by Zhang and Zhang and Xin [46,106]. Such a power structure risks overlooking community interests, which in turn can impede the sustainable development of historic areas, as pointed out by Chang [107].

The boundaries of historic districts offer a means to measure the external landscape effects of historical facilities. Historical facilities are defined by their impact on the prices of other buildings through enhancing their views. Koster, van Ommeren et al. found that affluent families are more willing to pay for views of historical facilities and thus tend to locate themselves within historic districts. This helps to explain the significant spatial income disparities within cities [108]. Furthermore, spontaneously formed community associations can play a positive role in conservation efforts. Poole and Appler have indicated that these associations contribute effectively to the protection of historic areas [109]. The current community participation mechanism has flaws. Government-led models limit residents'

involvement and neglect their interests [40]. Participation evaluation is insufficient, and improvement measures lack focus. A fair mechanism and better evaluation can increase participation and protect community interests.

5. Conclusions

5.1. Comparative Analysis with Related Bibliometric Studies

This study employs CiteSpace to conduct a bibliometric analysis of studies on historic district conservation, demonstrating uniqueness in research methods, data sources, and conclusions compared to existing studies.

For example, Ginzarly [35] conducts research solely with HUL as the core. Chen's [110] research is solely concentrated on the realm of urban design. Similarly, the study by Mehrdad Chahardowli et al. [111] is narrowly focused on the field of Sustainable Regeneration. Undoubtedly, these research foci are essential and represent emerging research areas in recent years. During analysis, research only focuses on a limited number of concepts related to HUL. In contrast, this study integrates two major databases, Web of Science and Scopus, which enrich the data sources. Meanwhile, this study adopts the semantic network analysis method and incorporates 12 related terms, such as "historic district" (frequency: 62), "historic urban landscape" (frequency: 44), and "historic conservation area" (frequency: 17), into a unified analytical framework. Through the keyword co-occurrence network (Figure 7 shows this content), the dynamic relationships among these terms can be clearly presented. The study finds that the correlation strength between "historic district" and "urban regeneration" (frequency: 15) is significantly higher (co-occurrence strength: 0.19) than that between HUL and other terms, breaking through the research limitations of focusing only on a single theoretical concept.

In this study, through multidisciplinary cross—analysis, it has been identified that "green/sustainable science/technology" (with a frequency of 73) and "urban studies" (with a frequency of 72), among other research contents beyond traditional historical blocks, are developing rapidly in this field, breaking through the limitations of a single discipline such as architecture or planning.

5.2. Key Conclusions of Historic District Conservation Research and Their Reflections in Practice

Since the turn of the 21st century, research on historic district conservation has emerged as a critical global issue, focusing on balancing cultural heritage preservation with urban sustainable development. Through CiteSpace visualization analysis, this study systematically mapped the research trajectory, hotspots, and challenges in this field, yielding the following core conclusions:

- Conceptual Development and Application Dilemmas

Since the early 20th century, the concept of historic districts has undergone continuous evolution through dynamic interactions between international conservation charters and localized practices. UNESCO's Historic Urban Landscape (HUL) Framework (2011) redefines historic districts as "multilayered socio-ecological systems" that integrate natural topography, cultural heritage, and contemporary urban functions. This framework advocates for holistic conservation that balances physical preservation with social sustainability [112]. However, its implementation encounters significant challenges due to disparities in legal systems, cultural interpretations, and disciplinary approaches across regions [35]. A paradigmatic example lies in China's institutional response: the Regulations on the Protection of Famous Historical and Cultural Cities, Towns, and Villages (2008) established a "historic and cultural district" (historic and cultural blocks) system rooted in the principle

of "organic renewal". This approach emphasizes incremental urban regeneration while maintaining cultural authenticity, contrasting sharply with Europe's community-driven revitalization models that prioritize resident participation and adaptive reuse [17,50].

- Research Achievements and Disciplinary Trends

Since 2015, research on historic district conservation has experienced exponential growth, reflecting its increasing prominence in academic discourse. China has emerged as a leader in applying technical methods such as GIS and space syntax to conservation practice [38], whereas European and American studies prioritize theoretical innovation within the Historic Urban Landscape (HUL) framework [15]. High-impact journals including *Sustainability* and *Landscape and Urban Planning* reflect the interdisciplinary nature of this field, integrating urban studies, environmental science, and heritage management [57,62]. Through the combination of bibliometric analysis of research and historical documents, it can be found that in the process of research in this field, international historical documents such as the 2022 ICOMOS report "Urban Heritage for Resilience" show consistency in the bursts of research hotspots with the keyword "Resilience". This indicates that international treaties have a convergence in the main focus directions of this field. At the same time, the rapid expansion of research in this field in China shows that the development of this field, which has extremely strong local characteristics, is greatly influenced by the authorities.

- Research Clusters and Methodological Innovations

Through keyword co-occurrence and co-citation analysis, this study identifies four core clusters: urban morphological evolution, sustainable technology applications, community participation mechanisms, and disaster resilience assessment. Notably, emerging methods like deep learning and social network analysis are infiltrating traditional fields. For instance, space syntax quantifies street vitality [45], while machine learning models assist fire risk assessments [39].

- Gap between Theory and Practice and Future Directions

Despite abundant research, historic district conservation faces challenges of "theoretical advancements outpacing practical implementation". For example, the HUL framework is often reduced to "landscape beautification projects" in developing countries due to economic pressures [79]; community participation mechanisms remain policy-level rhetoric, limiting residents' decision-making power [46]. Future research should prioritize adaptive theory development and promote "technology institution culture" synergistic innovation [19].

6. Discussion

The conservation of historic districts in the 21st century stands at a critical juncture. Emerging trends bring both opportunities and challenges. This section delves deeper into these aspects, building on the conclusions drawn earlier.

6.1. Trends: Future Prospects for Historic District Conservation

- Strengthening of Holistic and Comprehensive Conservation

The evolution of the historic district concept, especially the advent of the HUL framework, has ushered in a new trend of holistic and comprehensive conservation. This trend will become even more prominent in the future. With the growing global focus on climate change, the concept of resilience within the HUL framework will be a core focus of future research and practice [113]. Most historic districts are in vulnerable areas of cities [53]. Thus, it is urgent to boost their resilience physically, socially, and economically. Future efforts will

center on integrating sustainable and resilient design into historic buildings, optimizing urban infrastructure against climate impacts, and enhancing community-based resilience.

- Increasing Significance of Interdisciplinary Research

Research in historic district conservation is becoming increasingly important, which is a significant future trend [114]. As research deepens, it is clear that a single discipline cannot offer comprehensive and effective solutions. So, the in-depth integration of disciplines like urban planning, architecture, environmental science, and sociology is essential. For example, combining environmental science with architecture and urban planning can aid in better assessing climate change impacts on historic buildings and landscapes and developing practical protection strategies. Integrating sociology with heritage conservation can mobilize local communities, increase their participation, and improve conservation effectiveness. In the future, more interdisciplinary projects are expected, with multidisciplinary teams collaborating closely in all aspects of conservation, from planning to implementation and monitoring, to provide comprehensive solutions.

- Development Opportunities from New Technologies

In the context of rapid technological development, new technologies have greatly influenced historic district conservation and brought new opportunities. In digital technology, laser scanning can create high-precision digital archives of historic districts, providing data for conservation and restoration [43,115]. VR and AR technologies allow people to experience historic districts immersively, raising public awareness of historical culture and enlivening the cultural tourism industry [116]. In big data and AI, big data analysis helps managers understand district usage and needs for better resource allocation. AI algorithms can diagnose building diseases and recommend restoration plans, improving conservation efficiency. Additionally, sensor-based intelligent monitoring systems can monitor building safety and environmental changes in real time, achieving dynamic protection.

6.2. Challenges: Barriers to Effective Conservation

- Challenge of Defining the Concept Clearly

The concept of historic districts has been evolving and expanding. The HUL concept, for example, includes multi-dimensional urban features [13]. While this shows a deeper understanding, it also blurs the concept. Different regions and disciplines have different interpretations and applications. In future research, it is crucial to clarify the boundaries and core elements while enriching the concept to form a clear and universal definition. This requires considering the uniqueness of historic districts in different regions and conducting in-depth research from multiple disciplines. For instance, by comparing characteristics of historic districts in various cultural backgrounds, common elements can be identified for a unified concept. Also, clear definition criteria should be established to standardize its use in research and conservation, avoiding confusion and inappropriate strategies.

- Challenge of Disciplinary Integration

Current historic district conservation research involves multiple disciplines. Each discipline's research has its own perspective, and there are potential conflicts when these findings are applied together. For example, urban planning's focus on function and space may conflict with architecture's need to preserve building authenticity. Environmental science emphasizes ecological sustainability, while sociology focuses on community needs, making it hard to balance in practice. In the future, disciplinary integration needs to be strengthened. An interdisciplinary research framework should be built to enhance communication and cooperation. One way is to form interdisciplinary teams for joint projects

to explore integrated applications. Another is to promote interdisciplinary theoretical innovation to develop comprehensive theories for resolving research conflicts.

- Challenge of Technology Application and Problem Simplification

With technological progress, research in historic district conservation has seen improved technical means like 3D modeling, big data analysis, and AI. These technologies support complex problem-solving, but conservation problems are becoming more complex, involving cultural, social, economic, and environmental factors. A key future challenge is to use advanced technologies to simplify problems and make conservation decisions more scientific and efficient. For example, big data analysis can extract key information from large amounts of data, and AI algorithms can optimize conservation plans. Also, the combination of technology and practical application should be enhanced to make technology more targeted and effective in solving real-world problems, preventing a disconnect between technology and actual needs.

The challenges in historic district conservation in the 21st century call for the joint efforts of academia, government agencies, social organizations, and the public. Through strengthening theoretical research, promoting disciplinary integration, and optimizing technology application, effective conservation and sustainable development of historic districts can be achieved.

6.3. Limitations

This study has certain limitations, which are mainly reflected in three aspects: data sources, research methods, and research conclusions.

In terms of data sources, the CiteSpace software focuses on English-language research. The purpose is to avoid the interference of sample differences in different databases in the research of global trends, because data noise can obscure the research results. For example, there are at least 2000 papers on this topic in the Chinese database of CNKI. However, this data selection method is likely to cause language bias and lead to the neglect of non-English-language research. Given the regional characteristics of historic district conservation, it is crucial to include national and local documents. Analyzing only the literature in the Web of Science database makes it likely to miss important information.

Regarding research methods, this study has a certain degree of dependence on the parameters of CiteSpace. Taking the Kleinberg burst detection model as an example, in order to balance the presentation of detection results and significant but mild trends, the current study sets the γ parameter to 0.2. If the γ value is too low (such as 0.1), it will generate too many detection results that include minor fluctuations. If it is too high (such as 0.5), some significant but mild trends may be excluded from the analysis. This shows that parameter settings have a great impact on the results, and there is a risk of bias.

In terms of research conclusions, this study is based on bibliometric analysis, which has limitations when applied to the actual conservation of historic districts. Although bibliometric analysis can reveal research trends and hotspots, it is difficult to present the complex actual situations. The actual conservation work involves many factors such as local culture, economy, and policy implementation, which are not fully reflected in bibliometric analysis, thus limiting the wide applicability of the research conclusions.

Author Contributions: L.G.: Conceptualization, Methodology, Investigation, Writing—original draft, Writing—review & editing. M.X.: Supervision, Project administration, Funding acquisition, Writing—review & editing. J.L.: Data curation, Formal analysis, Visualization, Writing—review & editing. J.M.: Resources, Writing—review & editing. All authors have read and agreed to the published version of the manuscript.

Funding: This research received no external funding.

Data Availability Statement: No new data were created or analyzed in this study. Data sharing is not applicable to this article.

Conflicts of Interest: The authors declare no conflict of interest.

References

1. Dimelli, D. Modern Conservation Principles and Their Application in Mediterranean Historic Centers—The Case of Valletta. *Heritage* **2019**, *2*, 787–796. [CrossRef]
2. Hoagland, A.K. Where is the history in historic districts?: Introduction. *Public Hist.* **2010**, *32*, 11. [CrossRef]
3. Ronchini, C. Cultural paradigm inertia and urban tourism. In *The Future of Tourism: Innovation and Sustainability*; Springer: Berlin/Heidelberg, Germany, 2019; pp. 179–194. [CrossRef]
4. Aylworth, S. A Multifaceted Approach to Historic District Interpretation in Georgia. *Public Hist.* **2010**, *32*, 42–50. [CrossRef]
5. Mumford, E.P. *The CIAM Discourse on Urbanism, 1928–1960*; MIT Press: Cambridge, MA, USA, 2002.
6. Hamer, D. Learning from the past: Historic districts and the new urbanism in the United States. *Plan. Perspect.* **2000**, *15*, 107–122. [CrossRef]
7. Petzet, M. Principles of preservation: An introduction to the international charters for conservation and restoration 40 years after the Venice Charter. In *International Charters for Conservation and Restoration*; Monuments and Sites; ICOMOS: München, Germany, 2004; Volume 1, pp. 7–29.
8. Cucco, P. Dalla Conservazione Integrata di Amsterdam (1975) all'Integrated Approach to Cultural Heritage (2020). Nuove prospettive nello scenario di cambiamenti globali. *Esempi Archit. Int. J. Archit. Eng.* **2020**, *2*, 1–10.
9. Médard, C. City planning in Nairobi. In *Nairobi Today*; Mkuki na Nyota Publishers: Nairobi, Kenya, 2010; pp. 25–60.
10. ICOMOS International Scientific Committee; ISPRS Permanent Committee (ISC). *Charter for the Conservation of Historic Towns and Urban Areas. Adopted by ICOMOS General Assembly*; ICOMOS: Paris, France, 1987.
11. Stovel, H. Origins and influence of the Nara document on authenticity. *APT Bull.* **2008**, *39*, 9–17.
12. Truscott, M.; Young, D. Revising the Burra Charter: Australia ICOMOS updates its guidelines for conservation practice. *Conserv. Manag. Archaeol. Sites* **2000**, *4*, 101–116. [CrossRef]
13. Martini, V. The Historic Urban Landscape (HUL) as a new approach to the conservation of historic cities. *Landsc. Imagin.* **2012**, 579.
14. De Marco, L.; Hadzimuammedovich, A.; Kealy, L. *ICOMOS-ICCROM Guidance on Post-Disaster and Post-Conflict Recovery and Reconstruction for Heritage Places of Cultural Significance and World Heritage Cultural Properties*; ICOMOS & ICCROM: Paris, France, 2023.
15. Ghanbari, E.; Lotfi, S.; Sholeh, M. HUL values in practice: A character area designation model for the conservation of built heritage in less-developed regions. *J. Cult. Herit.* **2024**, *70*, 41–53. [CrossRef]
16. United Nations Educational, Scientific and Cultural Organization. Recommendation on the historic urban landscape. In Proceedings of the Records of the General Conference 36th Session, Paris, France, 25 October–10 November 2011.
17. Fan, L. International influence and local response: Understanding community involvement in urban heritage conservation in China. *Int. J. Herit. Stud.* **2014**, *20*, 651–662. [CrossRef]
18. Zhang, D.; Xu, S. Humanistic needs and satisfaction study of multi-users in historic districts based on cognitive psychology. *Psychiatr. Danub.* **2021**, *33* (Suppl. S8), 681–693.
19. Zhou, Y. The political economy of historic districts: The private, the public, and the collective. *Reg. Sci. Urban Econ.* **2021**, *86*, 103583. [CrossRef]
20. Chen, C. Science mapping: A systematic review of the literature. *J. Data Inf. Sci.* **2017**, *2*, 1–40.
21. Chen, C. *CiteSpace: A Practical Guide for Mapping Scientific Literature*; Nova Science Publishers: Hauppauge, NY, USA, 2016.
22. Zhao, Y.; Li, J.; Tao, C.; Ding, R. Research hotspots and trends of cardiopulmonary exercise test: Visualization analysis based on citespace. *Med. Nov. Technol. Devices* **2022**, *16*, 100191. [CrossRef]
23. Chen, C. Visualizing Patterns and Trends in Scientific Literature. Citespace 2012. Available online: http://cluster.cis.drexel.edu/~cchen/citespace/ (accessed on 19 March 2025).
24. Small, H. Co-citation in scientific literature-new measure of relationship between 2 documents. *J. Am. Soc. Inf. Sci.* **1973**, *24*, 265–269. [CrossRef]
25. Chen, C. CiteSpace II: Detecting and visualizing emerging trends and transient patterns in scientific literature. *J. Am. Soc. Inf. Sci. Technol.* **2006**, *57*, 359–377. [CrossRef]

26. Jia, G.L.; Ma, R.G.; Hu, Z.H. Review of Urban Transportation Network Design Problems Based on CiteSpace. *Math. Probl. Eng.* **2019**, *2019*, 5735702. [CrossRef]
27. Chen, C.; Ibekwe-SanJuan, F.; Hou, J. The structure and dynamics of cocitation clusters: A multiple-perspective cocitation analysis. *J. Am. Soc. Inf. Sci. Technol.* **2010**, *61*, 1386–1409. [CrossRef]
28. Chen, Y.; Wang, Y.P.; Zhou, D. Knowledge Map of Urban Morphology and Thermal Comfort: A Bibliometric Analysis Based on CiteSpace. *Buildings* **2021**, *11*, 427. [CrossRef]
29. Azkarate, A.; Azpeitia, A. Paisajes urbanos históricos¿ Paradigma o subterfugio. In *Alla Ric. Di Un Passato Complesso. Contrib. Onore Di Gian Pietro Brogiolo Per Il Suo Settantesimo Compleanno*; Universidad de Zagreb: Zagreb, Croatia, 2016; pp. 307–326.
30. Pavlik, J.B.; Zhou, Y. Are historic districts a backdoor for segregation? Yes and no. *Contemp. Econ. Policy* **2023**, *41*, 415–434. [CrossRef]
31. Hu, H. Tourism development of historic and cultural district based on tourists' experience. *Econ. Res. Guide* **2010**, *109*, 97–99.
32. Acharya, S.K. Urban development in post-reform China: Insights from Beijing. *Nor. Geogr. Tidsskr. Nor. J. Geogr.* **2005**, *59*, 228–236. [CrossRef]
33. Qian, Z. World Heritage Site inscription and waterfront heritage conservation: Evidence from the Grand Canal historic districts in Hangzhou, China. *J. Herit. Tour.* **2021**, *16*, 684–704. [CrossRef]
34. Li, S.; Nobuo, A.; Ruoran, W.; Xu, S. Development of cultural heritage conservation planning in China. *Plan. Perspect.* **2024**, *39*, 925–943. [CrossRef]
35. Ginzarly, M.; Houbart, C.; Teller, J. The Historic Urban Landscape approach to urban management: A systematic review. *Int. J. Herit. Stud.* **2019**, *25*, 999–1019. [CrossRef]
36. Kleinberg, J. Bursty and hierarchical structure in streams. In Proceedings of the Eighth ACM SIGKDD International Conference on Knowledge Discovery and Data Mining, Edmonton, AB, Canada, 23–26 July 2002; pp. 91–101.
37. García-Hernández, M.; De la Calle-Vaquero, M.; Yubero, C. Cultural heritage and urban tourism: Historic city centres under pressure. *Sustainability* **2017**, *9*, 1346. [CrossRef]
38. Tang, J.; Long, Y. Measuring visual quality of street space and its temporal variation: Methodology and its application in the Hutong area in Beijing. *Landsc. Urban Plan.* **2019**, *191*, 103436. [CrossRef]
39. Granda, S.; Ferreira, T.M. Assessing vulnerability and fire risk in old urban areas: Application to the historical centre of Guimarães. *Fire Technol.* **2019**, *55*, 105–127. [CrossRef]
40. Li, J.; Krishnamurthy, S.; Roders, A.P.; Van Wesemael, P. Community participation in cultural heritage management: A systematic literature review comparing Chinese and international practices. *Cities* **2020**, *96*, 102476. [CrossRef]
41. Liu, J.; Yang, L.; Xiong, Y.; Yang, Y. Effects of soundscape perception on visiting experience in a renovated historical block. *Build. Environ.* **2019**, *165*, 106375. [CrossRef]
42. Taylor, K. The Historic Urban Landscape paradigm and cities as cultural landscapes. Challenging orthodoxy in urban conservation. *Landsc. Res.* **2016**, *41*, 471–480. [CrossRef]
43. Li, M.; Liu, J.; Lin, Y.; Xiao, L.; Zhou, J. Revitalizing historic districts: Identifying built environment predictors for street vibrancy based on urban sensor data. *Cities* **2021**, *117*, 103305. [CrossRef]
44. Zhu, X.; Chiou, S.-C. A study on the sustainable development of historic district landscapes based on place attachment among tourists: A case study of Taiping old street, Taiwan. *Sustainability* **2022**, *14*, 11755. [CrossRef]
45. Lyu, Y.; Malek, M.I.A.; Jaàfar, N.H.; Sima, Y.; Han, Z.; Liu, Z. Unveiling the potential of space syntax approach for revitalizing historic urban areas: A case study of Yushan Historic District, China. *Front. Archit. Res.* **2023**, *12*, 1144–1156. [CrossRef]
46. Zhang, W.; Xin, J. Green Spaces and the Spontaneous Renewal of Historic Neighborhoods: A Case Study of Beijing's Dashilar Community. *Sustainability* **2023**, *15*, 16566. [CrossRef]
47. Wu, F.; Qin, S.; Su, C.; Chen, M.; Wang, Q.; Zhang, Q. Development of evaluation index model for activation and promotion of public space in the historic district based on AHP/DEA. *Math. Probl. Eng.* **2021**, *2021*, 6590699. [CrossRef]
48. Wang, Y.; Jin, C.; Xu, D.; Wang, T.; Wang, B. Analysis of Multi-Dimensional Layers in Historic Districts Based on Theory of the Historic Urban Landscape: Taking Shenyang Fangcheng as an Example. *Land* **2024**, *13*, 1736. [CrossRef]
49. Kou, H.; Zhou, J.; Chen, J.; Zhang, S. Conservation for sustainable development: The sustainability evaluation of the xijie historic district, dujiangyan city, China. *Sustainability* **2018**, *10*, 4645. [CrossRef]
50. Yung, E.H.K.; Chan, E.H.W.; Xu, Y. Sustainable Development and the Rehabilitation of a Historic Urban District - Social Sustainability in the Case of Tianzifang in Shanghai. *Sustain. Dev.* **2014**, *22*, 95–112. [CrossRef]
51. Akbar, S.H.; Iqbal, N.; Van Cleempoel, K. Saddar bazar quarter in Karachi: A case of British-era protected heritage based on the literature review and fieldwork. *Heritage* **2023**, *6*, 3183–3210. [CrossRef]
52. Anderheggen, S. Four Decades of Local Historic District Designation: A Case Study of Newport, Rhode Island. *Public Hist.* **2010**, *32*, 16–32. [CrossRef]

53. Beeson, S.T.; Lombardi, A.; Korkmaz, K.A. Condition Assessment of Cultural Heritage Buildings in the Historic Strand District of Galveston. In Proceedings of the International Conference on Protection of Historical Constructions (PROHITECH), Athens, Greece, 25–27 October 2021; pp. 816–827.
54. Septianto, E.; Poerbo, H.W.; Firmansyah; Martokusumo, W. Understanding the attractiveness of types of historic districts in Bandung: Implementing heritage conservation based on public perception. *J. Asian Archit. Build. Eng.* **2024**, 1–16. [CrossRef]
55. Zhao, S.; Marzuki, A.; Rong, W.; Ran, X. An empirical application of the consumer-based authenticity model in heritage tourism of the George Town historic district, Penang, Malaysia. *Heliyon* **2024**, *10*, e38254. [CrossRef] [PubMed]
56. Zhang, M.; Zhang, Y.; Fang, X.; Wang, X. A 3D spatial diagnostic framework of sustainable historic and cultural district preservation: A case study in Henan, China. *Buildings* **2023**, *13*, 1344. [CrossRef]
57. Li, H.Y.; Wang, F. Cultural Identity and Continuity-Case Study of Authentic Conservation of Xi'an Bei Yuan Men Historic District. *Appl. Mech. Mater.* **2013**, *357*, 1840–1846. [CrossRef]
58. Leng, H.; Shi, T.; Zhao, J. Study on Authenticity Protection and Restoration of Residential Historic District. *Appl. Mech. Mater.* **2013**, *357*, 1886–1889. [CrossRef]
59. Zhang, J.J.; Zhang, J.; Huo, X.W.; Zheng, W.H.; Zheng, X.; Zhang, M.M. Research on the positioning of protection and utilization of historic districts under big data analysis. In Proceedings of the 26th International Symposium of ICOMOS/ISPRS-International-Scientific-Committee-on-Heritage-Documentatio n (CIPA) on Digital Workflows for Heritage Conservation, Ottawa, ON, Canada, 28 August–1 September 2017; pp. 731–735.
60. Gao, Y.C.; Liu, S.; Wei, B.; Zhu, Z.N.; Wang, S.S. Using Wi-Fi Probes to Evaluate the Spatio-Temporal Dynamics of Tourist Preferences in Historic Districts' Public Spaces. *Isprs Int. J. Geo-Inf.* **2024**, *13*, 244. [CrossRef]
61. Xie, H.; He, Y.; Wu, X.Y.; Lu, Y. Interplay between auditory and visual environments in historic districts: A big data approach based on social media. *Environ. Plan. B-Urban Anal. City Sci.* **2022**, *49*, 1245–1265. [CrossRef]
62. Pan, Y.; Nik Hashim, N.H.; Goh, H.C. Public perception of cultural ecosystem services in historic districts based on biterm topic model. *Sci. Rep.* **2024**, *14*, 11717. [CrossRef]
63. Pickard, R. Area-based protection mechanisms for heritage conservation: A European comparison. *J. Archit. Conserv.* **2002**, *8*, 69–88. [CrossRef]
64. Akl, M.H.; Sheta, S.A.; ElGizawi, L. Application of BIM/GIS-based Integrated Models on the Historic Urban Districts of Rosetta City, Egypt. *Ital. J. Plan. Pract.* **2023**, *13*, 24–46.
65. Ding, F.; Ren, Y.Y.; Goudos, S.; Zhao, Y. Analysis of Public Space in Historic Districts Based on Community Governance and Neural Networks. *IEEE Access* **2023**, *11*, 81021–81032. [CrossRef]
66. Lee, T.M. The Spatial Form of Traditional Taiwanese Townhouses: A Case Study of Dihua Street in Taipei City. In Proceedings of the 7th European-Mediterranean International Conference (EuroMed), Nicosia, Cyprus, 29 Octber–3 November 2018; pp. 322–333.
67. Liang, W.; Ahmad, Y.; Mohidin, H.H.B. Spatial form and conservation strategy of Sishengci historic district in Chengdu, China. *Heritage* **2023**, *6*, 891–903. [CrossRef]
68. Zhu, X.Q.; Sun, J.J.; Fu, J.Y. Research on Mixed Vitality of Historic District and Space Mode Optimization: A Comparison between Hefang Street and Xinyifang in Hangzhou. *Appl. Mech. Mater.* **2013**, *357–360*, 1724–1729.
69. Yang, M. Variability of Land Surface Temperatures in Beijing's Historic Districts. *Sens. Mater.* **2024**, *36*, 3147–3165. [CrossRef]
70. Fan, R.B.; Li, X.M. Exploration on Traditional Courtyard Micro-Climate Characteristics and Improvement Method-Case Study of No. 6 Courtyard of Chang'anxue Alley in Xi'an Sanxuejie Historic District. *Appl. Mech. Mater.* **2013**, *357*, 1918–1927. [CrossRef]
71. Volkova, A.; Krupenski, I.; Kovtunova, N.; Hlebnikov, A.; Masatin, V.; Ledvanov, A. Converting Tallinn's historic centre's (Old Town) heating system to a district heating system. *Energy* **2023**, *275*, 127429. [CrossRef]
72. Dai, L.L.; Xu, B.X.; Wu, B.H. Assessing sustainable development of a historic district using an ecological footprint model: A case study of Nanluoguxiang in Beijing, China. *Area* **2017**, *49*, 94–105. [CrossRef]
73. Egusquiza, A.; Lückerath, D.; Zorita, S.; Silverton, S.; Garcia, G.; Servera, E.; Bonazza, A.; Garcia, I.; Kalis, A. Paving the way for climate neutral and resilient historic districts. *Open Res. Eur.* **2023**, *3*, 42. [CrossRef]
74. Si, S.; Li, J.Q.; Wang, Y.Z.; Liu, L. Thinking Critically through Key Issues in Improving the Effectiveness of Waterlogging Prevention and Control System in China's Historic Districts. *Sustainability* **2022**, *14*, 2913. [CrossRef]
75. Tahoon, D.M.; Abdel-Fattah, N.A.; Hegazi, Y.S. Social vulnerability of historic Districts: A composite measuring scale to statistically predict human-made hazards. *Ain Shams Eng. J.* **2023**, *14*, 102002. [CrossRef]
76. Zhao, L.; Lou, S.J. The Road of Complexity, The Road of Rehabilitation-Discussion of Detailed Planning for Protection and Renovation of the Southeast Area in the Ancient City of Liaocheng. *Appl. Mech. Mater.* **2012**, *174–177*, 2440–2446. [CrossRef]
77. Wang, Y.J. Urban design of historic districts based on action planning. *Open House Int.* **2018**, *43*, 43–51. [CrossRef]
78. Heath, T.; Oc, T.; Tiesdell, S. *Revitalising Historic Urban Quarters*; Routledge: London, UK, 2013; pp. 13–48.

79. Nasser, N. Planning for urban heritage places: Reconciling conservation, tourism, and sustainable development. *J. Plan. Lit.* **2003**, *17*, 467–479. [CrossRef]
80. Chen, Z.R. Observing the Frame of Creative Clusters/Groups: A Case Study of Historic Districts in Tainan City. In Proceedings of the 2018 1st IEEE International Conference on Knowledge Innovation and Invention (ICKII), Jeju, Republic of Korea, 23–27 July 2018; pp. 168–171.
81. Ochsner, J.K. The past and future of Pioneer Square: Historic character and infill construction in Seattle's First Historic District. *Change Over Time* **2017**, *7*, 320–343. [CrossRef]
82. Shi, Y.; Hu, X.Y.; Yang, J.Y. "Embedding" Updating Strategy Research of Urban Historic district-Taking South Historical District of Nanjing as example. *Appl. Mech. Mater.* **2013**, *397-400*, 712–716. [CrossRef]
83. Li, G.H.; He, N.; Zhan, C.H. Evaluation of tree shade effectiveness and its renewal strategy in typical historic districts: A case study in Harbin, China. *Environ. Plan. B-Urban Anal. City Sci.* **2022**, *49*, 898–914. [CrossRef]
84. Huang, J.; Hu, X.; Wang, J.Q.; Lu, A.D. How Diversity and Accessibility Affect Street Vitality in Historic Districts? *Land* **2023**, *12*, 219. [CrossRef]
85. Renne, J.L.; Listokin, D. Transit-oriented development and historic preservation across the United States: A geospatial analysis. *Transp. Res. Interdiscip. Perspect.* **2021**, *10*, 100373. [CrossRef]
86. Zhang, N. A preliminary study of slow traffic system to activate the vitality of historic districts take Wuhan Tanhualin historic district as an example. In Proceedings of the IOP Conference Series: Earth and Environmental Science, Chongqin, China, 20–22 November 2020; p. 012206.
87. Deng, Z.; Chen, D.; Qin, X.; Wang, S. Comprehensive assessment to residents' perceptions to historic urban center in megacity: A case study of Yuexiu District, Guangzhou, China. *J. Asian Archit. Build. Eng.* **2021**, *20*, 566–580. [CrossRef]
88. Sun, H.; Chen, Y.H. Research on the evaluation model of non-motorized tavel environment in historical districts considering riding speed. *Civ. Eng. J. Staveb. Obz.* **2024**, *33*, 591–606. [CrossRef]
89. Oba, T.; Iseki, H. Transportation Impacts on Cityscape Preservation: Spatial Distribution and Attributes of Surface Parking Lots in the Historic Central Districts. *J. Urban Plan. Dev.* **2020**, *146*, 04020014. [CrossRef]
90. Wen, Z.H.; Zhao, J.T.; Li, M.Z. A Study on the Influencing Factors of the Vitality of Street Corner Spaces in Historic Districts: The Case of Shanghai Bund Historic District. *Buildings* **2024**, *14*, 2947. [CrossRef]
91. Chen, Y.X.; Shu, B.; Chang, H.T. Exploring Architectural Shapes Based on Parametric Shape Grammars: A Case Study of the "Three Lanes and Seven Alleys" Historic District in Fuzhou City, China. *Buildings* **2023**, *13*, 2063. [CrossRef]
92. Ren, L.; Wu, Y.; Wang, Z. Sustainable Development of Historic Districts: From Cultural Resources to Cultural Narrative. In Proceedings of the IEEE Eurasia Conference on Biomedical Engineering, Healthcare and Sustainability (IEEE ECBIOS), Okinawa, Japan, 31 May–3 June 2019; pp. 83–86.
93. Been, V.; Ellen, I.G.; Gedal, M.; Glaeser, E.; McCabe, B.J. Preserving history or restricting development? The heterogeneous effects of historic districts on local housing markets in New York City. *J. Urban Econ.* **2016**, *92*, 16–30. [CrossRef]
94. Gilderbloom, J.I.; Hanka, M.J.; Ambrosius, J.D. Historic preservation's impact on job creation, property values, and environmental sustainability. *J. Urban.* **2009**, *2*, 83–101. [CrossRef]
95. Shipley, R.; Jonas, K.; Kovacs, J.F. Heritage Conservation Districts Work: Evidence from the Province of Ontario, Canada. *Urban Aff. Rev.* **2011**, *47*, 611–641. [CrossRef]
96. Zahirovic-Herbert, V.; Gibler, K.M. Historic district influence on house prices and marketing duration. *J. Real Estate Financ. Econ.* **2014**, *48*, 112–131. [CrossRef]
97. Heintzelman, M.D.; Altieri, J.A. Historic preservation: Preserving value? *J. Real Estate Financ. Econ.* **2013**, *46*, 543–563. [CrossRef]
98. Leichenko, R.M.; Coulson, N.E.; Listokin, D. Historic preservation and residential property values: An analysis of Texas cities. *Urban Stud.* **2001**, *38*, 1973–1987. [CrossRef]
99. Winson-Geideman, K.; Jourdan, D.; Gao, S. The Impact of Age on the Value of Historic Homes in a Nationally Recognized Historic District. *J. Real Estate Res.* **2011**, *33*, 25–47. [CrossRef]
100. Shen, S.; Zhao, J.; Xu, J.; Guo, J.; Shi, L. Understanding tourism development of historic districts from a representational perspective. *J. Tour. Cult. Change* **2016**, *14*, 291–306. [CrossRef]
101. Liu, J. Tourism Revitalization of Historic District in Perspective of Tourist Experience: A Case Study of San-Fang Qi-Xiang in Fuzhou City, China. In *Global Hospitality and Tourism Management Technologies*; de Pablos, P.O., Zhao, J., Eds.; IGI Global: Hershey, PA, USA, 2012; pp. 151–164.
102. Xie, Y.-F.; Li, L.; Guo, Y.-D.; Sun, X.-P.; Zhang, Y.-J. Sustainable Tourism-Oriented Conservation and Improvement of Historical Villages in the Urbanization Process: A Case Study of Nan'anyang Village, Shanxi Province, China. In *Urbanization and Locality: Strengthening Identity and Sustainability by Site-Specific Planning and Design*; Springer: Berlin/Heidelberg, Germany, 2016; pp. 187–203. [CrossRef]

103. Luo, H.; Chiou, B.-S. Framing the hierarchy of cultural tourism attractiveness of Chinese historic districts under the premise of landscape conservation. *Land* **2021**, *10*, 216. [CrossRef]
104. Araya, A.; Naoi, T.; Iijima, S. The Effects of Westerners' Presence on Japanese Evaluations of a Historic District: The Case of Takayama City. *J. Travel Tour. Mark.* **2016**, *33*, 628–644. [CrossRef]
105. Poulios, I. Discussing strategy in heritage conservation: Living heritage approach as an example of strategic innovation. *J. Cult. Herit. Manag. Sustain. Dev.* **2014**, *4*, 16–34. [CrossRef]
106. Zhang, X. Conversation on saving historical communities: A participatory renewal and preservation platform. In *IOP Conference Series: Materials Science and Engineering*; IOP Publishing: Bristol, UK, 2017; p. 082053.
107. Chang, H.-F. Development and Construction of Public Awareness of Community Characteristics Kaohsiung City's Historic District Industrial Recycling Case. In Proceedings of the 2013 International Conference on the Modern Development of Humanities and Social Science, Hong Kong, China, 1–2 December 2013; pp. 420–422.
108. Koster, H.R.; van Ommeren, J.N.; Rietveld, P. Historic amenities, income and sorting of households. *J. Econ. Geogr.* **2016**, *16*, 203–236. [CrossRef]
109. Poole, L.A.R.; Appler, D.R. Building a Local Preservation Ethic in the Era of Urban Renewal: How Did Neighborhood Associations Shape Historic Preservation Practice in Lexington, Kentucky? *J. Urban Hist.* **2020**, *46*, 383–405. [CrossRef]
110. Chen, D. Examining urban design strategies in historic districts: A systematic literature review. *Proc. Inst. Civ. Eng. Urban Des. Plan.* **2024**, *177*, 232–239. [CrossRef]
111. Chahardowli, M.; Sajadzadeh, H.; Aram, F.; Mosavi, A. Survey of Sustainable Regeneration of Historic and Cultural Cores of Cities. *Energies* **2020**, *13*, 2708. [CrossRef]
112. Bandarin, F.; Van Oers, R. *The Historic Urban Landscape: Managing Heritage in an Urban Century*; John Wiley & Sons: Hoboken, NJ, USA, 2012.
113. Duangputtan, P.; Mishima, N. Adapting the Historic Urban Landscape Approach to Study Slums in a Historical City: The Mae Kha Canal Informal Settlements, Chiang Mai. *Buildings* **2024**, *14*, 1927. [CrossRef]
114. Makhzoumi, J.; Al-Harithy, H.; Bazzi, M. Contextualizing UNESCO's Historic Urban Landscape Approach: A Framework for Identifying Modern Heritage in Post-Blast Beirut. *Land* **2024**, *13*, 2241. [CrossRef]
115. Lin, Y.; Zhang, M.; Yi, C.; Zhang, Y.; Xiong, J.; Lv, L.; Peng, X.; He, J. Sustainable Urban Regeneration with Wind and Thermal Environment Optimization: Design Roadshow of a Historic Town in China. *Coatings* **2024**, *14*, 1593. [CrossRef]
116. González-Albornoz, P.; López, M.I.; Carmona, P.; Rubio-Manzano, C. Digitalization and Spatial Simulation in Urban Management: Land-Use Change Model for Industrial Heritage Conservation. *Appl. Sci.* **2024**, *14*, 7221. [CrossRef]

Disclaimer/Publisher's Note: The statements, opinions and data contained in all publications are solely those of the individual author(s) and contributor(s) and not of MDPI and/or the editor(s). MDPI and/or the editor(s) disclaim responsibility for any injury to people or property resulting from any ideas, methods, instructions or products referred to in the content.

MDPI AG
Grosspeteranlage 5
4052 Basel
Switzerland
Tel.: +41 61 683 77 34

Buildings Editorial Office
E-mail: buildings@mdpi.com
www.mdpi.com/journal/buildings



Disclaimer/Publisher's Note: The title and front matter of this reprint are at the discretion of the Guest Editors. The publisher is not responsible for their content or any associated concerns. The statements, opinions and data contained in all individual articles are solely those of the individual Editors and contributors and not of MDPI. MDPI disclaims responsibility for any injury to people or property resulting from any ideas, methods, instructions or products referred to in the content.





Academic Open
Access Publishing

mdpi.com

ISBN 978-3-7258-5158-4